CHAPTER I

MINE AIR

1.1 COMPOSITION OF MINE AIR

Dry atmospheric air has the composition as given in Table 1.1. Composition of wet air is of course different depending on the moisture content.

Table 1.1 : Composition of Atmospheric Air

Components	% by volume	% by mass
Oxygen (O_2)	20.95	23.15
Carbon dioxide (CO_2)	0.03	0.046
Nitrogen (N_2)	78.09	75.52
Argon (Ar) and other rare inert gases like krypton, neon, xenon etc.	0.93	1.284
Total	100.00	100.00

Mine air on the other hand, invariably contains some impurities. Even in the least contaminated state, mine air contains more carbon dioxide than ordinary atmospheric air as there is no plant world underground to reconvert carbon dioxide to oxygen. Moisture content of mine air is also normally higher than that of surface air.

Impurities in mine air can be classified as: (a) non-toxic but explosive gases like methane (CH_4), acetylene (C_2H_2), hydrogen (H_2) and higher hydrocarbons; (b) toxic gases like carbon dioxide (CO_2), radon and its daughter products; (c) acutely poisonous gases like carbon monoxide (CO), nitrous fumes (NO_2), sulphur dioxide (SO_2), sulphuretted hydrogen (H_2S) and sometimes arsene and phosphene; (d) vapours of water, hydrocarbons (fuels and lubricants) and sometimes of metals like mercury or lead; (e) suspended fine liquid droplets such as fog due to condensed water-vapour or mist of fine oil droplets from drills etc., and (f) solid impurities such as dust, smoke and organisms.

Scanned with CamScanner

Of these, most important impurities affecting the health of the workers are the toxic and poisonous gases and vapours and pathogenic dusts. Mists of oil and water-vapour fogs are mainly nuisances. Smoke (from diesel engine exhaust, blasting or fires) is a minor irritant while organisms are of little consequence in mines.

1.2 OXYGEN (O_2, Molecular mass—32)

This is a colourless, odourless and tasteless gas of a specific gravity (relative to air) equal to 1.105, i.e., slightly heavier than air. One m^3 of oxygen at 273.15 K and 101.33 kPa has a mass of 1.426 kg. Oxygen has low solubility, 3 volumes being dissolved in 100 volumes of water at 293K. It supports life and combustion and hence is essential in sufficient quantities in any atmosphere where men work.

Oxygen deficiency in mine air occurs chiefly due to (a) oxidation of combustible substances like timber and minerals like coal, pyrites etc., as well as (b) addition of large quantities of gases such as methane, carbon dioxide etc., in the mine, though breathing of men, burning of flame-safety lamps and working of internal-combustion engines contribute to a lesser extent to the depletion of oxygen in mine air. Fires and explosions underground lead to a rapid development of large oxygen deficiencies.

1.2.1 Physiological Effects of Oxygen Deficiency in Air

During normal functioning of the lung, oxygen from the air is absorbed by the haemoglobin of the blood forming oxyhaemoglobin which soon parts with the oxygen to restore the broken-down cells of the body. In turn the blood gives out carbon dioxide which is exhaled. Thus the exhaled air contains less oxygen (15.5–18%) and an increased amount of carbon dioxide (2.6–6.6%). The rate of breathing as well as the quantity of carbon dioxide exhaled vary according to the rate of work of the man. Table 1.2 gives some relevant data about respiration. It is seen from the table that when doing hard work, a man breathes about $60 \times 10^{-3} m^3$ of air per minute. But the rate of inhalation may increase considerably when he is working very hard though such high rates are sustained only for a short time. According to Schneider, a breathing rate of 100 min^{-1} can be sustained for 15 minutes whereas that of 150 min^{-1} can be sustained for 1 to 2 minutes only.

Table 1.2 : Respiration Data

Nature of work	O_2 consumed in $m^3min^{-1} \times 10^{-3}$	CO_2 exhaled in $m^3min^{-1} \times 10^{-3}$	Respiratory quotient, CO_2 exhaled/ O_2 consumed	Quantity of air breathed in $m^3min^{-1} \times 10^{-3}$	Av. vol. of each breath in $m^3 \times 10^{-3}$	No. of breaths per minute
Rest in bed (1)	0.237	0.197	0.83	7.7	0.457	16.8
Rest standing (1)	0.328	0.264	0.81	10.4	0.612	17.1
Walking @3.2 km h^{-1}(1)	0.780	0.662	0.85	18.6	1.270	14.7
Walking @6.4 km h^{-1}(1)	1.595	1.395	0.88	37.3	2.060	18.2
Walking @8.1 km h^{-1}(1)	2.543	2.386	0.94	60.9	3.140	19.5
Rest (2)	0.303	0.227	0.75	5.3–14	0.42–0.75	12–18
Moderate rate of work(2)	2.121	1.909	0.9	49–63	1.58–2.10	30
Very vigorous work (2)	3.03	3.03	1.0	105	2.63	40

(1) Values obtained by Haldane at NTP.(273 K temperature and 101.33 kPa barometer)[1]
(2) Based on work of Forbes and Grove.[70]

Deficiency of oxygen in the air breathed has no serious effect if it is small. Breathing becomes faster and deeper at 17% O_2. At 15% there is dizziness, buzzing in the ears and rapid heart beat 13% leads to unconsciousness after prolonged exposure while at 10% unconsciousness follows in half an hour. At 7% there is heavy panting and palpitation, the face turns leaden blue and the senses get dulled and confused rapidly leading to unconsciousness. In air without any oxygen at all, a man becomes unconscious in forty seconds without warning because of anoxia.

The above physiological effects are with oxygen deficiency only, i.e. when the air contains only inert gases like nitrogen or methane and no asphyxiants like carbon dioxide or poisonous gases like carbon monoxide, nitrous fumes etc., which would worsen the effects. Men affected by severe oxygen deficiency usually suffer from convulsion and stoppage of respiration following unconsciousness. Heart beat may stop after a long exposure. If the heart beats, howsoever feeble it may be, animation can be effected by bringing the patient to fresh air immediately and applying artificial respiration. Symptoms of oxygen deficiency also depend on the partial pressure of oxygen which governs its absorption in the blood. Hence, a depression of barometric pressure at high altitudes enhances the effect of oxygen deficiency whereas an increase in barometric pressure at depth produces the reverse effect. It must be noted here that whereas carbon dioxide malady (see later) gives a distinct warning by heavy panting, oxygen deficiency may not give much warning.

It is prescribed by law in India[2] that mine air should contain atleast 19% of oxygen though this limit is 20% in the U.S.S.R. and 19.5% in the U.S.A.

Taking a hard working man to consume 2.5×10^{-3} m^3 min^{-1} of oxygen the required quantity of fresh air Q containing 21% O_2 needed to be supplied to the working place per minute so as to keep the level of O_2 concentration at 19% can be obtained from the oxygen balance equation per minute:

Amount of O_2 in intake air − amount of O_2 consumed = amount of O_2 in the exhaust air.

Or, $0.21\,Q-2.5\times10^{-3}=0.19Q$.

Or, $Q = \dfrac{2.5\times10^{-3}}{0.21-0.19} = 0.125$ m^3 min^{-1}

Note that there is no difference in the volume rate of the exhaust air and the intake air, since O_2 removed from the intake air by breathing is almost completely balanced by CO_2 produced.

Oxygen in excess of the percentage normally present in air has no harmful effect. However, continuous exposure to an atmosphere containing 80% oxygen for 48 hours produces irritating effects.

Example 1.1

A sample of mine air has the following volumetric composition: O_2—19.81%, CO_2—0.92%, CH_4—1.02% and N_2—78.25%. Calculate the composition by mass. What would be its composition (both by volume and by mass) if the air were saturated with water-vapour at the sampling temperature of 303K and atmospheric pressure of 101.33 kPa ?

At a given state, a certain volume of any gas contains the same number of molecules so that its mass is in proportion of its molecular mass.

Gas	% by volume V	Molecular mass M	VM	% by mass
O_2	19.81	32	633.92	22.00
CO_2	0.92	44	40.48	1.40
CH_4	1.02	16	16.32	0.57
N_2	78.25	28	2191.00	76.03
Total	100.00		2881.72	100.00

% by mass $= \dfrac{VM}{\Sigma(VM)}\times100$ is computed in the last column of the table above.

At a temperature of 303K saturated and barometer of 101.33 kPa (see psychrometric chart in Chapter III) 1 kg of dry air contains 28g of water-vapour, so that the mass of 1 kg of dry air when saturated =1028g. The composition by mass as also by volume calculated from the relation— % by volume$=\dfrac{m/M}{\Sigma(m/M)}\times100$ is given in the table below.

Scanned with CamScanner

Gas	Mass per kg of dry air, g	M	% by mass m	$\frac{m}{M}$	% by volume
O_2	220.0	32	21.40	0.6688	18.96
CO_2	14.0	44	1.36	0.0309	0.88
CH_4	5.7	16	0.55	0.0344	0.98
N_2	760.3	28	73.96	2.6414	74.89
H_2O	28.0	18	2.73	0.1517	4.29
Total	1028.0		100.00	3.5272	100.00

Example 1.2

A man when doing hard work in a confined space breathes 60.9×10^{-3} m³ of air per minute. He consumes 2.5×10^{-3} m³ of oxygen and produces 2.4×10^{-3} m³ of carbon dioxide per minute. Calculate the composition of the exhaled air and the quantity of fresh air necessary to be supplied so that the man is never left in an atmosphere containing more than 0.5% carbon dioxide. The composition of inhaled air is as given in Table 1.1.

In a minute, the man inhales $60.9\times10^{-3}\times0.2095=12.76\times10^{-3}$ m³ of O_2. But he consumes 2.5×10^{-3} m³ of O_2 so that the O_2 still present in exhaled air

$$=(12.76-2.5)\times10^{-3}=10.26\times10^{-3}\ \text{m}^3.$$

CO_2 present in exhaled air

$$=2.4\times10^{-3}+0.0003\times60.9\times10^{-3}=2.42\times10^{-3}\ \text{m}^3.$$

N_2 (inclusive of other inert gases) undergoes no change

$$=60.9\times10^{-3}\times0.7902=48.12\times10^{-3}\ \text{m}^3.$$

Total volume of exhaled air

$$=(10.26+2.42+48.12)\times10^{-3}=60.8\times10^{-3}\ \text{m}^3.$$

∴ The composition of exhaled air is

$$O_2 = \frac{10.26\times10^{-3}}{60.8\times10^{-3}}\times100 = 16.88\%$$

$$CO_2 = \frac{2.42\times10^{-3}}{60.8\times10^{-3}}\times100 = 3.98\%$$

$$N_2 = \frac{48.12\times10^{-3}}{60.8\times10^{-3}}\times100 = 79.14\%$$

$$\text{Total } 100\ \%$$

In order to maintain the percentage of CO_2 at 0.5% in the air, the man should exhale an amount of carbon dioxide that forms $0.50-0.03=0.47\%$ of the air supplied.

Since the man exhales 2.4×10^{-3} m³ of carbon dioxide per minute the fresh air supply per minute $=2.4\times10^{-3}\div0.0047=0.5106$ m³.

1.2.2 Detection of Oxygen Deficiency

A good warning of oxygen deficiency is given by oil lamps which exhibit a regular fall in their luminous intensity with oxygen deficiency (with 19% O_2, the luminous intensity drops to two-thirds its value in normal air) and are extinguished at 17% oxygen, but acetylene (carbide) lamps can burn even with 12 to 13% oxygen and hence are of no warning value. Briggs devised an attachment by which the air inlet to a safety lamp can be throttled. The degree of throttling required to extinguish the flame gives a measure of the oxygen content of the air. Portable oxygen indicators and monitors with warning devices (when the oxygen content falls below a predetermined level) are also in use in various parts of the world. A Russian portable detector uses the principle of oxidation of copper by the O_2 present in the sampled air in the presence of ammonium chloride with excess ammonia. The reduction in the volume of the air sample after oxidation and the consequent vacuum created is indicated on a manometer which can be graduated in percentage of oxygen. However, the flame-safety lamp still serves as the most prevalent indicator of oxygen deficiency.

1.3 NITROGEN (N_2, Molecular mass--28)

This is a colourless, odourless and tasteless gas, lighter than air (sp. gr.=0.967). It does not support life or combustion and is inert. It has low solubility, 100 volumes of water dissolving 1.5 volumes of nitrogen at 293K.

Nitrogen is produced in mines by the decomposition of organic substances, blasting with explosives (1 kg of nitroglycerine releases 0.64m³ or gases including 0.135m³ of N_2) and as emission from strata.

Scanned with CamScanner

Nitrogen has no harmful effect on the human system except that at higher concentrations, it leads to oxygen deficiency with consequent physiological effects.

1.4 METHANE (CH_4, Molecular mass—16)

Methane is a colourless and odourless gas with a specific gravity equal to 0.559. One m^3 of methane at NTP (273.15K and 101.33kPa) has a mass of 0.716 kg. That is why it has a tendency to accumulate in cavities at the roof of drives. It is slightly soluble in water, 100 volumes of water dissolving 3.3 volumes of methane at 293K. It burns with a blue flame producing carbon dioxide and water.

$$CH_4 + 2O_2 = CO_2 + 2H_2O \quad (1.1)$$

The above equation indicates the end products while in reality, the process is a chain reaction proceeding through several intermediate steps. Under suitable conditions, the reaction gets self-accelerated leading to an explosion and this is the most hazardous character of methane which has engaged the attention of mining engineers.

The combustion of methane in air can be expressed as

$$CH_4 + 2(O_2 + 4\,N_2) = CO_2 + 2\,H_2O + 8\,N_2 \quad (1.2)$$

taking air to contain one volume of O_2 and four volumes of N_2. It is clear from the equation that proper oxygen balance occurs when methane content of air is one-eleventh or 9.5% by volume. That is why this concentration forms the most explosive mixture of methane in air. One kg of methane on complete combustion releases 55685kJ of heat as compared to 2428 kJ produced by a kg of gunpowder and 6280 kJ produced by a kg of nitroglycerine. However, methane explosions are not as violent as that of commercial explosives since the density of the most explosive methane-air mixture is only 1.15 kg m^{-3} at 293K as compared to a density of 1000 kg m^{-3} for black powder and 1600 kg m^{-3} for nitroglycerine.

The explosibility of methane in air depends on the composition of the mixture. In normal air, methane concentrations upto 5% lead to no explosion, though the mixture can burn. Also concentrations higher than 14% do not form explosive mixtures as the excess methane absorbs a substantial amount of heat (methane has a specific heat equal to 2.47 kJ kg^{-1} K^{-1} compared to 0.96 kJ kg^{-1} K^{-1} for air) and decomposes to C_2H_2 and H_2. At such high

concentrations, the oxygen content of air becomes too low for complete combustion of methane which then burns producing CO and H_2. Air containing 25% methane will extinguish a flame as its oxygen content will be reduced to about 15%.

$$CH_4 + O_2 = CO + H_2 + H_2O \quad (1.3)$$

The explosibility limits stated above are for mixtures of methane and air with normal oxygen content. The effect of the percentage of oxygen in air on the limits of explosibility is shown in Fig. 1.1 (*Coward Diagram*). It is clear that with deficiency of O_2 the limits of explosibility narrow down and there is no explosion possible below an O_2 content of about 12%, whatever may be the methane concentration. Similarly presence of excess inert gases like CO_2 or N_2 or water vapour narrows down the limits of explosibility.

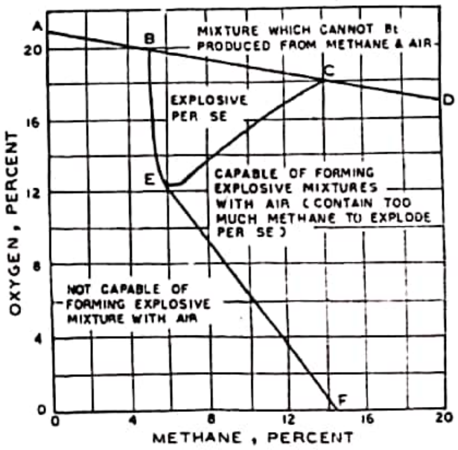

Fig. 1.1 Coward diagram.

The limits of explosibility on the other hand expand if methane is associated with other combustible gases such as ethane, hydrogen etc., depending on their relative concentration and individual limits

Scanned with CamScanner

of explosibility. The limit of explosibility 'x' of a mixture of combustible gases can be computed from the *Le Chatelier Equation*

$$x = \frac{100}{V_1/x_1 + V_2/x_2 + V_3/x_3 \ldots\ldots} \% \qquad (1.4)$$

where V_1, V_2, V_3 ..... are the percent by volume of the different combustible components ($V_1+V_2+V_3 \ldots\ldots = 100\%$) and x_1, x_2, x_3 ......, the limits of explosibility of the corresponding components. The limits of explosibility of some of the commonly associated gases are : CO, 12.5–74% ; H_2, 4.1–74% ; acetylene, 2.5–65% ; ethane, 3.2–12.5%. Presence of dispersed coal dust also reduces the lower limit of explosibility of methane to 3% with 5gm^{-3} of dust and to 2% with 10gm^{-3}.

Ignition of methane usually occurs between 923 and 1023K, but these limits can expand substantially depending on the source and method of ignition, methane content of air, presence of other impurities, surrounding temperature and pressure etc. For example, hot surfaces like that of an iron wire gauge used in a safety lamp ignite methane at a much higher temperature of 1473K compared to a flame. This fact together with the quick heat dissipation by the wire gauge (because of the large surface) does not allow the temperature to rise to the extent needed to cause explosion of the methane outside a safety lamp.

The most important characteristic of the ignition of methane is the delay between the ignition and the application of the heat source termed the *lag on ignition*. This is because of the fact that methane starts dissociating and burning only after absorbing a certain quantity of heat, i.e. 92.53kJ mol^{-1}. This property is utilized in designing safe explosives which produce a very short-duration flame. The lag falls considerably with rise in temperature of the source of ignition from about 10s at 923K to only about 1s at 1273K. It also falls with increasing pressure, but to a much lesser extent. The presence of hydrogen or other combustible gases reduces the lag so much so that the presence of 30% H_2 in the methane completely eliminates the lag on ignition.

It is well known that the rate of diffusion of gases into air is inversely proportional to the square root of their densities (Graham's Law). Methane, being light, diffuses fairly quickly compared to other heavier gases. The Prussian Firedamp Commission[1]

found that methane released into still air in quantities corresponding to 3 to 5% took three hours for nearly complete and four hours for complete diffusion. That is why methane evolved in goaf and other unventilated parts of a mine soon finds its way into the general body of air.

Methane is inert as far as physiological action is concerned, but, when present in large quantities in air, can cause serious oxygen depletion. There have been instances when men have put their heads into cavities in the roof filled with methane and have become unconscious in no time.

1.5 FIREDAMP

Firedamp implies a gas or a mixture of gases which in combination with air can cause an explosion. Usually it refers to the gases exuded from the strata, containing mainly methane (80-96%) with other minor contaminants such as nitrogen, carbon dioxide, ethane, ethylene and occasionally carbon monoxide and sulphuretted hydrogen. Normally 10% of nitrogen, 5% of higher hydrocarbons and 3-5% of carbon dioxide may be found in firedamp, though as much as 20% of nitrogen and 50% carbon dioxide have been recorded. Firedamp emitted from coal beds is often saturated with water-vapour.

1.5.1 Occurrence of Firedamp

Firedamp or methane is usually found in coal mines and sometimes in tunnels passing through carbonaceous shales. It has occasionally been recorded in some metalliferous mines of gold, copper, silver, lead, tin, zinc, quicksilver, salt, sulphur, iron, clay etc. Methane found in the Far East Rand gold mine is often associated with large quantities of hydrogen. In some Pennsylvanian coal mines, methane has been found to contain as much as 10% or more ethane, owing to the coal measure strata being associated with petroleum bearing rocks.

Vegetable matter composed mainly of cellulose $(C_6H_{10}O_5)_2$ and lignin decompose by bacterial action under confinement of superincumbent sediments producing methane and carbon dioxide:

$$(C_6H_{10}O_5)_2 = 5\,CH_4 + 5\,CO_2 + 2C \;.. \qquad (1.5)$$

or

$$2(C_6H_{10}O_5)_2 = 7\,CH_4 + 8\,CO_2 + 3\,H_2O + C_9H_6O \qquad (1.6)$$

Scanned with CamScanner

The process continues as the coal matter is subjected to higher pressures and temperatures, though with lesser intensity. In the early stages of coalification, much of the methane escapes owing to poor confinement, but it is largely retained in higher-rank coals such as bituminous coals and anthracites. It is a common observation that high-rank coals contain more methane and low-rank coals, more carbon dioxide.

Methane occurs in coal or in the adjacent strata either as free gas filling in pores, cracks etc., or as sorbed gas. Sorbed methane, in turn, chiefly occurs adsorbed on the surface of coal (by a process of physical bonding) though it occurs partly in the absorbed state when the gas is diffused into the coal structure forming a sort of solid solution. Russian work[3] shows that the relative contents of sorbed and free methane depends on the depth or in other words the temperature and pressure of the coal, the latter increasing with depth. Experiments by Palvalev[4] show that at a pressure of 2.5 MPa, one tonne of coal can hold 9m^3 of methane by adsorption and 3.54m^3 in the pore space while at a pressure of 100 MPa, it can hold 18.33m^3 by adsorption and 70.85m^3 in the pore space. This is because of the fact that coal surfaces get saturated with adsorbed methane at a pressure of 7-15 MPa when methane molecules penetrate into the interlamellar space in coal not accounted for by its porosity determined in the usual process at atmospheric pressure.

Though coals usually have a low porosity (8-10% occasionally rising to 20-25% particularly in lower-rank coals), the pores are very fine, thus offering a large surface area (of the order of 160-230 million m^{2}t^{-1}) for adsorption. But a fair portion of the gas remains confined in the coal due to its low permeability. It has been observed that pieces of coal still retain about one-third of their methane content even after twenty years of storage.

1.5.2 Migration of Methane

Desorption of methane occurs on release of confining pressure when the gas tends to migrate to the low-pressure zone. Though macrocracks and fissures provide channels for speedy migration, slow migration does take place by permeation through micropores and microcleavages. Methane also migrates in the adsorbed state along the pore surfaces till it reaches the low pressure zone where it ultimately gets desorbed.

Geological structures like faults and joints often provide major channels for gas migration. Dykes and sills may sufficiently weaken the contact zone of the coal formation to provide a path for methane migration. Folded structures lead to gas migration with the methane generally accummulating at the crest of anticlines and domes while synclines are relatively depleted of gas.

1.5.3 Methane Content of Coal

The methane content of coal, defined as the volume (m^3) of gas in a unit mass (t) of virgin coal under natural conditions, depends on the degree of coalification or rank of coal, higher-rank coals containing more methane. The extent of prior migration governed by geological structures, depth from the surface and the duration of the denudation cycle also controls the gas content to a considerable degree.

Graham[6,7] found the gas content of small lumps of coal to range from 0.36 to 16.8m^{3}t^{-1}. Russian work[3] shows that gas content of coal ranges upto 30-40m^3 t^{-1} occasionally rising to 50-60m^3 t^{-1} in very porous and fissured coals.

The method commonly used for measuring gas content is the direct method where a core sample of coal is taken to the laboratory in a sealed container and measured for the amount of methane desorbed after crushing. It has been observed by Bertard *et al*,[8] that a sample collected beyond a depth of two to six metres from an exposed face gives a practically constant desorbable concentration. Hence samples in order to be reliable must be collected beyond this depth. However, there is a certain volume of gas desorbed during the time between extraction of the sample from the seam and its enclosure in the container as well as in the container before laboratory testing. While the second quantity can be measured, the first can be estimated taking the desorbed quantity to be proportional to the square root of time. However, the method gives a lower estimate of the actual gas content of coal. Attempts have been made to account for the methane liberated during coring by measuring the methane dissolved in the drilling fluid, but to no specific advantage.

An indirect method of estimating the methane content of coal is by measuring the shut-in pressure in boreholes drilled into coal and correlating it with the methane content. Measurements by U.S.B.M.[9] in boreholes drilled from the surface to virgin seams

Scanned with CamScanner

show that the pressure is slightly less than the hydrostatic pressure. They, therefore, developed an empirical correlation between the depth of hole and the gas content in the form

$$V = \frac{Ah}{1+Bh} \tag{1.7}$$

where V = volume of adsorbed gas,

h = depth of hole,

and A and B are constants.

So far we have considered the gas content of coal in normal conditions. But in certain special cases such as in geologically disturbed areas where the coal is highly crushed containing a large proportion of voids, the gas content may substantially increase. Moreover such gas is generally in a free state and can be easily emitted into mine excavations.

1.5.4 Emission of Methane

It is common observation that the volume of gas emitted into the mine atmosphere far exceeds the methane content of the coal mined, the latter accounting for only 20-30% of the total gas emission. The rest of the gas obviously comes from the exposed ribs of coal and adjacent strata. In the Donets basin, U.S.S.R.,[3] it is estimated that of the total quantity of methane emitted into the mine only 10-15% come from broken coal, 40-50% from exposed surfaces of the seam being worked and the rest from the surrounding rock inclusive of the unworked seams emitted partly through the face (20%) and partly through the waste (25-35%). The rate of gas emission varies widely from mine to mine and even in the different districts of the same mine from very low values to even 250-300m^3t^{-1} of coal mined.

Indian coal mines are classified into three groups of gassiness based on the rate of methane emission : (a) *degree I*—upto 1$m^3 t^{-1}$, (b) *degree II* 1-10$m^3 t^{-1}$, (c) *degree III*—greater than 10$m^3 t^{-1}$. Though all coal mines fall into one or the other of the above three groups, there are very few highly gassy mines worked in this country yet. Table 1.3 lists a few highly gassy mines with their rates of methane emission.

Table 1.3 : Rates of Methane Emission in Some Indian Coal Mines

Sl No.	Mine	Seam	Rate of methane emission, $m^3 t^{-1}$
1.	Bhatdee	Mahuda Top	20 – 35
2.	Muslia	Ghusic	180 – 240
3.	Chinakuri	Dishergarh	20 – 35
4.	Amlabad	XIV	150 – 180
		XVI	30 – 35

Methane is emitted chiefly by a process of *slow exudation* from the seam and adjacent strata when fresh surfaces of coal and other methane-bearing formations are exposed during the process of working. Pulverization of coal during cutting, loading, transportation etc. causes desorption of methane. The size of coal produced has a great influence on the amount of gas emitted at the face. While large lumps release only 2% of their total gas content in the first ten minutes, coals of 0.25-1 mm size release 40% and of < 0.25 mm size, 66%. However, it is the exposed coal surface after mining that produces the major part (50 – 75%) of the gas rather than the mined coal, though the rate of emission fast decreases (75 – 83% of the total amount of gas emitted from exposed surfaces is exuded during the first hour or two after exposure).

Apart from the gas desorbed at the face, a fair amount of gas may get released when the coal gets crushed due to stress concentration near the front abutment. This finds its way partly to the face (depending on the permeability of coal, that increases with crushing) and partly to cavities and cracks in the superjacent strata. Depending on the method of mining, particularly roof control, and consequent breakage of the superjacent strata, a fair amount of gas may get released from these strata and find its way to the face and return-gates through the goaf. The greater the content of coaly matter in these strata, the greater is the amount of gas released from them. Though ordinary shales are estimated to contain only 0.08$m^3 t^{-1}$ of adsorbed methane carbonaceous shales contain around 1.98 – 2.8$m^3 t^{-1}$, the amount increasing with the carbon content of shale. In view of the large volume of superjacent strata

Scanned with CamScanner

involved, this source of methane can be substantial. The flow of gas from the waste to the face can be substantial (upto 50% or even more) under conducive ventilation systems.

The emission of methane at the coal face is therefore controlled by the following factors :

(a) *Gas content of coal.* As has been said earlier, the gas content of coal *in situ* depends chiefly on depth though other geological factors can introduce a variation even within the precincts of the same mine. The rate of gas emission can therefore be expressed as a simple function of depth.

$$q = \frac{q_o (H-H_o)}{a} \tag{1.8}$$

where q = gas emission at depth H, $m^3 t^{-1}$

q_o = gas emission at depth H_o, $m^3 t^{-1}$

and a = constant giving the rate of increase of methane emission.

The value of a varies widely from 5m to 40m from field to field.

(b) *Permeability of coal.* This controls migration of gas to the face. It is the cracks and fissures produced by mining stresses that mainly control the immediate migration of gas to the face rather than the permeability of virgin coal.

(c) *Density of coal beds or highly carbonaceous strata in the coal measure.* This gives a measure of the total gas that can be possibly released to the mine.

(d) *Method of mining.* This affects the rate of methane emission to a large extent. In a retreating method of mining, the gas emission at the face has been found to be much less (almost half) as compared to an advancing method of mining as in the previous case much gas is already released from the development openings prior to extraction.

The type and degree of mechanization affects the emission rate by way of controlling the degradation of coal. Coal-cutting machines cutting a thicker kerf release more methane than those cutting a thinner kerf. Ploughs cause much less methane emission than cutterloaders that pulverize coal. Blasting with cardox, hydrox [redacted] explosives.

The system of ground control also affects methane emission profoundly. Though it is claimed that the high stress concentration at the front abutment closes the pores and cracks thus preventing

gas migration from the seam to the face, the fracturing of the coal between the face and the front abutment causes a large release of methane. The gas emission is thus a function of the size of this fractured zone, which again depends on the thickness of the seam, strength of coal and the rock pressure. It is a common experience that with caving, where there is greater crushing of coal and breakage of superjacent strata, gas emission is much higher than with solid stowing.

An increased level of production and a high rate of face advance release a larger volume of methane per unit time, but the rate of emission per unit output is found to decrease with a faster rate of face advance, possibly because of the mined coal being removed from the face before releasing much of its gas content.

Normally the maximum amount of methane emission takes place at the face during the cutting shift, obviously owing to the greater amount of coal degradation. It is less in the loading shift and is further reduced during the packing shift in a cyclic system of working as at a longwall face. If working is suspended for a week, the rate of emission of methane is observed to decrease by 17 to 61%. Longer periods cause further decrease, though the rate of decrease progressively slows down. However, some pits do not show much variation in the amount of gas evolved from the mine during working and idle periods. Such occurrences may be due to large feeders of gas which continue blowing irrespective of whether the mine is working or is idle.

(e) *System of ventilation.* The system of face ventilation does affect the amount of gas emitted at the face. With an advancing face, a bidirectional ventilation system causes a certain amount of leakage of air from the intake to the return gate through the goaf, thus helping in removing some gas from the goaf directly to the return gate. This, in effect, reduces the gas emitted at the face. A boundary ventilation system however drives a fair amount of the gas from the waste to the face causing a high gas concentration at the return end of the face.

With a retreating face, the effect is reverse. A bidirectional ventilation system causes more gas emission at the face as compared to a unidirectional system.

The quantity of ventilation has been found to have some effect on the rate of gas emission. Though in most cases the methane concentration in the return is decreased by an increased quantity

Scanned with CamScanner

of ventilation, the absolute volume of methane emitted generally increases. This is because of the increased volume of air finding new paths of ventilation through the goaf and in the process removing the gas present therein. Depending on the method of ventilation and the relative amount of gas in the goaf, the methane concentration in the return air may rise, but the effect is generally temporary with the methane emission falling to the normal after the newly ventilated part of the goaf has been cleared of gas, though occasionally a somewhat higher level of methane emission may persist.

Emission of methane adsorbed in coal is little affected by changes in barometric pressure which are of the order of only 3.5 kPa. However, lowering of the barometric pressure does cause expansion of gas from cavities, goaves etc. into the workings which may be dangerous.[10] Changes in ventilation pressure affect methane emission in the same way as changes in barometric pressure, but they are much smaller (about one-tenth of the normal changes in barometer) in value and hence have little effect.

With commonly prevalent bidirectional system of ventilation, nearly half of the methane evolved from coal at an advancing longwall face is emitted at the face whereas the rest finds its way through cracks and cavities in the roof and the goaf or pack to the return airway. The emission of gas in the return gate, is however restricted to a distance varying from 100-400 metres from the outbye end of the face. In case of retreating longwall mining, most of the gas is emitted at the face.

The emission of gas in development headings is more than the general rate of gas emission in the mine since the emission from the face is augmented by the emission from the exposed surfaces of coal in the development opening. Skochinsky and Komarov[3] give the following relation for estimating the gas emission from a development opening :

$$q = \frac{4q'A}{24 \times 60} \text{ m}^3 \text{ min}^{-1} \quad (1.9)$$

where q = the rate of methane emission in the development opening,

q' = methane emission of the seam being worked, m^3t^{-1}

and A = mean 24-hourly output of coal from the development face, t.

The above relation, however, holds for an opening which has been driven for a period of atleast five months. For lesser periods of four, three, two or one month the quantity is to be multiplied by the factors 0.93, 0.87, 0.75 and 0.50 respectively.

Another type of gas emission from strata is in the form of *blowers* or *feeders* which continuously blow, sometimes at a fairly high pressure, for a few minutes to several years. One at the Cymmer colliery, South Wales, U.K. has been feeding gas with 97.5% methane at the rate of 22.7 m^3h^{-1} for over seventy years. Such large blowers are usually met with in sinking shafts or cross-measure drifts driven through porous and permeable beds such as of sandstone above coal seams. The gas in such beds is usually that which migrated from the coal seam through faults, cracks etc. Smaller and short-lived feeders may be met with inside the mine-workings and near the face. These owe their origin to the gas accumulated in faults, crevices, bed-separation cavities etc. The effective way of dealing with blowers is to seal the area off and pipe the gas to the surface.

Since blowers can be generally associated with geological structures, precautions should be taken when advancing towards such structures in a mine. This can be done by drilling advance boreholes fitted with blowout preventers at the collar.

Sometimes, methane may be given out from the strata in violent *outbursts* which emit large volumes of gas in a short time along with a lot of small coal and fine dust. One such outburst that occurred at the Valleyfield colliery, U.K. in 1911[5] caused the advance of a level by three metres upto a small fault throwing out about ninety tonnes of small coal and killing three men. In another case in a Belgian mine more than 120 persons were killed when there was a methane outburst liberating 339800m^3 of gas. The 1958 explosion at the Chinakuri pit is supposed to have followed a gas outburst.

Outbursts generally occur in the vicinity of areas of geological disturbance owing to the sudden release of confined gas in the disturbed zone, as the confining pressure is released by a working approaching the area. Some, however, contend that the pressure of desorption of methane by release of rock pressure can cause an outburst. Sudden fracture of overhanging roof and consequent crushing of coal have been advanced as a possible cause of methane outburst. Though these phenomena of rock pressure may lead to

Scanned with CamScanner

burst of coal, with rapid desorption of methane, they cannot be strictly considered as methane outbursts. Outbursts are less common in longwall workings as the advanced crushing of strata beyond the face releases the gas to roof cavities, thus preventing outbursts at the face.

No specific characteristics can be attributed to coal seams liable to methane outburst, but highly gassy seams of low volatile coal with disturbed geological structure can be subject to sudden outbursts. It is therefore advisable to look for preliminary signs such as increased gas emission, changes in structure and thickness of the seam, decrease in the strength of coal, manifestation of increased rock pressure such as gripping of drill rods in the hole being drilled or microseismic noise, when mining in these seams.

Various measures have been taken to deal with methane outbursts. In the anthracite mines of South Wales, U.K., long holes of large diameter are drilled ahead of face-advance so as to safely drain the gas. A method called *shock blasting* or *volley firing* was used in some French mines to prevent outbursts. This has been successfully used later in Belgian, Silesian and Ruhr collieries. Here, a face is drilled with a round of holes which are charged and simultaneously blasted electrically from the pit-top after all men have been withdrawn from the mine. This releases a large quantity of gas from the coal ahead of the face and makes it safe for further advance by normal methods upto a certain distance (3 to 4m). The increase in the gas content of the air at the face from a decimal percentage to almost 100% is so rapid that no explosion occurs due to the limits of explosibility being passed too quickly. Mining of adjacent protective seams also helps in reducing outbursts in hazardous seams.

The danger due to gas emission in a mine is enhanced if the coal dust in the mine is explosive so much so that a minor gas explosion can set off a major coaldust explosion. Thus a rate of gas emission, which is considered dangerous in bituminous-coal mines, may be tolerable in anthracite mines where the dust is less explosive.

Example 1.3

Samples of air collected in the intake and return gates of an advancing longwall face show 0.2 and 0.7% CH_4 respectively. Calculate the methane emission per tonne of coal mined, if the production from the face averages 1000 t per day and an air quantity of 20 $m^3\ s^{-1}$ circulates along the face.

Quantity of methane picked up by the air

$$= \frac{20(0.7-0.2)}{100} = 0.1\ m^3\ s^{-1}$$

$$= 8640\ m^3 \text{ per day.}$$

$$\therefore \text{ emission of methane per tonne of coal } = \frac{8640}{1000}$$

$$= 8.64 m^3$$

1.5.5 Dealing with Firedamp in Mines

Most of the methane evolved in mines is in the form of slow exudation or small feeders.

This gas is diluted and carried away by the ventilating current of air, the quantity of which should be such that the gas is diluted to a safe limit. As has been already stated, methane diffuses into the air at a fairly fast rate. However, diffusion of methane into still air rarely occurs in mines except at dead ends or in cavities in the roof where the air is still. The general mechanism of dilution of gas in normal mine roadways or at the face where turbulent flow occurs ($Re > 2000$) is by turbulent diffusion which is 100–1000 times faster than molecular diffusion. The distance required for complete mixing of methane in air by turbulent diffusion in a duct is given by equation 1.10[11] with an accuracy of $\pm 2\%$.

$$L \simeq 22\ r/\sqrt{f} \tag{1.10}$$

where L = distance from source of gas,

f = dimensionless resistance coefficient, (f commonly varies between 0.012 and 0.12—see Fig. 4.6)

and r = radius of the duct.

The above equation holds good for flow in a smooth circular duct where the gas issues axially from a point at the centre of the duct. In case of non-central discharge of gas the length will be more whereas for ducts with rough sides or with bends and obstructions the length will be less. Tests in mines show that complete mixing takes place at a distance of fourteen roadway-diameters in case of steel-arched roadways.

Scanned with CamScanner

Small quantities of methane entrapped in roof cavities soon get diluted by diffusion, but when methane is constantly fed into these cavities by blowers, it may be necessary to erect a hurdle sheet in order to divert the ventilating current into the cavity to clear the gas. Sometimes it may be necessary even to install a small blower for clearing such gas accumulation

Methane accumulates in dead ends if the ventilation of the dead end is stopped, the quantity accumulating increasing with time until the gas spills out to the main airways. Dangerous accumulation of gas can occur if there is recirculation of air by the auxiliary fan ventilating the dead end.

Clearance of such accumulated gas has to be done judiciously in order to avoid formation of large volumes of explosible methane-air mixtures. Though accumulated gas in the dead end may have a concentration well above the upper limit of explosibility it can form explosive mixtures on dilution with fresh air. It is therefore advisable to clear the gas by continuous auxiliary ventilation only if the accumulation is relatively small (less than for three hours in headings not exceeding 50m in length). With larger accumulations, intermittent ventilation becomes necessary. Long headings containing large quantities of gas are best cleared in sections from the outbye end by extending the length of ventilation ducting in successive stages.

1.5.6 Streaming and Layering of Methane

Because of low density, methane has a tendency for streaming particularly in steeply dipping roadways. Methane emitted at the roof travels up the dip in a layer near the roof depending on the velocity of air-current and the roughness of the roof With turbulent air-flow and a rough roof with obstructions such as roof bars etc. the tendency to streaming is reduced. If the air-current travels down the dip, it breaks up streaming and carries the methane down the dip. The critical velocity for such breaking up of streaming depends on the dip and varies from 0.04 m s^{-1} for a slope of 1 in 100 to 1.45 m s^{-1} for a slope of 1 in 2.8 (0.35 rad) in smooth airways. The tendency for streaming is greater with an up-the-dip air velocity where the critical velocity becomes higher.

Stable methane layers can also develop at the roof of horizontal airways depending chiefly on the rate of gas emission, particularly at the roof, the velocity of air and the size of the airway, though

other factors affecting methane layering are the roughness of the airway surface, presence of bends, obstructions etc. nearby and the nature and location of the sources of methane emission.

In large airways with relatively low average air velocity, there occurs at the roof a laminar boundary sublayer of sufficient thickness where the velocity is very low. Any methane emitted into this boundary sublayer cannot get diluted by turbulent diffusion and hence forms into a layer sometimes upto one metre in thickness which moves in the direction of the air-current but at a slower velocity. The percentage of methane in the layer gradually decreases from the top downwards with almost pure methane occurring against the roof.

The stability of methane layers as well as their length is indicated by a dimensionless *layering number*

$$L = \frac{v}{(4.32Q/W)^{1/3}} \qquad (1.11)$$

where v = average velocity of air, m s^{-1},

Q = quantity of methane emitted into the airway, $m^3\,s^{-1}$,

W = width of airway, m

and the constant 4.32 is the product of g, the acceleration due to gravity and the ratio of the density difference between air and methane to the density of air.

A layering number exceeding two in a horizontal airway causes turbulent diffusion and breaks up the methane layer. However, a layer of sufficient length still forms. There is generally a sharp decrease in the length of the layer (from the source to the point where the mean concentration of methane in the layer is 5%) with an increase in the layering number beyond five and hence this should be taken as a desirable value, provided the required air velocity to obtain this value is not prohibitively high. The desirable layering number in inclined airways depends on the direction of air-flow. While for ascensional ventilation, the desirable layering number is around eight, for descensional ventilation, it is less than that for horizontal airways.

The problem of methane layering becomes important in highly gassy coal mines, particularly where large-sized and duplicate airways cause reduction in air velocity. Such layers pose a constant explosion hazard and have to be suitably dealt with.

Scanned with CamScanner

As has been said earlier, increase of air velocity alone may not always suffice for breaking up of methane layers. Vertical or inclined hurdle sheets placed across the airway a little below the roof help in diverting the main air-current to the roof and breaking up the layer, but they offer substantial resistance to air-flow in the roadway. Better effect can be achieved by the use of delta-shaped vortex generators. These low streamlined bodies having a pointed leading edge and a flat trailing edge are placed in the air-stream with their plane making a small angle with the horizontal and with the trailing edge a little below the roof. As the air-stream meets the leading edge of this delta-shaped body, a vortex is generated on its lower side which travels along the surface until it bursts near the roof, thus breaking up the methane layer.

Where compressed-air supply is available, venturi blowers can be used for breaking up methane layers. Small 100mm diameter venturi blowers fed by 3mm jets of compressed-air have been found to be sufficiently powerful to break up layers as much as 70m in length. Such venturis should be earthed in order to guard against electrostatic sparking and as an additional measure of safety, a ring of water jets may be provided around the compressed-air jet.

Methane drainage or any other measure taken to reduce the rate of methane emission from the strata helps in minimizing the occurrence of methane layering.

Dilution of methane to a safe limit is practicable when the quantity of methane emitted is relatively small. With large quantities, the air quantity required for proper dilution will be prohibitive in which case attempt should be made to reduce the rate of methane emission from the strata.

Rate of gas emission can be controlled by a suitable selection of mining method, length of face, rate of face advance, type of mechanization, method of ground control etc. But these may have an adverse effect on output. Prior working of an adjacent less-gassy seam (protective seam) helps in reducing the rate of gas emission. Infusion of the seam ahead of the face with water or foam has been successfully used for reducing methane emission at the face by way of sealing the pores in coal and preventing gas migration to the face.

However, the surest way of bringing down the rate of methane emission in highly gassy seams is by methane drainage. Apart from minimizing the hazards associated with a high rate of methane emission, methane drainage often yields valuable quantities of methane which can be used as fuel.

1.5.7 Methane Drainage

Methane has been successfully drained from coal seams in many countries and utilized for industrial as well as household purposes. It is considered wise to aaopt methane drainage in all seams with a gas emission exceeding 20-25m^3 t^{-1}. Methane drainage has, however, not been tried in this country yet though some highly gassy seams are being evaluated for the purpose.

Methane drainage was first adopted in working mines where the common methods were (a) cross-measure borehole method, (b) superjacent heading method or Hirschbach method and (c) pack-cavity method. Of late, methods have been adopted to drain methane from virgin seams and from development workings.

Cross-measure Borehole Method. The cross-measure borehole method (Fig. 1.2) has been a very common method where cross-measure boreholes are drilled from roadways in a working seam, usually the tail gate of an advancing longwall face. The holes are drilled either upwards or downwards, the former being more common because methane usually accumulates in the bed-separation cavities in the roof of the seam and is driven out of these cavities as the roof breaks and collapses. The holes are inclined depending on the dip of the strata. In flat seams the inclination is generally

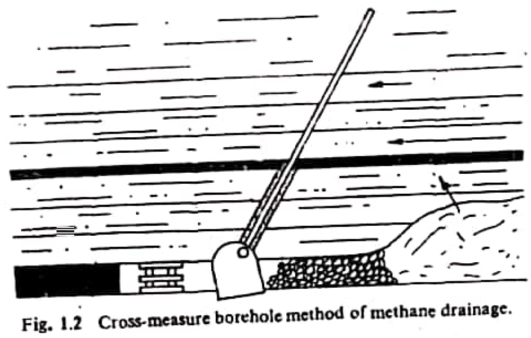

Fig. 1.2 Cross-measure borehole method of methane drainage.

at an angle of 0.87 to 1 rad (50°–60°) from the horizontal over the waste. An inclination of less than 0.79 rad (45°) produces less gas, causes greater dilution of the gas (because of the larger leakage of air into the hole) and increases the chances of jamming of the bore-rods in the hole. Sometimes good results have been claimed with holes inclined towards the face but such holes have been found to yield more diluted and a smaller quantity of gas in British coal mines.[12]

Placing of boreholes should normally be in the return since the ventilating pressure drives the gas in the goaf towards the return airway. Sometimes the dip of a seam may affect the natural flow of methane towards the rise side of the face. Besides, the haulage in the intake makes it difficult for the bulky drill to operate due to lack of space. All these considerations normally weigh in favour of putting the boreholes in the return. However, in South Wales, U. K., boreholes in the intake have been found to yield more gas than those in the return. The boreholes are usually 65-90mm in diameter and are spaced at intervals of 20 to 30m along the road so that they are not too close to each other to be very costly nor are they too far apart for adequate drainage. Their length varies from 15 to 100m (commonly 30-45m) depending on the presence of superjacent gas-bearing seams which have to be intersected for drainage. When such seams are not present, long holes do not have any advantage, as at greater heights the size of bed-separation cavities and the quantity of gas accumulated in them become too meagre. The holes are started off with a diameter of 115mm and collar pipes, 10m long and 90mm in diameter are cemented to them before they are drilled to the full length. The holes for methane drainage need special drilling machines capable of drilling long holes of large diameter cheaply. One such machine which has been found to be quite suitable is the 4.5kW Nusse and Graffer Fortschritt PIV/6 pneumatic-powered rotary drill having a rotational speed of 250π–500π rad min^{-1} (125–250 r.p.m.) and using multi-point fir-tree type of bits.

There is no definite relation between the face advance and the emission of methane from a borehole, but usually the rate of gas emission rises for the first two weeks until a maximum is reached at a distance of 30 to 50m from the face, after which the rate of emission falls. A suction of less than a hundred to a few thousand pascals is necessary to drain the gas, the usual suction being

1000 to 1500 Pa. The suction should be high enough to overcome the friction of the pipe ranges, but, at the same time, should not be so high that air may leak into the goaf and dilute the methane.

Hirschbach Method. In the Hirschbach method, headings with cross-sectional area of 5 to 7m² are driven at a height of about 25 to 30m on top of the working seam. They are so positioned that their vertical projections lie midway between the gate roads in the working seam (Fig. 1.3). It is always better to locate the drive in a coal seam at least 0.3–0.4m in thickness, if such a seam is available. Otherwise, they may be driven in stone. However, to effect economy an already existing drift or one driven for some other purpose may be chosen for methane drainage. Both along-the-seam and cross-measure boreholes are drilled from these headings as shown in the figure. Then the headings are sealed at the outbye end by dams

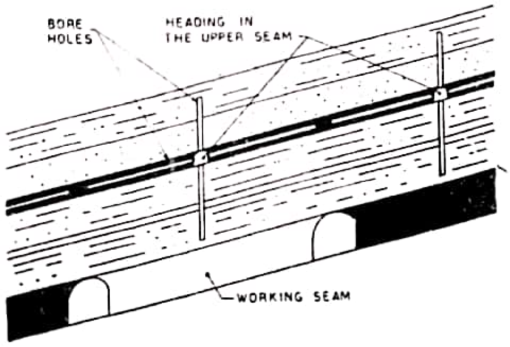

Fig. 1.3 Hirschbach method of methane drainage.

(Fig. 1.4) through which pipes are left. Methane is drawn from the headings through these pipes by applying a suction of 2–3 kPa.

Pack-cavity Method. In the pack-cavity method, corridors or webs parallel to the face are left in solid pack at intervals of about 40m and within 20m from the intake-and return-gate roads. These are connected by pipes to a main pipe range in the return airway and the gas is collected by applying a suction head of 250 to 350 Pa.

Scanned with CamScanner

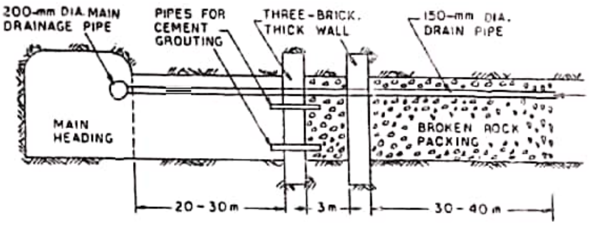

Fig. 1.4 Sealing dam.

The individual pipes from boreholes or pack cavities etc. are usually connected to a main pipe range, 150 to 300mm in diameter through pressure gauges, orifice-type flow meters, water-drain taps, sampling taps and valves etc. (Fig. 1.5). The mains are fitted with flame traps or flashback arresters both at the inbye and the outbye sides of the exhauster which may be at the surface or underground. Usually provision is made for automatic closing of solenoid-operated valves in the mains in case methane-air mixture approaches the limits of explosibility, particularly where the gas is fed to boilers. A minimum limit of 30% methane is prescribed by German regulations. The solenoids are operated by calorimeters, which indicate the methane-air ratio.

Sometimes filled-in goaves and the broken strata in worked-out mines may contain methane which may be drained by suitably sealing off the area. The Old Boston Colliery at Lancashire, U.K., has been sealed by concrete plugs in the shafts, with drain pipes left in them. The mine evolves practically pure methane which is expected to last for many years. In recent years goaves have been drained in the U.S.A. through vertical boreholes drilled from the surface.

Of all the above methods the cross-measure borehole method is the simplest and cheapest, but its yield of gas is less than the Hirschbach method which yields the maximum quantity of gas with a high methane percentage. This justifies the high cost of driving headings and boreholes in an upper seam in this method. Perfect sealing of headings may not be possible with this method when the seam underneath is goaved, but good results have been achieved by cement grouting the ground around the seal. Another advantage of the Hirschbach method is that the driving and drilling

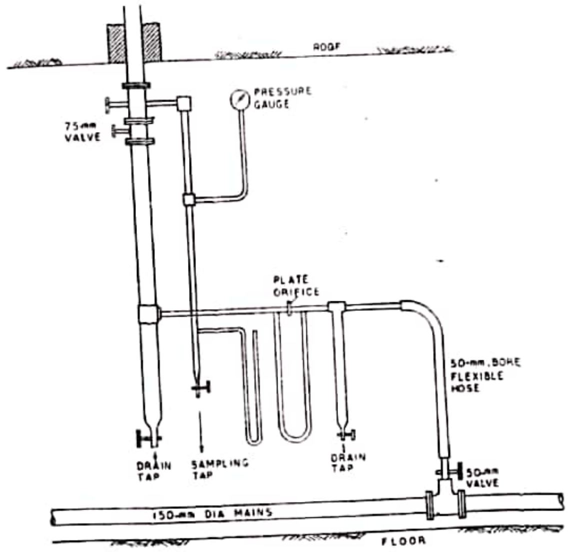

Fig. 1.5 Methane drainage pipe manifold.

operations are done outside the seam and hence do not interfere with normal mining operations. For retreating longwall and board-and-pillar workings, the Hirschbach method is the only suitable method. However, this method is not very successful, when the seam being worked has a massive sandstone cap. Enough roof fissures are not developed with such a roof, as a result of which the gas flows more easily to the face than to the drainage drift. The pack-cavity method yields the minimum quantity of gas which is often much diluted. In this method, only a closely controlled small suction head can be applied to prevent air leaking into the goaf causing spontaneous heating as well as the dilution of gas drained. It is for this reason that the pack-cavity method, though it involves the least cost and is the easiest, can be applied with any success only where good packing by hydraulic or pneumatic stowing is done. The quantity of methane drained by the cross-measure

Scanned with CamScanner

borehole method has been found to be such that the methane discharged into the ventilation system is decreased by 50–60% or sometimes more. However, it is estimated that due to the applied suction, the methane emission from the strata increases by about 15% over the normal emission without methane drainage.

Degassing of Coal Seams before Working. The methods adopted for degassing of coal seams before working include (a) regularly spaced vertical boreholes drilled to the seam from the surface, (b) long (150-250m) drainage holes drilled in the seam from the bottom of a large-diameter (2m) vertical borehole, (c) flanking holes drilled from development headings in coal and (d) blocking of the seam.

Drainage of virgin seams by vertical holes from the surface requires close spacing of holes, if the seam is not very permeable and hence is generally costly. The second method has been found quite successful in draining a large portion of gas (60–70%) in one of the Pittsburgh coal seams, but it involves a high cost. The cost can, however, be distributed if the large-diameter vertical borehole can be utilized subsequently, for example, as a ventilation shaft. Flanking holes drilled from the sides of roadways or from stables on either side of the roadways are generally 10-15m long and inclined at an angle of 0.26–0.35 rad (15–20°). Though they remove some amount of gas, much of its still gets into the roadways emitted from their surface. Flanking holes, however, have been successfully utilized in draining methane from specifically gassy areas such as fault zones from roadways running parallel to them. In the last method, the coal seam is blocked into suitable rectangular areas by development openings on all sides. Long holes are drilled into the block of coal and the whole area isolated by erection of stoppings and drained.

1.6 TESTING OF FIREDAMP

Indian law does not permit the methane concentration to exceed 0.75% in the return of a ventilation district or 1.25% in any part of the mine.

No shot is allowed to be charged, stemmed or fired at a place where inflammable gas is detected* or at any other place on its return. It is also required that electric power be cut off from a district where the percentage of inflammable gas exceeds 1.25%.

Where electricity is used in gassy mines, the percentage of inflammable gas is required to be determined on the intake side of the first working face and on the return of the last working face of a district every thirty days so long as the concentration does not exceed 0.6% beyond which weekly determinations become essential. If however the percentage exceeds 0.8% such determinations have to be done daily. For this reason it is essential to detect the presence of firedamp and ascertain its quantity at various working places in a mine.

1.6.1 Testing by Safety Lamp

Flame-safety lamps have been used for testing firedamp ever since their invention in 1815. Even today they are very commonly used for the purpose in Indian coal mines, chiefly due to the non-availability of reliable methanometers in sufficient number.

The principle depends on the fact that when a methane-air mixture comes in contact with the flame of the safety lamp, the gas in the vicinity of the flame burns forming a blue cap on the flame. The height of the cap depends on the percentage of methane, since at low percentages, the heat of combustion is not sufficient to ignite the gas beyond the limits of the cap. However, the greater the percentage of methane the greater is the heat produced by its burning and hence the greater is the height of the cap so much so that at about 5% methane (lower limit of explosibility of methaneair mixture), the burning gas fills the wire gauze of the lamp and the flame is extinguished. That is why it is always better to raise a safety lamp slowly upwards when testing for firedamp so that there is no chance of the lamp getting extinguished by suddenly entering a zone of high concentration of gas near the roof.

In the usual testing procedure known as cap test, the wick of the lamp is lowered until only a white fleck or a line in case of a flat wick is left at the tip of the reduction zone (the colourless zone). The lamp is slowly raised. The percentage of the gas present is indicated by the height of the cap produced by the burning methane which is usually of a blue-grey colour. Fig. 1.6 gives the height

*This has been clarified by the Chief Inspector of Mines, through personal communication, to actually mean detection by a flame-safety lamp which is equivalent to a methane concentration of 1.25% as determined by sensitive methanometers.

Scanned with CamScanner

of the cap at various percentages of methane in an Ashworth-Happlewhite–Grey lamp[13] with a 12.5mm wide wick and burning an equal mixture of colza and paraffin. The height of the cap however depends on the following :

(a) *Nature of the wick*, i.e. *round or flat*. Round wicks are used in Germany in preference to flat wicks as it is easy to trim them and they give a more suitable testing flame than flat wicks, but flat wicks have been claimed to give a more definite indication of the percentage by way of not only the height of cap, but also the shape of the cap.

(b) *Width of the wick*. The wider the wick the longer is the cap. A rough rule is that the height of the cap equals the width at 2%, one and a half times the width at 3% and twice the width at 4% of methane.

(c) *Nature of fuel used in the lamp*: Lamps burning fuels with high boiling point, such as paraffin or mineral colza and paraffin, usually give a 2.5mm high testing flame whereas with low-boiling-point fuels such as naphtha and colzalene the testing flame is higher, i.e. 3.8mm. So also the height of cap increases with fuels of lower boiling point for the same percentage of methane.

Though the *cap test* with a reduced flame gives a more accurate test for methane, it is often customary to carry out an *accumulation test* first with a luminous flame of a standard height. This test may then be checked by the cap test. The luminous-flame test

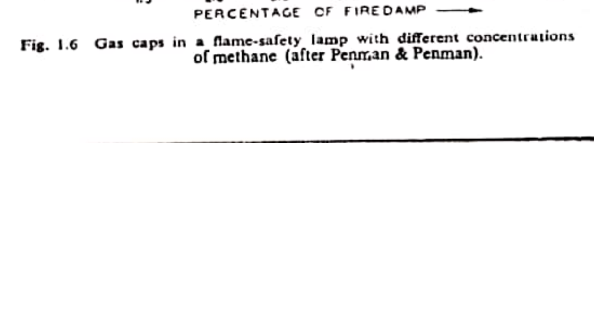

Fig. 1.6 Gas caps in a flame-safety lamp with different concentrations of methane (after Penman & Penman).

gives a better indication of methane since it produces more heat inside the lamp which causes better lamp ventilation resulting in a larger quantity of methane being drawn inside the lamp. For the same reason, the longer the flame, the better is the indication. With the same concentration of methane, a 34mm high flame produces three times the elongation produced with a 12mm high flame. The luminous-flame test is carried out without necessitating a dark surrounding and there is no chance of the flame going out when the flame size is reduced as may occur in the cap test. That is why it is better to have an indicating test with a luminous-flame followed by a cap test if necessary. However the luminous flame begins to spire at 3% CH_4 and may be extinguished at a higher percentage. Hence it is necessary to slowly raise the lamp in this case too, closely watching the behaviour of the flame all the time.

It is clear from Fig. 1.6 that a normal flame-safety lamp can not measure methane concentrations below 1.5% with any degree of accuracy. It is therefore quite inadequate to measure the statutory permissible concentrations in a mine for which more accurate methanometers have to be used.

To increase the sentitivity of the flame so as to test small percentages of gas, a prevalent German and Russian practice (originated by Rosen in 1929[14]) was to introduce a *salt pearl* at the end of a wire into the wick so that the pearl remained unaffected in the reduction zone when the lamp burned normally : but when the flame was reduced for testing, the salt pearl came to the oxidizing zone and was vaporized thus giving the testing flame a bright yellow rim. The cap, due to the burning of methane, appears above this rim in yellowish grey colour and can be readily distinguished against the bright yellow rim. It is possible to measure $<1\%$ CH_4 with the use of a salt pearl. A salt pearl usually lasts for two shifts and is easy to replace.

Brigg's copper loop acts on a similar principle, imparting a bright colour to the testing flame but is rarely used. Special designs of oil-safety lamps suitably adapted for testing small concentrations of firedamp such as Cunningham-Cadman, Cowles and Stokes gas-testing lamps are of only historical interest today. The first uses the principle of coloring the flame and the other two get a better and longer testing flame by using a low-boiling fuel such as alcohol or hydrogen.

Scanned with CamScanner

Misra[15] developed a thermoelectric attachment to a flame-safety lamp which could be used with a luminous flame to give a a fairly accurate estimate of the methane concentration in mine air even at low percentages. The M.R.E. Butane Lamp also works on a similar principle.

However, all these attachments to a flame-safety lamp have not found favour in practice, particularly with the development of accurate portable methanometers. Many firedamp detectors using various physical properties of methane-air mixture such as density, refractive index, thermal conductivity, inflammability, change of volumè on combustion, catalytic combustion, diffusion, acoustic properties, absorption of infra-red rays etc. have been designed ; but only a few of them have been developed into sturdy portable methanometers fit for use in gassy mines.

Methanometers are of two main types : the automatic and the estimating types. The automatic detectors give a signal when the gas percentage in the air reaches a certain predetermined value. In the British coal mines, it is required by law that for every eight persons at a longwall face there shall be a firedamp detector and one of eight such detectors shall be an automatic one. In board-and-pillar workings, there shall be a detector at each working place and one out of four such detectors shall be of an automatic type. In any case, there shall be at least one automatic detector provided in the workings. A safety lamp must be provided near an electric motor and electricity must be cut off if it detects fire-damp nearby.

Of late there is an increasing trend to have recording methanometers installed at vital parts of a mine to keep a continuous record of the methane content of the mine air. Telemetering devices can be incorporated so that recording can be made centrally on the surface. Monitoring of the methane concentration so as to automatically cut off power supply to a district when the methane concentration therein exceeds a predetermined safe value is also finding increasing use, particularly in highly gassy mines.

1.6.2 Automatic Detectors

Ringrose Automatic Firedamp Alarm. This consists of a combined electric lamp and firedamp alarm. The electric circuit of this device is given in Fig. 1.7. A heating filament F is provided in a

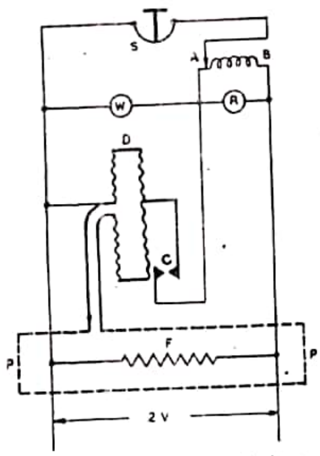

Fig. 1.7 Ringrose automatic firedamp alarm (diagrammatic).

porous pot P which is filled with the surrounding mine air by diffusion. The filament is heated by applying a current from a 2-V battery which also supplies the main lamp W. Normally only the white lamp W glows though both W and the red lamp R are in series, because W has a current capacity of only 0.3A while that of the red lamp is 0.7A. The hot filament ignites the methane-air mixture which burns producing carbon dioxide and water-vapour. The latter condenses causing a reduction in volume of the combustion products by two-thirds and thus producing a partial vacuum in the porous pot. As a result, the aneroid diaphragm D contracts, thus closing the contacts C which causes the red lamp R to glow by short-circuiting the current across W which is then extinguished. Simultaneously a coil B in parallel with R pulls a contactor A and establishes a permanent circuit through R through switch S. The red lamp is extinguished and the white lamp relighted by opening the switch S. The contacts C are so set that they come together only if a certain minimum percentage of methane is present in the air. Usually this is set at 1.25% methane. The porous pot is covered by wire gauzes which make it flameproof.

Scanned with CamScanner

The *Ringrose methanometer* (non-automatic type) uses the same principle, but here, the partial vacuum in the porous pot is indicated in a manometer which is calibrated in percentage of methane.

Naylor Spiralarm. This is another automatic detector (Fig. 1.8) consisting of a safety lamp which has a bimetallic spiral attached above the flame. The flame is normally kept at a constant height indicated by a pointer. With the percentage of methane in air rising, the flame increases in height and heats the spiral which uncoils so that at a predetermined percentage such as 1.25% or 2% the uncoiling of the spiral is sufficient to make a contact that makes an alarm lamp placed at the bottom of the detector glow.

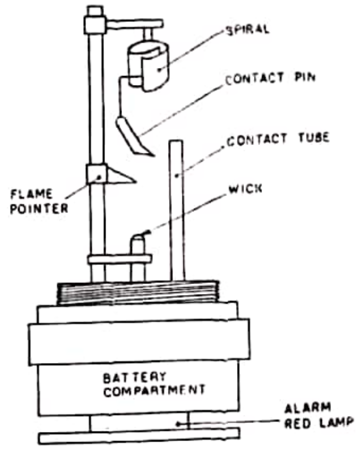

Fig. 1.8 Naylor spiralarm (diagrammatic).

Of late, several automatic methane alarms utilizing the rise in temperature on combustion of methane have been developed. Of these, the more commonly used ones such as the M.S.A. automatic firedamp detector or the Warnex manufactured by Drager uses a Wheatstone bridge circuit to measure the change in resistance of an electric filament heated by catalytic combustion of methane-air mixture over it. While the former gives a visual signal of a flashing light, the latter gives both visual and audible signals when the methane concentration exceeds a preset value.

In some Japanese firedamp alarms, thermisters are used to signal the rise in temperature by combustion of methane while in an English Electric firedamp alarm thermocouples are used.

1.6.3 Non-automatic Detectors

McLuckie Detector. This utilizes the principle of reduction in volume of methane-air mixture on combustion. The apparatus is contained in an aluminium case 100mm square in cross-section and 300mm high and takes 7 minutes for a reading. There are two compartments of equal volume, one, the combustion chamber N and the other, the compensating chamber M (Fig. 1.9). In the beginning, all the taps are opened and firedamp is drawn into the combustion chamber by squeezing the rubber aspirator a few times. Then the taps are closed and two minutes are allowed for both the chambers to attain the same temperature. After this, the taps opening the chambers to the atmospheres, i.e. taps B and C are opened for a short while for bringing the pressure inside the two

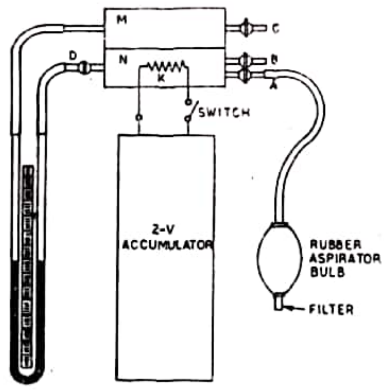

Fig. 1.9 MacLuckie methane detector (diagrammatic).

chambers to the atmospheric level before being finally closed. The switch is then closed to let the platinum coil K get heated for two minutes, after which it is opened. The chambers are allowed to cool and equalize in temperature for another two minutes. Now tap D is opened and the liquid in the right limb of the manometer rises. The percentage of methane is read off from a calibrated scale which is graduated to read up to 3.3% methane.

Detectors using change in resistance of a wire on heating by combustion of methane. Methanometers based on this principle are by far the most prevalent today almost all over the world. The *M.S.A. methanometers* are of this type. The instrument consists essentially of a balanced Wheatstone bridge circuit (see Fig. 1.10) supplied by a battery. The detector filament is of activated platinum which when heated sufficiently burns the firedamp whereas the compensating filament is made of deactivated platinum that has no action on the methane-air mixture. The only source of inaccuracy in this instrument is the physical deterioration of the platinum filament due to catalytic combustion of methane in its contact which alters its resistance and hence the balance of the bridge circuit. Specially activated filaments with relatively low operating temperatures and low rates of physical deterioration are now in use. The activated Pt filament is embedded in a pellet

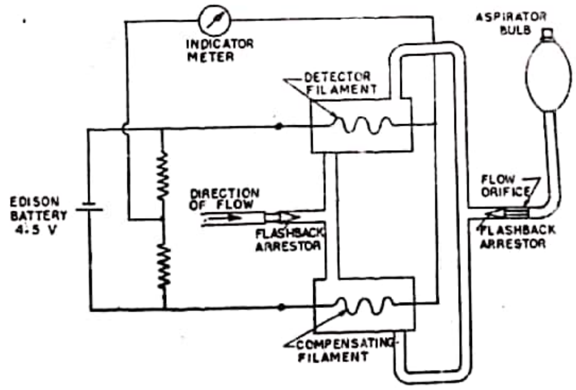

Fig. 1.10 M. S. A. methanometer (diagrammatic).

of alumina coated with finely divided palladium catalyst which lowers the temperature at which CH_4 is oxidized to around 623K so that the evaporation of Pt at this low temperature becomes negligible. The compensating filament on the other hand has a solution of potassium dichromate in place of palladium. This prevents the oxidation of CH_4 below 1173K. Even then it is always advisable to adjust the zero error, if any, in fresh air at the beginning of each shift. While taking a reading, firedamp is drawn over the filaments by squeezing the aspirator bulb. There are two flashback arresters provided on both sides of the detector filament. The detector filament gets heated up by the burning of methane and thus the bridge is unbalanced. This imbalance is recorded on the indicator meter which is calibrated to read the methane percentage directly. There are two scales provided, one for reading up to 2% methane and the other, up to 5% methane.

The recent-model (D-6) methanometers are fairly light (weighing only 0.47 kg) having a rechargeable battery and a telescopic probe for testing in remote roof cavities. A reading with these methanometers hardly takes 1.5–2 minutes.

The *KSA—01 methanometer* developed by the C.M.R.S. (India) and manufactured by K.S. Associates, the S.M.R.E. (U.K.) methanometer, the Verneuil V-54 (French) methanometer and the G-70 (F.R.G.) methanometer are some of this type.

Some Japanese instruments use thermisters in place of filaments to measure the temperature of combustion and hence the percentage of methane.

Methanometers using the property of thermal conductivity. These are of more recent origin and are based on the principle that a heated wire when exposed to different compositions of methane-air mixtures cools to different extents depending on the thermal conductivity of the mixture. The cooling alters the resistance of the wire which is measured by a Wheatstone bridge circuit. Fig 1.11 illustrates the electrical circuit of a methanometer of this type manufactured by Siemens and Halske. The two measuring filaments *g* mounted on opposite arms of the bridge are enclosed in aluminium chambers which can be filled by the methane-air mixture to be tested. The compensating filaments *f* on the other hand are sealed in similar aluminium chambers containing atmospheric air. The filaments are heated to a temperature of about 343K by current from a battery *a* through a circuit having a control

Scanned with CamScanner

rheostat *e* and an ammeter *b*. Potentiometer *c* is for adjustment of the zero error.

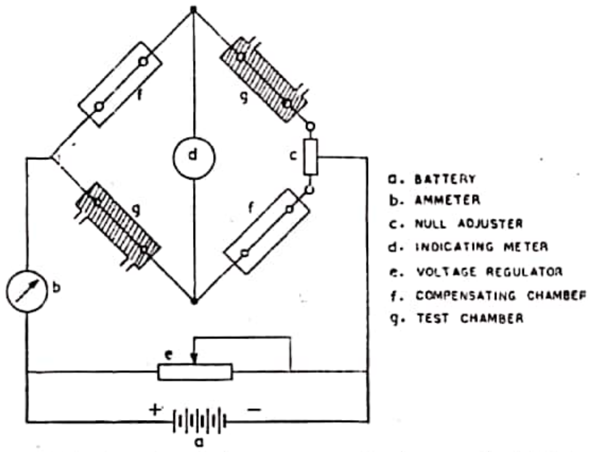

Fig. 1.11 Electrical circuit of Siemens and Halske thermal conductivity-type methanometer.

The instrument is claimed to give fairly quick readings (15-18 s per reading), but the readings are affected by presence of CO_2 and moisture. Hence absorbent tubes for CO_2 and moisture are provided along with a dust filter at the inlet. The instrument is temperature compensated but the null point is affected by pressure and has to be adjusted for variations in barometric pressure.

The *Auer methanometer* uses the above principle to measure methane concentration in the 0-5% range while for 0-2% range, it uses the principle of catalytic combustion. M.S.A. also have a methanometer of this type designed to measure 0-100% methane with a lower sensitivity of 5% methane.

Firedamp Interferometer. This is an instrument which utilizes the difference in refractive indices of methane and air for the estimation of the percentage of methane in mine air. The Zeiss interferometer is a compact and portable instrument measuring 200 × 100 × 40mm in a suitable leather case with a carrying strap. It gives a quick reading with an accuracy of 0.1% for an instrument reading between 0-10% methane. There are also more accurate instruments reading between 0-5% as also less accurate ones with a larger range of 0-100%.

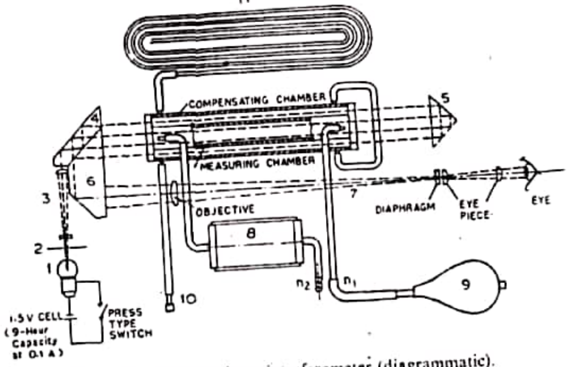

Fig. 1.12 Zeiss firedamp interferometer (diagrammatic).

The instrument (Fig. 1.12) consists of a 1.5-V, 0.1-A torch-type bulb 1 which sends in a beam of light through a slit 2 and a collimator 3 to a mirror 4. The ray gets reflected from the back surface of the mirror which is completely silvered. A part of this reflected ray passes through the front surface of the mirror (which is partly silvered) and enters the measurement chamber whereas the other part gets reflected from the front surface and again from the back surface of the mirror before entering the compensating chamber. The two rays get reflected again from a prism 5 at the other end of the two chambers and retraverse the chambers and the mirror before they join in the prism 6. The two rays traverse equal path between splitting and reuniting. So, they should normally have no phase difference and hence should not interfere. However, by giving a slight tilt either to the mirror or to the prism 5, they can be made to interfere and the interference figure is observed through a telescope 7 which has a graduated scale at the diaphragm. The interference figure consists of an initial dark band followed by

Scanned with CamScanner

successive coloured bands. The dark band is set to the zero of the scale before observation by a zero-error adjusting knob provided on the instrument. This should be done in fresh air.

During observation mine air is sucked (by squeezing about five times the rubber aspirator bulb 9 attached to nipple n_1) into the measurement chamber through an absorption tube 8 containing an equal mixture of sodalime and calcium chloride with two cotton-wool filters at both ends. The absorption tube scrubs the mine air of its dust, moisture and carbon dioxide content. The compensation chamber is filled with fresh air on the surface by removing the stopper 10 and sucking in air by means of an aspirator bulb attached there. At the other end, the compensating chamber is connected to the atmosphere by a long tube of narrow cross-section 11 for equalization of pressure.

When the observation chamber is filled with methane-air mixture whose refractive index is higher than that of pure air, the dark band of the normal interference figure shifts in proportion to the methane content and this can be read on the scale which is calibrated directly in percentages of methane.

The instrument can also determine the carbon dioxide content of mine air. For this, the aspirator bulb is attached to the nipple n_2 instead of to n_1, so that the measurement chamber is filled with both methane and carbon dioxide. The reading will give the total percentage of methane and carbon dioxide as the refractive indexes of the two gases differ very little from each other. The percentage of carbon dioxide can be obtained by deducting the methane percentage from this figure. For obtaining the true value however, it is necessary to reduce the carbon dioxide percentage so obtained by 5%.

Large variations of temperature and presssure from those at which the instrument is calibrated (293K and 101.33 kPa), affect the interferometer reading when the reading has to be multiplied by a correction factor so as to give the true value. The correction factor F is given by.

$$F = \frac{0.346T}{P} \tag{1.12}$$

where T and P are the measurement temperature (in K) and pressure (in kPa) respectively. It is also necessary to add another absorption tube if the atmosphere contains more than 0.4% of carbon dioxide.

The greatest disadvantage of the instrument is its lack of accuracy when the mine air contains gaseous impurities other than moisture, carbon dioxide and methane. Hydrogen particularly has the opposite effect of methane and can give a completely wrong picture, if present in sufficient quantity. There are many other makes of interferometers such as Riken, Toka etc., which have been found to be equally effective.[16]

Of the above methanometers, the McLuckie type[17] is the heaviest and largest in size. It takes the longest time for one determination and has to be held vertical during observation. That is why it is rarely used today in spite of its high accuracy (±0.05% as compared to ±0.05-0.1% of catalytic-combustion- and thermal-conductivity-type methanometers and ±0.1% for interferometers[18]). Ringrose methanometers also suffer from heaviness and longer reading time. Thermal-conductivity methanometers and interferometers, though, light and quick in reading are subject to errors due to temperature and pressure variations as well as to the presence of impurities like CO_2 and water-vapour. The catalytic-combustion type of instruments on the other hand are more or less free from these defects and are both portable and reasonably quick in operation. That is why they are finding increasing use all over the world today.

An *acoustic methanometer*[19] has been designed to measure high percentages of methane in pipe ranges used for methane drainage, but no model for measuring low concentrations in mine air is available.

Misra *et al.*,[20] established the velocity of propagation of ultrasonic waves as an effective measure of methane concentration in air, but no instrument has been built utilizing this principle.

1.6.4 Recording Methanometers

Safety in Mines Research Board Firedamp Recorder. This is a continuous recorder based on the principle of operation of both Ringrose and McLuckie detectors. Here, a pump forces the methane-air mixture, into a thick-walled cylinder of a capacity of 15cm³ and with three ports, each fitted with valves. One of the ports is connected to the pump, the second to the atmosphere and the third to an aneroid diaphragm. The three valves are operated by cams in a sequence such that at first the pump port is closed and the other two ports opened after the cylinder is filled with gas so

Scanned with CamScanner

that the cylinder and aneroid are at atmospheric pressure. Then all the ports are closed and the gas is burned by passing current through a heating coil in the cylinder. After an allowance of two minutes for cooling, the third operation opens the aneroid port which makes the diaphragm collapse to an extent, depending on the methane percentage. The degree of collapse expressed as the percentage of methane is recorded on a twentyfour-hour chart worked by a clockwork. The methane percentage is recorded at intervals of three minutes and the maximum percentage that can be recorded is 3.5%.

Other firedamp recorders of a similar type include the *Ringrose* and *Maihak Mono* recorder which work on a similar principle as the Ringrose firedamp alarm. Another recorder consists of a small flame lamp burning butane.[21] The temperature of the flame can be controlled for varying conditions of ambient temperature, humidity and butane pressure. A set of thermocouples records the temperature of the flame. Methane in air increases the flame temperature which is recorded by the thermocouples. The voltage scale is so calibrated as to give the percentage of methane directly.

Methane recorders based on catalytic combustion have also been designed and put to use. A significant development has been the use of the property of absorption of infra-red rays (of a particular wave length) by methane for the design of recording methanometers. Fig. 1.13 illustrates a French instrument of this type.

Two infra-red emitters S_1 and S_2 are arranged over a rotating shutter driven by a synchronous motor. The reference chamber C_1 contains fresh air and the test chamber C_2 is filled with the methane-air mixture to be tested. There are two receiver chambers R_1 and R_2 separated by a steel diaphragm D which is a few micrometres in thickness. A perforated plate E acting as the second electrode of a capacitor is separated from D by a small distance (a few hundredths of a mm). The higher the methane content in C_2, the weaker is the infra-red radiation received in R_2. This causes a differential pressure on diaphragm D which vibrates at the frequency of the shutter and at an amplitude depending on the methane content. The vibrations alter the capacitance of the capacitor which is amplified and recorded. The signal can be suitably amplified to trip a circuit breaker and cut off power supply to a district when the methane content exceeds a certain predetermined level.

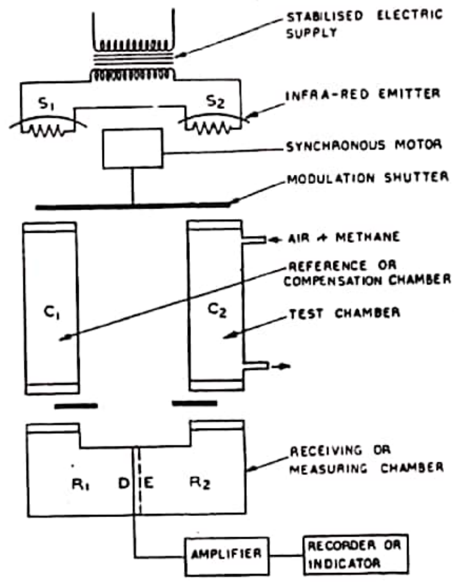

Fig. 1.13 Infra-red-type methane recorder (diagrammatic).

These recorders have been fairly widely used in Europe. It is significant to note that in 1967 there were 250 *Unor* (infra-red type) recorders installed in Germany as compared to only 184 Mono instruments.

1.7 CARBON DIOXIDE (CO_2 Molecular mass—44)

It is a colourless and odourless gas with specific gravity equal to 1.529. It does not support life or combustion. Water at 293K absorbs 0.88 times its own volume of carbon dioxide forming carbonic acid. The solubility increases with decrease in temperature so much so that at 273K water can absorb as much as 1.71 times its own volume of carbon dioxide. Carbon dioxide has a mildly toxic physiological effect. It causes irritation of the mucous membranes of the eyes, mouth and nose and produces a sensation

Scanned with CamScanner

of burning when the concentration exceeds 5-10%. It increases the rate and depth of breathing resulting in the labouring of the lung. At 2%, the depth of breathing increases by 50% and at 3%, by 300%. At 6% panting occurs and 10% produces a narcotic effect characterized by headache, dizziness and sweating. Haldane states that unconsciousness occurs at 11%, but death follows only after a few hours' exposure to this condition. The effects are however more serious if high carbon dioxide content of the air is associated with oxygen deficiency. In Indian coal mines, the carbon dioxide content of mine air is not allowed to exceed 0.5% whereas at Witwatersrand the limit is 0.2%.

Carbon dioxide occurs in both coal and metal mines and is produced by the exhalation of men, burning of lights, exhaust of internal-combustion engines, decay of timber, oxidation of coal, blasting of explosives and mine fires, explosions, etc. It is sometimes given off by the strata by the action of acid water on limestone or other carbonates. In British coal mines, carbon dioxide is evolved from the strata along with methane in such quantities that it comprises normally 3-5% of the firedamp in the mines. In some French coalfields, carbon dioxide is given off the coal bed in blowers or as outbursts. It is supposed to have been originated in limestone beds below the coal seam and migrated and accumulated in crevices in the seam. In Russian coal mines the CO_2 emitted ranges from 1.5 $m^3\,t^{-1}$ of daily output to as high as 15 $m^3\,t^{-1}$.

The relative importance of the different sources of CO_2 varies from mine to mine. An average miner breathes out about 0.05-0.06m^3 of CO_2 per hour while a flame lamp burning 6-7 g of fuel per hour produces 0.01m^3 of CO_2. An internal-combustion engine liberates about 0.08m^3 of CO_2 per hour per kW and a kg of gelatine dynamite, 0.25m^3. In metal mines, men, lamps and explosives produce about one-third of the total CO_2 produced, but in coal mines these sources contribute only a minor fraction of the order of one-tenth to one-twentieth though instances are there where the fraction can go up to one-third.

1.8 BLACKDAMP

This is a miner's term indicating a gaseous mixture which extinguishes lamps without at the same time causing any explosion or having any marked toxic effect. It usually means a mixture of carbon dioxide and nitrogen in which carbon dioxide may vary

from 5 to 90%. Haldane gives the average composition of blackdamp at 13% carbon dioxide and 87% nitrogen. Blackdamp is usually heavier than air, but becomes lighter when the percentage of carbon dioxide in it falls below 5.25%.

Example 1.4

The analysis of a sample of air from old workings is reported as follows : O_2—16.52%, CO_2—3.1%, CH_4—2.45% and N_2—77.93%. Find the percentage of air and blackdamp in the sample as well as the composition of blackdamp.

Taking air to contain 20.95% O_2, 0.03% CO_2 and 79.02% N_2, we have in the sample

$$\frac{16.52}{20.95} \times 100 = 78.85\% \text{ air,}$$

$$\frac{16.52}{20.95} \times 79.02 = 62.31\% \ N_2 \text{ in the air,}$$

$$\text{and } \frac{16.52}{20.95} \times 0.03 = 0.02\% \ CO_2 \text{ in the air.}$$

$$\text{Excess } N_2 = 77.93 - 62.31 = 15.62\%$$

$$\text{and excess } CO_2 = 3.1 - 0.02 = 3.08\%.$$

Blackdamp (mixture of excess N_2 and CO_2) = 15.62+3.08 = 18.70%

Composition of blackdamp :

$$N_2 = \frac{15.62}{18.70} \times 100 = 83.53\% \text{ and}$$

$$CO_2 = \frac{3.08}{18.70} \times 100 = 16.47\%.$$

1.9 AFTERDAMP

This refers to the air after a methane or coaldust explosion. It often contains an appreciable quantity of carbon dioxide along with some carbon monoxide, methane and unspent normal air. A typical composition of afterdamp consists of 30-50% residual

Scanned with CamScanner

air, 58-44% free nitrogen, 8-4% carbon dioxide and 4-2% carbon monoxide. Afterdamp is usually very poisonous due to the presence of carbon monoxide in it.

1.9.1 Detection of Carbon Dioxide

The presence of carbon dioxide is usually deduced from oxygen depletion indicated by the extinguishing of oil lamps at 17-17.5% oxygen. The light output of an oil lamp is diminished by 3.5% with every decrease of 0.1% in the oxygen content of the air. Carbon dioxide also turns lime water milky and this property can be used for its detection in mines.

Portable instruments have been devised for estimating small percentages of CO_2 in mine air. A simple device used in the U.S.S.R. comprises 10cm³ of a violet-red solution of phenolphthalein ($C_{20}H_{14}O_4$) and soda contained in a 110cm³ flask. A known volume of mine air is drawn through the solution by squeezing a rubber aspirator bulb of 70cm³ capacity a few times. The number of squeezes needed to completely bleach the solution gives a measure of the CO_2 content. The phenolphthalein solution is prepared by dissolving 53 mg of anhydrous soda in 10cm³ of water and adding to it one mg of phenolphthalein. The liquid is further diluted by adding fifty times its volume of freshly boiled and cooled distilled water (to expel any CO_2 already dissolved in the water).

With the above solution, the relation between the number of squeezes of the aspirator bulb and CO_2 content is as follows :

Number of squeezes of the aspirator	2-3	4-6	6-7	8-10
Approximate CO_2 content, %	0.3-0.25	0.2	0.15	0.1

Another portable CO_2 analyser employs a solid chemical absorbent of CO_2 in a closed chamber. A known volume of air is drawn into the chamber. On absorption of CO_2, a vacuum is produced in the chamber which is indicated in a manometer graduated directly in percentage of CO_2. Portable interferometers have also been designed for the estimation of CO_2 in mine air.

A colorimetric detector tube using hydrazine (NH_2NH_2) and crystal violet has been developed by Drager which gives an indication of CO_2 content in mine air by the length of tube over which there is a colour change to bluish violet. The tube is operated in conjunction with a bellow-type pump.

1.10 CARBON MONOXIDE (CO, Molecular mass—28)

Also known as whitedamp, it is a colourless and odourless gas slightly lighter than air (sp. gr.=0.972) and slightly soluble in water (100 volumes of water at 293K dissolving only 2.3 volumes of carbon monoxide). It burns in air with a blue flame and is explosive in presence of air at concentrations between 12.5% and 75%, the temperature of ignition being 873K. Carbon dioxide is reduced to carbon monoxide in presence of carbon at temperatures exceeding 773 to 873K.

Carbon monoxide is a deadly poisonous gas because the haemoglobin in the blood has 250-300 times greater affinity for carbon monoxide forming carboxyhaemoglobin than, for oxygen forming oxyhaemoglobin. Thus if carbon monoxide is breathed in large quantities for a sufficiently long time, the tissues, particularly those of the brain, get damaged due to lack of oxygen. The blood cells also get damaged after long exposure to carbon monoxide. As a result, the patient suffers from headache, nausea, overstraining of the heart, mental disorder, loss of memory, paralysis, temporary blindness etc. leading to unconsciousness. A person affected by carbon monoxide does not realize it himself and his mental disorder makes him work harder so much so that he may have to be forcibly carried away. Carbon monoxide imparts a bright pink colour to the blood and the patient looks fresh and flushed.

The best remedy for carbon monoxide poisoning is to quickly remove the patient to fresh air and administer pure oxygen. The patient has to be kept warm by covering him with blankets. A stimulant like black coffee is very helpful. Sometimes a small percentage (2-3%) of carbon dioxide mixed with oxygen gives a better effect as it stimulates the rate and depth of breathing. It is often difficult to recover from carbon monoxide poisoning and even if a person recovers, he remains ill from several hours to several days, depending on the degree of exposure, because of permanent tissue damage.

A harmless concentration of carbon monoxide for prolonged exposure is claimed to be 0.0016% by Skochinsky and Komarov.[3] Prolonged exposure to a concentration of 0.01% can cause chronic poisoning, though it can be tolerated for six hours at a stretch

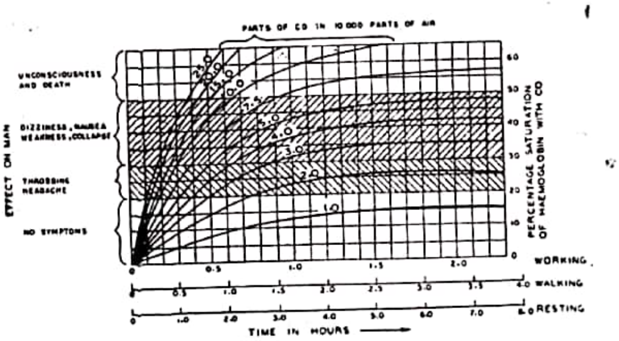

Fig. 1.14 Physiological effects of carbon monoxide (after T.D. Spencer)

beyond which a slight headache results on exertion. 0.02% causes headache, palpitation and giddiness after two hours. 0.1% results in unconsciousness after one and half hours while 0.4% can be fatal in a few minutes. Burrel, while testing the susceptibility of canaries to carbon monoxide, withstood a carbon monoxide concentration of 0.25% for twenty minutes but suffered from nausea and headache for a few hours afterwards. A concentration of 1% causes 60 to 80% blood saturation in a few seconds which is fatal. Fig. 1.14 illustrates the physiological effects of carbon monoxide as recorded by T. D. Spencer.[22] It is seen from the figure that the percentage of blood saturation which determines the symptoms is mainly a function of time and concentration of carbon monoxide. The rate of saturation of the blood is rapid initially, but slows down with time until ultimately a steady state of saturation is achieved. Hard work as well as high temperature and humidity of the ambient air increases the rate of absorption of carbon monoxide in the blood so that under such conditions, the patient gets affected much more rapidly. CO concentration in mine airways should not be allowed to exceed 0.005%. This is the threshold value also tentatively accepted by ACGIH (American Conference of Governmental Industrial Hygienists).

Carbon monoxide is usually found in the normal return air of deep coal mines in very small quantities and the ratio of carbon monoxide produced to oxygen absorbed is constant. Any change

in this ratio indicates spontaneous heating. Carbon monoxide is a product of active fires in coal mines and is invariably present in fatal quantities in afterdamp. Coal dust explosions produce more carbon monoxide that firedamp explosions. Timber fires can be dangerous sources of CO in metal mines. It is also present in appreciable quantities in the exhaust gases of diesel locomotives or other diesel engines. Another source of carbon monoxide is blasting particularly if the explosive has a shortage of oxygen. Normally though most commercial explosives are oxygen balanced, they produce certain amount of CO depending on the state of detonation and confinement of charge. An explosive fired in a hole in a strong rock produces less CO than in a weak rock. Blasting in coal produces more CO than in other rocks. Burning of explosive produces large quantities of CO. Normally an ammonia gelatine explosive produces 0.003-0.009m^3 of CO per kg of explosive blasted.

1.10.1 Detection of Carbon Monoxide

The simplest method of detecting carbon monoxide is to expose a bird or a mouse in a cage to the atmosphere containing the gas. Birds are more sensitive than mice and even among birds certain types such as canaries and muniahs give much better indication of carbon monoxide poisoning and hence are commonly used. These birds are normally so restless and active that even slight effects of carbon monoxide poisoning are noticeable in them. Such birds, when exposed to carbon monoxide, get affected more quickly than human beings. Hence a man testing for carbon monoxide with a bird gets enough time to move to safety after the bird gets affected. Burrel found that canaries exposed to 0.09% carbon monoxide showed very slight distress after exposure for one hour ; at 0.15% they were distressed after three minutes and fell from the perch after eighteen minutes ; at 0.2% they were distressed in one and a half minutes and fell from the perch in five minutes and at 0.29% they fell from the perch in two and a half minutes only. However, Spencer's[22] work shows that canaries can be a useful aid in detecting carbon monoxide in concentrations greater than 0.175% when the canary drops from the perch in a much shorter time than is required to make a working man unconscious, but below this concentration, canaries become less sensitive. The lowest concentration that makes a canary fall off the perch is 0.125% whereas a man can become unconscious with as low a concentration as 0.04-0.05%. However, for atmospheres containing more than 0.175% carbon monoxide, as is met with in rescue work, a bird cage is a good indicator. An oxygen cylinder supplied at the top of the bird cage helps in reviving the bird so that the same bird can be used over and over again.

The poor indication given by birds at low concentrations of CO which are yet highly poisonous has led to the adoption of other more accurate methods of CO detection, though bird cages are still carried by rescue parties.

The property of blood turning pink by absorbing carbon monoxide has been used for testing the gas. The air containing carbon monoxide is drawn through a light straw coloured solution of blood and the coloration produced compared with a standard colour chart calibrated for different concentrations of the gas. This method gives good accuracy[23] within the range of 0.01 to 0.2% carbon monoxide.

Modern CO detectors, however, use detector tubes containing a suitable gel such as alumina, silica gel, pumice stone etc. impregnated with a chemical which reacts with the CO of mine air to produce a colorimetric change. The estimation of the percentage of CO can be on the basis of matching the changed colour with standard shades calibrated against the percentage of CO or noting the length of tube over which the change of colour has occurred, the latter being more foolproof to read.

The detector tubes are sealed at both ends and store well for two years in this condition. During use the ends are broken and mine air is drawn through the tube by means of 1 to 10 squeezes of a rubber aspirator having an air displacement of 50 to 200cm³. These aspirators, though commonly used, can cause 5-15% error in the volume of air drawn. The bellow-type pump used with the Drager detector (Fig. 1.15) and the diaphragm pump used with the Auer detector are superior. The most accurate, however, is the piston type of pump used with some American and Japanese detectors. The reacting chemical in the tube is usually protected from the effect of moisture and other reacting gases, if any, by a suitable length of guard gel at either end.

The sensitivity of these detectors is generally high though the accuracy is much dependent on the detector-tube size, flow rate, volume of air sampled as well as the grain size, degree of packing, surface characteristics and purity of the gel used in the detector tube. A few typical detectors are described below.

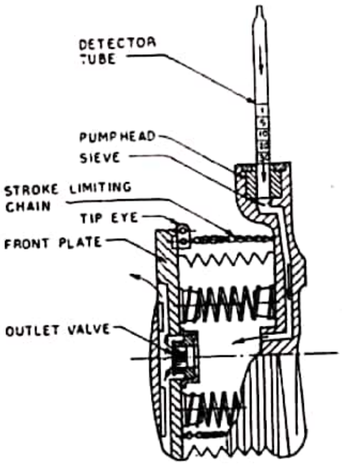

Fig. 1.15 Bellow-type pump used with Drager CO-detector tube.

The Hoolamite Tube. This consists of a glass tube filled with iodine pentoxide and fuming sulphuric acid (containing 47% SO_3) soaked in pumice stone. A known volume of air is sucked through the tube by operating a rubber aspirator for a fixed number of times when the carbon monoxide in the air reduces the iodine pentoxide liberating iodine and the grey colour of the reagent in the tube turns green, brown or black depending on the concentration. The concentration of carbon monoxide is obtained by comparing the colour produced with a standard colour chart provided with the instrument. A tube containing activated charcoal is usually introduced between the intake and the hoolamite tube in order to prevent gases other than carbon monoxide from reaching it. The hoolamite tube can estimate carbon monoxide concentration within the range of 0.1 to 1% and is not sensitive at low concentrations.[24]

Scanned with CamScanner

The M.S.A. Ammonium-Palladium-Complex Colorimetric Detector. Another colorimetric carbon monoxide detector developed by Shepherd of the National Bureau of Standards, U.S.A. during World War II and now extensively used in the U.S.A. consists of a glass tube containing yellow silica gel impregnated with palladium sulphate and ammonium molybdate. Mine air is drawn into the tube by an aspirator bulb through glass fibre and silica gel at the end of the tube so as to absorb gases other than carbon monoxide. Carbon monoxide in air reacts with the ammonium-palladium complex producing oxides, predominantly that of molybdenum, which turn the yellow colour to shades of green depending on the concentration of carbon monoxide. The percentage is obtained by comparing with a colour scale provided with the instrument. The instrument is sensitive to a concentration of 0.001% carbon monoxide and can detect within a range of 0.01 to 0.04%.

Anil automobile detector is of this type and can detect CO normally in the range of 10-1000 p.p.m., though with the use of the special C.M.R.S. appliance, it is claimed to be able to read down to even 2 p.p.m.

The P. S. Detector. This detector, manufactured by Siebe Gorman and Co. Ltd., Britain, consists of a glass tube containing silica gel impregnated with light yellow potassium palladium sulphite with silica gel at both ends for absorbing other gases. A fixed volume of air (120 cm³) is drawn through the tube at a constant rate over a period of two minutes through a calibrated orifice by operating a rubber aspirator. Carbon monoxide in the air turns the light yellow colour of potassium palladium sulphite to brown and the length of staining from one end of the tube indicates its concentration. Usually a graph showing the relation between the percentage of carbon monoxide and the length of stain is provided with the instrument. The instrument can read down to a concentration of 0.005% carbon monoxide with an accuracy of ±20% of the reading while at the upper end it can indicate a concentration up to 0.12%. The Drager CO detector is of a similar type.

The Hopcalite Detector. The generation of heat on the oxidation of carbon monoxide to carbon dioxide has been utilized by a detector manufactured by the Mine Safety Appliance Co., U.S.A. It consists of an analysing cell containing hopcalite, a specially prepared mixture of manganese dioxide and copper oxide. Air

is drawn into the cell by a hand operated pump. Carbon monoxide in the air is catalytically oxidized by hopcalite and the rise in temperature so produced is recorded by a thermocouple connected in series to a meter which is calibrated in the percentage of carbon monoxide. The instrument can read 0.005 to 0.015% carbon monoxide. A continuous-recording carbon monoxide indicator based on this principle has been developed by the U.S. Bureau of Mines for use in vehicular tunnels. Detectors using this principle are also in use in the U.S.S.R.

1.11 SULPHURETTED HYDROGEN (H_2S, Molecular mass—34)

Also known as stinkdamp, it smells like rotten egg and has a sweetish taste. It is slightly heavier than air with a specific gravity of 1.175 and burns with a light blue flame. It is soluble in water, one volume of water being capable of dissolving two and a half volumes of sulphuretted hydrogen at 293K. It is combustible and has a wide explosibility range of 4.3 to 45.5%. It is poisonous in nature, even more so than carbon monoxide and the allowable maximum concentration for prolonged exposure is 0.001% as recommended by ACGIH though the Russians fix it at 0.00066%. 0.005-0.01% affects a person in a half to one hour, the symptoms being irritation and inflammation of the eyes and irritation of the respiratory tract. An exposure for an hour to a concentration of 0.02-0.03% causes marked symptoms while an exposure to a concentration of 0.05-0.07% leads to serious poisoning in thirty minutes to one hour. A concentration of 0.1-0.3% causes rapid paralysis of the respiratory centre leading to asphyxia and death.

Sulphuretted hydrogen is rarely found in mines, sometimes occurring in afterdamps and gob fires in sulphurous coal. Methane blowers and outbursts occasionally give out small quantities of sulphuretted hydrogen. Sulphuretted hydrogen is usually produced in metal mines by the action of acid water on iron pyrites [$FeS_2+2H_2O=Fe(OH)_2+H_2S+S$], gypsum etc., by the imperfect detonation of gun powder and by blasting in heavy sulphide ores. H_2S can also be produced by rotting of timber in water. Considerable quantities of sulphuretted hydrogen have been found in acid mine water particularly if such water has been lying stagnant in poorly ventilated areas. The gas being highly soluble in water is usually dissolved in the stagnant water and can be released in dangerous quantities by a slight disturbance, such as the fall of a

Scanned with CamScanner

piece of rock into the water. Seven miners were gassed to death in 1932 in a South African metal mine when tapping a large body of water which had been standing for ten years in old workings.

Sulphuretted hydrogen is easily detected by its typical odour of rotten egg at very low concentrations such as 0.000075%. However, the smell is not perceptible at high concentrations due to the senses of smell and vision being impaired. An easy test for this gas is to expose a filter paper soaked in lead acetate solution to an atmosphere containing it when the filter paper turns brown and subsequently black within one to two minutes if the concentration is dangerous. The M.S.A. H_2S tester is an accurate instrument for detecting small percentages of sulphuretted hydrogen. It is a tube-type detector consisting of a glass tube filled with white granules of activated aluminium oxide coated with silver cyanide. When air containing sulphuretted hydrogen is drawn through the tube, the gas combines with silver cyanide forming black silver sulphide which turns the granules grey-black. The percentage is indicated by a scale placed alongside the tube which measures the length of the tube up to which the change of colour has taken place. Similar detectors are also manufactured by Auer and Drager and have also been developed by C.M.R.S. using different chemicals like compounds of lead (Drager) or bismuth (C.M.R.S.).

1.12 NITROUS FUMES (NO_2, Molecular mass—46)

These are rarely found in mines and consist mainly of nitric oxide, nitrogen dioxide and nitrogen tetroxide. The original product is usually nitric oxide (NO) which quickly combines with oxygen to form red fumes of nitrogen dioxide (NO_2) which have a pungent smell like that of fuming nitric acid. As nitrogen dioxide cools down it is slowly converted into colourless nitrogen tetroxide (N_2O_4). Nitrous fumes are highly soluble in water and can be effectively allayed by water spraying. Nitrous fumes are very poisonous, the maximum tolerable concentration for long exposure being 0.00025% as tentatively accepted by ACGIH. Concentrations of 0.025-0.075% are rapidly fatal. Men affected by nitrous fumes show immediate symptoms of cough, nausea, choking, perspiration and headache, but later develop serious bronchial troubles such as bronchitis and bronchopneumonia which may prove fatal within 48 hours. It has been claimed by Canadian investigators[25] that small quantities of nitrous fumes stimulate the development and growth of silicosis in dusty atmospheres. In Indian mines a tolerable concentration of nitrous fumes is taken as 0.0005% though in the U.S.S.R. it is still lower at 0.00025%.

These are usually formed when explosives containing nitroglycerine (particularly dynamite) undergo combustion instead of detonation as may sometimes occur with weak detonators. It has been found that nitroglycerine when properly exploded produces 63.2% carbon dioxide and 31.6% nitrogen but when burning in its own gases, as occurs in a confined space such as a drill hole, it produces 35.9% carbon monoxide and 48.2% nitric oxide. Besides, nitroglycerine explosives with oxygen imbalance produce noxious fumes, an excess of oxygen producing nitrous fumes and a deficiency, carbon monoxide. Normally detonated ammonia gelatine explosives produce about 0.003m³ of nitrous fumes per kg of explosive. Nitrous fumes may also be found in small quantities in the exhaust fumes of diesel locomotives. The most vulnerable places in a mine where nitrous fumes may be found in fatal quantities are shafts and tunnels where heavy shot firing takes place in a confined space.

The common test for nitrous fumes consists of exposing a filter paper soaked with starch and potassium iodide solution to the fumes. The filter paper turns blue by the liberation of iodine if nitrous fumes are present. Tube-type detectors indicating the percentage of nitrous fumes by the length of change in colour in the tube are also available. One such tube manufactured by Drager uses diphenyl benzidine as the reactant.

1.13 SULPHUR DIOXIDE (SO_2, Molecular mass—64)

This is a colourless gas with a very suffocating odour. It is much heavier than air (sp.gr.—2.264) and is highly soluble in water, one volume of water dissolving 40 volumes of sulphur dioxide at 293K. It is found in minute quantities in afterdamp in some coal mines, but occurs abundantly in sulphide-ore mines with fires. Blasting in rich sulphide ores also produces SO_2. Explosion of sulphide dust which results from blasting produces large quantities of SO_2 and H_2S. Sulphur dioxide is an irritant like nitrous fumes and its permissible maximum limit of concentration for prolonged exposure is 0.0005% as recommended by ACGIH (0.0007% in the U.S.S.R.). A concentration of 0.015-0.019% is fatal within a half to one hour.

Scanned with CamScanner

It is easily detected by its odour even at low concentrations of 0.0005%. However, tube-type detectors using iodine, starch and KI as reagents are available for more accurate estimation. In fact many companies like Drager, Auer, M.S.A. etc., have multigas detectors which can be used for testing of SO_2, H_2S, NO_2 and even CO by simply changing the detector tube.

Other poisonous gases like ammonia, phosphine, arsine, etc., are rarely found in mine air, but should be guarded against because of their adverse physiological effects. The maximum allowable concentrations of these gases for prolonged exposure are 85, 7 and 3 p.p.m. respectively. Radon and its daughter products are commonly found in mines of radioactive minerals. Their concentration should not be allowed to exceed 3700 $s^{-1}m^{-3}$ (10^{-1} μ Ci m^{-3}) for prolonged exposure.

1.14 SAMPLING AND ANALYSIS OF MINE AIR

1.14.1 Sampling of Mine Air

Spot samples at predetermined places in mine airways are usually collected for routine analysis of mine air. Occasionally where variation in composition is expected over the cross-section of the airway, the inlet of the sample holder may be traversed over the cross-section of the airway in a regular fashion during the period of sampling. Where distinct variation in composition exists as in an airway showing methane layering, spot samples at several spatial intervals have to be taken at the airway cross-section.

For analysis in the Haldane apparatus, the quantity of sample needed is very small and 70 cm³ is enough for three analysis, but for Orsat apparatus 250-500 cm³ is needed. Gas-sample holders of both displacement or vacuum type are generally of 250-300 cm³ capacity. For CO analysis 500 cm³ of sample should always be collected.

Glass is the most suitable material for the sample holder. But it is fragile and needs careful handling. Metallic holders are preferable from this point of view, but the stop valves of these holders tend to leak if not properly fitted and greased. Iron or even tinned iron is unsuitable as it readily absorbs O_2 in the sample. Brass, zinc and other non-ferrous metals can be used, but if H_2S and NO_2 are present, copper or copper alloys become unsuitable then glass becomes the only choice. Rubber or polythene should not be used as gases diffuse through them.

Collection of samples from mine airways can be done by (a) water or salt-solution displacement, (b) air displacement by sucking through mouth or by aspiration through a rubber aspirator or a hand or foot-operated pump and (c) in evacuated sample holders. The displacement-type sample holder whether of glass or metal is usually in the form of a cylinder with an inlet and outlet tube at either end fitted with airtight stop cocks (see Fig. 1.16). When such sample holders are not readily available, ordinary bottles of sufficient size can be used for collecting the air sample by simply emptying out the liquid contained in them at the spot of sampling. The bottles are then properly sealed with vaselined stoppers which may be further secured by rubber holding straps. The evacuated sample holders are usually in the form of glass bulbs with an attached glass tube, which has a jet drawn out at the end. After evacuation by a vacuum pump, the jet is sealed. The sample rushes into the bulb by breaking the tip of the seal at the sampling spot. The tube is then closed by a suitable rubber cap or waxed stopper.

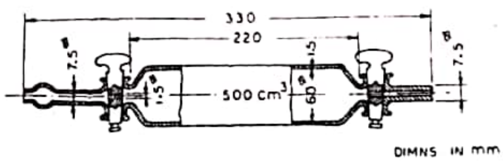

Fig. 1.16 Displacement-type glass sample holder.

Water displacement is unsuitable when CO_2 is to be accurately determined since the latter is readily soluble in water. A 22% aqueous solution of common salt is preferable in such cases. For accurate analysis by Haldane apparatus samples may be collected by displacement of mercury. When collecting by air displacement, sufficient air should be drawn through the sample holder in order to fully flush the holder as well as the connecting tubes with the gas being sampled.

Collection of samples of air from behind fire seals poses no problem when there is a positive pressure inside the seal. Stoppings showing high leakages into the sealed area (i.e. negative pressure inside the seal) should be avoided. If there is a temporary stopping behind the seal, it is necessary to pierce this stopping by a copper rod and insert a long tube through the sampling pipe in the seal so that it reaches well inside the fire area beyond the temporary stopping. It is important to ensure that this tube is fully flushed before collecting the sample.

1.14.2 Analysis of Mine Air

Normally concentrations of gases like oxygen, carbon dioxide, methane, carbon monoxide and nitrogen which are the common constituents of mine air are to be determined by mine-air analysis. It is only occasionally that a mine-air sample may be analysed for a rare constituent like H_2S, SO_2 or NO_2 which are more easily estimated by accurate spot detectors. Chemical analysis of mine air is accurate and is still widely used but is time-consuming and requires a large sample. That is why physical methods of analysis by infra-red analysers and gas chromatographs are becoming more popular today in spite of their high costs. The common chemical gas-analysis apparatus is the Orsat apparatus though for small samples, Haldane apparatus is used.

Orsat Apparatus. For rough and routine mine-air analysis, the Orsat apparatus fitted with a combustion pipette serves the purpose. It (Fig. 1.17) consists of a burette D of 100 cm³ capacity graduated to read down to 0.1 cm³. The burette is surrounded by a water jacket F for maintaining a constant temperature and is connected at the lower end by a long rubber tubing to a bottle E containing a sodium chloride solution. There are two pipettes, A and B, and a combustion chamber C connected to the burette through taps T_1, T_2 and T_3 respectively. The manifold connecting the burette and the pipettes is made of capillary tube in order to reduce the dead space in the apparatus. The pipette A contains a solution of 66g of caustic potash (KOH) dissolved in 200cm³ of distilled water for absorbing carbon dioxide and the pipette B, a solution of alkaline pyrogallol (formed by dissolving 10g of pyrogallic acid in 100cm³ of nearly saturated KOH solution) for absorbing oxygen. The pipettes are charged with glass tubes in order to increase the surface area of contact and help absorption of the gas in the absorbent solution. The pipettes are filled with the respective solutions up to fixed marks 'a' and 'b' about midway on the main limbs while the other limbs meant for adjusting the level of solution in the pipettes are closed at the top by suitable stop cocks G when not in use. This prevents the deterioration of the reagents by coming in contact with atmospheric air. Sometimes, the tops of these limbs may be covered by a rubber bladder in order to prevent contamination by air. The combustion chamber is filled with mercury and has a platinum coil for heating purposes.

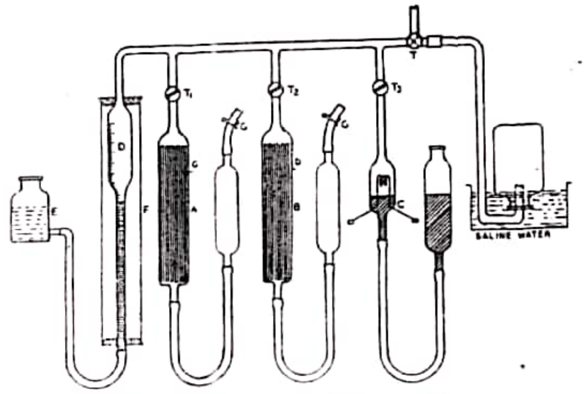

Fig. 1.17 Orsat apparatus (diagrammatic).

Gas from the sampling bottle is collected over saline water in the burette by suitably connecting the three-way tap T between the sampling bottle and the burette and lowering the bottle E. At first a small volume of gas is drawn into the burette. The gas so collected is likely to be contaminated by the air present in the apparatus and hence it is driven out of the apparatus through the tap T. Two to three such purgings are necessary before finally collecting the sample in the burette. Tap T is then closed and the water level brought to the same in both D and E so as to bring the gas to atmospheric pressure and read its volume. Usually for convenience of calculation, 100cm³ of gas is taken in the burette.

The gas is then introduced into the caustic potash pipette by opening tap T_1 and raising the bottle E which is raised and lowered for a few times so that the gas gets thoroughly mixed up with the reagent in the pipette. The gas is then brought back into the burette and tap T_1 closed when the reagent level in pipette A reaches the

Scanned with CamScanner

point 'a'. The gas in the burette is brought to the atmospheric pressure by making the liquid levels in D and E coincide with each other before reading the volume. The process is repeated until there is no further reduction of volume. The difference between the initial volume and that after absorption in caustic potash gives the carbon dioxide content of the sample.

If the gas contains methane or carbon monoxide, it is then passed into the combustion bulb and ignited there by heating the coil to white heat by passing electric current from a 6-V accumulator. The combustible gases burn, consuming a part of the oxygen of the sample. However, in case the methane content of the sample is greater than 5% (the lower limit of explosibility) the gas has to be diluted with a known volume of extra air freed from carbon dioxide and other impurities in order to avoid explosion in the combustion chamber. The contraction in the volume of the sample after combustion is noted. The sample is then passed into the caustic potash pipette and the amount of absorption, i.e. the volume of carbon dioxide produced after combustion is noted. From these, the percentage of carbon monoxide or methane can be calculated as follows :

$$CH_4 \text{ (1 vol)} + 2O_2 \text{ (2 vol)} = CO_2 \text{ (1 vol)} + \underset{\text{(2 vol condensed)}}{2H_2O} \qquad (1.13)$$

Or, when one volume of methane burns it consumes two volumes of oxygen and causes a reduction in volume equal to twice the volume of methane. Also, combustion of one volume of methane produces one volume of carbon dioxide.

$\therefore$ vol of $CH_4 = \frac{1}{2}$ (contraction in vol after combustion) ; also, vol of CH_4 = vol of absorption or vol of CO_2 produced after combustion.

In case of carbon monoxide,

$$2CO \text{(2 vol)} + O_2 \text{(1 vol)} = 2CO_2 \text{(2 vol)} \qquad (1.14)$$

There is a reduction of one volume or the reduction in volume after combustion is equal to half the volume of carbon monoxide. Also, the volume of absorption or the volume of carbon dioxide produced after combustion is equal to the volume of carbon monoxide.

If the gas contains both methane and carbon monoxide, the calculation will be as follows :

Let there be x cm³ of CH_4 and y cm³ of CO.

Contraction after combustion $= 2x + \frac{1}{2}y \qquad (1.15)$

and CO_2 produced after combustion $= x + y \qquad (1.16)$

From the above two equations, the volume of methane and carbon monoxide can be calculated. Also, the volume of oxygen consumed in combustion is obtained by adding half the volume of carbon monoxide to twice the volume of methane.

The next step is to pass the sample into the pipette containing alkaline pyrogallol where the rest of the oxygen is absorbed. The contraction in volume after absorption in pipette B gives the volume of the remainder of oxygen after combustion. The total oxygen content of the air is obtained by adding the two quantities. The volume of nitrogen is determined by difference. Sometimes, particularly for flue-gas analysis, the combustion tube may be replaced by a third pipette containing cuprous chloride solution (12g cuprous chloride dissolved in 20cm³ of concentrated HCl) in which copper wires are introduced to keep it in reduced condition. Carbon monoxide is absorbed in this pipette and its volume in the sample, so determined.

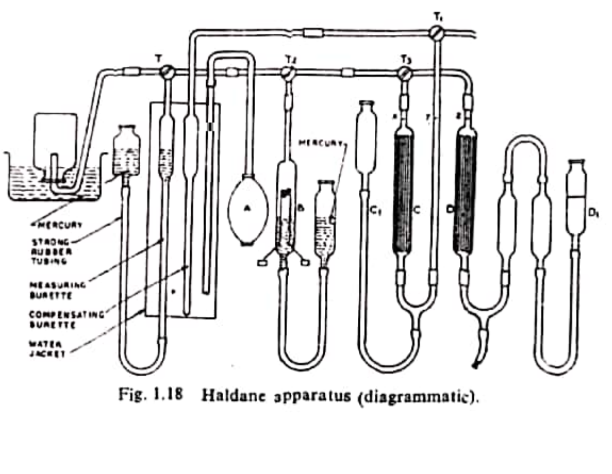

Fig. 1.18 Haldane apparatus (diagrammatic).

Haldane Apparatus. This is a more accurate apparatus for analysing mine air. There are two sizes. one, a large laboratory type and the other, a small portable type. the main differences between the two being the degree of accuracy and the capacity of the burette which is $10cm^3$ in the small one and $20cm^3$ in the larger one.

The apparatus is similar in principle to the Orsat apparatus. It essentially consists of a measuring burette (Fig. 1.18) graduated to read a minimum quantity of $0.01cm^3$ in the small appratus and $0.001cm^3$ in the larger one and a compensating burette to take into account the variations in the atmospheric conditions such as temperature, barometric pressure and humidity. Both the burettes are water jacketed, the water being constantly stirred by blowing air by a rubber aspirator A so as to equalize the temperature throughout the jacket.

Here also there are two pipettes, one containing a 36% solution of caustic potash for the absorption of carbon dioxide and the other, a solution of alkaline pyrogallol for the absorption of oxygen. The surface of the pyrogallate solution exposed to the atmosphere is usually covered by a layer of liquid paraffin in order to prevent oxidation of the reagent.

In the beginning, the three-way tap T_1 is so adjusted as to connect the compensating burette and the caustic potash pipette to the atmosphere. By adjusting taps T, T_2 and T_3 the main limbs of the caustic potash pipette C and the pyrogallate pipette D are connected to the atmosphere. The levels of reagents in the two limbs of the caustic potash pipette as well as in the pyrogallate pipette are brought to the marks X, Y and Z respectively by adjusting vessels C_1 and D_1. Tap T_1 is now turned so as to connect the compensating burette with the caustic potash pipette and is maintained in this position throughout the analysis.

The sample is then drawn into the burette, the transfer being made over mercury. For accuracy, it is desirable that the manifold connecting the burette and the pipettes be filled with an inert gas like nitrogen before the sample is collected for analysis. For this reason, a certain volume of air is first drawn into the apparatus. It is then passed into the caustic potash and pyrogallate pipettes successively in order to remove the carbon dioxide and oxygen present in it. The remaining nitrogen is now allowed to fill the apparatus. Here also the same order as in the Orsat apparatus,

i.e. initial absorption of carbon dioxide followed by combustion, absorption of carbon dioxide so produced and finally the absorption of oxygen, is followed. Care is always taken to repeat each operation till constancy of volume is reached.

The sample is collected in the burette by suitably turning tap T to connect the burette to the sampling bottle. The height of the mercury levelling vessel is so adjusted as to bring the levels of mercury in the burette and the levelling vessel to nearly the same. Tap T is now turned to connect the burette with the caustic potash pipette. It is better to maintain a slightly positive pressure in the burette by keeping the mercury level in the levelling vessel slightly higher than in the burette so that no reagent from the pipette gets into the connecting tubes, care being taken at the same time to see that the sample does not get into the caustic potash pipette. The height of the levelling vessel is now finely adjusted until the reagent level in C is brought back to X. The volume of sample in the burette is read. It is then passed into the caustic potash pipette several times before it is finally brought back into the burette. The level of reagent is brought to Y by adjusting C_1 if necessary. The mercury levelling vessel is then adjusted until the reagent level in C coincides with X when the volume in the burette is read. The process is repeated till a constant volume is obtained. The difference in volume between the first and the second reading gives the carbon dioxide content of the sample.

It takes a longer time for the absorption of oxygen in the pyrogallate solution so that it is necessary to keep the sample in contact with the pyrogallate solution for a few minutes. After absorption in pyrogallate the sample is brought back into the burette, the levelling vessel being so adjusted as to bring back the reagent level in D to Z. Tap T_3 is now turned to connect the burette with the potash pipette and the volume in the burette is read after the levels of potash solution are brought back to X and Y. Calculation of the composition is done as with the Orsat apparatus.

Where the sample contains three combustible gases such as methane, carbon monoxide and hydrogen, a separate analysis is done for the total oxygen content of the sample before combustion. The following example illustrates the calculation of the composition of a sample of mine air as analysed by the Haldane apparatus.

Scanned with CamScanner

Example 1.5

First analysis

Vol of sample taken $= 15.00\ cm^3$

Vol after absorption of CO_2 $= 14.71\ cm^3$

$\therefore$ Vol of $CO_2 = 0.29\ cm^3$ $= \frac{0.29 \times 100}{15.00} = 1.93\%$

Vol after absorption of O_2 $= 11.78\ cm^3$

$\therefore$ O_2 absorbed $= 2.93\ cm^3$ $= \frac{2.93 \times 100}{15} = 19.53\%$

Second analysis

Vol of sample taken $= 20.00\ cm^3$

Vol after absorption of CO_2 $= 19.62\ cm^3$

$\therefore$ CO_2 absorbed $= 0.38$ $= \frac{0.38 \times 100}{20} = 1.90\%$

Vol after combustion $= 19.14\ cm^3$

$\therefore$ contraction on combustion $= 0.48\ cm^3 = \frac{0.48 \times 100}{20}$

$= 2.40\%$

Vol after absorption of CO_2 $= 18.87\ cm^3$

$\therefore$ CO_2 formed $= 0.27\ cm^3$ $= \frac{0.27 \times 100}{20} = 1.35\%$

Vol. after absorption of O_2 $= 15.44\ cm^3$

$\therefore$ O_2 absorbed $= 3.43\ cm^3$ $= \frac{3.43 \times 100}{20} = 17.15\%$

O_2 used in combustion $= 19.53 - 17.15 = 2.38\%$

We have already discussed the reaction when methane and carbon monoxide burn in air. For hydrogen the reaction is

$$2H_2\ (2\ \text{vol}) + O_2\ (1\ \text{vol}) = 2\ H_2O\ (\text{condensed}) \qquad (1.17)$$

There is a contraction of three volumes or the volume of hydrogen is equal to two-thirds of the volume of contraction after combustion. Therefore,

$$\text{Total contraction after combustion} = 2CH_4 + \tfrac{1}{2}CO + \tfrac{3}{2}H_2 = 2.40\% \qquad (1.18)$$

$$CO_2 \text{ formed after combustion} = CO + CH_4 = 1.35\% \qquad (1.19)$$

$$O_2 \text{ consumed in combustion} = 2CH_4 + \tfrac{1}{2}CO + \tfrac{1}{2}H_2 = 2.38\% \qquad (1.20)$$

Subtracting eqn 1.20 from eqn 1.18 we get $H_2 = 0.02\%$.

Substituting the value of H_2 in eqn 1.18 and multiplying both sides by 2, we get

$$4.80 = 4CH_4 + CO + 0.06$$

or

$$4.74 = 4CH_4 + CO \qquad (1.21)$$

Subtracting eqn 1.19 from eqn 1.21, we have, $3\ CH_4 = 3.39$ or $CH_4 = 1.13\%$.

Substituting this value in eqn 1.19 we have

$$CO = 1.35 - 1.13 = 0.22\%$$

Therefore, the composition of the sample is :

Oxygen	19.53%
Carbon dioxide	1.90%
Carbon monoxide	0.22%
Methane	1.13%
Hydrogen	0.02%
Nitrogen (by difference)	77.20%
Total	100.00%

Bone and Wheeler Apparatus. This apparatus is different from the above two in that it brings back the sample in the burette to the same volume after each absorption and combustion and that the absorption or reduction in volume is calculated from the variation of pressure which is recorded by a mercury manometer. The advantages claimed by this method are that (a) a smaller volume of gas is needed for the complete analysis, (b) a small volume of reagent is used for absorption and is discarded after each analysis thus ensuring fresh reagent being used for each analysis and (c) the volume of each measurement being constant, any error in the graduation of the burette does not affect the accuracy of the analysis. Also, additional provision is made on this apparatus for the determination of hydrogen sulphide and unsaturated hydrocarbons.

1.14.3 Determination of Carbon Monoxide

A very accurate apparatus for determining carbon monoxide in very small quantities down to the range of 0-50 parts per million with an accuracy of the order of one part per million is the *iodine pentoxide apparatus* developed by Adams and Simmons. It is based on the principle of *Graham's apparatus* that carbon monoxide on

Scanned with CamScanner

being passed over iodine pentoxide liberates iodine which when absorbed in potassium iodide solution and titrated against a standard solution of sodium thiosulphate with starch as indicator gives a measure of carbon monoxide

$$I_2O_5+5CO \;=I_2+5CO_2 \qquad (1.22)$$

The apparatus (Fig. 1.19) consists of a burette for measuring the sample. The burette is water jacketted and is provided with a three-way tap T for connecting it either to the atmosphere or to the purifying train.

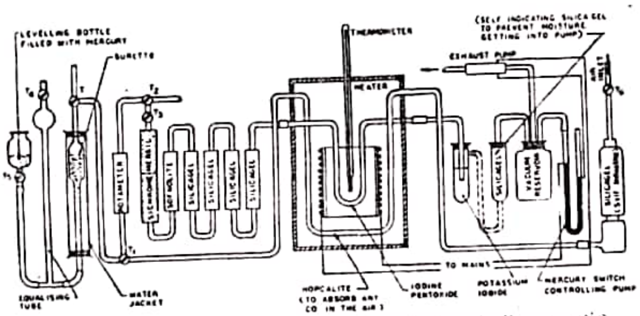

Fig. 1.19 Adams and Simmons apparatus for analysing CO (diagrammatic).

In the beginning the iodine pentoxide tube is filled with 10g of pure iodic acid. Taps T_6, T_1, T_2 and T_3 are opened so as to connect the purifying train to the air inlet. The pump is started and the air speed adjusted till the rotameter shows an air movement of 50-60cm³ min⁻¹. The heater is gradually raised to a temperature of 503 – 508K over a period of forty-five minutes to one hour and maintained at the temperature for half an hour when the iodic acid is converted to iodine pentoxide. The heater is then cooled to 423K and the air allowed to pass for another fifteen minutes before the pump is stopped and the potassium iodide bubbler removed, emptied, washed with distilled water and refilled with potassium iodide solution. The pump is restarted and 2000cm³ of air passed through the system again. Now the potassium iodide solution should not show any blue coloration on testing with starch. The potassium iodide solution is again tested for any trace of iodine

after passing another 5000cm³ of air. If it still shows a negative result, the analysis is started.

A certain volume of sample is taken in the burette through tap T which is then closed. Tap T_4 is opened and the sample brought to the atmospheric pressure by adjusting the height of the levelling bottle. Taps T_4 and T_5 are then closed and tap T turned to connect the burette with the purifying train by also opening taps T_1, T_2 and T_3. The levelling bottle is then raised to a height slightly above that of T and the tap T_5 slightly opened so as to give a positive pressure to the sample in the burette. The vacuum reservoir is of course disconnected from the potassium iodide tube which should open to the atmosphere before the gas is passed into the purifying train.

Opening of tap T_5 is so adjusted as to give a flow of 40-70cm³ min⁻¹. After the sample has been passed, taps T and T_5 are closed, T_1 is turned to connect the burette with the air inlet and 200cm³ of pure air (after passing through silica gel and hopcalite) is drawn into the burette by opening taps T and T_5 and lowering the mercury levelling bottle. This air is then passed through the purifying train by suitably adjusting taps T and T_1. This process is repeated twice or thrice in order to purge the apparatus completely of any gas from the sample.

The solution of iodine in potassium iodide is then titrated against N/560 sodium thiosulphate solution with 3 to 4 drops of 1% starch solution as indicator. Since 1cm³ of sodium thiosulphate solution is equivalent to 0.1cm³ of carbon monoxide at 273.15K and 101.33kPa barometer, the volume of carbon monoxide can easily be obtained from the amount of thiosulphate used to neutralize the iodine.

1.14.4 Infra-red Gas Analysers

These are fairly extensively used today for routine analysis of methane and other mine gases in Britain and other countries of Europe. The method is very quick and has an accuracy of the order of 0.1%.

Infra-red spectrometry[27] utilizes the principle that a particular gas or liquid absorbs radiation of a particular wave length, e.g. carbon dioxide absorbing radiations of 4.2μm and methane, of 7.5μm wave lengths. When an incident beam of this particular wave length passes through a cell containing the gas, it is partly

Scanned with CamScanner

extinguished, the amount of extinction being governed by Beer's law which is as follows :

$$I = I_o e^{-aLc} \quad (1.23)$$

where

I_o = intensity of incident beam,
I = intensity of transmitted beam,
a = absorbancy index or molar absorption coefficient,
L = optical path or length of cell
and c = molar concentration (kmol m^{-3})

Beer's law does not hold good very accurately for gases as the value of a for gases depends to some extent on the pressure of the gas and the presence of other diluents. However, calibration curves for common mine gases can be drawn with known concentrations and the analysis of the sample obtained by comparison with these calibration curves.

The infra-red spectrometer is a complicated and costly apparatus consisting essentially of (a) a source of infra-red radiation of sufficient range of wave length so as to cover all the gases present in the sample, (b) a slit and a collimator which produce a narrow beam of parallel rays, (c) a prism which disperses the beam to its components with various wave lengths, (d) an absorption cell for holding the sample and (e) the receiver which records the intensity of transmitted radiation. By rotating the prism, a beam of a particular wave length can be made to traverse the absorption cell which should have windows of suitable material that does not absorb the radiation. For wave lengths between 3μm and 9μm, fluorite windows are used while for wave lengths of 8–16μm and 15–20μm respectively, rock salt and sylvine are used. The prism is also constructed of the same material as the windows. The receivers can be either-bolometers or thermocouples used in conjunction with suitable amplifiers in order to produce measurable voltages.

1.14.5 Gas Chromatography

A rapid development in gas analysis has been the use of the technique of gas chromatography.[28] This method is capable of analysing mine gases with accuracy from small samples. Though the method is finding increasing use for common mine gases, chromatographs for analysis of rarer constituents like CO, H_2S, SO_2, NO_2 etc. in minute concentrations have to be more sophisticated.

Gas chromatographs[29, 30] essentially comprise a column containing a stationary phase over which passes a mobile phase of carrier gas from a suitable supply source through a pressure regulator. The sample to be analysed is introduced into the carrier gas in an injection chamber immediately before the column. A suitable detector for recording the concentration of the component gases is provided after the column.

The column is by far the most important part of the gas chromatograph and is responsible for the elution or separation of the individual constituents of a gaseous mixture. It contains an adsorbent which retains different gases for different durations in the column. As a result, the gaseous components which have the least retention time come out first followed by those with longer retention times thus resulting in the separation of the individual gases. The detector then senses and records the concentration of these individual gases in the form of Gaussian curves (against time), the heights of which or preferably the areas under which give, by suitable calibration, the concentration of the gas detected.

The stationary phase can be either an inactive solid support like diatomite coated with a thin liquid film or an active solid adsorbent like molecular sieve (dehydrated alumina silicates of Na and Ca), silica gel, alumina etc. For analysis of permanent gases, such as O_2, N_2, CO, NO, CH_4 etc. as is generally required in mines, solid adsorbents are commonly used.

The carrier gas usually chosen for permanent gases is hydrogen or helium which have high thermal conductivity compared to the gas to be detected so that high sensitivity can be obtained with thermal conductivity detectors commonly used for permanent gases. These detectors comprise thermal conductivity cells or katharometers having elements of heated wire or thermisters. As gases of different thermal conductivity pass over the element, it cools to different extents as a result of which the resistance of the element changes. The change in resistance is recorded through a bridge circuit and amplifier.

Thermal conductivity detectors are not very sensitive for trace components, in spite of more sensitive thermal conductivity

Scanned with CamScanner

detectors having been developed of late. Minor quantities of permanent gases can be detected by gas-density balance, but even these are unsuitable for trace components. Special types of detectors may be used for specific gases. For example, electron-capture detectors are very sensitive for NO_2 and halogenated compounds. Flame-ionization detectors can be used for hydrocarbons and microcoulometric detectors for compounds of sulphur. Lovelock-type helium-ionization detectors are by far the most sensitive for trace concentrations of permanent gases, but they make the whole instrument highly sophisticated and costly.

It is difficult to analyse a condensible gas like CO_2 or unsaturated hydrocarbons along with the other permanent gases present in mine air with a single column. Molecular sieves, though good for separating the permanent gases have an unusually high retention time for CO_2. In such cases dual columns, one of silica gel for separating CO_2 from air (O_2 and N_2 of air do not get separated here) and the other of molecular sieve for separating the permanent gas components of air such as O_2, N_2, CH_4, etc. are used. Of late, columns of porous polymer beads (Poropak) have been used with suitable temperature programming to analyse the complete range of possible mine gases like oxygen, nitrogen, carbon dioxide, carbon monoxide, methane, nitrous oxide, nitrogen dioxide, sulphur dioxide, hydrogen sulphide, water and ammonia.

There are many other instrumental methods of gas analysis. Instruments utilizing physical properties of gases such as density, sonic velocity, thermal conductivity, refractive index (interferometry), paramagnetic susceptibility etc. have been developed for analysing binary systems of gases, but are not suitable for complete mine-air analysis.

A very accurate method of getting a quantitative estimation of the various gaseous components of mine air even at minute concentrations is by *mass spectrometry*. The instrument basically comprises an electron beam which ionizes the molecules of the gas sample to be analysed. The ionized gases are then separated by subjecting them to a magnetic field which deflects the different ions to different extents depending on their mass to charge (m/e) ratio. An ion detector then records the concentration of the various components in the form of a mass spectrum with different peaks. However, mass spectrometers are extremely costly and have not found common use for mine-air analysis.

EXERCISE 1

1.1 The analysis of a sample of mine air gives 19.75% O_2, 77.95% N_2, 0.4% CO_2 and 1.9% CH_4. Determine the percentage and composition of black damp in the same.

1.2 How long could a man remain conscious in a heading 2×2.5m in cross-section when it has been sealed by a fall 10 m behind the face? The air in the heading contains 20.1% O_2 and 0.1% CO_2. Assume unconsciousness to follow 7% O_2 or 10% CO_2 in the air. The average O_2 breathing rate of the man may be assumed at 240 cm^3 min^{-1} with a respiratory quotient (CO_2 produced by O_2 inhaled) of 0.82. Determine if O_2 deficiency or the effect of CO_2 will have the dominating influence.

1.3 The instantaneous rate of liberation of methane in a room being advanced by a continuous miner varies from 1.5–7.5 m^3 min^{-1}. Calculate the required rate of supply of fresh air to the face in order to keep the methane concentration below 0.75%.

1.4 Oxidation of sulphides in a stope liberates 0.005 m^3 of SO_2 per minute. Calculate the rate of fresh air supply required to dilute the gas to the permissible concentration of 0.0005%.

1.5 0.1 m^3 of CH_4 is emitted per minute at a coal face mined by a continuous miner which also generates 10^{11} particles of dust of respirable size range per minute. Calculate the ventilation required to dilute the impurities to 0.5% CH_4 and 850 p.p.c.c. for dust taking the general body of mine air to contain 0.1% CH_4 and 200 p.p.c.c. dust.

1.6 An advancing longwall face with a daily production of 1500 tonnes of coal emits 30 m^3 of CH_4 per tonne of coal. Calculate the ventilation necessary to keep down the methane concentration at 0.75%.

1.7 A sample of air from a coal mine when analysed by a Haldane apparatus gives the following readings:

Initial volume of sample	..	19.962 cm^3
After CO_2 absorption	..	19.882 cm^3

Scanned with CamScanner

After combustion	..	19.602 cm³
After post-combustion		
CO_2 absorption	..	19.462 cm³
After O_2 absorption	..	15.799 cm³

Calculate the composition of the mine air assuming CH_4 and CO to be the possible combustible gases.

1.8 A sample of mine air from the gob gives the following results in two analyses :

First Analysis :

Volume of sample taken	..	18.00 cm³
Volume after absorption of CO_2		17.86 cm³
Volume after absorption of O_2	..	14.17 cm³

Second Analysis :

Volume of sample taken	..	19.95 cm³
Volume after absorption of CO_2		19.79 cm³
Volume after combustion	..	19.29 cm³
Volume after post-combustion		
CO_2 absorption	..	19.04 cm³
Volume after absorption of O_2	..	15.44 cm³

Find the composition of the mine air assuming H_2, CO and CH_4 to be the only combustible components present.

1.9 A sample of mine air analysed on the Orsat apparatus gave the following readings. Calculate its composition by volume and by mass.

Sample taken	..	99.8 cm³
After absorption in KOH	..	97.6 cm³
After combustion	..	95.1 cm³
After absorption in KOH	..	93.7 cm³
After absorption in alkaline pyrogallol	..	77.3 cm³

CHAPTER II

DUST IN MINES

2.1 THE HAZARD OF DUST

Most mining operations produce dust which, when air-borne, becomes a serious hazard to the health of the workers. Besides, inflammable dusts, as that of coal and sulphide ores can lead to disastrous explosions. However, explosive dusts are outside the scope of this book and we shall confine ourselves to the treatment of respirable dusts only in this chapter. The problem of dust has been there since the early days of mining, but in recent times, with the introduction of mechanization in mines, it has become a greater menace than ever, since machine operations usually throw up much more dust than hand operations ordinarily do.

Dusts of any kind when inhaled in large quantities lead to the development of respiratory diseases such as chronic bronchitis and pneumokoniosis. Pneumokoniosis is a general term used for occupational lung disease due to dust and has been redefined by the ILO working group in 1971[31] as the accumulation of dust in the lungs and tissue reactions to it. Specific names such as silicosis, asbestosis, siderosis, talcosis etc. have been used to indicate pulmonary diseases caused by specific dusts such as of silica, asbestos, iron oxides, talc etc. Metal fumes are also known to cause specific lung diseases. Besides radioactive dusts of uranium or thorium ores as well as other toxic dusts of ores (mainly oxides and carbonates of beryllium, arsenic, lead, chromium, vanadium, mercury, cadmium, antimony, manganese, tungsten, nickel, silver etc.) are also harmful to the human system and have to be guarded against.

2.2 PNEUMOKONIOSIS

From a pathological point of view, pneumokoniosis can be divided into two groups : (a) collagenous and (b) noncollagenous. Non-collagenous pneumokoniosis is caused by nonfibrogenic dusts and is characterized by (i) alveolar architecture remaining in tact,

Scanned with CamScanner

After combustion	..	19.602 cm^3
After post-combustion		
CO_2 absorption	..	19.462 cm^3
After O_2 absorption	..	15.799 cm^3

Calculate the composition of the mine air assuming CH_4 and CO to be the possible combustible gases.

1.8 A sample of mine air from the gob gives the following results in two analyses :

First Analysis :

Volume of sample taken	..	18.00 cm^3
Volume after absorption of CO_2		17.86 cm^3
Volume after absorption of O_2	..	14.17 cm^3

Second Analysis :

Volume of sample taken	..	19.95 cm^3
Volume after absorption of CO_2		19.79 cm^3
Volume after combustion	..	19.29 cm^3
Volume after post-combustion CO_2 absorption	..	19.04 cm^3
Volume after absorption of O_2	..	15.44 cm^3

Find the composition of the mine air assuming H_2, CO and CH_4 to be the only combustible components present.

1.9 A sample of mine air analysed on the Orsat apparatus gave the following readings. Calculate its composition by volume and by mass.

Sample taken	..	99.8 cm^3
After absorption in KOH	..	97.6 cm^3
After combustion	..	95.1 cm^3
After absorption in KOH	..	93.7 cm^3
After absorption in alkaline pyrogallol	..	77.3 cm^3

CHAPTER II

DUST IN MINES

2.1 THE HAZARD OF DUST

Most mining operations produce dust which, when air-borne, becomes a serious hazard to the health of the workers. Besides, inflammable dusts, as that of coal and sulphide ores can lead to disastrous explosions. However, explosive dusts are outside the scope of this book and we shall confine ourselves to the treatment of respirable dusts only in this chapter. The problem of dust has been there since the early days of mining, but in recent times, with the introduction of mechanization in mines, it has become a greater menace than ever, since machine operations usually throw up much more dust than hand operations ordinarily do.

Dusts of any kind when inhaled in large quantities lead to the development of respiratory diseases such as chronic bronchitis and pneumokoniosis. Pneumokoniosis is a general term used for occupational lung disease due to dust and has been redefined by the ILO working group in 1971[31] as the accumulation of dust in the lungs and tissue reactions to it. Specific names such as silicosis, asbestosis, siderosis, talcosis etc. have been used to indicate pulmonary diseases caused by specific dusts such as of silica, asbestos, iron oxides, talc etc. Metal fumes are also known to cause specific lung diseases. Besides radioactive dusts of uranium or thorium ores as well as other toxic dusts of ores (mainly oxides and carbonates of beryllium, arsenic, lead, chromium, vanadium, mercury, cadmium, antimony, manganese, tungsten, nickel, silver etc.) are also harmful to the human system and have to be guarded against.

2.2 PNEUMOKONIOSIS

From a pathological point of view, pneumokoniosis can be divided into two groups : (a) collagenous and (b) noncollagenous. Noncollagenous pneumokoniosis is caused by nonfibrogenic dusts and is characterized by (i) alveolar architecture remaining in tact,

Scanned with CamScanner

(ii) minimal stromal reaction consisting mainly of reticulin fibres and (iii) reversibility of dust reaction. Examples of noncollagenous pneumokoniosis are stannosis caused by tin oxide and barytosis caused by barium sulphate. Collagenous pneumokoniosis is characterized by (i) permanent alteration or destruction of alveolar architecture, (ii) collagenous stromal reaction of moderate to maximal degree and (iii) permanent scarring of lungs. It may be caused by fibrogenic dusts or altered tissue response to non-fibrogenic dusts. Silicosis and asbestosis are caused by fibrogenic dusts while complicated coal miners' pneumokoniosis or progressive massive fibrosis is an altered tissue response to a relatively non-fibrogenic dust. In practice distinction between collagenous and noncollagenous pneumokoniosis is difficult and continued exposure to the same dust such as coal dust may cause transition from non-collagenous to collagenous form.

2.3 SILICOSIS

Of all the types of pneumokonioses met with in mines, silicosis is the most dangerous since it can affect people fatally and is progressive in nature. There have been cases when a patient has complained of the symptoms of silicosis even after he had left the dusty operation for several years. Silicosis is characterized by the development of nodular fibrosis in the lung tissue. The nodules appear as protrusions in the lung tissue and histologically consist of a concentric development of fibrous tissue. They may at times be thrown into sharp relief by emphysema or collapse of the surrounding lung tissue. Calcarious development at the centre of the nodules is noticed in certain cases. Pathologically and symptomatically silicosis can be divided into the following three stages. In the *first stage* dyspnoea (inelasticity of the lung) and shortening of breath is noticed only on exertion. There may be a slight dry cough but chest expansion is rarely minimized. Radiographs of the lung show discrete circular shadows of nodules of a maximum diameter of 2mm. The *second stage* is characterized by well-established dyspnoea and cough with impaired chest expansion. The radiograph shows diffuse nodulation with a tendency to coalescence. Dyspnoea leads to total incapacity in the *third stage* when the radiograph shows areas of massive consolidation. Silicosis, particularly in the advanced stages, is usually associated with tuberculous infection which may modify the symptoms.

The cause of nodular fibrosis is believed to be the toxic action of high polymers of silicic acid.[32, 33] Particles of free silica (SiO_2) dissolve in the lung fluid forming silicic acid which, in turn, undergoes high polymerization when the initial pH(2) of silicic acid passes through a value of 5.5 to 6 corresponding to a stage of high polymerization of silicic acid as it tends to reach the lung pH of 7.

There has been no approved cure, so far, of silicosis, though its associated tuberculosis is amenable to treatment. Aluminium prophylaxis and therapy for the treatment of silicosis have been tried in Canada and some other countries since 1937 with encouraging results, but they have yet to find wide application in mines. The principle of aluminium therapy depends on the fact that particles of metallic aluminium or amorphous hydrated alumina when engulfed in the same phagocyte cell along with silica dust, neutralize the effect of silica, thus arresting further progression of fibrotic tissue reactions. Mature nodules become static and immature lesions of the early stage of fibrosis get resolved. Aluminium ordinarily has no toxic effect on lung tissue but excessive doses make the lung more susceptible to tuberculous infection. Aluminium dust is retained in the lung for a fairly long time extending even up to a year, and can hence act as a prophylactic agent against later inhalation of silica dust. Recently[34] aqueous solution of chlorhydroxy-allantoinate of aluminium and colloidal solution of aluminium hydroxide administered in the form of aerosol showed both prophylactic as well as stabilizing action on silicotic lesions, while the solution itself was completely inocuous.

Experiments have been carried out in Germany[35] for preventing dangerous silica dust from reaching the alveoli of the lung (where they could produce silicosis) by artificially increasing their size. This is done by releasing a large quantity of fine aerosol (0.05 μm size) of sodium chloride into the dusty air. Owing to Brownian motion, several particles of sodium chloride coagulate with each dust particle. The hygroscopic salt absorbs moisture when passing through the moist respiratory tract and makes the dust particles grow in size by condensation of water on them. Though encouraging results have been obtained from experiments on animals, the effect of the method on men has not yet been fully tried out.

Scanned with CamScanner

2.4 ASBESTOSIS

Asbestosis is pathologically and to some extent symptomatically distinct from silicosis. Pathologically, asbestosis involves the development of tough areas in the lung due to the presence of fibrous tissue. The fibrosis in asbestosis is different from the nodular fibrosis typical of classical silicosis. The lung radiograph shows a diffuse ground glass or cobweb-like appearance. Here the fibrosis is believed to be caused by the mechanical action of long asbestos fibres which get lodged in the alveolar walls causing morbid growth of fibrous tissue in the region. As a result, the alveolar walls or the septa separating alveoli get thickened owing to the presence of both asbestos fibres and asbestosis bodies. This is substantiated by the fact that the fibrosis-producing character of asbestos is almost completely eliminated if the asbestos is thoroughly pulverized so that no particle in it exceeds two micrometres in length. Emphysema is usually present in asbestosis with many pleural adhesions. The common symptoms of asbestosis are dyspnoea and non-productive cough. Often the clinical symptoms may be more pronounced than those in classical silicosis although the lung radiographs of asbestosis are less severe than those of classical silicosis. Progress of fibrosis in asbestosis has been found to be more rapid than in silicosis, so much so that a person may die of asbestosis within five years of the onset of symptoms. Asbestosis, however, makes the lung less susceptible to tuberculosis than does silicosis.

Apart from dusts of free silica and asbestos, other dusts such as that of chromite, iron ore, kaolin, barytes etc. produce pneumokonioses which usually do not show fibrosis and are generally non-progressive and non-disabling, though pigmentation and consequent thickening of alveolar walls do occur. Fibrosis however develops if these dusts contain some amount of free silica.

2.5 COAL MINERS' PNEUMOKONIOSIS

In the simplest form of coal miners' pneumokoniosis, coal dust usually collects at a number of foci all over the lung around the small bronchioles and their accompanying arteries and a network of reticulin fibres is developed all around these foci. The air spaces around the coal foci get dilated leading to focal emphysema. The

usual symptoms of coal miners' pneumokoniosis are dyspnoea, cough with coal-black sputum and emphysematous chest. This, however, results in only slight disablement after long exposures, unless associated with other complications such as tuberculous infection, which is usually associated with advanced coal miners' pneumokoniosis. In fact, the relatively fewer occurrences of pneumokoniosis in low-rank coal mines as compared to anthracite mines have been found to be due to the fact that vitricin in low-rank coals contains antibiotics which inhibit tubercular infection. Prolonged exposure, however, may lead to collagenous pneumokoniosis. When coal dust contains sufficient silica dust, development of progressive nodular fibrosis, characteristic of classical silicosis, occurs.

2.6 PHYSIOLOGICAL PROPERTIES OF DUST

2.6.1 Composition

The properties of dust affecting the development and severity of lung diseases are chiefly composition, size and concentration though particle shape is also an influencing factor. Acicular quartz crystals of South African gold mines have been found more violent than uniformly crystalline quartz of the Kolar Gold Field. Chemical and mineralogical composition of the dust particles determine the degree of virulence. While minerals like silica and asbestos are extremely hazardous, minerals like haematite have been reported to have a prophylactic effect on toxic dusts. The Silicosis Research Institute, Bochum[36] allots different hazard factors to different minerals in estimating the dust value which should always be less than a threshold limit value. However, free crystalline silica in any dust has been almost universally accepted as the most important hazard component of any dust. It can, by association, make any type of pneumokoniosis disabling. Thus it becomes necessary to ascertain the free silica content of any dust in order to assess its physiological importance.

It often becomes a problem to estimate the quartz (free silica) content of fine dust. Petrological microscopes fail to identify particles below 5μm in size. The U. S. Bureau of Mines have used immersion oils of refractive index 1.56, equal to that of quartz, to get an estimation of quartz particles on a dust slide by differential counting under the microscope. But this measurement can also include any other mineral of similar refractive index. Successful chemical methods of determining the free silica content of a mineral dust have been developed. Precise estimation of the quartz content of any dust is possible by X-ray diffraction analysis, infra-red spectrography and differential thermal analysis, though the methods involve costly equipment.

It must be borne in mind that it is the composition of the dust reaching the lung and not that of the air-borne dust or the mineral or rock producing the dust, that is important, since the composition can vary considerably for these conditions. For example, a sandstone with greater than 90% quartz produces dust with only 25% free silica in the size range below 5μm.

2.6.2 Size of Particle

This is the most important parameter of dust that governs its physiological effect. Most authors[37, 38] are agreed that the maximum tissue damage is caused by dusts of about one micrometre size and it decreases with particles of both higher and lower sizes. According to Hatch, tissue damage is negligible for particles above 2 to 3μm size. This is mainly because of the fact that large particles of 5μm size and above are usually trapped in the upper respiratory tract, such as the large bronchi, trachaea etc. whereas only particles of one micrometre or lesser size reach the alveoli of the lung. Again, of the latter, the maximum retention occurs for 1μm particles whereas 0.25μm particles lend themselves least to retention. This will be clear from Fig 2.1.[39] The percentage of retention again increases with ultrafine particles, whose deposition is governed more by Brownian motion than gravitational settling, but tissue damage caused by very fine particles is neglible, probably because of the fact that very fine particles are too quickly dissolved to produce any toxic effect. In practice, all dust below 5μm size is usually considered to be dangerous.

The 1959 Johannesburg Pneumokoniosis Conference adopted a 'respirable fraction' of dust cloud as defined by a sampling efficiency curve (see Fig. 2.2) passing through the points (1μm, 100%), (5μm, 50%) and (7μm, 0%) where the X-axis represents the equivalent particle diameter (taken as the diameter of a spherical particle of unit density having the same settling velocity in air as the particle

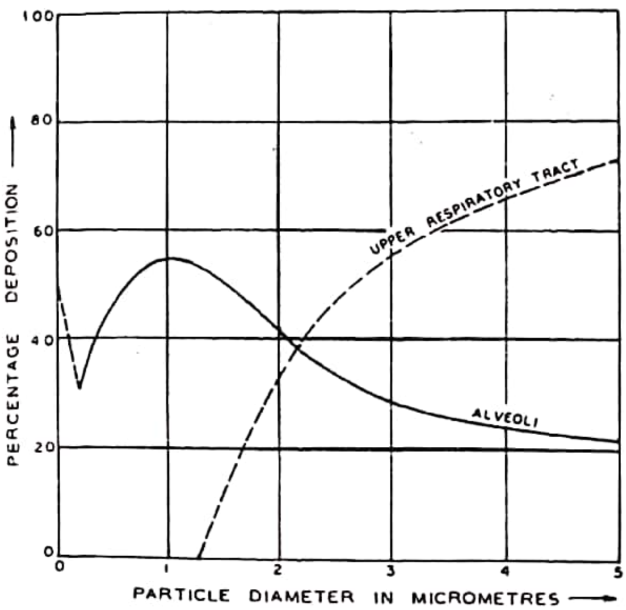

Fig. 2.1 Retention of mineral dust in human respiratory system.

in question) and the Y-axis, the collection efficiency. This curve simulates the size separation and deposition in the lung taking into account the particle size, shape and density. This size fraction is generally adopted today in designing modern gravimetric dust sampling instruments.

2.6.3 Concentration

Concentration of dust can be expressed as (a) mass of dust per unit volume of air, (b) number of particles per unit volume and (c) surface area of particles per unit volume. Mass concentration was the earliest-adopted indicator of dust hazard when sugartube method of dust sampling was prevalent in South Africa. But the

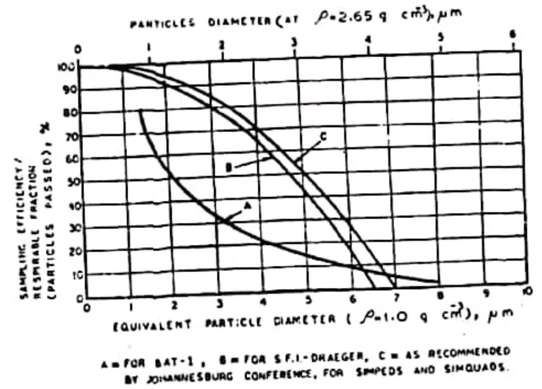

Fig. 2.2 Dust separation curves.

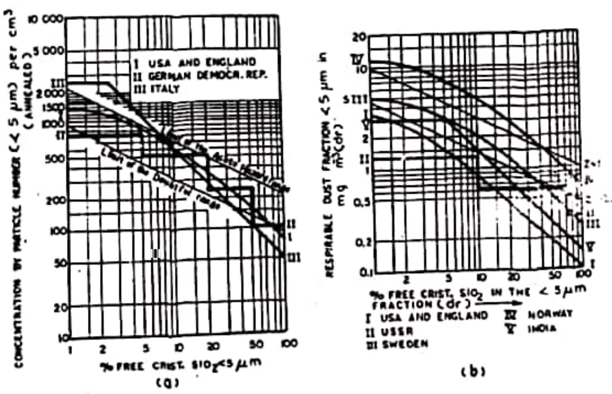

Fig. 2.3 Maximum allowable concentration of dust (MAC) in different countries :
(a) particle number concentration,
(b) mass concentration.

total mass of a dust cloud could give a very wrong estimate of its harmfulness since only a few large particles can completely outweigh the effect of a large number of particles of respirable size. For example, a 10μm particle weighs 8000 times as much as a 0.5 μm particle of the same dust. There was then a shift towards adopting the particle-number concentration in the respirable size range as a danger criterion and several sampling instruments, some of which were highly accurate, were designed to measure this concentration. Arbitrarily safe values of the *maximum allowable concentration* (MAC) based on particle-number count were prescribed in different countries based on different sampling instruments (see Fig. 2.3a). However, there was no good correlation established between particle-number concentration and incidence of pneumokoniosis.

Today therefore mass concentration, of course, in the respirable size range, has been reestablished as a danger criterion mainly based on its correlation with the incidence of pneumokoniosis established from recent studies in several European countries. The Johannesburg Pneumokoniosis Conference also recommended adoption of mass concentration of the respirable fraction for coal dust while for silica dust, the surface-area concentration of the respirable fraction was recommended.

King[38] has shown that toxicity of silica dust is more closely associated with the surface area of particles than the other parameters. This is understandable since solubility is dependent on the exposed surface of the particles, but it is difficult to measure surface area. The tyndalloscope is the only instrument today that gives an estimate of particle-surface-area concentration in terms of intensity of scattered light and is fairly widely used in West Germany. Particle-surface-area concentration, however, can be estimated from the particle-number concentration provided a complete size-frequency analysis of the dust cloud in the respirable size range is available and of late much research has been directed to developing quicker and more foolproof (free from personal error) methods of particle-size-frequency analysis.

Table 2.1 gives an interesting study by Goldstein and Webster[40] on the effect of intratracheally injected quartz particles of various sizes on fibrosis development in rats. It is interesting to see the correlation observed between the mass of injected dust and the incidence of fibrosis.

Scanned with CamScanner

Table 2.1 : Effect of Particle Size of Dust on Fibrotic Development in Rats

Size range, μm	Mass of dust injected, mg	Surface area, cm^2	Number of particles	Percentage of animals showing group 3 or 4 fibrosis
<1	14	600	4000×10^8	6
1—3	46	600	100×10^8	77
2—5	93	600	5×10^8	85

The MAC values based on mass concentration of the respirable fraction of dust for different quartz content is given in Fig. 2.3(b) for different countries. In India, the MAC or threshold value of respirable dust ($<5\mu m$ in size to be sampled by an NCB/MRE 113 A or equivalent gravimetric sampler) has been tentatively fixed for atleast a period of five years by a circular issued in 1975 by the DGMS at 3mg m^{-3} for dusts having $\leq 5\%$ free silica as in thec ase of coal mines. For metalliferous mines where the dust contains $>5\%$ free silica, the limit shall be determined by the relation

$$\text{Threshold value} = \frac{15}{\%\ \text{respirable quartz or free silica}}\ \text{mg m}^{-3} \qquad (2.1)$$

2.6.4 Time of Exposure

Experiments on animals show that larger lung dosages of dust produce faster development of silicosis and the same holds true for men also. While with exposure to large dust concentrations, it takes only a year or a few years for the development of nodular fibrosis, the period of exposure required for the development of silicosis progressively increases with decreasing concentration. It must be noted here that the human respiratory system has a certain capacity for disposing of inhaled dust. The coarse dust deposited in the upper respiratory tract is moved upwards by ciliary action and ultimately discharged through the sputum. Normally, wandering phagocyte cells engulf the fine particles reaching the alveoli and remove them to the lymph nodes where fibrosis may develop. It is when the lymph nodes are fully saturated that fibrosis develops in the alveolar walls in the lung.

It is thus obvious that the time of exposure to a certain dust concentration is an important factor in the development of pneumokoniosis and it is logical to correlate the incidence of pneumokoniosis with the cumulative dust exposure, which can be easily calculated from the length of employment of the worker if the average (weighted) shift concentration of dust to which the worker is subjected is known. It is with this objective in view that a 'dust sum' parameter obtained by multiplying the concentration parameter with the number of shifts over which the miner has been exposed to the dusty atmosphere was introduced by the Dust and Silicosis Control Centre at Essen, W. Germany. In any case, in accordance with the Johannesburg Pneumokoniosis Conference recommendations, the MAC all over the world today is taken as the time-weighted average level of dustiness over a sufficiently long period, usually an eight-hour working shift and long-duration sampling instruments have been developed to directly measure this shift-average concentration.

2.7 DYNAMICS OF SMALL PARTICLES

Any effective measure of dealing with dust in mines involves a thorough understanding and utilization of the dynamic properties of fine particles and this aspect will be dealt with here. Other physical properties of dust such as optical, electrical etc. are also utilized for sampling, separation etc. but these will be dealt with when considering their utilization.

Small particles have a relatively high surface area per unit mass. If a centimetre cube of quartz is comminuted to particles of $1\mu m^3$ size, there will be 10^{12} particles with a total surface area of $6m^2$ as compared to only $6cm^2$ surface area of the original cube. Owing to the large surface area, there is a greater viscous resistance to the motion of small particles in air as compared to large ones. A small particle falling in the gravitational field of the earth will be opposed by the viscous resistance of air which will increase with increasing velocity of the particle until the particle has no acceleration. The resistance of air then balances the gravitational force and the particle falls at a constant velocity called the *terminal settling velocity*. The terminal velocity of fine particles is very small, being of the order of centimetres or even millimetres per hour and that is why particles of fine dust, when once air-borne, remain in suspension for a long time.

Scanned with CamScanner

Viscous resistance to a particle in motion is given by the equation

$$R = \frac{C_D \, \rho_a A v^2}{2} \qquad (2.2)$$

(compare with eqn 4.32)

where R = resistance,
ρ_a = density of air,
A = projected surface area of the particle,
v = velocity of the particle relative to air
and C_D = drag coefficient.

C_D is not constant, but varies with the Reynolds number and the shape of the particle. For values of *Re* (Reynolds number) greater than 10^3 (up to a maximum limit of 2.5×10^5), C_D is reasonably constant and has an average value of 0.44 for spheres. This is the regime of turbulent motion where the resistance is proportional to the square of the velocity (Newton) and eqn 2.2 can be written as

$$R = \frac{0.44\pi\rho_a \, D^2 v^2}{8} \qquad (2.3)$$

where D = diameter of the particle.

For $Re < 3.0$, C_D can be taken to vary inversely with *Re* given by the equation $C_D = 24/Re$ for spherical particles.

Or, $$R = \frac{24\mu}{vD\rho_a} \times \frac{\pi\rho_a \, D^2 v^2}{8} = 3\pi\mu Dv \qquad (2.4)$$

The above equation, as developed by Stokes, holds good for streamline flow where the resistance varies directly as velocity. It must be noted here that whereas for turbulent motion the resistance is governed by air density and is independent of viscosity (see eqn 2.3), for streamline motion (eqn 2.4) the reverse is the case. For intermediate values of *Re*, the resistance depends on both viscosity and density of air. Here, C_D is a complex function of *Re* and is given by the approximate relation $C_D = 14/Re^{\frac{1}{2}}$ for which

$$R = 5.5\rho_a^{\frac{1}{2}} \mu^{\frac{1}{2}} D^{\frac{3}{2}} v^{\frac{3}{2}} \qquad (2.5)$$

2.7.1 Terminal Settling Velocities

As has been said earlier, a falling particle attains the terminal velocity when the gravitational force balances the air resistance.

So, for turbulent motion,

$$\frac{\pi D^3}{6}(\rho - \rho_a)\, g = \frac{0.44\pi\rho_a \, D^2 \, v_t^2}{8}$$

Or, $$v_t = \left\{\frac{3Dg(\rho-\rho_a)}{\rho_a}\right\}^{\frac{1}{2}} \qquad (2.6)$$

where v_t = terminal velocity,
ρ = density of particle
and g = acceleration due to gravity.

Similarly for streamline motion,

$$v_t = \frac{D^2(\rho - \rho_a)g}{18\mu} \qquad (2.7)$$

and for intermediate motion,

$$v_t = \frac{0.209\,(\rho - \rho a)^{\frac{2}{3}}\, g^{\frac{2}{3}}\, D}{(\rho_a \mu)^{\frac{1}{3}}} \qquad (2.8)$$

In the above equations, ρ_a is very small compared to ρ so that $\rho - \rho_a$ can be approximately taken as equal to ρ. Again assuming values of ρ_a = 1.2 kg m^{-3}, g = 9.81 m s^{-2} and $\mu = 1.8\times10^{-5}$ Pa s for ordinary temperatures, the above equations can be simplified for spherical particles as :

for turbulent motion,

$$v_t = 4.95\,\rho^{\frac{1}{2}} D^{\frac{1}{2}} \qquad (2.9)$$

$$\left(\frac{v_t D \rho_a}{\mu} > 10^3 \quad \text{or,} \quad D > \frac{0.021}{\rho^{\frac{1}{3}}}\right)$$

for streamline motion $v_t = 3.03\times10^4\,\rho D^2$ (2.10)

$$\left(D < \frac{1.141\times10^{-3}}{\rho^{\frac{1}{3}}}\right)$$

and for intermediate motion, $v_t = 34\,\rho^{\frac{2}{3}} D$ (2.11)

$$\left(\frac{1.141\times10^{-3}}{\rho^{\frac{1}{3}}} < D < \frac{0.021}{\rho^{\frac{1}{3}}}\right)$$

where v_t = terminal velocity in ms^{-1}
D = diameter of particle in m
and ρ = density of particle in kg m^{-3}.

Scanned with CamScanner

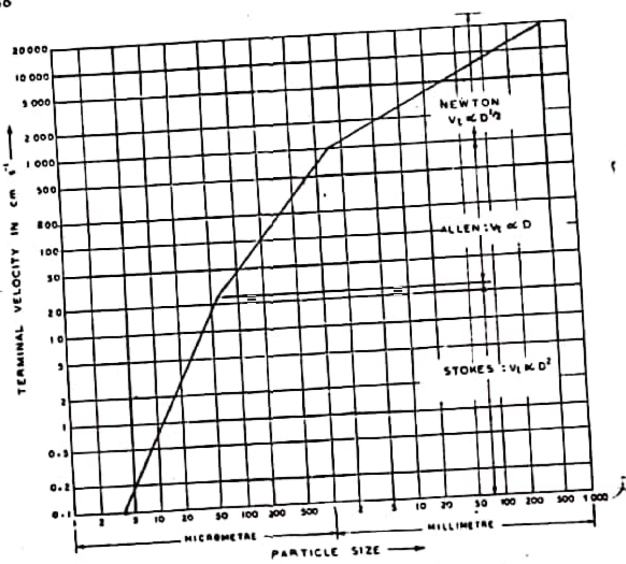

Fig. 2.4 Terminal velocities of quartz particles in air.

The settling velocity for particles of irregular shape is however slightly lower than that for spherical ones. Fig. 2.4 gives the terminal velocities for different sizes of crushed quartz particles in air.[42]

Stokes' law of gravitational settling (eqn 2.7) does not hold good for very fine particles, since when particles become small compared to the mean free path of gas molecules, the viscous resistance decreases and consequently the terminal velocity increases. For such particles Cunningham developed the following relation :

$$v_c = v_s\left(1+1.7\frac{l}{D}\right) \tag{2.12}$$

where v_c = true terminal velocity,
v_s = terminal velocity as calculated by Stokes' equation (eqn 2.7)

and l = mean free path of the gas molecules
$\simeq 10^{-7}$ m under ordinary atmospheric conditions.

For particles above 0.5μm in size, v_c differs very little from v_s, though it is about five times as high as v_s for 0.05μm particles.

Example 2.1

Calculate the terminal settling velocity for 1μm and 0.1μm diameter particles of quartz (sp. gr. = 2.6) in air.

Density of particle $\rho = 2600$ kg m^{-3}.

For both the particle sizes, particle diameter

$$D < \frac{1.141\times10^{-3}}{\rho^{\frac{1}{3}}}$$

Hence Stokes' law is applicable.

For 1μm particles, terminal velocity

$v_s = 3.03\times10^4\times2600\times10^{-12} = 78.78\times10^{-6}$ m s^{-1}.

For 0.1μm particles however, Cunningham's correction will be necessary. For this size of particles

$v_s = 3.03\times10^4\times2600\times10^{-14} = 0.79\times10^{-6}$ m s^{-1}.

$v_c = v_s\,(1+1.7\, l/D) = 0.79\times10^{-6}\,(1+1.7\times10^{-7}/10^{-7})$

$= 2.13\times10^{-6}$ m s^{-1}, taking mean free path of gas molecules,

$l = 10^{-7}$ m.

2.7.2 Brownian Motion

Owing to their small mass, submicroscopic particles (below 1μm in size) are imparted a random motion by gas molecules bombarding on them. The amount of displacement x in time t is given by Einstein as follows :

$$x = \sqrt{\frac{RT}{N}\cdot\frac{2t}{3\pi\mu D}}\times10^{9}\mu\text{m} \tag{2.13}$$

where R = universal gas constant = 8314.4 J kmol^{-1} K^{-1},
T = temperature in K,
N = number of gas molecules in 1 kmol = 6.06×10^{26},
μ = viscosity of gas = 1.8×10^{-5} Pas for air at ordinary temperatures,
and D = diameter of particle in μm.

For very fine particles obeying Cunningham's law, eqn 2.13 can be modified to

$$x = \sqrt{\frac{RT}{N}\cdot\frac{2t}{3\pi\mu D}\left(1+1.7\frac{l}{D}\right)}\times10^{9}\mu\text{m} \tag{2.13a}$$

Scanned with CamScanner

Table 2.2[43] gives the displacement of spherical silica particles of various sizes by Brownian motion as compared to gravitational settling. It will be noted that as the particle size increases, the effect of Brownian motion becomes negligible as compared to gravitational settling.

Table 2.2 : Effect of Size on the Relative Displacement of Fine Particles of Silica due to Gravitational Settling and Brownian Motion

Diameter of particles in μm	Distance fallen in 1 second in μm	Brownian displacement in 1 second in μm
0.1	2.1	36.3
0.2	5.7	21.1
0.4	17.4	13.1
0.6	35.1	10.1
0.8	59.1	8.5
1.0	88.0	7.5
1.5	189.0	5.9
2.0	327.0	5.1
2.5	500.0	4.6
3.0	720.0	4.1
4.0	1250.0	3.5
5.0	1940.0	3.1

2.8 SAMPLING OF AIR-BORNE DUST

We have seen that air-borne dust is of considerable danger to the health of miners. In order to effect suitable preventive and suppressive measures for allaying dust in a mine it is essential to have a suitable device to estimate or sample air-borne dust likely to be breathed by miners. The following facts must be considered in the choice of a sampling instrument :

(a) Whether the parameter of dust assessed is a true measure of the danger to health. This necessitates that the sample should be able to give a knowledge of the necessary dust concentration in the dangerous size range. Mass concentration of the respirable fraction of dust is widely accepted today as the relevant concentration. However, in the absence of an agreed international standard on MAC values and sampling instruments as well as in view of the not too conclusive correlation between different dust parameters and incidence of pneumokoniosis uniformly applicable to all types of dusts established yet, particle concentration with particle-size-frequency distribution and surface-area concentration still continue to be assessed. Also, the sample should be able to give an assessment of the dangerous component of dust as regards composition. This necessitates adequate volume of sample to be collected for chemical and mineralogical analysis.

(b) The duration of sampling should be such as to give a true picture of dustiness of any mining operation or place of work without necessitating a large number of samples to be taken. The present trend is to obtain a continuous sample over at least a working shift.

(c) The sample should be representative of the dust cloud in the breathing zone of the worker.

(d) The sampling instrument should be easily portable and robust for rugged underground conditions and should require minimum maintenance ; it should be operated with minimum skill ; it should have self-contained power supply and should render the measurement of dust in as little time as possible without involving too much accessory work.

In this connection it should be noted that whereas more precise and accurate instruments for dust sampling are essential for laboratory and research work, for routine dust analysis a balance must be struck between accuracy on one hand and cost, skill in operation, quickness and easy manipulation on the other.

2.9 DURATION AND INTERVAL OF SAMPLING

Dust production in any mining operation varies a great deal with time and the variation is greatly irregular due to irregularities in normal cycles of operation. Hence the time and duration of sampling should be very carefully chosen to give a fairly accurate estimation of the dustiness of any particular operation over a long period. A true estimate can however be obtained by a continuous

Scanned with CamScanner

sampling device working over the whole shift or even over several shifts. From this a true shift mean or, in general terms, a true period mean can be obtained. A mean close to the true period mean can be obtained by taking a large number of short-duration samples over the period, the deviation approaching zero as the number approaches infinity ; but it is impracticable.

Snap samples or samples taken over a short duration are liable to deviate a great deal from the true average at a source of dust production owing to large variations in the rate of dust production at the source and to get a close approximation to the true mean, a fantastically large number of samples will be necessary. Kitto and Beadle,[44] advocating a new form of thermal precipitator, give the following figures (Table 2.3) for the performance of a thermal precipitator for different durations of sampling as compared to one sampling continuously over a period of two hours.

Table 2.3 : Performance of a Thermal Precipitator for Different Durations of Sampling

Duration of sampling in minutes	5	10	15	20	30	40	60
Percentage standard deviation	35.5	28.4	29.7	25.7	21.6	22.7	4.4

They suggest that a sampling period of ten minutes will reasonably represent the true mean with the result falling within 20% of the average in two out of three cases.

2.10 POSITION OF SAMPLING

Because of the intermittent dust production in any mining operation and the irregular nature of air movement governing the dust distribution at the face, it is very hard to select the correct part of the face where a true representative sample can be obtained.

Dawes, Maguire and Tye[45] show that there is a great variation in samples taken at different sections of the working face near the source of production of dust. The variation, however, gets gradually attenuated as the sampling points are receded farther along the return airway. This is due to the longitudinal and lateral mixing of the dust in the air-stream. If the Reynolds number characterizing the air-flow is well above the critical number, which is generally the case with any mine-ventilation system, complete mixing takes place at a distance of five to ten roadway diameters. Thus it is possible to get a more average dust sample beyond the mixing zone than near the source. Any temporary variation in dust production at the source tends to be attenuated with increasing distance from the source. Due regard of course is to be paid to any admixing with dust from other sources. With velocities prevalent in mine airways, gravitational settling of dust is slow, particularly so for the pathogenic size of $<5\mu m$ and it is possible to get a representative sample at a distance of 6-15m away from the face.

While considering the positioning of sampling points, it must be borne in mind that the uniformity of distribution of dust in an air-stream is dependent on the uniformity of flow in the airway and in order to get a representative sample, it is necessary to collect the sample in a straight portion of the airway at least ten diameters away from any bend or major obstruction.

Another factor which should be borne in mind when collecting a sample of dust from air is that the sampling velocity should be, as far as practicable, equal and equidirectional to the velocity of air from which the sample is being collected. This is essential for minimizing the loss of particles by inertial separation before entry into the sampler.

The best sample having direct relevance to health hazard is one collected at the breathing point of the worker. This has led to the development of personal dust samplers which collect a sample of the respirable dust fraction over a sufficiently long period, usually a shift.

2.11 METHODS OF SAMPLING

Based on the principle of operation, the present-day air-borne dust sampling methods can be classed as follows : (a) filtration, (b) sedimentation, (c) inertial precipitation, (d) thermal precipitation, (e) electrical precipitation and (f) optical methods based on light scattering.

Scanned with CamScanner

2.11.1 Filtration

Filtration has been the earliest method of sampling. Sugartubes were used on the Witwatersrand till 1919 when they were replaced by konimeters. Sugartubes had only 87% filtration efficiency by weight for silica dust and a fair amount of fine dust of the respirable size range escaped collection. Other soluble filtering media like potassium nitrate, salycilic acid[14] etc. were tried to improve filtration efficiency. Early nonsoluble filters tried were of cotton wool, flannel etc., but today synthetic membrane filters having pore size down to 0.01μm have been developed. Paper thimbles are claimed to have 98% filtration efficiency.

Earlier, filtration method was primarily used to collect large samples of the order of 50mg or more for chemico-mineralogical analysis. Mass concentration could be determined by differential weighing of the filter before and after collection of the sample, but this concentration was of little value since it covered the entire particle size range, i.e. inclusive of all the particles above the respirable size range. Attempts have been made to obtain the mass concentration in the respirable size range from dust samples collected on soluble filters, by dissolving the filters and separating the -5μm particles by sedimentation. However, this does not give a true picture of the mass concentration of the respirable fraction in the air-borne dust since the aggregates present in the air-borne dust cloud which are normally treated as single particles of the aggregate size in the respiratory system, invariably break up in the process of solution and separation so that an overestimation of the mass concentration of the respirable fraction is obtained.

Particle concentration and size distribution have been determined by spreading a certain amount of dust collected on the filter on a glass slide in a solution of Canada balsam in xylol (the dust gets fixed in Canada balsam when the xylol evaporates) and examining it under a microscope. But proper dispersal of dust on a microscope slide by this method is difficult and errors creep in due to both small particles flocculating and aggregates breaking up.

Instruments based on the principle of filtration include the Soxhlet and Gothe filters which use paper thimbles, the Siter filter using a synthetic membrane filter and the microsorban filter using a low-resistance soluble filter. Air is drawn through the first two by a compressed-air-operated ejector, a uniform flow rate being maintained by the use of an orifice or nozzle, so that the total volume

of air sampled can be calculated from the sampling duration. The third, which has a low-resistance filter, is run by a high-volume electrically operated blower with a flow meter.

Filtration has become important in recent times owing to the adoption of the mass concentration of the respirable size fraction as the relevant dust parameter signifying hazard. The sampling instruments commonly known as gravimetric dust samplers use an elutriator of gravitational-settling or cyclone type which separates out dust particles above respirable size range and the respirable size fraction is collected on a membrane or glass-fibre-paper filter in a suitable holder. The filter can be weighed before and after sampling to get the mass of dust collected. Today matched-weight filters are available which obviate double weighing.

Gravimetric dust samplers. These are of two main types: (a) those using a gravitational-settling type of elutriator and those using cyclones for elutriation. The MRE dust sampler (type 113A) and the S.F.I-Drager sampler belong to the former type while the SIMPEDS (Safety in Mines Personal Dust Sampler) and SIMQUADS (Safety in Mines Quarry Dust Sampler) in U.K., BAT-I in Germany and the American gravimetric dust samplers, belong to the latter type. While the former are relatively bulky and serve as good long-duration fixed-point dust samplers, the latter are usually light (except for BAT-I) and can be mounted on a miner's safety helmet or clipped to his coat lapel so as to be near his breathing point. That is why they are generally chosen for personal dust samplers.

The British gravimetric dust samplers with both gravitational-settling and cyclone type of elutriators are claimed to give a dust separation curve closely matching the one recommended by the Johannesburg Conference (curve C in Fig. 2.2). The S.F.I-Drager sampler gives a curve (curve B in Fig. 2.2) which differs only slightly from the above. But the BAT-I sampler as also the American samplers give a different separation curve as indicated by curve A in Fig. 2.2. However, this curve is closer to the alveolar dust retention curve (see Fig. 2.1).

MRE 113A sampler. This is the type of instrument recommended for use in Indian mines. Manufactured by Casella, England, this sampler (Fig. 2.5) is a fixed-point instrument comprising a horizontal elutriator (1) provided with a slotted resistor plate (2) to minimize the effects of cross air-flow at the front end. At the rear end,

Scanned with CamScanner

the elutriator is connected to a filter holder (4) which in turn, is connected to the diaphragm pump (5) driven by a DC motor (8) through gears and crank (7). The pump draws in mine air through the elutriator and then through the filter and discharges it to the atmosphere through a flow smoothener and a flow meter which indicates if the correct flow rate is maintained. A counter geared to the pump records the total flow in litres and can be reset to zero after every reading. The motor is supplied from a 900-mAh capacity nickel-cadmium rechargeable battery through an intrinsically safe circuit. The current consumption is 65mA so that the instrument can be safely worked for a twelve-hour period. The instrument made of stainless steel is 230 × 120 × 175mm in size and weighs 4.1 kg.

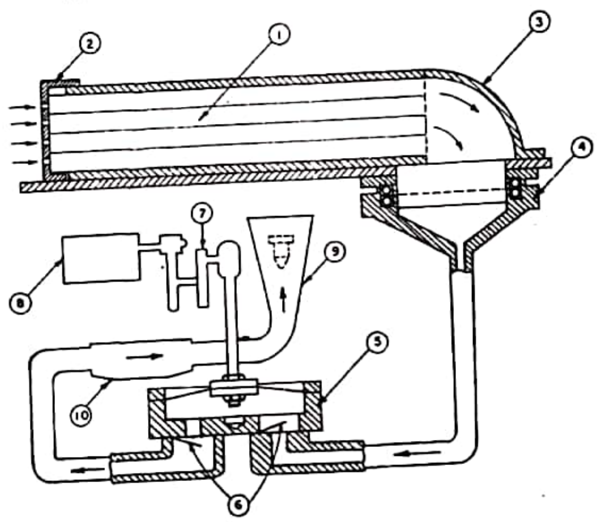

1. HORIZONTAL ELUTRIATOR
2. SLOTTED RESISTOR PLATE
3. TRANSFER HOOD
4. FILTER HOLDER
5. DIAPHRAGM PUMP
6. FLAP VALVES
7. ADJUSTABLE CRANK
8. ELECTRIC MOTOR
9. FLOW METER
10. SMOOTHENING DEVICE

Fig. 2.5 Gravimetric dust sampler-type MRE 113A.

The instrument is normally provided with a four-channel elutriator which performs according to the recommended separation curve C in Fig. 2.2. Provision is also there for fitting it with an eight-channel elutriator which separates out all particles of $<5\mu m$ equivalent diameter. Fiftyfive-mm diameter filters of either glass-fibre paper (Whatman type GF/A) or constant-weight membrane filters (German MF 500) mounted in reloadable stainless steel holders are used for collecting samples. The pump is normally set to have an aspiration rate of 2.5×10^{-3} m^3 min^{-1} $\pm$ 4%. The instrument is claimed to give highly repeatable readings with a standard deviation of 8%.

Simpeds 70 Mk 2 and Simquads. These are personal dust samplers operating on the same principle and using cyclone elutriators. While the elutriator-filter unit of Simpeds is mounted on the miner's helmet by the side of the lamp, that of Simquads is usually clipped to the jacket lapel of the miner. Also the pump in Simpeds is mounted on the cap lamp battery which supplies power to it. The pump unit of the Simquads on the other hand is mounted on a three-cell nickel-cadmium battery which can be strapped on to the belt of the miner

The instrument essentially consists of a small (80 × 45 × 45mm) cyclone-filter unit through which air is drawn at the rate of 1.9×10^{-3} m^3 min^{-1} by a diaphragm pump through a suitable damper (for smoothening pulsating flow) and a flow indicator. A figure-counter geared to the pump records the time of operation of the sampler. The filter is cassette mounted for easy handling and is usually an organic membrane filter or a glass-fibre filter of 37mm diameter. The instrument draws a current of 90mA and can easily operate over a shift.

BAT-I. This is a German instrument using a cyclone elutriator. Air is drawn through the sampler by a compressed-air ejector at the rate of 4 m^3 h^{-1}. The flow-rate is monitored by a manometer indicating the pressure drop across the cyclone. The instrument is, however, comparatively bulky and hence used as a fixed-point sampler.

Respirable dust monitor RDM-201. This is a gravimetric sampler developed in the U.S.A. which gives an automatic digital readout of the mass concentration of the respirable dust by a beta-ray absorption technique. The instrument comprises a cyclone elutriator which separates the coarse fraction and a filter which collects the

Scanned with CamScanner

respirable fraction. The mass of dust deposited on the filter per unit area is obtained from the absorption of β-radiations from a carbon-14 source as measured by a Geiger counter.

β-radiation attenuation is governed by the law

$$N/N_o \doteq e^{-\mu \frac{m}{A}}$$

$$\text{Or, } m = \frac{(\ln N_o - \ln N)\, A}{\mu} \qquad (2.14)$$

where N_o and N are the beta counts before and after deposition of dust on the filter, μ is the characteristic absorption coefficient of the β-radiation, m is the mass of dust deposited on the filter and A is the area of the filter. The mass concentration is computed automatically by the instrument by monitoring the flow-rate and the duration of sampling. The beta source ($37 \times 10^5\ s^{-1}$) is harmless and has a large half life of 5700 years.

2.11.2 Sedimentation

Green[50] utilized gravitational settling for estimating the dust content of air. In this method, a certain volume of air is caught in a vertical cylinder and the dust in it is allowed to settle by gravity on to a glass slide placed at the bottom of the cylinder. The slides are then examined under the microscope for determining particle concentration and size. For accurate results, it is essential to control the temperature of the cylinder in order to avoid convectional air movement inside the cylinder. This method has been claimed to give almost 100% efficiency for particles greater than 0.2μm size, but it requires a long time of settling under rigorous laboratory condition. The slotted-duct dust sampler, developed by Boddy[51] is a long-duration sampler based on the principle of sedimentation.

However, the sedimentation method requires tedious microscopic counting and sizing and is subject to personal error.

2.11.3 Inertial Precipitation

Dust sampling instruments using inertial precipitation are based on three principles : impaction, impingement and centrifuging. Konimeter is the most widely used instrument utilizing impaction. The *cascade impactor* developed by May[47] and later modified by Sonkin[48] collects the dust sample in separated size ranges, but has

not been successful owing to the limited size range of particles collected. The midget impinger uses the second principle while the *conifuge* developed by Sawer and Walton[49] is based on the principle of centrifuging. This instrument collects a size-graded spectrum

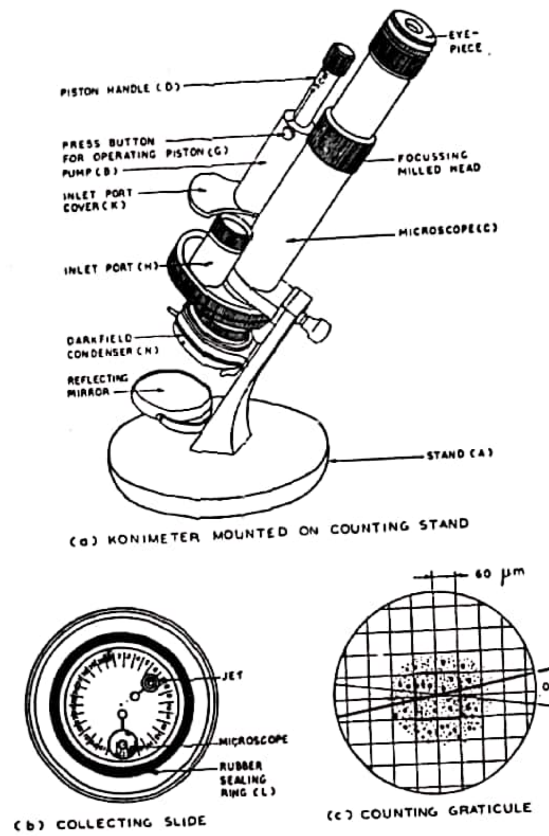

Fig. 2.6 Zeiss konimeter.

of dust, but its high speed of rotation confines it to the laboratory only. A recently developed German gravimetric dust sampler TBF-50 operates on the principle of centrifugal separation and precipitation.

Konimeter. Originally developed by Sir Robert Kotze in 1916, this has been a widely used instrument, for routine dust sampling purposes. It essentially consists of a piston pump by operating which a certain volume of mine air can be made to impinge on a glass slide coated with a suitable dust collecting adhesive. The dust which gets deposited on the slide is counted under a microscope which, in most makes, forms an integral part of the instrument.

Fig. 2.6(a) shows a Zeiss konimeter mounted on a counting stand (A). It consists essentially of the pump (B) and the microscope (C). By pressing the piston handle (D) to the lowest position against the action of the spring (E) (see Fig. 2.7), the piston moves to the bottom of the cylinder and is retained there by the catch (F). The piston is released by pressing the button (G) which releases the catch and thus lets the spring push up the piston to the top position thus sucking in a certain volume of air through the suction port (H). In the Zeiss konimeter, the pump can be set to sample 5cm³, 2.5cm³ or 1cm³ of air by suitably setting the piston handle. Dust-laden mine air enters through the inlet port which is made funnel shaped in order to avoid inertial separation of dust at the entrance. The air impinges on the glass slide (J) (Fig. 2.7) through a tapered jet (I) which has a diameter of 0.5mm and is placed 0.5mm away from the glass slide. When no sampling is done, the inlet port is closed by a cap (K) for protecting it from dust.

The glass slide is coated with a thin layer of an adhesive such as pure white vaseline or petroleum jelly. It is essential to clean the slide first by washing it with warm soapy water and then cleaning with xylol. Sometimes it may be necessary to boil the slide with dilute hydrochloric acid (25% solution) in order to clean it properly. The vaseline can be smeared on the glass by the tip of a finger covered with tissue paper when only a pin-head size drop of vaseline is sufficient. Care is taken to wipe off all excess vaseline by a clean tissue paper. A better way, however, is to dissolve vaseline in xylol or toluene (2g of vaseline dissolved in 100cm³ of xylol gives a suitable solution) and pour the solution on the glass slide. The solvent, on evaporation, leaves a thin coating of vaseline on the glass slide. When the dust-laden air impinges on the slide, the dust gets deposited on the slide due to its inertia while the clean air goes out into the pump cylinder through the annular opening around the jet. The glass slide is held tight against a rubber ring (L) thus making the space between the slide and the jet air-tight. The glass slide [Fig. 2.6 (b)] is divided into 30 divisions (36 in Sartorius konimeter and even 42 in some instruments) which are numbered. By rotating the glass slide, a particular division can be brought under the sampling jet for collection of the sample, thus enabling 30 samples to be collected on the same slide.

After the sample has been collected, it is brought under the microscope by suitably turning the glass slide and the particles are counted. The microscope comprises a 16-mm objective and a 15x eye-piece giving a total magnification of 200. The eye-piece contains a graticule [Fig. 2.6 (c)] where two opposite sectors, each covering $\pi/10$ rad (18°) are marked out. It is sufficient to count the particles in these two sectors and multiply the figure by 10 so as to get the total count with an accuracy of $\pm 12\%$. The narrow space between the close parallel lines in the graticule represents 5μm so that while counting, particles greater than 5μm in size can be left out. Besides, there are parallel lines at right angles to each other and spaced 60μm apart covering the whole graticule in order to get the total count over the whole field of vision, if necessary.

The slide can be counted under light-field or dark-field illumination, a substage condenser (N) with its centre covered being provided for the latter purpose. Dark-field counting shows up more particles (down to 0.2μm size) than light-field counting and hence should be adopted whenever possible.

The Sartorius mining-type konimeter (Fig. 2.7) has an additional feature that it has a bell (O). Before sampling, the instrument is held by the handle (P) and the konimeter, pulled out of the bell by releasing the spring-loaded catches (not shown in the figure) until it slides down and rests on the retaining pins (Q). Then the konimeter is pushed back to the original position with a certain volume of mine air entrapped in the bell. Sixty seconds are allowed for the large particles to settle before the sample is taken. The instrument is thus very suitable for mine air heavily laden with dust, i.e. of the order of 4000-5000 p.p.c.c. (particles per cubic centimetre) which cannot be counted on the ordinary konimeter. Besides, the covers of the pump and glass slide provided in this type make it sturdy. The instrument may or may not be provided with an attached

Scanned with CamScanner

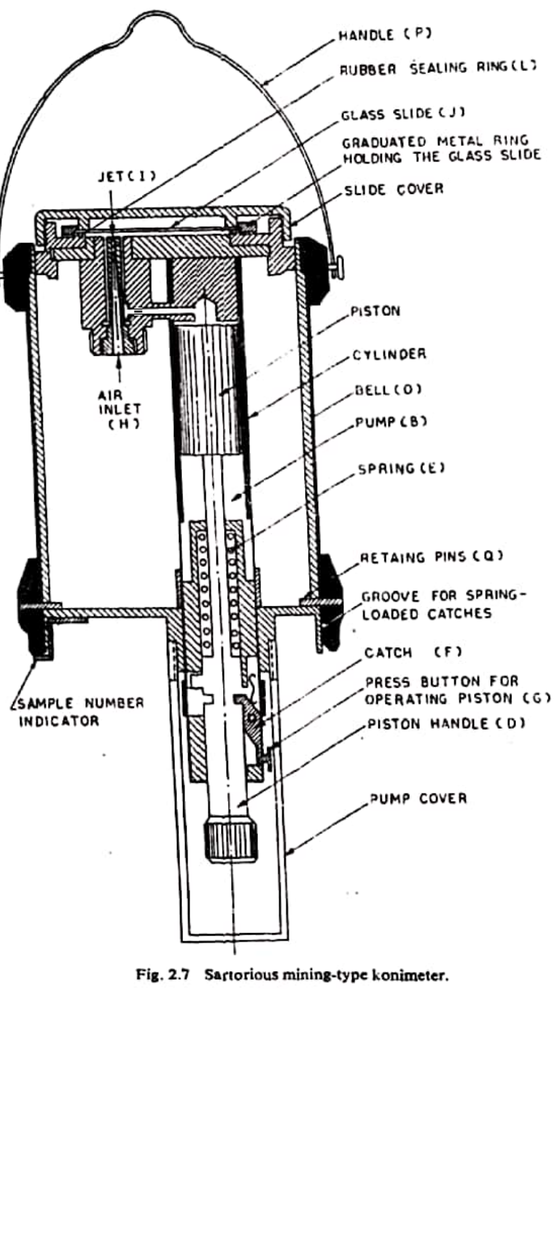

Fig. 2.7 Sartorious mining-type konimeter.

microscope, the slide being examined under an ordinary microscope in the latter case. Separate microscopic examination of the slide becomes preferable where the slide is to be heat and acid treated before counting.

In South African mines where the insoluble silica component of the dust is very important, the konimeter slide is usually incinerated first to remove carbonaceous matter and then immersed in dilute hydrochloric acid to remove soluble particles (usually crystallized from drilling water).

The konimeter is a light, handy instrument requiring no power source and is easy to operate. A large number of samples can be taken at a time and an on-the-spot estimation of the particle concentration obtained with instruments having attached microscopes. The konimeter slide can be heat and acid treated to eliminate carbonaceous and soluble particles, that are not hazardous to health.

But its main defect is that it gives the particle-number concentration and the estimated concentration is relative rather than absolute. Even then no definite sampling efficiency has been established for the konimeter[11] though early workers had found the efficiency varying between 50 and 65%. It is a snap sampling device collecting only $5 cm^3$ of air sample over an extremely short period of one-fourth of a second, so that a large number of samples would be needed to get a reliable value for the shift-average concentration. The high impaction velocity of the order of $100 ms^{-1}$ breaks up aggregates of particles and possibly even large particles, thus overestimating the danger to health. This is clearly established from the fact that a konimeter sample shows three times as many particles below $2 \mu m$ as that collected by a thermal precipitator from the same dusty atmosphere.[42] The sample collected in a konimeter is inadequate for chemical analysis. Besides, microscopic counting is tedious and subject to personal error, though of late attempts have been made to subject konimeter slides to automatic counting. One such device comprises an electronic scanner which comprises a television camera that sends pulses from dust particles to a photomultiplier for amplification and counting. Though the scanner can count very fine particles, a lower limit to the particle size counted has to be set in order to avoid noise pulses showing up as dust particles.

Midget Impinger. This is an instrument commonly used in the U.S.A. It consists of a hand-cranked four-cylinder pump which

Scanned with CamScanner

sucks in air at a vacuum of 3kPa. The vacuum is maintained constant by a suitable spring-loaded valve. The sample is collected in a graduated flat-bottom cylindrical glass flask (Fig. 2.8) which contains a known volume (10-15cm^3) of dust-free water or alcohol. The pump is connected at B and the air to be sampled is drawn in through A which has its bottom end shaped into a suitable nozzle (about 1mm in diameter) so as to pass a quantity of 2.85×10^{-3} m^3 min^{-1}. The impingement velocity is about seventy metres per second.

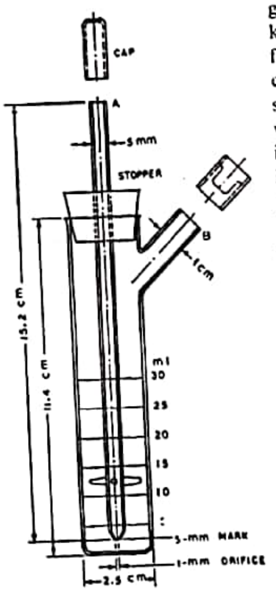

Fig. 2.8 Midget impinger flask.

The dust-laden air from the nozzle impinges on the bottom of the flask and the dust is collected in the collecting fluid. The quantity of air sampled is obtained by noting the time of sampling and the flow-rate of the nozzle. A portion of the dust-laden fluid is filled into a counting cell usually 1mm deep which is then covered with a cover slip. The cell is allowed to stand for about half an hour to allow the dust particles to settle to the bottom of the cell when it is counted under a microscope. The settling time can be reduced using a 0.1mm deep counting cell.

Impinger dust samples are usually counted under light field with a 16-mm objective and 20x eye-piece which show up particles down to 1μm size. Dark-field counting can reveal particles down to 0.1μm size but it is not desirable to use dark-field counting since the collecting efficiency of the impinger falls rapidly for particles below 1μm size and there is usually a much larger number of fine particles produced than originally present in the sample due to the breaking up of aggregates by impingement. Usually a microprojector giving an ultimate magnification of 1000 is used for making the microscopic counting easy.

Recently the U.S. Bureau of Mines have successfully used an automatic electronic counter, the *Coulter Counter* to obviate microscopic counting. The counter gives the total count as well as a size analysis of the particles. The midget impinger sample comprising dust particles suspended in an electrolyte is made to pass through an aperture. When a dust particle passes through the aperture it displaces a part of the electrolyte thus changing its conductivity. The change in resistance produces an electric pulse proportional to the volume of electrolyte displaced. The pulses are sorted to twelve different size ranges by a discriminating circuit. With a 3μm aperture, particles down to 0.6μm equivalent spherical diameter can be counted at a very high speed.

The midget impinger, though not as handy as the konimeter, collects a more representative sample over a longer duration of ten minutes to three hours depending on the dust concentration in the air. However, it has a low collecting efficiency of the order of 40%. It also causes breaking up of aggregates by impingement.

TBF-50. The TBF-50 inertial gravimetric dust sampler, recently developed in Germany, comprises two cyclones, the first one separating the coarse fraction of dust which is normally removed in the upper respiratory tract. The second cyclone is claimed to collect dust particles of size normally getting deposited in the lung, while the finest fraction escaping collection in the second cyclone simulates the fine particles that escape deposition in the lung and are thrown out with the exhaled air.

The instrument aspirates air at the rate of 0.05m^3 min^{-1} by a Ni-Cd-battery-powered electric blower or a compressed-air ejector. The dust collected in the cyclones is washed and filtered on a previously weighed membrane filter for determination of mass concentration.

2.11.4 Thermal Precipitation

This method utilizes the principle that when a body surrounded by dusty air is heated, a dust-free zone is produced around the hot body, the extent of the dust-free zone depending on the temperature gradient between the hot body and the surrounding air. If such a zone (Fig. 2.9) is intercepted by two glass cover slips and a current of dusty air allowed to enter the space between them in the direction shown, the dust in the air gets deposited on the cover slips at the points A and A' where it remains attached by molecular attraction.

Scanned with CamScanner

The velocity of thermal precipitation for microscopic particles with relatively small temperature gradients is given by Davies[42] as follows :

$$v = \frac{3.6\times10^{-6}}{T}\cdot\frac{dT}{dx} \tag{2.15}$$

where v = precipitation velocity in m s^{-1},
T = temperature in K
and dT/dx = temperature gradient in K m^{-1}.

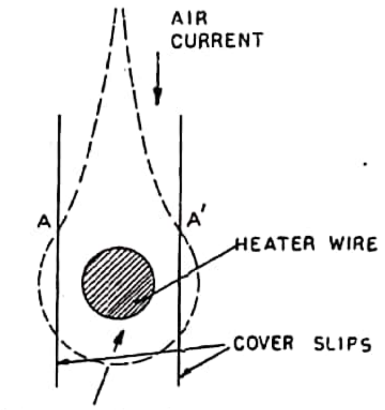

Fig. 2.9 Dust-free space around a hot body.

Though the phenomenon of thermal precipitation was discovered by Aitken and first utilized by Whytlaw-Gray and Lomax, it was Green and Watson who designed the thermal precipitator in its present form in 1935. The thermal precipitator is claimed to have 100% efficiency in collecting all dust particles below 5μm size which are indeed the particles dangerous to health.

The instrument consists essentially of a precipitator head (Fig. 2.10) which comprises a nichrome wire, heated electrically to a temperature of about 373K by current from a 2-V cap-lamp battery. The temperature of the wire is maintained constant by keeping the heating current constant (normally at 1.2A) by adjusting a variable

resistance put in series with the heater wire. An ammeter indicates the heating current. The heater wire is held between the brass blocks of the precipitator head, separated from them by two thin insulating strips on either side. The strips also serve as spacers between the wire and the thin glass cover slips which are inserted into the cylindrical openings in the precipitator head on either side of the wire and are held in position by two cylindrical brass plugs. The brass plugs also serve in conducting away the heat from the glass cover slips, thus maintaining a constant thermal gradient. A thermal gradient of the order of 400×10^{3} Km^{-1} is obtained.

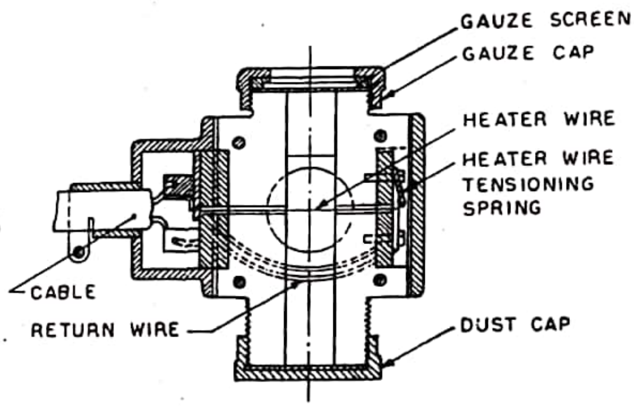

Fig. 2.10 Thermal-precipitator head.

The precipitator head is normally screwed on the top of a water aspirator consisting of a flat water tank of 300cm^3 capacity which has a discharge nozzle at the bottom fitted with a tap. The nozzle is designed to allow a rate of flow of 7cm^3 min^{-1} which creates a sampling velocity of 1.4 m min^{-1} through the sampling slot of 0.51 × 9.5-mm cross-section. The tank in recent designs is made of a small height and large cross-sectional area in order to minimize the variation in the head of water causing flow and hence the rate of flow. The rate of flow should not be too fast as such an air velocity imparts a high momentum to the dust particles which may penetrate the dust-free zone and thus escape precipitation. Too low a rate of

Scanned with CamScanner

flow, on the other hand, causes an unnecessary increase in the sampling time. Usually the rate of flow does not fall below 6.5cm³ min⁻¹. On opening the tap, water from the tank runs out and fills the 100cm³ measuring cylinder at the bottom (Fig. 2.11). At the same time air to be sampled is drawn into the tank through the precipitator head where all the dust is precipitated. The volume of air sampled is given by the volume of water collected in the measuring cylinder. Normally the air inlet into the precipitator head is covered with a wire gauze for preventing very large particles of dust entering the precipitator head. The whole instrument is provided with a suitable light carrying box and when sampling, it can

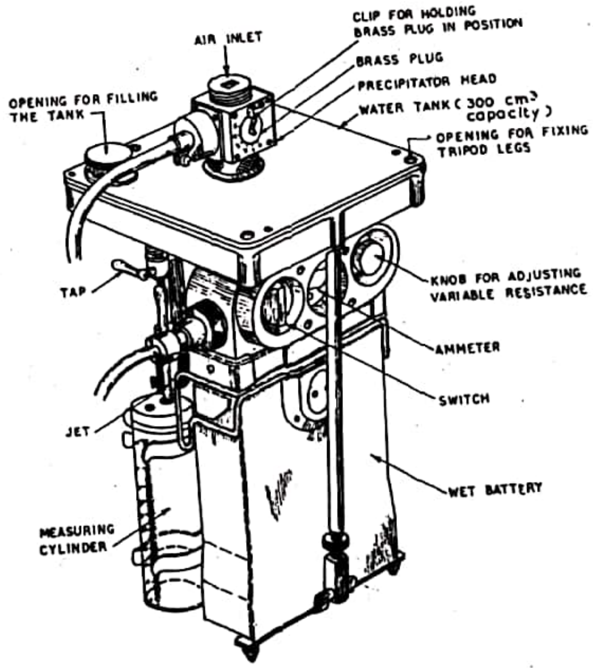

Fig. 2.11 Thermal precipitator.

be taken out of the box and mounted on a tripod stand or slung from chains. When taking a sample, the wire is first heated for two minutes, before the aspirator tap is opened. The duration of sampling depends on the dust concentration. For high concentrations, it may be only ten minutes while for low concentrations, it may be as high as thirty minutes.

After the sample has been collected on the cover slips, the latter are mounted on a 75×25mm microscope slide and waxed to it so that the dust is enclosed between the two glass surfaces. The slide is then counted under a high-power microscope using a 2-mm oil-immersion objective and a 12x occular so as to get a magnification of 1000. Counting is done with the help of a suitably calibrated graticule introduced in the eye-piece. The number of particles within the area of the graticule is counted. Several spots uniformly distributed along the length and breadth of the dust strip are counted for getting a representative value. The particle concentration is obtained by using the following relation :

$$c = \frac{2NLB}{AV} \tag{2.16}$$

c = concentration in p.p.c.c.,
N = total number of particles counted,
L = length of the dust strip on the cover slip in mm,
B = breadth of the dust strip on the cover slip in mm,
A = total area in mm² over which counting has been done
= area of the graticule × no. of spots counted
and V = volume of sample collected in cm³.

It is necessary to count both the cover slips, though a total count of 200 particles is sufficient for reasonable accuracy.

Size analysis is best done with the help of a *Patterson and Cawood graticule* (Fig. 2.12) where several circles of different diameters are marked alongside the graticule. These circles should be calibrated for the magnification used with the help of a stage micrometer. The dust particles are visually matched with these circles so that the projected surface area of a particle, as observed under the microscope, equals that of the circle. The diameter of the circle then gives the diameter of the particle. This diameter, as against the statistical diameter which is measured as the dimension of a particle in a fixed direction, say, along the horizontal

Scanned with CamScanner

cross-hair, is a more useful parameter since it corresponds to the effective diameter as obtained from the rate of settling according to Stokes' law.

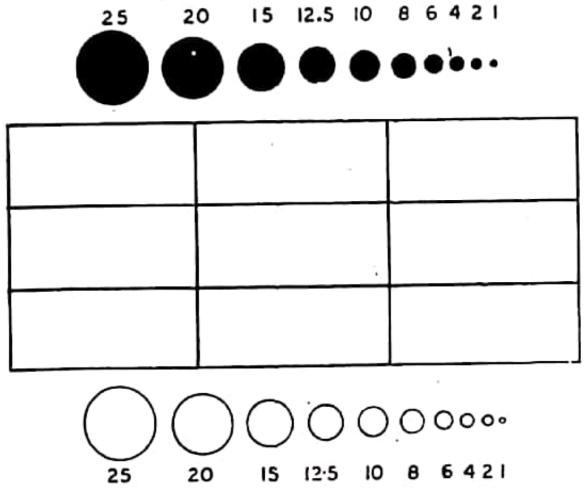

Fig. 2.12 Patterson and Cawood graticule.

The thermal precipitator has a high collection efficiency. The low velocity of sampling does not break up aggregates and a fairly representative sample over a reasonably long duration is obtained. Precipitator heads with rotatable plugs which can collect six samples on a pair of coverslips have been developed. Of late, thermal precipitators have been designed for sampling over a shift or even twenty-four hours.[52] Dust slides can be incinerated and acid-treated if necessary. However, microscopic counting of the dust particles is tedious and subject to personal error.

Automatic electronic devices have been developed for counting and sizing of dust samples collected by the thermal precipitator. A diffraction size-frequency analyser developed in South Africa has been claimed to give an accurate measure of the size distribution of the dust sample as well as the respirable surface area of the dust. An opaque film of aluminium is deposited on the thermal precipitator slide by volatilizing the metal from a hot filament in vacuo. On washing the slide with a detergent solution, the dust particles are removed leaving their replica on the slide. The diffraction pattern formed by the apertures is printed out on a digital recorder at the rate of one sample per second. A size-frequency analysis is obtained by incorporating wave-vector filters in the optical system. Beadle[53] developed a photoelectric apparatus which gives an estimation of the surface-area concentration of the dust particles. The apparatus measures the amount of light extinguished by the dust strip on the thermal precipitator slide which is related to the projected surface area of the particles. However, the concentration so determined is dependent on the degree of polydispersity of the dust sample.

For dusts whose pathogenic effect is determined by the particle surface area, the thermal precipitator in conjunction with an automatic electronic size frequency and surface-area analyser offers a very accurate sampling instrument, though its size and cost may limit its use to research laboratories only.

2.11.5 Electrical Precipitation

This utilizes the well-known principle of electrical precipitation which is described later. The electrical precipitator essentially consists of a charging wire maintained at a high negative potential of about 12000 volts and surrounded by an earthed concentric cylinder. Dust-laden air is drawn through the cylinder by a fan at a constant rate. The dust particles when passing through the instrument, get charged and are drawn to and precipitated on the inner surface of the earthed cylinder.

This instrument, like the filtration devices, has a large sampling capacity and is suitable for collecting large quantities of dust for chemical analysis. The mass concentration can also be determined by noting the difference in weight of the cylinder before and after collection of dust. The instrument has a high collecting efficiency, but the high voltage used in it makes it unsuitable for use in coal mines where filters are preferred.

Gravimetric dust samplers utilizing electrical precipitators have been developed where the coarse fraction of the air-borne dust is first removed in a cyclone separator and the respirable fraction is collected in the electrical precipitator for estimation of mass concentration by differential weighing.

2.11.6 Optical Method

This method utilizes the property of scattering of light by a suspension of fine particles. For particles large enough compared to the wave length of light, i.e. particles above 1μm in diameter, the intensity of scattered light is roughly given by the relation

$$\frac{I_s}{I_0} = KND^2 \tag{2.17}$$

where I_s = intensity of scattered light,
I_0 = intensity of incident light,
N = number of particles per unit volume,
D = diameter of particles

and K = constant depending on the refractive index, absorption coefficient and shape of the particles as well as the wave length of light, angle of scattering and the distance of the point of observation from the dust cloud. For particles smaller than the wave length of light, Rayleigh's law that $I_s \propto D^6$ holds good. However, in polydisperse dust clouds in mines, the intensity of light scattered by the large particles is so high compared to that by fine particles that the law of scattering as given in equation 2.17 can be easily adopted for such clouds. The equation shows that the intensity of scattered light is proportional to the surface area of the particles, a fact well borne out in practice.

Tyndalloscope. The first instrument based on this principle was the Tyndall meter designed by Tolman and Vliet in 191[illegible] where the intensity of light scattered at right angles to the incident beam was measured. Today the Tyndalloscope (Fig. 2.13) is very commonly used in German coal mines for routine dust sampling purposes. The instrument consists of a chamber open to the dusty atmosphere. A part of a collimated beam of light from a lamp is allowed to pass through the dust cloud while the other part passes through a filter consisting of a polariser and a rotatable analyser. The light scattered by the dust cloud at an angle of 0.524 rad (30°) to the direction of incidence is observed on one half of the field of an eye-piece, the other half showing the part of the beam passing

through the filter. The analyser is rotated until the intensity of light on both the halves of the eye-piece is equalized. The intensity of scattered light and hence the dust concentration is then directly

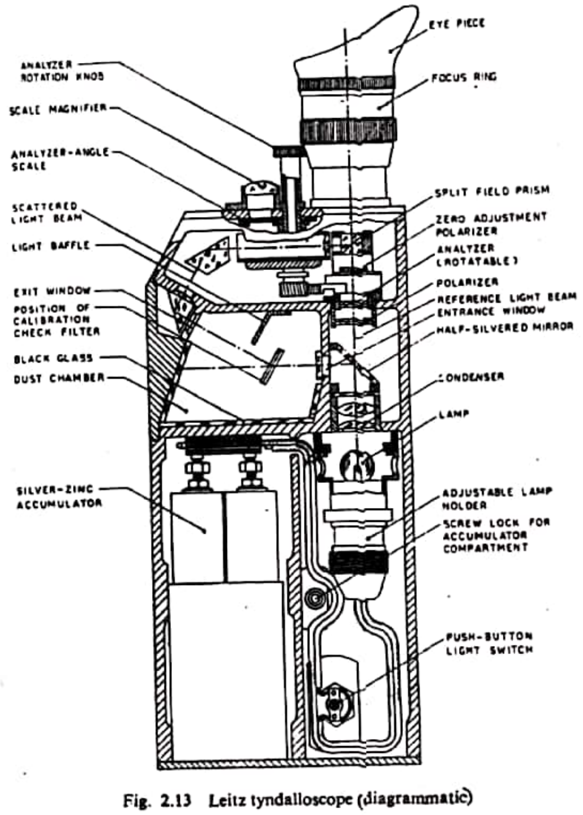

Fig. 2.13 Leitz tyndalloscope (diagrammatic)

proportional to $\sin^2\alpha$ where α is the angle through which the analyser is rotated.

The Tyndalloscope has been widely used in the German mines chiefly because of its cheapness as well as quickness and ease of operation. Besides, it gives an estimate of the dust level in terms of surface-area concentration. But it has certain substantial drawbacks. The law of proportionality between the dust concentration and the intensity of scattered light depends on many variable factors such as refractive index, absorption coefficient and shape of the particles. Besides, the degree of polydispersity or the size distribution of particles in the dust cloud affects the intensity of scattered light to a large extent, so much so, that it is necessary to draw separate calibration curves, not only for dusts of different nature but also for dusts with various degrees of polydispersity as may be produced in different types of mining operation. This is well exemplified in Table 2.4[43] which gives the concentration and degree of polydispersity of dust produced by various mining operations on the Witwatersrand.

Table 2.4 : Degree of Polydispersity of Various Types of Dust

Size of particles in μm	Ore bin dust		Blasting dust		Drilling dust	
	Concentration (p.p.c.c.)	%	Concentration (p.p.c.c.)	%	Concentration (p.p.c.c.)	%
<0.2	182	8.0	13 020	11.9	1 266	53.6
0.2	315	13.8	19 140	17.5	483	20.3
0.4	285	12.6	17 170	15.7	234	
0.8	262	11.5	13 240	12.1	111	4.7
1.2	225	9.9	9 080	8.3	61	2.6
1.6	214	9.4	6 460	5.9	47	2.0
2.0	164	7.2	7 110	6.9	54	2.3
2.5	141	6.2	6 560	6.5	35	1.5
3.0	134	5.9	6 460	5.9	28	1.2
4.0	146	4.6	5 690	5.2	28	1.2
⩾5.0	207	9.1	5 470	5.0	14	0.6

Again, the amount of light scattered is considerably increased by the presence of other particles in the atmosphere such as fine droplets of water or particles of salt resulting from their evaporation, fine droplets of oil from pneumatic machines and other fumes and smoke which are not uncommon in mines. It is for these reasons that Tyndalloscope readings have to be used in conjunction with another dust sampling instrument such as the konimeter to get an estimate of the dust level.

Recently dust monitoring Tyndallometers giving an automatic record of respirable dust concentration have been developed, but they are still subject to errors due to variations in the nature and degree of polydispersity of dust.

Simslin (*Safety in Mines Scattered Light Instrument*). This is a British instrument using the Tyndall effect. It (Fig. 2.14) comprises a collimated beam of near-infra-red light passing through a dust chamber. The direct beam is shielded while the light scattered over a cone angle of 0.698 rad (40°) is measured by a photomultiplier tube which feeds a chart recorder. Dusty air is drawn through the instrument at the rate of 1.5×10^{-3} m^3 min^{-1} through a single-duct elutriator to remove the coarse fraction of dust so that the instrument gives a measure of the dust concentration over the respirable size range. However, it is subject to the same errors as the recording Tyndallometer.

The Royco Particle Counter.[55] This is a unique instrument using the light scattering property of dust to get the particle-number concentration as well as the size distribution. A stream of dusty air

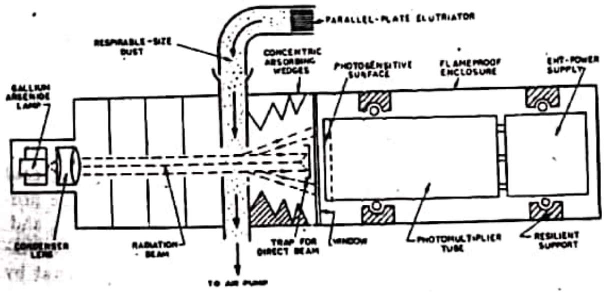

Fig. 2.14 Simslin dust sampler (optical principle).

is drawn through the instrument by a vacuum pump at a rate which can be varied from 0.28×10^{-3} to 2.8×10^{-3} m^3 min^{-1}. The light scattered by the air-borne dust particles at $\pi/2$ rad to the incident beam is directed through an optical system to a photomultiplier tube which emits a train of pulses. The amplitude of the pulse is proportional to the projected surface area of the particle and the number of pulses corresponds to the number of particles. The pulses are fed to an amplifier and height discriminator for size analysis and the results are reported on a digital meter or strip-chart recorder. Particle sizes between 0.3 and 10μm can be recorded by the instrument.

Holographic System. A different optical system which has been developed for counting and size analysis of a suspended cloud of aerosols consists of a pulsed ruby laser illuminating the particles. The light diffracted from the cloud forms ring-like wave interference patterns on a photographic film which gives a permanent record of these patterns called the 'hologram'. A three-dimensional image of the dust cloud is then reconstructed from the hologram by another laser beam. This can be magnified 300 times by a Vidicon camera tube and television monitor. Individual particles can be focused and displayed on a screen for visual analysis. However, the existing instruments are capable of recording particles above 3μm size only and hence are not suitable for mine-dust analysis.

2.12 PREVENTION AND SUPPRESSION OF DUST

Successful dealing with dust in mines in order to keep its concentration in the mine air below the dangerous limit consists of (a) prevention of the production of dust, (b) prevention of the dust, already formed, getting air-borne and (c) dilution and suppression of the air-borne dust.

2.13 PREVENTION OF THE FORMATION OF DUST

Dust is mainly produced by mining operations like drilling, coal cutting and blasting, though a small amount of dust may be produced by the crushing of mineral during free fall at chutes and transfer points. Crushing of coal pillars by rock pressure is an important source of dust production. Size reduction of mineral by crushing produces a considerable amount of dust.

Production of fine dust during drilling can be minimized by using sharp bits so that there is more of chipping than of grinding action. Sufficient thrust on the bit and suitable arrangement for the clearance of cuttings from the hole help in reducing dust production. There is no difference in rotary and percussive drilling as regards the quantity of pathogenic dust produced by them. Dust production in rotary drilling is inversely proportional to the rate of penetration, though it varies directly with the speed of rotation. Thus high thrust at a low rotational speed produces the minimum dust. Coal cutting machines should have sharp picks and the chain should always be equipped with the complete set of picks for minimizing dust production. The chain should not run at an excessive speed in comparison with the advance of the machine and arrangement should be made for cleaning the gummings so that they do not recirculate and get crushed.

Dust produced by blasting can be minimized by suitably controlling the pattern of holes and the quantity and strength of the explosive used so that excessive fragmentation is avoided. The number of blastings should be kept down to the minimum and efforts should be made to confine shot-firing to relatively idle periods, such as in between the shifts when only a small number of workers may be exposed to the heavy dust concentration produced by blasting.

Free fall of material at the face, during transport and at transfer points should be reduced as far as practicable. The system of haulage should be designed, installed and used with a view to minimizing spillage. It is a good practice to keep ore bins, chutes etc. always full in order to minimize dust production by free fall of mineral. Crushers, if installed underground, should be so isolated that the dust produced by them does not get into the general mine air. The right method of working with adequate roof-control helps in reducing production of dust by reducing crushing of pillars.

2.14 PREVENTION OF DUST GETTING AIR-BORNE

This involves measures for suppressing the dust at the source of production and removing or consolidating the dust already deposited.

2.14.1 Drilling

Suppression of dust produced by drilling is achieved mainly by adopting wet drilling. Wet drilling has proved very effective in dust suppression. Whereas the dust concentration during dry drilling may be as high as 5000 p.p.c.c. or more, it is brought down to only 200 to 400 p.p.c.c. by the use of wet drilling. For wet drilling to be effective, the pressure of water should be sufficient, but too high a pressure reduces the rate of penetration by cushioning the cutting action and hence should be avoided. A good pressure is about 75 kPa less than the pressure of air (i.e. 400-500 kPa). The amount of water fed into the hole should be at least 3×10^{-3} m^3 min^{-1} for effecting proper dust suppression.

Wet percussive drills commonly used today incorporate an internal water feed arrangement where water is fed at the shank end of the hollow drill steel by means of a water tube passing through the piston of the drill and entering into the drill steel up to a length of about ten millimetres from the shank end. In such drills it is essential that no compressed air gets into the water-stream as this causes the formation of air bubbles. Any dust caught in these air bubbles gets released into the atmosphere when such bubbles break. That is why wet drills are nowadays invariably provided with vent holes in the front head of the drill for releasing the leaking air into the atmosphere. In addition, it is better to provide a rubber nipple at the end of the water tube where it enters the drill steel in order to seal the junction so that no air can enter the drill steel.

Another method of feeding water into the drill steel commonly used in Germany and South Wales, U.K. is through an *external flush-head* provided at the shank end of the drill steel (Fig. 2.15). A portion of the shank near the shoulder is rounded off to fit into the flush-head. There is an annular chamber in the flush-head, sealed on both sides by rubber rings and connected to the water channel in the drill steel by a hole on the side of the steel. Water is fed into the drill steel through this chamber. The advantage of the external flush-head is that it can be used with any type of drill. Special construction of the drill, as in the internal water-feed system, is unnecessary so that simpler, lighter and cheaper drills can be used. Chances of air getting into the water-stream is completely eliminated with the external flush-head.

Nowadays rotary drills have also been fitted with external flush-heads for water flushing through hollow drill steels. However, external flush-heads usually cause a loss of energy varying from

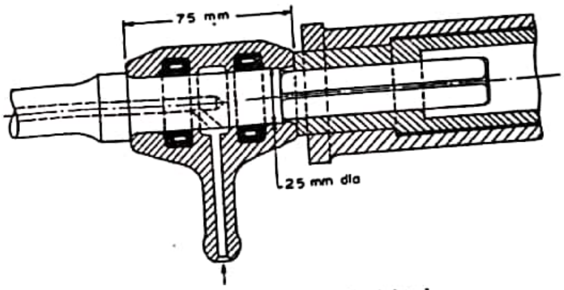

Fig. 2.15 External water flush-head.

5 to 15% due to friction between the shank and the flush-head.

Where water is scarce, foam can be used for suppressing dust. Foam is usually produced by adding a small quantity (usually 1%) of a foaming agent like pyrene to water. Burdekin and Broomhead[64] claim that there is little difference in the effectiveness of water and foam in dust suppression in drilling though foam is costlier.

Wet drilling has been very successful in allaying dust to a safe concentration. Still constant efforts have been made to develop other means of dust suppression with dry drilling because of the following reasons : (a) dry drilling causes less bit wear (bit wear with dry drilling is one-third to half of that due to wet drilling) and has a higher rate of penetration than wet drilling ; (b) wet drilling produces sloppy working conditions, particularly when drilling upward holes as in roof bolting ; (c) in deep and hot mines, wet drilling causes discomfort by increasing the humidity of the mine air ; (d) clayey and shaly beds, when saturated with water from wet drilling, become weak thus having a deleterious effect on roof control.

The early designs of dry extractors consisted essentially of a hood sealing off the mouth of the hole and provided with two holes, one for the passage of the drill steel and the other connected to a suitable exhaust system for cleaning the dust from the hole. The *Kelly dust-trap* commonly used in the U.S.A. in nineteen hundred and thirties consisted of a heavy metal shield connected to an ex-

Scanned with CamScanner

haust system through a settling chamber and a filter. The *Belgian hood* which was quite popular in the U.K. and Europe consists of a tapered steel spiral fitting into the collar of the hole and constrain-ed by it, allowing sufficient clearance at the centre for the move-ment of the drill steel. The spiral has a flexible rubber cowl which forms an air-tight seal against the rock face and the cuttings are drawn away through a rubber hose. The dusty air exhausted from the hole is cleaned by a suitable dust-trap.

The dust-trap usually consists of a compressed-air ejector sucking in air through one or more concentric bag filters. The coarse particles of dust are usually removed by inertial separation before filtration. Fig. 2.16 illustrates a Koningsborn dust extractor. Here, the dust-laden air enters tangentially into a conical hopper below the filters, thus causing centrifugal separation of the coarse particles. The whole trap is made in two parts, the upper part con-taining the ejector and dust separation devices and the lower part, a dust collecting drum which can be sealed and hauled away for disposal of dust. A good practice is to silt the dust in the drum by water before it is disposed of. The efficiency of this dust-trap is about 98% and it consumes about 0.33 cubic metres of air per minute. It has a capacity of 24 metres of drilling.

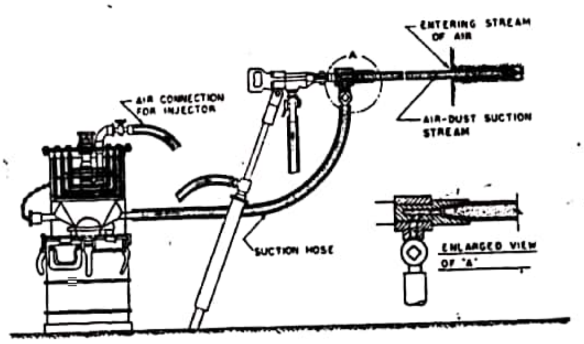

Fig. 2.16 Koningsborn dry dust extractor.

Hoods with dust-traps have, in certain cases, been very efficient in suppressing dust. They are, however, not much used now mainly because of the fact that it is difficult to maintain an air-tight seal

between the hood and the irregular rock face. Besides, hoods can-not be effectively used during collaring. It becomes difficult to maintain the alignment of the hole as the operator cannot see its mouth when using a hood. That is why today most of the dry dust extractors use the principle of extracting the dust from the hole through a hollow drill steel by means of a suitable exhaust system.

The *Holman dryductor drill* uses this principle. Here, a compressed-air ejector (eductor) sucks in the dust from the hole through the drill steel and a duct in the body of the drill. The dust-laden air then passes through a system of cyclones and filters for separating the dust (Fig. 2.17). Alternatively, a dust-trap as des-cribed earlier can be used for extracting the dust. The ejector con-sumes about 1.5 to 2 cubic metres of air per minute at a pressure of 500-600 kPa and produces a vacuum of the order of 25-30 kPa. The dust suppression efficiency of the dryductor is fairly high com-pared to wet drilling at suitable air pressure. In one case,[37] drilling with the dryductor produced a dust concentration of only 200 p.p.c.c. as compared to 750 p.p.c.c. produced by wet drilling with a Holman silver bullet drill under similar conditions. Besides, the dryductor gives a much faster rate of penetration as the cutting face is always maintained clean by the rapid removal of the cuttings. However, drilling with the dryductor is suitable for dry rocks only, since drilling in wet strata causes choking of the hole in the drill steel thereby reducing the dust suppression efficiency.

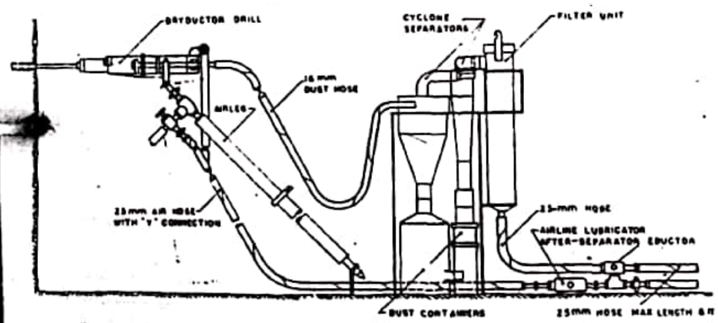

Fig. 2.17 Holman dryductor drill with dust extractor.

Scanned with CamScanner

Another method used in Germany draws the dust from the hole through the hollow drill steel and then through a suction-head ('A' in Fig. 2.16) into a suitable dust-trap. This method can be adopted for any type of drill, percussive, rotary or rotary-percussive, without needing special construction of the drill. There are, however, chances of the suction passage getting choked by dust separating out from the air-stream when the latter takes a sharp turn at the suction-head.

With both dry and wet drilling, it is necessary to make the dust suppression measures foolproof by suitably interlocking the air supply to the drill with the dust suppression measure. Thus in a wet drill the air cannot be turned on without turning on the water and in dry drilling, no drilling can progress without ensuring the necessary suction.

Example 2.2

A wet drill drilling at a drift face produces a dust concentration of 400 p.p.c.c. in the respirable size range while the dust concentration rises to 700 p.p.c.c. if the drilling is done dry. Calculate the amount of dust of respirable size produced per minute in either case if the drift face is ventilated by a tube delivering $2.5 m^3 s^{-1}$ of fresh air. Also calculate the efficiency of dust suppression by wet drilling.

With wet drilling, the dust produced per minute

$$= 400 \times 10^6 \times 2.5 \times 60 = 6 \times 10^{10} \text{ particles.}$$

Dust produced per minute with dry drilling

$$= 700 \times 10^6 \times 2.5 \times 60 = 10.5 \times 10^{10} \text{ particles.}$$

$\therefore$ Efficiency of dust suppression

$$= \frac{10.5-6}{10.5} \times 100 = 42.86\%.$$

2.14.2 Coal Winning

Winning of coal by coal-cutting machines, continuous miners' or pneumatic picks produces a lot of dust. Dust produced by pneumatic picks can be reduced by about 50% by using wet pneumatic picks. Suppression of dust produced by coal-cutting machines is usually done by water sprays incorporated in the machine. There

are usually four or five jets, 6mm in diameter provided at different parts of the jib for spraying the gummings at the source of production. These sprays are usually fed by internal water feed-pipes fitted inside the jib. The water is supplied at a pressure of 150-350 kPa and its consumption is about $65 \times 10^{-3} m^3$ per tonne of cuttings produced. The reduction in dust concentration by wet cutting varies between 80 to 90% of the dust produced by dry cutting.

Wetting agents have been used to reduce the surface tension of water and thus enable it to wet more dust. But they have to be added in very small quantities and this causes difficulty in suitably controlling their addition to the water-stream. Besides, field tests[58, 59] have shown that addition of wetting agents causes no significant reduction in the dust production. On the other hand, if wetting agents are at all used, they should be of such composition as is not injurious to health. Foam produced by dissolving a small quantity (1 to 2%) of a foaming agent like 'Pyrene' in water and then blowing compressed-air through it has been used instead of water, but it does not present any marked advantages.

2.14.3 Loading

Much dust can be raised by loading dry material. That is why it is desirable to wet the muck pile by water sprays before loading.

2.14.4 Water Infusion

Cleavages and cracks in coal seams usually contain a large quantity of fine dust which is set free during the process of winning. Such dust can be suitably allayed by infusing the coal with water under pressure. Usually holes 50mm in diameter and 1.8m long are drilled at 3 to 5m interval along a face. The holes should be drilled at right angles to the cleavage planes ; thus it may be necessary to drill holes inclined to the face (flanking holes). A suitable seal (Fig. 2.18) is placed somewhere midway in the hole, the exact positioning of the seal being determined experimentally so that sufficient pressure can be applied without causing leakage from the hole. The water pressure should be sufficient to force water along the cleavage planes, but not enough to infuse water into the roof or floor. The pressure requirements in British coal mines vary from 250 kPa to 4 MPa, depending on the nature of coal, though pressures as high as 27 MPa have been used in Germany.

Scanned with CamScanner

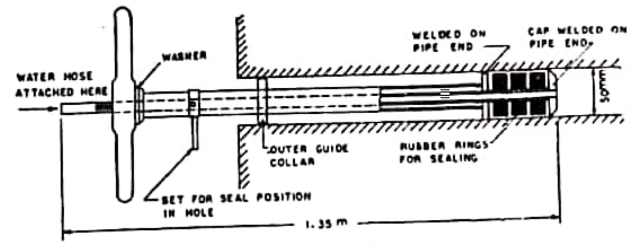

Fig. 2.18 Water-infusion tube

The average amount of water consumed is about 10×10^{-3} m^3 per tonne of coal produced. Long holes drilled parallel to and at a distance of about 1.5m from longwall faces have also been successfully infused.

In British coal mines, water infusion has been claimed to achieve about 75% reduction in the dust concentration at the face. In addition to suppressing dust, water infusion loosens the coal to some extent, thus making its winning easier.

2.14.5 Pulsed Infusion

The loosening of coal with water infusion led to the development of pulsed infusion. Here, a pulse or shock is imparted to the water in the hole by firing an explosive charge in it so that the loosening effect is enhanced in addition to suppressing dust. Flanking holes inclined at an angle of 0.8 rad ($\simeq 45°$) to the face are commonly used for pulsed infusion. They are about 2-3.5m long and spaced at 1.8m intervals. The holes are first charged with the requisite quantity of explosive and then the infusion tube is inserted, the seal tightened and the hole infused with water under pressure for about 15 to 20 minutes before the shot is fired. Normal infusion tubes fitted with suitable non-return valves to guard against the shock wave damaging the pipe lines may be used, though special types of tubes are also in use. Infusion pressures up to 3 MPa have been used and for such high pressures, suitable explosives capable of withstanding water under pressure have to be chosen. Usually barytes-sensitized gelatinous explosives such as 'hydrobel' are used in conjunction with submarine type of detonators.

Pulsed infusion may be sufficient to blast coal in the solid depending on the nature of coal, but it is also extensively used for blasting undercut faces. The amount of explosive used for solid blasting is about 250 to 350g per hole. Sometimes pulsed infusion with a lesser quantity of explosive (150–250g) may be done in the solid in order to loosen the coal sufficiently and make it amenable to winning by coal ploughs or cutter-loaders. Long holes drilled parallel to the face at a distance of 1.5m have been fired by pulsed infusion. Here, the hole is stemmed at one end and infused from the other. Explosive charges are placed at intervals of 1.8m along the hole and are connected to each other by a detonating fuse such as 'Cordtex'.

2.14.6 Water Stemming

This consists of stemming a shot hole after charging with a plastic or p.v.c. bag (usually 0.15mm thick) filled with water. Water, owing to its incompressibility, gives a better confinement to the charge so that a better efficiency of blasting is obtained. This usually results in a saving of about 25% in the explosive consumption. Water stemming produces less dust, the reduction in the dust concentration being 50-70% of the dust produced by blasting with ordinary clay stemming.

2.15 REMOVAL OF DEPOSITED DUST

Often, dust deposited on the floor of mine roadways can become air-borne by high velocity air-current, trampling by men etc. A vacuum-cleaning device has been designed for removing the dust deposited on roadways. The dust is delivered first to a cyclone for the separation of coarse particles and then to a filter for collecting the finer dust.

2.16 CONSOLIDATION OF ROADWAY DUST

The best method of preventing roadway dust getting air-borne is to consolidate it. The simplest method of consolidation is by wetting the dust with water sprays, but water sprays alone do not produce good wetting of all deposited dust and a large quantity of water may be needed for producing effective results. Besides, water evaporates quickly needing very frequent spraying. Two common methods of consolidating roadway dust are (a) the calcium

Scanned with CamScanner

chloride method commonly used in British coal mines and (b) the salt crust process sometimes used in Germany.

2.16.1 Calcium Chloride Method

This method utilizes the principle of keeping the dust constantly and thoroughly wetted so that it takes on the consistency of a paste. To this end, the dust is first sprayed with water mixed with a suitable wetting agent and then sprinkled over with calcium chloride. Calcium chloride, being hygroscopic, absorbs moisture from the air and keeps the dust wet. Subsequent trampling by men further helps in the consolidation of the dust.

Normally, the floor is first covered with a layer of stone dust of a minimum thickness of 25 to 50mm, the work progressing in the direction of the ventilation current. Then a solution of a wetting agent (a 3 to 5% solution of Teepol or Lissapol N has been found to be suitable) is sprayed at the rate of 6.5×10^{-3} m^3 per square metre of floor area and the roadway allowed to dry for an hour or so. Next it is again sprayed with the solution of the wetting agent at the rate of 6.5×10^{-3} to 10×10^{-3} m^3 per m^2 in order to ensure thorough penetration of the dust by the wetting agent. After this preliminary treatment, the roadway is left for 2 to 3 hours and then flaked calcium chloride is spread on the floor. The amount of calcium chloride depends on the relative humidity of the air and generally varies between 2 to 7% of the dust. Deliquescence of the calcium chloride becomes complete after about 36 hours, after which the roadway can be opened for traffic. Dust deposited on the roof and sides of a roadway can be consolidated by spraying it with a calcium chloride paste.

A single treatment lasts for a period which may be anything from a couple of months to a year depending on the rate of deposition of dust. The method is unsuitable for a heavy rate of deposition so that it becomes imperative to use this method of consolidating roadway dust only in conjunction with suitable suppressive measures adopted at the face and other points of dust generation.

2.16.2 Salt Crust Process

Here, unlike the calcium chloride method, the dust is bound up in the form of a hard crust. The method consists of sprinkling common salt on the dust and then spraying it with water. Initially water amounting to about 15% of the weight of the salt used is

sprayed. The salt dissolves and penetrates into the dust, but soon, the water starts evaporating, thus causing the salt to recrystallize and form a hard crust on the surface. Particles of dust are trapped in the growing salt crystals and thus consolidated.

As fresh dust is deposited on the crust, it becomes necessary to respray it so that the salt can dissolve and recrystallize entrapping the freshly deposited dust. The amount of water to be sprayed subsequently should be such that it ensures a high rate of crystallization, maintaining at the same time a firm crust. The salt crust process has been found to be unsuitable for very high (>75%) and very low (<55%) humidities and because of this many German mines are now using the calcium chloride process.

2.17 DILUTION AND SUPPRESSION OF AIR-BORNE DUST

The simplest way of reducing the concentration of dust in air to a pathologically safe limit is to dilute it by increasing the quantity of ventilation. This, however, is limited to dealing with relatively small concentrations of dust, since large concentrations would require a large quantity of air which not only would increase the cost of ventilation but also create high air velocities which may raise deposited dust thus producing the opposite effect.

Supression of air-borne dust, can be classified into two methods : (a) wet suppression and (b) dry suppression.

2.17.1 Wet Suppression of Dust

This usually utilizes sprays of water for wetting fine particles suspended in the air. The wetted particles grow in size and are easily separated out by gravitational settling. Sometimes, particularly with mist spray, the spray may be directed against a surface such as a wall or a curtain of brattice so that the separation of the wetted particles is enhanced owing to impingement. Fine atomized sprays or mist sprays having droplets of about 60 μm diameter have been found to be much more effective in wetting suspended dust than coarse sprays. Atomized sprays can be produced by swirl-type or impingement-type pressure nozzles or by pneumatic atomizers. Pressure nozzles for producing fine droplets usually require high water pressure (of the order of 4-5 MPa) and very small nozzle diameter (0.2-0.5mm). This requires the nozzles to be very carefully finished. Slight nozzle wear destroys the uniformity of atomization.

Scanned with CamScanner

That is why pneumatic atomizers consisting of a spray of water and compressed-air through small-diameter nozzles (1mm diameter) are preferably used in mines for producing mist cones. The droplet size in pneumatic sprays depends on the relative volume of water and air as well as the velocity of the mixture through the nozzle, the droplet size decreasing with increased amount of compressed-air and increased velocity (for details of performance of atomizers, the reader is referred to 'Atomisation and Spray Drying' by W.R. Marshall, Jr.).

Water sprays have been effectively used for suppressing dust on haulage roads and at chutes, transfer points, ore bins, skip loading stations etc. Regular spraying of shaft sets suppresses the dust collected on them thus preventing it from getting air-borne.

Dust produced during blasting in a heading or drive can be effectively suppressed by providing a suitable arrangement of sprays. Fig. 2.19 illustrates arrangements of mist curtain as commonly used in German mines for suppressing air-borne dust

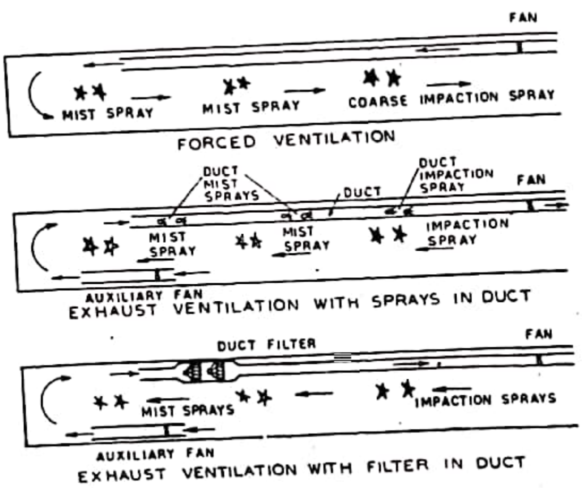

Fig. 2.19 Mist curtains for removal of air-borne dust after blasting.

after blasting (it is compulsory to use mist curtains in stone headings). Generally, the dusty air, after blasting, is driven by an auxiliary fan through a 20-30m long zone of fine mist sprays succeded by coarse impaction sprays in about 15 minutes time. With careful installation and maintenance, the mist curtain method can have a dust suppression efficiency of 60-80% for particles in the respirable size range.

Wet dust suppression, though by far the cheapest, is however undesirable in deep and hot mines where it may worsen the environmental condition by increasing the humidity. Besides, water affects soft floors. Dust allayed by water can again become air-borne if allowed to dry up. Water has a deleterious effect on machinery and conveyors etc. Due to these reasons, dry dust suppression measures are adopted in many mining operations. Steam has been used successfully for suppressing dust at loading stations, tipplers etc. on the surface. Jets of steam at a pressure of 1MPa are allowed to impinge on the dust as it is raised. Steam is more efficient in suppressing dust and 1kg of water as steam is equivalent to 20 kg of water in its ability to suppress dust. With a suitable arrangement of steam jets, a reduction of 40-50% in the dust concentration has been achieved at surface tipplers at Bedwas colliery, S. Wales, U.K.

2.17.2 Dry Dust Suppression

This usually consists of exhausting the dusty air from the point of operation and then separating the dust from the air by inertial separation, filtering, electrical precipitation etc. so that the cleaned air can be recirculated. Means of dry dust suppression are commonly used in mines at transfer points, ore bins, crusher stations and even for cleaning the air after blasting in headings.

2.17.3 Exhausting Dusty Air

The kinetic energy imparted to fine particles during their production is so small (due to the small mass of the particles) and the air resistance to their projection so great (due to their relatively large surface area) that the former plays a very insignificant role in their dispersal which is almost entirely controlled by air movement. It is thus necessary to control the movement of air at the source of production in order to check dispersal of fine dust into air.

Scanned with CamScanner

Most ore handling processes cause some amount of air movement about them. The most important and clearly understood air movement is, however, that induced by a stream of falling material. The quantity of air moved by a stream of falling material or *pulvation* is a complex function of the area of opening available to air-flow, height of fall, quantity of material falling, size, shape and consistency of the stream, size of material and shape of the flow path and hence is difficult to predict from theoretical considerations. It is, however, possible to measure the quantity of air moved by tracer gas technique in which a certain non-hazardous gas like carbon dioxide is introduced at the entrance of the induced air-flow at a constant rate and the concentration of gas at the exit of the induced air-stream is determined. The rate of induced air-flow can then be calculated as given in Chapter VIII. Table 2.5[42] gives the rate of air-flow induced by crushed rock falling through chutes as measured by this technique.

Table 2.5 : Rates of Air-flow Induced by Crushed Rock falling in Chutes

Vertical fall, m	Material flow, $t\ h^{-1}$	Aggregate size	Air displacement, $m^3\ s^{-1}$
9	40-50	Fine	0.224-0.364
9	37-200	Fine	0.280-1.240
3	50-60	Coarse-medium	0.216-0.224
3.6	120	Coarse 20% and medium 80%	0.302
3.6	77-120	Coarse-medium	0.140-0.224
3.6	160	Coarse 50% medium 30% and fines 20%	0.199-0.294

Anderson[60] gives the following empirical relation for the estimation of the induced flow-rate Q :

$$Q = 0.283\ \frac{A^2RH^2}{D}\ m^3\ min^{-1} \tag{2.18}$$

where A = enclosure opening upstream, i.e. where the air is induced into the system by the falling material, m^2,

R = rate of material flow, $t\ h^{-1}$,

H = height of fall, m

and D = average particle diameter, m.

When the stream comes to rest, the falling material gets compacted and the air entrained in it is violently expelled (referred to as *splash*), carrying with it a lot of dust. The aim of any dust control measure should be to avoid or effectively deal with such a splash. The splash can be prevented easily in enclosed systems by suitably exhausting the induced air drawn into the system. At mines, such enclosed systems are offered by chutes, crusher stations, storage bins etc. Here the quantity of exhaust air necessary should be sufficient to overcome the induced air movement. A much larger quantity is also not desirable since it might create large air velocities within the enclosure, capable of raising dust. It is a good practice to keep down the amount of dust picked up by the exhaust air as far as possible, since it causes less damage to the exhaust pipes and minimizes the problem of air cleaning. It is for this reason that the air velocities in exhaust pipes should be kept low. Fig. 2.20

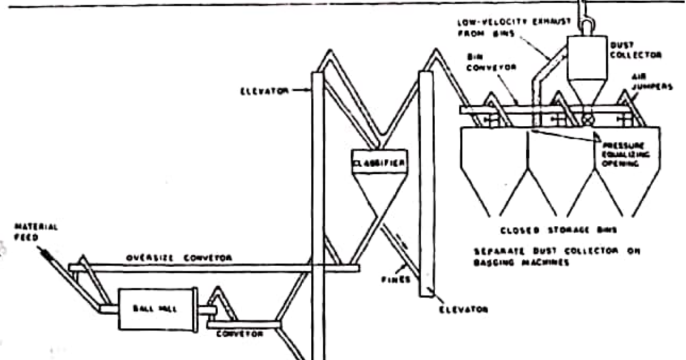

Fig. 2.20 Diagrammatic layout of a grinding mill with completely enclosed low-velocity exhaust ventilation system.

Scanned with CamScanner

shows such an exhaust system. It is to be noted that at all points where free passage of air is likely to be obstructed by the material closing the opening, air jumpers are provided for connecting the enclosure to the exhaust system. All air jumpers and the main exhaust pipe should preferably have an inclination greater than 1 rad ($\simeq 60°$) with the horizontal so that the dust separated from the air-stream in these pipes can easily gravitate down into the system.

However, all dusty operations cannot be completely enclosed and in such cases the released dusty air has to be effectively drawn away by an exhaust hood. Open exhaust hoods are much less efficient since they draw in unnecessary air from all around the dusty zone (see Fig. 2.21). The efficiency of exhaust hoods increases to the extent they enclose the dusty operation.

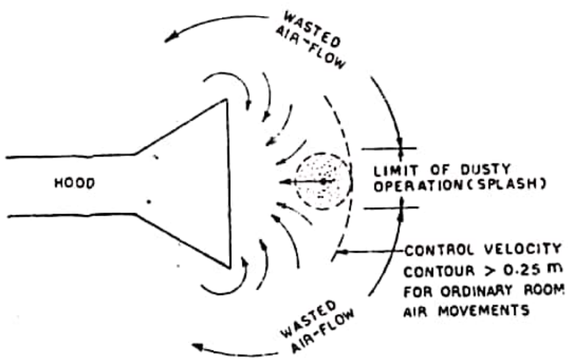

Fig. 2.21 Figure illustrating the effectiveness of an exhaust hood.

2.17.4 Design of Exhaust Hoods

The main consideration in designing exhaust hoods is the capture velocity produced by it. Flanged hoods are preferable to ordinary ones as they substantially modify the flow pattern so much so that for creating the same capture velocity in front of the hood, a flanged hood results in a 30% reduction in the total rate of flow. This will be amply clarified from Fig. 2.22. Dalla Valle[54] gives the

following general equation for calculating the air velocity at any distance x from the mouth of the hood along its axis.

$$v = \frac{Q}{10x^2 + A} \tag{2.19}$$

where v = velocity at a distance x,
Q = quantity of air flowing through the hood
and A = area of the hood opening.

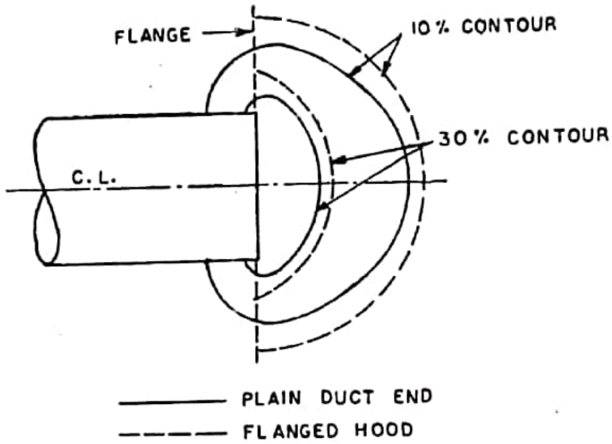

Fig. 2.22 Relative position of velocity contours for plain and flanged hoods.

The above equation holds approximately true for hoods of all shapes. When a hood is suspended over a flat surface, the velocity of air flowing through the open area between the hood and the flat surface is given by the following equation according to Dalla Valle.

$$v = \frac{0.71Q}{px} \tag{2.20}$$

where p = perimeter of the hood opening
and x = free distance below the hood.

It will be seen from the above equation that for a particular hood, the smaller the value of x, the larger is the capture velocity for the

Scanned with CamScanner

same rate of flow, which clearly indicates the desirability of the hood enclosing the dusty operation as far as practicable.

Depending on the nature of the dusty operation, the exhaust hood should be able to create an adequate capture velocity. Drinker and Hatch[42] have suggested the following capture velocities (Table 2.6) at the point of operation for effectively dealing with the dispersed dust.

Table 2.6 : Capture Velocities for Collecting Dispersed Dust

Condition of generation	Minimum air velocity, m s^{-1}	Process
Released with low air velocity	0.5-1.0	Paint spraying in booth, dumping dust into hopper.
Active generation	1.0-2.5	Stone cutting, rotating mixers, active barrel filling, conveyor loading.
Released with great force	2.5-10.0	Grinding, heavy crushing.

A more generally applicable method of estimating the quantity of exhaust hood ventilation is due to Hemeon. He suggests that the capture velocity at the farthest visible limit of travel of dusty air from the source (say a splash) where its directional energy is dissipated in turbulence, should be atleast 0.25 m s^{-1} for ordinary room air movements (see Fig. 2.21). The figure, however, has to be higher if there are stronger air-currents in the area. Dust resistance and fan size usually restrict the air velocity at hood entrance to about 15 m s^{-1} and to ensure a capture velocity of the order of 1 m s^{-1} at the source of dust, the hood has to be placed at a distance of only $1.2D$ from the source, where D is the side of a square hood (see equation 2.19).

The shape of a hood does not materially affect the velocity distribution at the entrance, but a suitably shaped hood with the sides of the opening converging on the duct helps in reducing the pressure loss at the entrance and hence decreases the power cost of ventilation. The shock pressure loss for exhaust hoods can be calculated from equations 4.34, 4.60 and 4.64 knowing the edge

condition and the velocity of air in the exhaust duct. The values of N_c and N_e in such a case are equal to 0 and 1 respectively since there is free entry of air into the hood. For a plain hood, which is nothing but the extension of the exhaust pipe, a value of $Z=3.8$ can be adopted for which X becomes 0.92 ; or the shock loss at the hood is 0.92 times the velocity head in the duct. For a plain hood with flanges, the value of Z can be taken as equal to 2.5 when X becomes 0.35. Alden,[61] however, gives the value of X for entry into flanged pipes to be equal to 0.49. Hoods with sides of the opening converging to the duct (Fig. 2.23) can be likened to flanged pipes and the value of $X=0.49$ adopted for them since the angle of convergence is usually too large to cause any reduction in the value of X.

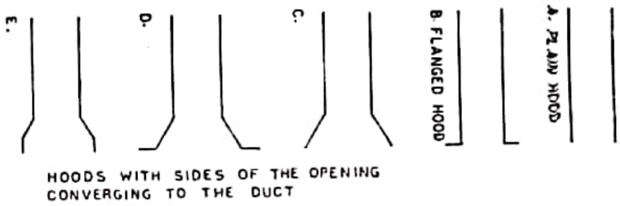

Fig. 2.23 Types of exhaust hoods.

The exhaust pipes used with such hoods should be of sufficient size so that the velocity of air in them is adequate to transport the dust carried in the air. The air velocity necessary for transporting dust vertically upwards should exceed the terminal settling velocity of the largest particle in the dust cloud (see equations 2.9 to 2.11). This velocity is usually more than sufficient for horizontal transport of dust. In practice, a velocity of 15 to 20 metres per second is usually maintained in the exhaust duct.

Having decided on the velocity in the duct, one can easily calculate the size of the fan necessary for the exhaust system by knowing the resistance of the system. It is often necessary to provide a suitable damper in the system in order to prevent overloading of the motor, if the system resistance is less than the estimated value. But this is a wasteful process and a better method of control is the reduction of the speed of the fan. The fan and ducting should

Scanned with CamScanner

be suitably earthed in order to prevent the development of high electrostatic charges, particularly when handling inflammable matter such as coal dust.

2.17.5 Design of Enclosures for Conveyor Transfer Points, Screens and Crushers

These are common sources of dust generation in mines and associated plants and mills. All these sources are usually covered by hoods placed close to the source almost enclosing it and connected to exhaust systems. The volume of air to be exhausted is generally arbitrarily fixed at 35-50 m^3 min^{-1} per m width of belt in case of belt conveyors, 0.5 m^3 min^{-1} per m^3 volume of bins or 15.0 m^3 min^{-1} per m^2 screen area for screens. Sometimes, the quantity is fixed on the basis of an arbitrary air velocity of 2-2.5 m s^{-1} at the enclosure opening. Wright[80] suggests a volume of 45 m^3 min^{-1} per m^2 of enclosure or hood opening (both on upstream and downstream side) in addition to the quantity obtained from equation 2.18. It must, however, be borne in mind that, to keep this quantity within reasonable limits, the value of A in equation 2.18 should be as small as possible, preferably restricted to 0.15 m^2 per m width of belt.

Equation 2.18 holds for material transfer from belt to belt or chute to belt, but where the belt or chute discharges into a bin where the entrained air cannot escape at the downstream end and undergoes a reversal of direction on hitting the bin, the quantity required is only $Q/2$. The value of H is normally taken equal to half the bin height.

In case of screens, at least three points of exhaust have to be provided :

(i) At the point of discharge of belt or chute on the the screen—the screen is completely covered by a hood and the area A is the feed belt or chute opening.

(ii) At the point of discharge of oversize to belt or bin.

(iii) At the point of discharge of undersize to belt or bin.

In either of the latter two cases, the screen hood peripheral opening is taken equal to A for calculation of quantity. In view of the usually large size of screen, this area becomes substantially large even for a 25mm hood peripheral opening, which has to be scrupulously maintained narrow.

Similarly, crushers should be provided with two points of exhaust. The crusher top should be completely closed and exhausted. Windows for inspection and clearing blockage may be left but they should be kept closed during normal operation for proper dust control. The point of transfer of crushed ore to belt is separately enclosed and exhausted. While equation 2.18 can be used for computing the quantity for the hood at the crusher top, the quantity required at the crusher discharge point is normally less (by one-third) than the quantity calculated by the same equation even when taking A equal to the crusher throat opening, since the flow path is very much constricted and offers a high aerodynamic resistance.

2.17.6 Disposal of Dusty Air

The simplest way to dispose of dusty air is through a stack or a long pipe which discharges the air at a remote point where air pollution is inconsequential. Such stacks vary in height from 15m upwards. The dust concentration at any point downwind of a stack depends on the stack height, the rate of dust emission from the stack and the wind velocity.

Stacks can conveniently dispose of dusty air where there are no extensive residential areas nearby, but in large inhabited areas such as cities, stacks will be prohibitively tall if air pollution in the vicinity is to be avoided. In such cases it becomes necessary to clean the dusty air before it is disposed of. With a rate of dust emission from the stack of 1 g s^{-1} and a wind velocity of 1 m s^{-1} there is a maximum dust concentration of 0.09 mg m^{-3} at a distance of about 1200m from a 50m high stack. The concentration decreases on both sides of this peak, it being only 0.01 mg m^{-3} at a distance of 500m as well as 7000m from the stack. The peak concentration is more and occurs at a lesser distance from the stack, with smaller stack heights. With the above rate of dust emission and wind velocity, the peak concentration is 0.25 mg m^{-3} occuring at a distance of 500m from the stack with a 20m high stack while with a 10m high stack, the corresponding figures are 1.2 mg m^{-3} at 160m. The dust concentration of course varies inversely as the wind velocity.

2.18 AIR CLEANING

The methods commonly used for cleaning air of its dust load are

Scanned with CamScanner

(a) gravitational cleaning, (b) inertial cleaning, (c) scrubbing, (d) filtration and (e) electrical precipitation.

2.18.1 Gravitational Settling

Here the dust-laden air is led through a settling chamber (Fig. 2.24) where the dust settles down by gravity. For a dust particle at the top of the chamber to settle down to the bottom, its time of retention in the chamber t should be equal to h/v_t, where v_t=terminal settling velocity of the particle and h=height of settling chamber.

$$\text{Again,} \quad t = \frac{l}{v_a} = \frac{lhb}{Q} \qquad (2.21)$$

where v_a = velocity of air in the chamber,
l = length of chamber,
b = breadth of chamber
and Q = quantity of air flowing.

From the above relations we get

$$hb = \frac{Q}{v_a} \qquad (2.22)$$

$$\text{and} \quad h/l = \frac{v_t}{v_a} \qquad (2.23)$$

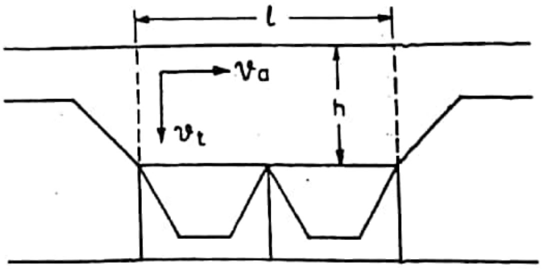

Fig. 2.24 Settling chamber (diagrammatic).

For good settling, the flow in the chamber should be laminar, but this is difficult to achieve in practice since it would involve a

large cross-section for the chamber. A suitable velocity is of the order of 0.3 m s^{-1} though larger velocities of 1.5 m s^{-1} or more are used in practice due to limitations of space and cost. Because of this there is usually some turbulence in the setttling chamber and the terminal settling velocity should be multiplied by a suitable eddy factor when designing settling chambers. For a velocity of 0.3 m s^{-1}, it is customary to take an eddy factor of 0.5. Again, for uniform flow through the chamber, which is necessary for good settling, it is better to have the breadth of the chamber nearly equal to its height. Settling chambers are suitable for large particles only since for small particles, they will have to be too long.

Example 2.3

Design a settling chamber for separating quartz dust down to 50μm size from a stream of air flowing at the rate of 3 m^3 s^{-1}.

Let us assume v_a = 0.3 m s^{-1}
and $h = b$

From equation 2.10 the terminal settling velocity of 50 μm particles in still air = 0.19 m s^{-1}, assuming ρ = 2500 kg m^{-3}. Therefore the actual settling velocity v_t = 0.5×0.19
=0.095 m s^{-1}, assuming an eddy factor of 0.5.

$$\text{From equation 2.22, } hb = h^2 = \frac{Q}{v_a} = \frac{3}{0.3} = 10,$$

$$\text{or, } h = b = 3.16\text{m}.$$

$$\text{From equation 2.23, } h/l = \frac{v_t}{v_a}$$

$$= \frac{0.095}{0.3} = 0.32$$

$$\text{Therefore,} \quad l = \frac{h}{0.32} = \frac{3.16}{0.32} = 9.9\text{m}.$$

2.18.2 Inertial Settling

The simplest form of inertial cleaner is illustrated in Fig. 2.25. Here the dust-laden air is deflected downwards by a baffle. The air sheds its dust load when it takes a sharp turn to rise up again in the chamber. A low rising velocity helps in further separation of dust by gravitational settling. This sort of collector has a good

Scanned with CamScanner

efficiency on weight basis for heavy dust loading, but is unsuitable for either low dust loading or fine particles.

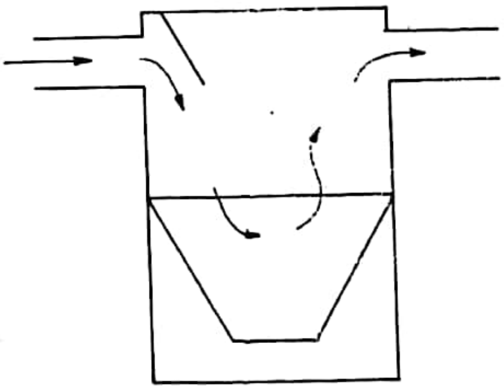

Fig. 2.25 Inertial cleaner (diagrammatic).

2.18.3 Cyclone

The most common type of inertial cleaner is the cyclone separator (Fig. 2.26). Here, the dust-laden air is imparted a rotating motion by virtue of its tangential entry into the cyclone. Owing to this rotational motion, the dust particles are subjected to a centrifugal force which imparts them a radial acceleration. This radial acceleration is much higher than the acceleration due to gravity. The air-stream entering the cyclone travels down in an outer vortex or spiral during the course of which it deposits its dust load on the walls of the

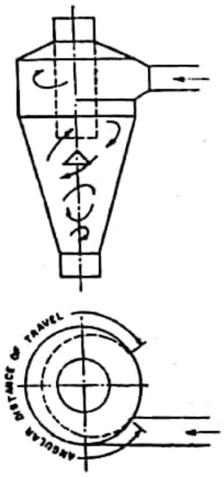

Fig. 2.26 Cyclone separator (diagrammatic).

cyclone and the clean air travels up again in an inner vortex before entering the exit duct.

The centrifugal force F acting on a dust particle moving with an angular velocity ω is given by the relation

$$F = \frac{\pi D^3}{6}(\rho-\rho_a) r\omega^2 \qquad (2.24)$$

where r = radius of curvature of the path of the particle,
D = diameter of the particle,
ρ = density of the particle
and ρ_a = density of air.

For attaining the terminal centrifugal settling velocity, F must be equal to the air resistance which, for spherical particles in streamline motion, is equal to $3\pi\mu D v_c$ (see equation 2.4)

$$\text{or,} \quad \frac{\pi D^3}{6}(\rho-\rho_a) r\omega^2 = 3\pi\mu D v_c$$

$$\text{or,} \quad v_c = \frac{r\omega^2(\rho-\rho_a)D^2}{18\mu} \qquad (2.25)$$

where v_c = centrifugal settling velocity.

Combining equations 2.25 and 2.7 we have

$$v_c = \frac{r\omega^2}{g} v_t = \frac{v^2}{rg} v_t \qquad (2.26)$$

where v_t = terminal velocity of gravitational settling
and v = linear velocity of the rotating gas-stream.

Equation 2.26 shows that for any particle size, the centrifugal settling velocity can be increased by either increasing the speed of rotation of the air-stream or by decreasing the value of r. It is for this reason that smaller cyclones are more efficient than larger ones. The factor v^2/rg is termed the *separation factor*.

Rosin, Rammler and Intelmann[54] have given the following equation for determining the smallest size of particle separated by a cyclone.

$$D^2_{min} = \frac{9\mu D_0}{2\pi N v(\rho-\rho_a)(4r/D_0)^n} \qquad (2.27)$$

where D_{min} = minimum diameter of particle removed,
D_0 = diameter of the exit duct of the cyclone,
N = equivalent number of turns of the gas-stream in the inner spiral of the cyclone (this is constant for all cyclones of similar proportions and ranges from 0.5 to 3.0),

Scanned with CamScanner

r = radius at which the spiral velocity is equal to the cyclone entrance velocity v

and n = an exponent varying between 0.5 and 0.7.

The above equation clearly shows that the efficiency of cyclones for collecting fine particles increases with rise in the spiral velocity as well as the depth of the cyclone.

The pressure loss in a cyclone is given by the following relation developed by First.[42]

$$\Delta P = \left[12 \frac{(b/k)h_i}{D_e^2} \Big/ \left(\frac{h}{D}\right)^{\frac{1}{3}} \left(\frac{h_c}{D}\right)^{\frac{1}{3}} \right] P_v \qquad (2.28)$$

where P_v = inlet velocity pressure,
ΔP = pressure loss in the cyclone,
b = width of cyclone inlet,
h_i = height of cyclone inlet,
h = height of cylindrical outer shell,
h_c = height of cone,
D = diameter of the outer cylinder
and K = a dimensionless factor depending on the cyclone inlet and having a value of 0.5 for cyclones without inlet vanes, 1.0 for inlet vanes that do not expand the entering air-stream or extend to exit-duct wall and 2.0 for inlet vanes which extend across the entire annular space.

Generally, pressure consumption in cyclones varies from 350 Pa in low-efficiency cyclones to about 1kPa for cyclones with higher efficiency.

There are two types of cyclones : the high-efficiency type and the low-efficiency type. The former are narrow (100-600mm dia.) and tall cyclones with high spiral velocities. They have good efficiency for fine particles though they offer a higher resistance and can handle a smaller quantity of air. One design by King[43] (Fig. 2.27) is claimed to have an efficiency of 95% for particles below 10 μm size with an outer vortex velocity of 18 m s^{-1} and a cyclone diameter of 300mm. The efficiency is 92% for a cyclone of 1200mm diameter. For smaller particles of less than 5 μm size, it becomes necessary to use a vortex velocity of 24 m s^{-1} for satisfactory results. The low-efficiency cyclones are, however, more generally used since cyclones are commonly used as primary collectors. These are usually of

large size capable of handling large quantities of air and offer a low resistance. Their efficiency is, however, 70-80% for mineral dust (<100 μm size) and they fail to catch particles less than 10 μm in diameter. The design of such cyclones is more or less standardized nowadays, a common design having the outer cylindrical shell 2 to 3 entrance-pipe diameters in length and about twice as much in diameter. The cone is about three times the length of the cylindrical shell. The outlet duct has the same area as the inlet duct and extends about half diameter into the cone. An inverted cone 30% smaller than the outlet, and placed three-fourths outlet diameter below the exit has been found to improve efficiency.

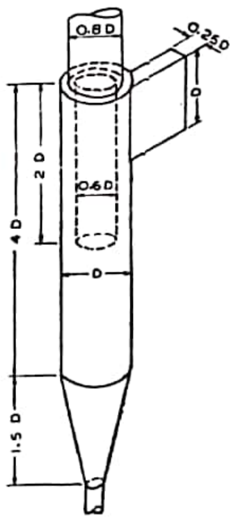

Fig. 2.27 High-efficiency cyclone separator designed by King.

2.18.4 Scrubbing

Scrubbing utilizes the principle of wetting the dust particles in order to facilitate their separation by both gravitational and inertial settling. It is very difficult to wet all dust particles. A simple spray wets only 50% of the particles of any mineral dust. A greater contact between the sprayed water and the dust particles is, however, obtained in scrubbers. Use of wetting agents in traces sometimes helps in wetting mineral dust, but large quantities of wetting agents cause foaming.

Scrubbers are of two main types : (a) mechanical centrifugal scrubbers and (b) inertial scrubbers. Wet rotoclones are typical examples of the former where the dusty air is sprayed as it meets the blades of the exhauster. In the simplest form of the latter type the dusty air is led tangentially into a cylinder at its bottom and then sprayed. There is a variety of commercial scrubbers using this principle where the air-stream is given more directional changes.

Scanned with CamScanner

Scrubbers, in general, operate well on heavy loadings of coarse dust. Their performance is poor for fine particles though exceptions have been claimed. The water consumption in scrubbers usually varies between one fourth to half of the mass of air handled. Scrubbers have a relatively short life, because of corrosion and wear of the internal parts.

2.18.5 Filtration

The mechanism of dust precipitation on filters comprises mainly impingement and diffusion, though electrostatic attraction may play an important role. Precipitation by impingement is by inertial separation of dust from a fast-moving stream of dust-laden air, when it meets with an obstruction. The efficiency of filtration by impingement is a function of the following dimensionless parameters :

$$\eta = f(P_i, Re, D/2r) \tag{2.29}$$

where η = efficiency of filtration,

P_i = impingement parameter $= \dfrac{\rho D^2 v}{18 \mu r}$,

Re = Reynolds number $= \dfrac{v D \rho_a}{\mu}$,

r = radius of obstruction, say, the fibres in a cloth filter,

v = air velocity approaching the fibre,

ρ_a = density of air,

μ = viscosity of air,

D = diameter of particle

and ρ = density of particle.

The efficiency of filtration by diffusion on the other hand given by the equation 2.29 when P_i is replaced by P_d, the diffusion parameter which is equal to $K/(vD^2r)$, where K is a constant depending on the diffusion coefficient. It will thus be seen that whereas the efficiency of filtration by impingement varies directly with the square of the particle diameter and the air velocity, that by diffusion varies inversely with these quantities and the filtering efficiency is the minimum for a particular value of vD^2. In other words, for a fixed air velocity, the filtering efficiency will be the minimum for a certain diameter of particle. For a velocity of say 0.015 m s^{-1} (a velocity commonly used in filtration) the minimum efficiency is

obtained for a particle of 0.1 μm size and the efficiency goes on increasing with increasing particle size. It is worth noting that whereas filtering by diffusion is more important for very fine particles at low velocities, the opposite is the case for filtration by impingement. For mine dusts which contain only a small fraction of very fine particles of <0.1 μm diameter, the major mechanism of filtration is impingement and for such a condition, the efficiency of filtration can be increased by increasing the air velocity. This is the practice in case of saw dust or metal filing filters soaked with oil, but in dry fibrous filters or cloth filters, a high velocity is undesirable since it blows off the precipitated dust. Besides, a high air velocity builds up a heavy dust load on the filter in a short time thus needing too frequent cleaning. In practice, air velocities through dry filters are maintained in the streamline regime of flow. In both the cases of filtration by impingement or diffusion, the efficiency of filtration increases with decreasing r so that for high efficiency, fine fibres are desirable.

The above treatment of filtration efficiency is for filtration through a single layer of fibres. For a thick bed of filter the filtration efficiency is given by the equation

$$\eta = 1 - e^{-\Upsilon l} \tag{2.30}$$

where $\Upsilon = \dfrac{1-P}{P} \cdot \dfrac{K}{\pi r^2}$,

l = thickness of filter,

P = porosity

and K is a complex function of particle size, air velocity as well as P and r.

The above equation shows that the efficiency increases exponentially with the thickness of the filter, a fact well borne out in practice.

A common way of judging the efficiency of a filter is by noting its resistance to air-flow. The resistance of a new filter is fairly low, but it builds up as dust goes on accumulating on it with time. This increase in resistance is given by Dalla Valle as follows :

$$\Delta P = \frac{K c\, v^2 t^2}{D^2} \tag{2.31}$$

where ΔP = increase in the pressure loss in the filter in time t,

c = dust loading, i.e. the mass of particles per unit volume of air,

Scanned with CamScanner

v = air velocity,
D = diameter of particles
and K = a constant depending mainly on the particle size, its value increasing with decreasing particle size.

It is seen that the resistance rises fast with fine particles and with high dust loadings. Thus it is desirable to leave a certain amount of coarse dust in the air entering the filters when primary cleaners such as cyclones are used before filters. It has been found that the initial resistances and filtering efficiencies of different cloth filters vary considerably, but when these filters have been loaded with dust to the same extent of rise in resistance they attain similar filtering efficiencies. This relationship between resistance and efficiency however, does not hold good for dissimilar filtering materials for which separate resistance-efficiency relationships should be established.

Cloth Filters. Heavy (350 g m^{-2}) cotton fabrics are most commonly used for filter cloth because of their cheapness. Woolen fabrics, however, have a higher filtering efficiency because of the fineness of their fibres, though they are costlier. Filter cloth is usually felted since woven fabric tends to open up gradually and leak. Both screen and bag-type filters are used, the latter being more commonly used in mines.

Flannel-bag filters have been extensively used on the Witwatersrand gold field for filtering dust-laden air from ore bins. Because of the low filtering velocity, a large filtering surface becomes essential and for this reason it often becomes necessary to have serveral bags operating in parallel. Dusty air is blown into the bags (usually 400-550mm in diameter and 6m long) at a rate that generates a filtering velocity of the order of 0.10 to 0.12 m s^{-1}. Both forcing and exhausting fans are used for air movement, though the latter handle clean air and hence are subject to less wear. The filters are loaded till they absorb a pressure of about 600 Pa when they are changed for cleaning. Changing of bags is done every day. Bag filters have been found to last from a year to two years if properly maintained. They are usually treated with a preservative like 'Cuprinol' for protection against fungus. Cleaning of bags by shaking reduces their life, though this is the method often adopted. An ingenious method adopted in South Africa is to turn the bag inside out and alternately inflate and deflate it. Self-cleaning filters using a reverse jet of air have been developed.

The efficiency of bag filters on the Witwatersrand has been found to be fairly high after use for some time and it is essential to leave some dust in the filter while cleaning so as to maintain a good filtering efficiency. Table 2.7 gives the filtering efficiency of flannel bags.

Table 2.7 : Filtering Efficiency of Flannel-Bag Filters

Time of Operation in hours	Filtering efficiency, %	Pressure drop, Pa	Filtering velocity, m s^{-1}
new	20	49	—
1/2	74	196	0.17
2	88	245	0.15
10	99	440	0.13

Woolen fabric filters, mainly of the screen type, are used extensively in German coal mines for filtering dusty air from skip-loading points, crusher stations, pneumatic stowing areas etc. A filtering device for cleaning air after blasting in headings is gaining favour in German coal mines because of the humid condition created by wet suppression measures. The heading is sealed off by a suitable curtain and a fan forces the dusty air through a woolen filter having an area of 60 m^2 at the rate of 5 m^3 s^{-1}. The filter has an initial resistance of 186 Pa rising to 608 Pa in three weeks' time before it is cleaned. The cleaning is done by blowing back compressed-air along with rapping of the filter, the dust being collected in a pan. The filter has a life of about three years. The efficiency of the filter is 99% (on mass concentration basis) while the efficiency of the whole installation is 90%, chiefly because of leakage at the curtain.

Saw-dust and Metal-shaving Filters. Filters made of saw dust and metal shavings impregnated with old oil have been successfully used in some Australian mines. Saw-dust filters are also commonly used on the Witwatersrand where horizontal beds of saw dust, 37mm in thickness are laid on 2mm screens. The saw dust is well graded, its size varying between 3 and 12mm. Dusty air is fed from the top so as to give a filtration velocity of 0.3 m s^{-1}. Higher velocities of the order of 0.5 m s^{-1} give good efficiencies, but cause channelling and hence are not used. Usually two such beds 0.6 to 0.9 m vertically apart are required for good efficiency. The pressure consumed by these filters is higher, i.e. from 1 to 1.5 kPa.

Scanned with CamScanner

The efficiency of saw-dust filters is initially low, particularly for fine particles, but it increases to 90-100% after 2 to 3 weeks' use. The saw dust is changed when the resistance increases to 1.5 kPa, but changing becomes infrequent with periodical raking of the saw dust which prevents its clogging. The saw dust should be sprayed with water before raking.

2.18.6 Electrical Precipitation

Electrical precipitators have got a great scope for use in metal mines for cleaning air passing from one section to another or at shaft-loading stations, crusher houses etc. They have been successfully installed in some of the South African gold mines. They can be so designed as to handle large quantities of air since they permit an air velocity up to 1 m s^{-1} through them at a fairly low resistance (below 100 Pa). Hence the cost of operation of the fan drawing air through them is lower than that with filters or cyclones. The electrical power cost is very little. Though their initial cost is comparatively high, it has been claimed to be redeemable within a period of seven years from the savings in their operating cost. They have a high efficiency, i.e. of the order of 90% for particles of all sizes, though electrical precipitators can be designed to attain an efficiency as high as 99.9%, if cost is no consideration.

Electrical precipitators essentially consist of a narrow discharge electrode which is maintained at a high DC voltage (usually negative) and a collecting electrode which is grounded. There are two types of arrangements. In the tube type of precipitator, the discharge electrode is in the form of a stiff wire and the grounded electrode, in the form of a cylinder concentrically surrounding it. In the plate type, there is a set of parallel wires (discharge electrodes) in between parallel plates which serve as the collecting electrodes.

The air around the discharge electrode gets ionized owing to corona discharge and in its turn charges the dust particles contained in it. The charged dust particles then travel to the ground electrode at a rate given by the equation

$$v = \frac{En'\epsilon}{3\pi\mu D} \qquad (2.32)$$

assuming streamline motion of the particles,

where v = terminal velocity of particle,
E = voltage gradient between the electrodes (usually a voltage gradient of 300 kV m^{-1} is used),
n' = total number of unit charges ϵ on the particle,
μ = viscosity of air
and D = diameter of particle.

n' depends on several factors such as the particle diameter, its dielectric constant and the time of charging and is given by the equation

$$n'\epsilon = \left[1+2\left(\frac{k-1}{k+2}\right)\right] \cdot \frac{ED^2}{4} \cdot \left(\frac{\pi u n \epsilon t}{1+\pi u n \epsilon t}\right) \qquad (2.33)$$

where k = dielectric constant,
n = number of ions per unit volume,
u = mobility of ions
and t = time of charging.

It has been found in practice that terminal velocity of settling in electrical precipitators is usually in the turbulent regime when a more appropriate equation for v is

$$v = \frac{4.26}{D}\sqrt{\frac{En'\epsilon}{\pi\rho_a}} \qquad (2.34)$$

where ρ_a = density of air.

The efficiency of collection of electrical precipitators is given by the following equations due to Deutsch[54]

$$\frac{c_0 - c}{c_0} = 1 - e^{-(2vL/xv_a)} \text{ for cylinders} \qquad (2.35)$$

and

$$\frac{c_0 - c}{c_0} \approx 1 - e^{-(vL/xv_a)} \text{ for wire-and-plate system,} \qquad (2.36)$$

where c_0 = concentration of dust entering the precipitator,
c = concentration leaving it,
x = distance between electrodes,
L = length of collector,
v_a = air velocity
and v = terminal velocity as obtained from equation 2.32.

2.18.7 Sonic Separation

Suspended fine particles have a tendency to flocculate when they are subjected to high-frequency (10000-20000 Hz) sound waves. The flocculated particles can then be separated by gravitational or

Scanned with CamScanner

inertial settling. The use of high-power ultrasonic generators may lead to the development of suitable ultrasonic dust separators, but no commercial models are available yet.

2.19 DUST MASKS

Even with sufficient measures for suppressing dust, the worker in certain mining operations such as chute loading, grizzley operation etc. is usually subjected to a dangerous concentration of dust due mainly to his proximity to the dusty operation. It is advisable for such persons to wear dust masks even though they might cause a certain amount of discomfort.

A lot of work has been done in designing suitable dust respirators. They usually consist of a light face-piece made of rubber, aluminium or plastic with a sponge-rubber lining for an air-tight fit when the knitted cotton face-straps are tightened. Both permanent and removable filters are used, the latter being more common as they are easily changed. Cotton, wool, paper, asbestos etc. have been used as filtering material. The M.A.S. 'dust foe-66' respirator which is commonly used in the U.S.A. for mine dusts contains a resin-coated fabric filter. The resin is electrostatically charged in order to increase the filtering efficiency by aiding electrostatic precipitation of dust. The respirator is very light, weighing only 85 g. All dust respirators have to satisfy the U.S. Bureau of Mines standard efficiency test which lays down that no more than 4mg of dust should pass through the filter in 30 minutes when exposed to a dust concentration of 50 ± 10 mg m^{-3}.

EXERCISE 2

2.1 Calculate the terminal settling velocity of 0.3 μm diameter particles of limestone dust of specific gravity 2.78 in air. What will be the error if the terminal velocity were calculated by Stokes' law without Cunningham's correction ? What will be the terminal velocity of 15 μm diameter particles of the same material in air ?

2.2 Calculate the quantity of air that may be circulated at a coal face to dilute the dust produced by cutting to the permissible level of 3 mg m^{-3} for particle size below 5 μm, if the cutting operation produces 2.1 g of dust below 5 μm size every minute. The air entering the face may be taken to have a dust load of 0.8 mg m^{-3} in the size range of $<5\mu$m.

2.3 A 2×1.2m screen is covered by an exhaust hood. The gap between the hood and the screen at the periphery is 35mm. Calculate the quantity of air to be exhausted per minute in order to maintain an inward air velocity of 0.25 m s^{-1} in the gap. Also calculate the size of the exhaust duct and the pressure loss in the hood assuming the shock factor for the hood to be 0.5 with respect to duct velocity which may be assumed at 20 m s^{-1}.

Scanned with CamScanner

CHAPTER III

MINE CLIMATE

3.1 PHYSICAL PROPERTIES OF MINE AIR

Mine air is essentially a mixture of permanent gases like oxygen and nitrogen, with some water-vapour. At the prevalent temperatures and pressures in the mines it behaves as an ideal gas. The percentages of cxygen and nitrogen in mine air rarely vary much from the usual, but the moisture content changes substantially depending on physical conditions.

3.2 PRESSURE

Pressure of a fluid on a surface with which it is in contact is the normal force exerted by the fluid per unit area of the surface. Pressure can be expressed in absolute measure when it gives the difference in the pressure of the fluid and that of complete vacuum. Often pressure is expressed with reference to the local atomspheric pressure as datum in which case it is called the *gauge pressure*. Gauge pressure is in fact the difference between the absolute pressure and the atmospheric pressure.

Pressure can again be divided into (a) *static pressure* and (b) *velocity pressure* the sum of the two being called the total pressure. The static pressure of compressed air inside a sealed vessel is shown on a pressure gauge or manometer connected to the vesse! at any point. It acts equally on all directions. If a hole is made in the wall of this vessel, air rushes out with a velocity depending on the static pressure inside the vessel. If the vessel wall is thin, the entire static pressure P_s is converted to velocity pressure P_v given by the expression $P_v = \rho v^2/2$ where v is the velocity of flow through the hole and ρ=density of air.

On the other hand if the air is let out from the pressure vessel through a length of narrow pipe, a manometer connected to a normal hole in the wall of the pipe at a certain distance from its junction with the vessel will indicate a static pressure (a hole normal to the direction of flow will record no component of velocity pressure) lower than P_s by the velocity pressure of air in the pipe at

the point and the pressure loss between the vessel and the point of measurement because of flow.

The static pressure indicated above is positive since it is higher than the atmospheric pressure. If the vessel were evacuated, instead of being pressurized, to a pressure lower than the atmospheric, the static pressure in the vessel will be negative.

The S. I. unit of pressure is Pa (pascal=N m^{-2}) which equals kg m^{-1} s^{-2} in basic units. Water gauges are commonly used for measurement of ventilation pressure in mines and the readings are generally obtained in mm w.g., 1 mm w.g. being equal to g (=9.8) Pa.

Pressure is sometimes expressed in terms of *head* which is the height of a column of fluid exerting the pressure at its bottom. If we consider a column of air of density ρ and height h, the pressure P at its bottom is equal to its weight over unit area.

$$P = \rho hg,$$
$$\text{or } h = P/\rho g \tag{3.1}$$

3.3 BAROMETRIC PRESSURE

Barometric pressure or atmospheric pressure of air at any point is the weight of the column of atmospheric air per unit area over that point. Thus, it varies with the elevation of the point and the meteorological conditions. Barometric pressure at different depths or elevations can be determined from the following relation after Laplace.[42]

$$Z = \frac{K\alpha T(1+K_1 \cos 2\phi - K_2 \cos^2 2\phi)}{(1-0.378\, e/B)}\left(1+\frac{Z}{r}\right)\log\frac{B_2}{B_1} \tag{3.2}$$

where h_1 = elevation of the upper station in metres,
h_2 = elevation of the lower station in metres,
Z = $h_1 - h_2$,
B_1 = atmospheric pressure (the barometer reading after correction for temperature and gravity) at the upper station in kPa,
B_2 = atmospheric pressure at the lower station in kPa,
B = mean atmospheric pressure in kPa = $\frac{B_1+B_2}{2}$,
r = mean radius of the earth = 6367 324 m,

Scanned with CamScanner

T = mean temperature of the air column between the altitudes h_1 and h_2 in K.
e = mean vapour pressure of the air column in kPa,
ϕ = latitude of the station in rad,
K = barometric constant = 18 400 m,
α = coefficient of expansion of air = 0 003 665

and K_1 and K_2 are constants depending on the shape of the earth and are equal to 0.002 64 and 0.000 007 respectively. The above relationship can be simplified with a reasonable degree of accuracy compatible with mining calculations to

$$Z = 67.4\, T \log (B_2/B_1) \tag{3.3}$$

At mean sea level at $\pi/4$rad (45°) N latitude and at 273.15 K (0°C) temperature the mercury barometer reads 760mm. Taking density of Hg = 13 596 kg m^{-3} at 273 15 K and g (acceleration due to gravity) = 9.806 65 m s^{-2}, this pressure is equal to 0.76 × 13.596 × 9.806 65 = 101.33 kPa = 1013.3 mbar (millibar). Thus 1 mm Hg = 1.333 3 mbar = 133.33 Pa.

The atmospheric pressure is accurately measured by a mercury barometer. This essentially consists of a trough of mercury, over which is inverted a graduated tube filled with mercury. The tube is sealed at the upper end and the open lower end is under mercury in the trough. The pressure of the mercury column in the tube at its base then balances the atmospheric pressure, which is read directly in terms of the height of the column.

3.3.1 Fortin Barometer

This is the commonest type of mercury barometer. It consists of a glass tube encased in a brass tube which protects the glass and carries the graduated scale. The glass tube is inverted over a cistern containing mercury. The level of mercury in the cistern can be varied by an adjusting screw so that the level can always be set to the zero of the scale. This enables the scale on the brass tube to read the height of the mercury column directly.

3.3.2 Kew-pattern Barometer

This, on the other hand, has a fixed cistern where the level of mercury in the cistern can not be adjusted. So, when the level of mercury in the tube changes due to variation of barometric pressure there is a change in the level of mercury in the cistern also. The

amount of this change depends on the relative diameter of the cistern. If A_1 is the internal cross-sectional area of the tube and A_2, that of the cistern (excluding the outer cross-sectional area of the tail of the tube), then a rise of 1 mm in the tube will cause a fall of A_1/A_2 mm in the cistern so that the total rise in the barometer reading will be $(A_1+A_2)/A_2$ mm. Or, in other words, for a barometric rise of 1 mm, the level of mercury in the tube will rise by $A_2/(A_1+A_2)$ mm. To avoid computation after reading, the scale in such a barometer is graduated in units of $A_2/(A_1+A_2)$ standard units so that it gives the barometric reading directly. The value of $A_2/(A_1+A_2)$ is usually kept between 0.95 and 0.99.

Mercury barometer readings have to be corrected for temperature and gravity in order to get the atmospheric pressure in standard units, i.e. reduced to standard conditions of temperature and gravity (273.15 K and 9.806 65 m s^{-2}). The temperature correction is given by the relation

$$c_T = -\frac{B(\alpha_m - \alpha_b)(T-273.15)}{1+\alpha_m(T-273.15)} \tag{3.4}$$

where c_T = temperature correction in kPa,
B = observed barometer reading in kPa,
α_m = coefficient of expansion of mercury = 0.000 1818,
α_b = coefficient of linear expansion of brass = 0.000 0184,
and T = temperature in K.

The gravity correction is given by the equation

$$c_g = \frac{B'(g_1-g_0)}{g_0} \tag{3.5}$$

where c_g = gravity correction in kPa,
g_1 = gravity at the place of observation,
B' = observed barometer reading corrected for temperature
and g_0 = standard gravity, i.e. average gravity at m.s.l. at $\pi/4$ rad (45°) N latitude = 9.806 65 ≃ 9.81 m s^{-2}.

g_1 can be measured or calculated from the relation

$$g_1 = g_0\,(1-0.002\,64 \cos 2\phi + 0.000\,007 \cos^2 2\phi) - 3.086\times10^{-6}\, h \tag{3.6}$$

Scanned with CamScanner

where ϕ is the latitude in rad and h, the altitude of the place above mean sea level in metres.

Example 3.1

A Fortin barometer installed at a mine reads 99.72 kPa. Calculate the atmospheric pressure at the mine, if the mine is located at an altitude of 330m from the mean sea level at 0.337 rad (19°–20′) N latitude. The thermometer on the barometer records a temperature of 294.15 K.

Correction for temperature from equation 3.4

$$= -\frac{99.72\ (0.000\ 1818-0.000\ 0184)\ (294.15-273.15)}{1+0.000\ 1818\ (294.15-273.15)} = -0.34 \text{ kPa.}$$

Value of g from equation 3.6

$$= 9.806\ 65\ \{1-0.002\ 64\times\cos\ (2\times0.337) + 0.000\ 007\times\cos^2\ (2\times0.337)\} - 3.086\times10^{-6}\times330$$

$$= 9.785\ 45 \text{ m s}^{-2}.$$

Correction for gravity$=(99.72-0.34)\ (9.785\ 45-9.806\ 65)/9.806\ 65$
$= -0.22$ kPa.

So, corrected barometer reading or the atmospheric pressure
$=99.72-(0.34+0.22)=99.16$ kPa.

3.3.3 Aneroid Barometers

Mercury barometers have an accuracy of $\pm$ 0.025 mm Hg or $\pm$ 3.33 Pa, but are not very portable or sturdy in construction. Hence for mining purposes, aneroid barometers are commonly used. The aneroid (Fig. 3.1) consists of a concentrically corrugated, evacuated chamber normally kept from collapsing by a spring inside it. It, however, collapses or expands under increasing or decreasing atmospheric pressure, the distortion being transmitted through a sensitive spring and a series of levers and chains to a pointer moving on a graduated scale. The distortion is thus magnified about 200 times and can be easily read. The accuracy of aneroids is of the order of $\pm$ 6.66 Pa. In more sensitive instruments measuring smaller ranges of pressure, the accuracy has been improved to $\pm$3.33 Pa.

However, the aneriod is subject to errors due to the following:

(a) *Creep*. This is the reading of the barometer lagging behind the actual pressure when there is a considerable change of pressure.

The error due to creep depends on the amount of change of pressure and the time allowed before taking the reading. For accurate reading, sufficient time commensurate with the pressure change should be allowed before taking a reading with an aneroid.

(b) *Set*. Sometimes a major change in temperature or pressure may cause a permanent set in the distortion of the chamber thus necessitating frequent checking of the instrument against a standard control instrument, particularly when working over a large range of temperature and pressure.

(c) *Variation of Temperature*. This can affect the reading of the aneroid substantially if the change in temperature is large. Normally, aneroids are suitably compensated for temperature by incorporating a bimetallic link in its design or by leaving a certain volume of gas inside the collapsible chamber, but even with temperature-compensated aneroids, it has been found that a variation of temperature of 14 K can cause an error of 66.6 Pa. This error again varies with pressure. Thus, it is necessary to correct the barometer reading in accordance with the calibration of the instrument at known temperatures.

Paulin Aneroid and Askania Statoscope. Both of these (the latter covering a small range of pressure) try to avoid the error due to creep. Here, the distortion of the diaphragm is brought back to

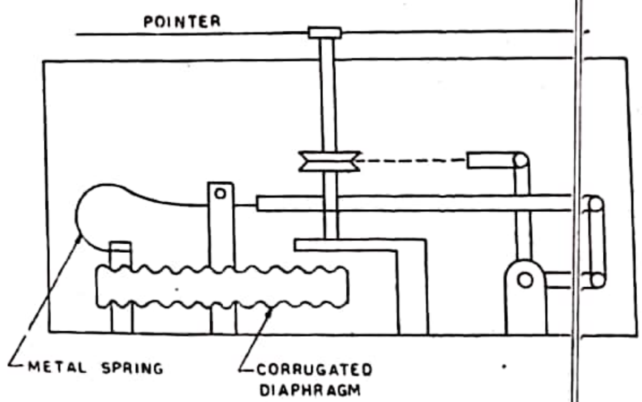

Fig. 3.1 Aneroid barometer (diagrammatic)

Scanned with CamScanner

zero by varying the tension on a sensitive spring. Hence the diaphragm is always kept at the null position and the reading of pressure obtained from the amount of adjustment to the spring. Fig. 3.2 shows an Askania statoscope. When the collapsible chamber D is acted upon by pressure (say high pressure) the pointer P moves down the scale S which has a range of only 66.6 Pa. By adjusting the knob K, the tension of the spring can be suitably varied so as to bring back the pointer to the zero position. The turning of the knob is recorded on the scale S' which is directly graduated in the units of barometric pressure.

3.3.4 Barographs

These are used for continuous recording of the atmospheric pressure. They utilize the same principle as the aneroid and consist

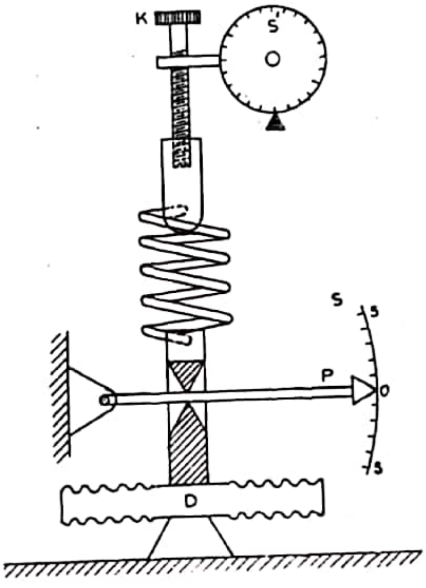

Fig. 3.2 Askania statoscope.

of a series of evacuated chambers which increase their sensitivity so that the distortion can be utilized to work a marker pen on a continuously moving chart that records the barometric pressure.

3.3.5 Hypsometers

Hypsometers are not used for mining purposes as accurate temperature measurement is not possible underground. It should be noted that a change in pressure of the order of 100 Pa changes the boiling point of water by only 0.03 K.

As a rough rule barometric pressure is taken to rise at the rate of 10.9 Pa per metre depth.

3.4 TEMPERATURE

Temperature of mine air is commonly measured by a mercury thermometer. Alcohol thermometers, though more sensitive because of the coefficient of expansion of alcohol being six times as high as that of mercury, are much less accurate. Alcohol has, however, a lower freezing point of 173 K as compared to about 233 K of mercury and alcohol thermometers find more suitable use in low-temperature ranges. Normally, temperature of mine air refers to the dry-bulb temperature. To get a correct reading of the dry-bulb temperature of the air the thermometer should be held at least 315 mm away from any surface so that the reading is not affected by the heat radiated to or from the surface. The bulb of the thermometer should also be perfectly dry. The sensitivity of thermometers commonly used in mines varies from 0.2 to 0.5 K as the thermometers of higher sensitivity usually cover a smaller range of temperature.

Sometimes in the assessment of the environment in a narrow space underground where radiation of heat from the rock walls is significant it may be necessary to measure the *radiant temperature*. This may be done by covering the thermometer bulb by a black globe.

3.5 SOURCES OF HEAT IN MINE AIR

3.5.1 High Temperature of Surface Air

Surface air entering the mine can carry with it some heat if the surface temperature is high compared to the underground temperature.

3.5.2 Heat due to Auto-compression

As the air descends the downcast shaft, it gets compressed by the weight of the shaft air-column approximately at the rate of 1.1 kPa per 100m depth and its potential energy is converted to heat energy. Provided no work is done by the air descending the shaft, (i.e. the flow is frictionless and non-accelerative) and no heat or moisture is lost or gained by the air, the compression of air in the downcast shaft will be reversible adiabatic following the relation

$$\frac{T_2}{T_1} = \left(\frac{P_2}{P_1}\right)^{\frac{\gamma-1}{\gamma}} = \left(\frac{V_1}{V_2}\right)^{\gamma-1} \quad (3.7)$$

where T = temperature in K,
γ = C_p/C_v = 1.404 for dry air (γ varies slightly with the moisture content of air, but for mining purposes it can be taken as equal to 1.4),
V = specific volume (volume of unit mass of air),
P = barometric pressure and subscripts 1 and 2 indicate the state of air at the shaft-top and -bottom respectively.

The rise in temperature due to auto-compression at any depth can be determined from equation 3.7 by finding the barometric pressures at the shaft-top and at that depth (the latter can be found from equation 3.2) or from specific volumes (or densities, since density $\rho = \frac{1}{V}$) at the two points. Under similar assumptions, the rise in temperature due to auto-compression can also be obtained by equating the potential energy with enthalpy change (see the general energy balance equation 4.1. Under the assumptions made $dQ=0$ as no heat is transferred, $dW=0$ as no work is done and $dKE=0$ as the flow is non-accelerative so that $dH=-dPE$)

$$hg = \Delta H = C_p \Delta T \quad (3.8)$$

where ΔT = rise in temperature in K,
ΔH = change in enthalpy, J kg^{-1}
h = depth of shaft in m
and C_p = specific heat of air in J kg^{-1} K^{-1}.

The rise of temperature with depth by auto-compression as given by equations 3.7 and 3.8 does not change when there is friction in the shaft resulting in a pressure drop. The whole process can then be considered as frictional adiabatic, a combination of reversible adiabatic compression from P_1 to P_2 resulting in a rise in temperature from T_1 to T_2 coupled with an irreversible adiabatic expansion at constant temperature T_2 from P_2 to P_3, P_2-P_3 being the shaft pressure drop.

Taking g=9.81 m s^{-2} and C_p =1005 J kg^{-1} K^{-1} in equation 3.8, it is seen that the rise in the dry-bulb temperature of air due to auto-compression is 0.976 K per 100m depth.

The *wet-bulb temperature* of air also rises with depth, though at a lesser rate depending on the surface dry-bulb and wet-bulb temperatures. For prevalent summer conditions in India the wet-bulb temperature may rise at the rate of 0.3 to 0.25 K for every 100m depth. The above rates of rise in air temperature hold when there is no addition of moisture in the shaft, but with the evaporation of moisture in the shaft, the rate of increase in the dry-bulb temperature with depth falls sharply. In such cases the adiabatic index γ in equation 3.7 may be replaced by a variable polytropic index n. In dry shafts n approaches γ, but in wet shafts n can be equal to 1 (isothermal compression) or even less than 1 because of evaporation of water in the downcast shaft which lowers the dry-bulb temperature. Observations at a very wet Indian mine (Chinakuri No. 1 and 2 pits) give a value of n=0.905 in November and 0.709 in April in the downcast shaft. This is because there is a fall in the dry-bulb temperature of the air as it descends from the surface to the pit-bottom owing to excessive evaporation, even though the shaft is fairly deep (611m).

In the upcast shaft however, n has a higher value of 1.25, since the upcast air is almost saturated with water so that its temperature is not affected by evaporative cooling. For similar reasons, the polytropic index is lower in summer, when the air, being at a higher temperature, is able to evaporate more moisture in the shaft.

It must be remembered that in wet downcast shafts, though there may be only a very small rise (there may even be a fall in very wet shafts) in the dry-bulb temperature, there is indeed a substantial amount of latent heat added to the mine air. The rate of rise in wet-bulb temperature remains the same irrespective of the amount of moisture added in the shaft, unless of course there is heat transfer from the strata in addition to heating due to auto-compression.

Scanned with CamScanner

In old rock formations like those of the Kolar Gold Field the geothermal gradient is flat so that the rise in rock temperature with depth almost equals the rise in air temperature due to auto-compression, so that the heat transfer from the strata in the downcast shaft is insignificant compared to the heat of auto-compression. But in the coal fields where the geothermal gradient is steep, there may be substantial heat transfer from the strata as the depth increases. This will cause a steeper rise in the wet-bulb temperature so that intolerable wet-bulb temperatures may be obtained at the downcast shaft-bottom at relatively shallower depths compared to the Kolar Gold Field.

Similar to the heating of air due to auto-compression in the downcast shaft, adiabatic expansion and consequent cooling take place as the upcast air ascends to the surface. However, since most mine workings are concentrated at the bottom levels, the cooling through adiabatic expansion compensates for only a small fraction of the heat gained by adiabatic compression. On the Witwatersrand Gold Field this compensation was about 16.7% at a depth of 1829m and only 11.1% at a depth of 2743m.

3.5.3 Heat from Rock

Heat flows out of the hot core of the earth at almost a constant rate of 0.05 W m^{-2} over most of the earth's surface. As a result, the rock temperature is found to rise as we go deeper down the earth's crust. The rate of increase of temperature with depth is called the *geothermic gradient*. The geothermic or geothermal gradient varies from place to place and is dependent on the physical properties of the rock such as thermal conductivity, specific heat and density which govern the rate of heat transfer in the rock. The geothermic gradient is steeper, or the rise in temperature with depth faster for rocks of lower thermal conductivity such as coal-measure rocks than for rocks of higher thermal conductivity. Other minor factors which affect the geothermic gradient are the age of the rock and the presence of dykes, sulphide ore bodies etc. nearby. The surface air temperature at any place varies during the course of the year, but the ground temperature at a depth of about 15m from the surface remains constant throughout the year. This temperature is usually the average annual temperature at the surface and hence varies from place to place depending on the climate. It is 301.5 K on the Kolar Gold Field but only 277.6 K in the Canadian

gold mining districts. The geothermic gradient at any place is thus the rate of rise in temperature above this temperature.

Table 3.1 gives the geothermic gradient in some mining districts of the world, although a range varying from 1K/11m to 1K/140m has been recorded.

Table 3.1 : Geothermic Gradient in Various Mining Districts of the World

Mining district	Geothermic gradient
Lancashire coalfields, U.K.	1K/34 m
Hollinger and McIntyre, Canada	1K/122.4 m
Witwatersrand, S. Africa	1K/109.8 m
Kolar Gold Field	1K/91.1 m
Indian coalfields	1K/38.4 m

Geothermic gradient is determined by observing the virgin-rock temperature at various depths in a mine. For obtaining accurate virgin-rock temperatures, readings should be taken at the bottom of boreholes where the temperature of the rock is not affected by ventilating air-currents. The depth of the borehole required for accuracy depends on the time for which the rock face has been exposed. On the Witwatersrand Gold Field it has been found that the minimum depth of boreholes required for accuracy is 9m. It can be reduced to 6m in case of freshly exposed rock surfaces, but for good results, a hole of 15-30m depth is recommended. The United States Bureau of Mines,[43] on the other hand, observes that the virgin-rock temperature can be measured approximately accurately by inserting a 250mm long psychrometric thermometer mounted in a groove on a 19mm diameter wooden rod into a 1.5-1.8m deep drillhole at a rapidly advancing face. An allowance of one hour after the drilling is made for the dissipation of the heat of drilling in the rock. Ten minutes are sufficient for the thermometer to pick up the rock temperature and the fall of temperature on withdrawal of the thermometer from the hole is very slow so that a quick reading gives the rock temperature with a reasonable

Scanned with CamScanner

accuracy. The rate of cooling of the thermometer can be further reduced by covering the bulb of the thermometer with a heat insulating material such as rubber. The accuracy is, however, much hampered if cooled air circulates at the face at a high velocity. Similar results have been obtained at North Staffordshire Colliery, U.K.,[64] where 1.2m long and 44mm diameter blastholes in coal were sufficient to record the virgin-rock temperature satisfactorily provided the rate of advance of the heading was maintained at 0.9m day^{-1}. It was found that at a depth of 0.9m, the strata temperature was not affected by the air temperature over a period ranging from 2 to 17 hours of exposure, as long as the difference between the strata temperature and the air temperature did not exceed 10 K. The measurement of temperature in this case was done with a sensitive thermocouple.

The South African practice[43] is more accurate and uses a finely graduated maximum thermometer inserted in a groove on a 32mm diameter wooden rod (Fig. 3.3). The thermometer is chilled in an ice box before inserting in the hole which should be 38mm in diameter. The bulb and the portion of the stem where the thermometer is to be held by fingers are covered by rubber sleeves in order to insulate them against sudden rise of temperature. The borehole should be properly cleaned. A dry hole is preferred to a wet hole. The thermometer is inserted at the bottom of the hole by screwing in the required number of extension rods to the one holding the thermometer and pushing it inside the hole. It is left inside the hole for at least 48 hours (sometimes even for four days) before it is taken out, chilled and read.

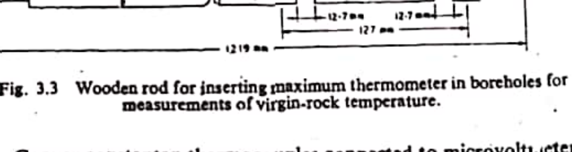

Fig. 3.3 Wooden rod for inserting maximum thermometer in boreholes for measurements of virgin-rock temperature.

Copper-constantan thermocouples connected to microvoltmeters or thermisters connected to a suitable bridge circuit can be used instead of thermometers for rock temperature measurement. The

thermocouple or thermister head is embedded in a short metallic cylinder which is inserted into a borehole in the rock with the help of a mounting rod or tube. Digital quartz thermometers which give a digital indication of the temperature down to 0.001 K can also be used for rock temperature measurement. They utilize the change in resonant frequency of quartz crystal with temperature and give a linear temperature characteristic They are not affected by noise and cable resistance.

In virgin areas deep prospecting boreholes are commonly used for the measurement of the virgin-rock temperatures at regular depth intervals with the help of suitable temperature probes.

Heat Transfer from the Rock to the Mine Air. This is mainly through direct heat transfer from the exposed rock surface to the air. When the rock surface is dry, the heat transfer is mainly through convection and raises the sensible heat of the air, but when the rock surface is wet a substantial amount of water evaporates into the air thus leading to both sensible and latent heat transfer.

In very wet mines where a lot of water may flow out of the strata, a substantial amount of strata heat is transferred to the air through the strata water flowing along the airways to the pit-bottom sumps. The strata water oozes out almost at the virgin-rock temperature and by the time it reaches the sumps, it may attain a temperature equal to or slightly higher than the return air temperature so that the heat transfer through strata water equals $C_{pw}(T_v - T)$ (where C_{pw} =specific heat of water, T_v =virgin-rock temperature and T=temperature of water entering the sump) per unit mass of water flowing out.

Direct heat transfer from the rock to the mine air is governed by the rate of heat transfer within the rock mass and the heat transfer from the rock wall of the excavation to the mine air. The rate of sensible heat transfer from the rock wall to the air is a linear function of the difference between the temperature of the rock wall and the mean air temperature as well as the *coefficient of heat transfer*

$$q=\alpha(T_s-T_a) \tag{3.9}$$

where q = rate of heat transfer, i.e. the amount of heat flow per unit area per unit time,

α = coefficient of heat transfer and T_s and T_a are teh rock-wall and air temperatures respectively.

Scanned with CamScanner

The coefficient of heat transfer or the *thermal emmisivity* is a complex function of the properties of the rock surface, the moisture content, temperature and velocity of air as well as the size of the airway.

Quasi-empirical relations based on Reynolds' analogy have been developed for predicting values of α for turbulent flow in pipes and these can be used for mine airways for accurate estimation of α. One such relation due to Colburn[67] is as follows :

$$St \cdot Pr^{\frac{2}{3}} = \frac{f}{8} \tag{3.10}$$

where St = Stanton number

$$= \frac{\alpha}{C_p G} = \frac{\alpha}{C_p\ \rho_a v},$$

C_p = specific heat of air at the mean air temperature.

G = mass velocity = $v\ \rho_a$,

ρ_a = average density of air,

v = average velocity of flow,

Pr = Prandtl number

$$= \left(\frac{\mu\ C_p}{k_a}\right)_F,$$

k_a = thermal conductivity of air,

μ = viscosity of air,

f = Darcy-Weisbach resistance coefficient of the airway and subscript F denotes the values of the fluid properties at the arithmetic average of the surface and mean air temperatures often referred to as the *film temperature*.

For prevalent temperatures in mine airways Pr can be taken equal to 0.72 so that equation 3.10 reduces to

$$\alpha = \frac{f\ C_p\ \rho_a v}{6.4} \tag{3.11}$$

The rate of heat-flow in the rock is a complex function of the thermal diffusivity of the rock, the difference in the rock and the air temperature, thermal emmisivity of the rock surface, the distance from the rock wall and the time of cooling.

The *thermal diffusivity* of a rock is given by the relation

$$d = \frac{k}{C\rho} \tag{3.12}$$

where d = thermal diffusivity of the rock,

k = thermal conductivity of the rock,

C = specific heat of the rock

and ρ = density of the rock.

Coefficient of thermal conductivity or simply *thermal conductivity* is defined as the amount of heat-flow through a unit thickness of material over an unit area per unit time for a unit temperature difference and is given by the equation $q = kAt.\ dT/l$,

where q = amount of heat flowing,

A = area,

t = time,

dT = temperature difference

and l = thickness of material.

Thermal conductivity depends on the isotropy of the rock (anisotropic rocks have different coefficients of thermal conductivity in different directions : as for example, the conductivity along bedding planes in sedimentary rocks or cracks and cleavages in other rocks is more than that across them), temperature and pressure of the rock and the nature of the rock. The coefficient of thermal conductivity is the highest for metals and the lowest for gases. For rocks, it depends to a large extent on the pore space, the more porous rocks having less thermal conductivity. Table 3.2 gives the thermal conductivity and thermal diffusivity for various rocks.

Increase in temperature causes decrease in thermal conductivity to the tune of 0.225–0.306% per K for most rocks except for coal where there is an increase of thermal conductivity at the rate of 0.104% per K. Pressure increases thermal conductivity and it has been found that the rate of increase of thermal conductivity with pressure for fine-grained sandstone is of the order of 1% per 6.9 MPa.

Scanned with CamScanner

Table 3.2 : Thermal Conductivity and Thermal Diffusivity of Rocks[5]

Rock	Thermal conductivity, (kJ m^{-1} s^{-1} K^{-1}) $\times 10^{-4}$	Thermal diffusivity, (m^2 s^{-1} $\times$ 10^{-7})
Granite	18.84-27.21	9.0-13.0
Diorite	23.03	12.0
Gneiss	22.19	12.0
Quartzite	37.26-75.78	16.0-33.0
Limestone	18.00-28.89	8.0-13.0
Sandstone	20.93-28.89	10.0-14.0
Shale	7.95-19.26	4.0-9.6
Siltstone	15.91	7.8
Coal	3.56-4.61	2.2-2.8
Sand	2.60	2.4
Broken shale	1.88	3.3
Broken coal	0.71-1.05	1.6-2.3

When a fresh opening is made in a mine, there exists a large difference of temperature between the rock wall and the air as a result of which heat flows into the air at a very high rate and the rock, in turn, is cooled to a certain distance. With time, the rock gets cooled to a greater distance and the rock-wall temperature falls so that the rate of heat-flow decreases. In active mines therefore, the maximum amount of heat is transferred from the rock to the mine air in stopes where large virgin-rock surfaces are continually exposed to the air-current. Roadways have a fairly high rate of heat transfer initially but the rate falls with the ageing of the airway.

Heat Transfer in Mine Airways. Let us, as an ideal case, consider a mine airway to be a hollow circular cylinder surrounded by an infinite homogeneous mass maintained at a constant temperature T_v (virgin-rock temperature). If now a current of air at temperature T_a enters the cylinder, it can be shown mathematically that at any

time t the temperature T_s of the surface of the airway at the entrance will be given by the equation

$$T_s - T_a = (T_v - T_a)\,\phi\,(x,y) \qquad (3.13)$$

where $\phi\,(x, y)$ is a function of x and y,

$$x = \frac{kt}{C r^2 \rho}\ , \text{ and } y = \frac{r\alpha}{k}$$

and r = radius of the airway.

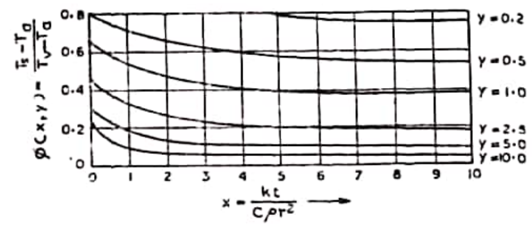

Fig. 3.4 Value of ϕ (x, y) for various values of x and y (after Hitchcock and Jones).

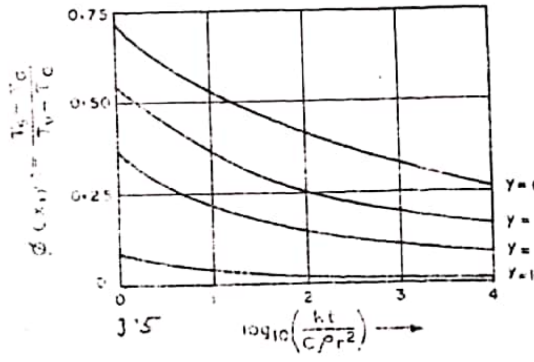

Fig. 3.5 Value of ϕ (x, y) for various values of x and y (after Hitchcock and Jones).

Figs. 3.4 and 3.5 show the value of $\phi\,(x, y) = (T_s - T_a)/(T_v - T_a)$ for various values of x and y as computed by Jaeger and Hitchcock and Jones.[65] It will be seen from the figures that with increase of time, T_s falls at first rapidly and then slowly so that after the lapse of an inifinitely large time, T_s approaches T_a when the heat-flow from the strata to the air ceases. The rate of heat transfer q from the strata to the air at any time at the entrance of the airway is given by the equation

$$q = \alpha (T_s - T_a)$$
$$= \alpha (T_v - T_a)\, \phi (x, y) \qquad (3.14)$$

As the air moves along the airway it picks up heat from the strata and its temperature rises. If we consider a small length of airway dL in traversing which there is a rise of dT in the temperature of air, then

$$qpdL = Q\rho_a C_p\, dT \qquad (3.15)$$

where p = perimeter of the airway
and Q = quantity of air flowing per unit time.

Combining equations 3.14 and 3.15 we have

$$\frac{dT}{T_v - T} = \frac{pky\phi (x, y)\, dL}{Q\rho_a\, C_p r} \qquad (3.16)$$

where T is the air temperature at any point along the airway.

The air temperature T_L at any time t at a distance L from the entrance of the airway is given by integrating equation 3.16 between the limits 0 and L.

Or,

$$T_v - T_L \approx (T_v - T_o)\, e^{-\frac{pky\,\phi (x, y)\, L}{Q\rho_a\, C_p r}} \qquad (3.17)$$

This equation has been found by Hitchcock and Jones[65] to satisfactorily predict air temperatures along an experimental dry airway. Equation 3.17 shows that as the distance increases, the temperature of air rises rapidly in the beginning and then slowly until T_L approaches T_v when L tends to infinity. Again it is seen that the greater the value of Q, the less is the value of T_L, which suggests that circulation of a large quantity of air through an airway of a certain length helps in keeping the air temperature down. Hitchcock and Jones found that the temperature at a point in a drive fell to 300.9 K after two years of development, the virgin-rock temperature being 302.9 K; but after only 6 days of completion of the drive and establishment of through ventilation in it, the temperature fell to 297.4 K. This is because of the fact that during

development, the volume of air circulating in the drive was much smaller (only 2.3 $m^3\,s^{-1}$ producing an air velocity of only 0.15 m s^{-1}) than when through ventilation was established in it.

Also we see that in deep and hot mines, it is desirable to conduct the air to the face in the shortest intake with a minimum cross-sectional area so that the surface area through which heat transfer takes place is minimized. Smooth airway surfaces reduce heat transfer and hence are desirable for intakes. The high power cost of ventilation through an intake of reduced cross-section can be partly compensated by increasing the size of the return airway or having multiple return airways. This causes greater heat transfer in the return airways which is rather desirable, since it aids natural ventilation by heating up the return air.

The above considerations apply to dry airways only. If, however, moisture evaporates from the surface of the airway, it considerably increases the rate of heat transfer by extracting the latent heat of evaporation from the rock. As a result, the circulating air picks up a greater amount of heat.

The combined sensible and latent heat transfer in wet airways is given by the relation[68]

$$q = \alpha (T_s - T) + f_w\, l\, \epsilon \{e'(T_s) - e\} \qquad (3.18)$$

where T = dry-bulb temperature of air,
f_w = fraction of airway surface that is wet,
l = latent heat of evaporation of water,
ϵ = coefficient of mass transfer,
$e'(T_s)$ = saturation vapour pressure at T_s which can now be considered as an overall surface temperature for both dry and wet portions of the rock
and e = vapour pressure of air.

At commonly prevalent temperatures in mines (290-310 K) $e'(T_s)$ can be given by the approximate relation

$$e'(T_s) = a\, T_s^2 + b\, T_s + c \qquad (3.19)$$

where a, b and c are constants having values of 0.002 133, −1.121 64 and 147.83 respectively with T_s in K and e' in kPa.

e is given by the relation

$$e = 461.9 \times 10^{-6}\, m'T \text{ kPa} \qquad (3.20)$$

where m' = absolute humidity in g m^{-3}.

Scanned with CamScanner

The coefficient of mass transfer is a similar function of flow parameters as the coefficient of heat transfer.
The Stanton number in equation 3.10

$$St = \frac{Nu}{Re \cdot Pr} \tag{3.21}$$

where Nu = Nusselt number $= \frac{\alpha D}{k}$,

D = airway diameter

and Re = Reynolds number of flow

$= \frac{v D \rho_a}{\mu}$.

A similar group to the one on the right hand side of equation 3.21 i.e. $Sh/(Re . Sc)$ can be used to correlate the mass transfer coefficient.

Similar to the Colburn heat transfer equation 3.10 we can write for mass transfer

$$\frac{Sh}{Re . Sc} \cdot Sc^{2/3} = \frac{f}{8} \tag{3.22}$$

$$\text{Or, } \left(\frac{\epsilon R T P_{am}}{v B}\right)\left(\frac{\mu}{\rho_a D_m}\right)^{0.67} = \frac{f}{8} \tag{3.23}$$

where Sh = Sherwood number $= \frac{\epsilon R T P_{am} D}{D_m B}$,

Sc = Schmidt number $= \frac{\mu}{\rho_a D_m}$,

R = gas constant for air = 287.1 J kg^{-1} K^{-1},

T = temperature of air (mean),

P_{am} = logarithmic mean partial air pressure

$= \frac{(B-e)-(B-e')}{ln \frac{(B-e)}{(B-e')}}$,

B = atmospheric pressure,

e' = saturated vapour pressure at the temperature of the evaporating film of water,

e = vapour pressure of air flowing

and D_m = mass diffusivity of water-vapour into air = 0.092 m^2 h^{-1} at 298 K.

Since values of e' and e are relatively small compared to that of B,

the ratio P_{am}/B can be taken equal to unity in which case equation 3.23 reduces to

$$\epsilon = \frac{f}{8}\left(\frac{v}{RT}\right)\left(\frac{\rho_a D_m}{\mu}\right)^{0.67} \tag{3.24}$$

In terms of the heat transfer coefficient,

$$\epsilon = \left(\frac{\alpha}{C_p \rho_a}\right)\left(\frac{B}{R T P_{am}}\right)\left[\left(\frac{C_p \mu}{k_a}\right)\left(\frac{\rho_a D_m}{\mu}\right)\right]^{0.67} \tag{3.25}$$

The variation in the dry-bulb temperature along the airway can now be obtained from equation 3.15 which can be rewritten as

$$p\alpha (T_s - T)\, dL = \rho_a C_p Q dT \tag{3.26}$$

Similarly the rise in the absolute humidity of air along the airway can be written as

$$f_w p \,\epsilon\, [e'(T_s) - e]\, dL = Q\, dm' \times 10^{-3} \tag{3.27}$$

$$\text{or, } f_w p \,\epsilon\, [a T_s^2 + b T_s + c - 461.9 \times 10^{-6}\, m'T]\, dL = Q\, dm' \times 10^{-3} \tag{3.28}$$

substituting the values of $e'(T_s)$ and e from equations 3.19 and 3.20 respectively.

The solution of the above differential equations needs the estimation of T_s at different times. This can be done by adopting the standard solution given by equation 3.13 provided a notional value of T_a is adopted taking into account both sensible and latent heat transfer. This can be done by combining equations 3.9 and 3.18, so that

$$T_a = T - \frac{f_w l \epsilon}{\alpha}[e'(T_s) - e] \tag{3.29}$$

Evaluation of T_s from equation 3.13 assuming current value of air temperature for T_a ignores the cooling history of the airway. Starfield[68] developed the following approximate relation based on Duhamel's theorem for taking into account the cooling history of the airway which can be solved numerically :

$$T_{s_n} = T_s [1 - \phi(x, y)] + \frac{1}{2} \sum_{i=0}^{n-1} \left(T_{a_i} \; T_{a_{i+1}}\right)[\phi(x, y)_{n-1} - \phi(x, y)_{n-i-1}] \tag{3.30}$$

where the subscript n denotes the value of a variable at a time $n\,\delta t$ after the opening of the airway, δt being a given interval of time.

Scanned with CamScanner

For the same moment of time equation 3.29 can be written as

$$T_{a_n} = T_n - \frac{f_w\, l\, \epsilon}{\alpha}\left[aT^2_{s_n} + b\, T_{s_n} + c - 461.9\times 10^{-6}\, m'_n\, T_n\right] \quad (3.31)$$

Thus T_a for any moment of time (say, the present) can be built up from equations 3.30 and 3.31 at the start of the airway where $L = 0$, if the air temperature and humidity at the time of commissioning of the airway is known.

For variations along the airway let us denote the value of the variables at a distance δL from the start of the airway by an asterisk, e.g. T_n^*. Assuming the variations to be nonlinear, the following equations can be written for the values of T_n^* and m'^*_n :

$$T_n^* = T_n + \tfrac{1}{2}\,\delta L\left(\frac{dT_n}{dL} + \frac{dT_n^*}{dL}\right) \quad (3.32)$$

and $$m'^*_n = m'_n + \tfrac{1}{2}\,\delta L\left(\frac{dm'_n}{dL} + \frac{dm'^*_n}{dL}\right) \quad (3.33)$$

These equations in conjunction with equations 3.26 and 3.27 as well as equations 3.30 and 3.31 with and without asterisks lead to the solution of $T_{s_n}^*$, m'^*_n and T_a^* at $L=\delta L$. Similarly values of these variables can be built up for other values of L along the airway.

The method of solution is obviously very lengthy and needs the help of a digital computer. However, it is quite versatile in as much as it can incorporate variations in the values of f_w (i.e. wetness of the airway), the quantity of flow Q and the virgin-rock temperature T_v (this can occur along inclined airways) both along the airway as well as in time. Variations in input air temperature and humidity can also be accounted for. Addition of heat from other sources, such as auto-compression, machinery etc. can be taken into account by modifying equation 3.26 as follows

$$\{p\alpha\,(T_s - T) + q'\}\; dL = \rho_a\, C_p\, Q\, dT \quad (3.34)$$

where q' = rate of addition of heat from other sources over the length dL.

Somewhat simpler relations have been suggested by Ramsden for heat and mass transfer along wet roadways from which dry-bulb temperature and mixing ratio gradients along the roadway can be predicted. A wet roadway has been considered to have a portion of its surface dry with a surface temperature T_s and the remaining portion wet having a surface temperature T'_s which are approximately related to the dry- and wet-bulb temperatures of air (T and T' respectively) by the relation

$$T_s - T_s' = T - T' \quad (3.35)$$

An equation similar to 3.26 can be written as

$$p\alpha\,[(T_s - T)\,(1 - f_w) + (T_s' - T)\, f_w]\; dL = \rho_a\, C_p\, Q\, dT \quad (3.36)$$

T_s in the above equation can be obtained from equation 3.13 which can be written as

$$T_s = T + \phi\,(x,y)\,(T_v - T) \quad (3.37)$$

Combining equations 3.36 and 3.37, we have

$$\frac{dT}{dL} = \frac{p\alpha\phi\,(x,y)}{\rho_a\, C_p\, Q}\left[(T_v - T) - \frac{f_w}{\phi(x,y)}\,(T - T')\right] \quad (3.38)$$

The mixing ratio gradient is given by the relation

$$\frac{dm}{dL} = \frac{0.7\alpha_c\, p\, f_w}{B\,\rho_a\, Q}\left[e'(T_s') - e'(T)\right] \quad (3.39)$$

where α_c = convection heat transfer coefficient and is given by the relation

$$Nu = \frac{\alpha_c\, .\, D}{k_a} = 0.023\, Re^{0.8}\, .\, Pr^{0.4} \quad (3.40)$$

$$e'(T_s') = 0.6105 \exp\left[\frac{17.27\,(T_s' - 273.15)}{T_s' - 35.85}\right] \text{kPa} \quad (3.41)$$

$$e'(T) = 0.6105 \exp\left[\frac{17.27\,(T - 273.15)}{T - 35.85}\right] \text{kPa} \quad (3.42)$$

f_w in this set of equations as also in the equations of Starfield is an imponderable, difficult to estimate from visual observation of the roadway. It is best determined experimentally from heat transfer studies in actual roadways.

Heat Transfer in an Advancing Stope. A stope differs in shape from an ordinary airway and keeps on advancing into virgin rock. The rate of heat transfer in it depends on the rate of stope advance and time apart from the shape and size of stope and the rock and air characteristics. However, with a given rate of face advance, a 'recurring state' will be reached in the stope, characterized by a cyclic repetition of thermal gradient around the stope

Scanned with CamScanner

after each blast, a certain time after the start of the stope in virgin rock.

A simplified method of calculation of the rate of heat transfer in such a recurring state has been given by Starfield[89] by considering a short length of an idealized stope where the total amount of heat transferred has been taken as the sum of heat transferred from the face AB, hanging wall AD, footwall BC and the broken rock at the face (see Fig. 3.6). No heat transfer is assumed to take place beyond a certain distance from the face ($AD=l$) which approximately corresponds with the position of the scatter wall.

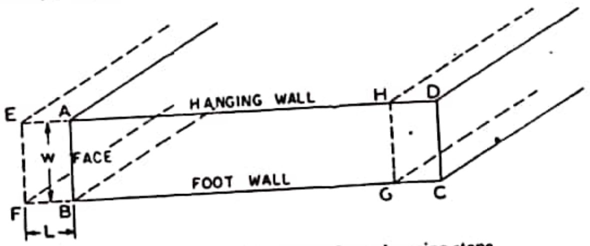

Fig. 3.6 Heat transfer model of an advancing stope.

The total flow of heat $q_F(t)$ from a unit length of face over the cycle time t is given by the relation

$$q_F(t) = Wk\int_0^t \left(\frac{\partial T}{\partial x}\right)_{x=0} dt \tag{3.43}$$

where W=height of face=AB,

x =distance ahead of face in the rock

ahd T =rock temperature.

The above expression can be evaluated with the help of a digital computor by solving the rock heat conduction equation

$$\frac{\partial^2 T}{\partial x^2} = \frac{1}{d}\cdot\frac{\partial T}{\partial t} \tag{3.44}$$

subject to the conditions

(i) $k\dfrac{\partial T}{\partial x} = \alpha(T - T_a)$ at $x=0$, where T_a = temperature of air entering the stope,

(ii) $T_{(x,t)} \to T_v$ the virgin-rock temperature as $x \to \infty$ and

(iii) $T_{(x,o)} = T_{(x+L,t)}$, where L=length of face advance in each cycle (condition for recurring state).

With faster rate of face advance $q_F(t)$ achieves a maximum value $q_{max}(t)$ given by the relation

$$q_{max}(t) = Wkth(T_v - T_o) f(h\sqrt{d.t}) \tag{3.45}$$

where $h = \dfrac{\alpha}{k}$.

The function f has been calculated and plotted by Starfield in Fig. 3.7. He has also calculated the value of $q_F(t)/q_{max}(t)$ for different rates of face advance and plotted it in Fig. 3.8 against two dimensionless parameters $L/\sqrt{d.t}$ and $h^2 d.t$ so that $q_F(t)$ can be calculated from $q_{max}(t)$ obtained from equation 3.45.

Heat transfer from hanging wall which is similar to that from foot wall is a two-dimensional problem and hence more difficult to solve even on a computer. A simplified approach has been given by Starfield who divides the stope width l to N sections each of length L so that $N = \dfrac{l}{L}$ and considers heat transfer from each section to be independent of the other.

In the recurring stage the total heat transfer from the hanging wall over a period t, $q_H(t)$ is given by the relation

$$q_H(t) = q_{max}(Nt)\,\frac{L}{W} \tag{3.46}$$

where $q_{max}(Nt)$ can be estimated from equation 3.45 by substituting Nt for t so that

$$q_H(t) = lk\,t\,h(T_v - T_o) f(h\sqrt{l d.t/L}) \tag{3.47}$$

$f(h\sqrt{l d.t/L})$ can be obtained from Fig. 3.7 by reading $h\sqrt{l d.t/L}$ in place of $h\sqrt{d.t}$.

The maximum amount of heat that can be transferred by broken rock at the face (for the condition where all the heat is transferred from the broken rock to the ventilating air before the former is removed from the face) is the difference between the heat content of the face rock (of a volume WL) and that transferred from the face over a period t.

Thus $q_R(t) = k\,W L(T_v - T_o)/d - q_F(t)$ (3.48)

Scanned with CamScanner

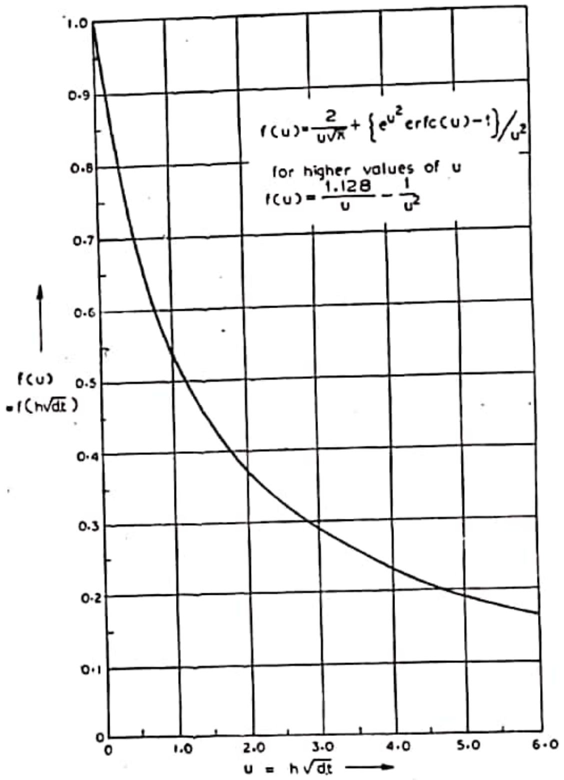

Fig. 3.7 $f(h\sqrt{d.t})$ vs $h\sqrt{d.t}$ (after Starfield).

where $q_R(t)$= maximum possible heat transfer from the broken rock.

The total heat transferred per unit length of face over the cycle time t is thus given by

$$q(t) = q_F(t) + 2q_H(t) + q_R(t) \tag{3.49}$$

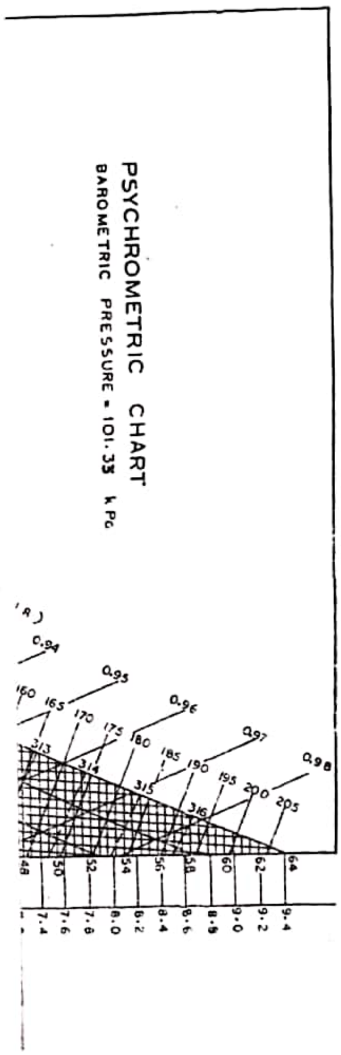

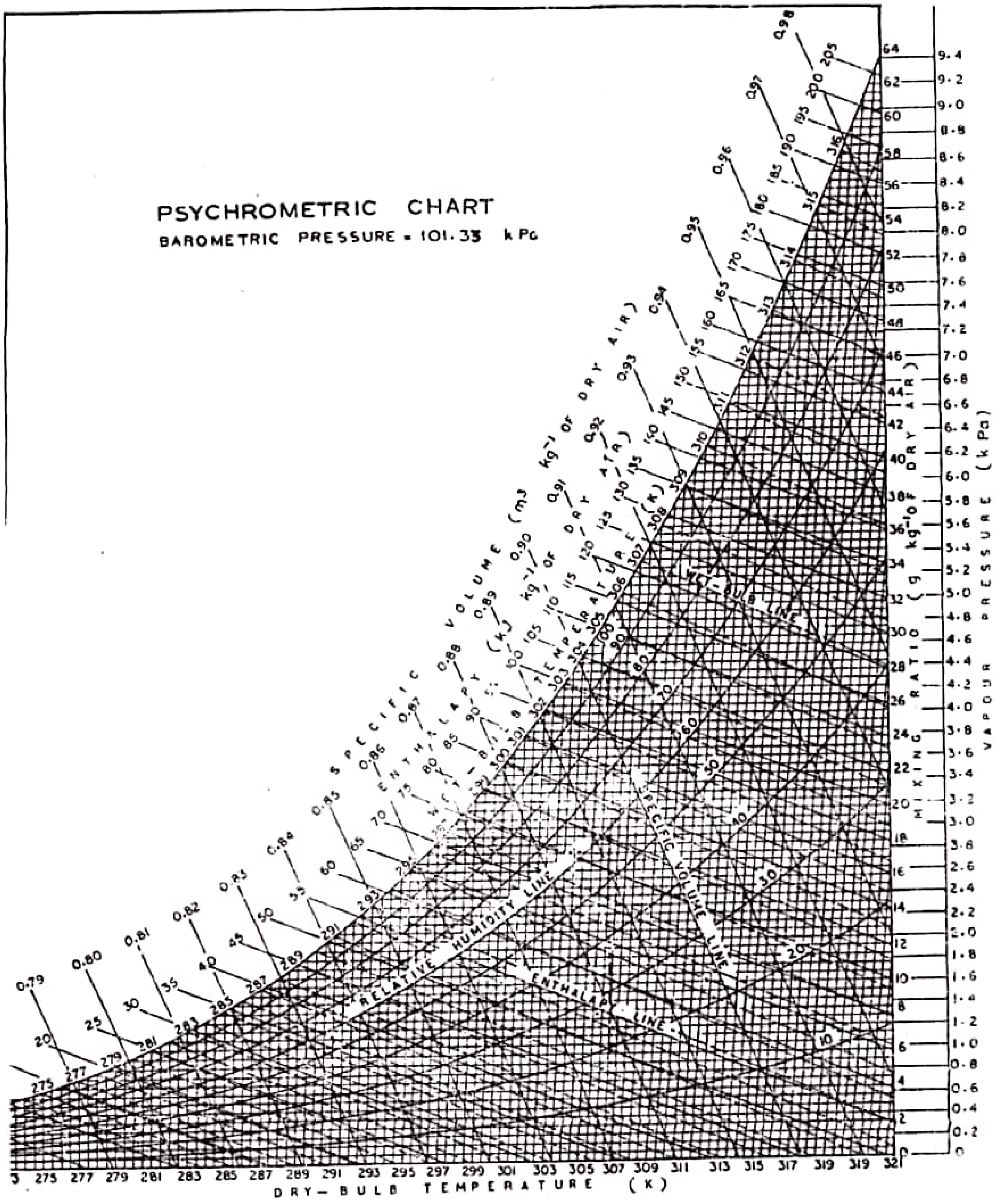

Fig. 3-9 Psychrometric Chart

Scanned with CamScanner

where q_r = heat pick-up in kW per 100m length of airway. Note that it is independent of the air-flow rate in the airway, though strictly speaking a higher flow rate leads to an increased heat pick-up from the rock, partly because of increased value of α (see equation 3.11) and partly because of slower rate of temperature rise of the air along the roadway.

f_w = wetness factor = zero for dry airways and 1 for very wet airways. For a wet floor and dry roof and sides f_w can be taken equal to 0.25.

n = age of roadway in years,

k = thermal conductivity of rock, kW m^{-1} K^{-1},

p = perimeter of the airway, m,

T_v = virgin-rock temperature, K

and T = dry-bulb temperature of air, K.

For stopes, Whillier [134] recommends the following equation :

$$q_s = 0.11\,(1+0.05\,W)\,(T_v-T)\sqrt{\frac{L_m}{10}\cdot\frac{L_s}{50}\cdot\frac{k\rho C}{13}} \qquad (3.59)$$

where q_s = heat pick-up from the rock in the stope in kW per m of face length,

W = stoping width, m,

L_m = average monthly face advance, m,

L_s = stope span (average distance from centre gully to stope face,

ρ = density of rock, kg m^{-3}

and C = specific heat of rock, kJ kg^{-1} K^{-1}.

In both the above equations, the dry-bulb temperature of air, T has to be estimated (at least every 100m or so in roadways). While stope wet-bulb temperatures can be fixed at tolerable limits or somewhat less than that and the dry-bulb temperature taken as 2 K higher than the wet-bulb temperature, in roadways the dry-bulb temperature has to be estimated, say, from equation 3.38. In finished stopes, the heat pick-up is estimated by assuming L_m=1.

The rate of heat pick-up at a development end (up to 50m behind the face) in a drive or tunnel is higher and can be estimated from the equation[135]

$$q_e = L_d\,(T_v-T)\left(\frac{p}{12}\right)^{1.3}\left(\frac{k\rho\,C}{13}\right)^{0.8} \qquad (3.60)$$

Scanned with CamScanner

where q_e = rate of heat pick-up in the vicinity of the development end, kW

and L_d = daily rate of face advance, m.

3.5.4 Heat from Men

Heat is produced by men through the process of metabolism. Even a man at rest produces quite an appreciable quantity of heat by basal metabolism. Weeks[43] estimates the heat produced by basal metabolism (when food is withheld for a specific length of time) at 46.5 Wm^{-2} of body surface. Du Bois[43] gives the following formula for calculating the body surface of a man.

$$A = 0.2024m^{0.425} \times h^{0.725} \tag{3.61}$$

where A = area of the body surface in m^2,

m = mass of the body in kg

and h = height of the body in m.

Average men have a body surface of 1.8-1.9m^2 so that they have a basal metabolic rate of 84-88 W.

When doing hard work, however, the heat produced by the body is much more than that produced by basal metabolism and sometimes it may be as much as ten times the latter. The heat-engine efficiency of the human body, i.e. the ratio of the work done by the man in a certain time to the amount of heat produced by him in excess of that due to basal metabolism in that time is found to be only 20%. Assuming the above heat-engine efficiency of the human body the heat produced by an average man doing moderate work of 45 W is of the order of 310 W or about 165-170 W m^{-2} of body surface. Wyndham gives the following typical metabolic heat rates for different rates of work :

Nature of work	Light work (e.g. winch driving)	Moderate work (e.g. sweeping, fitting)	Hard work (e.g. tramming, shovelling)
Metabolic heat rate, W m^{-2} of body surface	90	180	270

3.5.5 Heat Produced by Machinery

This can be a large source of heat particularly in highly mechanized mines. Most of the power input to electric- or I.C.

engine-powered machinery in a mine appears as heat at one stage or the other.

Almost all the work done by face machinery for cutting, drilling, loading and transport is frictional except for that part of the work done against gravity in lifting material, as may sometimes happen in loading or conveying. Hence, most of the power input to such machinery is converted to heat partly in the machine itself (equivalent to the inefficiency of the machine) and partly through frictional work. Most of the heat produced by the face machinery goes to raise the temperature of the air at the face.

In hoists or pumps, work is done mainly against gravity. Here, only that part of the power input which is spent up in the motor or engine and gearing as well as in doing frictional work appears as heat. A 2000 kW internal hoist running at 60% overall efficiency will add 800 kW of heat to the mine air at the site of the hoist in addition to the heat produced by frictional work in the shaft. Assuming 10% of the work output of the hoist to be spent on overcoming friction, a further 120 kW of heat is added in the shaft. On the other hand, a haulage engine pulling tubs on level ground converts all of its power input to heat, a part of it being put into the air at the engine and the rest as frictional heat in the haulage road. It is a good practice to dispose of heat from large hoists, pumps or haulage engines directly to the return air by ventilating the engine rooms by a separate split of air-current. The frictional heat in haulage roads can be prevented from getting at the face by installing haulages in the return, a fact worth considering in deep mines. This becomes all the more important for locomotive haulage where all the heat is added to the air in the haulage road.

Diesel locomotives, being much less efficient than electric locomotives of either trolley-wire or battery type, produce more heat for the same power. It must be borne in mind that the heat produced by diesel locomotives is equal to the heat content of the fuel consumed. The heat content of normal diesel fuel is about 44 MJ kg^{-1}. A diesel locomotive consumes about 0.26 kg of fuel per kWh so that the heat generated is 2.93 kW per kW of locomotive power. However, since the locomotive does not work all the time, the average heat generated by a diesel locomotive is of the order of 1 kW per kW of rated engine power.

Almost all the work done by a fan is converted to heat except for the part used for increasing the kinetic energy of air as the air

Scanned with CamScanner

undergoes adiabatic compression. The same is the case with compressors. There is an increase in the air temperature of 0.826 K for every kPa pressure developed by the fan. That is the reason why it is better to locate booster fans on the return and to install exhaust fans rather than forcing fans as main mine ventilators at the surface.

Compressed-air machinery add no heat to the mine air. Compressed-air machines like rock drills which do frictional work add heat to the rock face equivalent to the work done, but this is fully compensated by the expansive cooling of the exhaust air.

Assuming the air velocity at the drill inlet and exhaust to be the same and neglecting the work of feed thrust on the drill, the general energy balance equation (4.1) yields

$$-dW = dH = C_p\,dT \tag{3.62}$$

where dW = work done,
dH = change in enthalpy of compressed-air between drill inlet and exhaust,
dT = change in temperature of compressed-air between drill inlet and exhaust
and C_p = specific heat of compressed-air.

When a compressed-air machine does work against gravity, however, there is a positive cooling of the mine air. It is for this reason that compressed-air hoists are often preferred to electric hoists inside deep and hot mines even though the latter are more efficient.

On the other hand compressed-air in pipes does add a certain amount of heat to the mine air. Compressed-air is often generated at fairly high temperatures if proper after-cooling arrangement is not there. This hot compressed-air further gains heat due to autocompression in the pipe range in the shaft. As the compressed-air goes down the shaft, it gives up heat to the ventilating air as a result of which some of the moisture in the compressed-air condenses thus generating heat. The overall heat addition to the mine air from compressed-air is thus given by the relation,

$$q = M\{C_p(T_1 - T_2) + \frac{l}{1000}(m_1 - m_2) + hg\} \tag{3.63}$$

where q = heat lost by compressed-air in W,
M = mass flow rate of compressed-air in kg s^{-1},
C_p = specific heat of compressed-air $= 1005$ J kg^{-1} K^{-1},

T_1 and T_2 are temperatures in K of the compressed-air pipe at the shaft-top and shaft-bottom respectively,
l = latent heat of evaporation of water in J kg^{-1}
and h = depth of shaft in m and m_1 and m_2 are moisture contents in g kg^{-1} of dry compressed-air at the top and bottom of the shaft respectively.

Example 3.2

A fan ventilating a heading through a duct of 600mm diameter circulates 4 m^3 s^{-1} of air at the face. Calculate the heat added to the air by the fan, if the input power of the fan is equal to 2.9 kW.

Cross-sectional area of the duct $= \frac{\pi}{4}(0.6)^2 = 0.283$m^2.

$\therefore$ Velocity of air in the duct $= \frac{4}{0.283} = 14.13$m s^{-1}.

Kinetic energy of air leaving the duct

$$= \frac{1}{2} mv^2 \text{ W}$$

$$= \frac{4 \times 1.2 \times (14.13)^2}{2} = 479 \text{ W}$$

where m = mass or air in kg flowing per second,
v = velocity of air in m s^{-1}
and the density of air is assumed to be equal to 1.2 kg m^{-3}.

Energy input to the fan converted to heat

$$= 2900 - 479 = 2421 \text{ J}$$

3.5.6 Heat from Lights

This becomes significant if carbide lamps are used. Cooke[43] estimates that a carbide lamp consuming 156g of carbide per shift produces 96.5 J of heat per second although according to Jeppe,[43] its power may be as high as 204.7 W when the lamp burns at full brightness. A candle produces 25-35 J, an electric cap lamp (two-cell type), 2.6 J and an ordinary electric bulb, 40 J every second dep·nding of course on the current and voltage.

3.5.7 Heat due to Oxidation

This is a major source of heat in coal mines, particularly in seams liable to spontaneous heating. In coal mines, 80-85% of the

Scanned with CamScanner

heat added to the air can be traced to this source. Neglecting the amount of oxygen consumed by men and flame lamps, i.e. assuming all the oxygen consumed in a mine to be utilized in the oxidation of coal, Haldane states that a fall of 0.1 in the percentage of oxygen in the air between the intake and return airways produces enough heat to raise the air temperature by 7K.

It may be noted here that in coal mines desorption of methane from coal produces a certain degree of cooling by extracting 835-1025 kJ of heat per m^3 of methane desorbed.

Heat due to oxidation is not usually appreciable in metal mines where a small quantity of heat may be produced by the oxidation of timber. But in some mines producing sulphidic ores, spontaneous heating of the sulphides may add a considerable amount of heat to the air. Heat due to oxidation of coal is 8.79 MJ m^{-3} of O_2 absorbed while that for oxidation of pyrites[1] is 18 MJ m^{-3}.

3.5.8 Heat due to Blasting

This can be of considerable magnitude. Ewing and Egan[43] estimate the heat produced by blasting in a mine milling 101 600 tonnes per month to be 316.5 MJ h^{-1} on an average, but since the blasting is confined to an hour or so per day, the actual heat produced in that hour is of the order of 5.3-6.3 GJ. However, this heat is dissipated away by the ventilating current before men return to work after blasting.

3.5.9 Heat Caused by Rock Movement

Moss[43] has shown that the actual heat addition to the air on account of the movement of strata in coal mines is only 1% of the total heat added to the air, although theoretically it should be of the order of 9% in consideration of the rock masses involved. This is believed to be due to most of the heat being dissipated in the broken rock mass itself.

The relative importance of the various sources of heat in a metal mine is evident from the following example. A section of a mine on the Witwatersrand[43] had 4500 men, each with a carbide lamp. The number of electrical units consumed were 822 000 kWh per month and the quantity of ventilating air was 151 $m^3 s^{-1}$. The depth to the top of the section was 1524m and the total heat taken up by the air as calculated from the air temperature was 11.56 MW. The distribution of heat was as given in Table 3.3.

Table 3.3 : Distribution of Heat from Various Sources in a Mine

Source	Heat produced in MW	Heat produced in % of total
Auto-compression	2.42	21
Human beings	1.58	14
Carbide lamps	0.90	7
Power	1.32	12
Rock and other sources (by difference)	5.34	46
Total	11.56	100

A more recent study by the author in one of the highly mechanized copper mines of Zambia producing about 15 000t per day from a depth of 600 to 900m from the surface shows that 46.65% of the total heat picked up from the mine is produced by diesel and electric machinery (including electric lighting), 12.05% by auto-compression and 40.12% is from rock of which 68% is from stopes and the rest, from development openings. Only 1.18% is produced by men and their cap lamps. The proportion is estimated to change at greater depth where the heat from rock and auto-compression will increase.

Example 3.3

A downcast shaft is 300m deep. The barometer reads 102 kPa at the shaft-top. The surface air temperature being 295 K, calculate the air temperature at the bottom of the shaft assuming the temperature of the air to be affected by auto-compression only.

As a rough estimate, the rise in the temperature of air due to auto-compression

$$= 0.96 \times 3 = 2.88 \text{ K}.$$

Therefore, the mean temperature of the air column

$$= 295 + 1.44 = 296.44 \text{ K}$$

Let B = barometric pressure at the shaft-bottom.

$$\therefore 300 = 67.4 \times 296.44 (\log B - \log 102)$$

$$\text{or } B = 105.6 \text{ kPa}.$$

Scanned with CamScanner

Now let T = temperature at the shaft-bottom in K.

$$\therefore T = 295 \left(\frac{105.6}{102}\right)^{(1.4-1)/1.4}$$
$$= 297.99\text{K}.$$

Using the relation given in equation 3.8, the rise in temperature

$$= \frac{300 \times 9.81}{1005} = 2.93 \text{ K}$$

Therefore, $T = 295 + 2.93 = 297.93$K.

3.6 MOISTURE CONTENT OF MINE AIR

Mine air always contains some amount of moisture. There is a maximum quantity of moisture which can be contained in any space of gas, air or even vacuum at a certain temperature. When the air at a particular temperature contains the maximum amount of water-vapour it can hold, it (or rather the space) is called saturated and can pick up no more water-vapour at that temperature. On the other hand, if the air can still pick up some more water-vapour at the prevailing temperature, it is called unsaturated. The capacity of air for containing water-vapour increases with temperature and hence if saturated air is heated up without adding any extra moisture to it, it becomes unsaturated. Conversely, if unsaturated air is cooled, its degree of saturation increases until it is fully saturated at a certain temperature. If the cooling proceeds beyond this temperature, the air gives up water-vapour which condenses into mist or dew. This temperature at which the air attains saturation is called the *dew point*.

Saturated air at a certain temperature holds a fixed amount of moisture. This quantity remains the same if the temperature is raised without further addition of moisture. If on the other hand moisture is added as the temperature rises, the air picks up more moisture until it gets saturated at the higher temperature.

Moisture content of air can be expressed in the following terms: (a) *vapour pressure*, (b) *saturation deficit*, (c) *relative humidity*, (d) *dew point*, (e) *specific humidity*, (f) *mixing ratio* and (g) *absolute humidity*. Each of the above units except the relative humidity specifies the moisture content completely, the relative humidity alone requiring the temperature to be given in addition.

3.6.1 Vapour Pressure

This is the partial pressure of water-vapour present in a certain volume of air or space. When a gas or mixture of gases such as air is confined in a given space in a container it exerts a certain pressure on the walls of the container. When another gas or water-vapour is allowed to diffuse into it and occupy the same space, the pressure on the container walls is the sum of the partial pressures (the pressure exerted by the individual gas if it occupies the container alone) of the component gases.

Since at a certain temperature and atmospheric conditions the barometric pressure does not change, addition of water-vapour to dry air reduces its partial pressure and hence its density. Again, water-vapour has a lower density than dry air. Hence the overall density of air is reduced by the addition of water-vapour. The vapour pressure is the maximum when the air is saturated at a certain temperature. It should be noted that the *saturation vapour pressure* varies with temperature only and is independent of the presence of other gases and vapours. The saturated vapour pressure of air for various temperatures have been experimentally determined and are given in Table 3.4.[62] Empirical relations (equations 3.19 and 3.41) have been fitted to these data and can be used for the calculation of saturation vapour pressure.

3.6.2 Saturation Deficit

This is the difference between the saturation vapour pressure at the temperature of observation and the actual vapour pressure and is measured in any pressure unit.

3.6.3 Relative Humidity

This is the ratio of actual vapour pressure to the saturation vapour pressure at the temperature of observation (dry-bulb temperature) expressed as a percentage. For temperatures prevalent in mines, this can be taken equal to the *saturation ratio* which is the ratio of the mass of moisture per unit mass of dry air to the mass of moisture required to saturate the air at the temperature of observation.

$$\text{Saturation ratio} = \left(\frac{622e}{B-e}\right) \Big/ \left(\frac{622e'}{B-e'}\right) = \frac{(B-e')e}{(B-e)e'} \qquad (3.64)$$

(see later)

Scanned with CamScanner

Now let T = temperature at the shaft-bottom in K.

$$\therefore T = 295\left(\frac{105.6}{102}\right)^{(1.4-1)/1.4}$$

$$= 297.99\text{K}.$$

Using the relation given in equation 3.8, the rise in temperature

$$= \frac{300\times 9.81}{1005} = 2.93 \text{ K}$$

Therefore, $T = 295 + 2.93 = 297.93$K.

3.6 MOISTURE CONTENT OF MINE AIR

Mine air always contains some amount of moisture. There is a maximum quantity of moisture which can be contained in any space of gas, air or even vacuum at a certain temperature. When the air at a particular temperature contains the maximum amount of water-vapour it can hold, it (or rather the space) is called saturated and can pick up no more water-vapour at that temperature. On the other hand, if the air can still pick up some more water-vapour at the prevailing temperature, it is called unsaturated. The capacity of air for containing water-vapour increases with temperature and hence if saturated air is heated up without adding any extra moisture to it, it becomes unsaturated. Conversely, if unsaturated air is cooled, its degree of saturation increases until it is fully saturated at a certain temperature. If the cooling proceeds beyond this temperature, the air gives up water-vapour which condenses into mist or dew. This temperature at which the air attains saturation is called the *dew point*.

Saturated air at a certain temperature holds a fixed amount of moisture. This quantity remains the same if the temperature is raised without further addition of moisture. If on the other hand moisture is added as the temperature rises, the air picks up more moisture until it gets saturated at the higher temperature.

Moisture content of air can be expressed in the following terms: (a) *vapour pressure*, (b) *saturation deficit*, (c) *relative humidity*, (d) *dew point*, (e) *specific humidity*, (f) *mixing ratio* and (g) *absolute humidity*. Each of the above units except the relative humidity specifies the moisture content completely, the relative humidity alone requiring the temperature to be given in addition.

3.6.1 Vapour Pressure

This is the partial pressure of water-vapour present in a certain volume of air or space. When a gas or mixture of gases such as air is confined in a given space in a container it exerts a certain pressure on the walls of the container. When another gas or water-vapour is allowed to diffuse into it and occupy the same space, the pressure on the container walls is the sum of the partial pressures (the pressure exerted by the individual gas if it occupies the container alone) of the component gases.

Since at a certain temperature and atmospheric conditions the barometric pressure does not change, addition of water-vapour to dry air reduces its partial pressure and hence its density. Again, water-vapour has a lower density than dry air. Hence the overall density of air is reduced by the addition of water-vapour. The vapour pressure is the maximum when the air is saturated at a certain temperature. It should be noted that the *saturation vapour pressure* varies with temperature only and is independent of the presence of other gases and vapours. The saturated vapour pressure of air for various temperatures have been experimentally determined and are given in Table 3.4.[62] Empirical relations (equations 3.19 and 3.41) have been fitted to these data and can be used for the calculation of saturation vapour pressure.

3.6.2 Saturation Deficit

This is the difference between the saturation vapour pressure at the temperature of observation and the actual vapour pressure and is measured in any pressure unit.

3.6.3 Relative Humidity

This is the ratio of actual vapour pressure to the saturation vapour pressure at the temperature of observation (dry-bulb temperature) expressed as a percentage. For temperatures prevalent in mines, this can be taken equal to the *saturation ratio* which is the ratio of the mass of moisture per unit mass of dry air to the mass of moisture required to saturate the air at the temperature of observation.

$$\text{Saturation ratio} = \left(\frac{622e}{B-e}\right)\Big/\left(\frac{622e'}{B-e'}\right) = \frac{(B-e')e}{(B-e)e'} \qquad \textbf{(3.64)}$$

(see later)

Scanned with CamScanner

Table 3.4—Pressure of Aqueous Vapour over Water in kPa

Temperature in K	0.0	0.1	0.2	0.3	0.4	0.5	0.6	0.7	0.8	0.9
273	0.605	0.609	0.613	0.617	0.622	0.626	0.631	0.635	0.640	0.645
274	0.650	0.655	0.659	0.664	0.669	0.674	0.679	0.684	0.689	0.693
275	0.698	0.703	0.708	0.714	0.719	0.724	0.729	0.734	0.739	0.745
276	0.750	0.755	0.761	0.766	0.771	0.777	0.782	0.788	0.794	0.799
277	0.805	0.810	0.816	0.822	0.828	0.833	0.839	0.845	0.851	0.857
278	0.863	0.869	0.875	0.881	0.888	0.894	0.900	0.906	0.913	0.919
279	0.925	0.932	0.938	0.945	0.951	0.958	0.965	0.971	0.978	0.985
280	0.992	0.999	1.006	1.013	1.019	1.026	1.034	1.041	1.048	1.055
281	1.062	1.069	1.077	1.084	1.091	1.099	1.106	1.114	1.121	1.129
282	1.136	1.144	1.152	1.160	1.167	1.175	1.183	1.191	1.199	1.208
283	1.216	1.224	1.232	1.240	1.249	1.257	1.266	1.274	1.283	1.291
284	1.300	1.309	1.318	1.326	1.335	1.344	1.353	1.362	1.371	1.380
285	1.389	1.398	1.408	1.417	1.426	1.436	1.445	1.455	1.464	1.474
286	1.483	1.493	1.503	1.513	1.523	1.533	1.543	1.553	1.563	1.573
287	1.584	1.594	1.604	1.615	1.625	1.636	1.646	1.657	1.668	1.679
288	1.690	1.701	1.712	1.723	1.733	1.744	1.756	1.767	1.779	1.790
289	1.802	1.813	1.825	1.836	1.848	1.860	1.872	1.884	1.896	1.908
290	1.920	1.932	1.945	1.957	1.969	1.982	1.995	2.007	2.020	2.032
291	2.045	2.059	2.072	2.085	2.098	2.111	2.124	2.137	2.151	2.164
292	2.178	2.191	2.205	2.219	2.233	2.246	2.261	2.275	2.289	2.304

Table 3.4 (Contd.)—Pressure of Aqueous Vapour over Water in kPa

Temperature in K	0.0	0.1	0.2	0.3	0.4	0.5	0.6	0.7	0.8	0.9
293	2.318	2.332	2.347	2.361	2.376	2.391	2.406	2.421	2.436	2.451
294	2.466	2.481	2.496	2.512	2.527	2.543	2.558	2.574	2.590	2.606
295	2.621	2.637	2.653	2.670	2.686	2.703	2.719	2.736	2.752	2.769
296	2.786	2.803	2.820	2.837	2.854	2.872	2.889	2.906	2.924	2.941
297	2.959	2.977	2.995	3.013	3.031	3.050	3.068	3.086	3.105	3.123
298	3.142	3.161	3.180	3.199	3.218	3.237	3.257	3.276	3.295	3.315
299	3.335	3.354	3.374	3.394	3.414	3.435	3.455	3.476	3.496	3.517
300	3.538	3.558	3.579	3.600	3.622	3.643	3.664	3.686	3.707	3.729
301	3.751	3.773	3.795	3.817	3.839	3.862	3.884	3.907	3.930	3.953
302	3.976	3.999	4.022	4.045	4.068	4.091	4.115	4.139	4.163	4.187
303	4.211	4.235	4.260	4.285	4.309	4.334	4.359	4.384	4.409	4.434
304	4.460	4.485	4.510	4.536	4.562	4.588	4.614	4.641	4.667	4.693
305	4.720	4.747	4.774	4.801	4.828	4.855	4.883	4.910	4.938	4.966
306	4.994	5.022	5.050	5.079	5.107	5.136	5.165	5.194	5.223	5.252
307	5.282	5.311	5.340	5.370	5.400	5.430	5.461	5.491	5.522	5.553
308	5.584	5.614	5.645	5.676	5.708	5.740	5.771	5.803	5.835	5.867
309	5.900	5.933	5.965	5.998	6.031	6.064	6.097	6.130	6.164	6.198
310	6.232	6.266	6.300	6.335	6.369	6.404	6.439	6.474	6.509	6.544
311	6.580	6.615	6.651	6.687	6.723	6.760	6.797	6.834	6.871	6.908
312	6.945	6.982	7.020	7.057	7.095	7.133	7.172	7.210	7.249	7.288

Scanned with CamScanner

Table 3.4 (Contd.)—Pressure of Aqueous Vapour over Water in kPa

Temperature in K	0.0	0.1	0.2	0.3	0.4	0.5	0.6	0.7	0.8	0.9
313	7.327	7.366	7.405	7.445	7.484	7.524	7.564	7.605	7.645	7.686
314	7.726	7.768	7.809	7.850	7.892	7.934	7.976	8.018	8.060	8.103
315	8.146	8.188	8.231	8.274	8.318	8.362	8.406	8.450	8.494	8.539
316	8.584	8.629	8.674	8.719	8.765	8.810	8.856	9.902	8.948	8.995
317	9.042	9.089	9.136	9.183	9.231	9.279	9.327	9.375	9.423	9.472
318	9.521	9.570	9.619	9.669	9.719	9.769	9.819	9.870	9.920	9.971
319	10.022	10.073	10.125	10.176	10.228	10.281	10.333	10.386	10.439	10.492
320	10.546	10.599	10.653	10.707	10.761	10.815	10.870	10.926	10.981	11.037
321	11.092	11.148	11.205	11.261	11.318	11.375	11.432	11.489	11.547	11.605
322	11.663	11.722	11.780	11.839	11.898	11.958	12.018	12.078	12.138	12.198
323	12.259	12.320	12.381	12.443	12.505	12.567	12.629	12.692	12.755	12.818

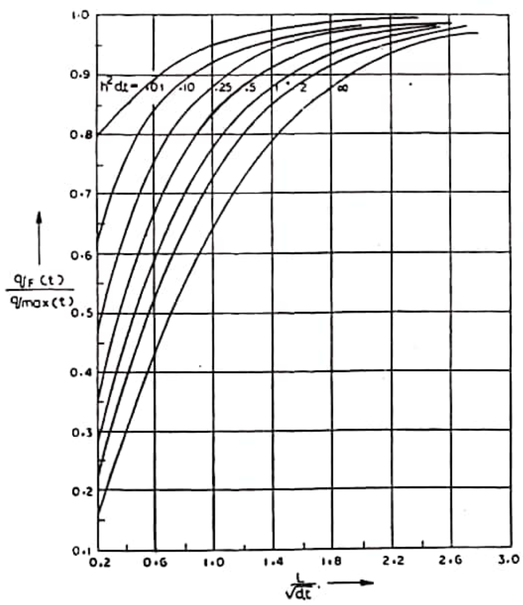

Fig. 3.8 $q_F(t)/q_{max}(t)$ vs $L/\sqrt{d.t}$ (after Starfield).

and that over unit time,

$$q = \frac{q_F(t) + 2q_H(t) + q_R(t)}{t} \tag{3.50}$$

In cut-and-fill method of stoping filling follows face advance. The fill face will release a certain amount of sensible and latent heat. For computing this the fill face can be assumed to be at the same surface temperature as the last section of the hanging wall.

The heat transferred from the last section of the hanging wall over time t

$$q_{HN}(t) = \frac{L}{W} \cdot \{q_{max}(Nt) - q_{max}(\overline{N-1} \cdot t)\} \tag{3.51}$$

The heat transfer from unit area per unit time

$$q_{HN} \approx \frac{q_{max}(Nt) - q_{max}(\overline{N-1}\,.\,t)}{t\,W} \tag{3.52}$$

The surface temperature of the hanging wall T_s can now be determined from the relation

$$q_{HN} = \alpha (T_s - T_o) \tag{3.53}$$

Taking the same surface temperature for the fill face, the sensible heat transfer from the fill face over the period t will be given by

$$q_{FL}(t) = W \alpha (T_s - T_o) \tag{3.54}$$

so that the total sensible heat transfer per unit length of stope face per unit time

$$q_T = \frac{q_F(t) + 2q_H(t) + q_R(t) + q_{FL}(t)}{t} \tag{3.55}$$

Let this cause a rise in the dry-bulb temperature of the air of ΔT.

Then $q_T = C_p\, \rho_a\, Q\, \Delta T$ (3.56)

where Q = air-flow rate along the stope.

At the end of the unit length of face the dry-bulb air temperature now becomes $T_o + \Delta T$. This air temperature can now be used for calculating the heat transfer from the next unit length of the face and the process continued till the dry-bulb air temperature at the return end of the stope face is obtained.

The change in the absolute humidity and hence in the wet-bulb temperature along the face can be similarly obtained by solving the equation

$$W \epsilon \{e'(T_s) - e\} = Q\, \Delta m' \times 10^{-3} \tag{3.57}$$

where $\Delta m'$ = change in the absolute humidity of the air, for each unit length of face.

The above methods of computing heat addition in wet roadways and stopes in mines are highly complicated and need substantial amount of digital computation. Simplified empirical relations have been developed in South African gold mines for estimation of heat transfer in roadways, stopes and development ends.

Ramsden[133] developed the following relation for wet airways :

$$q_r = 5.57\,(f_w + 0.255)\,(T_r - T)\left(\frac{p}{12}\right)^{0.437}\left(\frac{n}{3}\right)^{-0.147}\left(\frac{k}{5.5\times10^{-3}}\right)^{0.853} \tag{3.58}$$

$$\therefore \frac{\text{saturation ratio}}{\text{relative humidity}} = \left\{\frac{(B-e')e}{(B-e)e'}\right\} \Big/ \left(\frac{e}{e'}\right) = \frac{B-e'}{B-e} \tag{3.65}$$

where B = barometric pressure, e = vapour pressure and e' = saturation vapour pressure.

Since e and e' are too small in comparison with B, $B-e$ and $B-e'$ can be considered to be equal and hence saturation ratio can be taken equal to relative humidity.

3.6.4 Dew Point

For any vapour pressure e, a temperature T_d can be found at which the saturation vapour pressure is equal to e. T_d is called the dew-point temperature.

3.6.5 Specific Humidity

The specific humidity is defined as the mass of water-vapour present in a unit mass of air (mass of air includes that of dry air as well as of moisture). The specific humidity is related to vapour pressure by the relation

$$S = 622\,\frac{e}{B - 0.378e} \tag{3.66}$$

where S = specific humidity in g kg^{-1}.

It is assumed that water-vapour has a density equal to 0.622 times that of air at the same temperature and pressure.

3.6.6 Mixing Ratio

This is a quantity similar to the above and is defined as the mass of water-vapour per unit mass of dry air,

$$\text{or,}\quad m = 622\,\frac{e}{B-e} \tag{3.67}$$

where m = mixing ratio in g kg^{-1}.

3.6.7 Absolute Humidity

This unit is less commonly used nowadays. It is defined as the mass of water-vapour per unit volume of air and is given by the relation

$$m' = \frac{10^{6} e}{461.9T} \tag{3.68}$$

Scanned with CamScanner

where m' = absolute humidity in g m^{-3},
T = temperature in K
and e = vapour pressure in kPa.

3.6.8 Measurement of Humidity

There are several methods for the measurement of humidity. They are listed below in order of their use.

(1) Thermodynamic method (the psychrometer).

(2) Methods using hygroscopic substances (the hair hygrometer etc.)

(3) Condensation method (the dew-point hygrometer).

(4) Absorption methods :
   (a) Chemical (volumetric and gravimetric)
   (b) Electrical (change of resistance, change of dielectric constant).

(5) Diffusion methods.

(6) Optical methods.

Of these, the thermodynamic method is the only method used in mines and will be discussed here.

Psychrometers record the dry-bulb and the wet-bulb temperatures of the air from which the vapour pressure or the other units of humidity can be calculated.

3.6.9 Wet-bulb Temperature

This is the temperature recorded by a thermometer whose bulb is covered with a thin cotton gauze which is dipped at the lower end into water so that the surface of the bulb is kept moist by capillary action. If such a thermometer is placed in unsaturated air, the latter will pick up moisture from the bulb of the thermometer. As a result, its temperature in the vicinity of the bulb will fall owing to the loss of the latent heat of evaporation until the air gets saturated. Once the air is saturated there will be no further evaporation and cooling of the thermometer when it will show a constant temperature. This temperature is the wet-bulb temperature.

Thus the wet-bulb temperature, in conjunction with the dry-bulb temperature, gives a measure of the degree of saturation or the relative humidity of the air. If the temperature of saturated air is raised without further addition of moisture, both its dry-bulb

and wet-bulb temperatures rise (the latter at a slower rate) and its relative humidity falls, but the dew point of the air remains constant. If water is evaporated into unsaturated air its dry-bulb temperature falls by evaporative cooling, the wet-bulb temperature remains constant and the dew point rises until it reaches the wet-bulb temperature at the point of saturation. At such a point the dry-bulb temperature is equal to the wet-bulb temperature.

The vapour pressure can be calculated from the dry- and wet-bulb temperatures using the following relations:

(1) $$e=e'-0.0012B\,(T-T')\left(1+\frac{T'-273.15}{610}\right) \tag{3.69}$$

for an air velocity of 0-0.5 m s^{-1}

(2) $$e=e'-0.0008\,B\,(T-T')\left(1+\frac{T'-273.15}{610}\right) \tag{3.70}$$

for an air velocity of 1-1.5 m s^{-1}

(3) $$e=e'-0.000\,656\,B\,(T-T')\left(1+\frac{T'-273.15}{610}\right) \tag{3.71}$$

for an air velocity > 3 m s^{-1}

where T = dry-bulb temperature in K,
T' = wet-bulb temperature in K,
e = vapour pressure of the air,
e' = saturated vapour pressure at temperature T'
and B = barometric pressure in the same units as e and e'.

For temperatures between 274 K and 322 K and pressures between 85 and 115 kPa the following relation is accurate within a limit of variation of 1.1% and hence can be suitably used for mining calculations.

$$e=e'-0.000\,66\,B\,(T-T') \tag{3.72}$$

The moisture content of mine air can also be obtained from psychrometric tables or charts.

Fig. 3.9 gives a psychrometric chart for an atmospheric pressure of 101.33 kPa. The chart shows the vapour pressure, moisture content (mixing ratio), specific volume and relative humidity for various dry-bulb and wet-bulb temperatures. In addition, enthalpy of moist air is also plotted on the chart.

The chart even though drawn for a barometric pressure of 101.33 kPa, can be used for easy calculation of the tehrmodynamic state of mine air with a tolerable degree of accuracy. However, for greater accuracy, the vapour pressure e read from the chart can be corrected for any barometric pressure B by the relation

Scanned with CamScanner

$$e(B) = e+0.000\,66\,(T-T')\,(101.33-B) \qquad (3.72a)$$

where $e(B)$ = vapour pressure at barometer B.

Change of state of air for different thermodynamic processes such as heating, cooling etc. can be directly marked on the psychrometric chart as illustrated in Fig. 3.10.

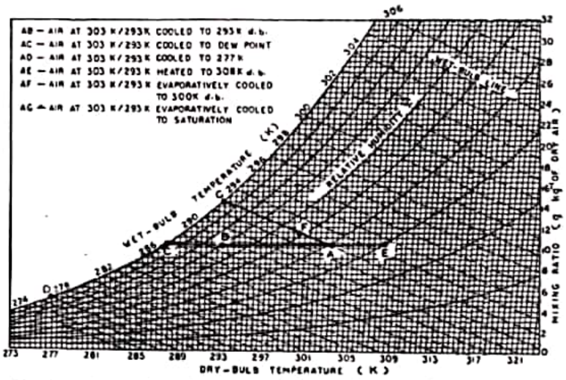

Fig. 3.10 Thermodynamic processes illustrated on a psychrometric chart.

Example 3.4

From the psychrometric chart determine the change in the moisture content of air evaporatively cooled to saturation from 304 K d.b. (dry-bulb) and 297 K w.b. (wet-bulb). Also show that 'evaporative cooling' is actually a process of heating.

Referring to Fig. 3.9, air at 304/297 K on being evaporatively cooled, will proceed along the wet-bulb line until it meets the 100% relative humidity line when it will be saturated at 297 K.

At 304/297 K moisture content of air = 15.75 g kg^{-1} of dry air.

At 297 K saturated, moisture content = 18.75 g kg^{-1} of dry air.

$\therefore$ Change in moisture content

$= 18.75 - 15.75 = 3$ g kg^{-1} of dry air.

Enthalpy at 304/297 K = 71.6 kJ kg^{-1} of dry air.

Enthalpy at 297 K saturated = 72.0 kJ kg^{-1} of dry air.

This clearly suggests that there is an addition of heat $= 0.4$ kJ kg^{-1} of dry air.

Example 3.5

Air at 302/292 K is cooled by chilled water at 277 K in a shell-and-tube-type heat exchanger. The temperature of water leaving the exchanger is 288 K and the rate of water circulation is 2 kg s^{-1}. Find the wet- and dry-bulb temperatures of cooled air if air circulation through the heat exchanger is 8 m^3 s^{-1} measured at the inlet. What will be the temperature of cooled air if the rate of water circulation is increased to 4 kg s^{-1}?

Assume the heat exchanger to be 90% efficient.

Heat extracted from the air by the circulating water $= (288-277)\times 2\times 4.19\times 0.9 = 82.96$ kJ s^{-1} for a water circulation rate of 2 kg s^{-1} and $= (288-277)\times 4\times 4.19\times 0.9 = 165.92$ kJ s^{-1} for a circulation rate of 4 kg s^{-1} taking specific heat of water $= 4.19$ kJ kg^{-1} K^{-1}.

Air at 302/292 K has a specific volume

$= 0.868$ m^3 kg^{-1} of dry air (from psychrometric chart).

$\therefore$ dry air-flow rate $= \dfrac{8}{0.868} = 9.22$ kg s^{-1}.

Enthalpy of air at 302/292 K (from psychrometric chart)

$= 53.21$ kJ kg^{-1} of dry air.

Enthalpy extracted from air by circulating chilled water

$= \dfrac{82.96}{9.22} = 9$ kJ kg^{-1} of dry air for a water-flow rate of 2 kg s^{-1}

and $= \dfrac{165.92}{9.22} = 18$ kJ kg^{-1} of dry air

for a water-flow rate of 4 kg s^{-1}.

$\therefore$ Resultant enthalpy of cooled air

$= 53.21 - 9 = 44.21$ kJ kg^{-1} of dry air for a water-flow rate of 2 kg s^{-1}

and $= 53.21 - 18 = 35.21$ kJ kg^{-1} of dry air for a water-flow rate of 4 kg s^{-1}.

The moisture content of air remains unchanged on cooling in a shell-and-tube-type heat exchanger until it gets saturated at the dew point after which the air will give up some condensed water and follow the 100% relative humidity line on further cooling. It must be noted here that in contrast to this, moisture content of air increases due to evaporation of water when the cooling is done in spray-type coolers and the air follows the wet-bulb temperature line until it is saturated at the wet-bulb temperature when it follows

Scanned with CamScanner

the 100% relative humidity line on further cooling. If cooling proceeds to a sufficiently low temperature the ultimate state point is the same no matter what the method of cooling is (compare the paths ACD and AGD for cooling of air from A to D in Fig. 3.10).

Mixing ratio of air at 302/292 K

$=9.5$ g kg^{-1} of dry air.

For this mixing ratio and an enthalpy of 44.21 kJ kg^{-1} of dry air the air has a dry-bulb temperature of 293.5 K and a wet-bulb temperature of 289 K (from psychrometric chart), but for an enthalpy of 35.21 kJ kg^{-1} of dry air, the air gets cooled beyond the dew point. From the intersection of the enthalpy line (35.21 kJ kg^{-1} of dry air) and 100% relative humidity line, the temperature of cooled air is read as 285.5 K saturated.

Example 3.6

Air at 307/302 K mixes with air at 275 K saturated in the proportion of 6 : 2 by mass on dry air basis. Find the temperature and humidity of the mixed air. What will be the temperature and humidity of the mixed air if the mass ratio of the two streams of air were reversed?

When the two air-streams mix, heat will be given up by the hotter stream of air and taken up by the cooler stream until their dry-bulb temperatures become equal. This will be the dry-bulb temperature, of the mixed air. There will be no change in the total moisture content or enthalpy until and unless the mixture is cooled beyond the dew point when condensed water will separate out of the mixed air thus reducing its moisture content and enthalpy (that removed by the condensed water). The mixed air will then be saturated at the weighted average dry-bulb temperature.

The weighted average dry-bulb temperature of the two streams of air

$$=\frac{307\times6+275\times2}{8}=299 \text{ K}$$

when they mix in proportion of 6 : 2. This will be the dry-bulb temperature of the mixed air.

Mixing ratio of air at 307/302 K

$=23.5$ g kg^{-1} of dry air

and at 275 K saturated $=4.5$ g kg^{-1} of dry air.

Resultant mixing ratio of the mixed air

$=(23.5\times6+4.5\times2)/8=18.75$ g kg^{-1} of dry air.

For this mixing ratio and a dry-bulb temperature of 299 K the wet-bulb temperature=297.5 K (from psychrometric chart).

When the proportion of the two mixing air-streams is reversed,

the weighted average dry-bulb temperature $=\dfrac{275\times6+307\times2}{8}$

$=283$ K

The weighted average mixing ratio $=(23.5\times2+4.5\times6)/8$ $=9.25$ g kg^{-1} of dry air. Since this is higher than the maximum possible mixing ratio of 7 g kg^{-1} of dry air at 283 K, some water will condense out of the mixed air which will be saturated at 283 K.

3.6.10 Instruments for Measuring Relative Humidity of Mine Air

The Fixed or *Non-ventilated Hygrometer.* This is fixed at a suitable place in the mine so as to be well ventilated by the mine air-current. It consists of two thermometers mounted side by side, the bulb of one being exposed to the air and that of the other covered with a thin gauze of muslin, the lower end of which is dipped in a container filled with water. Distilled water or rain water (not mine water) should be used in the container as impurities in water affect its rate of evaporation. The surface of the muslin should be clean and the muslin should be changed from time to time. Care should be taken to wipe all dirt and moisture from the surface of the dry bulb. When taking readings underground, the lamp should not be held too close to the hygrometer. It should preferably be held on the leeward side of the hygrometer so that the heat given out by it does not affect the thermometers. This instrument reads the dry- and wet-bulb temperatures from which the humidity can be obtained by referring to psychrometric tables or charts.

Whirling Hygrometer or *Sling Psychrometer.* A defect of the fixed hygrometer is that unless it is placed in an air-current with a velocity of 3 m s^{-1} or more, the moisture evaporated from the wet bulb surrounds both the dry and wet bulbs, thus affecting the readings slightly. Besides, the evaporative cooling of the wet bulb may also affect the dry-bulb temperature with low air velocity. That is why the whirling hygrometer is commonly used in mines for better accuracy. This (Fig. 3.11) consists of a dry- and a wet-bulb thermometer as in a fixed hygrometer and is provided with a handle for whirling it at a rate of 20 rad s^{-1} ($\simeq$200 r.p.m.) which produces a relative air velocity of 3 m s^{-1}

Scanned with CamScanner

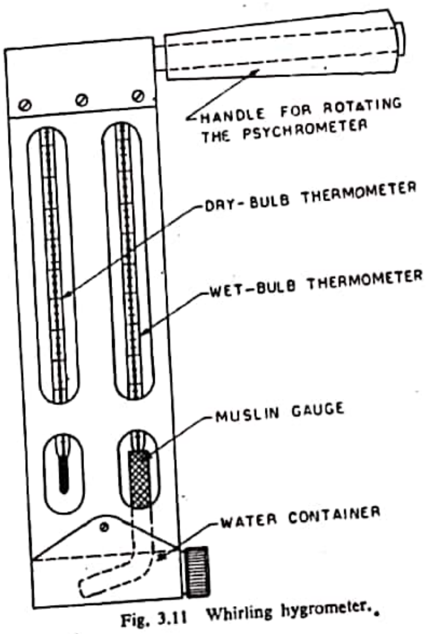

Fig. 3.11 Whirling hygrometer.

Assmann Psychrometer. This is an aspiration psychrometer with the bulbs of the thermometers ventilated by a fan operated by a clock-type spring. The bulbs of the thermometers are covered with metal sleeves whose outer surfaces are bright chromium-plated in order to prevent radiation from surrounding surfaces affecting the readings of the thermometers. For the same reason it is desirable to hold the psychrometer away from the body of the observer and other surfaces. The fan should be run for three minutes before taking a reading. For accuracy, an occasional checking and control of ventilation speed is essential.

3.6.11 Hygrometric Surveys

Hygrometric survey in mines is normally carried out to check and control the environmental conditions at various parts of the

mine so as to maintain the mine atmosphere (wet-bulb temperature and air velocity or effective temperature) within statutorily permissible limits. It is generally carried out by whirling hygrometers, the survey proceeding in a regular manner from the top of the downcast shaft to that of the upcast shaft. Readings must be taken at all splits, points of leakage, haulages, compressors etc., before and after wet sections of roadways and in fact at all places where the temperature and humidity of the mine air are to undergo a marked change. Psychrometric readings should be accompanied by measurements of pressure and quantity of air flowing.

When psychrometric survey results are to be used for heat transfer studies in the mine, it is necessary to note the time of the psychrometer reading. Simultaneously a control psychrometer is read at the surface at regular time intervals so that the survey readings can be corrected for variation of temperature and humidity of surface air with time.

3.7 DENSITY OF AIR

Density (mass per unit volume) of air varies with its temperature, pressure and moisture content. Within the range of temperatures and pressures met with in mines, air can be considered as a perfect gas so that the ideal gas law can be applied to it. Let us first consider dry air.

$$PV_0 = R_0T \tag{3.73}$$

where P = pressure of air in Pa,

V_0 = volume of 1 kmol of air in m^3,

T = temperature of air in K

and R_0 = universal gas constant = 8314.4 J kmol^{-1} K^{-1}.

Taking air to have the composition by volume as given in Table 1.1, and molecular masses of O_2, CO_2, N_2 and Ar (including other rare gases) as 32, 44, 28 and 40 respectively the molecular mass of air.

$$= \frac{20.95\times32+0.03\times44+78.09\times28+0.93\times40}{100}$$

$$= 28.955$$

$\therefore$ characteristic gas constant of air

$$R_a = \frac{8314.4}{28.955} \simeq 287.1 \text{ J kg}^{-1}\text{ K}^{-1}.$$

Equation 3.73 can be written as follows in terms of characteristic gas constant of air :

$$PV = R_aT \tag{3.74}$$

Scanned with CamScanner

where V = specific volume of air
(volume per unit mass) in $m^3 kg^{-1}$.

Using the value of R_a in equation 3.74, we have

$$V = 287.1\ T/P \tag{3.75}$$

Or, ρ_a (density of dry air in kg m^{-3}) = $P/287.1\ T$

$$= 1000\ B/287.1\ T \tag{3.76}$$

where B = barometric pressure in kPa.

For moist air the density depends on the amount of moisture in the air or the vapour pressure. Consider 1 m^3 of moist air. Both dry air and moisture occupy the same volume. The mass of dry air and moisture in this volume will depend on their partial pressures, $B-e$ for dry air and e for water-vapour.

$$\text{Mass of dry air} = \frac{1000\ (B-e)}{287.1\ T}\ \text{kg}$$

$$\text{and mass of water-vapour} = \frac{1000\ e}{R_w\ T}\ \text{kg}$$

where R_w = characteristic gas constant for water-vapour

$$= \frac{R_0}{18} = \frac{8314.4}{18} = 461.9\ \text{J kg}^{-1}\ \text{K}^{-1} \tag{3.77}$$

and e is in kPa.

Total mass of moist air

$$= \frac{1000\ (B-e)}{287.1\ T} + \frac{1000\ e}{461.9\ T}$$

$$= \left(\frac{B-0.378\ e}{287.1\ T}\right) 10^3\ \text{kg}$$

Since this is the mass of 1 m^3 of moist air, the density of moist air

$$\rho = \left(\frac{B-0.378\ e}{287.1\ T}\right) 10^3\ \text{kg m}^{-3} \tag{3.78}$$

Example 3.7

Calculate the density of air at a barometric pressure of 101.325 kPa and dry- and wet-bulb temperatures of 299 and 296 K respectively.

From equation 3.72 vapour pressure $e = 2.6$ kPa.

If ρ = density of air, then from equation 3.78

$$\rho = \frac{(101.325-0.378\times2.6)\ 1000}{287.1\times299} = 1.17\ \text{kg m}^{-3}.$$

Specific Weight of Air. The specific weight of air which is defined as the weight of air per unit volume is given by the relation

$$\gamma = \rho\ g\ \text{N m}^{-3} \tag{3.79}$$

with ρ in kg m^{-3} and g in m s^{-2}.

It is obvious that while density does not change with change of gravity, specific weight does.

Specific Gravity. The specific gravity of any gas or mixture of gases generally refers to the ratio of the density of the gas or mixture of gases to that of air at the same temperature and pressure (usually standard temperature and pressure). Since 1 kmol of any gas (ideal) at a given temperature and pressure has the same volume (1 kmol at STP has a volume of 22.4137 m^3), the specific gravity of any gas is then the ratio of its molecular mass to the molecular mass of air.

For example the specific gravity of water-vapour

$$= \frac{18}{28.955} = 0.622$$

Specific gravity of solids, however, is the ratio of the density of solid to that of water at 277.15 K (=1000 kg m^{-3}). The specific gravity therefore numerically equals the density expressed in t m^{-3}.

3.8 SPECIFIC HEAT

The specific heat of air is the amount of heat required to raise the temperature of a unit mass of air by one kelvin. The specific heat at constant volume C_v is less as the heat here is required only to raise the temperature (internal energy) of the air. But the specific heat at constant pressure C_p is comparatively more since in this case the heat has not only to raise the temperature, but also to do work for the expansion of the air. For ideal gases $C_p - C_v = R_a$, but for real gases $C_p - C_v > R_a$ since there is not only external work of expansion but also internal work done to overcome intermolecular cohesion when the air expands at constant pressure. For air C_p is roughly equal to 1005 J kg^{-1} K^{-1} while C_v is roughly equal to 712 J kg^{-1} K^{-1}.

Specific heat varies with temperature and can be given by the following simple relations for the range of temperatures commonly met with in mines.

(a) $C_{pa} = 995.68 + 0.029\ T$ J kg^{-1} K^{-1} (3.80)

(b) $C_{pv} = 1553.7 + 0.645\ T + 35\ 169/T$ J kg^{-1} K^{-1} (3.81)

Scanned with CamScanner

where C_{pa} = specific heat of air,
C_{pv} = specific heat of water-vapour
and T = temperature in K.

3.9 ENTHALPY

Enthalpy (sometimes called total heat) is defined by the equation

$$H = U + PV \tag{3.82}$$

where H = enthalpy,
U = internal energy,
P = pressure (absolute)
and V = specific volume.

Differentiating the above equation, we get

$$dH = dU + PdV + VdP \tag{3.83}$$

From the First Law of Thermodynamics

$$dq = dU + PdV \tag{3.84}$$

where dq = amount of heat exchanged.

Combining equations 3.83 and 3.84, we have

$$dq = dH - VdP \tag{3.85}$$

For incompressible flow in an open system, as in a mine, there is no change of pressure on heating. Hence the change in enthalpy equals the amount of heat added to the air.

Enthalpy is a function of the state of the air and hence a change in enthalpy is dependent on the initial and final states and not on the process of change. For an ideal gas change in enthalpy is given by the relation

$$dH = C_p\, dT \tag{3.86}$$

Normally enthalpy of air at 273.15 K (0°C) is assumed to be zero and the enthalpy at any particular state is given by the sum of the sensible heat of dry air, the latent heat of water-vapour and the sensible heat of water-vapour. Let us first consider unsaturated air. If 1 kg of dry air contains, say m g of water vapour at T K, the enthalpy will be given by the relation

$$H = C_{pa}(T-273.15) + 0.001\, m\, C_{pv}(T-273.15) + 0.001\, ml \text{ kJkg}^{-1} \text{ of dry air} \tag{3.87}$$

where C_{pa} = specific heat of dry air, kJ kg^{-1} K^{-1},
C_{pv} = specific heat of water-vapour, kJ kg^{-1} K^{-1},
and l = latent heat of evaporation of water, kJ kg^{-1}.

We have said that C_p varies with temperature. The latent heat of evaporation of water l also varies with temperature. For temperatures between 273 and 373 K the following relation can be assumed to hold good with reasonable accuracy.

$$l = 3.1636 \times 10^6 - 2428\ T \text{ J kg}^{-1} \tag{3.88}$$

The enthalpy of water-vapour at any particular state is constant, whatever way the change in state might have been achieved. In other words, the enthalpy in the above case will be the same in the two different hypothetical cases, i.e. if (a) the water were vaporized completely at 273.15 K and the vapour then raised to T K or (b) it were raised to the temperature T K in the liquid state and then vaporized at that temperature. In the former case the value of l in equation 3.87 is that corresponding to 273.15 K and those of C_{pa} and C_{pv} corresponding to the average temperature $(273.15+T)/2$ K (more correctly the value of $C_p\,(T-273.15)$ in equation 3.87 should be $\left(=\int_{273.15}^{T} C_p\, dT\right)$. In the latter case the equation will be

$$H = C_{pa}(T-273.15) + 0.001 m C_{pw}(T-273.15) + 0.001\ ml \tag{3.89}$$

where C_{pw} = specific heat of water in liquid form
= $4820.5 - 2.18\, T$ J kg^{-1}K^{-1},
l = latent heat at T K

and C_{pa} and C_{pw} correspond to $(273.15+T)/2$ K.

Generally however, fair accuracy is achieved by using equations 3.87 or 3.89 with the following values of l, C_{pa}, C_{pv} and C_{pw} for the range of temperatures commonly met with in mines :

l = 2.5×10^6 J kg^{-1},
C_{pa} = 1005 J kg^{-1} K^{-1},
C_{pv} = 1860 J kg^{-1} K^{-1},
and C_{pw} = 4186.8 J kg^{-1} K^{-1}.

Enthalpies of moist air as calculated on the above basis are plotted in Fig. 3.9.

In case of supersaturated air where there is some water existing in liquid form in saturated air, the enthalpy will be given by the relation

$$H = C_{pa}(T-273.15) + 0.001\, m'\, C_{pv}(T-273.15) + 0.001\, m'l + 0.001\, m''\, C_{pw}(T-273.15) \text{ kJ kg}^{-1} \text{ of dry air} \tag{3.90}$$

where m' = amount of water-vapour in the saturated air in g kg^{-1} of dry air
and m'' = amount of liquified water-vapour in g kg^{-1} of dry air, so that
$m' + m''$ = total moisture content of air.

3.10 EFFECT OF HEAT AND HUMIDITY ON THE MINER

It has been said earlier that the human body produces a lot of waste heat by the process of metabolism which has to be dissipated into the surrounding mine air.

The major part of the heat produced by the body is dissipated from the surface of the skin by radiation, convection and evaporation of sweat, though a very small part is dissipated from the lung through exhaled air. The heat transfer from the inner parts of the body to the skin is through the blood circulatory system, although conduction accounts for a minor part.

When the temperature of the atmosphere is 298 K or less, the normal blood circulation of the body along with conduction is sufficient to transfer the heat from the inner parts of the body to the surface of the skin. The heat transfer from the skin to the ambient air at these temperatures is mainly by convection and radiation. But above 298 K, the heat transfer to the skin has to be faster. Here, the vaso-motor control comes into operation, dilating the size of blood vessels and thus ensuring larger blood circulation to the skin. As the temperature rises above 302 K, the sweat glands start functioning and now the heat transfer from the skin is mainly by the evaporation of sweat.

When the dry-bulb temperature of the mine air exceeds the body temperature (310.05 K) the body can give away heat to the surrounding atmosphere by the evaporation of sweat only.

3.10.1 Effect of High Wet-bulb Temperature

The rate of evaporation of sweat depends on the moisture content of the ambient air and the air velocity. Though the relative humidity of air is specified by the difference in the dry-bulb and wet-bulb temperatures, it is the wet-bulb temperature, that greatly influences the rate of evaporative cooling of the human body. At high wet-bulb temperatures the rate of cooling gets reduced. As a result, the body temperature rises as shown in Table 3.5.

The rise in the temperature of the body varies from person to person and depends on the degree of acclimatization. A moderate rise in the body temperature of the order of 1.4 K is not harmful, but when the body temperature rises above 312 K and/or the heart rate exceeds 140 beats min^{-1} heat intolerance, that may ultimately lead to heat stroke, appears.

Table 3.5 : Rise in Body Temperature with Wet-bulb Temperature

Wet-bulb temperature in K	Rise in body temperature in K
Up to 302.15	0.11 - 0.66
302.65 - 304.85	0.33 - 0.77
305.35 - 307.65	0.66 - 1.55
Above 307.65	1.44 - 1.90

Various authorities have given different tolerable limits of wet-bulb temperature. Haldane[43] puts it at 304.3 K for partially acclimatized men at rest in still, saturated air. With a high dry-bulb temperature, however, this value could be somewhat more. Caplan reported that with the prevalent high dry-bulb temperatures in the Kolar Gold Field of the order of 316-322 K, cases of heat stroke were frequent at wet-bulb temperatures of 307.5-308.5 K but were rare below a wet-bulb temperature of 305.5 K. A study in South Africa revealed that the probable risk of heat stroke rose sharply when the wet-bulb temperature exceeded 305.15 K, but was low when the wet-bulb temperature was between 300.15 K and 304.15 K. Fatal heat stroke risks were negligible below 302.5 K w.b. and non-fatal heat stroke risks were negligible below 300.15 K.

3.10.2 Acclimatization

Acclimatization plays an important role in the human tolerance of high wet-bulb temperatures. The first physiological response of the human body to very hot and humid atmosphere is the dilation of the blood vessels in the skin, but the volume of the fluid in the blood circulatory system does not immediately increase as a result of which the heart-rate shoots up to 160-180 beats min^{-1}. After two to three days of acclimatization, however, the circulatory volume builds up and consequently the heart-rate falls to 120 beats min^{-1}. In addition sweating begins earlier and the rate of sweating increases.

A system of acclimatization has been satisfactorily adopted in South African gold mines where the worker is made to work at a

Scanned with CamScanner

controlled rate for four hours a day in a chamber with a saturated air temperature of 305.15 K and an air velocity of 0.5 m s^{-1}. The work rate is gradually increased to a maximum (rate of oxygen consumption = 1.4 l min^{-1}) on the last day over a period of eight days. This system has been claimed to satisfactorily acclimatize Bantu miners for the following combinations of work and wet-bulb temperature :

(a) Light work (0.65 l min^{-1} oxygen consumption) at 307.15 K.
(b) Moderate work (0.95 l min^{-1} oxygen consumption) at 305.15 K
(c) Hard work (1.45 l min^{-1} oxygen consumption) at 304.15 K.

Worse wet-bulb temperatures can be tolerated by these acclimatized workers at reduced work rate, higher air velocity of 1-1.5 m s^{-1} or with the use of a micro-climate cooling system.

It must, however, be noted here that the capacity for acclimatization varies from person to person and some persons never really get acclimatized. Besides acclimatization is a temporary phenomenon and the effect is lost if the worker is taken out of the hot and humid conditions for about a month or so.

3.10.3 Effect of Air Velocity

Higher air velocity aids evaporative cooling, by removing the saturated air from the immediate vicinity of the body surface. However it has been seen that though an increase in air velocity up to 1 m s^{-1} markedly affects the comfort condition, the effect is less felt above this velocity and is negligible beyond a velocity of 3 m s^{-1}. On the other hand, velocities greater than 2 m s^{-1} are uncomfortable as they raise dust. High velocities of the order of 3m s^{-1} or more, when coupled with a high dry-bulb temperature of the order of 322 K and a low relative humidity, cause burning sensation and a rise of body temperature by too rapid evaporation of sweat and may ultimately result in heat stroke.

3.10.4 Heat Stroke

Heat stroke results from the breakdown of the temperature regulating mechanism of the body when the body temperature shoots up. In the early stages, it is characterized by mental excitement followed by restlessness, intolerance and delirium. Vomiting is a usual symptom. Muscular cramps and loss of body fluid occur [illegible] temperature rises above 313 K, the skin

becomes hot, dry and gritty ; the pulse becomes fast and irregular and the respiration, stertorous. At 314.25 K unconsciousness occurs and the skin turns blue due to cyanosis. If no measures are taken to reduce the temperature, death occurs due to asphyxia at 316.5 K.

People having constipation and alcoholics are more prone to heat stroke. People in febrile conditions having an initial body temperature above the normal develop very high temperatures under heat stroke conditions. It has been observed in South African mines that workers with low body weight who normally have low work capacity fall an easier prey to heat stroke. Gross overweight with low work capacity also makes the worker prone to heat stroke. Older men (over 45 years of age) are more liable to heat stroke than younger men.

The patient suffering from heat stroke should be stripped naked and laid down. Cold water should be poured over the body accompanied by vigorous fanning. The hair should be cropped short and ice bag applied to the head until temperature comes down to 312 K when the body should be covered by a thin blanket. Utmost caution is necessary for a day or two as the symptoms of heat stroke are likely to relapse.

3.10.5 Changes in Cardio-vascular System

Under hot and humid conditions, more blood is supplied to the skin and hence the cardiac rate and output increase so much that beyond the critical temperature cardiac failure may result. This leads to decreased blood pressure which causes less blood circulation. As a result, heat exhaustion symptomized by fatigue, nausea, giddiness and headache occurs leading under more severe conditions to vomiting and blurred vision. The ultimate stage is heat collapse which results in unconsciousness. In severe cases of collapse, the skin becomes cold and clammy and the pulse cannot be felt. It is however less severe than heat stroke though the conditions producing it are the same.

3.10.6 Changes in Water and Chloride Metabolism

There is a great loss of water from the body when there is excessive sweating. At 307 K a resting man may sweat at the rate of 120 cm^3 per hour though when doing hard work the sweat rate may increase to 850 cm^3 h^{-1}. Beyond this however, the sweat

Scanned with CamScanner

output decreases due to fatigue of the sweat glands. Haldane states that there have been cases where a man produces as much as 2.94 kg of sweat per hour when doing hard work in a very hot atmosphere, though the average sweating rate of acclimatized men varies between 0.45 and 0.7 kg h^{-1}. The loss of sweat is usually made up by drinking water, but the maximum a man can drink at hot temperatures is estimated at 700 cm^3 h^{-1}. Drinking in excess of this may result in vomiting and the water may not be able to get into the body and the circulatory system owing to the lack of sufficient blood supply to the alimentary canal. Excessive loss of water causes dehydration of the body characterized by sunken eyes and inelastic skin, high body temperature and may lead to the failure of blood circulation.

Man has enough sodium chloride reserve in the body (28g in blood and 57g in the tissues) and this is normally replenished by the usual daily intake of 14 to 24g. The loss of sodium chloride in 100 cm^3 of sweat amounts to 0.5g only. Hence an occasional excessive sweating cannot deplete the chloride reserve of the body to any appreciable extent unless there is heavy sweating over a long period aided by further chloride loss through vomiting or diarrhoea. The effects of chloride depletion are fatigue, nausea, vomiting and cramps.

3.10.7 Mental Fatigue

This is the outcome of continued undersupply of blood to the brain which causes mental depression, neglect of work and a rebellious attitude that may lead to strikes. Carelessness due to mental fatigue is a potential cause of accidents. It is interesting to note that after the installation of the air-conditioning plants at the Kolar Gold Field there was a sharp fall in the number of accidents underground.

3.10.8 Fall of Working Efficiency

The working efficiency of man falls with increasing temperature and humidity of the ambient air. Caplan and Lindsay state that at the Kolar Gold Field the efficiency of workers in a 3-hour shift (in a high dry-bulb temperature) starts falling at a slow rate when the wet-bulb temperature exceeds 301.5 K. Beyond 305 K, the fall is rapid as would be evident from Table 3.6.

Table 3.6 : Working Efficiency at Various Wet-bulb Temperatures

Wet-bulb temperature in K	Working efficiency (%)
306.8	75
308.2	50
310.1	25

Fig. 3.12 gives the working efficiency of miners in South African gold mines at various wet-bulb temperatures on the basis of work output at 300.15 K being considered as 100%.

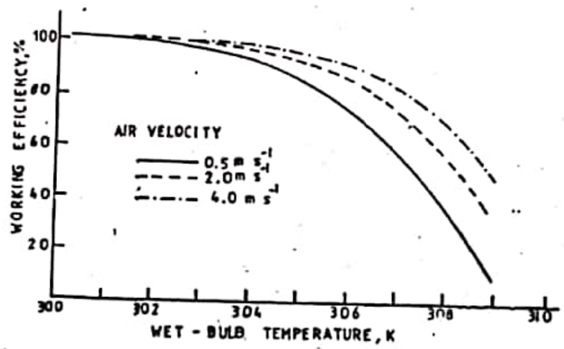

Fig. 3.12 Working efficiency vs wet-bulb temperature (after Wyndham).

3.11 COOLING POWER OF MINE AIR

The cooling power of mine air depends mainly on the wet-bulb temperature and the air velocity. The dry-bulb temperature affects the cooling power only a little except in cases of high dry-bulb temperature coupled with low wet-bulb temperature and high air velocity. So, the cooling power of mine air on the human body can be expressed in terms of wet-bulb temperature and air velocity and in fact, in most of the mines the wet-bulb temperature alone can be taken as a fair measure of comfort conditions. Other measures have, however, been developed to define the cooling power of mine air more exactly.

Scanned with CamScanner

3.11.1 Kata Thermometer

The kata thermometer developed by Hill *et al.*, as early as 1916 is a glass thermometer (Fig. 3.13) with a 40mm long and 20mm diameter bulb filled with coloured alcohol connected to a 200mm long stem having two smaller bulbs or reservoirs at the top and the bottom ends. The stem has two marks at 308 and 311 K in between the two bulbs. When taking a reading with the kata thermometer, the bulb is first heated by dipping it in hot water so that the liquid rises to the top reservoir. The bulb is then taken out of water, wiped with a dry cloth and is allowed to cool in the mine air. The time taken by the thermometer to cool from 311 K to 308 K is noted. The kata cooling factor which gives the amount of heat lost per cm^2 of the surface of the bulb in cooling from 311 to 308 K is usually written on the kata thermometer. This factor divided by the time taken for the cooling gives the rate of heat loss from the kata thermometer.

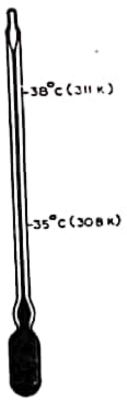

Fig. 3.13 Kata thermometer

The dry-kata reading gives an estimate of the heat loss from the surface of the bulb due to radiation and convection and hence is of little importance, particularly under hot and humid conditions where most of the heat loss from the human body is through evaporation. All the same Hill advocates a dry-kata reading of not less than 250 W m^{-2} for good working conditions.

The wet-kata reading is obtained by covering the bulb of the kata thermometer by a wet muslin. The idea is to make it resemble the human body which loses heat by radiation, convection as well as evaporation. The wet-kata cooling power is related to the wet-bulb temperature and the air velocity by the following relations.

$$K = (14.65+35.59\, v^{1/2})\,(309.65-T') \qquad (3.91)$$

for air velocities < 1 m s^{-1}

$$\text{and} \quad K = (4.19+46.05\, v^{1/2})\,(309.65-T') \qquad (3.92)$$

for air velocities > 1 m s^{-1}

where K = kata cooling power of air or the heat loss in W m^{-2},

v = velocity of air in m s^{-1}

and T' = wet-bulb temperature in K.

It has been said earlier that a moderately working man produces about 165 W m^{-2} of waste heat which has to be dissipated. In other words, a kata value of 165 W m^{-2} should be sufficient for cooling a moderate worker, but it has been found that the rate of cooling of the kata thermometer is much faster compared to the human body, i.e. the cooling air is not 100% efficient for the human body as compared to a kata thermometer. This is due to the fact that the kata thermometer is much smaller compared to the human body and has a smaller volume to surface area ratio. Also, the convection coefficient of a kata thermometer is twice as high as that of a nude body. The body surface is rarely completely sweat-covered as the wet kata. Because of clothing, air cannot get access to the whole body surface. Besides, the factor of acclimatization of the human body too contributes to the difference between the cooling effect of mine air on the kata thermometer and the human body.

Many authors put the kata cooling efficiency of air at only 20% which means that for comfortable working, the minimum wet-kata reading should be 165×5=825 W m^{-2}. Bedford and Worner[43] give the following work output for various wet-kata readings (Table 3.7).

Table 3.7 : Variation of Work Output with Wet-Kata Reading

Wet-kata reading, W m^{-2}	Rest time in min h^{-1}	Relative work output (%)
778.7	7.3	100
611.3	6.7	94
540.1	9.0	91
452.2	10.0	82
376.8	11.1	81
268.0	22.4	59

Orenstein and Ireland also give the lower limit of wet-kata cooling power for comfortable working condition as 628 W m^{-2}.

However, the kata cooling power is not always consistent. The kata factor varies with temperature. A variation of 10% occurs if the air temperature changes from 283 to 303 K. Moreover, with low air velocities and large differences between dry- and wet-bulb

Scanned with CamScanner

temperatures, the wet-kata cooling power has a considerably low value. This is due to the fact that in an unventilated or poorly ventilated wet-bulb thermometer (which the kata is in a way) the moisture evaporated surrounds the bulb and hence the thermometer gives a higher reading for the wet-bulb temperature than the true value. Because of this higher estimation of the wet-bulb temperature by the kata thermometer, the cooling power shown by it is less. This is illustrated by the following example. At a wet-bulb temperature of 306.5 K and an air velocity of 0.51 m s^{-1} the kata readings were 159, 130 and 71 W m^{-2} for differences between dry- and wet-bulb temperatures of 0, 5.56 and 16.67 K respectively whereas for the same wet-bulb temperature and with an air velocity of 5.1 m s^{-1} the kata readings for all dry-bulb temperatures remained constant at 159 W m^{-2}. Thus it will be seen that the kata thermometer overestimates the effect of air velocity and underestimates that of temperature and humidity of the mine air as regards its cooling power.

It is for these reasons that the kata thermometer offers no better measure of the cooling power of mine air than wet-bulb temperature, hence its use has long been discontinued in many parts of the world.

3.11.2 Effective Temperature

In 1925 Yaglou developed the effective temperature scale. This scale reduces any environmental condition of dry- and wet-bulb temperatures and air velocity to a thermo-equivalent condition of still, saturated air at a certain equivalent temperature called the effective temperature. In other words, the feeling of warmth of a worker under the condition of the said dry- and wet-bulb temperatures and air velocity is the same as at the equivalent temperature in still, saturated air. The scale is computed by subjecting men to a certain air condition (dry- and wet-bulb temperatures and air velocity) in one room and then letting them into another adjacent room where the air is still and saturated. The saturated temperature at which the feeling of warmth by the man is the same as at the given air condition, is the effective temperature. Fig. 3.14 gives the effective temperature scale for men stripped to the waist.

This scale was held by the British Royal Commission on Safety in Coal Mines to be superior to wet kata estimation under extreme conditions of heat and humidity.

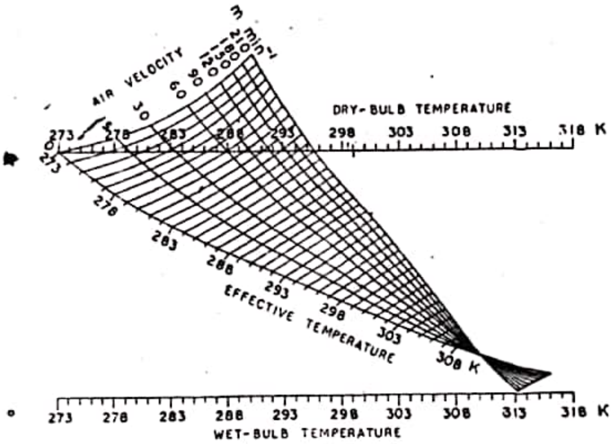

Fig. 3.14 Effective temperature scale for men stripped to the waist.

However, the effective temperature is subject to the feeling of warmth by men which not only depends on the individual but also his immediate past experience or extent of acclimatization. It is also subject to the following criticism :

(a) It gives insufficient weight to the deleterious effect of low air velocities below 0.5 m s^{-1} in hot and humid environments.
(b) It exaggerates the effect of high dry-bulb temperatures at air velocities in the range of 0.5-1.5 m s^{-1}.
(c) It underestimates the harmful effect of high air velocities above 1.5 m s^{-1} at extremely high temperatures exceeding 322 K.
(d) Climates of similar physiological severity as assessed by rectal temperature, heart rate etc. do not always have the same effective temperatures, especially in severe heat stress.

Like wet-bulb temperature, the effective temperature gives an assessment of the cooling power of the environment irrespective of the working rate of man. Different limits of effective temperature could be set for different work rates but such limits would have to

Scanned with CamScanner

be empirical. Yaglou and Drinker gave the following comfortable limits of effective temperature for men and women in light clothing engaged in sedentary occupation :

Season	Effective temperature, K		
	Lower limit	optimum	upper limit
Summer	291	294	299
Winter	288	290	296

For men acclimatized in tropical conditions, the upper limit rises to 300 K which can also be taken as the upper limit for mine workers.

Carrier gives the following working efficiency for industrial workers at different effective temperatures :

Table 3.8 : Working Efficiency at Different Effective Temperatures

Effective temp., K	Working η, %	Effective temp., K	Working η, %
294	100	308	50
300	90	311	30
305	70		

Fig. 3.15 gives the working efficiency of South African miners at various effective temperatures.

3.11.3 Predicted Four-hour Sweat Rate (P_4SR)

A physiological index of comfort in a certain environment called the 'predicted four-hour sweat rate' was developed by the Medical Research Council of Great Britain on the basis of large-scale tests in London and Singapore between 1947 and 1953. The predicted four-hour sweat rate can be read from nomograms prepared by the Council from the various variables affecting the index : dry-bulb

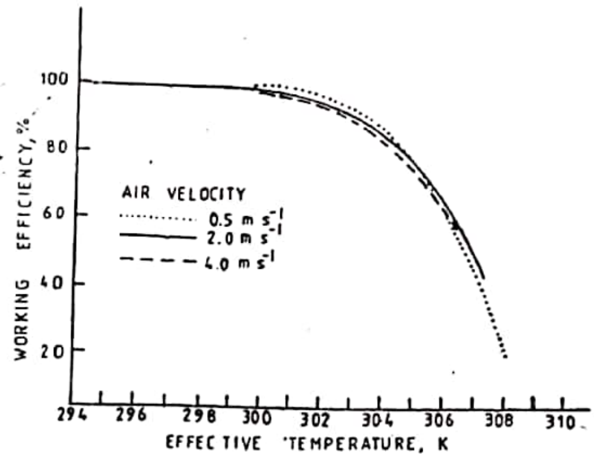

Fig. 3.15 Working efficiency vs effective temperature (after Wyndham).

temperature of air, wet-bulb temperature of air, radiant temperature, air velocity, rate of work, nature of clothing. The method is claimed to be very reliable, but even here, errors may creep in due to variable work output and physical fitness of different men. Besides, the calculation is complicated and involves the measurement of several factors. It is perhaps because of this reason that P_4SR has found little acceptance in mines.

3.11.4 Specific Cooling Power

The specific cooling power of mine air is defined by Mitchell and Whillier[132] as the maximum rate of heat transfer from 1 m^2 of the human body surface to the surrounding air under any environmental condition defined by dry-bulb temperature, wet-bulb temperature, velocity of air, radiant temperature, atmospheric pressure and the skin temperature. The following empirical relations were developed from extensive studies for different modes of heat transfer :

$$R = 17\times 10^{-8}\,(0.5\,T_r + 154.1)^3\,(T_s - T_r) \tag{3.93}$$

$$C = 8.3\,(B/10\;1.3)^{0.6}\,v^{0.6}\,(T_s - T_a) \tag{3.94}$$

and $$E = \frac{15\ 100}{B} (B/101.3)^{0.8}\ v^{0.6}\ (e'_s - e) \tag{3.95}$$

where R, C and E are maximum rates of heat transfer by radiation, convection and evaporation respectively in W m^{-2},

B = barometric pressure in kPa,
T_r = radiant temperature, K,
T_a = dry-bulb temperature of air, K,
T_s = temperature of the skin, K,
e = vapour pressure of air, kPa,
e'_s = saturated vapour pressure at the skin temperature, kPa,
and v = air velocity, m s^{-1}.

The specific cooling power of the air $= R+C+E$ (3.96)

This specific cooling power should equal or exceed the metabolic heat rate for any work rate in order to dissipate all heat produced by the human body. However, to avoid excessive heat strain, the skin temperature has to be maintained at a certain level. It has been seen that acclimatized men in equilibrium in hot environments showing only a mild heat strain have mean skin temperatures close to 308.2 K irrespective of air temperatures, humidity, air speed or work rate.

Taking 308.2 K as the acceptable skin temperature, and with the approximations of $T_r = T_a$, $B = 100$ kPa and $T_a = T' + 2$ where T' is the wet-bulb temperature of air, a chart (Fig. 3.16) was prepared giving specific cooling power as a function of wet-bulb temperature and air velocity. For most mine environments where the difference between T_a and T' is small (taken here as 2 K), these charts will give a good estimate of the cooling power of air. The chart also provides the design comfort environment (dry-bulb and wet-bulb temperatures and air velocity) for any work rate for the purpose of the calculation of cooling load when air cooling becomes necessary.

For example, for hard work (metabolic rate of 270 W m^{-2} at a place with a prevalent air speed of 0.5 m s^{-1}, the tolerable wet-bulb temperature will be 300.5 K (the dry-bulb temperature being 302.5 K). If, however, the air speed could be raised to 2.5 m s^{-1}, the tolerable wet-bulb limit will rise to 305 K.

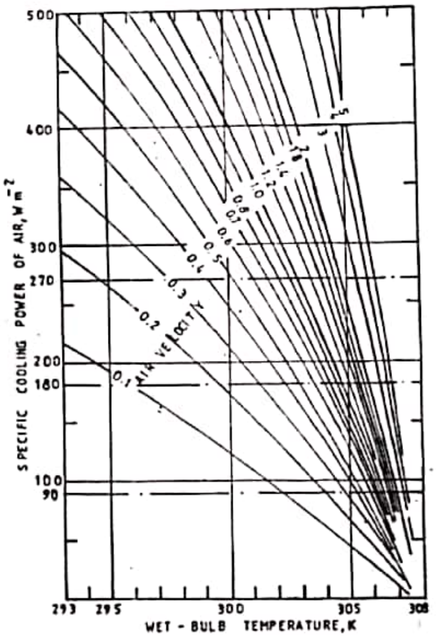

Fig. 3.16 Specific cooling power of air at different wet-bulb temperatures and air velocities (after Wyndham).

3.12 METHODS OF IMPROVING THE COOLING POWER OF MINE AIR

As surface air enters a mine through a downcast shaft, its temperature rises due to auto-compression. Strata heat may also add to the air temperature in deep mines. The latter will, however, vary from season to season depending on the surface air temperature. As the air travels from the downcast shaft-bottom to the working face, its temperature will further rise due to heat added from the rock. While the rate of temperature rise will be somewhat slower in the intake airway, it will be higher across the workings which on advancing continuously expose virgin-rock faces to the air-current. The air, however, rarely acquires the virgin-rock temperature (v.r.t.)

Scanned with CamScanner

at the face except in relatively shallow and poorly ventilated mines. If the temperature of air is less than the v.r.t. as it leaves the workings, there will be a further rise in its temperature in the return up to the upcast shaft-bottom (assumed to be at the same elevation as the downcast shaft-bottom) though at a very slow rate owing to the small difference in the rock and air temperatures. However, in bidirectional system of ventilation, there may actually be a fall in the air temperature along the return owing to leakage of cooler air from the intake. As the air rises in the upcast shaft, there is a fall in its temperature due to auto-expansion, but it has a temperature still higher than that of the atmosphere except in very shallow mines where the rock temperature may be lower than the surface air temperature so that there is heat transfer from the air to the rock.

The above is the case in dry mines. But in wet mines (most mines are wet), there may be very slight rise in the dry-bulb temperature of the air (in fact there may be a fall in extremely wet shafts) at the downcast shaft-bottom. But the wet-bulb temperature rises substantially increasing the relative humidity of the air. Strata heat addition in the intake raises the dry-bulb temperature, but lowers the relative humidity so that the air is capable of picking up more moisture if the intake roadway is wet. In relatively dry faces there is a rise in saturation deficit owing to rapid addition of strata heat. In the return airway however, addition of moisture may decrease the dry-bulb temperature while raising the wet-bulb temperature so that the air is nearly saturated as the upcast shaft-bottom. Auto-expansion in the upcast shaft cools the air often below the dew point causing water to condense in the upcast shaft. In deep and wet mines, the condensed water literally pours down the upcast shaft.

Fig. 3.17 illustrates the air temperature variation in a deep and highly wet coal mine in India (Chinakuri No. 1 & 2 pits) while Fig. 3.18 illustrates the annual variation of the upcast and downcast pit-bottom temperatures at the same mine.

Fig. 3.17 also gives the variation in the enthalpy and moisture content of the air as it traverses the mine. With an intake of 80 $m^3\,s^{-1}$ as measured at the downcast shaft-bottom (specific volume $=0.854\ m^3\,kg^{-1}$ of dry air) the dry air-flow rate is 93.7 $kg\,s^{-1}$. The heat added to the air between the downcast shaft-top and upcast shaft-bottom is $93.7\ (99.65-52.35)\times10^{-3}=4.43$ MW. A part of

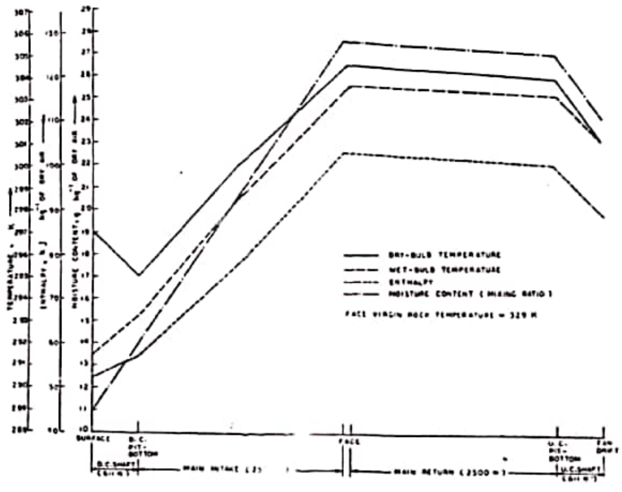

Fig. 3.17 Variation of dry- and wet-bulb temperatures at Chinakuri No. 1 and 2 pits (November, 1975) ; Face V.R.T.=329 K.

this heat is given up in the upcast shaft so that the total heat removed from the mine$=93.7\ (89.60-52.35)\times10^{-3}=3.49$ MW.

There is an addition of $93.7\ (14-11)=281.1$g of moisture per second in the downcast shaft, while total addition of moisture up to the upcast shaft-bottom is $93.7\ (26.8-11)=1480.5\ g\,s^{-1}$. Of this $93.7\ (26.8-24)=262.4\ g\,s^{-1}$ condenses in the upcast shaft and is carried back into the mine. It is significant to observe that the ventilating air acts as a water pump in the mine, removing in the above case $93.7\ (24-11)\times3600\times10^{-6}=4.385$ t (or m^3) of water in an hour. The quantity would be higher with higher air-flow rates.

The methods of improving the cooling power of mine air include (a) increasing the quantity of ventilating air, (b) circulating drier air and (c) cooling or refrigeration of the circulating air (including the use of devaporized compressed-air).

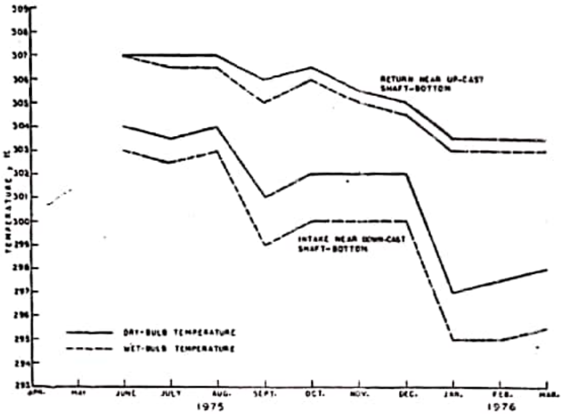

Fig. 3.18 Annual variation of temperatures at d.c. and u.c. shaft-bottoms at Chinakuri No. 1 and 2 pits (1975-76).

3.12.1 Increased Quantity of Air

This should be the first to be tried for improving hot and humid conditions in mines. The increased quantity of air not only dilutes the heat produced in the mine but also produces a higher air velocity which improves the cooling power of mine air. There is a minimum quantity of air required for a mine for supporting men and flame lamps and for diluting dust and gases to a safe concentration. In shallow mines this quantity is usually sufficient for dealing with the heat also. However, in deep mines an extra quantity may be necessary for suitably dealing with the heat produced in the mine. It is difficult to assess the exact quantity of air required because of the fact that a variety of factors such as the temperature of the air entering the mine, the quantity of heat addition from different sources, the wetness of the mine and the efficiency of air distribution underground affect it and many of these factors are variable. All the same a fair estimate of the heat addition in a mine from different sources should be made and the quantity requirement for the dilution of this heat evaluated before deciding on any additional measure for improving the cooling power of mine air.

Taking a minimum air velocity of 0.5 m s^{-1} in any part of the mine and considering provision of comfortable environment for hard work (metabolic rate of 270 W m^{-2}), the maximum allowable wet-bulb temperature in any part of the mine will be 300.5 K (see Fig. 3.16).

It would be advisable to design the ventilation system on the basis of this wet-bulb temperature even though the wet-bulb temperature permissible by law is higher, i.e. 303.5 K in India. The allowable enthalpy of air then corresponds to the wet-bulb temperature of 300.5 K and dry-bulb temperature of 302.5 K. It may be noted here that the enthalpy of air is primarily dependent on the wet-bulb temperature (see the psychrometric chart—Fig. 3.9 and mark the near parallelism of the wet-bulb line and the enthalpy line) and even if the dry-bulb temperature were somewhat more or less than 2 K higher than the wet-bulb temperature in any part of the mine, the error introduced by the above assumption of the dry-bulb temperature will be negligible.

If q is the amount of heat added in any part of the mine per unit time (kW), then for heat balance

$$M \cdot H_a = q + M\,H_i \tag{3.97}$$

$$\text{Or,}\quad Q = \frac{q}{(H_a - H_i)\rho'}\ \text{m}^3\ \text{s}^{-1}$$

where M = mass flow-rate of dry air, kg s^{-1},
= $Q\rho'$,
Q = quantity of air flowing, m^3 s^{-1},
ρ' = apparent density, kg of dry air per m^3 of moist air,
H_a = allowable enthalpy of air, i.e. at 300.5 K wet-bulb and 302.5 K dry-bulb temperatures, kJ kg^{-1} of dry air
and H_i = enthalpy of in-flowing air, kJ kg^{-1} of dry air.

At one mine on the Witwaterstrand Gold Field the quantity of air was increased from 40.6 m^3 s^{-1} to 135 m^3 s^{-1} and a refrigeration plant was installed simultaneously to improve conditions of temperature and humidity in the mine. The total heat extracted by the increased quantity of air was 3.49 MW, nearly twice as much as extracted by the refrigeration plant alone (1.55 MW). The wet-kata reading improved from 289 to 523 W m^{-2} with a 30% increase in the production efficiency. There was a reduction in the cases of heat stroke by two-third and a considerable reduction in the rates of accident and sickness.

However, the increase in volume has its limitations. In very hot and humid mines where an increased air velocity produces little bodily comfort, an extra volume of air will be of no help. Moreover mine airways should be large enough to take the extra quantity of air without causing excessive frictional pressure loss and excessive air velocity. High pressure loss increases the power cost of ventilation and high air velocity raises dust in the roadways. Hence both of these are undesirable.

We have seen earlier that the wet-bulb temperature of air entering a downcast shaft rises steadily with depth. At a certain depth therefore the wet-bulb temperature may reach a level which will lead to the face wet-bulb temperature exceeding the tolerable limit. In such cases ventilation alone will not be sufficient to alleviate the face environmental conditions.

3.12.2 Drying of Mine Air

It has already been said that a fairly high dry-bulb temperature can be tolerable if the relative humidity or the wet-bulb temperature is low. That is why in deep and hot mines where the air temperature is high, maintaining the air dry helps a great deal in improving the working conditions. There is no economical process of drying the air as such except by refrigeration. Drying of mine air by passing it over dessicants like calcium chloride, magnesium chloride or silica gel becomes very costly and the advantage gained by drying is greatly compensated by the heat produced by absorption which raises the temperature of air. However, care can be taken to see that the air does not pick up moisture in the mine and hence is maintained dry. This is done by adopting dry mining. Although dry mining is harmful from the point of view of dust hazard, it is worthwhile to find out suitable dry dust-collecting means rather than to use water for dust suppression in very hot mines. However, if the strata ooze out water, it is very difficult to control the humidity of the mine air. Spraying of fuel oil over the surface of airways has been found to considerably reduce evaporation from the surface. Experiments with a roadway-surface sprayed with fuel oil and then with water showed that it took the water one whole shift to evaporate whereas ordinarily it would have evaporated in 10 to 15 minutes. Sometimes it may be economical to line the major airways with concrete with suitable drain pipes installed in it to drain off the water from behind the lining and thus prevent moisture evaporating into the mine air. Covering up of water drains goes a long way in minimizing evaporation of moisture into the mine air.

3.12.3 Refrigeration

Refrigeration of mine air is necessary when its temperature becomes excessive so that no further increase in the quantity of air would improve environmental conditions. Refrigeration plants are usually designed to produce tolerable environmental conditions throughout the year at the working places in the mine. Normally, the air is cooled and dehumidified so that it is saturated at 275 to 278 K. It is then conducted to the working faces as such or after mixing with a stream of uncooled air so as to obtain the desired face temperatures. Hence a refrigeration plant should be designed to have a capacity, sufficient for cooling the farthest face under the worst surface-temperature conditions as may occur in the summer. The refrigerators installed on the Witwatersrand have usually a heat extracting capacity of 3.7 MW per 100 $m^3 s^{-1}$ of air entering the mine. They cool the surface air at 292.5 K dry-bulb and 289.5 K wet-bulb temperatures to 274.8 K saturated. The first refrigerator installed in India at Oorgaum mine cooled air from 296 K wet-bulb to 277.5 K saturated, the refrigerator capacity being approximately 5.58 MW per 100 $m^3 s^{-1}$ of air (the actual amount of heat extracted was 3.95 MW from 71.4 $m^3 s^{-1}$ of air flowing through the mine).

Calculation of Cooling Load of a Refrigerator. The cooling load of a refrigeration plant for any part of the mine is calculated so as to provide comfortable environmental conditions (300.5 K w.b. and 302.5 K d.b.) assumed earlier for ventilation requirement calculations. Heat-flow into the mine air from different sources has been discussed earlier. On the basis of this study an estimate of the total heat (both sensible and latent) added to the mine air in this part q is made. The required cooling load q_c is then given by the heat balance equation

$$q_c = q + Q\,\rho'\,(H_i - H_a)\ \text{kW} \tag{3.98}$$

The heat content of the air flowing into the mine varies from season to season and the cooling load should be calculated for the maximum heat content of the in-flowing air (occuring in the summer). However, it is necessary to determine the cooling load for

Scanned with CamScanner

different seasons, particularly when the variation is large, so that the refrigeration plant can be designed in multiple units. While the entire plant may work in the worst conditions, a part of it may be shut down during colder seasons.

In working mines, the heat content of the air reaching the workings gives the sum of the heat content of the ambient air entering the mine and the heat added in the mine so that the cooling load is estimated by deducting from it the heat content of the air desired to be circulated at the face. However, it must be noted here that while a spot cooler designed to cool the air at any particular face will handle the air supplied to that face only and hence will have a lesser total cooling load, a surface refrigeration plant will have a larger cooling load depending on the quantity of air entering the mine.

Refrigeration Process. The commonest type of refrigeration plant used at mines is of the vapour-compression type. In this type a liquid refrigerant is allowed to evaporate and extract the latent heat of evaporation from the mine air. To achieve this at temperatures as near the atmospheric as possible, the refrigerant is compressed. For example, liquid ammonia evaporates at 239.8 K absorbing a latent heat of evaporation of 1.37 MJ kg^{-1} of liquid ammonia at atmospheric pressure but at an absolute pressure of 406 kPa the evaporating temperature is 272.04 K and the latent heat 1.27 MJ kg^{-1}. For economy, the refrigerant is used in a cyclic system where it is condensed after evaporation and reused. Thus a complet evapour-compression refrigeration system comprises an evaporator where the liquid refrigerant evaporates by extracting the latent heat from the air it cools, a compressor for compressing the refrigerant vapour in order to raise its temperature of condensation and a condenser to turn the vapour refrigerant into liquid again. In addition, a receiver for storing the liquid refrigerant and an expansion valve for reducing the pressure and controlling the flow-rate of the refrigerant are needed.

The theoretical vapour-compression cycle is shown in Fig. 3.19 which gives the *P-H* (pressure-enthalpy) diagram for the cycle. Constant temperature lines are vertical in the liquid phase and horizontal in the liquid+vapour phase. Usually a dry compression (where the compression is in the vapour phase—the line 3-4 in Fig. 3.19) is preferred for better life of the compressor even though it has a little less coefficient of performance. A reference to Fig. 3.19

shows the evaporation represented by the line 2-3. The line 3-4 shows the compression of the refrigerant vapour. It is not isentropic (3-4") because of lost work in the compressor. The line 4-1 gives the condensation of the refrigerant and 1-2, the throttling process which cools the refrigerant. Both evaporation and condensation are isothermal. In the process of throttling or expansion, a part of the liquid refrigerant evaporates drawing the latent heat of evaporation from the liquid refrigerant so that its temperature falls, but as a result this part of the liquid refrigerant looses its ability to extract heat in the evaporator.

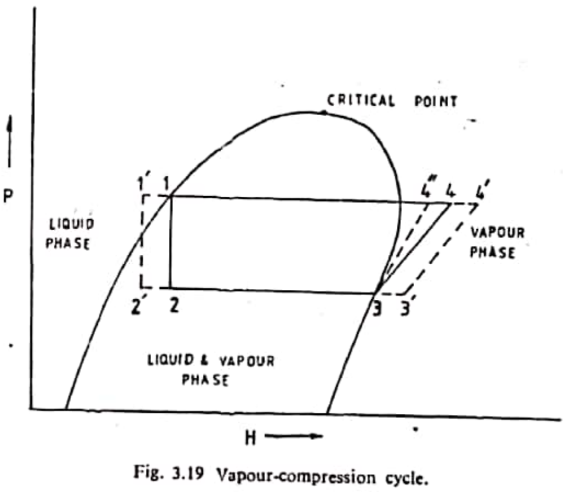

Fig. 3.19 Vapour-compression cycle.

In order to increase the coefficient of performance in actual refrigerators, the refrigerant may be sub-cooled in the condenser to 1' and superheated in the evaporator to 3' before being compressed.

The heat absorbed during evaporation

$$q_e = H_3 - H_2 \text{ kJ kg}^{-1} \text{ of refrigerant} \qquad (3.99)$$

where H is the enthalpy and the subscripts refer to the points on the *P-H* diagram. The amount of heat rejected during condensation is given by

Scanned with CamScanner

$$q_c = H_4 - H_1 \text{ kJ kg}^{-1} \quad (3.100)$$

$H_1 = H_2$ since no work is done during the throttling process and only sensible heat is converted to latent heat.

The work of compression W is given by the relation

$$W = q_c - q_e = H_4 - H_3 \text{ kJ kg}^{-1} \quad (3.101)$$

assuming no heat gain or loss during compression.

The *cooling load* or *rating* of the refrigerator is the rate of heat removal in the evaporator in kW. It is often expressed in refrigeration tonne (Rt) which is equal to a rate of heat removal of 3.5 kW. The mass of refrigerant required to be circulated

$$M_r = \frac{1}{H_3 - H_1} \text{ kg s}^{-1} \text{ for every kW of cooling load}$$

$$= \frac{3.5}{H_3 - H_1} \text{ kg s}^{-1} \text{ per Rt} \quad (3.102)$$

The theoretical compressor volume (piston displacement) is obtained by multiplying the mass of the refrigerant circulated by the specific volume of the refrigerant which can be obtained from the pressure-enthalpy (Mollier) diagram of the refrigerant (see Fig. 3.20 for such a diagram for Freon 12). Hence theoretical piston displacement

$$= \frac{1}{H_3 - H_1} \cdot V_3 \text{ m}^3 \text{ kW}^{-1} \quad (3.103)$$

The power consumption of the compressor

$$= \frac{H_4 - H_3}{H_3 - H_1} \text{ kW for every kW of cooling load}$$

$$= \frac{3.5\,(H_4 - H_3)}{H_3 - H_1} \text{ kW Rt}^{-1} \quad (3.104)$$

The *coefficient of performance* of the refrigeration plant

$$= \frac{\text{heat absorbed in evaporator}}{\text{net work supplied}}$$

$$= \frac{H_3 - H_1}{H_4 - H_3} \quad (3.105)$$

Heat removed through condenser which is theoretically equivalent to the heat absorbed in the evaporator plus the work of compression

$$= \frac{H_4 - H_1}{H_3 - H_1} \text{ kW per kW cooling of load} \quad (3.106)$$

Compressor. For most large-capacity mine refrigeration plants, reciprocating compressors or centrifugal compressors are generally

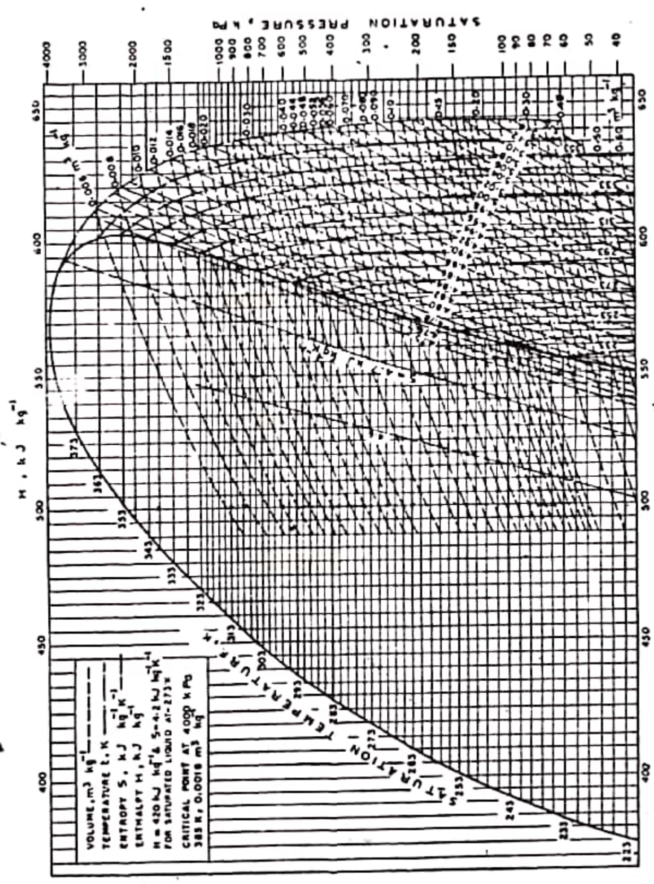

Fig. 3.20 Mollier (pressure enthalpy) diagram for Freon 12

Scanned with CamScanner

used. Rotary compressors are limited to small sizes only (fractional-tonnage refrigerators). Reciprocating compressors used in refrigeration plants are generally electrically driven, of high speed (up to 370 rad s^{-1} or 3500 r.p.m.) and are usually air or water cooled. Centrifugal compressors of single to eight stages have been used. They have higher speed than reciprocating compressors That is why they are more compact. There are no rubbing parts like valves, piston rings, etc. and hence the efficiency is maintained over the whole life of the plant and also the gas is delivered in a steady stream which does not come in contact with contaminating lubricating oil.

Refrigerant. A good refrigerant should have a large latent heat of evaporation and should evaporate and condense as near atmospheric temperature and pressure as possible. Ammonia and fluorinated hydrocarbons like Freon 11, 12 etc. are suitable refrigerants. Although carbon dioxide can reduce compressor size because of its low specific volume, it is not suitable for use at mines, because of its low critical temperature (304.5 K) and toxicity.

Ammonia has the largest latent heat of evaporation and is cheap, but is toxic and corrosive for brass and copper. However, leakage of ammonia can be easily detected by smell and corrosion can be avoided by selecting suitable material for construction of the refrigerator. That is why it is commonly used in surface refrigeration plants. On the other hand, Freon is a non-toxic refrigerant and is therefore commonly used in underground air-cooling plants even though it is costlier than ammonia. Freon 11 (trichloro-monofluoro-methane) is generally used in centrifugal compressors while Freon 12 (dichloro-difluoro-methane), in reciprocating compressors.

Condensers and Evaporators. Condensers are generally of the shell-and-tube type. Evaporative condensers, where the hot refrigerant vapour passes through finned tubes on which water is sprayed by circulating pumps and there are fans to blow air over the condenser tubes, are generally restricted to smaller plants not exceeding 350 kW (100 Rt) in capacity. Such condensers do not need any further cooling of condenser water. But for larger plants, the heated water from the condenser has to be cooled either in spray ponds or cooling towers.

Evaporators are similar to shell-and-tube type condensers in construction. Their design should be such as to allow the boiling

of the refrigerant with minimum drop of pressure as well as ensure efficient removal of heat from the medium being cooled.

The design of evaporators and condensers is based on the rate of heat transfer. The mass flow-rate of cooling water M_w in the condensers is given by the relation

$$M_w = \frac{q}{4.1868\,(T_2-T_1)}\ \text{kg s}^{-1} \tag{3.107}$$

where q = the rate of heat removal in kW

$$= \frac{H_4-H_1}{H_3-H_1} \times \text{cooling load,} \tag{3.108}$$

T_2 is the temperature of water at the condenser outlet and T_1, that at the condenser inlet in K.

The surface area of heat transfer, from which the number and size of tubes (in case of shell-and-tube type condenser) can be calculated, is given by the relation

$$q = \alpha A \,\Delta T_m \quad \text{kW} \tag{3.109}$$

where A = the surface area of heat transfer in m^2,

ΔT_m = the log mean temperature difference in K

$$= \frac{\Delta T_1-\Delta T_2}{\ln(\Delta T_1/\Delta T_2)} = \frac{\Delta T_1-\Delta T_2}{2.3\log(\Delta T_1/\Delta T_2)} \tag{3.110}$$

ΔT_1 and ΔT_2 = difference of temperature between water and refrigerant at the inlet and outlet of the condenser respectively,

and α = the overall heat transfer coefficient in kJ m^{-2} s^{-1} K^{-1}.

α is usually calculated from test data on the type of condenser as well as the water-refrigerant system.

αA can, however, be estimated from the relation

$$\frac{1}{\alpha A} = \frac{1}{\alpha_i A_i} + \frac{1}{\alpha_f A_i} + \frac{t}{k A_m} + \frac{1}{\alpha_o A_o} \tag{3.111}$$

where α_i = heat-transfer coefficient at the inner surface of the tube (convective) $\simeq \dfrac{21.4(T_m-206.48)v_w^{0.8}}{D_i^{0.2}}$ $\text{Wm}^{-2}\text{K}^{-1}$ (3,112)

Scanned with CamScanner

A_i = area of the inner surface of the tubes, m^2,
D_i = inner tube diameter, m,
T_m = mean water temperature, K,
v_w = velocity of flow of water in the tubes, m s^{-1},
α_f = heat-transfer coefficient because of scale deposit on the inner surface of the tube. $\frac{1}{\alpha_f}$ called the fouling factor can be taken equal to 0.0001 m^2 K W^{-1} for clean tubes, 0.0002 m^2 K W^{-1} for dirty tubes and 0.0005 m^2 K W^{-1} for very dirty tubes,
t = thickness of tubes,
k = thermal conductivity of tube material = 380 W m^{-1} K^{-1} for copper and 44 W m^{-1} K^{-1} for cupronickel (90 : 10),
A_m = mean heat transfer surface area, m^2,
A_o = area of the outer surface of tubes, m^2
and α_o = heat-transfer coefficient at the outer surface of the tubes (condensation). This has to be obtained from test data.

Equation 3.109 can also be used for designing the evaporator. The mass flow-rate of brine or cooling medium M_c is computed from the relation

$$M_c = \frac{q}{C\,(T_2-T_1)} \text{ kg s}^{-1} \tag{3.113}$$

where q = rate of heat transfer in the evaporator or the cooling load, kW,
C is the specific heat of the brine in kJ kg^{-1} K^{-1} and T_2-T_1 is the fall of temperature of the brine in the evaporator.

Coolers. The cooling of the air can be direct or indirect. Direct cooling where the air flows directly over the evaporator tubes is adopted only in small units such as spot coolers. In the indirect system an intermediate cooling medium like brine or water is used. This medium is cooled in the evaporator and in turn, cools the air in the cooler unit. Brine is preferred to water when the air is cooled to a fairly low temperature (near about the freezing point of water) because brine has a lower freezing point, and hence is less likely to freeze in the pipelines. Calcium chloride and sodium chloride

solutions are the common brines used as they remain liquid under all temperatures they are subjected to, are non-corrosive, have a relatively high specific heat and are fairly stable.

Generally two types of coolers are used in mine refrigeration plants, spray type and pipe-nest type. In the spray-type cooler, the chilled cooling medium from the evaporator is sprayed through nozzles along a chamber through which the air passes. The moisture from the air in this case condenses and contaminates the brine. Besides, the particles of liquid moisture and brine get carried into the mine with the air-stream, so that one has invariably to use a scrubber to separate as much of these particles as possible. That is why spray coolers are seldom used when brine is the cooling medium since a part of the brine is always lost and the rest gets diluted by water condensed from the air needing a concentration plant, even though they have the distinctive advantage of cheapness and low resistance to air-flow.

The pipe-nest type of cooler keeps the brine out of physical contact with the air and hence from contamination. But such coolers are costlier and offer substantial resistance to air-flow (as much as 1000 Pa may be lost in the cooler). However, there is no loss of brine. On the other hand, water condensed from the air in the cooler is pure and can be used as make-up water in the cooling tower or spray pond.

A suitable practice would be to have two coolers placed in series ; one of the spray type using water as the cooling medium and the other of the pipe-nest type using brine as the cooling medium. The air passes through the spray-type cooler first. The water in this cooler is not chilled to a very large extent so as to avoid any chance of freezing. Such a combined cooler is cheaper than a simple pipe-nest cooler and offers less resistance to air-flow while avoiding the disadvantage of the spray cooler.

The rate of heat transfer from the cooling liquid (brine or chilled water) to the air q is given by the relation

$$\begin{aligned} q &= M_c\ C\,(T_{co}-T_{ci}) \\ &= M_a\,(H_i-H_o)-0.001\,M_a C_{pw}\,(m_i-m_o)(T_{wo}-273.15)\,\text{kW} \end{aligned} \tag{3.114}$$

where M_a = mass flow-rate of dry air, kg s^{-1},
T_{ci} and T_{co} = temperature of cooling liquid at the inlet and outlet of the cooling coil respectively, K,

Scanned with CamScanner

H_i and H_o = enthalpy of air entering the cooling chamber and leaving it, kJ kg^{-1} of dry air,
m_i and m_o = mixing ratio of air entering and leaving the cooling chamber, g kg^{-1} of dry air,
C_{pw} = specific heat of condensed water, kJ kg^{-1} K^{-1}
and T_{wo} = temperature of condensed water, K.

For spray-type cooling chambers using chilled water, an equation similar to equation 3.114 can be written.

From the energy balance principle

$$M_a H_i + M_{wi} C_{pw} (T_{wi} - 273.15)$$
$$= M_a H_o + M_{wo} C_{pw} (T_{wo} - 273.15) \tag{3.115}$$

and from conservation of mass

$$M_{wi} = M_{wo} - 0.001\, M_a (m_i - m_o) \tag{3.116}$$

where M_{wi} and M_{wo} are the mass flow-rate of water into and out of the chamber and C_{pw} = specific heat of water.

Hence $q = M_{wi} C_{pw} (T_{wo} - T_{wi})$

$$= M_a (H_i - H_o) - 0.001\, M_a C_{pw} (m_i - m_o)(T_{wo} - 273.15) \text{ kW} \tag{3.117}$$

The design of the cooling chamber is subject to the limitations of the second law of thermodynamics :

(a) the wet-bulb temperature of air leaving the cooling chamber cannot be lower than the temperature of cooling liquid entering the chamber,

(b) the temperature of cooling liquid leaving the chamber cannot be higher than the wet-bulb temperature of air entering the chamber.

The design of cooling coils, i.e. the total pipe-nest surface area required can be done with the use of equations 3.109 and 3.110 where ΔT_1 and ΔT_2 can be approximately taken as the difference between the wet-bulb temperature of air and the temperature of the cooling liquid at the inlet and outlet of the cooling coil respectively.

Cooling Towers. Heated condenser water has to be cooled for reuse in a cyclic system. At the surface, spray ponds or cooling towers of standard design may be used, but underground cooling towers have to be properly located and designed depending on the amount of heat to be extracted, and temperature, humidity and flow-rate of air available for cooling. Most spray towers are located in parts of shafts or winzes where the condenser water is sprayed at the top and works its way down through sets of screens, with the cooling air flowing upwards under the ventilating pressure of

the mine. Fig. 3.21 gives some installations of this type. Occasionally a horizontal spray chamber may be used with induced draft.

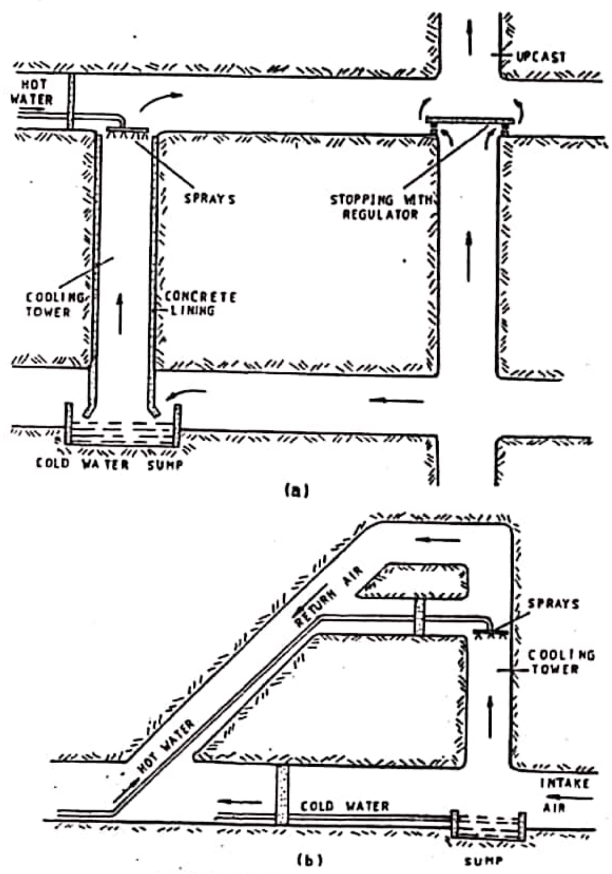

Fig. 3.21 Underground cooling towers.

The limitations of the second law of thermodynamics that the water cannot leave the tower at a temperature lower than the wet-bulb temperature of the entering air and the wet-bulb temperature of the air leaving the tower cannot exceed the temperature of water entering the tower should always hold in designing these cooling towers. Equation 3.117 used for coolers can also be used for cooling towers, though the heat transfer in this case is in the opposite direction (i.e. from water to air).

Cooling towers are usually designed to cool condenser water by 7 to 9 K. Air velocities in cooling towers vary between 2.5 to 7.5 m s^{-1}, the higher velocities giving greater retention time for the droplets of water, but velocities greater than 9 m s^{-1} are undesirable as they tend to carry away a large amount of water droplets.

Mine Refrigeration Plants. Mine refrigeration plants are of three types depending on their location : surface plants, underground plants (centrally located) and spot coolers. It is very essential for economy to maintain a high *positional efficiency* of the refrigeration plant. Obviously spot coolers which are located at the face have the maximum positional efficiency as they supply the cooled air directly to the face, but they meet with the difficulty of disposing of the heat extracted from air at the face. This heat can best be disposed of if a direct return airway (not ventilating any other district) is available nearby. Otherwise the heat extracted from one face may be carried to another face or even recirculated to the refrigeration plant in which case the effect of cooling at the face will be reduced. Spot coolers are used generally for cooling remote development headings, engine houses etc. They are semi-portable and have small capacity. Reciprocating compressors are commonly used. Both direct and indirect cooling (usually with water as a cooling medium) are used depending on the size. The quantity of air-flow through the spot cooler should not exceed half the quantity passing through the airway in order to prevent recirculation of air through the cooler.

Surface refrigeration plants are of relatively large capacity running into megawatts. For deep mines, however, their positional efficiency falls where it may be more profitable to have central underground refrigeration plants. Underground refrigeration plants are generally of smaller capacities and face the problem of suitably disposing of the heat extracted from the air.

A very suitable system is the *divided installation* (of the refrigerator and the cooler) which incorporates the advantages of both surface and underground plants.

The first surface refrigeration plant was installed at the Morro Velho Mine, Brazil in 1920. In 1929, the same mine installed the first underground refrigeration plant. The first mine air-conditioning plant in India was installed in 1936 at the Oorgaum Mine, Kolar Gold Fields. The surface refrigeration plants at mines today are mostly of the ammonia type although at the Robinson Deep Mine, South Africa there is a Carrene plant on the surface.

Champion Reef Mine, K.G.F., India. A typical ammonia plant installed on the Gifford Shaft at this mine is illustrated in Fig. 3.22. The plant has a capacity of 3.7 MW (1060 Rt) cooling 70.82m^3 s^{-1} of air from 294.25 K wet-bulb to 277.5 K saturated.

Here, ammonia is first compressed by a reciprocating compressor driven by a 300 kW, 31 rad s^{-1} (300 r.p.m.) motor. The compressed gas then passes through the oil separator which extracts any oil picked up from the compressor cylinder. The oil-free gas is now cooled to liquifaction in the condenser by circulating cold water by three 22-kW pumps each having a capacity of 6.06 m^3 min^{-1}. The cooling water extracts the heat of compression of the

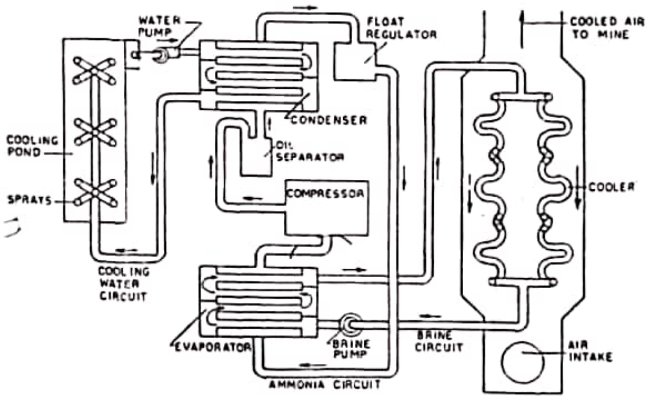

Fig. 3.22 Schematic diagram of the surface air-conditioning plant at Champion Reef mine, K.G.F.

gas as well as the latent heat of evaporation of ammonia. The liquid ammonia is then fed through the float regulator to the evaporator. The float regulator so adjusts the flow that a constant level of liquid ammonia is maintained in the evaporator. The compressor in its backward stroke causes a partial vacuum in the cylinder, as a result of which a part of the liquid ammonia in the evaporator is vaporized and drawn into the cylinder to be compressed again. After the extraction of heat from ammonia the cooling water gets warm and is cooled again in a spray pond. The condenser and evaporator are of the shell-and-tube type.

A weak calcium chloride brine solution (sp. gr. 1.22) is circulated through the evaporator by three brine circulation pumps each having a capacity of 4.9 m^3 min^{-1}. The brine on leaving the evaporator gets cooled and the cold brine is then circulated through the cooler which consists of a large coil of 38mm bore steel pipes. Air to be cooled is blown over the cooler pipes by a 2-stage

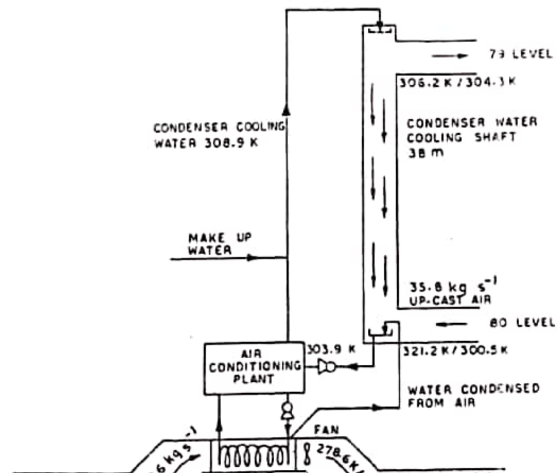

Fig. 3.23. Schematic diagram of the underground air-cooling plant at Champion Reef mine, K.G.F.

propeller fan of 2400mm diameter. The brine, after cooling the air gets warm and has to be cooled again by the vaporization of liquified ammonia in the evaporator.

An underground refrigeration plant has also been installed at this mine. This was necessary because the south section workings had 329.8 K d.b. and 306.5 K w.b. temperatures in spite of the surface cooling plant. The plant is situated at a depth of 2318m from the surface and has a capacity of cooling 9.44 m^3 s^{-1} at 305.9 K d.b. and 293.2 K w.b. to 276.5 K saturated. The plant consists of a three-cylinder compressor with Freon 12 (dichloro-difluoro-methane, CCl_2F_2) as refrigerant. The condensing water is cooled by spraying it in an upcast shaft. Fig. 3.23 gives the layout of the plant.

Robinson Deep Mine, S. Africa. The principle of operation of the Carrene plant on Turf shaft at the Robinson Deep Mine, S. Africa is similar except that here centrifugal compressors are used to compress the refrigerant, Carrene No. 2 (trichloro-fluoro-methane, $CFCl_3$). It has been found that for the same capacity, centrifugal compressors take less space than reciprocating compressors. The cooler is different from the one described above. Here, the cold brine, instead of being circulated through tubes on the path of the air-current, is sprayed into the air.

The whole plant consists of three Carrier centrifugal refrigeration circuits leading from a common spray pond. Each of these three units can be operated singly or together to cool the air in stages. Each unit consumes 112 kW in the two-stage centrifugal compressor. The brine pumps are 250mm centrifugal ones, each consuming 112 kW at 153 rad s^{-1} (1460 r.p.m.) and delivering 10.5 m^3 min^{-1} against a head of 41.2m. The cooling water pumps are 200mm centrifugal ones driven by 56 kW motors running at 154 rad s^{-1} (1470 r.p.m.) and delivering 9 m^3 min^{-1} against a head of 26m. There are two fans circulating the air. Each of the fans is driven by a 75 kW motor running at 76 rad s^{-1} (725 r.p.m.).

Surface Plants vs Underground Plants. Surface plants have the advantages of (a) simplicity, (b) convenience of operation and inspection, (c) safety, (d) cheapness (as they use cheap refrigerants like ammonia) and (e) ease in the disposal of waste heat into the air. Besides, surface refrigeration plants aid in producing a large natural ventilating pressure because of the large difference in the downcast

Scanned with CamScanner

and upcast air temperatures so much so that in deep mines, mechanical ventilation may become unnecessary after the installation of surface air-conditioning plants.

On the other hand, underground refrigerators may slightly reduce the natural ventilating pressure. The main disadvantage of surface refrigerators is their low positional efficiency which is defined as the ratio of the effective cooling units produced at the working face, i.e. the difference in the heat content of the face air before and after the installation of the refrigerator to the total cooling units produced by the refrigerator. Positional efficiency of surface plants increases with time, since the rock through which the cooled air is carried to the face gets progressively cooled. However, the rate of increase of positional efficiency decreases with time so much so that after a certain time the increase in positional efficiency can be considered as negligible. The positional efficiency in surface plants usually varies from 35% upwards, a lower positional efficiency being considered unsatisfactory. In very hot and deep mines, particularly where the working faces are far off from the shaft, cool air from the surface refrigeration plants picks up much heat before it reaches the working place. It may be noted here that in deep shafts auto-compression alone can use up a major part of the cooling produced by the surface cooling plant. The problem will be more acute if the mine is wet. Under such conditions an underground plant will have a higher positional efficiency by being nearer the face.

Besides, surface plants pose some difficulties in feeding the cooled air into the mine. The commonest way is to feed a quantity of cooled air, slightly less than the quantity circulating through the mine into the downcast shaft at a depth of 30m or more from the shaft collar so that a small quantity of unconditioned surface air always enters the mine at the top of the intake shaft. Alternatively, the cooled air can be fed at the top of the downcast shaft which should then be covered with a suitable leakproof air-lock. Whereas the former method needs a close control of the quantity of cooled air fed into the mine and incurs some loss of cooling by dilution with unconditioned air, the latter needs an air-lock which is very inconvenient in a hoisting shaft. Besides, it is difficult to prevent leakage of cooled air through the air-lock.

Underground refrigeration plants have high positional efficiency if suitably sited. It has been found in deep mines that if a face is laterally over 1000m away from the bottom of the downcast shaft (where the underground refrigeration plants are usually situated), the positional efficiency becomes unsatisfactorily low. In such cases the plant has to be located nearer the face.

Underground refrigeration plants have the following disadvantages: (a) They have to use non-toxic refrigerants like Freon which costs four times more than ammonia, commonly used in surface plants. Also, it is difficult to prevent the leakage of refrigerant and Freon, being odourless, is less likely to be detected if leaking in a large quantity. Moreover the non-toxic refrigerants are less commonly available. (b) The problem of dissipating the heat extracted from the air is difficult and heavy pumping expenses might have to be incurred. Sometimes if suitable underground positions for spray cooling of water are not available, the water may have to be pumped to the surface for cooling thus involving a high cost of pumping. Besides, spray cooling of water in upcast shafts or airways increases the humidity of the upcast air which then becomes unsuitable for ventilating upper levels. Also, the condenser water gets fouled by picking up dust from the air and may lead to the corrosion of pipes. (c) In dry and dusty mines, dust deposits on the surface of the tubes in the cooler thus reducing the efficiency of heat transfer and necessitating frequent cleaning for ensuring good operation. (d) There is difficulty in suitably locating an underground excavation and such excavations are costly. (e) Supervision of plant is difficult. (f) In mines susceptible to rock burst, the excavation housing the refrigerator may be subjected to high stresses set up by the differential cooling of the surrounding rock thus resulting in rock bursts. (g) Underground plants are usually of small capacity (up to 1.75 MW) and hence a single plant may not be able to serve the whole mine. (h) In case of a breakdown of the refrigeration plant underground, the working condition soon becomes unbearable whereas with a surface plant the downcast shaft serves in extracting heat from the intake air for a considerable period. The sides of the shaft get substantially cooled by the cool air from the surface refrigeration plant over the years. The extent of cooling is the maximum near the top of the shaft and decreases as the depth increases. When the plant stops, the sides of the shaft absorb heat from the air for a time which is usually sufficient for the plant to be put back in operation.

Divided Installation. Here the major part of the refrigeration plant excepting the cooler unit is located at the surface so that the

Scanned with CamScanner

heat extracted from the air can be easily disposed of to the atmosphere. But the cooler is located underground. The cooling medium (brine or water) from the evaporator is carried in insulated pipes to the cooler underground and returns through another range of pipes, thus forming a closed circuit. The pumping cost in this case is low as the two columns of down-going and up-coming cooling medium almost balance each other and the power required for pumping is for overcoming pipe friction only. A divided-installation plant has high positional efficiency, faces no difficulty in disposing of extracted heat and obviates the need of surface air-locks, but its main disadvantage is the high cost of high-pressure insulated pipelines required for conducting the coolant underground. Besides it is difficult to adopt such a system for very deep mines owing to the very high pressures the ranges would be subjected to. A typical example of divided installation is offerred at the Lesliegeois Colliery, Belgium, where the virgin-rock temperature at the bottom horizon (at a depth of 1010m) is 318 K. A surface ammonia plant of 2.42 MW capacity cools 200 m^3 min^{-1} of water to 274.25 K. The chilled water is taken down the shaft through insulated pipes. To avoid the passage of high-pressure chilled water through the heat exchangers underground the water is passed through a Pelton turbine whereby its pressure is reduced. The Pelton turbine drives a pump which pumps the warm water to the surface. The pressure lost in the turbine, pump and water pipes is made up by an electric motor of 180 kW. The chilled water from the turbine goes to a reservoir from where it is distributed to coolers located near the face.

At Butte mine, Montana, U.S.A. the summer surface temperatures are 305.4 K d.b. and 288.6 K w.b. with a dew point of 277.6 K which means that the air is very dry. The cooling medium is water. It is cooled by spraying it in a surface cooling tower through which is circulated a current of air. The air is precooled by passing it over the cooled water pipes. The cool water at 276.4 K is taken down the shaft which is 1220m deep, in insulated pipes and is used to cool the air there. The cooling achieved underground is from 302.6 K w.b. to 294.3 K w.b. In winter the surface temperature is very low which makes cooling unnecessary. This is a typical example of evaporative cooling of air which is sufficiently dry.

Air-conditioning in Deep Coal Mines. Air-conditioning in deep and hot coal mines poses a slightly more difficult problem than in

metalliferous mines, as surface refrigeration plants have much lower positional efficiency in coal mines. This is because of the following reasons : (a) For the same depth, the heat produced in coal mines is more because of the higher strata temperature (geothermic gradient in coal measure strata is usually steeper as is evident from Table 3.1) and larger surface area of rock exposed even though the thermal diffusivity and hence the rate of heat transfer in coal measure strata is less. (b) Coal mines are usually more wet and hence a large quantity of moisture is evaporated into the cooled air thus increasing its relative humidity. (c) A lot of heat is produced in coal mines by the oxidization of coal. Because of these reasons it is better to have an underground cooling plant in a coal mine, preferably with the cooler unit (the heat exchanger between coolant or cooling medium and air) as near the face as possible.

Spot Coolers. For ventilating hot faces, small-capacity spot coolers are becoming popular both in coal and metal mines. These are semi-portable and have a cooling capacity generally varying from 50-200 kW (15-55 Rt). There are two types of spot coolers : (a) where the direct evaporation of the refrigerant cools the air (generally confined to the smaller ones), and (b) where an intermediate coolant such as water is used. The units usually consist of reciprocating compressors driven by electric or compressed-air motors. Cooling of the compressed refrigerant is done in air-cooled condensers. A typical direct-evaporation unit consisting of a V-8 compressor driven by a 25 kW motor along with a condenser and oil separator measures 1700mm in length, 750mm in width and 1450mm in height. The cooled refrigerant passes through an evaporator fitted inside the ducting of a forcing fan supplying air to the face. The evaporator has a cooling surface of 40 m^2 approximately which is capable of transferring 46 kJ m^{-2} h^{-1} K^{-1} to the air flowing at the rate of 2.67 m^3 s^{-1}. The pressure required for the air-flow is 735 Pa. The spot coolers, though having the advantage of cooling the face, leave the rest of the mine hot. However, a useful gain associated with spot coolers is that cool air helps in condensing moisture on dust particles thus helping in dust supression at the face. Table 3.9 lists a few spot coolers.

Other methods of mine air-cooling include the use of devaporized compressed-air, ice or liquid air as well as regenerative cooling.

Scanned with CamScanner

Table 3.9 : Spot Coolers

Country	Make	Cooling capacity, kW	Remarks
East Germany (GDR)	WK 1205	128	Compact, portable and suitable for coal mines
West Germany	KR 150	181	,,
-do-	KR 200	233	,,
U.S.S.R.	WK 42	49	,,
U.S.S.R.	KP Sch.-I	73	,,
U.K.	J. E. Hall	16	,,
India	Voltas 33 TR	115	Semi-portable, suitable for metal mines only.
-do-	Voltas 100 TR	350	Stationary, suitable for metal mines only.

3.12.4 Regenerative Cooling

This is only in the theoretical stage of development and has yet to be adopted in practice. If a certain gas of high density and low specific heat such as carbon dioxide is circulated in a closed circuit down the upcast shaft and up again through the downcast shaft, then the heat developed due to auto-compression of carbon dioxide will be dissipated into the upcast air while the cooling due to auto-expansion will cool the downcast air. This not only produces cooling of the downcast air but also increases the natural ventilation.

3.12.5 Devaporized Compressed-air

Ordinarily, compressed-air when escaping from a pipe does practically no work and hence does not produce any cooling. However, compressed-air is saturated at its usual supply pressure of 500 kPa. Its degree of saturation is reduced to 20% on expansion to free air so that it reduces the overall relative humidity and the wet-bulb temperature when mixed with the main air-current. A 9% addition of compressed-air usually reduces the w.b. temperature of the main air-stream by 1 K. This practice however is very uneconomical.

Wet compressed-air reduces the efficiency of drills etc. by washing away the lubricant. It also causes rusting in the pipe ranges.

Compressed-air, when it expands by doing work, as for instance in an air motor, cools down and any moisture present in it may freeze to ice depending on the degree of expansion. This restricts the design of air motors to low expansion types where full work can not be derived out of the compressed-air. Morever, aqueous vapour in compressed-air carries the latent heat of evaporation into the mine. This heat is given up to the air when water-vapour condenses during the use of compressed-air for doing work and this neutralizes to a large extent the expansive cooling produced by the compressed-air. It has been found that the temperature of expanded exhaust air with saturated compressed-air is about 11.1 K higher than that with devaporized compressed-air. It is for these reasons that devaporized compressed-air is far superior to ordinary compressed-air in improving the cooling power of mine air.

Devaporization is done by overcompressing the air by about 50% over the normal working pressure of 500-650 kPa and then passing it through a heat exchange system where the overcompressed air is cooled by a current of cool devaporized compressed-air. The cooled overcompressed-air is now employed to run an air motor. In doing so it expands to the normal working pressure and also cools to 273 K. At this temperature, all the moisture in the compressed-air is liquified and removed from it. The dry and cool compressed-air is now circulated through the heat exchanger to cool the overcompressed-air.

The devaporized compressed-air is now sent down the mine where it is used to run air motors, drills etc. at the face. The exhaust air from these machines gets substantially cooled by expansion. This, coupled with the dryness of the air helps in keeping down the temperature and humidity at the face.

This system, inspite of its limited capacity for cooling the mine air as a whole, produces good cooling at the face where it is most required. The extra power required in devaporizing the compressed-air is only 10% in case of reciprocating compressors and 12.5% in case of centrifugal compressors. However, the main disavantage of the devaporized compressed-air plant is its comparatively high cost and low efficiency of performance.

3.12.6 Ice and Liquid Air

Cooling of mine air at the face by the use of ice or liquid air becomes very costly.

Scanned with CamScanner

The comparative cost of cooling mine air by various methods is given by Dobson[43] as follows :

Table 3.10 : Comparative Cost of Various Methods of Cooling

Method of cooling	Cost in P MJ^{-1}
Additional ventilation+ (where feasible)	0.038-0.076
Compressed-air through nozzle	4.76
Compressed-air doing work	1.12
Cooling with chilled water+ (as at Butte—not universally feasible)	0.19
Liquid air	17.9-24.1
Ice	0.79
Dehumidified compressed-air+	0.38-0.76
Ammonia plant at K.G.F•	0.26
Carrene plant at Turf shaft•	0.36
Underground or surface refrigeration plant (average)+	0.57

+ Estimated by Peele
• Estimated by McIntyre

Example 3.8

Calculate the capacity of an underground refrigeration plant for a mine circulating 70 $m^3\ s^{-1}$ of air measured in the downcast shaft. The summer temperatures of the intake air are 300.2 K d.b. and 295.8 K w.b. and the barometric pressure at the plant site is 110.66 kPa. It is required to cool the air to 277.4 K saturated.

At temperature 300.2 K d.b. and 295.8 K w.b. vapour pressure $e_1 = 2.45$ kPa.

Mixing ratio $m_1 = \dfrac{622e_1}{B-e_1} = 14.08$ g kg^{-1} of dry air.

C_{pa_1} (specific heat of dry air)for the temperature range 273.15 K to 300.2 K

$$= 995.68+0.029\left(\frac{273.15+300.2}{2}\right)$$

$$= 1004\ J\ kg^{-1}\ K^{-1}$$

C_{pv_1} (specific heat of water-vapour) for the range 273.15 to 300.2 K

$$= 1553.7+0.645\left(\frac{273.15+300.2}{2}\right)+\frac{35\ 169}{(273.15+300.2)/2}$$

$$=1861.3\ J\ kg^{-1}\ K^{-1}.$$

l (latent heat of vaporization) at 273.15 K$=2.5004\times10^6$ J kg^{-1}.

Therefore enthalpy of air at 300.2 K d.b. and 295.8 K w.b.

$$H_1=C_{pa_1}(T_1-273.15)+0.001m_1C_{pv_1}(T_1-273.15)+0.001m_1l$$

$$=1.004\ (300.2-273.15)+0.001\times14.08\times1.861\ (300.2-273.15)+0.001\times\ 14.08\times2500.4=63.07\ kJ\ kg^{-1}\text{ of dry air.}$$

At temperature 277.4 K saturated, vapour pressure e_2=0.837 kPa.

Mixing ratio $m_2 = \dfrac{622e_2}{B-e_2}=4.74$ g kg^{-1} of dry air.

Amount of liquified vapour $m_3=m_1-m_2=9.34$ g kg^{-1} of dry air.

C_{pa_2} (specific heat of dry air) over the range 273.15 to 277.4 K

$$= 995.68 + 0.029\left(\frac{(273.15+277.4)}{2}\right)=1003.7\ J\ kg^{-1}\ K^{-1}.$$

C_{pv_2} (specific heat of water-vapour) over the range 273.15 to 277.4 K

$$= 1553.7+0.645\ (273.15+277.4)/2+\frac{35\ 169}{(273.15+277.4)/2}$$

$$= 1859\ J\ kg^{-1}\ K^{-1}.$$

C_{pw_2} (specific heat of liquified water-vapour) over the range 273.15 to 277.4 K

$$= 4820.5-2.18\ (273.15+277.4)/2=4220.4\ J\ kg^{-1}\ K^{-1}.$$

Enthalpy at 277.4 K saturated,

$$H_2=C_{pa_2}(T_2-273.15)+0.001\ m_2\ C_{pv_2}\ (T_2-273.15)+0.001\ m_2\ l +0.001\ m_3\ C_{pw_2}(T_2-273.15)$$

$$=16.32\ kJ\ kg^{-1}\text{ of dry air.}$$

∴ The difference in enthalpy for 1 kg of dry air when it cools from 300.2/295.8 K to 277.4 K saturated$=63.07-16.32=46.75$ kJ.

The density of dry air at 300.2/295.8K

$$= \frac{B-e_1}{287.1\times300.2}\times10^3\doteq1.26\ kg\ m^{-3}.$$

Scanned with CamScanner

70 m³ of air will contain $70 \times 1.26 = 88.2$ kg of dry air. Therefore the total heat to be extracted from the air

$$= 46.75 \times 88.2$$

$$= 4123.4 \text{ kJ s}^{-1} = 4.12 \text{ MW} \qquad (1180 \text{ Rt}).$$

Example 3.9

A longwall face circulating 20 m³ s⁻¹ of air has 308/303.5 K d.b./w.b. air temperatures at the return gate end. A spot cooler is to be installed to cool the air supplied to the face so that the maximum wet-bulb temperature at the face is 302.5 K. Find the cooling load. The evaporator temperature is to be 275 K and the condenser temperature, 311 K. Calculate the amount of refrigerant required, capacity and power of compressor and the rate of heat removal in the condenser with Freon 12 as the refrigerant.

Referring to psychrometric chart (Fig. 3.9) enthalpy at 308/303.5 K = 101.74 kJ kg⁻¹ of dry air.

When this air is cooled to 302.5 K wet-bulb, its dry-bulb temperature will be 303.5 K and enthalpy = 97.13 kJ kg⁻¹ of dry air. Specific volume of air at 308/303.5 K = 0.908 m³ kg⁻¹ of dry air.

$$\therefore \text{ Cooling load} = \frac{20\,(101.74-97.13)}{0.908}$$

$$= 101.54 \text{ kW} = 29 \text{ Rt}.$$

Now referring to the Mollier diagram for Freon 12 (Fig. 3.20) for a condenser temperature (saturation) of 311 K, the enthalpy of the refrigerant $H_1 = 455.1$ kJ kg⁻¹ of refrigerant. On throttling the refrigerant cools to 275 K without change of enthalpy.

On evaporation (to saturation assumed, though in practice evaporation may proceed a little beyond this state for drier operation of the compressor) the enthalpy increases so that

$$H_3 = 575.3 \text{ kJ kg}^{-1}.$$

From equation 3.102, mass of refrigerant required

$$= \frac{1}{H_3 - H_1} = \frac{1}{575.3-455.1}$$

$$= \frac{1}{120.2} = 0.0083 \text{ kg s}^{-1} \text{ per kW of cooling load}$$

$$= 0.0083 \times 101.54 = 0.843 \text{ kg s}^{-1} \text{ for the plant.}$$

Specific volume of refrigerant at entry to compressor $V_3 = 0.055$ m³ kg⁻¹ (from Mollier diagram).

∴ Compressor capacity

$$= \frac{1}{120.2} \times 0.055 \times 101.54 = 0.046 \text{ m}^3\text{s}^{-1}$$

(see equation 3.103).

Enthalpy of refrigerant after compression (assumed isentropic) $H_4 = 592.9$ kJ kg⁻¹.

∴ Compressor power

$$= \frac{(592.9-575.3) \times 101.54}{120.2} = 14.87 \text{ kW}$$

(see equation 3.104).

Rate of condenser heat removal (from equation 3.106)

$$= \frac{(592.9-455.1) \times 101.54}{120.2}$$

$$= 116.4 \text{ kJ s}^{-1} \text{ (kW)}.$$

Example 3.10

The following measurements were made on an underground air-cooling plant. Calculate the coefficient of performance of the plant. Also check if all the measurements are correct.

Evaporator water flow-rate = 28.5 kg s⁻¹.
Evaporator inlet water temperature = 297.3 K.
Evaporator delivery water temperature = 282.5 K.
Compressor motor output power = 524 kW.
Condenser water flow-rate = 67.6 kg s⁻¹.
Condenser inlet water temperature = 311.9 K.
Condenser delivery water temperature = 319 K.

Evaporator rate of heat exchange $= 28.5 \times 4.187\,(297.3-282.5)$
$= 1766$ kW

taking specific heat of water = 4.187 kJ kg⁻¹ K⁻¹.

$$\text{Coefficient of performance} = \frac{\text{cooling at evaporator}}{\text{input power to compressor}}$$

$$= \frac{1766}{524} = 3.37$$

taking input power of compressor = output power of compressor.

Condenser heat exchange rate

$$= 67.6 \times 4.187\,(319-311.9) = 2009.6 \text{ kW}.$$

Condenser heat removal = evaporator heat removal + compressor heat = 1766 + 524 = 2290 kW.

Thus there is some measurement error somewhere.

Scanned with CamScanner

EXERCISE 3

3.1 The following are the readings of a barometer and thermometer at the base camp and the face of a mine located on a hill-top. Calculate the elevation of the mine face above the base camp. Neglect moisture content of air.

	Barometer reading, kPa	Thermometer reading, K
Base camp	100.1	305
Mine face	98.3	298

3.2 How much heat is added to the mine air by (a) a 300 kW underground pump pumping 6m^3 of water per minute through a height of 150m ; (b) a diesel truck running on level ground and consuming 9.5 kg of fuel per hour on the average, the calorific value of fuel being 42.6 MJ kg^{-1} ; (c) a 46 kW direct-driven surface forcing fan circulating 60 m^3 s^{-1} of air through the mine at a static pressure of 900 Pa. Assume 6m diameter shafts.

3.3 Air at 305 K d.b./294 K w.b. enters a 610m deep shaft which is very wet so that it gets 95% saturated with water-vapour at the shaft-bottom. Calculate the dry-and wet-bulb temperatures of air at the shaft-bottom, taking auto-compression to be the only source of sensible heat.

3.4 Find the dry-and wet-bulb temperatures of the resulting air when 2 m^3 of air at 297.5 K saturated mixes with 5 m^3 of air at 308 K d.b./302 K w.b. temperatures every second. The barometer reads 101.33 kPa.

3.5 Find the mass of dry air in 5.1 m^3 of moist air at 310 K d.b./301 K w.b. temperatures.

3.6 What is the amount of heat extracted when 1 m^3 of air at 310 K d.b./301 K w.b. is cooled to 305 K d.b.? What is the wet-bulb temperature? What would be the amount of heat extracted if the air were cooled further to 278 K saturated? What would be the mass of water-vapour condensed in the process?

3.7 Air at 309 K d.b./297 K w.b. is being cooled to a dry-bulb temperature of 302 K by spraying water into it. What would be

its wet-bulb temperature? What is the change in its density if the barometer reads 101.33 kPa?

3.8 Using the psychrometric chart find the percentage of error that may be introduced by not taking into account the dry-bulb temperature in calculating the heat extraction capacity of a refrigeration plant for cooling air from 291 K w.b. to 277 K saturated. The likely range of variation of the dry-bulb temperature is upto 321 K.

3.9 A hygrometer reads 303 K d.b./293 K w.b. Find the effective temperature if the air velocity is 1 m s^{-1}. What air velocity would ensure an effective temperature of 294 K ?

3.10 Calculate the enthalpy of air at 307 K d.b./302 K w.b. temperatures at a barometric pressure of 101.33 kPa where the vapour pressure is 3.7 kPa. Assume specific heat of air=1005 J kg^{-1} K^{-1} specific heat of water-vapour=1860 J kg^{-1} K^{-1} and latent heat of vaporization of water=2.5×10^6 J kg.$^{-1}$

3.11 A pump chamber has 4 large pumps each of water power = 940 kW and input power = 1010 kW. 18 m^3 s^{-1} of air at 305.5 K d.b./300.4 K w.b. enters the chamber to ventilate it. Calculate the outlet temperatures of the air as well as the amount of cooling needed to restore the air temperature to the inlet conditions.

3.12 The following measurements were made on a cooling plant. Calculate the duty of the cooling plant (evaporator heat exchange), the condenser heat exchange and the compressor power input.

Evaporator water flow-rate		=	28.7 kg s^{-1}
Evaporator water temperature			
	inlet	=	295.9 K
	delivery	=	280.3 K
Condenser water flow-rate		=	107.1 kg s^{-1}
Condenser water temperature			
	inlet	=	310.1 K
	delivery	=	315.3 K

Scanned with CamScanner

CHAPTER IV

AIR-FLOW THROUGH MINE OPENINGS

When a viscous fluid like air flows through a mine airway, it meets with a resistance to flow due to viscous shear, eddies and separation. It has to do some frictional work as a result of which a part of its pressure energy is converted to entropy energy.

4.1 GENERAL ENERGY BALANCE EQUATION

Consider a unit mass of air (or any fluid) flowing steadily through an open system, say a mine airway, per unit time.

The general energy balance equation for a small section of the system can be written as :

$$dQ - dW = dH + dPE + dKE \quad (4.1)$$

where dQ = heat added to or removed from the section (from outside the system),

dW = external work done on or by the fluid in the section (e.g. work done by a fan in moving air or by compressed-air running a motor),

dH = change in enthalpy of the fluid across the section,

dPE = change in potential energy of the fluid across the section,

= gdh,

dKE = change in kinetic energy of the fluid across the section = $d\left(\frac{v^2}{2}\right) = vdv$,

g = acceleration due to gravity,

h = elevation of the fluid

and v = velocity of the fluid.

This equation holds for frictional or frictionless flow ; for compressible or incompressible flow.

Enthalpy comprises a useful 'pressure' energy component VdP and a useless 'entropy' energy component TdS.

Or, $$dH = VdP + TdS \quad (4.2)$$

where V = specific volume of fluid,

T = temperature of the fluid,

dP = change in absolute pressure of the fluid,

and dS = change in entropy of the fluid.

The 'frictional work' is internal to the system where the useful pressure energy component of the enthalpy is converted to entropy energy. In other words, there is a rise in TdS component at the expense of VdP component, the value of dH remaining the same.

Again $$TdS = dQ + dF \quad (4.3)$$

where dF = frictional work.

Combining equations 4.1, 4.2 and 4.3 we have

$$-dW = VdP + dF + dPE + dKE \quad (4.4)$$

Note that this equation, though having no heat term, takes into account heat transfer from or to the surrounding.

When there is no external work, $dW = 0$

Or, $$VdP + dF + dPE + dKE = 0 \quad (4.5)$$

Integrating between the boundaries 1 and 2 of the system,

$$-\int_1^2 VdP = F_{1-2} + g(h_2 - h_1) + \frac{v_2^2 - v_1^2}{2} \quad (4.6)$$

Within the range of pressure change mine air is subjected to, it can be considered incompressible so that V in equation 4.6 can be taken as constant and the equation written in the form

$$V(P_1 - P_2) = F_{1-2} + g(h_2 - h_1) + \frac{v_2^2 - v_1^2}{2} \quad (4.7)$$

or $$\frac{P_1 - P_2}{\rho} = F_{1-2} + g(h_2 - h_1) + \frac{v_2^2 - v_1^2}{2}. \quad (4.8)$$

where ρ = density of the fluid = $\frac{1}{V}$.

Note that removal of the friction term F_{1-2} from equation 4.8 results in the well-known *Bernoulli equation* for frictionless flow of ideal fluids.

Now for flow in a horizontal airway of uniform cross-section where both $g(h_2 - h_1)$ and $\frac{v_2^2 - v_1^2}{2}$ equal zero, equation 4.8 reduces to

$$\frac{P_1 - P_2}{\rho} = F_{1-2} \quad (4.9)$$

Thus there is always a drop of pressure depending on the amount

Scanned with CamScanner

of frictional work along path of flow of a viscous fluid and the pressure drop is used as a measure of the resistance to flow.

4.2 LIMITS OF COMPRESSIBILITY

Mine air-flow is generally assumed incompressible. If we set 5% change in the value of V (or ρ) as the limit of incompressibility and assume a linear relationship between P and V, the limiting change in the value of P will then be 5%. Taking the initial pressure of mine air to be 100 kPa (of the order of 1 atomsphere), the limiting drop of pressure for incomprressible flow is 5 kPa. In other words, the flow can be considered incompressible if the fan pressure is < 5 kPa.

Looking at equation 4.8 it is clear that apart from F_{1-2}, the change in elevation and air velocity also change the pressure. For a 5 kPa limit of pressure change, the change in elevation required is $5000/(\rho.g)=425$m taking $\rho=1.2$ kg m^{-3} and g=9.8 m s^{-2}. For the same limit of pressure change, the change in velocity required

is $\sqrt{\dfrac{5000\times 2}{\rho}}=91$ m s^{-1}.

While air velocities in mines never reach 91 m s^{-1}, and fan pressures rarely exceed 5 kPa, shafts deeper than 425m are common. In such cases estimation of frictional work should be done from equation 4.6 instead of equation 4.8 taking into consideration the variation of V.

4.3 FLOW OF VISCOUS FLUIDS

A viscous fluid is one which has a certain degree of molecular cohesion and any deformation of it is associated with the establishment of shear stresses in the fluid. Let us consider a viscous fluid flowing along a stationary plane surface so that the flow at all points is parallel to the surface (Fig. 4.1). The velocity of the fluid in contact with the surface tends to equal that of the surface (which, in this case, is zero) because of molecular adhesion and there exists a velocity gradient in a direction perpendicular to that of flow. As we proceed farther away from the surface, each layer of fluid moves ahead of the preceding layer. As a result, a tangential shear stress is set up between the surface and the fluid as well as between the successive layers of the fluid. The amount of this shear stress is proportional to the rate of shear strain, the

constant of proportionality being termed the viscosity of the fluid by Newton.

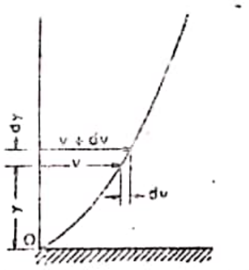

Fig. 4.1 Velocity gradient in viscous flow.

$$\tau=\mu\frac{dv}{dy} \tag{4.10}$$

where τ = tangential shear stress,

$\dfrac{dv}{dy}$ = velocity gradient (rate of shear strain)

and μ = absolute or dynamic viscosity of the fluid.

The S. I. Unit of absolute viscosity is Pas or Ns m^{-2} (kg m^{-1}s^{-1} in basic units). The commonly used CGS unit is poise (g cm^{-1} s^{-1} =0.1 Pas). Viscosity of a fluid is independent of pressure except at very high or very low pressures, but varies with temperature. Whereas the viscosity of liquids decreases with temperature, that of gases increases. Table 4.1 gives the viscosity, density and *kinematic viscosity* (=dynamic viscosity/density) of air at different temperatures at a standard barometer of 101.33 kPa and g_c (standard gravitational acceleration) =9.806 65 m s^{-2}.

4.4 LAMINAR FLOW THROUGH PIPES

Let us now consider laminar flow of a fluid through a horizontal circular pipe of uniform cross-section.

When the flow is laminar parallel to the axis of the tube, there is no shear stress in the direction perpendicular to the axis of the tube and hence no pressure gradient in that direction, but pressure gradient dP/dx exists in the direction of flow due to viscous shear. If now we consider the forces acting on a cylindrical fluid element of

Scanned with CamScanner

Table 4.1 Viscosity and Density of Air at Different Temperatures[72]

Temp., K	Viscosity μ, Pas $\times 10^{-5}$	Density ρ, kg m^{-3}	Kinematic viscosity $\nu = \mu/\rho$, m^2 s^{-1} $\times 10^{-4}$
273	1.711	1.295	0.132
278	1.734	1.269	0.137
283	1.759	1.248	0.141
288	1.783	1.227	0.145
293	1.807	1.207	0.150
298	1.831	1.186	0.154
303	1.854	1.166	0.160
313	1.902	1.130	0.168
333	1.998	1.062	0.188
353	2.089	1.001	0.209
373	2.176	0.944	0.231
473	2.583	0.743	0.348
573	2.947	0.614	0.480
673	3.278	0.521	0.629
773	3.584	0.454	0.790

radius r and length L (see Fig. 4.2), in the direction of flow, we have, for equilibrium,

$$\pi r^2 P - \pi r^2 \left(P + \frac{dP}{dx} L \right) - 2\pi r L \tau = 0$$

or
$$\tau = -\frac{dP}{dx} \frac{r}{2} \tag{4.11}$$

At the centre line, $\tau = 0$ since $r = 0$, but at the boundary, τ is the maximum and is equal to

$$\tau_o = -\frac{dP}{dx} \cdot \frac{r_o}{2} \tag{4.12}$$

where r_o = radius of the pipe.

Since $\tau = -\mu \dfrac{dv}{dr}$, equation 4.11 becomes $\dfrac{dv}{dr} = \dfrac{dP}{dx} \cdot \dfrac{r}{2\mu}$.

Integrating with respect to r, we have,

$$v = \frac{dP}{dx} \cdot \frac{r^2}{4\mu} + C.$$

When $r = r_o$, $v = 0$ and $C = -\dfrac{dP}{dx} \cdot \dfrac{r_o^2}{4\mu}$.

Substituting this value of C in the above equation, we have

$$v = -\frac{1}{4\mu} \cdot \frac{dP}{dx} (r_o^2 - r^2) \tag{4.13}$$

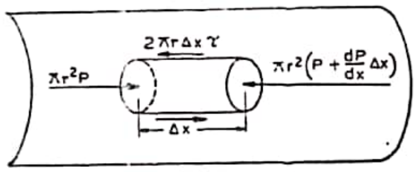

Fig. 4.2 Pressure acting on a cylindrical element of fluid subjected to viscous flow in a pipe.

The above equation is that of a parabola (Fig. 4.3), or the velocity distribution curve for the whole pipe is a paraboloid of revolution for which the average velocity

$$\bar{v} = \frac{v_{max}}{2} = -\frac{dP}{dx} \cdot \frac{r_o^2}{8\mu}$$

$$\text{or,} \quad -\frac{dP}{dx} = \frac{8\mu\bar{v}}{r_o^2} = \frac{32\mu\bar{v}}{D^2} \tag{4.14}$$

where D = diameter of the pipe.

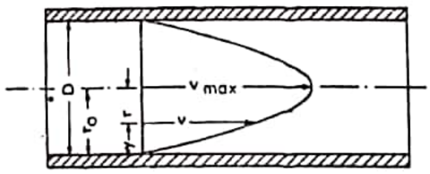

Fig. 4.3 Velocity distribution in a pipe with laminar flow.

Since the pipe is of uniform cross-section, the above equation can be integrated with respect to x over a pipe length L to give

$$\Delta P = \frac{32\mu\bar{v} L}{D^2} \tag{4.15}$$

Scanned with CamScanner

This is the *Poiseuille equation* which gives the estimate of the pressure drop for laminar flow of viscous fluids through pipes.

4.5 TURBULENT FLOW

So far, we have considered laminar flow where the fluid moves steadily in parallel streamlines or laminae of streamlines. Here the viscosity of the fluid plays the most important role in determining the flow pattern. Under certain conditions of flow, the laminar flow pattern becomes disturbed and unstable when eddies are formed resulting in the intermingling of fluid between adjacent laminae. Such a flow is called turbulent flow. Fluid turbulence involves a complex pattern of motion which can be likened to molecular motion on a greatly enlarged scale. There is a much greater rate of dissipation of energy in turbulent flow, as a result of which the pressure gradient is steeper than with laminar flow.

4.6 REYNOLDS NUMBER

The nature of flow of a fluid (laminar or turbulent) is governed by a dimensionless parameter called the Reynolds number, which is equal to

$$\frac{vD\rho}{\mu} = \frac{vD}{\nu}$$

where v = velocity of flow
D = diameter of the duct in case of flow through a duct,
ρ = density of the fluid,
μ = viscosity of the fluid
and $\nu = \frac{\mu}{\rho}$ = kinematic viscosity.

The Reynolds number determines the relative influence of viscosity on the flow pattern. The larger the Reynolds number, the lesser is the influence of viscosity on the flow pattern and at high Reynolds numbers, the viscous resistance to deformation becomes less important in comparison to inertial resistance to acceleration, which is a function of the fluid density.

As Reynolds number increases beyond a certain critical limit, laminar flow becomes unstable. This limit, however, depends on the nature of disturbances in the flow. It has been physically possible to maintain laminar flow at as high a Reynolds number

as 40 000 by having a thoroughly undisturbed flow, but this value decreases with the presence of disturbances until at a lower critical limit (which occurs at a Reynolds number of 2000) disturbances of any magnitude are eventually dampened by viscosity so that a laminar flow is obtained.

Example 4.1

Determine the nature of flow in a mine airway of 2.2×1.8 m size if the velocity of air in the airway is 0.5 m s^{-1}. Calculate the maximum velocity at which the flow still remains truly laminar. Assume the air to be at an atmospheric pressure of 101.33 kPa and at a temperature of 303 K.

Equivalent diameter of the airway $= 4\,\frac{A}{P} = \frac{4 \times 2.2 \times 1.8}{2(2.2+1.8)} = 1.98$ m.

From Table 4.1, $\nu = 0.16 \times 10^{-4}$ m^2 s^{-1}.

Therefore, Re (Reynolds number) $= 0.5 \times 1.98/(0.16 \times 10^{-4}) = 61875$.

So, the flow is turbulent.

For the flow to be laminar, i.e. $Re \leqslant 2000$,

maximum velocity $= 2000 \times 0.16 \times 10^{-4}/1.98 = 0.016$ m s^{-1}.

4.7 BOUNDARY LAYER

When a real or viscous fluid flows past a solid boundary, its velocity at the contact with the boundary is reduced to that of the boundary. The velocity increases as we proceed away from the boundary until beyond a certain zone or layer adjacent to the boundary, almost the free stream velocity is obtained. This layer has been termed by Prandtl as the boundary layer. The boundary layer may be laminar or turbulent depending on the Reynolds number characterizing flow. This is illustrated in Fig. 4.4, where let us consider the flow of a fluid past a streamlined strut at a velocity v_0. If only viscous effects are taken into account, the lateral velocity distribution will be according to curve I or, the velocity will be zero at the boundary, increasing uniformly away from it to the value v_0. On the other hand, if only accelerative effects are taken into account the velocity distribution will be as shown in curve II. Curve I corresponds to a value of Re below the critical limit whereas curve II corresponds to an infinitely high value of Re. For an intermediate value of Re, however, the velocity distribution will follow an intermediate curve, e.g. curve III. Curve I shows a laminar boundary layer while curve III, a turbulent one.

Scanned with CamScanner

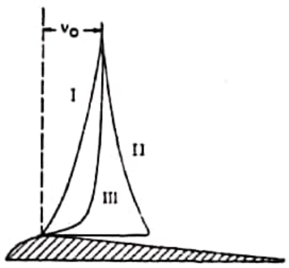

Fig. 4.4 Velocity gradients for different types of flow.

4.7.1 Laminar and Turbulent Boundary Layers in Pipes

In case of flow through pipes, the boundary layer extends all over the cross-section of the pipe since the velocity of flow increases from zero at the boundary to the maximum at the centre of the pipe. With laminar flow the velocity distribution across the pipe is given by curve I in Fig. 4.5 which is a parabola. The boundary layer in this case is a laminar boundary layer. As the value of *Re* increases, turbulence sets in and the velocity distribution becomes as shown in curve II which follows the relation

$$\frac{v}{\bar{v}} = \sqrt{f}\,(2.15 \log \frac{y}{r_o} + 1.43) + 1 \qquad (4.16)$$

where f=the Darcy-Weisbach resistance coefficient (see later). For flow at the centre of the pipe where $y=r_o$, equation 4.16 reduces to

$$\frac{v_{max}}{\bar{v}} = 1.43\sqrt{f} + 1 \qquad (4.17)$$

In this case also, there exists a boundary layer extending from the boundary to the centre of the pipe but different in nature from the laminar boundary layer. This is termed the turbulent boundary layer. However, with turbulent flow in smooth pipes, there exists a very thin laminar sublayer near the boundary where the velocity distribution follows the parabolic curve.

4.7.2 Flow in Rough Pipes

When the walls of a pipe are rough, the laminar sublayer at the boundary is broken up and the entire boundary layer becomes a turbulent one. Such a case usually occurs if the magnitude of roughness exceeds six times the thickness of the laminar sublayer for a particular Reynolds number.

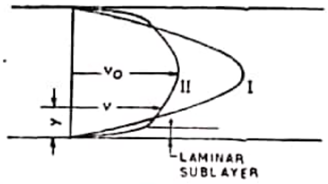

Fig. 4.5 Laminar and turbulent boundary layer.

4.8 RESISTANCE OF SMOOTH-WALLED PIPES

In turbulent flow the shear force is no longer a function of viscosity alone. However, whether for laminar or turbulent flow the boundary shear stress τ_o is a function of a dimensionless parameter f called the Darcy-Weisbach resistance coefficient.

$$\tau_o = \frac{f\rho v^2}{8} \qquad (4.18)$$

Since, in a horizontal pipe of uniform cross-section, the boundary shear is in equilibrium with the force due to pressure gradient along the pipe,

$$\tau_o \pi DL = -\frac{dp}{dx} L \frac{\pi D^2}{4}$$

Substituting $\triangle P_f$ for $-\frac{dp}{dx}L$ and solving for τ_o, we get

$$\tau_o = \triangle P_f \frac{D}{4L} \qquad (4.19)$$

Combining equations 4.18 and 4.19, we have

$$\triangle P_f = f\frac{L}{D}\frac{v^2\rho}{2} \qquad (4.20)$$

Equation 4.20 gives the pressure drop in pipes due to frictional resistance alone, since it has been developed for a horizontal pipe of uniform cross-section where there is no change in potential and kinetic energy of the fluid flowing. In pipes with potential and

Scanned with CamScanner

kinetic energy changes the pressure drop will be given by equation 4.8 expressed as follows in terms of pressure :

$$P_1 - P_2 = \triangle P_f + g(h_2 - h_1)\rho + \frac{v_2^2 - v_1^2}{2}\rho \qquad (4.21)$$

$$\text{where } \triangle P_f = \text{frictional pressure drop} = \frac{flv^2\rho}{2D}$$

$$= F_{1-2}\,\rho \qquad (4.22)$$

Both the equations 4.20 and 4.21 hold for incompressible flow where there is no change in the density of air, but where compressibility effects are significant, the change in pressure has to be estimated from the integration of the general energy balance equation 4.5 (see Appendix I).

4.8.1 Resistance Coefficient

The resistance coefficient f is a function of the Reynolds number. For values of Re less than 2000,

$$f = \frac{64}{Re} \qquad (4.23)$$

This relationship follows from the equation of Poiseuille (equation 4.15) :

$$\Delta P = \frac{32\mu vL}{D^2} = \frac{64\mu}{vD\rho}\cdot\frac{L}{D}\cdot\frac{\rho v^2}{2}$$

$$= \frac{64}{Re}\cdot\frac{L}{D}\cdot\frac{\rho v^2}{2} = f.\frac{L}{D}\cdot\frac{\rho v^2}{2}.$$

For values of Re greater than 2000, the value of f is given by the following empirical relationship due to *Blasius* :

$$f = \frac{0.316}{Re^{\frac{1}{4}}} \qquad (4.24)$$

The above equation holds true up to a value of $Re = 100\,000$, beyond which f is given by the *Karman-Prandtl resistance equation* for turbulent flow in smooth pipes :

$$\frac{1}{\sqrt{f}} = 2\log(Re\sqrt{f}) - 0.8 \qquad (4.25)$$

It is found, both from theoretical considerations and experimental work, that the resistance coefficient is related to the thickness of the boundary sublayer by the equation

$$\frac{\delta}{r_o} = \frac{65.6}{Re\sqrt{f}} \qquad (4.26)$$

where δ = thickness of the boundary sublayer.

Curve ABCDE in Fig. 4.6 gives the values of f for various values of Re in the case of flow in smooth pipes. Fig. 4.6a gives an enlarged plot of the Karman–Prandtl equation 4.25.

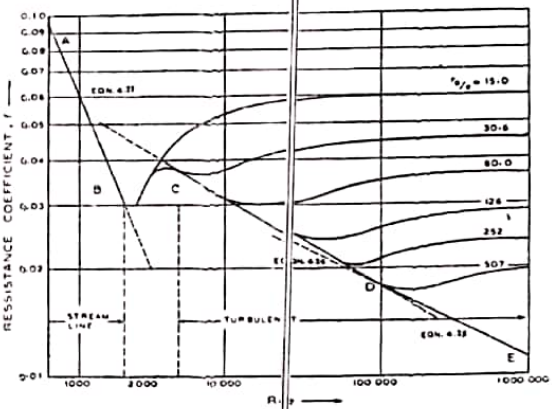

Fig. 4.6 Variation of resistance coefficient with Reynolds number for smooth and rough pipes (after Nikurdase).

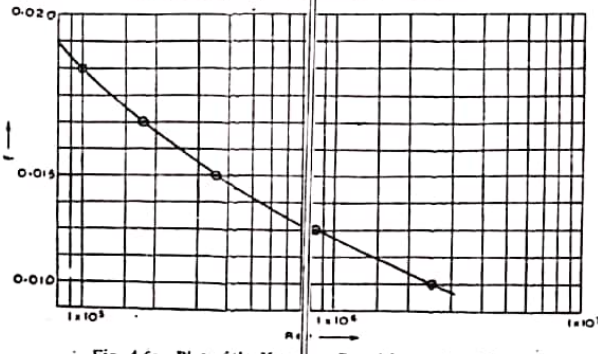

Fig. 4.6a Plot of the Karman-Prandtl equation 4.25.

Example 4.2

The average air velocity as measured in a 2.0m diameter smooth-lined airway is 0.01 m s⁻¹. What is the maximum velocity of flow and where does it occur in the airway? If the average velocity is raised to 0.5 m s⁻¹, what would be the maximum velocity and what would be the thickness of the laminar sublayer at the boundary?

Taking ν for air = 0.000 016 m² s⁻¹,

$$Re = \frac{\bar{v}D}{\nu} = \frac{0.01 \times 2.0}{0.000\,016} = 1250,$$

for an average velocity of flow $\bar{v} = 0.01$ m s⁻¹.

The flow is laminar for which the maximum velocity $v_{max} = 2\bar{v}$ = 0.02 m s⁻¹ and it occurs at the centre of the airway.

For $\bar{v}$ = 0.5 m s⁻¹,

$$Re = \frac{0.5 \times 2.0}{0.000\,016} = 62\,500.$$

Or, the flow is turbulent, for which

$$v_{max} = \bar{v}\,(1.43\sqrt{f} + 1).$$

But, for this value of Re,

$$f = \frac{0.316}{Re^{1/4}} = \frac{0.316}{(62\,500)^{1/4}} = 0.02.$$

$$v_{max} = 0.5\,(1.43\sqrt{0.02} + 1) = 0.6 \text{ m s}^{-1}.$$

Thickness of the boundary sublayer

$$\delta = \frac{65.6\, r_0}{Re\sqrt{f}} = \frac{65.6 \times 1.0}{62500 \times \sqrt{0.02}} = 0.007\ 42 \text{ m}$$

where r_0 = radius of the airway = 1.0 m.

4.9 RESISTANCE OF ROUGH-WALLED PIPES

As has already been said, no boundary sublayer is formed in pipes with sufficiently rough walls. The resistance coefficient in rough pipes is hence independent of Reynolds number at values of Re which, in smooth pipes, produce a boundary sublayer of a thickness less than one-sixth of the magnitude of roughness e (Fig. 4.7). In such cases f is given by the *Karman-Prandtl equation*

$$\frac{1}{\sqrt{f}} = 2 \log \frac{r_0}{e} + 1.74 \qquad (4.27)$$

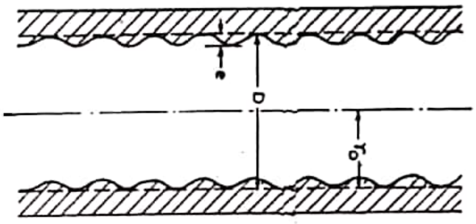

Fig. 4.7 Boundary roughness in a pipe (diagrammatic).

Values of f for various magnitudes of pipe roughness as determined experimentally by Nikurdase in artificially roughened pipes are given in Fig. 4.6. It will be seen that pipes which are considered rough at a certain value of Re, behave as smooth pipes at lower values of Re. This happens because, with Re decreasing, the thickness of the laminar sublayer increases as compared to the value of e so much so that at a value of e/δ less than 6, f practically ceases to be independent of Re and at values of e/δ less than $\frac{1}{4}$, the relationship between f and Re becomes as for smooth pipes. For the intermediate range ($\frac{1}{4} < e/\delta < 6$), f is a complex function of e and Re and can be obtained from Fig. 4.6. For values of Re below 2000, however, all pipes whether smooth or rough follow the same curve.

4.10 FLOW IN CONDUITS OF VARIED SHAPES

We have so far considered flow in circular pipes. Flow in pipes of other shapes differs very slightly and for all practical purposes, the resistance equation 4.20 for circular pipes, holds good for all cross-sectional shapes when D is taken as the equivalent diameter given by the relation

$$D = \frac{4A}{p} \qquad (4.28)$$

where A = cross-sectional area of the pipe

and p = wetted perimeter of the pipe.

Scanned with CamScanner

4.11 AIR-FLOW THROUGH MINE OPENINGS

Mine airways can be considered as very rough conduits with incompressible flow so that equation 4.20 can be used for calculating the frictional pressure drop

$$\Delta P_f = \frac{fLpv^2\rho}{8A} \qquad (4.28a)$$

Flow of air in mine airways is rarely laminar ($Re \leqslant 2000$) except for leakage through goaf or loose waste packs. It is usually, highly turbulent, where the value of f is determined by equation 4.27. The frictional pressure loss is proportional to the square of the velocity of air. However, in some mine airways with very low air velocities of the order of 1.2 m min^{-1}, the Reynolds number falls between 2000 and 4000 when the pressure loss is neither proportional to the velocity, as in the case of laminar flow (see equation 4.15) nor to the square of velocity, as in the case of highly turbulent flow. In such cases the pressure loss can be expressed in terms of v by the relation

$$P \propto v^n$$

where n varies between 1.6 and 1.9 ; but such cases are rare in mines and the pressure loss involved in these cases is small.

Equation 4.20 can be written in the form

$$\Delta P_f = \frac{kLp\,v^2}{A} = \frac{kSv^2}{A} = \frac{k\,S\,Q^2}{A^3}\ \text{Pa} \qquad (4.29)$$

where Q = flow through the airway, m^3 s^{-1},
S = Lp = area of the rubbing surface, m^2
and k = coefficient of friction = $f\rho/8$ N s^2 m^{-4} (=kg m^{-3}) (4.30)

Like f, k depends on the degree of roughness of the mine airway at high values of Re. Effect of density variation can generally be neglected so that k remains a constant for a particular type of airway (degree of roughness). Equation 4.29, therefore, finds common use in mine ventilation calculations.

4.11.1 Flow through Ventilation Ducts

Flow through ventilation ducts commonly used for auxiliary ventilation in mines can be likened to that in smooth pipes, when

the resistance coefficient is governed by equations 4.24 and 4.25. The friction pressure loss in such ducts can be calculated by substituting the value of f from equation 4.24 in equation 4.20 which will then give

$$\Delta P_f = \frac{0.316}{Re^{\frac{1}{4}}} \cdot \frac{L}{D} \cdot \frac{v^2\rho}{2} \qquad (4.31)$$

or, $\Delta P_f \propto v^{1.75}$

More generally however, $\Delta P_f \propto v^n$ where n varies from 1.71 to 1.83 between values of Re equal to 3000 and 400 000. Holdsworth *et al*[13] give a general value of $n = 1.9$ for coal-mine ducts.

Example 4.3

What is the pressure required to circulate 20 m^3 of air per second, through a mine airway 300m long, 2.5m high and 3m wide? The coefficient of friction of the airway is 0.01 N s^2 m^{-4}. Calculate the Darcy–Weisbach resistance coefficient for the airway taking the air density at 1.2 kg m^{-3}. It is proposed to increase the quantity to 30 m^3 s^{-1} by widening the roadway. Calculate the volume to be stripped. Assume applied pressure to remain constant.

$$\text{Pressure required} = \frac{0.01\,(2.5+3)2\times300\times20^2}{(2.5\times3)^3}$$

$$= 31.29\ \text{Pa.}$$

Darcy-Weisbach resistance coefficient

$$f = \frac{8k}{\rho} = \frac{8\times0.01}{1.2} = 0.066.$$

Taking applied pressure and coefficient of friction to remain the same, let the width be increased to Wm.

$$\therefore\ 31.29 = \frac{0.01\,(2.5+W)\,2\times300\times30^2}{(2.5W)^3}$$

Or, W = 4.2m (from a graphical solution of the equation).
The volume to be stripped
$= 4.2\times2.5\times300 = 3150$ m^3.

Scanned with CamScanner

Example 4.4

A smooth steel duct 450×600mm in size circulates 0.5 m^3 of air per second. Calculate the coefficient of resistance of the duct and the friction pressure loss in a 100m length of the duct.

The equivalent diameter of the duct $= \dfrac{4\times 0.45\times 0.6}{2\,(0.45+0.6)} = 0.5143$m.

Velocity of air in the duct $= 0.5/(0.6\times 0.45) = 1.85$ m s^{-1}.

Therefore, $Re = 0.5143\times 1.85/0.000\,016 = 59\,466$

assuming $\nu = 0.16\times 10^{-4}$ m^2 s^{-1} (see Table 4.1).

For this value of Reynolds number, equation 4.15 due to Blasius holds true.

Or, resistance coefficient $f \approx 0.316/Re^{\frac{1}{4}} = 0.020\,24$.

Friction pressure loss from equation 4.20a $= f\,L p\,v^2\,\rho/8A$

$$= \frac{0.020\,24\times 100\times 2(0.45+0.6)\times(1.85)^2\times 1.2}{8\times(0.45\times 0.6)} = 8.08 \text{ Pa},$$

assuming $\rho = 1.2$ kg m^{-3}.

If we assume a value of $k = 0.002\,94$ Ns^2 m^{-4} (see Chapter VIII) for smooth ducts, then from equation 4.29,

pressure loss $= 0.002\,94\times 100\times 2(0.45+0.6)\times(1.85)^2/(0.45\times 0.6)$

$= 7.83$ Pa.

Example 4.5

Calculate the pressure required to circulate 3000 m^3 min^{-1} of air through a 2500m long tunnel of

(a) 3×3m cross-section with $k = 0.0098$ N s^2 m^{-4}
and cost of driving = 400.00 Rs m^{-1}

(b) 3.5×3.5m cross-section with $k = 0.0098$ N s^2 m^{-4}
and cost of driving = 500.00 Rs m^{-1}

and (c) 3×2.5m smooth-lined cross-section with $k = 0.0039$ N s^{-2} m^{-4} and cost of driving and lining = 650.00 Rs m^{-1}

Which will be the most economical of the three if the tunnel is to have a life of 12 years. Assume cost of power to be 9 P kW^{-1} h^{-1}, fan efficiency = 75%, motor efficiency = 92% and the safe rate of interest for present value calculation, 4%. The present value of Re. 1.00 per annum for 12 years at 4% compound interest is Rs. 9.39.

Case (a)

$$\text{Pressure required} = \frac{0.0098\times 2(3+3)\times 2500\,(3000/60)^2}{(3\times 3)^3}$$

$= 1008.2$ Pa $= 1.0082$ kPa.

$$\text{Air power} = \frac{3000}{60}\times 1.0082 = 50.41 \text{ kW}.$$

$$\text{Power input to the motor} = \frac{50.41}{0.75\times 0.92} = 73.058 \text{ kW}.$$

Annual consumption of electric power

$= 73.058\times 24\times 365 = 639.988\times 10^3$ kWh.

Annual power cost $= 639.988\times 10^3\times 0.09 =$ Rs. 57 598.92

Present value of annual power cost over 12 years $= 57\,598.92\times 9.39$

$=$ Rs. 540 853.86.

Capital cost for driving $= 2500\times 400.00$

$=$ Rs. 1 000 000.00.

Total cost $= 1\,000\,000.00 + 540\,853.86$

Rs. 1 540 853.86.

Case (b)

$$\text{Pressure required} = \frac{0.0098\times 2(3.5+3.5)\times 2500(3000/60)^2}{(3.5\times 3.5)^3}$$

$= 466.5$ Pa $= 0.4665$ kPa.

$$\text{Air power} = 0.4665\times\frac{3000}{60} = 23.325 \text{ kW}.$$

$$\text{Power input to the motor} = \frac{23.325}{0.75\times 0.92} = 33.8 \text{ kW}.$$

Annual consumption of electric power

$= 33.8\times 24\times 365 = 296.088\times 10^3$ kWh.

Annual power cost $= 296.088\times 10^3\times 0.09 =$ Rs. 26 647.92.

Present value of annual power cost over 12 years

$= 26\,647.92\times 9.39 = 250\,223.97$.

Capital cost of driving $= 2500\times 500 =$ Rs. 1 250 000.00.

Total cost $= 1\,250\,000.00 + 250\,223.97 =$ Rs. 1 500 223.97.

Scanned with CamScanner

Case (*c*)

$$\text{Pressure required} = \frac{0.0039 \times 2(3+2.5) \times 2500(3000/60)^2}{(3 \times 2.5)^3}$$

$$= 635.56 \text{ Pa} = 0.6356 \text{ kPa}.$$

$$\text{Air power} = \frac{3000}{60} \times 0.6356 = 31.78 \text{kW}.$$

$$\text{Power input to the motor} = \frac{31.78}{0.75 \times 0.92} = 46.06 \text{ kWh}.$$

Annual power consumption $= 46.06 \times 24 \times 365 = 403.4856 \times 10^3$ kWh.
Annual power cost $= 403.4856 \times 10^3 \times 0.09 =$ Rs. 36 313.70.
Present value of annual power cost over 12 years
$= 36\,313.70 \times 9.39 =$ Rs. 340 985.64.
Capital cost for driving and lining $= 2500 \times 650 =$ Rs. 1 625 000.00.
Total cost $= 1\,625\,000.00 + 340\,985.64 =$ Rs. 1 965 985.64.
Alternative (*b*) is the most economical.

4.11.2 Shock Resistance

We have so far considered the case of frictional resistance to flow in pipes (due to boundary shear), but if the pipe contains an obstruction on the path of flow, which not only exposes an extra boundary to flow but also causes eddies and separation in the wake of the obstruction, there occurs a pressure loss across the obstruction. The resistance so offered by the obstruction is commonly termed as shock resistance. Shock pressure loss also occurs at points of change in cross-sectional areas as well as bends where eddies are formed and separation takes place. Note that the term 'frictional work' used in the general energy balance equation 4.4 covers both frictional resistance and shock resistance.

4.11.3 Drag of Immersed Bodies

The total longitudinal force exerted by a moving fluid on an immersed body is evidently the sum of the longitudinal components of all normal and tangential stresses on the boundary surface. If we consider a thin plate immersed in a fluid so that its plane is parallel to the direction of flow, the effect of drag due to the difference in normal stresses at the leading and trailing ends of the plate will be negligible and the drag in such a case can be considered to be almost entirely due to viscous boundary shear. But if the plate

is placed with its plane across the flow, the drag will be almost fully due to the difference in the normal forces acting on the front and the rear sides of the plate. The above two forms of obstruction represent two extreme cases. For intermediate forms of obstruction, the drag will be a combination of both *surface* or *frictional drag* (due to viscous boundary shear) and *form* or *pressure drag* (due to unbalanced normal forces). The object of streamlining an obstruction is to minimize the form drag, but there will still be some loss of pressure across it due to boundary shear which, in fact, increases with increase in the length of the obstruction. Hence for streamlined forms, there is an optimum length for which the total drag is the minimum.

If the total longitudinal force on the immersed body is F and the projected area of the body in a plane perpendicular to the direction of flow, A, then the loss of pressure $\triangle P_D$ across it is given by the relation

$$\triangle P_D = F/A = C_D \frac{v^2\rho}{2} \tag{4.32}$$

where C_D is the *drag coefficient*.

C_D is a function of Re (taking into account the diameter of obstruction) and the form of the body. Let us consider a spherical body. At very low values of Re (less than unity) where viscous drag is predominant, C_D is given by the relation

$$C_D = 24/Re \tag{4.33}$$

But as Re increases, viscous deformation gets confined to the front surface of the obstruction and accelerative effects causing separation and formation of a wake become predominant. When Re reaches a value of about 10^3 the viscous shear becomes very small (about 5%) in comparison with the drop of pressure at the wake. As a result, C_D becomes almost independent of Re having an average value of 0.44. On further increase of Re to 2.5×10^5 however, turbulence sets in the boundary layer and there is a sharp reduction of about 60% in the value of C_D because of the shifting of the point of separation further downstream. The extremely low drag coefficient of streamlined bodies at high Reynolds numbers is due to the minimization of separation at the wake which almost eliminates the form drag.

On the other hand, if the body is in the form of a circular disc with its plane perpendicular to the direction of flow, C_D becomes

Scanned with CamScanner

independent of *Re* at a much lower value of *Re* (beyond the region of deformation drag) because of the fact that the separation points in this case are fixed entirely governed by the form of the body.

For the high Reynolds numbers commonly met with in mines, C_D can be taken to depend mainly on the form of the body. Table 4.2 gives the values of C_D for infinitely long bodies of different cross-sections. They correspond to a Reynolds number nearly equal to that for a bunton in a mine shaft and hence can be generally used for buntons in shafts.

Table 4.2[75] : Drag Coefficients of Infinitely Long Bodies of Different Cross-sections

FORM OF CROSS-SECTION		C_D	FORM OF CROSS-SECTION		C_D
I	I GIRDER	2.75	▽	TRIANGLE	2.00
⊢⊣	I GIRDER	2.05	—	PLATE	1.98
□	RECTANGLE	2.05	┐	ANGLE	1.98
T	TEE	2.05	┘	ANGLE	1.82
△	TRIANGLE	1.55	▢	ROUNDED-SQUARE	1.35
◇	SQUARE	1.55	○	CIRCLE	1.20
∧	ANGLE	1.45		STREAMLINED SECTION AS PER FIGURE	1.05
□	CAPPED RECTANGLE	1.40			
				DUMB BELL	1.30

DIRECTION OF AIR-FLOW

4.11.4 Shock Loss at Area Changes and Bends

Shock loss due to changes in cross-sectional area of pipes can also be likened to pressure loss due to drag of immersed bodies. Here also, the pressure loss is proportional to the velocity pressure corresponding to the average velocity of flow and is given by the relation.

$$\Delta P_s = XP_v = X\frac{\rho V^2}{2} \tag{4.34}$$

where X is a dimensionless constant, called the *shock factor* and P_v = velocity pressure.

In this case also, X depends on both Reynolds number and the boundary geometry. At low Reynolds numbers, the viscous effect predominates whereas at high values of *Re*, such effects are subordinated to those of acceleration. Hence at Reynolds numbers prevalent in mine airways, the value of X can be considered to remain unaffected by Reynolds number. The boundary geometry affects the value of X in that, at an abrupt area change as shown in Fig. 4.15, X is affected almost entirely by separation losses whereas if the change in area were more gradual, the separation losses would have been less and pressure loss due to boundary shear would have contributed more to the total pressure loss.

Shock losses at bends are akin to those at area changes and are due to eddies and separation caused by the constriction of the effective area of flow at the bend.

4.12 PRESSURE LOSS IN A MINE AIRWAY

When determining the pressure loss in a projected mine airway, both friction and shock losses are to be taken into account. Normally they are determined independently of each other, i.e. the friction loss for the airway without the obstruction is determined first and then the shock loss due to the obstruction is determined and both are added together. This is however, not strictly accurate, since the velocity distribution and the nature of flow in a pipe are affected by the boundary roughness of the pipe and hence the shock factor is also affected. However, model studies[76] show that simple addition of friction and shock losses gives fairly accurate results for smooth airway surfaces, though the results become inaccurate for rough airways, in which case accurate estimation of the total pressure loss can be made only from measurements on geometrically similar models.

Slight bends or small area changes involving shock losses of only small magnitude often do not warrant their separate determination. They are usually included in the friction pressure loss by suitably increasing the value of the coefficient of friction k. Although both losses are different from each other in the sense that friction losses are mainly due to surface drag and shock losses, to form drag, the latter can be conveniently expressed in the form of the former without much inaccuracy and it is a general practice to express regularly intermittent shock losses of small magnitude in terms of friction loss.

Scanned with CamScanner

Taking the standard value of ρ equal to 1.2 kg m^{-3}, we have from equation 4.34

$$\Delta P_s = 0.6Xv^2 \text{ Pa} \tag{4.35}$$

where v is in m s^{-1}.

If k_s = the coefficient of friction corresponding to the shock loss, then from equation 4.29

$$k_s = \frac{0.6Xv^2A}{L\rho v^2} = 0.6X\frac{A}{L\rho} \tag{4.36}$$

If the shock loss per 100m length of airway is given by XP_v, then k_s will be equal to $0.006XA/p$. This value of k_s has to be added to the normal value of k due to surface friction in order to get the overall coefficient of friction for calculating the total pressure loss. In practice, field determination of the value of coefficient of friction for a particular type of airway usually records this overall coefficient of friction.

It is seen from equation 4.36 that k_s depends on the ratio A/p which is a function of the shape and size of the airway. Hence, the relative importance of k_s with respect to k will depend on the size of airway of a particular shape. Whereas for ducts or airways of 1m diameter $A/p=0.25$, for average mine roadways of 2.5m diameter or 2.5m square size, $A/p=0.625$. Hence, the relative importance of k_s for the former is much less compared to the latter so much so that small shock losses in narrow ducts can often be neglected as compared to the friction loss, but they cannot be neglected in large-size airways. For average mine airways of 2.5m diameter, where $A/p=0.625$, the value of k_s becomes 0.00375 X (where X is the shock factor per 100m length). This value can be generally applied for all rough-surfaced mine airways without introducing much error, since in such airways, the value of k_s is fairly small compared to that of k and the above generalization hardly introduces any appreciable error.

Sometimes, minor shock losses are accounted for by considering an increased length of the airway so that the friction loss over the extra length of the airway equals the shock loss. If L_s = the extra length of airway, then

$$L_s = \frac{0.6Xv^2A}{kpv^2} = \frac{0.6XA}{kp} \tag{4.37}$$

In general terms, pressure loss in a mine airway due to 'frictional work' ΔP can be given by the relation

$$\Delta P = \Delta P_f + \Delta P_s = \frac{kSv^2}{A} + 0.6Xv^2 \tag{4.38}$$

Estimation of ΔP therefore requires a knowledge of k and X for any airway.

4.12.1 Coefficient of Friction

The coefficient of friction for a mine airway can be estimated from equations 4.27 and 4.30 if an estimate of the degree of roughness e could be obtained, but it is not possible to find the value of e for mine airways accurately. It is more commonly determined from field measurements on similar airways.

4.12.2 Determination of 'k' from field measurements

This involves the field measurement of frictional pressure drop ΔP_f over a certain length of airway from which the value of f and hence k could be calculated if the velocity of flow v and the density of air ρ were also measured. ΔP_f itself cannot be measured directly unless the airway is horizontal and of uniform cross-section, but it can be obtained from the measurement of absolute pressures, elevations and air velocities at the beginning and the end of the airway with the help of equation 4.21 which can be written in the form

$$\Delta P_f = (P_1 - P_2) + g(h_1 - h_2)\rho + \frac{v_1^2 - v_2^2}{2}\rho \tag{4.39}$$

P_1 and P_2 in the above equation are absolute static pressures and can be measured by aneroid barometers.

But often for better accuracy of measurement, a suitable water gauge connected by tubes to the two ends of the airway is used for measuring the pressure difference between the two ends (see Chapter VIII). The tubes are usually made to face at right angles to the air-current so that the pressure difference measured is the static pressure difference. In such cases equation 4.39 is somewhat modified.

We know that $P = P_A + P_s$ (4.40)

where P_A = local atmospheric pressure

and P_s = gauge static pressure.

Scanned with CamScanner

Substituting in equation 4.39, we have

$$\Delta P_f = P_{A_1} + P_{s_1} - P_{A_2} - P_{s_2} + g(h_1 - h_2)\rho + \frac{v_1^2 - v_2^2}{2}\rho$$

$$= P_{s_1} - P_{s_2} + \frac{v_1^2 - v_2^2}{2}\rho \qquad (4.41)$$

since $P_{A_2} = P_{A_1} + g(h_1 - h_2)\rho$.

Again since $P_s + \frac{v^2\rho}{2} = P_s + P_V = P_T$, where P_V is the velocity pressure and P_T, the total pressure, equation 4.41 further reduces to

$$\Delta P_f = P_{T_1} - P_{T_2} \qquad (4.42)$$

The total pressure difference $P_{T_1} - P_{T_2}$ can be directly measured on the water gauge if the tubes at the two ends of the airway are made to face the air-current, but the result will not be accurate since, the velocity pressure varies widely over the airway cross-section. That is why it is more common to measure the static pressure difference by the gauge-and-tube method and determine the velocity pressure difference from measured average velocities to find the value of ΔP_f with the help of equation 4.41.

The above method of field measurement of ΔP_f presumes that there is no shock pressure loss in the airway. If however, there is a component of shock loss which can be independently estimated (see later), equation 4.39 will be modified as

$$\Delta P = \Delta P_f + \Delta P_s = P_1 - P_2 + g(h_1 - h_2)\rho + \frac{v_1^2 - v_2^2}{2}\rho$$

$$= \left(P_{A_1} + P_{s_1}\right) - \left(P_{A_2} + P_{s_2}\right) + g(h_1 - h_2)\rho + \frac{v_1^2 - v_2^2}{2}\rho \qquad (4.43)$$

and equation 4.42 as

$$\Delta P_f = P_{T_1} - P_{T_2} - \Delta P_s \qquad (4.44)$$

in order to obtain the value of ΔP_f.

Figs. 4.8 and 4.9 illustrate graphically the different components of pressure in equation 4.43. Fig. 4.8 illustrates a fan forcing air through an inclined airway and Fig. 4.9, a fan exhausting air from an inclined airway.

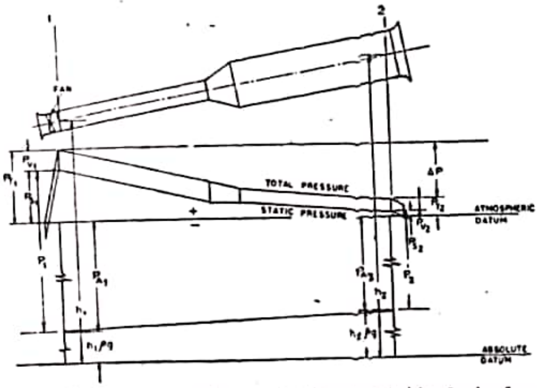

Fig. 4.8 Pressure gradient in a ventilation system with a forcing fan.

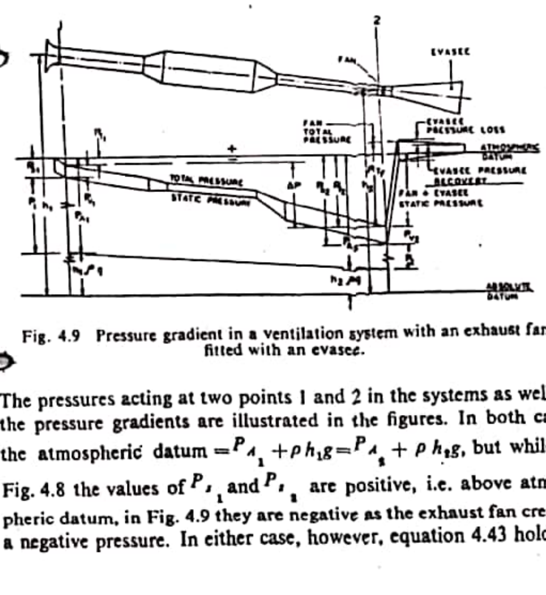

Fig. 4.9 Pressure gradient in a ventilation system with an exhaust fan fitted with an evasee.

The pressures acting at two points 1 and 2 in the systems as well as the pressure gradients are illustrated in the figures. In both cases the atmospheric datum $= P_{A_1} + \rho h_1 g = P_{A_2} + \rho h_2 g$, but while in Fig. 4.8 the values of P_{s_1} and P_{s_2} are positive, i.e. above atmospheric datum, in Fig. 4.9 they are negative as the exhaust fan creates a negative pressure. In either case, however, equation 4.43 holds.

Scanned with CamScanner

It should be noted here that just at the inlet to any of the above systems the static pressure as measured by a static or side tube is negative and numerically equal to the velocity pressure which is positive so that the total pressure at this point as measured by a pitot or facing tube is zero. On the other hand just at the outlet of the system, the static pressure is zero while the total pressure equals the velocity pressure.

Equation 4.43 is valid for incompressible flow only and cannot be used for deep shafts where compressibility effects are significant. Recourse has to be taken in such cases to the general energy balance equation 4.6 for the estimation of $\triangle P$. Expressing F_{1-2} in terms of $\triangle P$, we have

$$-\int_1^2 VdP=\frac{\triangle P}{\rho}+g\,(h_2-h_1)+\frac{v_2^2-v_1^2}{2} \qquad (4.45)$$

where ρ is the density of air at a certain reference point, normally taken at the fan inlet since determination of $\triangle P$ (or k) is used for the estimation of the required fan pressure.

The theoretical estimation of the term $-\int_1^2 VdP$ in the above equation is difficult as the process (of auto-compression or auto-expansion in the shaft) is never ideal. In working mines it is best

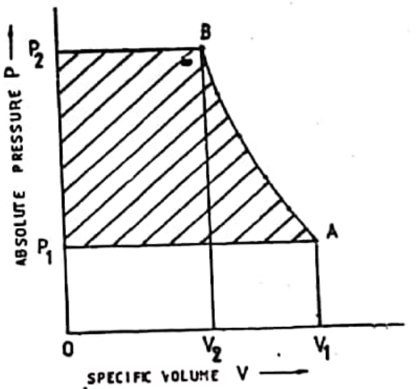

Fig. 4.10 *P-V* diagram for auto-compression of air in a downcast shaft.

to take measurements of P and V at different depths in the shaft and plot the P-V diagram (see Fig. 4.10). The value of $-\int_1^2 VdP$ then equals the area P_1ABP_2 (see equations 5.6 to 5.9 in Chapter V).

Where readings are available only at the top and bottom of the shaft $-\int_1^2 VdP$ can be obtained from the approximate relation

$$-\int_1^2 VdP=(P_1-P_2)\frac{V_1+V_2}{2} \qquad (4.46)$$

In known polytropic processes, however, the following relation can be used for greater accuracy

$$-\int_1^2 VdP=\frac{n}{n-1}\,(P_1V_1-P_2V_2) \qquad (4.47)$$

where n=polytropic index

$$=\left(\ln\frac{P_2}{P_1}\right)\Big/\left(\ln\frac{V_1}{V_2}\right)=\left(\ln\frac{P_1}{P_2}\right)\Big/\left(\ln\frac{V_2}{V_1}\right) \qquad (4.48)$$

Addition of moisture (or other gases) in the shaft can be taken into account by modifying equation 4.45 as follows, though the error involved is negligible :

$$-\int_1^2 VdP=\frac{\triangle P}{\rho}+g\,(h_2-h_1)+g\int_1^2 0.001\,m\,dh+\frac{v_2^2-v_1^2}{2} \qquad (4.49)$$

where m=mixing ratio in g kg^{-1} of dry air.

The specific volume V in this case is the apparent specific volume of moist air i.e. volume of moist air per unit mass of dry air given by the relation

$$V=\frac{287.1T}{1000(B-e)} \quad m^3\,kg^{-1} \qquad (4.50)$$

where B and e are the barometric pressure and vapour pressure in kPa and T, the temperature in K.

Sometimes regular intermittant shock losses occur superimposed on frictional losses as in timbered mine airways or shafts with buntons. It is difficult to estimate such shock losses independently and they are often incorporated in the coefficient of friction determined from field measurements on such airways.

The effect of such shock losses on the coefficient of friction can be illustrated by examining Fig. 4.11 which gives the variation in the value of k with spacing of timber sets as estimated by McElroy.[53]

Scanned with CamScanner

It will be seen from the figure that when the sets are placed skin to skin, there is no shock loss at all, and the value of k is the least. As the spacing increases, the value of k increases due to increased shock loss at each timber set up to a certain maximum, beyond which it starts falling again due to the obstructions being too far apart.

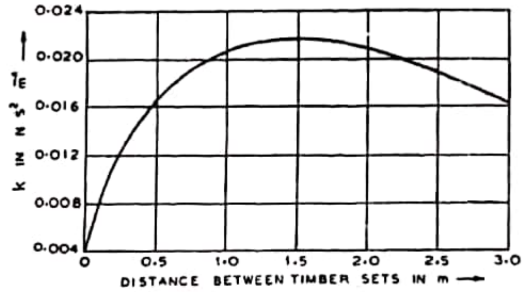

Fig. 4.11 Variation of the coefficient of friction of a timbered airway with spacing of sets.

Table 4.3 : Effect of the Magnitude and Spacing of Surface Roughness on the Value of k in Shafts

Shape of shaft	D/e	s/e	k, Ns² m⁻⁴
Circular	37	10.0	0.0118
,,	67	3.8	0.0137
,,	67	3.8	0.0127
,,	100	5.8	0.0147
Square	18	24.0	0.0294
,,	18	12.0	0.0382
,,	18	6.0	0.0392
,,	25	75.0	0.0098

A similar effect of shock loss on the value of k is illustrated in Table 4.3[75] where k has been estimated for shafts with obstructions in the form of ribs regularly spaced along the walls as would occur in case of shafts with timber sets or German tubbing. It is seen from the table that the value of k is not only a function of the surface

roughness D/e (where D=equivalent diameter and e=average magnitude of roughness of the wall surface) but also on the spacing of the ribs s or rather the ratio s/e.

Values of k for various types of airways have been determined by several authorities (Table 4.4), but they vary over a wide range. Hence, it may be advisable to determine the value of k, for the particular type of airway one has to deal with, from actual measurements on such airways, if available. It must be borne in mind that k depends on air density and if k determined for a particular air density ρ_0 is to be used at another air density, say, ρ_1, its value should be corrected by multiplying it by the ration ρ_1/ρ_0. If k has been determined at standard air density of 1.2 kg m⁻³ then

$$\rho_0=1.2, \text{ or } k=k_0\rho_1/1.2 \tag{4.51}$$

where k=coefficient of friction, corrected for air density ρ_1 and k_0= coefficient of friction at standard air density.

Table 4.4 : Values of k for Various Types of Airways

Type of airway	Value of k in Ns² m⁻⁴ or kg m⁻³ minimum	maximum	average	Authority
Roadways				
Smooth-lined				
(a) Without obstructions	0.001 86	0.003 73	0.002 75	McElroy and Richardson
(b) slightly obstructed	0.002 75	0.004 71	0.003 73	
(c) moderately obstructed	0.004 71	0.006 57	0.005 59	
Brick- or concrete-lined	—	—	0.002 16	Vogel
Concrete-lined (rectangular)	—	—	0.003 73	N.C.B.
Concrete-lined (arched)	—	—	0.003 73	Murgue
Unlined in sedimentary rock or coal				
(a) without obstructions	0.005 59	0.012 95	0.010 20	McElroy and
(b) slightly obstructed	0.006 57	0.013 93	C.011 18	Richardson
Unlined stone drift in coal-measure strata	0.008 93	0.010 40	0.009 81	Vogel
Unlined straight airways with fairly uniform sides (rectangular, coal measure rocks)	—	—	0.012 07	N.C.B.
Unlined rough airways (rectangular, coal measure rocks)	—	—	0.015 79	N.C.B.

Scanned with CamScanner

Type of airway	Value of k in $Ns^2 m^{-4}$ or $kg\ m^{-3}$			Authority
	minimum	maximum	average	
Unlined tunnel in rock (Rand gold field, slightly curved with a few sets)	0.010 40	0.010 79	—	Magasiner
Timbered airway (sets at 1.5m centre)				
(a) without obstruction	0.014 81	0.018 64	0.017 66	McElroy and Richardson
(b) slightly obstructed	0.015 79	0.020 50	0.018 64	McElroy and Richardson
(c) moderately obstructed	0.017 66	0.022 56	0.020 50	McElroy and Richardson
Rectangular airways supported with girders on brick or concrete walls	—	—	0.009 32	N.C.B.
Shafts				
Brick-lined	—	—	0.006 18	Flugge de Smidt and Polkinghorne
Brick-lined	—	—	0.003 92	Raux
Lined without bunton	—	—	0.003 43	Vogel
Lined with steel buntons	—	—	0.010 50	Vogel
Lined with wooden buntons	0.023 45	0.024 92	0.024 33	Vogel
Staple pit without bunton	0.019 42	0.025 80	0.022 56	Vogel
Staple pit with one cage compartment	0.082 80	0.094 27	0.088 29	Vogel
Staple pit with two compartments	0.052 48	0.066 90	0.059 74	Vogel

Air density depends on barometric pressure, temperature, humidity and the content of contaminating gases like methane in the air. These in normal cases, do not vary to any appreciable extent. Hence, the refinement of correcting k for density changes becomes unnecessary except when the value of k has to be projected for very deep mines where there is likely to be a large change in barometric pressure and temperature. However, it would be better to account for the density component in the value of k by computing k from field measurements under these conditions, if possible.

4.12.3 Shock Factor

Shock factprs for different shapes of obstructions, bends, area changes etc. are determined empirically mostly from model studies.

However, shock factors for any unique airway geometry occuring in the mine can be determined from field measurements with the help of equation 4.34 in conjunction with equation 4.43 or 4.44 which can be rewritten as

$$\triangle P_s = \frac{X\rho v^2}{2} = P_1 - P_2 + g(h_1 - h_2)\rho + (v_1^2 - v_2^2)\frac{\rho}{2} - \triangle P_f \quad (4.52)$$

$$\text{Or } \triangle P_s = \frac{X\rho v^2}{2} = (P_{T_1} - P_{T_2}) - \triangle P_f \quad (4.53)$$

It is of course necessary to independently estimate the value of $\triangle P_f$ for the airway over the measuring section.

4.12.4 Shock Factor for Bends

Shock losses at bends are mainly due to the constriction of the cross-sectional area of the air-stream at the bend and its subsequent expansion farther beyond the bend as shown in Fig. 4.12. Fig. 4.13 shows the various types of bends used in mine airways and ducts. Right-angle bends or elbows are most commonly used in mines. Normal bends have the outer corner rounded by a radial curve centred on the diagonal and the inner corner either rounded concentrically or square. With the square bends, the outer corner is square, but the inner corner may be square or may form a radial curve centred on the diagonal. The inner bevel bend is only a variation of the square bend. The crowded bend has the outer curve of a larger radius as compared to a normal bend. Venturi and

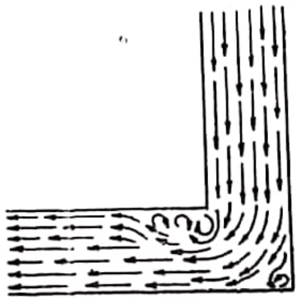

Fig. 4.12 Flow pattern at a bend.

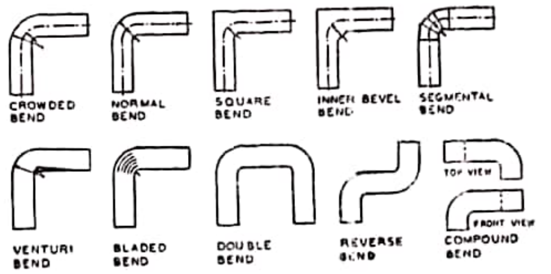

Fig. 4.13 Different types of bends.

bladed bends are specially designed for reducing shock loss in sharp bends. In the venturi bend, the cross-sectional area of flow at the entrance is gradually reduced to about two-thirds at the exit end of the bend. It is then increased gradually to the normal beyond the bend. The double, reverse or compound bends consist of two closely spaced single bends arranged as shown in Fig. 4.13.

The approximate shock factor for normal bends is given by the relation

$$X = \frac{0.25}{R^2\sqrt{a}} (2i/\pi)^2 \tag{4.54}$$

where X = shock factor,
R = radius ratio (see Fig. 4.14),
a = aspect ratio
and i = angle of deflection in rad.

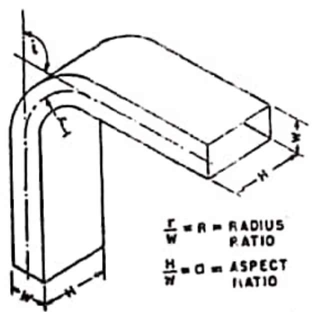

Fig. 4.14 Characteristics of a bend.

For right-angle bends in rectangular airways, equation 4.54 becomes

$$X = \frac{0.25}{R^2\sqrt{a}} \tag{4.55}$$

since $i = \pi/2$ and for square or circular airways, where $a = 1$,

$$X = \frac{0.25}{R^2} \tag{4.56}$$

The value of R is minimum for a square inner corner and is equal to $\frac{W/2}{W} = 0.5$. In such a case the value of X becomes the maximum (equal to 1). X decreases with increasing values of R and appreciable reduction in shock loss occurs with a value of $R = 1.5$ for which $X = 0.11$, but little practical advantage accrues from the value of R exceeding 2, i.e. the value of X decreasing below 0.06.

For square bends in rectangular airways,

$$X = \frac{0.6}{R\sqrt{a}} (2i/\pi)^2 \tag{4.57}$$

which reduces to

$$X = \frac{0.6}{R\sqrt{a}} \tag{4.58}$$

for right-angle bends and to

$$X = \frac{0.6}{R} \tag{4.59}$$

for right-angle bends in airways of square of circular cross-section.

Here also, the minimum value of R (for a square inner corner) is equal to 0.5 for which $X = 1.2$. This is the usual case with bends in mine airways. For a crowded bend, the value of X is obtained by arbitrarily increasing the value of X for a similar normal bend to an extent depending on the degree of crowding. Usually X is increased by 40% for 25% crowding on the outer radius of a normal bend. Inner bevel bends may be treated as square bends. Segmental bends have a shock factor slightly higher than that of a similar normal bend (i.e. with the inner and outer curves circumscribing the segments) because of the slight crowding on the outer radius. Common venturi bends can be considered as normal bends

Scanned with CamScanner

with a value of R=0.8 to 0.9 depending on the construction. Blades in bends divide it into sections having different values of R and a and the average shock factor for such bends is obtained by weighting the shock factors for different sections by their areas. The average has, however, to be increased slightly in order to account for the edge effect and excess rubbing surface so as to get an accurate estimation of the shock factor. It must be noted here that the vanes in a bend should not extend beyond the curved part in order that they do not unnecessarily increase the rubbing surface and hence the frictional pressure loss. Russian experiments show that 6-guide vanes placed at distances of 0.135D, 0.292D, 0.471D, 0.673D, 0.898D and 1.145D from the inner corner (D=diameter of the duct or the side in case of square duct) in an elbow with slightly rounded corners reduce the resistance of the bend from one-third to one-fourth. Guide vanes of aerofoil section are preferable. They should be equally spaced and be twice as many in number as ordinary vanes.

When bends discharge directly into the atmosphere, the shock loss is larger by about 50 to 80% than the usual shock loss at such bends. A double bend has a lower shock loss than two similar single bends because of the fact that the air after contraction at the first bend does not fully expand until after the second bend. A compound bend incurs nearly the same shock loss as two similar single bends while a reverse bend has a higher pressure loss. Numerous small bends involving deflections of less than 0.5 rad (30°) are often present in drives following the lode in metal mines. The shock loss at individual bends of such sinuous airways is too small to warrant calculation. In such cases an approximate integrated value of X over a length of airway may be taken.

With slightly sinuous airways, i.e. with a large-radius curve, a sharp bend of 0.26 rad (15°) deflection or a wall line close to the centre line every 30m; or, a small-radius curve, a sharp bend of 0.5 rad deflection or a wall line crossing the centre line every 60m, X=0.2 per 30m length. With highly curved airways, i.e. a continuous large-radius curve, a continuous curve with small deflections of 0.18-0.26 rad (10°-15°) every 6 to 9m, bends of 0.35-0.5 rad (20°-30°) deflection every 15-30m or a wall line crossing the centre line every 15m, X=0.5 per 30m. For intermediate conditions, X=0.3 per 30m.

Table 4.5 gives values of X for some types of bends.

Example 4.6

A mine airway, 2.1m wide, 2.4m high and 600m long, contains a normal bend with a deflection of $\pi/3$ rad and a radius of curvature of 3m. The airway passes a quantity of 9.5 $m^3\,s^{-1}$. Calculate the pressure loss in the airway as well as the resistance of the airway. Also, calculate the equivalent length of a straight airway of similar size and surface which will cause the same pressure loss. Assume the value of k to be equal to 0.0098 N $s^2\,m^{-4}$.

Friction pressure loss in the airway $= kSQ^2 / A^3$

$$=0.0098 \times 2(2.1+2.4)\times 600\times(9.5)^2/(2.1\times 2.4)^3=37.3 \text{ Pa.}$$

From equation 4.54, shock factor for the bend

$$=\frac{0.25}{(1.43)^2\sqrt{1.143}}\left(\frac{2\pi}{3\pi}\right)^2=0.0508$$

since radius ratio $R=3/2.1=1.43$ and aspect ratio $a=2.4/2.1=1.143$.

Therefore shock pressure loss due to the bend

$$=0.6\times 0.0508\left(\frac{9.5}{2.1\times 2.4}\right)^2=0.108 \text{ Pa.}$$

Or, total pressure loss=37.3+0.108=37.408 Pa.

$$\text{Resistance of the airway}=\frac{37.408}{(9.5)^2}=0.414 \text{ Ns}^2\text{ m}^{-8}.$$

Equivalent length of straight airway

$$=\frac{\Delta PA^3}{kpQ^2}=\frac{37.408\times(2.1\times 2.4)^3}{0.0098\times 2(2.1+2.4)\times(9.5)^2}$$

$$=601.7 \text{ m.}$$

4.12.5 Shock Factors for Area Changes

Shock losses at area changes depend only on A_c (cross-section of the flow-stream at the vena contractra) and A_e (see Fig. 4.15), but since A_c depends on the values of A_a and A_o, shock losses can be represented by velocity pressures at any of these four areas. The shock factor for *abrupt symmetrical area changes* is given by the following relations

$$X_o=(1/C-N_e)^2 \tag{4.60}$$

$$X_e=\frac{(1/C-N_e)^2}{N^2_e} \tag{4.61}$$

$$X_a=\frac{(1/C-N_e)^2}{N^2_c} \tag{4.62}$$

where X_o, X_e and X_a are shock factors corresponding to velocity pressures at sections with areas A_o, A_e and A_a respectively, $C=A_c/A_o$=coefficient of contraction, $N_e=A_c/A_e$=ratio of expansion and $N_c=A_o/A_a$=ratio of contraction.

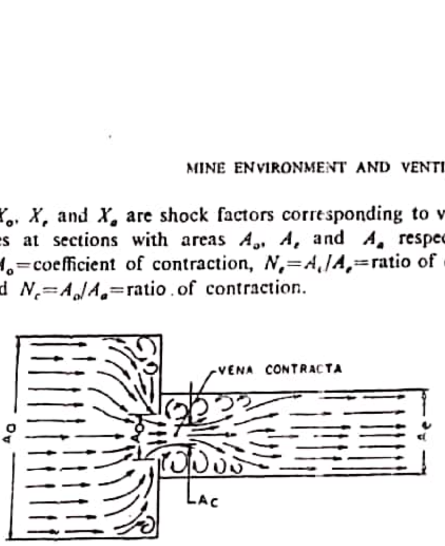

Fig. 4.15 Flow pattern at area change.

For *gradual symmetrical expansions*, the shock factor X' is given by the relation

$$X' = yX \tag{4.63}$$

where y=an empirical constant and X=shock factor for abrupt expansion.

The value of y depends on the included angle of divergence of the sides at the expansion. Test values of y are conflicting, but a practical minimum of 0.25 for an angle of 0.122 rad (7°) is widely accepted. Angles exceeding 0.5 rad (30°) offer no material advantage over abrupt expansion.

The coefficient of contraction C depends on several factors and is given by the relation

$$C = \sqrt{\left(\frac{1}{Z-ZN_c^2+N_c^2}\right)} \tag{4.64}$$

where Z is an empirical factor called the *contraction factor*. Z is affected by the edge conditions at the constriction, the abruptness of contraction and the form of contraction. For free contraction at a sharp edge, e.g. at entry into a pipe, Z averages 3.8. For abrupt symmetrical contraction, Z equals 1.5 for round edges as with round timber, 2.5 for square edges as in the case of sawn timber and 2.7 to 2.8 for absolutely sharp edges as found in plate orifices. The value of Z for gradual and symmetrical contractions such as bell-mouths is as low as 1.05. Fig. 4.16 gives the value of Z for various

included angles of convergence. The value of Z at zero angle is 1 and becomes about 2.5 at π rad.

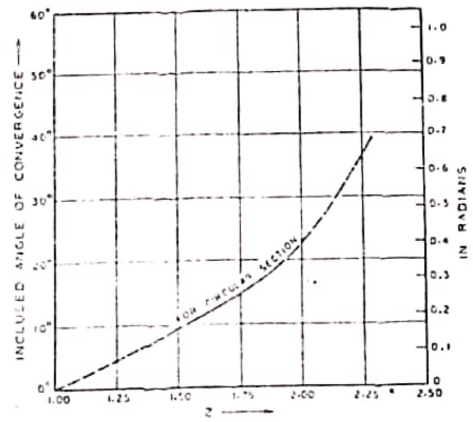

Fig. 4.16 Values of 'Z' for various values of the included angle of convergence.

4.12.6 Unsymmetrical Area Changes

Very few data regarding shock losses at unsymmetrical area changes are available, though shock losses at unsymmetrical contractions in ducts have been found to be more than that at symmetrical ones of similar area ratios. Some cases of unsymmetrical area changes as met with in mines are discussed below.

Shock loss at local enlargements in airways due to non-uniform drivage is negligible. When the length of the enlarged part is appreciable, shock loss occurs at both the ends of the enlarged section due to expansion and contraction respectively. However, this shock loss is compensated by the decrease in friction pressure loss resulting from the reduced velocity of air in the enlarged section. In such cases, it is sufficient to assume a friction loss for the whole length of the airway inclusive of the enlarged portion on the basis of the normal airway cross-section.

Scanned with CamScanner

Door Frames. These offer abrupt contraction and expansion usually on three sides (two sides and the top) in an airway. They can be likened to symmetrical area changes and the shock factor determined assuming a value of $Z=2.5$ for square-edged door frames without the door and $Z=2$ for similar door frames with door held in an open position.

Regulators. These are similar to door frames with square edges and the value of Z for them can be taken as equal to, or, in symmetrically placed regulators, slightly less than 2.5.

4.12.7 Obstructions in the Airway

Regular Obstructions. Props or bars in the midstream of a mine roadway or buntons in shafts pose such obstructions and in such cases, the value of Z is usually doubled, e.g. $Z=5$ for square-edged obstruction. Pressure loss at such obstructions can be more accurately calculated if C_D for the particular form of obstruction is known. Let us consider the case of a bunton in a shaft of a cross-sectional area A. If the projected frontal area of the bunton is A_1, then F, the drag force acting on the bunton is given by the relation

$$F=\Delta P_D A_1 = C_D A_1 P_v = \frac{C_D A_1 v^2 \rho}{2} \quad (4.65)$$

(see equation 4.32)

Or, ΔP_s, the shock pressure loss in the shaft due to the drag force is given by the relation

$$\Delta P_s = \frac{C_D A_1 v^2 \rho}{2A} \quad (4.66)$$

If the buntons are so spaced that the flow around one does not interfere with that around the adjacent ones, then the shock loss at each of them is independent of the other, but when the spacing is such that each bunton lies in the turbulent wake of the preceeding one, the value of shock loss for a bunton is less than as calculated from equation 4.66 and is given by the relation

$$\Delta P_s = \frac{C_D A_1 v^2 \rho \psi}{2A} \quad (4.67)$$

where ψ is called the shielding factor or interference factor. ψ is mainly a function of the spacing ratio s/W,

where s = spacing of buntons and

W = width of bunton.

However, other factors such as the shape of the buntons and their arrangement in the shaft, shape of the shaft, velocity profile in the shaft and Reynolds number of flow also affect ψ to some extent. Bromilow[76] has found the following empirical relation for ψ to hold good for a variety of shafts with a spacing ratio of 10 to 40, commonly met with in mines

$$\psi = 0.0035\, s/W + 0.44 \quad (4.68)$$

Mine Cars. A single car in a mine airway can be treated as an ordinary obstruction, but a train of mine cars causes the following pressure losses :

(a) shock loss due to abrupt contraction at the front of the train,

(b) shock loss due to abrupt expansion at the end of the train and

(c) friction loss due to the rubbing surface of the train.

In such a case, the value of Z at the contraction is taken equal to 5 for square edges and 3 for round edges. The shock loss at the expansion, however, is taken equal to that for a similar abrupt symmetrical expansion. The friction loss for the intermediate section can be more accurately calculated, but for ordinary purposes, where an accuracy of 5% is sufficient, it can be taken as $(2-N)/N^3$ times the normal friction loss, N being the ratio of the constricted area to the normal area of cross-section. Weeks[80] gives the following values of shock factor for mine cars of a projected area A_1 in airways of cross-sectional area A. For single cars $X=1.5$ for $A_1/A=0.15$ to 0.2 and $=3$ for $A_1/A=0.4$. For a train of five cars with $A_1/A=0.15$ to 0.2, $X=7$.

Conveyors in airways can be allowed for by reducing the cross-sectional area of the airway by about 0.9 m². *Cages* and *skips in shafts* can be treated as ordinary obstructions when stationary, but when they are in motion, the shock loss across them should take into account the relative velocity of air.

Irregular Intermittent Obstructions. Shock losses at irregular intermittent obstructions of a minor nature are difficult to calculate individually. They are more conveniently determined as the total shock loss over a certain length of airway. The following values of X can be assumed in practice: (a) For slight obstructions such as a trolley box, a water box, a large flanged pipe, occasional small roof falls, occasional small cross bars, hangers, props etc., $X=0.1$ for 30m length. (b) For obstructions of a moderate degree such

Scanned with CamScanner

as large ventilation ducts, occasional large cross bars or heavy hangers, frequent small roof falls, occasional constrictions etc., $X=0.3$ for 30m. (c) For a high degree of obstructions such as a combination of obstructions given above, large falls, occasional storage piles of timber or pipes, closely spaced cross bars, props or constrictions etc., $X=1.0$ for 30m.

4.12.8 Supported Airways

Regularly supported airways provide obstructions to the air-flow at the airway boundary and lead to drag loss, the magnitude of which depends on the projected surface area of the sets, average approach air velocity, drag coefficient of the sets (mainly dependent on the cross-sectional shape of the members) and the shielding effect due to aerodynamic interference between sets. The drag loss in supported airways is closely integrated with the friction pressure loss in the bare airway and it is customary to express the total pressure loss in terms of a combined resistance coefficient.

Xenofontowa *et al*[77] developed the following empirical relations for f from investigations in supported mine roadways.

For airways supported with 3-piece timber sets and steel arches

$$f = \frac{0.006\,54}{\left(0.205+0.12\log\dfrac{Ee}{sm_1\,m_2}\right)^2} \qquad (4.69)$$

for $s/e < 5$

$$f = \frac{0.006\,54}{\left(0.175+0.06\log\dfrac{Es}{5em'_1\,m_2}\right)^2} \qquad (4.70)$$

for $s/e > 5$

where s = spacing of timber or steel sets (centre to centre),
e = size of support (projecting into the airway),
f = coefficient of resistance,
E = $D/2e$,
D = equivalent diameter of airway $=4A/p$,
A = net cross-sectional area of airway (inside support),
p = perimeter of airway,
p' = perimeter of inside edge of support,

$$m_1 = 1 + \frac{0.12\,e}{s} - \sqrt{\left(\frac{0.24\,e}{s}\right)}$$

$$m'_1 = 1 + \frac{0.6\,e}{s} - \sqrt{\left(\frac{1.2\,e}{s}\right)}$$

and $m_2 = p'/p$.

For airways supported with bars only

$$f = \frac{0.006\,54}{\left(0.11 + 0.065\log\dfrac{Es}{e}\right)^2} \qquad (4.71)$$

These relations, however, do not take into account variations in the surface roughness of the bare airways and cross-sectional shape of the supports and hence are not universally applicable. Misra[78,79] gives the following theoretical relations for supported airways which are more universally applicable

$$f = \frac{C_D D\delta^2\left(1+\dfrac{A'}{A_c}\right)^2 A_1}{4\,A'\,s} + \frac{f_f\left(\dfrac{s-l}{s}\right)p_s + f_f\,p_e}{p} \qquad (4.72)$$

for $s \geqslant l$

$$f = \frac{\psi\, C_D\, D\delta^2\left(1+\dfrac{A'}{A_c}\right)^2 A_1}{4\,A'\,s} + f_f\frac{p_e}{p} \qquad (4.73)$$

for $s<l$

where C_D = experimental drag coefficient of the supporting member = 1.18 for square timber and 0.96 for round timber,
δ = ratio of the approach velocity over the sets to the average velocity in the bare airway,
A' = cross-sectional area of bare airway,
A_c = cross-sectional area of the air-stream at the vena contracta inside the set $=CA'$.
C = coefficient of contraction,
A_1 = projected frontal area of the sets,
l = length of aerodynamic influence of sets $\simeq 42\,e$,
p_s = setted portion of the perimeter of bare airway,
p_e = unsetted portion of the perimeter of bare airway,
and ψ = shielding factor.

Scanned with CamScanner

The experimentally determined value of ψ for different spacings (s/l) is given in Fig. 4.17.

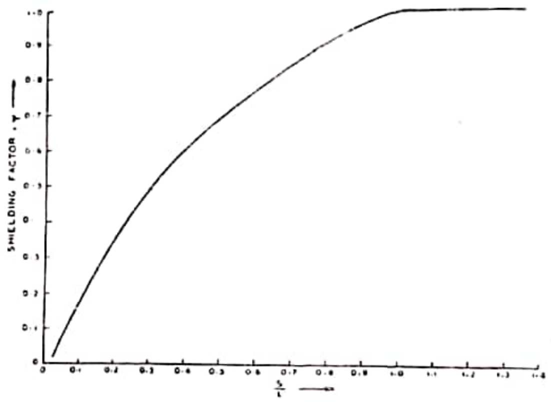

Fig. 4.17 Experimental values of shielding factor for different spacings of sets.

Example 4.7

An unlined roadway in hard rock, 2.8 × 3m in cross-section and 600m long has two right-angle square bends with square inner corners. It has also a door frame (without any door) of 1.5×2m size installed in a stopping. Calculate the pressure required to circulate 10 m³ s⁻¹ of air through the roadway.

Assuming coefficient of friction $k=0.0098$ N s² m⁻⁴ for unlined airway in hard rock, frictional pressure loss

$$\Delta P_f = \frac{0.0098\times 2(2.8+3)\ 600\times 10^2}{(2.8\times 3)^3} = 11.51 \text{ Pa}$$

Shock factor for each bend (from equation 4.58)

$$X_b = \frac{0.6}{R\sqrt{a}} = \frac{0.6}{0.5\sqrt{1.07}} = 1.16$$

since for a square inner corner, radius of bend $r=\frac{2.8}{2}=1.4$ m ;

or, $R=1.4/2.8=0.5$ and $a=3.0/2.8=1.07$.

Shock factor for the door frame (with respect to air velocity in the main airway)

$$X_a = \frac{\left(\frac{1}{C}-N_e\right)^2}{N_c^2} \qquad \text{(see equation 4.62)}$$

$$\text{where } C = \sqrt{\frac{1}{Z-ZN_c^2+N_c^2}}$$

$$= \sqrt{\frac{1}{2.5-2.5(0.357)^2+(0.357)^2}} = 0.658$$

taking the door frame to be square-edged for which $Z=2.5$,

$$N_e=N_c = \frac{1.5\times 2}{2.8\times 3} = 0.357.$$

$$\therefore \quad X_a = \frac{\left(\frac{1}{0.658}-0.357\right)^2}{(0.357)^2} = 10.61.$$

Total shock factor $X=10.61+1.16\times 2=12.93$.

$$\text{Shock pressure loss } P_s = 12.93\times\frac{1.2}{2}\times\frac{10^2}{(2.8\times 3)^2}$$

$= 10.99$ Pa

taking density of air $= 1.2$ kg m⁻³.

$\therefore$ Total pressure loss $= 11.51+10.99$

$= 22.5$ Pa.

Example 4.8

A vertical shaft 6m in diameter is connected at its bottom to a level plat 4.5×2.5m in cross-section. The flow in the shaft being 180 m³ s⁻¹, calculate the shock factor for the connection of the shaft with the plat with respect to the plat air-velocity, if the static-pressure difference between the shaft and the plat is measured at 310 Pa. Neglect friction loss.

$$\text{Velocity of air in the shaft} = \frac{180}{\frac{\pi}{4}(6)^2} = 6.36 \text{ m s}^{-1}.$$

Shaft velocity pressure $=0.6\,(6.36)^2=24.27$ Pa taking $\rho=1.2$ kg m⁻³.

Scanned with CamScanner

Velocity of air in the plat $= \dfrac{180}{4.5\times 2.5} = 16.0$ m s^{-1}.

Plat velocity pressure $0.6\,(16.0)^2 = 153.6$ Pa.

Pressure loss at the junction of the plat with the shaft

$=$ measured static pressure difference + shaft velocity pressure $-$ plat velocity pressure

$= 310+24.27-153.6 = 180.67$ Pa.

$$\text{Shock factor} = \frac{180.67}{\text{plat velocity pressure}}$$

$$= \frac{180.67}{153.6} = 1.176.$$

Example 4.9

Calculate the pressure loss across a bunton of I girder, 200×150 mm in size installed with its web parallel to the axis in the middle of a 6m diameter shaft, if the air velocity in the shaft is 6 m s^{-1}. What will be the pressure loss in the shaft due to such buntons placed regularly at intervals of 3m, if the shaft is 300m deep ?

From equation 4.66 pressure loss across the bunton

$$= \frac{C_D A_1 v^2 \rho}{2A} = 2.75\times 0.9\times (6)^2\times 1.2/(2\times 28.26)$$

$$= 1.89 \text{ Pa.}$$

since $C_D = 2.75$ (from Table 4.2)

$A_1 = 0.15\times 6 = 0.9$ m^2.

$A = 3.14\times (6)^2/4 = 28.26$ m^2

and ρ is assumed to be equal to 1.2 kg m^{-3}.

The actual pressure loss across a single bunton taking into account the interference of other buntons is given by the equation

$$\Delta P_s = \frac{C_D A_1 v^2 \rho \psi}{2A}$$

From equation 4.68

$\psi = 0.0035\, s/W + 0.44 = (0.0035\times 3/0.15) + 0.44 = 0.51$

$\Delta P_s = 1.89\times 0.51 = 0.964$ Pa.

So, total pressure loss in the shaft due to the buntons

$= 0.964\times 300/3 = 96.4$ Pa.

4.12.9 Shock Losses at Splits and Junctions

These shock losses are due to bending as well as area change.

Observation by various workers shows that there are greater eddies formed at splits than at junctions and hence there is a larger pressure drop at splits compared to junctions. In fact a gain in pressure may be observed under certain conditions due to ejector action at junctions.

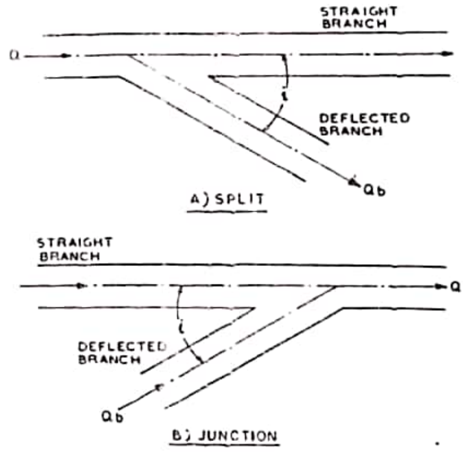

Fig. 4.18 Split and junction.

Hartman [81] gives the following relations for the shock factor for splits and junctions (Fig. 4.18) :

For splits

$$X = 0.5\left(\frac{Q}{Q_b} - 1\right)^2 \qquad (4.74)$$

for the straight branch

$$\text{and } X = \left(\frac{Q}{2\,Q_b}\right)^2 + \left(\frac{Q}{Q_b} - 1\right)^2 + X_b \qquad (4.75)$$

for the deflected branch.

For junctions

$$X=3.3\left(\tan\frac{i}{2}-0.67\right)\left[\frac{Q}{Q_b}\left(\frac{1}{C}-1\right)\right]^2 \qquad (4.76)$$

for the straight branch

$$\text{and } X=X_b-0.5\left(\frac{Q}{Q_b}-1\right)^{2.5} \qquad (4.77)$$

for the deflected branch,

where Q = total air-flow,

Q_b = air-flow in the concerned branch,

X_b = bend shock factor as determined from equation 4.57,

i = angle of deflection of the bend

and C = coefficient of contraction.

Both X and X_b relate to velocity pressure in the branch airway. Though equations 4.74 to 4.77 have been developed from model studies for equal cross-section of main and branch airways, the author claims that they can be used with varying cross-section of airways without much error.

Table 4.5 gives experimental values of X for some bends, splits and junctions as determined by Xenofontowa *et al*[77].

Junction of Fan-drift with Shaft. Air-flow from shafts to fan-drifts undergoes bending and often area change. However, the bend loss is more here because of eddies created in the dead end formed by the closed upper part of the shaft. Most shafts, however, are closed with a surface air-lock which admits a certain amount of leakage so that the leakage air-current joins the main air-stream at the junction of the fan-drift with the shaft. Losses at such junctions can be substantial in view of the large velocity of flow in the shaft which calls for their accurate estimation.

Skochinsky and Komarov[3] give the following values (Table 4.6) of X for right-angled junctions of shafts with fan-drifts with respect to fan-drift velocity for various fan-drift—shaft area ratios :

Table 4.5 : Experimental Values of 'X' for Bends, Splits and Junctions

NATURE OF BEND, SPLIT OR JUNCTION	SHOCK FACTOR X	NATURE OF BEND, SPLIT OR JUNCTION	SHOCK FACTOR X
RIGHT-ANGLE SQUARE BEND	1.40	RIGHT-ANGLE SPLIT	3.6
RIGHT-ANGLE BEND WITH ROUNDED INNER CORNER $R_i = W/3$ / $R_i = 2W/3$	0.75/ 0.52	RIGHT-ANGLE SPLIT	2.5
RIGHT-ANGLE BEND WITH BEVELLED INNER CORNER $\pi/4$ rod.	0.66	RIGHT-ANGLE SPLIT WITH BEVELLED CORNERS	1.5
RIGHT-ANGLE NORMAL BEND $R_i = W/3$, $R_o = 3W/2$, $R_i = 2W/3$, $R_o = 5W/3$	0.60 0.30	SPLIT AT 60° ($\pi/3$ rod)	1.5
RIGHT-ANGLE SQUARE BEND WITH AEROFOIL VANES	0.20	SPLIT AT 60° ($\pi/3$ rod)	1.0
RIGHT-ANGLE SQUARE BEND WITH ORDINARY VANES	0.35 TO 0.37	RIGHT-ANGLE JUNCTION	2.0
DOUBLE RIGHT-ANGLE SQUARE BEND, $l < 8W$	2.10	RIGHT-ANGLE JUNCTION	2.6
REVERSE RIGHT-ANGLE SQUARE BEND	2.40	RIGHT-ANGLE JUNCTION WITH BEVELLED CORNERS	1.0
COMPOUND RIGHT-ANGLE SQUARE BEND	2.80	JUNCTION AT 60° ($\pi/3$ rod) (WITH RESPECT TO V_1 OR V_3)	1.0
DOUBLE SQUARE BEND WITH 45° ANGLE OF DEFLECTION $l = 2W$, $l = 4$-$6W$	0.7, 1.1	JUNCTION AT 60° ($\pi/3$ rod)	1.5
ENTRY INTO CIRCULAR PIPE & RECTANGULAR PIPE	0.9 & 1.25	FOR CIRCULAR AND FOR RECTANGULAR	0.35 0.7
DEPENDING ON INCLUDED ANGLE AND LENGTH	0.05 TO 0.25	DEPENDING ON RADIUS	0.03 TO 0.13

(SHOCK FACTOR X WITH RESPECT TO V_2)

Table 4.6 : Shock Factors for Shaft-fan-drift Junctions

Fan-drift : shaft area ratio	X
0.25	0.82
0.30	0.85
0.40	0.90
0.50	0.96
0.60	1.03

Scanned with CamScanner

Recent work by Misra[134] on junctions of shafts and fan-drifts of equal rectangular cross-section shows that the shock factor rises from as low as 0.28 for a deflection angle $i=0.524$ rad (30°) to as high as 1.28 for $i=1.28$ rad (90°) ; the variation being non-uniform. The shock factor further rises with leakage at the shaft collar as evident from Fig. 4.19.

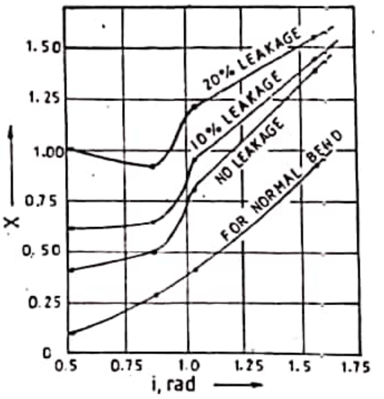

Fig. 4.19 Shock factor for shaft-fan-drift junction.

4.13 RESISTANCE OF AIRWAYS

We have seen that for most mine airways,

$$\Delta P_f = kS\, Q^2/A^3 \quad \text{(see equation 4.29)}$$

For a given airway or a ventilation system such as a mine at any particular stage of working k, S and A can be taken as constant and hence equation 4.29 can be written as

$$\Delta P_f = R_f Q^2 \tag{4.78}$$

where R_f is called the frictional *resistance* of the airway or the system. Combining equations 4.29 and 4.78 we have

$$R_f = \frac{kS}{A^3} = \frac{kpL}{A^3} \tag{4.79}$$

Similarly equation 4.35 can be written as

$$\Delta P_s' = 0.6 X v^2 = 0.6 X \frac{Q^2}{A^2} \tag{4.80}$$

Since for a given airway, the shock factor X and cross-sectional area A are constant

$$\Delta P_s = R_s\, Q^2 \tag{4.81}$$

where R_s = shock resistance

From equations 4.80 and 4.81

$$R_s = \frac{0.6\, X}{A^2} \tag{4.82}$$

For all practical purposes, the total resistance of the airway

$$R = R_f + R_s \tag{4.83}$$

But this is not strictly correct, since the surface roughness of an airway affects the velocity profile and hence the shock resistance. Though for small values of k (smooth airways) equation 4.83 gives fairly accurate results, for very rough airways scaled models may be used for accurate determination of the total resistance.

The unit of R in the S.I. system is N s^2 m^{-8}. The equivalence of some other prevalent units are 1 *Weisbach* (*Wb*)=9.81 N s^2 m^{-8}, 1*Murg*=0.00 981 N s^2 m^{-8} and 1 *Atkinson* (old British system)= 0.06 N s^2 m^{-8}. R, like k, is expressed at a certain air density and the following relation has to be used to determine R at any other air density

$$R = R_o\ \rho/\rho_o \tag{4.84}$$

where ρ is the observed air density, ρ_o=air density at which the resistance R_o was determined.

4.13.1 Determination of the Resistance of Airways

Resistance of airways can be estimated from a knowledge of k and X with the help of equations 4.79 and 4.82. It is, however, better to determine the resistance of typical airways from field measurements of pressure drop and quantity of flow

$$R = \frac{\Delta P}{Q^2} \tag{4.85}$$

Resistance of a group of airways in simple series or parallel connection can be easily calculated, if the resistance of each individual airway is known.

Airways in Series. When the airways are joined in series, the total pressure drop across all of them is the sum of pressure drops across each of them while the same quantity Q flows through each of them.

Scanned with CamScanner

$$\triangle P = \triangle P_1 + \triangle P_2 + \triangle P_3, \ldots\ldots + \triangle P_n \qquad (4.86)$$

Dividing both sides by Q^2, we have

$$\frac{\triangle P}{Q^2} = \frac{\triangle P_1}{Q^2} + \frac{\triangle P_2}{Q^2} + \frac{\triangle P_3}{Q^2}, \ldots\ldots + \frac{\triangle P_n}{Q^2}$$

Or, $R = R_1 + R_2 + R_3, \ldots\ldots, + R_n$ (4.87)

where R=combined resistance and R_1, R_2, R_3,........., R_n are the resistances of the individual airways.

Airways in Parallel. On the other hand, when the airways are joined in parallel, the pressure drop across all of them is the same, say, $\triangle P$ while quantities get distributed amongst them depending on their resistances. Using the same symbols as for airways in series,

$$\triangle P = R_1 Q_1^2 = R_2 Q_2^2, \ldots\ldots = R_n Q_n^2$$
$$= RQ^2 \qquad (4.88)$$

Again Q, the total quantity flowing through all the airways is given by

$$Q = Q_1 + Q_2 + Q_3, \ldots\ldots, Q_n \qquad (4.89)$$

Combining equations 4.88 and 4.89, we have,

$$\sqrt{\frac{\triangle P}{R}} = \sqrt{\frac{\triangle P}{R_1}} + \sqrt{\frac{\triangle P}{R_2}} + \sqrt{\frac{\triangle P}{R_3}} \ldots\ldots + \sqrt{\frac{\triangle P}{R_n}},$$

$$\text{or, } \frac{1}{\sqrt{R}} = \frac{1}{\sqrt{R_1}} + \frac{1}{\sqrt{R_2}} + \frac{1}{\sqrt{R_3}} \ldots\ldots \frac{1}{\sqrt{R_n}} \qquad (4.90)$$

4.13.2 Resistance of Leaky Airways

In airways where substantial leakage of air takes place through the walls (this becomes particularly important in case of airways in broken ground or bordering packs) or where several parallel leakage paths are offered by stoppings between parallel intakes and returns admitting sufficient leakage, the resistance of the airway is not governed by the simple relation $P = RQ^2$, even though the flow in the airway is turbulent in nature.

Theoretical analysis of leakage through such airways is given by Peascod and Keane,[82] who have expressed the leakage as a function of the resistance of the airway and that of the leakage path. However, it is difficult to estimate the latter without actually measuring the leakage. Fairly accurate estimation of the pressure drop ΔP in a leaky airway can be obtained from the relation

$$\Delta P = R\, Q_O Q_E \qquad (4.91)$$

where R = resistance of the airway,
Q_O = quantity measured at the beginning of the airway and
Q_E = quantity measured at the end of the airway so that leakage
$= Q_O - Q_E$.

Equation 4.91 can be expressed in the form $\triangle P = RQ_m^2$ (4.92)

where Q_m is the geometric mean of the quantities Q_O and Q_E

$$= \sqrt{Q_O\, Q_E}$$

Leakage in Ducts. Unlike leakage through strata, packs or a set of stoppings, leakage through the walls of a duct is mainly through leaky joints in new duct systems and through pitted walls in old corroded ducts. In either case the leakage can be likened to discharge through an orifice obeying the square law ($\triangle P = RQ^2$) of pressure drop.

Based on this principle Misra[83] developed the following relations for leakage in terms of the resistances of the duct and the leakage path

$$Q_O^3 - \frac{2}{R'_1 \sqrt{R'_2}} P_O^{3/2} = Q_E^3 \qquad (4.93)$$

$$\text{and } \left(\frac{1}{9} + \frac{1}{27}\cdots\right) - \log\left(\frac{Q_E}{Q_O}\right) - \left\{\frac{1}{9}\left(\frac{Q_E}{Q_O}\right)^3 + \frac{1}{27}\left(\frac{Q_E}{Q_O}\right)^6 \ldots\ldots\right\}$$
$$= \left(\frac{R_1}{2R_2}\right)^{1/3} \qquad (4.94)$$

where R_1 = resistance of the duct $= LR'_1$,
R_2 = resistance of the leakage path $= R'_2/L^2$,
R'_1 = resistance of the duct per unit length,
R'_2 = resistance of the leakage path per unit length of duct,
P_O = pressure developed by the fan connected to the duct
and L = length of duct.

The solution of equation 4.94 is plotted in Fig. 4.20. R_1 can be estimated for a smooth duct of any diameter by combining equations 4.20 and 4.78 as follows

$$R_1 = \frac{fLP}{2DA^2} \qquad (4.95)$$

Scanned with CamScanner

f in the above equation can be obtained from the Blasius (equation 4.24) or Karman-Prandtl (equation 4.25) equations depending on the value of Re. More approximately however, R_1 can be computed from equation 4.79 taking a value of k=0.0029 N s^2 m^{-4}. Knowing R_1, Q_O and Q_E, R_2 for any duct can now be obtained from equation 4.94.

Pressure drop in a leaky duct can then be obtained from equation 4.91 by substituting R_1 for R or from equation 4.93 but the latter gives an overestimated value.

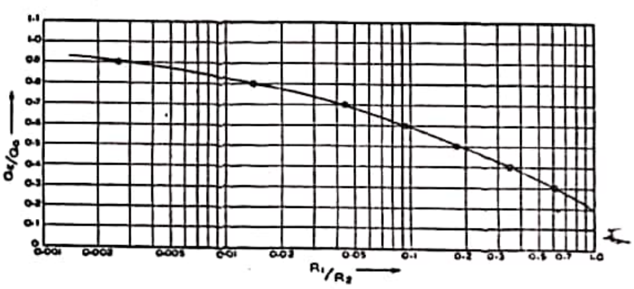

Fig. 4.20 R_1/R_2 vs Q_E/Q_O.

The National Coal Board (N.C.B.), U.K. expresses leakage in terms of a *leakage coefficient* which is defined as the quantity in cft/min leaking from a 100ft length of the duct with an applied pressure of 1 in w.g. The leakage coefficient so defined is related to R'_2 by the equation

$$R'_2 = \frac{25.4\times9.81\ (100\times0.3048)^2\times3600}{(0.02832\ Q_L)^2}$$

$$= \frac{1.04\times10^{12}}{Q_L^2} \qquad (4.96)$$

where Q_L= leakage coefficient.

N.C.B. considers it to be a good practice to have a leakage coefficient of 30 which corresponds to a value of R'_2=1.16×10^9 N s^2 m^{-8} per metre length of duct. The tolerable limit of leakage coefficient is 100 (R'_2=0.104×10^9 N s^2 m^{-8}).

It has been shown earlier that for turbulent flow in mine ducts, P is proportional to $Q^{1.9}$ and the leakage through duct walls has

been estimated by Holdsworth *et al*[77] to obey the law $P \propto Q^n$ where n varies between 1.4 and 2, but the assumption of the square law for both the cases in developing equations 4.93 and 4.94 does not introduce any appreciable error in the estimation of Q_E/Q_O, though it does overestimate the value of P_O.

Example 4.10

A district is supplied by a main intake and a main return airway running side by side at a distance of 30m and interconnected at 50m intervals. The stoppings in the interconnections allow some leakage so that the quantities measured at the inbye and outbye ends of the main intake are 5 and 7.5 m^3 s^{-1} respectively. Calculate the pressure across the main intake and return at the outbye end if the resistances of the main intake, main return and the working district are 7.5, 7.0 and 0.5 N s^2 m^{-8} respectively.

Pressure drop in the main intake
$= 7.5\times5\times7.5 = 281.25$ Pa.
Pressure drop in the main return
$= 7.0\times5\times7.5 = 262.5$ Pa.
Pressure drop in the workings
$= 0.5\times5^2 = 12.5$ Pa.
∴ Total pressure drop
$= 281.25+262.5+12.5$
$= 556.25$ Pa.

Example 4.11

A 3m long duct of 450mm diameter was closed at both ends and pressurized by compressed-air to a gauge pressure of 500 Pa. The pressure fell to 250 Pa after 10 s. Calculate the rate of leakage and the resistance of the leakage path assuming a square law for leakage. The barometric pressure is 101 kPa.

Volume of the duct $= \frac{\pi}{4}(0.45)^2\times3 = 0.477$ m^3.

Volume of free air in the duct at a gauge pressure of 500 Pa $= \frac{0.477\times101.5}{101}$
$= 0.4794$ m^3.

Volume of free air in the duct at a pressure of

$$250 \text{ Pa} = \frac{0.477 \times 101.25}{101}$$

$$= 0.4782 \text{ m}^3.$$

$\therefore$ Volume of free air leaked $= 0.4794 - 0.4782 = 0.0012 \text{ m}^3$.

$$\text{Rate of leakage} = \frac{0.0012}{10} = 0.000\ 12 \text{ m}^3 \text{ s}^{-1}.$$

Taking the leakage to occur at the squared mean root pressure of $\{(\sqrt{250} + \sqrt{500})/2\}^2 = 364.2$ Pa,

$$\text{resistance of leakage path} = \frac{364.2}{(0.000\ 12)^2}$$

$$= 2.53 \times 10^{10} \text{ N s}^2 \text{ m}^{-8}.$$

4.14 POWER OF VENTILATION

Power of ventilation or air power (AP) is the rate at which work is done to maintain the air-flow through a system, and is given by the relation

$$AP = -M \int V dP \quad (4.97)$$

where M = mass flow rate of air through the system.

For incompressible flow, equation 4.97 can be written as

$$AP = MV(P_1 - P_2) = Q(P_1 - P_2) \quad (4.98)$$

Neglecting change in potential and kinetic energy of air, equation 4.98 reduces to

$$AP = \Delta PQ \text{ W} = \Delta PQ \times 10^{-3} \text{ kW (see equation 4.43)} \quad (4.99)$$

where ΔP is in pascals and Q in $\text{m}^3 \text{ s}^{-1}$.

Since $\Delta P = RQ^2$

$$AP = RQ^3 \times 10^{-3} \text{ kW} \quad (4.100)$$

The required power output of the prime mover driving a fan causing the air-flow can be found by dividing the air power by the efficiency of the fan and gear.

4.15 EQUIVALENT ORIFICE

Murgue expressed the resistance of a mine or an airway in terms of the area of an equivalent orifice. Here, the resistance of a mine is expressed as the area of the orifice in a thin plate which offers the same resistance to air-flow as the mine.

Let Q = quantity of air flowing through the mine in $\text{m}^3 \text{ s}^{-1}$,

A = area of the orifice in m^2,

A_c = area of flow at the vena contracta in $\text{m}^2 = 0.6A$ ordinarily,

v = velocity of flow at the vena contracta

and h = head of air causing flow in m.

We know that for flow through an orifice,

$$v = \sqrt{(2gh)}, \quad (4.101)$$

or, $Q/A_c = \sqrt{(2gh)}$

Therefore, $A = Q/(0.6\ \sqrt{2gh}) = Q\sqrt{\rho g}/(0.6\ \sqrt{2gP})$

$$= Q\ \sqrt{\rho}/(0.6\ \sqrt{2P}) \quad (4.102)$$

where P = pressure causing flow in Pa.

Assuming the standard value of $\rho = 1.2 \text{ kg m}^{-3}$, equation 4.102 reduces to

$$A = 1.29\ Q/\sqrt{P} \quad (4.103)$$

or, expressing in terms of resistance,

$$A = 1.29/\sqrt{R} \quad (4.104)$$

where R = resistance of the mine in $\text{N s}^2 \text{ m}^{-8}$.

Equations 4.103 and 4.104 are generally used for calculating the size of regulators for control of flow in mine airways. However, these equations are valid for standard air density. In Indian mines where the temperature and humidity of the air are generally high, the value of ρ is less than 1.2 kg m^{-3}. Besides, the coefficient of contraction in a regulator depends on various factors such as Reynolds number of flow, shape and edge conditions of the opening as well as the opening-airway area ratio. A more practical value for the coefficient of contraction in a regulator is 0.63. Hence for the purpose of calculating regulator size, equations 4.103 and 4.104 can be modified as

$$A = 1.2\ Q/\sqrt{P} = 1.2/\sqrt{R} \quad (4.105)$$

4.16 CHARACTERISTIC OF AN AIRWAY OR MINE

The resistance of an airway, a system of airways or a mine can be expressed in graphical form by plotting the pressure drop ΔP against the rate of flow Q (see Fig. 4.21).

Since for most airways or systems of airways,

$\Delta P = RQ^2$ where R is the resistance of the airway or the system, the characterstic is usually a square parabola. However, the curve is steeper for high values of R and flatter for low values of R.

Scanned with CamScanner

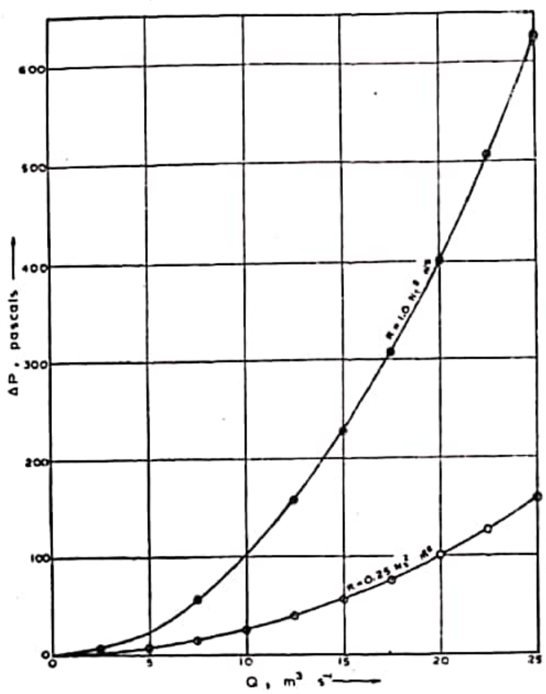

Fig. 4.21 Characteristics of airways.

Example 4.12

A fan delivers 4 $m^3 s^{-1}$ of air through a 500m long and 500mm diameter leakproof duct ventilating a heading. Taking the Darcy-Weisbach resistance coefficient f of the duct to be 0.02, calculate the size of the orifice which may be used with the duct to deliver the same quantity of air when its length is only 20m.

Cross-sectional area of the duct

$$= \frac{\pi}{4}(0.5)^2 = 0.196 \text{ m}^2.$$

Taking the fan pressure to remain constant, the same quantity will be delivered by the shorter duct when its resistance alongwith that of the orifice equals the resistance of the longer duct.

Resistance of a 500m duct

$$= \frac{fL\rho}{2DA^2} = \frac{0.02 \times 500 \times 1.2}{2 \times 0.5\,(0.196)^2}$$

$$= 312.37 \text{ N s}^2 \text{ m}^{-8}$$

taking density of air = 1.2 kg m^{-3}.

Resistance of a 20m duct

$$= 312.37 \times \frac{20}{500} = 12.49 \text{ N s}^2 \text{ m}^{-8}.$$

$\therefore$ Resistance of the orifice

$$= 312.37 - 12.49 = 299.88 \text{ N s}^2 \text{ m}^{-8}.$$

$$\text{area of orifice} = \frac{1.29}{\sqrt{299.88}} = 0.07 \text{ m}^2.$$

4.17 ECONOMIC DESIGN OF MINE AIRWAYS

Airways should always be designed for maximum safety and economy. For maximum economy, the cost of ventilation should be the minimum. The cost of ventilation consists of (a) the power cost and (b) the interest and amortization charges on the capital invested in the airway.

From equation 4.100, the air power is proportional to the resistance of the airway for a given quantity, or, in other words, the power cost of ventilation is a function of the resistance of the airway for a given quantity. By reducing the resistance of an airway one can reduce the power cost of ventilation, but this invariably involves an extra capital expenditure by way of increased cross-section of airway or lining. For maximum economy, a balance must be struck between the saving in the power cost and the extra capital expenditure incurred.

The various factors affecting resistance and hence the power cost of ventilation are as follows.

4.17.1 Size of the Airway

Examining equation 4.79 we see that

$R_f \propto 1/A^{5/2}$, since $p \propto \sqrt{A}$;

Scanned with CamScanner

or, the resistance and hence the power cost varies inversely as the five-halves power of the cross-sectional area of the airway.

4.17.2 Surface Character of Airway

For constant values of L, p and A, the resistance varies directly as k (see equation 4.79), the coefficient of friction which primarily depends on the surface character of the airway. The value of k for unlined airways is approximately five times that of smooth-lined ones. Hence, for the same size, a lined airway would incur only one-fifth of the power cost of an unlined one, though some extra capital has to be invested in the lining.

4.17.3 Shape of Airway

The resistance and hence the power cost varies directly as the perimeter of the airway for constant values of A and k. For any given area, the perimeter is the least for a circular shape and hence the circular shape is the most economic one for an airway from the point of view of power cost. However, for the usual shape of mine airways, the variation of power cost due to varying shapes is negligible. This would be evident from Table 4.7 which gives the shape factors for airways of various shapes.

Table 4.7 : Shape Factor for Various Shapes of Airways

Shape of airway	Shape factor ($p/\sqrt{A}$)
Circle	3.55
Regular hexagon	3.66
Arched section with a side ratio 1 : 1 and the arch having a radius of curvature = five times the side	3.87
Square	4.00
Rectangle with a side ratio of 1 : 1.25	4.03
" " " " 1 : 1.5	4.08
" " " " 1 : 2.0	4.26
" " " " 1 : 3.0	4.62

The factors discussed above mainly affect the frictional resistance, though the size of airways also affects shock resistance to

some extent, as shock resistance varies inversely as the square of the area of cross-section (see equation 4.82). The shape of the airways affects the shock resistance too in that it affects the aspect ratio at bends and the degree of symmetry at area changes. However, shock resistance as compared to frictional resistance becomes appreciable in case of sinuous airways with obstructions. Thus, for economizing on power cost of ventilation, airways should be so designed as to avoid bends, obstructions and area changes as far as practicable. Where unavoidable, bends should be of large radius and with small angles of deflection. Streamlining of area changes or obstructions in airways helps in reducing power cost of ventilation.

Covering of buntons with fairings reduces shock loss in shafts considerably and deserves serious consideration particularly in lined shafts where shock loss due to buntons is the major pressure loss. Fairings of 1.6m thick galvanized steel sheets on I-girder buntons as shown in Fig. 4.22 were installed at Kingshill No 3 shaft, U.K. Though they cost about £3-35p. (Rs. 54.00 approximately) per metre length, the capital invested was estimated to be recovered

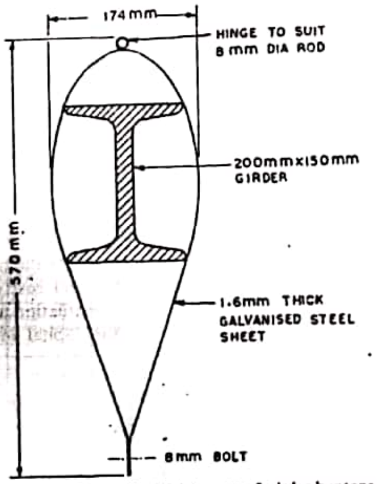

Fig. 4.22 Streamlined fairing over I-girder buntons.

from the saving in power cost within a period of 16 months. A new design of bunton fabricated out of steel sheet bent into a shape with a round top and bottom and vertical sides and with a single welding at the bottom has been used in some mines of South Africa for reducing resistance to air-flow. These buntons offer 60% less resistance to air-flow ($C_D = 1.1$) than corresponding I-girders ($C_D = 2.75$) and are only one-third in weight, though twice as stiff. Fig. 4.23 shows a design of a shaft which has dispensed with buntons.

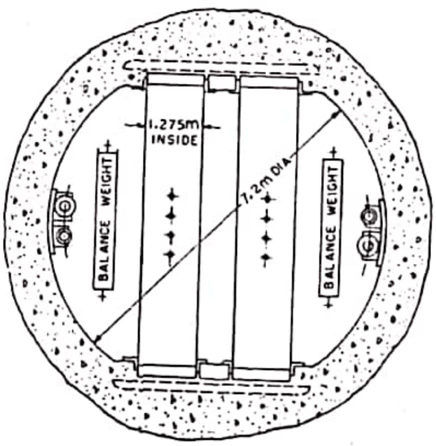

Fig. 4.23 Layout of shaft without buntons.

Misra[84] developed the following relation for the most economic size of airway, based on minimizing the total cost of ventilation, i.e., the sum of the annual power cost of ventilation and the annual interest and amortization charges on the capital invested on the airway :

$$\left(r' + \frac{r}{R^n - 1}\right) C_1 A^{7/2} + \frac{1}{2}\left(\left(r' + \frac{r}{R^n - 1}\right)\right.$$

$$\left.(C_1 + C_2) F t A^3 - \frac{21.9\, k F Q^3 C}{\eta} = 0 \right. \qquad (4.106)$$

where A = cross-sectional area of the airway in m^2,
r' = speculative rate of interest on capital = 10% usually,
r = safe rate for redemption of capital = 4% usually,
R = $r + 1$,
C_1 = cost of rock excavation in Rs m^{-3},
C_2 = cost of lining in Rs m^{-3},
C = power cost in Rs kW^{-1} h^{-1}
F = $p/\sqrt{A}$ = shape factor = 4 on the average,
p = perimeter of the airway in m,
t = thickness of lining in m,
k = coefficient of friction in N s^2 m^{-4},
η = efficiency of fan and motor,
Q = quantity flowing through the airway in m^3 s^{-1}
and n = life of the airway in years.

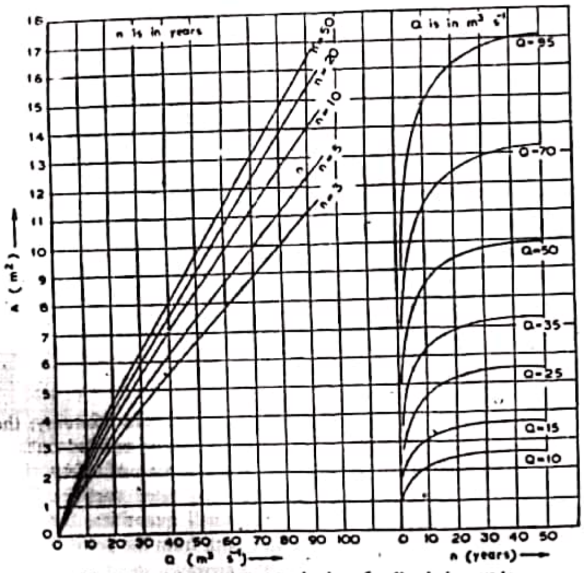

Fig. 4.24 The most economic size of unlined airways in coal-measure strata.

The above equation can be solved for the value of A for any given value of Q, assuming the values of the other variables for the particular condition. Figs. 4.24 and 4.25 give the most economic size of airway for different quantities and airway life for unlined airways in coal-measure strata and concrete-lined airways respectively, based on the following assumptions.[84]

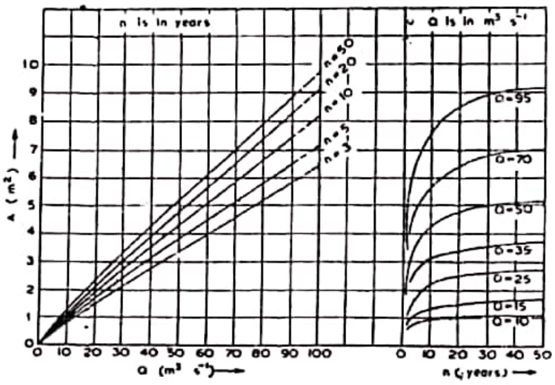

Fig. 4.25 The most economic size of concrete-lined airways.

k = 0.002 16 N s^2 m^{-4} for concrete-lined airways and 0.009 81 N s^2 m^{-4} for unlined airways in coal-measure strata,

C_1 = 60.00 Rs m^{-3},

C_2 = 100.00 Rs m^{-3} of concrete lining,

C = 0.09 Rs kW^{-1} h^{-1}

and η = 0.5 (50%).

It is evident from the figures that for maximum economy, the size of lined airways is much smaller than that of unlined ones, a fact deserving consideration from the point of view of safety, since large openings are more unstable and may need support. Thus whereas unlined openings may do for small quantities, for large quantities, lined airways are preferable both from the point of view of safety and economy. The life of the airway also affects its size. For temporary airways, it is not necessary to invest a large capital

either in excavating a larger cross-sectional area than is normally required or in lining the airway.

In the same way as there is an economically optimum size of any airway for a given flow-rate, an airway of any given size also has an economically optimum flow-rate or velocity of flow, though other technological and safety considerations may affect the optimum velocity.

EXERCISE 4

4.1 A rectangular smooth steel duct 600 × 400mm in cross-section and 200m long has air flowing through it. Calculate the pressure loss in the duct for the following flow-rates through it. Also calculate the value of the coefficient of friction k for the duct. Assume kinematic viscosity ν=0.000 016 m^2 s^{-1} and density ρ=1.2 kg m^{-3} for air.

(a) 0.6 m^3 min^{-1}, (b) 0.5 m^3 s^{-1} and (c) 3 m^3 s^{-1}.

4.2 Calculate the quantity that will flow through an airway 1500m long, 5m wide and 2m high with an applied pressure of 300 Pa across it if the pressure drop measured across a 200m length of an airway having similar rubbing surface but a cross-section of 3.5 × 2m is found to be 30 Pa with a flow of 20 m^3 s^{-1}.

4.3 40 m^3 s^{-1} of air flowing through a 4m diameter shaft absorbs a pressure of 490 Pa. Find the flow in the shaft when its diameter is enlarged to 6m assuming pressure drop across it to remain unchanged. Also find the pressure drop in the enlarged shaft if the flow is maintained at 40 m^3 s^{-1}.

4.4 A 200m long longwall face is ventilated by two gate roads each 300m long. Calculate the quantity that will flow along the face when a ventilating pressure of 150 Pa is applied across the gate roads at the outbye end. The face has a resistance of 0.6 N s^2 m^{-8} per 100m and the gate roads, 0.8 N s^2 m^{-8} per 100m length. Neglect leakage between gate roads

4.5 An unlined airway 350m long, 2.5m wide and 2.8m high has a sharp bend of 1.1rad deflection angle and a stopping with a sawn

Scanned with CamScanner

timber door frame (without door) 2 × 2m in size. Calculate the pressure drop in the airway for a flow of 10 m³ s⁻¹.

4.6 A 4 × 3m rectangular vertical shaft fully open at the collar is so fitted as to have a coefficient of friction k=0.0098 N s² m⁻⁴. The shaft delivers air into 15-level crosscut at a depth of 450m from the surface. Calculate the pressure drop in the shaft between the surface and the crosscut for a quantity of 100 m³ s⁻¹ entering the shaft. 20% of the air entering the shaft leaks through the upper level door 60m above 15-level.

4.7 A concrete-lined vertical circular shaft 300m deep and 5m in diameter is fitted with sets of two parallel buntons each 3.5m long spaced at 3m interval along the shaft. The buntons are of I-section with a flange width of 125mm facing air-flow. Calculate the shaft pressure loss for a flow of 80 m³ s⁻¹. Assume a Darcy-Weisbach resistance coefficient of 0.02 for bare concrete-lined shafts, a drag coefficient of 2.75 for I-section girders and an interference factor of 0.9.

4.8 A 200m advancing long longwall face worked with solid stowing is connected to 600m long trunk airways comprising a pair of intake and a pair of return airways separated by permanent stoppings by a pair of 150m long gate roads. The following are the quantity measurements in the different parts of the ventilation circuit. Calculate the pressure across the outbye ends of the trunk airways assuming the longwall face to have a resistance of 1.15 N s² m⁻⁸ and the gate and trunk airways, a resistance of 0.012 N s² m⁻⁸ per 100m. Take shock pressure losses to be 10% of the frictional pressure loss.

Location	Quantity m³ s⁻¹
Longwall face, inbye ends of intake and return gates	15
Trunk intakes just before their connection to the intake gate	23
Trunk returns at the outbye end	25

4.9 A shaft being sunk is being ventilated by two ducts in parallel, one 500mm in diameter and the other 600mm in diameter supplied from the same fan. It is proposed to replace the two ducts by a single duct of 1m diameter. Calculate the change in the quantity supplied to the face assuming the fan pressure to remain unchanged.

4.10 Three splits are ventilated from the inbye end of a pair of main intake and return airways connected to the downcast and upcast shafts respectively. The following gives the measured pressure drops and quantities :

Pressure drop between surface and intake-shaft bottom	= 160 Pa
Pressure drop between intake-shaft bottom and the inbye end of the main intake	= 200 Pa
Pressure drop between the inbye end of the main return and upcast-shaft bottom	= 180 Pa
Pressure drop across the splits	= 150 Pa
Fan-drift pressure	= 840 Pa
Flow in the three splits	= 16 m³ s⁻¹, 15m³ s⁻¹ and 12 m³ s⁻¹
Flow in the shafts	= 50 m³ s⁻¹
Flow at the outbye end in the main intake	= 45 m³ s⁻¹
Flow in the fan drift	= 56 m³ s⁻¹

Calculate (a) resistance of each of the splits, shafts and main intake and return airways, (b) leakage in various parts of the mine and the volumetric efficiency of the mine, (c) coefficient of friction for the main intake airway which is 3000m long and 2.5 × 3.5m in cross-section, and (d) the resistance as well as the equivalent orifice of the mine.

4.11 A shaft 200m deep and having a finished diameter of 4m has a coefficient of friction k=0.015 N s² m⁻⁴. Calculate the equivalent orifice of the shaft with the density of air flowing through it being equal to 1.15 kg m⁻³.

4.12 A fan ventilating a mine was circulating 75 m³ s⁻¹ at a pressure of 600 Pa. After a reorganization of the ventilation system the

Scanned with CamScanner

fan circulates 100 $m^3 s^{-1}$ at a pressure of 500 Pa. Calculate the change in the equivalent orifice of the mine, taking $\rho=1.2$ kg m^{-3}. Plot the new mine characteristic.

4.13 A rectangular roadway 4 × 2.5m in cross-section and 1000m long passes 7500 $m^3 min^{-1}$ of air. What would be the saving in power if (a) the entire length of the roadway is enlarged to a height of 3m maintaining the same width of 4m throughout, (b) the roadway is concrete-lined to a finished section of 3.5×2m throughout assuming the flow to remain unchanged and the coefficient of friction for unlined and concrete-lined roadways to be 0.01 and 0.003 N s^2m^{-4} respectively. Further assuming the cost of electric power to be 12 paise per unit and an overall fan and drive efficiency of 65%, calculate the most economic one of all the three alternatives if the cost of stripping is Rs 50.00 per metre and the cost of lining Rs 300.00 per metre length of the roadway which has an expected life of 15 years.

4.14 200 $m^3 s^{-1}$ of air downcasts through a shaft at a pressure drop of 3 kPa. It is required to increase the air flow to 300 $m^3 s^{-1}$. Streamlining of shaft equipment gives 40% reduction in the coefficient of friction. The efficiency of fan and motor being 70%, calculate the annual saving in power cost achievable by streamlining the shaft equipment if 1 kWh of power costs Rs 0.14.

4.15 A 1000m long and 3×4m cross-section drift is ventilated by a fan connected to two ducts of 400mm and 300mm diameter installed in parallel. Calculate the delivery through each duct if the fan pressure is 3 kPa assuming a coefficient of friction of 0.003 N s^2m^{-4} for the ducts and 0.01 N s^2 m^{-4} for the drift. What is the size of a single duct which may replace the two ducts without affecting the ventilation at the face? Neglect leakage.

CHAPTER V

NATURAL VENTILATION

Small and shallow mines are somtimes ventilated by natural means only though the ventilation in such cases is usually poor, fluctuates to a large extent and is even subject to reversal of direction. In cases of emergency such as fires underground, mechanical ventilation can be subjected to control while natural ventilation cannot be. It is for these reasons that all mines should preferably be mechanically ventilated. However natural ventilation does play a role in all mechanically ventilated mines.

5.1 CAUSES OF NATURAL VENTILATION

5.1.1 Temperature

Natural ventilation can be visualized to be caused by the difference in densities of air in the upcast and downcast shafts. The heavier air sinks down and the lighter air moves up thus setting up an air-current. The difference in air densities in the upcast and downcast shafts is mainly caused by the heating and rarefaction of air in the mine workings due to the addition of heat from rocks, men, machinery, lights, spontaneous heating etc. Autocompression in the downcast shaft changes the density of air according to the theoretical relation $\rho \propto P^{1/\gamma}$ the effect being maximum at the bottom of the shaft, but the reverse process takes place in the upcast shaft due to auto-expansion. So theoretically, there is no difference between the average air densities in the two shafts and hence no natural ventilation due to auto-compression and auto-expansion, though in practice a slight effect on natural ventilation is exerted by the two processes being non-isentropic and occuring at different average temperatures.

Apart from temperature, the following are the other factors affecting air density.

5.1.2 Moisture Content of the Air

Addition of moisture in the downcast shaft decreases the density of air as moisture is lighter than air, but this also causes evaporative cooling of the downcast air and consequent increase in its

Scanned with CamScanner

density so much so that, in effect, evaporation of moisture in the downcast shaft usually aids natural ventilation.

5.1.3 Barometric Pressure

It is well known that air density is a function of barometric pressure. If the mean barometric pressure of the downcast air column is higher than that of the upcast air column, it helps natural ventilation and vice versa. However, since barometric pressure rarely varies to any appreciable extent from place to place within the limits of a mining property, the effect of such variation on natural ventilation is negligible.

5.1.4 Addition of Gases

Methane emitted from the workings of coal mines reduces the density of return air thus aiding natural ventilation. This effect may, however, be slightly offset by the cooling of mine air produced by the desorption of methane. Large addition of carbon dioxide on the other hand has the opposite effect. Addition of compressed-air from the exhaust of the compressed-air machinery used underground, however, has little effect on the density of air.

5.1.5 Leakage

In multilevel mines, leakage of denser downcast air to the upcast shaft causes an increase in the density of upcast air, thus reducing natural ventilation. In view of the low efficiency of natural ventilation, of the order of 1.4 to 1.6% it is important to minimize leakage of air from the downcast to the upcast shaft in order to get the maximum benefit of natural ventilation.

5.1.6 Circulation of Refrigerated Air

Circulation of refrigerated air through the downcast shaft increases the density of downcast air thus aiding natural ventilation to a large extent.

5.1.7 Other Factors

Other factors such as spraying of water in the downcast shaft for preserving shaft timber from dry rot or minimizing fire hazard etc. or having steam pipes through the upcast shaft where steam is used underground (this is, however, a rare practice now) help natural ventilation by increasing the downcast air density or decreasing the upcast air density.

5.2 AMOUNT OF NATURAL VENTILATION

The quantity of air circulated by natural ventilation depends on the above factors, the most important of them being the heat added to the air from the strata in the workings. In shallow mines the natural ventilating pressure (this in turn determines the quantity depending on the mine resistance) may be of the order of a few pascals, but in deep and hot mines, it increases considerably varying from 250 Pa to even 750 Pa. In some hot and deep mines such as Robinson Deep on the Rand, South Africa, where refrigerated air is sent down the intake shaft, the N.V.P. is estimated to be of the order of 1200 Pa.

5.3 DIRECTION OF NATURAL VENTILATION

This depends mainly on the depth of the mine as the depth generally controls the amount of heat added to the mine air. In shallow mines, where the underground temperature is not very high, the surface temperature is the major contributing factor to the direction of natural ventilation. Let us consider two shafts with their collars at different elevations as illustrated in Fig. 5.1. Let the ground temperature be 298 K at an average depth of 20m from the surface and the geothermic gradient, 1 K for every 40m depth. Then the temperature at the bottom of the shaft A will be 299.5 K and that at the bottom of shaft B, 301.5 K. In summer, the surface temperature is higher than the average annual temperature of 298 K. Let us assume this to be 308 K. The average temperature of the air column in shaft B will then be 304.75 K and that in shaft A, 303.75 K, but in shaft A, the total air column balancing that in shaft B also includes a column of surface air equal in length to the difference in heights of the two shaft collars. Or, in other words, the effective average air temperature in shaft A will be (303.75 +308)/2=305.88 K which is higher than that in shaft B. Hence the air will flow down shaft B and up shaft A. In winter, however, the surface air temperature falls. Assuming the winter surface temperature to be 288 K the average temperature in shaft B will be 294.75 K and that in shaft A, 291.88 K so that air will flow down shaft A and up shaft B, thus resulting in the reversal of air-

Scanned with CamScanner

current. It will be evident from the above that the temperature in the shallower shaft is more affected by variations in surface temperature than in the deeper one. Hence, the deeper the shaft, the less is the effect of changes in surface temperature on natural ventilation.

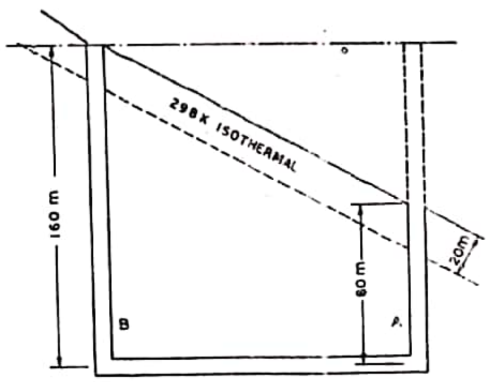

Fig. 5.1 Figure illustrating the development of natural ventilating pressure.

The reversal of air-current in shallow mines usually takes place seasonally, from summer to winter and vice versa, the intervening periods of spring and autumn being periods of stalemate with very little or no natural ventilation. Where there is a large diurnal variation of temperature, ventilation may be reversed during the course of the day.

We have considered shallow shafts with collars at unequal elevations. If the collars are at the same elevation, the average temperatures of the air columns in the two shafts become the same and there is no natural ventilation. However, when the surface-air temperature is less than the temperature of the workings, natural ventilation can continue in any one direction if initiated by some agency in that direction. In such a case, the downcast air column will be more affected by the surface-air temperature and hence will have a lower average temperature than the upcast air column and natural ventilation will occur. In deep mines where the temperature of the workings is always greater than that of surface atmosphere, natural ventilation continues in the same direction, but the quantity may vary depending on the average downcast air temperature which is affected by the surface temperature. There is hardly any variation in the upcast air temperature. The extent of variation of quantity will, however, depend on the depth of the shaft, deeper shafts having lesser variation. In one of the South African mines with 1200m deep shafts the winter N.V.P. was found to be greater than the summer N.V.P. by about 500 Pa. The summer N.V.P. at Chinakuri 1 and 2 pits with 611m deep shafts is 150 Pa while the winter N.V.P. is 285 Pa.

Although natural ventilating pressure in a mine is mainly generated in shafts, it is also generated in the workings if the air travelling through them traverses an inclined path. With normal ventilation of dip workings in an inclined seam or bed the cool intake air travels down an inclined airway to the face and gets heated up there so that the return air travelling up gets hot and rarefied. As a result, a positive N.V.P. which aids the N.V.P. produced in the shafts is generated in the workings. In case of rise workings however, a negative N.V.P. is produced which opposes the pit-bottom N.V.P. For similar reasons, a higher N.V.P. is produced in the workings with ascensional ventilation where the downcast air is taken directly to the bottom of the workings and allowed to travel up through them into the return, whereas with descensional ventilation, the N.V.P. produced in the workings is considerably less.

5.4 CALCULATION OF N.V.P. FROM AIR DENSITIES

Let the mean density of downcast and upcast air be ρ_D and ρ_U kg m^{-3} respectively.

Let the shafts be of equal depths, D m (or, D should be taken as equal to the difference in height between the higher shaft collar and the deepest ventilated point in the mine).

The N.V.P. $= D\ (\rho_D - \rho_U) g$ Pa (5.1)

Now $$\rho_D = \frac{(B_D - 0.378\, e_D) \times 10^3}{287.1\ T_D} \text{ kg m}^{-3} \quad (5.2)$$

and $$\rho_U = \frac{(B_U - 0.378\ e_U) \times 10^3}{287.1\ T_U} \text{ kg m}^{-3} \quad (5.3)$$

Scanned with CamScanner

where B_D and B_U are the mean barometer readings in kPa in the downcast and the upcast shafts respectively, e_D and e_U are the average vapour pressures of moisture in kPa in the downcast and upcast air respectively and T_D and T_U are the mean temperatures of the downcast and upcast air columns respectively in K.

For mine shafts in general, $B_D = B_U = B$ say. Further, let us neglect the effect of moisture. Then,

$$\text{N.V.P.} = Dg\left(\frac{B}{287.1\,T_D} - \frac{B}{287.1\,T_U}\right) \times 10^3$$

$$= \frac{gDB}{287.1} \quad \frac{T_U - T_D}{T_U \times D_D} \times 10^3 \text{ Pa} \tag{5.4}$$

Example 5.1

Calculate the natural ventilating pressure in a mine given the following data :

Depth of mine=300m
Pit-bottom barometer reading=101.27 kPa
Pit-top barometer reading=98.10 kPa
Average temperature in downcast shaft=304 K
Average temperature in upcast shaft=307 K

Using equation 5.4

$$\text{N. V. P.} = \frac{gDB}{287.1} \quad \frac{T_U - T_D}{T_U \times T_D} \times 10^3$$

$$= \frac{9.8 \times 300\left(\frac{101.27+98.1}{2}\right)}{287.1} \times \frac{(307-304)}{307 \times 304} \times 10^3$$

$$= 32.81 \text{ Pa.}$$

Example 5.2

Two vertical shafts each 6m in diameter and 300m deep are connected at the bottom by a level 2×2.5m in cross-section and 800m long. The average barometric pressure in the shafts being 101.325 kPa, calculate the velocity of flow in the level due to natural ventilation. Temperature measurements in the shafts are as follows:

Downcast shaft-top=293 K
Downcast shaft-bottom=296 K
Upcast shaft-top=303 K
Upcast shaft-bottom=303.5 K

The coefficient of friction k for the shafts is 0.004 N s^{2}m^{-4}, and for the levels, 0.01 N s^{2}m^{-4} Neglect shock losses.

$$\text{Average downcast shaft temperature} = \frac{293+296}{2} = 294.5 \text{ K}$$

$$\text{Average upcast shaft temperature} = \frac{303+303.5}{2} = 303.25 \text{ K.}$$

$$\text{N.V.P.} = \frac{9.8 \times 300 \times 101.325}{287.1} \quad \frac{(303.25-294.5)}{303.25 \times 294.5} \times 10^3$$

$$= 101.7 \text{ Pa}$$

Cross-sectional area of the level=5 m^2.
Perimeter of the level=9m.

Cross-sectional area of the shafts $= \frac{\pi}{4}(6)^2 = 9\pi$ m^2.

Perimeter of the shafts=6 π m.

Let v=velocity of flow in the level in m s^{-1}.

The quanity of flow=5v m^{3}s^{-1}.

$$101.7 = \frac{2 \times 0.004 \times 6\pi \times 300 \times (5v)^2}{(9\pi)^3}$$

$$+ \frac{0.01 \times 9 \times 800\,(5v)^2}{5^3} = 14.45\,v^2.$$

$$\text{Or, } v = \sqrt{101.7/14.45} = 2.65 \text{ m s}^{-1}.$$

Sometimes N.V.P. is expressed in terms of ***motive column*** that is the height of the air column in the downcast shaft which causes the natural ventilating pressure. In other words, motive column is the N.V.P. expressed in terms of the height of a column of air with a density equal to that of air in the downcast shaft.

Scanned with CamScanner

Or,

$$h = \frac{\text{N.V.P.}}{\rho_D g} \quad (5.5)$$

where h=height of motive column in m and N.V.P., ρ_D and g are expressed in Pa, kg m^{-3} and m s^{-2} respectively.

In most cases, results within 2-3% accuracy are obtained in the calculation of N.V.P. from the temperatures of shaft air-columns, but the mean temperatures should be determined carefully. In the upcast shaft, the temperature is very little affected by the surface temperature and a few widely spaced readings give a good average, if there is no leakage from the intake at any level. Downcast shafts are affected by variations in surface temperature and hence temperature measurements should be made at closer spacing particularly in the upper part of the shaft which is most affected by the surface temperature.

McElroy[83] states that differences in barometric pressure and moisture content of the two air columns affect the value of N.V.P. as calculated from shaft temperatures by not more than 5% each in naturally ventilated mines and not more than 10% each in mechanically ventilated deep and hot mines where it may be necessary to determine the air densities in the two shafts with greater accuracy.

Hinsley[87] suggested the use of the P-V diagram for the mine for a more accurate estimation of the power of natural ventilation. According to him, computation of N.V.P. from air densities, howsoever accurately the densities might have been measured, becomes anomalous in mechanically ventilated mines, though the error may not be very apparent in purely naturally ventilated mines. It is more logical to conceive of natural ventilation in terms of the rate of work done by the air rather than pressure, since the latter has no significance without the specification of density which varies from place to place in the mine. However, N.V.P. can always be estimated from the work of natural ventilation with respect to a reference air density.

5.5 DETERMINATION OF N.V.P. FROM THERMODYNAMIC CONSIDERATIONS

A mine can be likened to a heat engine with the following cycle : (a) Air (the working substance in this case) descending the down-

cast shaft undergoes auto-compression, as a result of which its pressure and temperature increase and specific volume decreases. (b) Heat is added from the rocks to the hot and compressed air as it travels through the mine workings thus increasing its temperature. As a result of this, its specific volume increases, but pressure decreases because of the air doing work against friction. (c) In the upcast shaft auto-expansion leads to an increase in its specific volume, but pressure and temperature fall. (d) Finally heat is rejected by the air at low temperature to the atmosphere which acts as the sink and the air returns to the atmospheric condition of pressure, specific volume and temperature thus completing the cycle.

5.5.1 The Work of Natural Ventilation—P-V Diagram

Let us consider a unit mass of dry air entering the downcast shaft and undergoing auto-compression. Assuming no heat or moisture exchange between the shaft wall and the air, this process of auto-compression is a frictional adiabatic, somewhat steeper than the reversible adiabatic (isentropic) curve AB in Figs. 4.10 and 5.2.

The flow work of air entering the shaft

$$W_{fli} = P_1 V_1 \quad (5.6)$$

(area OV_1AP_1 in Fig. 4.10)

The work done on the air by auto-compression

$$W_c = \int_1^2 P\,dV \quad (5.7)$$

(area V_1ABV_2 in Fig. 4.10)

The flow work out of the shaft

$$W_{flo} = -P_2 V_2 \quad (5.8)$$

(area OV_2BP_2 in Fig. 4.10)

∴ Total work done on the air in the downcast shaft

Scanned with CamScanner

$$W_{dc} = W_{fli} + W_c + W_{flo} = P_1V_1 + \int_1^2 PdV - P_2V_2$$

$$= -\int_1^2 VdP \qquad (5.9)$$

(area P_2BAP_1 in Fig. 4.10. Note that since the work is one of compression done on the air it is —ve.)

[$\int d(PV) = \int P\,dV + \int V\,dP$

also, $\int d(PV) = P_2V_2 - P_1V_1$

$\therefore \int P\,dV + \int V\,dP = P_2V_2 - P_1V_1$

Or, $P_1V_1 + \int P\,dV - P_2V_2 = -\int V\,dP$]

where P =absolute pressure of air,

V =specific volume (volume per unit mass) and subscripts 1 and 2 represent conditions at the downcast shaft-top and -bottom respectively.

Similarly the work done on the air in the mine workings

$$W_w = -\int_2^3 V\,dP \qquad (5.10)$$

(area P_2BCP_3 in Fig. 5.2)

and that in the upcast shaft

$$W_{uc} = -\int_3^4 V\,dp \qquad (5.11)$$

(area P_3CDP_4 in Fig. 5.2)

where subscripts 3 and 4 give conditions at the upcast shaft-bottom and -top respectively.

The total work done on the air in the mine

$$W_t = W_{dc} + W_w + W_{uc} = -\int_1^2 V\,dP - \int_2^3 V\,dP - \int_3^4 V\,dP \qquad (5.12)$$

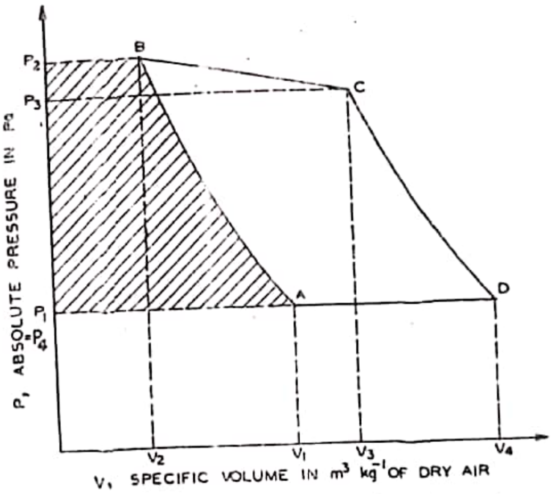

Fig. 5.2 *P-V* indicator diagram for a naturally ventilated mine.

(area ABCD in Fig. 5.2. Here P_1 is taken equal to P_4 since the upcast and downcast shaft-tops are assumed at the same elevation.)

When there is no external work done on the air (i.e. there is no fan in the ventilation system), the above work is the work of natural ventilation due to the addition of heat in the mine workings and can be equated to changes in potential and kinetic energy of air and frictional work (see equation 4.6).

Thus from the principle of general energy balance

$$-\int_1^2 V\,dp = (h_2 - h_1)\,g + \frac{v_2^2 - v_1^2}{2} + F_{1-2} \qquad (5.13)$$

$$-\int_2^3 V\,dp = (h_3 - h_2)\,g + \frac{v_3^2 - v_2^2}{2} + F_{2-3} \qquad (5.14)$$

and $$-\int_3^4 V\,dp = (h_4 - h_3)\,g + \frac{v_4^2 - v_3^2}{2} + F_{3-4} \qquad (5.15)$$

where h = elevation above a certain datum,
v = velocity of air,
F = 'frictional work',
and g = acceleration due to gravity.

Combining equations 5.13, 5.14 and 5.15 we have

$$F_{1-2}+F_{2-3}+F_{3-4}=(h_1-h_2)\,g-\frac{v_2^2-v_1^2}{2}-\int_1^2 V\,dP$$
$$+(h_2-h_3)\,g-\frac{v_3^2-v_2^2}{2}-\int_2^3 V\,dP$$
$$+(h_3-h_4)\,g-\frac{v_4^2-v_3^2}{2}-\int_3^4 V\,dP \quad (5.16)$$

Neglecting the kinetic energy terms in equation 5.16 and assuming $h_2=h_3$ and $h_1=h_4$

$$F_{1-4}=-\int_1^2 V\,dP-\int_2^3 V\,dP-\int_3^4 V\,dP=W_t \quad (5.17)$$

So far we have considered flow of dry air. When moisture is added in the mine airway, the energy balance equation has to be modified to take into account the change in the potential energy of moisture in addition to the changes in the potential and kinetic energy of air and 'frictional work'. Equations 5.13, 5.14 and 5.15 can then be re-written as

$$-\int_1^2 V\,dP=(h_2-h_1)\,g+g\int_1^2 0.001\,m\,dh+\frac{v_2^2-v_1^2}{2}+F_{1-2} \quad (5.18)$$

$$-\int_2^3 V\,dP=(h_3-h_2)\,g+g\int_2^3 0.001\,m\,dh+\frac{v_3^2-v_2^2}{2}+F_{2-3} \quad (5.19)$$

$$-\int_3^4 V\,dP=(h_4-h_3)\,g+g\int_3^4 0.001\,m\,dh+\frac{v_4^2-v_3^2}{2}+F_{3-4} \quad (5.20)$$

and equation 5.17 as

$$F_{1-4}=-\int_1^2 V\,dP-\int_2^3 V\,dP-\int_3^4 V\,dP-g\int_1^2 0.001\,m\,dh$$
$$-g\int_3^4 0.001\,m\,dh \quad (5.21)$$

since $g\int_2^3 0.001\,m\,dh=0$ with $h_2=h_3$

where m is the mixing ratio in g kg^{-1} of dry air.

It must be noted that V in this case is the apparent specific volume of moist air i.e. volume of moist air per unit mass of dry air.

5.5.2 Natural Ventilation with Mechanical Ventilation

When there is mechanical ventilation aiding natural ventilation, the *P-V* diagram becomes as shown in Fig. 5.3. Let us consider the case with an exhaust fan at the top of the upcast shaft. Here, the expansion curve CD extends down to E or, in other words, the pressure of air at the top of the upcast shaft P_4 is no longer equal to P_1 but less than P_1, P_1-P_4 being the depression created by the fan. The air is, however, compressed back by the fan to P_1, the atmospheric pressure, the compression following the curve

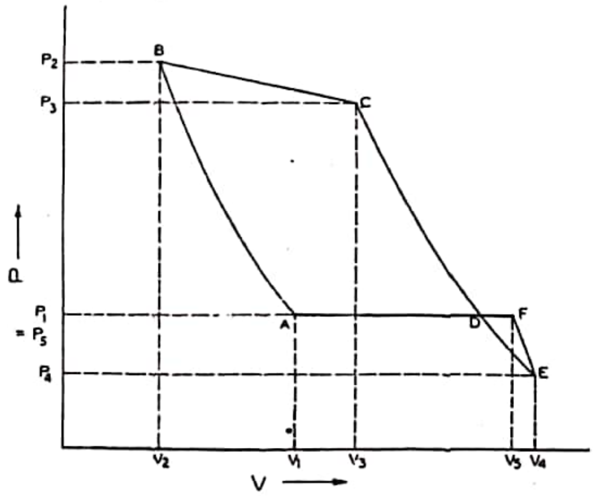

Fig. 5.3 Indicator diagram with fan ventilation.

EF. EF is slightly steeper than CE because of the extra work done against the internal friction of the fan. Referring to

Scanned with CamScanner

Fig. 5.3 the total work done by natural agency as well as the fan $\left(-\int_1^2 V\,dP - \int_2^3 V\,dP - \int_3^4 V\,dP\right)$ is given by the area $P_1ABCDEP_4$, out of which the work done by the fan alone $\left(W_f = -\int_4^5 V\,dP\right)$ is given by the area P_1FEP_4. So the work done by N.V.P. is given by the area ABCD – DEF, but since DEF is very small it can be neglected and the N.V.P. will then be calculated from the work done as represented by the area ABCD only. The energy equation for the compression of air in the fan can be written as follows neglecting the frictional work in the fan and change in potential and kinetic energy of air across the fan (see equation 4.4)

$$-W_f = \int_4^5 V\,dP \tag{5.22}$$

Adding equation 5.22 to equations 5.18, 5.19 and 5.20 and neglecting changes in kinetic energy we have the general energy equation for the whole process

$$F_{1-4} = -\int_1^2 V\,dP - \int_2^3 V\,dP - \int_3^4 V\,dP - \int_4^5 V\,dP$$
$$- g\int_1^2 0.001\,m\,dh - g\int_3^4 0.001\,m\,dh - W_f \tag{5.23}$$

5.5.3 Determination of N.V.P. from P-V Diagram

The accuracy of determination of N.V.P. from the P-V diagram of the mine depends on how accurately the P-V diagram is plotted. As has been said earlier, the processes of compression and expansion of air involved in an actual mine are not ideal and hence, theoretical prediction of the P-V diagram can never be very accurate. However, in existing mines an exact plot of the P-V diagram can be made from actual measurement of the absolute pressure by an aneroid barometer and estimation of apparent specific volume from barometric and hygrometric readings. Here again the degree of accuracy depends on how far apart readings of P and V are taken along the mine air circuit.

The apparent specific volume of air can be calculated from equation 4.50. In case of substantial addition of other gases in the mine, the apparent specific volume should take into consideration the partial pressure of these gases too. While the addition of lighter

gases like methane increases the specific volume, that of heavier gases like CO_2 decreases it. Addition of compressed-air makes no difference in the specific volume. However, in all cases extra work is done in lifting the additional amount of gas in the upcast shaft and equation 5.23 has to be modified to take this into account.

$$\text{Or, } F_{1-4} = -\int_1^2 V\,dP - \int_2^3 V\,dP - \int_3^4 V\,dP - \int_4^5 V\,dP$$
$$- g\int_1^2 0.001\,m\,dh - g\int_3^4 0.001\,m\,dh$$
$$- m'\,g\,(h_4 - h_3) - W_f \tag{5.24}$$

where m' is the mass of gas in kg added per kg of dry air.

The area of the indicator loop on the P-V diagram gives the power of natural ventilation and dividing it by a reference specific volume of air (usually at the fan inlet) gives the Natural Ventilation Pressure.

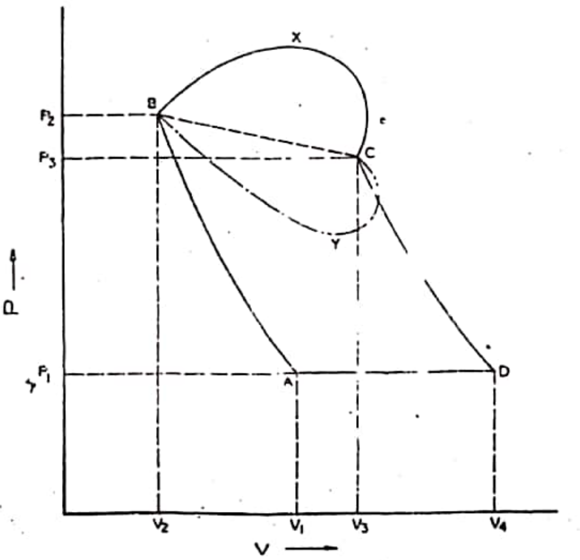

Fig. 5.4 Indicator diagram showing the effect of the dip and rise workings on natural ventilation.

Scanned with CamScanner

5.5.4 Variations in the P-V Diagram

Figs. 5.2 and 5.3 give the usual shape of the P-V diagram with level workings. With dip and rise workings, however, the curve BC does not drop uniformly but forms a loop as shown in Fig. 5.4 (BXC for dip workings and BYC for rise workings). Because of additional generation of natural ventilation power in dip workings, the area of the indicator loop increases while it decreases in the case of rise workings.

When air pressure changes sharply at any point in a mine such as across a regulator or a booster fan, there is also a change in the shape of the curve BC as shown in Fig. 5.5. The curve BMNC indicates a boosted district with MN representing the booster pressure, while the curve BXYC indicates a regulated district with XY representing the pressure drop across the regulator.

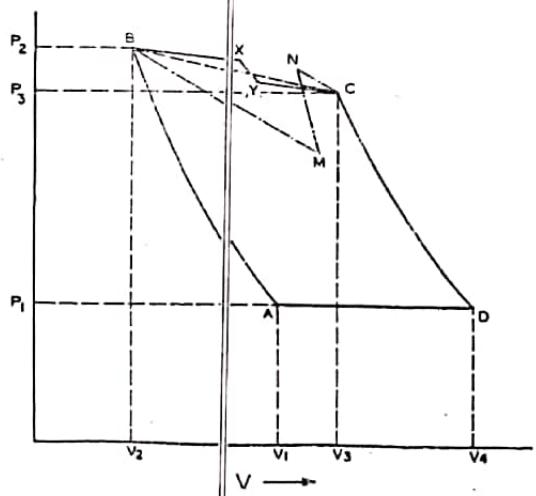

Fig. 5.5 Indicator diagram showing the effect of regulators and boosters on natural ventilation.

5.6 OTHER METHODS OF DETERMINING N.V.P.

Other practical methods used for finding N.V.P. in mines are as follows.

5.6.1 From Pressure and Quantity Measurements with Fan Running and Fan Stopped

With the fan running, the mine resistance

$$R = \frac{P_f + P_n}{Q_f^2} \tag{5.25}$$

and with fan stopped,

$$R = \frac{P_n}{Q_n^2} \tag{5.26}$$

where

P_n = N.V.P.,

P_f = fan pressure (fan-drift pressure),

Q_n = quantity flowing through the mine with fan stopped

and Q_f = quantity with fan running.

Combining equations 5.25 and 5.26, we get

$$P_n = P_f \frac{Q_n^2}{Q_f^2 - Q_n^2} \tag{5.27}$$

5.6.2 From Pit-bottom Pressures with Fan Running and Fan Stopped

Let p_n be the pit-bottom pressure with fan stopped and p_f, the pit-bottom pressure with fan running.

$$p_n = P_n - R_s Q_n^2 = P_n\left(1 - \frac{R_s}{R}\right) \tag{5.28}$$

where R_s = shaft resistance.

Similarly

$$p_f = \left(P_n + P_f\right)\left(1 - \frac{R_s}{R}\right) \tag{5.29}$$

Combining equations 5.28 and 5.29

$$\frac{p_f}{p_n} = \frac{P_n + P_f}{P_n}$$

$$\text{or, } P_n = \frac{P_f p_n}{p_f - p_n} \tag{5.30}$$

5.6.3 From Pressure across a Stopping in Fan Drift

N.V.P. can also be found out by erecting a stopping in the fan-drift (in fact in any part of the main circuit of ventilation) and measuring the pressure across the stopping with the fan idle, but this will vary from the N.V.P. measured with air flowing through the workings, since in the latter case, the difference in air densities causing natural ventilation will change as a result of the addition of a variable quantity of heat from outside depending on surface conditions.

5.6.4 From Fan Pressures and Quantities at Two Different Speeds

Another method of estimating N.V.P. is to measure the fan pressure (at the fan drift) and quantity at two different speeds of the fan. Let P_{f1} and P_{f2} be the fan pressures and Q_1 and Q_2 the quantities at speeds N_1 and N_2 respectively and R, the resistance of the mine. Then,

$$R = \frac{P_n + P_{f1}}{Q_1^2} = \frac{P_n + P_{f2}}{Q_2^2} \tag{5.31}$$

P_n can be found from the above equation.

However, all the above methods need the stopping or speed variation of the fan. Besides, the following sources of error are likely to occur: (1) The course of air may change, and the resistance of workings vary depending on whether the fan is running or is stopped. As a result of this both quantity and pit-bottom pressure may be affected. (2) The fan offers a considerable resistance to N.V.P. when stopped. This, however, does not occur in the case of section 5.6.3 where there is no flow of air. (3) Leakage of air round the fan may occur while the fan is running and stop when the fan stops. This affects the quantity actually flowing through the mine.

Example 5.3

The following are the readings of the fan-drift pressures and quantities with the fan running at two different speeds. Calculate the natural ventilation pressure. Also find the equivalent orifice of the mine.

Fan-drift pressure at a speed of 31.4 rad s^{-1}=650 Pa
Fan-drift quantity at a speed of 31.4 rad s^{-1}=84.8 $m^3 s^{-1}$
Fan-drift pressure at a speed of 34.5 rad s^{-1}=715 Pa
Fan-drift quantity at a speed of 34.5 rad s^{-1}=88.3 $m^3 s^{-1}$
Let P_n=N.V.P.
and R=resistance of the mine.

$$R = \frac{P_n + 650}{(84.8)^2} = \frac{P_n + 715}{(88.3)^2}$$

(see equation 5.31)

$$P_n = \frac{715\ (84.8)^2 - 650\ (88.3)^2}{(88.3)^2 - (84.8)^2}$$

$$=121.51 \text{ Pa.}$$

$$R = \frac{121.51+650}{(84.8)^2} = 0.107 \text{ N s}^2\text{m}^{-8}.$$

Equivalent orifice

$$A = \frac{1.29}{\sqrt{0.107}} = 3.94 \text{ m}^2$$

(see equation 4.104).

5.7 ARTIFICIAL AIDS TO NATURAL VENTILATION

5.7.1 Stacks or Chimneys

Stacks built on the top of upcast shafts aid natural ventilation, but their application is limited to shallow mines where the length of the stack can be fairly large in comparison to the depth of the shaft.

5.7.2 Furnaces

N.V.P. can be considerably increased by putting furnaces at the bottom of upcast shafts. In coal mines where cheap fuel is available, these were quite common before the introduction of fans, but were later discarded in favour of the latter on account of various dangers involved in having furnaces underground.

5.7.3 Use of Air, Water or Steam Jets and Falling Water

Jets pointing in the direction of air-flow or water falling along the direction of air-current helps natural ventilation to some extent which, though not substantial, aids in maintaining the direction of flow when there is a chance of reversal of air-current.

5.7.4. Surface Winds

These, if suitably directed into the mine, aid natural ventilation by adding velocity pressure to the N.V.P. Sometimes, if the mine exhaust is guided in the direction of surface wind, the latter produces a suction effect aiding natural ventilation. Surface wind velocities are, however, usually small and vary considerably in

Scanned with CamScanner

direction and amount and deflection of surface wind into a mine for aiding natural ventilation should be considered only when a steady flow of wind with little variation of direction occurs.

Example 5.4

The following data were obtained from an aneroid and hygrometer survey of a mine 600m deep. Calculate the Natural Ventilation Pressure, the power of the fan and the resistance of the mine when a quantity of 150 $m^3 s^{-1}$ (as measured at the fan inlet) circulates through the mine. Plot the *P-V* diagram.

Depth, m	Elevation, h, m	Dry-bulb temperature T, K	Wet-bulb temperature T', K	Barometric pressure, B, kPa	Vapour pressure, e, kPa	Mixing ratio, m, g kg^{-1} of dry air	Apparent specific volume V, $m^3 kg^{-1}$ of dry air
				Downcast shaft			
0	600	297.0	291.2	100.21	1.688	10.66	0.8[illegible]56
100	500	296.7	291.5	101.04	1.764	11.05	0.8[illegible]58
200	400	296.4	291.8	101.88	1.842	11.45	0.8[illegible]1
300	300	296.1	292.1	102.71	1.920	11.85	0.84[illegible]3
400	200	295.8	292.4	103.55	2.000	12.25	0.8[illegible]6
500	100	295.5	292.7	104.38	2.080	12.66	0.82[illegible]9
600	0	295.2	293.0	105.22	2.165	13.07	0.82[illegible]2
				Upcast shaft			
600	0	304.5	303.3	104.21	4.202	26.14	0.87[illegible]4
500	100	304.0	303.0	102.68	4.153	26.22	0.88[illegible]6
400	200	303.5	302.7	101.16	4.140	26.54	0.89[illegible]8
300	300	303.0	302.4	99.62	4.029	26.21	0.91[illegible]0
200	400	302.5	302.1	98.09	3.973	26.26	0.92[illegible]3
100	500	302.0	301.8	96.57	3.917	26.30	0.93[illegible]6
0	600	301.5	301.5	95.03	3.862	26.35	0.95[illegible]0
				Fan outlet			
0	600	308.1	303.7	100.21	4.093	26.48	0.92[illegible]

From the given data (d.b. and w.b. temperatures and barometric pressures at different depths) the vapour pressure, mixing ratio and apparent specific volume of air have been calculated with the help of equations 3.72, 3.67, and 4.50 and listed in the above table. The *P-V* diagram is plotted in Fig. Exp. 5.1.

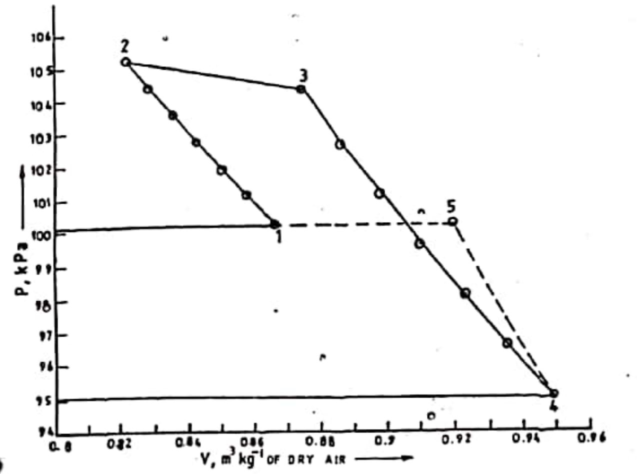

Fig. Exp. 5.1 *P-V* diagram for the mine.

Considering the compression of air in the fan to be polytropic, the polytropic index

$$n = \log\left(\frac{P_5}{P_4}\right) \Big/ \log\left(\frac{V_4}{V_5}\right) = \log\left(\frac{100.21}{95.03}\right) \Big/ \log\left(\frac{0.95}{0.92}\right) = 1.654$$

$-\int V\,dP$ is estimated from the simple relation

$$-\int V\,dP = \sum \left(P_n - P_{n+1}\right) \frac{V_{n+1} + V_n}{2}$$

where n refers to the number of the measuring point. The polytropic law has not been used here for the computation of $-\int V\,dP$ because the pressure differences involved are so small that they do not warrant the involved computation.

For the downcast shaft :

$$-\int_1^2 V\,dP = (100.21-101.04)\,\frac{0.866+0.858}{2}$$
$$+(101.04-101.88)\,\frac{0.858+0.851}{2}$$
$$+(101.88-102.71)\,\frac{0.851+0.843}{2}$$
$$+(102.71-103.55)\,\frac{0.843+0.836}{2}$$
$$+(103.55-104.38)\,\frac{0.836+0.829}{2}$$
$$+(104.38-105.22)\,\frac{0.829+0.822}{2}$$
$$=-4.226 \text{ kJ kg}^{-1} \text{ of dry air.}$$

$g\int 0.001\,m\,dh$ is estimated from the relation

$$g\int 0.001\,m\,dh = \sum 0.001\,g\,\frac{m_{n+1}+m_n}{2}\left(h_{n+1}-h_n\right)$$

Taking $g=9.8$ m s^{-2} and assuming datum at 600m level, we have for the downcast shaft

$$g\int_1^2 0.001\,m\,dh = 0.0098\Big[(500-600)\,\frac{10.66+11.05}{2}$$
$$+(400-500)\,\frac{11.05+11.45}{2}$$
$$+(300-400)\,\frac{11.45+11.85}{2}$$
$$+(200-300)\,\frac{11.85+12.25}{2}$$
$$+(100-200)\,\frac{12.25+12.66}{2}$$
$$+(0-100)\,\frac{12.66+13.07}{2}\Big]$$

$=-69.7$ J kg^{-1} $=-0.07$ kJ kg^{-1} of dry air.

$g\,(h_2-h_1)=9.8\,(0-600)=-5880$ J kg^{-1}
$=-5.88$ kJ kg^{-1} of dry air.

From equation 5.18 we have

$$F_{1-2}=-\int_1^2 V\,dP-g\int_1^2 0.001\,m\,dh-g\,(h_2-h_1)$$
$$=-4.226+0.07+5.88=1.724 \text{ kJ kg}^{-1} \text{ of dry air}$$

neglecting any change in kinetic energy.

For the workings :

$$-\int_2^3 V\,dP = (105.22-104.21)\,\frac{0.822+0.874}{2}$$
$$=0.857 \text{ kJ kg}^{-1} \text{ of dry air.}$$

Or, $F_{2-3}=0.857$ kJ kg^{-1} of dry air taking $h_2=h_3$ (see equation 5.19).

For the upcast shaft :

$$-\int_3^4 V\,dP=(104.21-102.68)\,\frac{0.874+0.886}{2}$$
$$+(102.68-101.16)\,\frac{0.886+0.898}{2}$$
$$+(101.16-99.62)\,\frac{0.898+0.910}{2}$$
$$+(99.62-98.09)\,\frac{0.910+0.923}{2}$$
$$+(98.09-96.57)\,\frac{0.923+0.936}{2}$$
$$+(96.57-95.03)\,\frac{0.936+0.95}{2}$$
$$=8.362 \text{ kJ kg}^{-1} \text{ of dry air.}$$

$$g\int_3^4 0.001\,m\,dh = 0.0098\Big[(100-0)\,\frac{26.14+26.22}{2}$$
$$+(200-100)\,\frac{26.22+26.54}{2}$$
$$+(300-200)\,\frac{26.54+26.21}{2}$$
$$+(400-300)\,\frac{26.21+26.26}{2}$$
$$+(500-400)\,\frac{26.26+26.30}{2}$$
$$+(600-500)\,\frac{26.30+26.35}{2}\Big]$$

$=154.62$ J kg^{-1} $=0.155$ kJ kg^{-1} of dry air.

Scanned with CamScanner

$g(h_4-h_3)=9.8\times600=5880$ J kg^{-1}=5.88 kJ kg^{-1} of dry air.

$\therefore\ F_{3-4}=8.362-5.88-0.155=2.327$ kJ kg^{-1} of dry air.

$F_{1-4}=F_{1-2}+F_{2-3}+F_{3-4}=1.724+0.857+2.327=4.908$ kJ kg^{-1} of dry air.

The fan work (taking polytropic compression with $n=1.654$)

$$W_f=-\int_4^5 V\,dP=\frac{n}{n-1}(P_4V_4-P_5V_5)$$

$$=\frac{1.654}{0.654}(95.03\times0.95-100.21\times0.92)$$

$$=-4.84 \text{ kJ kg}^{-1} \text{ of dry air.}$$

Now from equation 5.23

$$F_{1-4}=-4.226+0.857+8.362+0.07-0.155$$
$$=4.908 \text{ kJ kg}^{-1} \text{ of dry air, since}$$

$$-\int_4^5 V\,dP-W_f=0$$

$$\text{The total work}=\int_1^2 Vd_p-\int_2^3 Vd_p-\int_3^4 Vd_p$$

$$=-4.226+0.857+8.362$$
$$=4.993 \text{ kJ kg}^{-1} \text{ of dry air.}$$

Also the total work $=F_{1-4}+$ work of lifting water

$$=F_{1-4}+g\int_1^2 0.001\,m\,dh+g\int_3^4 0.001\,m\,dh$$

$$=4.908-0.07+0.155=4.993 \text{ kJ kg}^{-1} \text{ of dry air.}$$

The work of Natural Ventilation

$$=\left(-\int_1^2 VdP-\int_2^3 VdP-\int_3^4 VdP\right)-\int_4^5 VdP$$

$$=4.993-4.84=0.153 \text{ kJ kg}^{-1} \text{ of dry air.}$$

$\therefore$N.V.P. $=\frac{0.153}{0.95}=0.161$ kPa=161 Pa with respect to the air density at the fan inlet.

For a flow-rate of 150 m^3 s^{-1} at the fan inlet ($V=0.95$ m^3 kg^{-1}), the mass flow-rate of dry air

$$=\frac{150}{0.95}=157.895 \text{ kg s}^{-1}.$$

$\therefore$The power of the fan$=4.84\times157.895=764.21$ kW.

The pressure drop in the mine due to frictional work

$\Delta P=4.908/0.95=5.166$ kPa.

$\therefore$The resistance of the mine

$$=\frac{\Delta P}{Q^2}=\frac{5166}{150^2}=0.2296 \text{ N s}^2\text{m}^{-8}.$$

EXERCISE 5

5.1 The following are the barometer and psychrometer readings in different parts of a mine. Calculate the natural ventilating pressure, if the shafts are 300m deep.

Location	d.b. temperature, K	w.b. temperature, K	Barometer reading, kPa
Upcast shaft-top	304.5	304.5	101.06
Upcast shaft-bottom	306	305	104.39
Downcast shaft-top	297	288	101.06
Downcast shaft-bottom	301	294.5	104.39

Scanned with CamScanner

5.2 The upcast and downcast shafts at a mine are 800m deep and are similar aerodynamically (of same dimensions, nature of lining and equipment). The downcast shaft is used for hoisting from the bottom level while the upcast shaft from an intermediate level at a depth of 100m from the surface. The flow in the shaft is 6000 $m^3\ min^{-1}$ above the 100m level and 3000 $m^3\ min^{-1}$ below it. Water gauges at separation doors at 100m level and 800m level read 125.75mm and 135.9mm respectively while the fan-drift water gauge reads 127mm. Calculate the resistance of the shafts in Wb. as well as in S.I. units per 100m and the N.V.P. at the bottom level. Assume the N.V.P. to be in proportion of the depth of shafts. Take $g=9.8\ m\ s^{-2}$.

5.3. The following temperatures were measured in a mine 320m deep. Calculate the quantity of air that will flow through it due to natural ventilation if the mine has a resistance of 0.24 $N\ s^2\ m^{-8}$. The surface barometer reads 98.66 kPa and the barometric pressure rises by 1.15 kPa per 100m depth.

Temperature at the top of the downcast shaft	=301 K
Temperature in the intake to the bottommost level workings	=302 K
Temperature in the return of the above-mentioned workings	=306 K
Temperature in the surface fan drift	=305.5 K

Assume the mine to be dry.

5.4 A fan circulates 8500 $m^3\ min^{-1}$ of air through a mine at a fan drift pressure of 1.25 kPa. The flow through the mine reduces to only 2900 $m^3\ min^{-1}$ when the fan is stopped. Calculate the natural ventilating pressure.

CHAPTER VI

MECHANICAL VENTILATION

Natural ventilation alone is often inadequate and unreliable for mine ventilation. It is subject to much less control than mechanical ventilation. Artificial aids to natural ventilation are inefficient and often inapplicable. Hence mechanical ventilation is a common practice in almost all mines today. In the early days, common mechanical ventilators were the bellows, paddle wheels or reciprocating compressors, all of which were limited in capacity. This led to the development of centrifugal fans which were initially of the slow-rotating types and hence were extremely large and unwieldy in size. Today however, the commonly used mine fans are of both centrifugal and axial-flow types, the latter being more popular.

6.1 THEORY OF CENTRIFUGAL FANS

A centrifugal fan essentially consists of an impeller, rotor or wheel rotating inside a volute casing. The impeller, in turn, consists of several blades or vanes mounted on a central hub over the driving shaft. When the impeller rotates, air is drawn into it at the hub and is discharged at the periphery into the casing. Fig. 6.1 indicates an impeller of a centrifugal fan in which

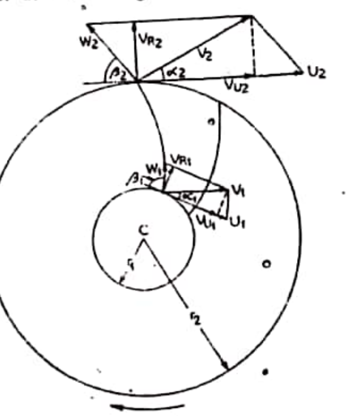

Fig. 6.1 Velocity triangles at the inlet and outlet of a centrifugal impeller.

U = the peripheral velocity of the impeller in m s^{-1},
V = the absolute velocity of flow in m s^{-1},
W = the relative velocity of flow in m s^{-1}, i.e. velocity of air relative to that of the impeller so that V is the resultant of W and U,
V_R = radial component of the absolute velocity of flow,
V_U = tangential component of the absolute velocity of flow,
r_1 = radius of the impeller inlet in m,
r_2 = radius of the impeller outlet in m,

and subscripts 1 and 2 indicate the flow conditions at the entrance and discharge of the impeller respectively.

Now consider a quantity of air Q passing through the impeller per unit time. The mass of this air is equal to $Q\rho$ kg s^{-1} where Q=quantity in m^3 s^{-1} and ρ=density of air in kg m^{-3}. This mass of air rotates in the impeller about the axis C. The torque τ causing this motion is given by the rate of change of angular momentum or moment of momentum from the inlet to the outlet of the impeller. The moment of momentum of air at the impeller inlet is equal to $Q\rho V_{U1}r_1$ since it is only the tangential component $Q\rho V_{U1}$ of the linear momentum $Q\rho V_1$ which is effective, the radial component $Q\rho V_{R1}$ having no moment about C. Similarly the moment of momentum of air at the impeller outlet is equal to $Q\rho V_{U2}r_2$. Or, the change of the moment of momentum from the impeller inlet to the impeller outlet, which is also the rate of change of moment of momentum since the change takes place in unit time, is equal to

$$Q\rho(V_{U2}r_2-V_{U1}r_1)$$

Or,

$$\tau=Q\rho(V_{U2}r_2-V_{U1}r_1) \text{ J} \tag{6.1}$$

The work done in the unit time or the power required to cause the motion that is power input to the impeller vanes is equal to the torque multiplied by angular velocity.

$$\text{Or,} \quad P=Q\rho\omega(V_{U2}r_2-V_{U1}r_1) \text{ W} \tag{6.2}$$

where ω = angular velocity in rad s^{-1}
and P = power input to the impeller vanes.

$$\text{Or,} \quad P=Q\rho(V_{U2}U_2-V_{U1}U_1) \tag{6.3}$$

since $\omega r=U$.

So, the theoretical head or the input head generated by the impeller

$$H_i=P/Q\rho g=(V_{U2}U_2-V_{U1}U_1)/g \text{ m} \tag{6.4}$$

where g=acceleration due to gravity in m s^{-2}. The above equation is know as Euler's equation. Now, if α is the angle between the directions of the absolute velocity of flow V and the tangential velocity U, equation 6.4 can be written as

$$H_i=(V_2U_2\cos\alpha_2-V_1U_1\cos\alpha_1)/g \tag{6.5}$$

since $V_{U2}=V_2\cos\alpha_2$
and $V_{U1}=V_1\cos\alpha_1$.

Also from the velocity triangles shown in Fig 6.1

$$W^2=U^2+V^2-2UV\cos\alpha$$

$$\text{or,} \quad UV\cos\alpha=(U^2+V^2-W^2)/2. \tag{6.6}$$

Substituting the above value of $UV\cos\alpha$ in equation 6.5 we get

$$H_i=\frac{U_2^2+V_2^2-W_2^2}{2g}-\frac{U_1^2+V_1^2-W_1^2}{2g}$$

$$=\frac{V_2^2-V_1^2}{2g}+\frac{U_2^2-U_1^2}{2g}+\frac{W_1^2-W_2^2}{2g} \tag{6.7}$$

The above equation shows that the input head is divided into three parts

(a) $\frac{V_2^2-V_1^2}{2g}$ which is the head representing gain in kinetic energy,

(b) $\frac{U_2^2-U_1^2}{2g}$ which is the head due to centrifugal force,

[Consider a small volume of air (Fig. 6.2) of a thickness dr and a unit cross-sectional area rotating about an axis C at a distance r from C. The volume of air=dr and its mass=$dr\rho$.

So, the centrifugal force acting on it=$dr\rho\omega^2r$. Since this force acts on unit area, it is also the centrifugal pressure which when expressed in terms of height of air column or head is equal to $dr\omega^2r/g$. The total centrifugal head developed as the air passes from the impeller inlet to discharge is equal to

$$\int_{r_1}^{r_2}\frac{dr\omega^2r}{g}=\frac{\omega^2r_2^2-\omega^2r_1^2}{2g}=\frac{U_2^2-U_1^2}{2g}\Bigg]$$

and (c) $\frac{W_1^2-W_2^2}{2g}$ which suggests a head conversion due to change of relative velocity from W_1 to W_2.

Scanned with CamScanner

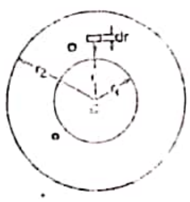

Fig. 6.2 Figure illustrating development of a centrifugal head in an impeller

However, no physical meaning can be attached to the last two terms, since the centrifugal head is not exactly equal to $(U_2^2-U_1^2)/2g$, as no particle of air moves at the peripheral speeds U_1 and U_2 and no diffusion takes place in a curved channel. It is thus convenient to take the last two terms jointly to represent an increase of pressure from the inlet to the outlet of the impeller.

It may, however, be noted here that the velocities used in Euler's equation are assumed to represent the average velocities over the cross-section perpendicular to the direction of flow. This assumption is not correct in practice though it has to be made for theoretical studies and design purposes. Since the true velocities are unknown, the value of H_t in Euler's equation as calculated from average velocities is usually higher than the true input head; or, in other words, the power input as calculated from Euler's equation is not the same as the true power input. So, to distinguish this theoretical head calculated from Euler's equation from the true input head, some authors designate it as Euler's head H_e. Equation 6.4 is then written as

$$H_e = \frac{V_{U2}\, U_2 - V_{U1}\, U_1}{g} \tag{6.8}$$

Now, if β is the external angle between the directions of W and U, then

$$V_U = U - V_R \cot\beta \tag{6.9}$$

Or, equation 6.8 becomes

$$H_e = \frac{U_2\,(U_2 - V_{R2}\cot\beta_2)}{g} - \frac{U_1\,(U_1 - V_{R1}\cot\beta_1)}{g} \tag{6.10}$$

Further assuming that the air has no prerotation before entering the impeller or, there is meridional entry into the impeller as shown diagrammatically in Fig. 6.3, we have

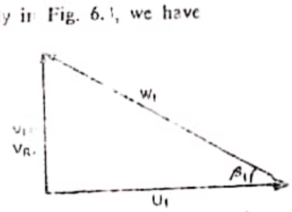

Fig. 6.3 Velocity triangle for meridional entry.

$$H_e = H_{e2} = \frac{U_2^2 - U_2 V_{R2}\cot\beta_2}{g} \tag{6.11}$$

since $\qquad V_{U1}=0$ and $V_{R1}=V_1$

In the above equation, U_2 is obtained from the rotational speed and the diameter of the impeller; β_2, from the inclination of vanes and V_{R2}, from the quantity of air flowing.

$$U_2 = 2\pi r_2\, n = \omega r_2 \tag{6.12}$$

where n = speed of the impeller in r.p.s.

Also, $V_{R2} = Q$/area of discharge of impeller $= Q/(2\pi\, r_2\, B)$ (6.13)

where B = width of impeller in m.

Or, $\qquad V_{R2} \propto Q$ for a particular impeller.

6.1.1 Theoretical Characteristics

Now plotting H_e against V_{R2} or Q we get the theoretical head characteristic of the fan. Equation 6.11 represents a straight line which cuts the H_e axis at U_2^2/g and the V_{R2} axis at

$$\frac{U_2^2}{g} \div \frac{U_2\cot\beta_2}{g} = U_2\tan\beta_2$$

which represents the maximum theoretical capacity. The slope of the line depends on the value of the angle β_2. U_2^2/g is the maximum

Scanned with CamScanner

head possible and is called the *theoretical shut-off head* which is the head developed when no air passes through the fan, or $Q=0$. The actual shut-off head H_s is, however, much less and bears a constant ratio with U_2^2/g ($H_s \doteq 0.585\ U_2^2/g$ for blowers of all specific speeds and discharge angles, β_2). For radial-bladed fans, i.e. for $\beta_2=\pi/2$ rad (90°), $H_e=U_2^2/g=$ constant, or the variation of quantity at constant speed of rotation of the impeller does not affect the Euler's head (see Fig. 6.4).

For $\beta_2<\pi/2$ rad (backward-bladed fans), cot β_2 is positive, or H_e decreases with increase of V_{R2} whereas for $\beta_2>\pi/2$ rad, cot β_2 is negative and hence H_e increases with increasing V_{R2}.

Where air enters the impeller with prerotation, we have at the inlet

$$H_{e1}=\frac{U_1^2 - U_1 V_{R1} \cot \beta_1}{g} \qquad (6.14)$$

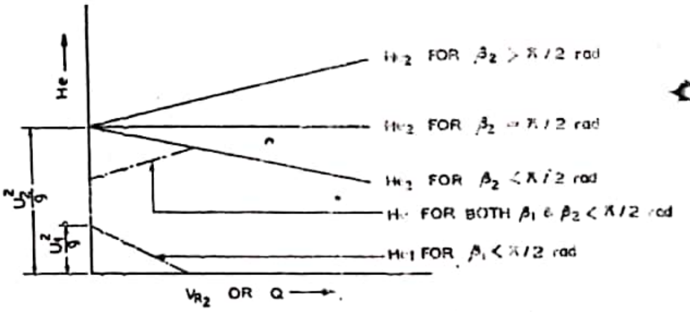

Fig. 6.4 Theoretical head characteristics of centrifugal fans.

This equation is similar to equation 6.11 and gives a similar straight-line characteristic cutting the H_e axis at U_1^2/g. It is illustrated by the broken line in Fig. 6.4 for $\beta_1<\pi/2$ rad. The characteristics for other values of β_1 are similar to those for the outlet condition. Equation 6.14 can be plotted on the H_e—V_{R2} diagram by suitably converting V_{R1} in the form of V_{R2} from the relation

$$\frac{V_{R1}}{V_{R2}}=\frac{\text{area of impeller outlet}}{\text{area of impeller inlet}}=\frac{2\pi r_2 B_2}{2\pi r_1 B_1}=\frac{r_2 B_2}{r_1 B_1} \qquad (6.15)$$

where B_1 and B_2 are the widths of the impeller at the inlet and outlet respectively.

Euler's head characteristic for the fan can then be obtained by deducting H_{e1} from H_{e2} to obtain H_e for various values of V_{R2} and then plotting H_e against V_{R2} (as shown by the line of dots and dashes in Fig. 6.4).

The theoretical power input to the fan can be obtained by multiplying H_e by $Q\rho g$, or in other words, by KV_{R2} where K is a constant depending on the impeller and density of air. For conditions assumed in equation 6.11, theoretical power

$$P_a = K\frac{(U_2^2 V_{R2}-U_2 V_{R2}^2 \cot \beta_2)}{g} \qquad (6.16)$$

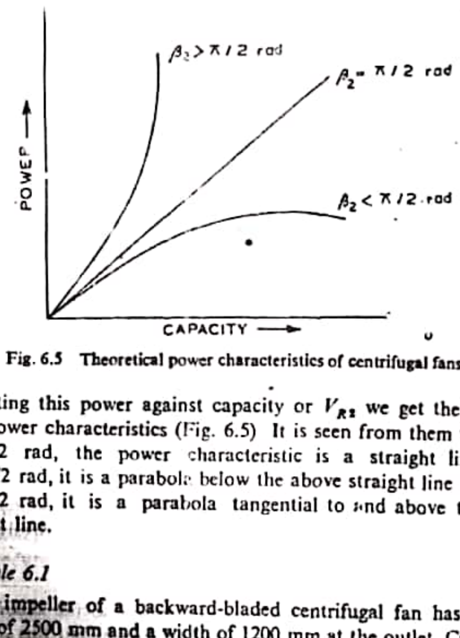

Fig. 6.5 Theoretical power characteristics of centrifugal fans.

Plotting this power against capacity or V_{R2} we get the theoretical power characteristics (Fig. 6.5). It is seen from them that for $\beta_2=\pi/2$ rad, the power characteristic is a straight line. For $\beta_2<\pi/2$ rad, it is a parabola below the above straight line and for $\beta_2>\pi/2$ rad, it is a parabola tangential to and above the said straight line.

Example 6.1

The impeller of a backward-bladed centrifugal fan has a diameter of 2500 mm and a width of 1200 mm at the outlet. Calculate the maximum theoretical head the fan will develop when rotating at a speed of 1760 rad min^{-1} (280 r.p.m.). Assume meridional entry into the impeller. What will be the theoretical head developed

Scanned with CamScanner

by the fan when circulating 50 m³ of air per second if the outlet vane angle is 1.13 rad ? What is the maximum theoretical capacity of the fan ?

Tangential outlet velocity $U_2 = \omega r_2 = \frac{1760}{60} \times \frac{2.5}{2} = 36.67$ m s⁻¹.

Maximum theoretical head $= U_2^2/g = 36.67^2/9.8 = 137.2$ m of air column $= 137.2 \times 1.2 \times 9.8 = 1613.5$ Pa,

assuming the density of air to be equal to 1.2 kg m⁻³.

At $Q = 50$ m³ s⁻¹, $V_{R2} = Q/(\pi D_2 B) = 50/(3.14 \times 2.5 \times 1.2)$
$= 5.308$ m s⁻¹.

Therefore theoretical head $H_e = (U_2^2 - U_2 V_{R2} \cot \beta_2)/g$
$= (36.67^2 - 36.67 \times 5.308 \times \cot 1.13)/9.8$
$= 127.83$ m of air column $= 1503.3$ Pa.

V_{R2} for maximum theoretical capacity $= U_2 \tan \beta_2$
$= 36.67 \times \tan 1.13 = 77.64$ m s⁻¹.

Therefore maximum theoretical capacity
$= 3.14 \times 2.5 \times 1.2 \times 77.64 = 731.37$ m³ s⁻¹.

6.1.2 Efficiencies

In practice, theoretical characteristics of a fan are never achieved due to various losses in the machine which can be classed as (a) hydraulic losses, (b) mechanical losses and (c) leakage losses. Hydraulic losses consist of losses due to skin friction and diffusion in the impeller and the rest of the passage between the two measuring points at the inlet and outlet of the fan and shock losses or eddy and separation losses at the impeller inlet and outlet, all of which contribute to the loss of head. *Hydraulic efficiency* is then defined as the ratio of the available total head to the input head.

$$\text{Or, } \eta_h = \frac{H}{H_i} \quad \frac{H_i - \text{hydraulic losses}}{H_i} \tag{6.17}$$

The ratio of the input head to Euler's head is usually referred to as *vane efficiency*, although there is no actual loss involved.

$$\text{Or, } \eta_{va} = \frac{H_i}{H_e} \tag{6.18}$$

Sometimes the ratio of the actual total head to the theoretical or Euler's head is termed as *manometric efficiency*, but this has no physical meaning, and hence serves no useful purpose

$$\eta_{man} = \frac{H}{H_e} = \eta_h \times \eta_{va} \tag{6.19}$$

Some (McFarlane[20], Hartman[21]) define manometric efficiency as the ratio of the actual head developed to the velocity head of air moving at the fan tip speed,

i.e $\eta_{man} = \frac{H}{U_2^2/2g}$ which is in fact twice the *head coefficient* defined later.

Leakage through clearances between the rotating and stationary parts of a turbo-machine causes capacity losses. If Q=actual developed capacity of the fan and Q_L=leakage capacity loss, then the *volumetric efficiency* is given by the relation

$$\eta_v = \frac{Q}{Q + Q_L} = \frac{Q}{Q_i} \tag{6.20}$$

Mechanical losses are losses of power due to friction at bearings and disc friction which though strictly a hydraulic phenomenon is grouped with mechanical losses since it is external to the flow through the fan and does not incur a loss of head. *Mechanical efficiency* is thus the ratio of the power actually absorbed by the impeller and converted into head to the power applied to the shaft.

$$\text{Or, } \eta_m = \frac{\text{input power} - \text{mechanical losses}}{\text{input power}}$$

$$= \frac{Q_i H_i \rho g}{\text{input power}} \tag{6.21}$$

The *gross* or *total efficiency* is the ratio of the power in the air to the input power (it is often called mechanical efficiency though obviously the term is not quite appropriate).

$$\text{Or, } \eta = \frac{QH\rho g}{\text{input power}} = \eta_h \times \eta_v \times \eta_m \tag{6.22}$$

Total efficiency is usually calculated on the basis of total head but when calculated on the basis of static head, it is called *static efficiency*. It is the total efficiency which is however used in design procedure.

6.1.3 Fan Characteristics

The most important characteristic of a fan is the head-capacity characteristic which determines its applicability to a particular mine characteristic, the other characteristics such as of efficiency-capacity and input power-capacity being of secondary importance.

Scanned with CamScanner

Attempts have been made to theoretically calculate hydraulic losses in a fan so as to predict its actual performance, which can help immensely in projecting new designs of fans ; but partly due to the inaccuracy in the estimation of hydraulic losses owing to the constant variation of the direction of air velocity in the impeller and the shape and size of the channel, and partly due to the availability of sufficient data today for estimating characteristics from existing types, approximate theoretical characteristics serve no useful purpose. However, a knowledge of the hydraulic losses in an impeller does help in understanding the nature of the actual head-capacity characteristic of a fan as compared to its theoretical characteristic.

As has been already said, the hydraulic losses in a fan include (a) the skin friction and diffusion losses in the impeller and the rest of the fluid path and (b) the eddy and separation losses at the impeller inlet and outlet. Some eddy losses also occur due to recirculation in the space between blades. This loss is very small when the fan runs at full capacity but becomes significant for operation at low volumes.

Friction loss in a channel can be obtained from the formula

$$h_f = fLv^2/2gD \qquad (6.23)$$

where

f = resistance coefficient,

D = mean equivalent diameter of the flow channel
= 4 × area/perimeter,

L = length of channel

and v = velocity at the section with mean equivalent diameter.

Because of the variation of the values of L and D for various parts of the flow channel and difficulties in their actual measurement as well as the problem of selecting a suitable friction coefficient f, the friction loss for the whole fluid path is usually expressed as a function of the quantity Q.

Or, $h_f = K_1Q^2$, where K_1 is a constant.

Similarly the diffusion losses can be expressed as

$$h_d = K_2Q^2$$

where K_2 again is a constant for a given type of machine.

Since both friction and diffusion losses vary as Q^2, they can be combined as $h_{fd} = K_3Q^2$ (6.24)

This equation is in the form of a parabola about the head axis.

In a given machine, the eddy and separation losses are a minimum for a particular capacity Q_s called the *shockless capacity* where the impeller inlet and outlet velocities agree with the vane angles. Any increase or decrease of the capacity causes increased shock loss. The shock loss is usually expressed as a function of the difference between the quantity and the shockless capacity.

Or, $h_s = K_4(Q - Q_s)^2$ (6.25)

The above equation is in the form of a parabola with its apex at Q_s.

Combining these two losses, we get the total hydraulic losses as shown in Fig. 6.6. It should be noted that the *best efficiency point* (b.e.p.) or the point of minimum hydraulic loss lies to the left of the shockless capacity since it is a function of both the friction and shock losses. Subtracting the hydraulic losses from the input head we get the actual head.

Or, $H = H_t - K_3Q^2 - K_4(Q - Q_s)^2$ (6.26)

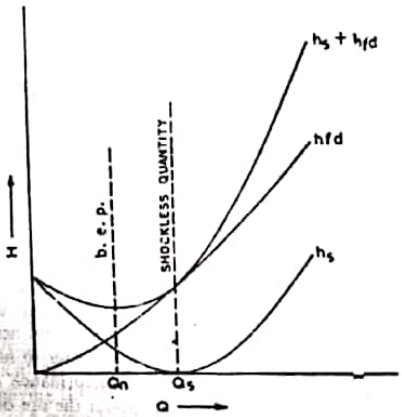

Fig. 6.6 Hydraulic losses in an impeller.

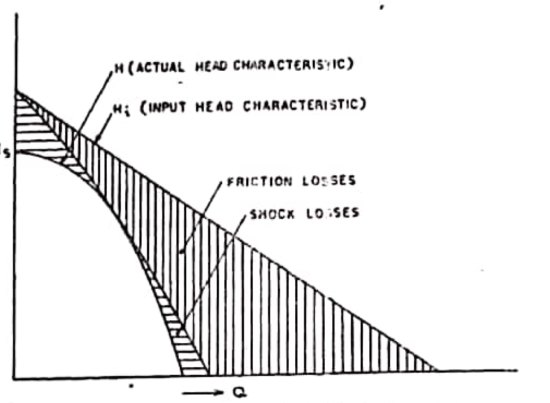

Fig. 6.7 Actual head characteristic of centrifugal fans.

This is graphically represented in Fig. 6.7. The H_i curve is plotted by fixing the point of its intersection with the Q axis at $Q=KV_{R2}=KU_2 \tan \beta_2$ which is the maximum capacity at zero head (the H_e and H_i curves intersect at zero head). The other point on the H_i curve is determined from the actual characteristic curve of a similar machine. The values of K_3 and K_4 are also determined from an actual characteristic curve, but these values are found to be inconsistent from fan to fan and even along the same curve.

The actual head can be expressed in the form

$$H=A\omega^2+B\omega Q+CQ^2 \tag{6.27}$$

where A, B, C are constants depending on fan design. The above equation gives the head-capacity curve for a constant speed, but for similar reasons as stated above, the equation is not of much practical use.

Actual characteristics are therefore drawn from test data on fans and hold good for other geometrically similar fans. The pressure, power and efficiency characteristics of fans are customarily drawn by the manufacturers on the basis of fan total head or pressure. But from the user's point of view it is better to have the fan static-pressure characteristic so that the performance of the fan alone connected to a mine or system (without the use of an evasee or diffuser) can be directly obtained. Even when a part of the velocity pressure of the fan is recovered in an evasee, the relevant characteristic is the combined fan static-pressure and evasee-pressure (recovery) characteristic.

Fan velocity-pressure characteristics are often provided alongwith fan total-pressure characteristics by the manufacturer so that fan static-pressure characteristics can be easily drawn by subtracting the velocity pressure from the total pressure for different quantities. Even otherwise the fan velocity-pressure characteristic can easily be drawn from a knowledge of the cross-sectional area of the fan outlet.

Figs. 6.8, 6.9 and 6.10 give typical actual characteristic curves[10] for forward-bladed, radial-bladed and backward-bladed fans respectively based on fan static pressure. The pressure or head characteristics of radial- and backward-bladed fans rise at first, but soon start falling with increase of capacity. On the other hand, the head characteristic of forward-bladed fans falls at first with increasing capacity until it flattens out or even shows a rising trend before starting to fall again. This indicates a lower loss of head at low capacities with forward-bladed fans as compared to the other types. This is mainly due to the forward-bladed fans having a large number of blades which help in reducing recirculation and the consequent losses. In all the types however, the operating point should be fixed to the right of the aerodynamic stall point P which is the point of reverse flexure, for at capacities less than this the performance of the fan becomes unstable and there occurs fluctuation of air velocity characterized by throbbing and noise. The power curves of both forward- and radial-bladed fans are rising, but this is not really a serious disadvantage if the operating point does not vary, or in other words, if the system characteristic does not change. The power characteristic of the backward-bladed fan is non-overloading in nature thus making the fan more suitable for operation over a wide range of quantity without the motor getting overloaded. The efficiency characteristics of all centrifugal fans are usually with a flat peak which means that good efficiency is maintained over a wide range of operation.

The major difference amongst the three types of fans is in their *head coefficient* ψ, the forward-bladed fan having the maximum head coefficient, the radial-bladed coming next and the backward-bladed fan having the least. For this reason, the tip speed required for developing a given head is about 35% higher with radial-bladed

Scanned with CamScanner

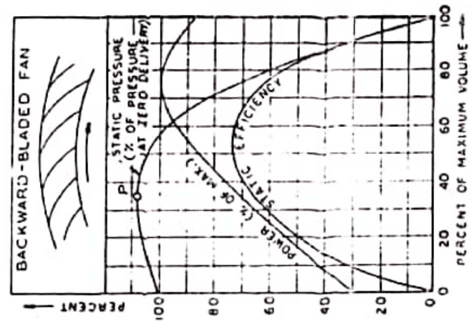

Fig. 6.10 Characteristics of a backward-bladed centrifugal fan (*after MacFarlane*).

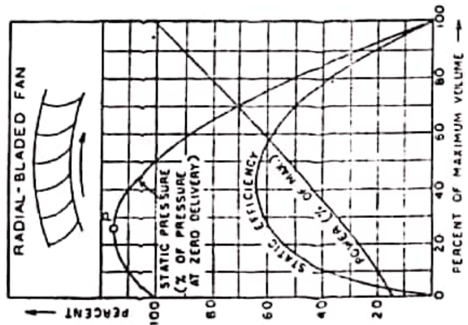

Fig. 6.9 Characteristics of a radial-bladed centrifugal fan (*after MacFarlane*).

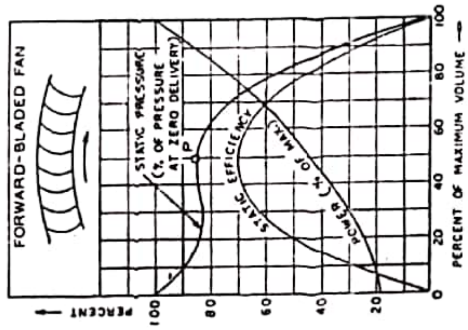

Fig. 6.8 Characteristics of a forward-bladed centrifugal fan (*after MacFarlane*).

fans and about 75% higher with backward-bladed fans than with forward-bladed fans. Normal welded and riveted construction with steel permits a maximum tip speed of 100 m s^{-1} which limits the maximum head developed to about 15 kPa in forward-bladed fans, 8 kPa in radial bladed fans and 4.8 kPa in backward-bladed fans. With special material and design of construction, the tip speed can be raised to 150 m s^{-1} which means that a forward-bladed fan can produce a pressure of 34 kPa, a radial-bladed one, 18 kPa and a backward-bladed fan 10.8 kPa. This necessarily means that the diameter of the fan and the rotational speed should progressively increase from forward- to backward-bladed fans in order to get a given duty of head. The capacity at a given static head for a certain wheel diameter is the highest with forward-bladed fans, intermediate with backward-bladed fans and the least with radial-bladed fans and hence from this point of view, the fan diameter for a given head-capacity duty is the least with forward-bladed fans, intermediate with backward-bladed ones and the largest with radial-bladed fans.

Table 6.1 lists the distinctive features of the three types of fans of ordinary steel plate construction.

Table 6.1[92]: Comparison of the Different Types of Centrifugal Fans.

	Forward-bladed	Radial-bladed	Backward-bladed
Number of blades	24-64	4-24	8-16
Internal eye diameter	0.87 D	0.5-0.75 D	0.65-0.8 D
Max. width (single-inlet)	0.56 D	0.35-0.45 D	0.25-0.3 D
Commercial size	76-3350mm	1520-2540mm	3050-3350mm
Peak head coefficient (based on static pressure)	1.1-1.3	0.55-0.7	0.35-0.4
Tip speed for 250 Pa pressure	13.7-12.7 m s^{-1}	19.5-17.3 m s^{-1}	24.4-22.8 m s^{-1}
Peak static efficiency	65-75%	60-75%	70-80%*
Trend of power characteristic	rising	rising	non-overloading
Wheel dia. D	minimum	maximum	intermediate
Space requirement	minimum	maximum	intermediate
Operating speed	minimum to moderate	moderate to minimum	maximum
Noise	least	intermediate	maximum

* Modern backward-bladed fans with aerofoil-section vanes made of steel sheets formed into a hollow fabricated construction are capable of developing static efficiencies as high as 82-83%.

Scanned with CamScanner

6.2 DESIGN OF CENTRIFUGAL FANS

The design or selection of a fan for a given set of conditions is based on affinity laws which give the relationship between the head, capacity, speed and size of the fan. These laws, established experimentally, are well borne out by theoretical laws of dynamic similitude obtained from the dimensional analysis of the variables affecting fan performance (for details see Reference 93). These laws are :

(a) When the speed of a given fan is changed, its head varies as the square of the speed, capacity (at impeller outlet), directly as the speed and power, as the cube of the speed.

or,
$$\frac{H_1}{H_2}=\frac{\omega_1^2}{\omega_2^2} \tag{6.28}$$

$$\frac{Q_1}{Q_2}=\frac{\omega_1}{\omega_2} \tag{6.29}$$

and
$$\frac{P_1}{P_2}=\frac{\omega_1^3}{\omega_2^3} \tag{6.30}$$

where ω=speed, H=head, P=power,

Q = capacity and subscripts 1 and 2 refer to the original and the new speed respectively.

(b) In case of two geometrically similar impellers (i.e., of the same specific speed) operating at the same speed, their heads are in the ratio of the square of the impeller outside diameter D, their capacities, in the ratio of D^3 and their power, in the ratio of D^5.

or,
$$\frac{H_1}{H_2}=\left(\frac{D_1}{D_2}\right)^2 \tag{6.31}$$

$$\frac{Q_1}{Q_2}=\left(\frac{D_1}{D_2}\right)^3 \tag{6.32}$$

and
$$\frac{P_1}{P_2}=\left(\frac{D_1}{D_2}\right)^5 \tag{6.33}$$

Equation 6.28 can be combined with equation 6.31 to give

$$\frac{H_1}{H_2}=\frac{\omega_1^2 D_1^2}{\omega_2^2 D_2^2} \tag{6.34}$$

or, $\frac{H}{\omega^2 D^2}$=constant for geometrically similar impellers. This term when multiplied by g is termed the *specific head*, which is a dimensionless characteristic describing the performance of an impeller.

Similarly combining equations 6.29 and 6.32 we have

$$\frac{Q_1}{Q_2}=\frac{\omega_1 D_1^3}{\omega_2 D_2^3} \tag{6.35}$$

or, $\frac{Q}{\omega D^3}$=constant for geometrically similar impellers. This term, called the *specific capacity*, is another dimensionless characteristic describing the performance of an impeller.

(c) When the diameter of an impeller is reduced (but not the width) at a given speed, its head decreases in the ratio of the square of the diameter, capacity, directly as the diameter and power, as the cube of the diameter. These relationships are, however, approximate, particularly for a large reduction in the impeller diameter. It must be noted that the two impellers in this case are not geometrically similar.

6.2.1 Specific Speed

Specific speed n_s, as defined by equation 6.36 is an important design factor and is used as a 'type number' for grouping impellers hydraulically. The specific speed of all geometrically similar impellers is the same and does not vary with variations in fan speed.

$$n_s=\frac{nQ^{\frac{1}{2}}}{H^{\frac{3}{4}}} \tag{6.36}$$

where Q and H represent the capacity and head at the best efficiency point in $m^3\ s^{-1}$ and m respectively and n is the speed in r.p.s.

When designing an impeller for a given head-capacity duty, first the rotational speed is fixed depending on the type and cost of drive (a higher rotational speed results in a smaller fan and cheaper drive). This, in turn, fixes the specific speed. Next step is to find

Scanned with CamScanner

out a suitable fan type from existing designs which has this specific speed at optimum efficiency, and a suitable head-capacity curve. Then the dimensions of the new impeller are obtained by applying either equation 6.34 or equation 6.35. It may be worth noting here that specific speeds of most centrifugal fans of high efficiency lie between 0.64 and 1.8 while the usual specific speed for axial-flow fans is about 4.5.

For a new design of an impeller, design factors established experimentally have to be used. Having fixed the specific speed as above, the next step is to decide on the impeller vane outlet angle β_2. This selection is based on the steepness of the head-capacity curve, operating range and the output desired for a given diameter at the selected speed of the impeller. It may be noted here that both head and capacity increase with β_2 or, in other words, high head and capacity can be obtained with a lower diameter and hence a lower peripheral speed of the impeller as β_2 increases ; but the efficiency falls with increasing β_2. It has been found with centrifugal pumps that optimum efficiency is obtained at $\beta_2=0.44$ rad (25°) and as it increases to 0.5π rad (90°), efficiency falls by 5 to 10 points. The same holds true for fans too. Knowing specific speed and β_2, two other vital dimensionless design factors, the head coefficient ψ and the capacity coefficient ϕ can be obtained from Fig. 6.11 which was prepared by Stepanoff[89] for centrifugal blowers and is found to hold good for certain designs of modern axial-flow and centrifugal fans. The figure gives the plot of dimensionless specific speed ω_s, instead of n_s. However, ω_s can be obtained from n_s from equation 6.38 by assuming a suitable b_2/D_m ratio (see Fig 6.12). In practice b_2 varies from 10% to 40% of D_m in centrifugal fans.

$$n_s=\frac{\text{r.p.s}\sqrt{\text{m}^3/\text{s}}}{\text{m}^{\frac{3}{4}}}=3.1275\left(\frac{b_2}{D_m}\right)^{\frac{1}{2}}\left(\frac{D_{ave}}{D_m}\right)^{\frac{1}{2}}\frac{\phi^{\frac{1}{2}}}{\psi^{\frac{3}{4}}} \quad (6.37)$$

(for derivation see Ref. 89)

For centrifugal fans, $D_{2i}=D_{2o}$ or $D_m=D_{ave}$ so that the ratio D_{ave}/D_m is equal to unity. The value differs from unity only in case of high specific speed axial-flow impellers as for example,

$$(D_{ave}/D_m)^{\frac{1}{2}}=0.964$$

for $n_s=4$.

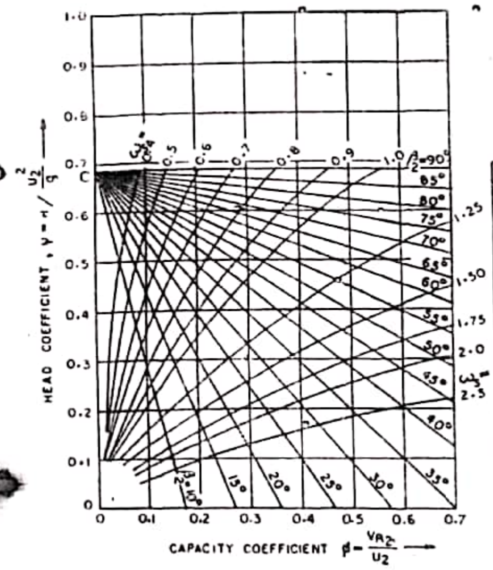

DEGREE	RADIAN
10°	0·175
15°	0·262
20°	0·349
25°	0·437
30°	0·524
35°	0·611
40°	0·698
45°	0·786
50°	0·873
55°	0·960
60°	1·048
65°	1·135
70°	1·222
75°	1·310
90°	1·397
85°	1·484
90°	1·571

Fig. 6.11 Values of ϕ and ψ for various values of β_2 and ω_s (*after Stepanoff*).

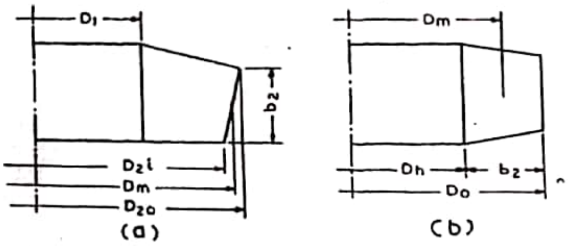

Fig. 6.12 D_m and D_{ave} of impellers :
(a) Centrifugal blower—$D_m^2=(D_{2i}^2+D_{2o}^2)/2$, $D_{ave}=(D_{2i}+D_{2o})/2$;
(b) Axial-flow fan—$D_m^2=(D_o^2+D_h^2)/2$, $D_{ave}=(D_o+D_h)/2$.

Scanned with CamScanner

Again, for similar impellers, the ratio b_2/D_m is constant so that the ratio $\phi^{\frac{1}{2}}/\psi^{\frac{3}{4}}$ gives a dimensionless type number defining the specific speed n_s. This ratio is called the *dimensionless specific speed* ω_s. Equation 6.37 can then be written as

$$n_s = 3.1275 \left(\frac{b_2}{D_m}\right)^{\frac{1}{2}} \left(\frac{D_{ave}}{D_m}\right)^{\frac{1}{2}} \omega_s \tag{6.38}$$

6.2.2 Head and Capacity Coefficients

These are dimensionless design constants which are found to form a continuous function of specific speed at a certain value of β_2 for a continuous row of fans of consistent design. The head coefficient is the ratio of the head at the operating point (best efficiency point) to Euler's head at zero capacity U_2^2/g.

Or

$$\psi = H \Big/ \frac{U_2^2}{g} \tag{6.39}$$

The capacity coefficient is defined by equation 6.40.

$$\phi = \frac{V_{R2}}{U_2} \tag{6.40}$$

A chart similar to that in Fig. 6.11 can be drawn from test data of any particular fan design (b_2/D_m). This is done as follows : The point $\phi = \tan \beta_2$ is marked on the ϕ axis and is connected to the point depicting the ψ and ϕ of the fan. The extension of this line will cut the ψ axis at a point corresponding to C in Fig. 6.11. This line can then give the design constants ψ and ϕ for fans with the given value of β_2 for any specific speed. Similar lines for other values of β_2 can be obtained by joining the point C with points representing $\tan \beta_2$ on the ϕ axis. Specific speeds (ω_s) for different points (ψ, ϕ) on any β_2 line can be obtained from the relation

$$\omega_s = \phi^{\frac{1}{2}}/\psi^{\frac{3}{4}}.$$

The ω_s lines on the chart are then drawn by interpolation. It must be noted here that such a chart will hold good contingent on the fact that other minor design factors such as impeller hub ratio, number of vanes and casing design are not altered to a great extent.

Knowing ψ, U_2 can be obtained from equation 6.39 and from U_2, D_2 can be found out with the help of the following equation :

$$U_2 = \pi D_2 n = \omega \cdot \frac{D_2}{2} \tag{6.41}$$

Next, V_{R2} is found from ϕ by using equation 6.40 and from b_2 the width of the impeller outlet is found by using the relation

$$V_{R2} = \frac{Q}{\pi D_2 b_2} \tag{6.42}$$

It should be noted here that the ratio b_2/D_2 so obtained must agree with the ratio previously assumed. b_2/D_2 can, however, be estimated from special charts showing the values of b_2/D_2 for various values of n_s and β_2 for the given fan type.

In Fig. 6.13, the head coefficient is plotted on the y-axis and the capacity coefficient on the x-axis. The Euler's head curve will cut the ψ-axis at $\psi = 1$, or $H_e = U_2^2/g$, and the ϕ-axis at $\phi = \tan\beta_2$ or $V_{R2} = U_2 \tan \beta_2$. The angle it will make with the ψ-axis, i.e. $\angle OYZ$ will then be equal to β_2 since $OY = 1$. The Euler's outlet-velocity triangle for a capacity ϕ will then be represented by the triangle OXY. However, this triangle is only theoretical in nature. The actual outlet-velocity triangle $OX'Y$ is obtained by plotting X' from the values of ψ and ϕ of the fan being designed and connecting it to O and Y. In this velocity triangle, OX' gives V_2 (actual absolute outlet velocity) and α_2, its angle of discharge into the volute. These two factors determine the design of the volute casing.

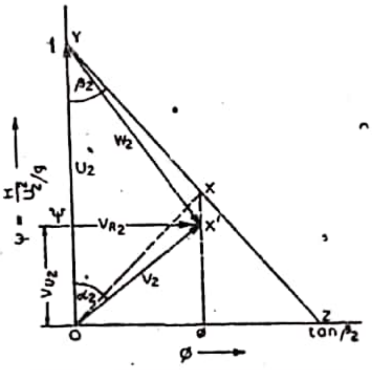

Fig. 6.13 Construction of the actual outlet velocity triangle.

By consulting Fig. 6.14 which gives the value of the volute velocity distribution factor $R_{v3}=V_3/V_2$ for different values of α_2,

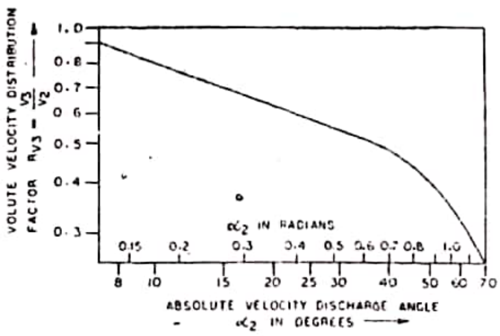

Fig. 6.14 Volute velocity distribution factors for various values of α_2 (*after Stepanoff*).

the suitable value of V_3 (the volute throat velocity) for the above values of V_2 and α_2 can be obtained and the volute throat area then decided upon from the relation : impeller capacity = volute capacity

or,
$$V_{R2}\,A_2 = V_3\,A_v \tag{6.43}$$
where A_2 is the impeller outlet area $=\pi D_2\,b_2$, and A_v is the volute throat area.

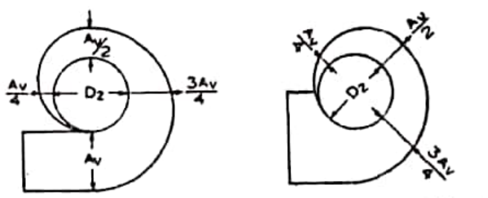

Fig. 6.15 Design of volute casing.

Then the design of a normal or abbreviated volute can be done as shown in Fig. 6.15. The normal volute is preferred for better efficiency, though where size of the fan is to be minimal, i.e. where

space is the main consideration, an abbreviated volute may be used. The final step is the establishment of the inlet-velocity triangle from which the value of β_1 can be obtained.

Usually in fan design practice, the ratio V_{R1}/V_{R2} varies from 1.3 for low specific speed fans (n_s=0.35) to nearly unity for fans with $n_s \geqslant 2.2$ or axial-flow fans. A suitable value of this ratio is selected depending on the specific speed of the fan being designed and the value of V_{R1} established thereform.

Also, V_{R1} is usually taken as equal to or slightly greater than the velocity through the impeller eye.

or
$$V_{R1} \geqslant \frac{4Q}{\pi D_1^2} \tag{6.44}$$

From the above equation and the relation $V_{R1}=Q/\pi D_1\,b_1$, D_1 and b_1 can be found and knowing D_1, U_1 can be calculated from the relation $U_1=\pi D_1\,n=\omega D_1/2$.

Now for efficiency, the ratio of the pitch-per-second P_{1s}, or the absolute entrance velocity for meridional entrance and the meridional velocity V_{R1} should be from 1.15 to 1.25. This ensures a nominal prerotation at the impeller entrance. Selection of the above ratio fixes P_{1s}. Then the inlet velocity triangle is constructed as shown in Fig. 6.16. Angle OXY in this triangle gives the angle β_1.

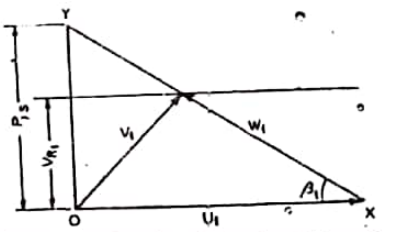

Fig. 6.16 Construction of the inlet velocity triangle.

The number of vanes is usually calculated by using the formula
$$\frac{l}{t} = 4.75\psi \tag{6.45}$$

Scanned with CamScanner

where l=the vane true length,

$t = \pi D_1/Z$

and Z=the number of vanes.

The number of vanes in small fans, however, is invariably less.

6.2.3 Design of Forward-bladed, Multi-vane Sirocco-type Fans

These fans represent a class by themselves. They are suitable for developing a high head for a particular size, the head coefficient for the b.e.p. operation of such fans being 1.1 for smaller units to 1.2 for larger ones ; but their efficiency is low compared to the backward-bladed centrifugal fans. These fans have an impeller diameter varying between 75mm and 3300mm and the average specific speed is round about 1.0 based on static head in metres of air column for single-inlet impellers. With double-inlet type, the capacity is doubled or n_s is multiplied by $\sqrt{2}$. Their efficiency based on static head is about 70%. One of the great drawbacks of the forward-bladed impulse type of fan is its limited range of operation. The fan becomes noisy on both sides of the best efficiency point. Besides, at higher pressures, the stall point is reached soon whereas at low heads the drive may become overloaded due to the sharply rising power-capacity characteristic.

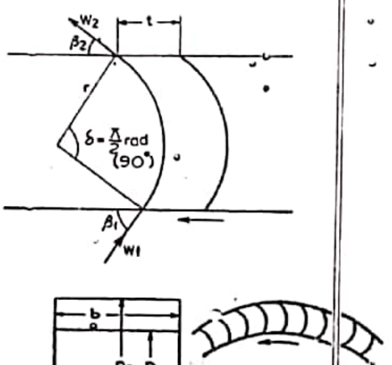

Fig. 6.17 Design factors of sirocco-type fan.

The mechanical and hydraulic design elements of impulse fans are well established within narrow limits so much so that designing such fans is a very easy affair.

Referring to Fig. 6.17, the radius of curvature of the vane is so fixed that $\delta=\pi/2$ rad and the inlet and outlet vane angles β_1 and β_2 are fixed by the ratio of D_1 and D_2 as follows :

$$\tan\beta_1 = \frac{D_2}{D_1} \text{ and } \tan\beta_2 = \frac{D_1}{D_2}$$

The ratio D_1/D_2 is usually taken between 0.8 and 0.95, the commonest ratio used being 0.875 for which β_1=0.86 rad (49°) and β_2=0.72 rad (41°). Now for designing a fan for an operative head H and capacity Q, we can base our design on head coefficient ψ which is known.

U_2 can be found out from ψ by using equation 6.39

Now $$U_1 = \omega D_1/2 = \frac{\omega D_1/2}{D_1/D_2} = \frac{\omega D_1/2}{0.875} \tag{6.46}$$

Sirocco-type fans are usually designed for meridional entry into the impeller as illustrated by the inlet velocity triangle shown in Fig. 6.3. It is clear from the figure that

$$V_{R1} = U_1 \tan\beta_1 = \frac{U_1}{D_1/D_2} = \frac{\omega D_1/2}{D_1/D_2} = \frac{\omega D_1/2}{0.875}$$

or, $$Q = V_{R1}\,\pi D_1 b = \frac{\pi D_1^2\,\omega b}{2\times 0.875} \tag{6.47}$$

For normal-capacity impulse wheels, the area of impeller inlet and that of the impeller eye should be equal or,

$$\pi D_1\, b = \frac{\pi D_1^2}{4}$$

or, in other words, $$b = \frac{D_1}{4} \tag{6.48}$$

An increase of the impeller width beyond this value will increase the capacity but not in proportion to the impeller width, and the efficiency may also fall. In practice however, one often finds widths varying from 0.4 D_1 to 0.8 D_1 for single-inlet fans.

Scanned with CamScanner

Substituting the value of b from equation 6.48 in equation 6.47, we get

$$Q = \frac{\pi D_1^3 \omega}{7} \tag{6.49}$$

The values of ω and D_1 can be found from equations 6.46 and 6.49.

If it is desired to limit ω or fix it on the basis of other considerations, D_1 can be calculated from equation 6.46. The only variable now in equation 6.47 for suitably adjusting Q to the desired capacity is b. In such a case however, the relation between b and D_1 as given in equation 6.48 will not hold good.

The number of vanes can be calculated from the equation

$$Z = \pi D_2/t \tag{6.50}$$

where Z = number of vanes
and t = vane spacing.

t is usually taken as $0.7\,r$ to $1.0\,r$ for large fans (about 760mm or more in diameter) and $2\,r$ to $2.5\,r$ for small fans, where r is the vane radius and is given by

$$r = (D_2 - D_1)/(2\sqrt{2}) \tag{6.51}$$

In practice, the number of vanes vary from 24 in small fans to 64 for larger ones with 760mm or larger impeller diameters.

Design of impellers for centrifugal fans is usually adjusted for simple construction by welding steel-plate parts. Such designs neither permit a good impeller approach nor any guidance inside the impeller to turn the flow through $\pi/2$ rad. Some improvement in efficiency can be achieved by using a conical hub and a venturi inlet. For minimizing leakage loss and hence bettering efficiency, there should be as little gap between the side of the stationary casing and the rotating impeller as possible. This is particularly so with low-specific-speed fans, though with high-specific-speed fans, which are of low-head and high-capacity type, this is not so very important. The maximum gap allowed between the impeller and the impeller inlet is of the order of 3mm for fans of about 760mm size (backward-bladed). It must be noted that proper axial alignment of the inlet and the wheel with minimal clearance between the two is very essential for backward-bladed fans, whereas forward-, and to a less extent, radial-bladed fans are less critical of such a provision.

6.2.4 Volute Design

The general equation of a volute spiral is

$$\theta = K \log \frac{r}{r_o} \tag{6.52}$$

where r is the distance of the casing from the centre of the wheel at any point at an angle θ from the zero point where $r = r_o$ = radius of the wheel + the minimum clearance between the wheel and the casing, and K is a constant.

The normal volute generally becomes too large. For this reason, commercial volutes are usually of the abbreviated design. The standard volute design (Fig 6.18) which is adopted for all fans by the National Association of Fan Manufacturers, U.S.A. and serves them remarkably equally is based on the relation

$$A_v = 1.5\,D^2 \tag{6.53}$$

where D is the diameter of the impeller.

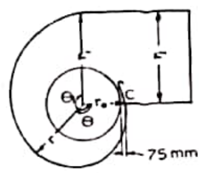

Fig. 6.18 Volute design.

This relation allows for a velocity head of only 10% of the static head at the volute throat. A clearance of, say, 75mm is maintained at the start of the scroll.

Referring to Fig. 6.18, at $\theta = 0$, $r_o = \frac{D}{2} + 75$mm and at θ_1, $r_1 = \sqrt{A_v}$ (assuming a square throat).

Therefore $$\theta_1 = K \log \frac{r_1}{r_o}$$

or, $$3\pi/2 = K \log \frac{\sqrt{A_v}}{\frac{D}{2} + 75} = K \log \frac{\sqrt{(1.5\,D^2)}}{\frac{D}{2} + 75} \tag{6.54}$$

Knowing D, the value of K can be determined from equation 6.54. This can then be substituted in the general equation of the spiral $\theta = K \log \frac{r}{r_o}$ to get the values of r at various values of θ for accurate construction of the scroll.

Usually a cut-off sheet C is extended up to 10-40% (the former for backward-bladed and the latter for forward-bladed fans) of the uncovered part following the trend of the spiral. The clearance between the tip of the cut-off sheet and the wheel is from 75-125mm with 900mm diameter fans, its value increasing or decreasing with larger or smaller-diameter fans. Exact proportion is unnecessary as noise rather than performance determines this distance. From noise point of view, the clearance between the tip of the cut-off sheet and the fan wheel should not be less than 7% of the wheel diameter. For the same reason, i.e. to reduce noise, the tip of the cut-off sheet is usually rounded or blunted.

Example 6.2

A single-inlet centrifugal fan, 0.95m in diameter and 0.3m in width rotating at a speed of 30π rad s^{-1} (15 r.p.s.) delivers $11.7 m^3$ of air per second at a pressure of 1.43 kPa at the b.e.p. It is required to design a fan to deliver 50 $m^3 s^{-1}$ at a pressure of 300 Pa.

If we take a geometrically similar fan, i.e. of the same specific speed, we have

$$n_s = \frac{15\sqrt{11.7}}{\left(\dfrac{1430}{1.2\times 9.8}\right)^{\frac{3}{4}}} = 1.4 = \frac{n\sqrt{50}}{(25.5)^{\frac{3}{4}}}$$

since 300 Pa = 25.5m air column of a density of 1.2 kg m^{-3}.

Or, $\quad n = 2.25$ r.p.s., or, $\omega = 4.5\pi$ rad s^{-1}

From equation 6.34 $\quad \dfrac{1430}{300} = \dfrac{30^2 \times (0.95)^2}{(4.5)^2 \times D_2^2}$,

or, $\quad D_2 = 2.9$m.

Hence the diameter of the fan will be fairly large. On the other hand if a higher speed of say 14π rad s^{-1} (7 r.p.s.) is assumed for the fan, then

$$n_s = \frac{7\sqrt{50}}{(25.5)^{\frac{3}{4}}} = 4.36$$

or, $\quad \omega_s = \dfrac{4.36}{3.1275\,(b_2/D_m)^{\frac{1}{2}}}$ (from equation 6.38, assuming D_{ave}/D_m to be equal to one).

or, $\quad \omega_s = \dfrac{4.36}{3.1275\,(0.3/0.95)^{\frac{1}{2}}} = 2.48.$

Now from Fig. 6.11

$\psi = 0.16$ and $\phi = 0.36$, if β_2 is taken as equal to 0.44 rad (25°). It may be noted here that in the first fan $\psi = 0.58$ and $\phi = 0.30$.

Now, $\psi = \dfrac{H}{U_2^2/g}$ or, $0.16 = \dfrac{25.5\times 9.8}{U_2^2}$ or, $U_2 = 39.5$ m s^{-1}

or, $\quad D_2 = \dfrac{2U_2}{\omega} = \dfrac{U_2}{\pi n} = \dfrac{39.5}{3.14\times 7} = 1.8$m.

The diameter could be further reduced by assuming a higher value of β_2. Note that the specific speed of the new fan is large suggesting that an axial-flow fan would be a better choice.

6.3 AXIAL-FLOW FANS

In general, axial-flow fans are machines with high capacity, low head and very high specific speed. Mostly they have a single stage, though for high heads, two- or three-stage fans are used in order to keep size and speed within reasonable limits. In view of the low head produced by axial-flow impellers, losses due to skin friction or drag losses become quite significant, necessitating proper streamlining and polishing of the impeller vanes. For this reason as well as for considerations of strength, vanes of axial-flow impellers take the form of aerofoils.

So far the design of axial-flow fans has generally been based on tested aerofoil sections, but today there are sufficient design data available for axial-flow fans which enable the designer to adopt the conventional design procedure used for centrifugal blowers and fans for axial-flow fans too. This involves the fixing of the specific speed and the vane angles at the various radii of the axial-flow impeller. Impellers so designed with either thin-plate vane section or aerofoil section do not show much variation in efficiency, but thin plates do not always have the necessary strength and hence aerofoil sections are selected. However, the vane thickness is gradually reduced from hub outwards, since thinner

Scanned with CamScanner

aerofoils have a higher lift-drag ratio. Thicker vanes, on the other hand, result in separation and noise with high-pressure and high-speed impellers. The maximum value of lift coefficient C_L is obtained at a vane thickness of 12% of the chord length l, the value decreasing for higher or lower thicknesses.

6.3.1 Aerofoils

Fig. 6.19 indicates an aerofoil which consists of a certain thickness of material concentrated about a mean line shown by dots and dashes. All good aerofoils have nearly the same variation of thickness along the mean line, the maximum thickness however being different for different profiles. For a detailed treatment of the geometry of aerofoil profiles the reader is referred to the N.A.C.A. technical reports on aerofoils. Aerofoil sections as used in aircraft wing design, which also have been used in the design of mine fans, have been adequately dealt with in Chapter VI of 'Theory of Flight' by Von Mises. The maximum distance from the mean line to chord l is called the vane camber (G in Fig 6.19) which is usually expressed as a percentage of l. It is also customary to state the position of the camber along the chord (as defined in the figure by l_c).

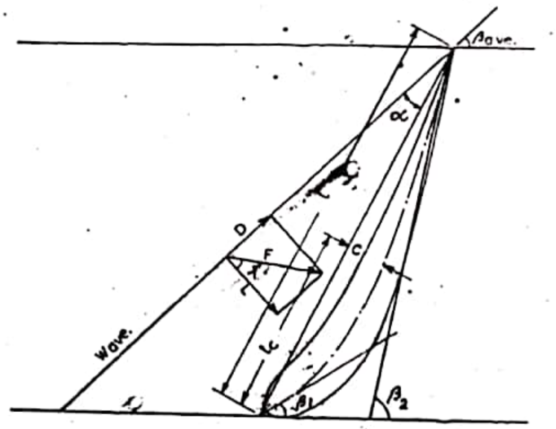

Fig. 6.19 An aerofoil (diagrammatic).

Angle α is called the angle of attack, i.e. the angle between the chord of the aerofoil and the direction of the average relative velocity of air W_{ave}.

The force F acting on an aerofoil exposed to air-flow can be divided into two components, one D, the drag component along the direction of W_{ave} and the other L, the lift component at right angles to it. The angle λ between F and L is called the gliding angle. These forces L and D can be evaluated from the formulae

$$L = C_L b l \rho W_{ave}^2 \tag{6.55}$$

and

$$D = C_D b l \rho W_{ave}^2 \tag{6.56}$$

where C_L and C_D are experimental coefficients called lift and drag coefficients respectively,

l=chord length,

b=width of aerofoil (or the vane length in a fan),

W_{ave}=undisturbed relative air velocity

and ρ=density of air.

Both C_D and C_L depend mainly on the aerofoil profile and the angle of attack α, which again is dependent on the values of β_1 and β_2.

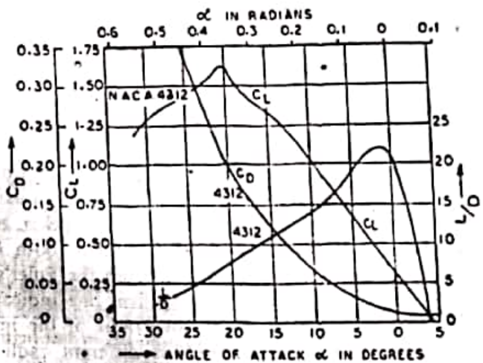

Fig. 6.20 Variation of lift and drag coefficients with angle of attack (*NACA report No. 460*)

Scanned with CamScanner

Fig 6.20 shows the values of C_D and C_L as well as of L/D for various values of α for a particular aerofoil. The L/D curve can be likened to the efficiency characteristic of a fan. Whereas lift contributes to the head generated by the fan, the drag component causes loss due to skin friction and eddies in the wake behind the vane. Hence it is necessary to have a high L/D ratio and the angle of attack should be fixed accordingly.

The theoretical head developed by the axial-flow fan is also given by Euler's equation

$$H_e = \frac{U_2 V_{U2}}{g} \qquad (6.57)$$

or,

$$H_e = \frac{U_2(U_2 - W_{U2})}{g} = \frac{U_2^2}{g} - \frac{U_2 W_{U2}}{g} \qquad (6.58)$$

Where U_2 is the tip speed of the impeller (see Fig 6.21).

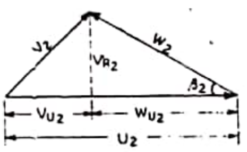

Fig. 6.21 Euler's outlet velocity triangle.

At zero capacity, $W_{U2}=0$,

$$H_e = U_2^2/g \qquad (6.59)$$

The above equations represent the condition at the tip of the vane or the outer diameter of the impeller (note that in axial-flow impellers, $U_2 = U_1$). At any other diameter of the impeller, both U_2 and W_{U2} change (for a normal design of impeller, both U_2 and W_{U2} vary directly as the diameter) and so does the Euler's head. This is illustrated in Fig. 6.22 where the firm line indicates the Euler's head at zero capacity for various radii of the impeller. The dotted line gives the Euler's head at different radii for a particular flow represented by W_{U2}. Both of these curves are square parabolas.

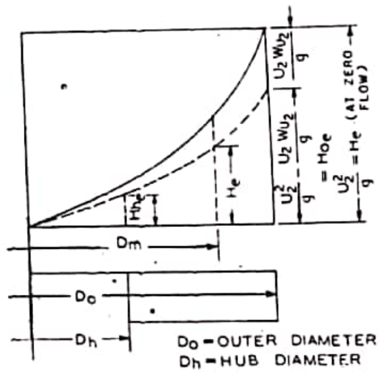

Fig. 6.22. Head generated at different diameters of an axial-flow impeller.

The head distribution along the radii is similar for both centrifugal and axial-flow fans, but in centrifugal fans, all particles of air entering at the hub or inlet leave the impeller at the outlet, or, in other words, they attain the outlet or peripheral Euler's head before leaving the impeller. In axial-flow fans however, a particle of air entering at a radius leaves the impeller at the same radius. So the heads developed at different radii are different, the impeller total head being an integrated average which is given by

$$H_e = \frac{H_{oe} + H_{he}}{2} \qquad (6.60)$$

Where H_{oe} and H_{he} are the heads at the periphery and the hub respectively.

This head occurs at the mean diameter $D_m \left(D_m = \sqrt{\frac{D_h^2 + D_o^2}{2}} \right)$ and so, for design purposes, the outlet conditions for an axial-flow impeller are taken at the mean diameter. As is evident, the integrated Euler's head in an axial-flow fan is much less than that in a centrifugal fan of the same size and that is why axial-flow fans have to run at a higher speed in order to produce the necessary head.

Scanned with CamScanner

6.3.2 Design of Axial-Flow Fans

All theoretical discussions and practical design of axial-flow fans assume a constant axial velocity through the impeller and this fact is corroborated by experimental results. A forced vortex theory of flow which is found to be the best suited for axial-flow fan design demands that (a) both inlet and outlet pitch remain constant for different radii so as to maintain a uniform axial velocity at all radii and (b) the outlet pitch be greater than the inlet pitch to provide the impelling action.

Pitch P at a certain diameter D is defined by the equation

$$P_1 = \pi D \tan \beta_1 \tag{6.61}$$

or,

$$P_2 = \pi D \tan \beta_2 \tag{6.62}$$

subscripts 1 and 2 indicating the inlet and outlet conditions respectively.

Multiplying both sides of equation 6.61 by the speed in r.p.s., we have

$$P_1 \times (\text{r.p.s.}) = \pi D\,(\text{r.p.s.}) \tan \beta_1$$

or,

$$P_{1s} = U \tan \beta_1 \tag{6.63}$$

where P_{1s} is the inlet pitch-per-second.

Writing equation 6.63 for the hub and outer diameter conditions, we have

$$P_{1s} = U_h \tan \beta_{1h} \tag{6.64}$$

and

$$P_{1s} = U_o \tan \beta_{1o} \tag{6.65}$$

Equations 6.64 and 6.65 define the inlet velocity triangles. With an axial inlet velocity, $P_{1s} = V_R$ or the velocity triangles are as given in Fig. 6.23, but with prerotation at inlet, the velocity triangles become as shown in Fig 6.24. However, an axial entry is usually assumed for axial-flow fan design.

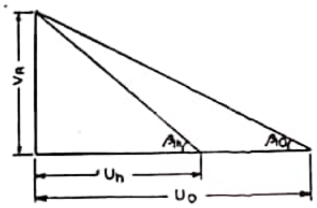

Fig. 6.23 Inlet velocity triangles with axial inlet velocity.

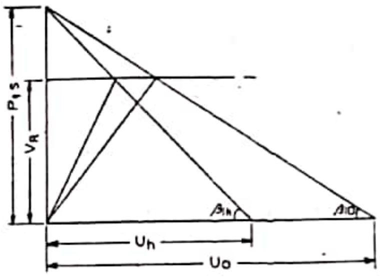

Fig. 6.24 Inlet velocity triangles with prerotation at the inlet.

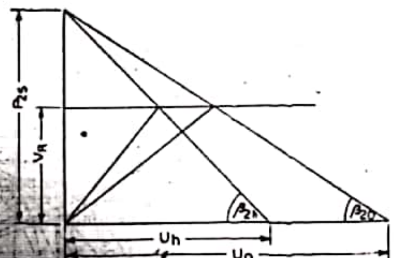

Fig. 6.25 Outlet velocity triangles.

The velocity triangles for the outlet conditions are given in Fig 6.25. It should be noted here that for providing impelling action the impeller vane angle should increase gradually from inlet to outlet i.e. $\beta_2 > \beta_1$ or, $P_{2_t} > P_{1_t}$. The ratio P_{2_t}/V_R is called the impelling ratio and is assumed as a design constant in axial-flow fan design.

Similar to the design of centrifugal fans, the design of a single-stage axial-flow fan for a given head-capacity condition starts by assuming the speed (r.p.s.) which in its turn fixes the specific speed. Since single-stage axial-flow fans have no inlet guide vanes, the entry to the impeller is axial. For such a condition, the design values of the head coefficient and capacity coefficient as given in Fig. 6.11 hold good for axial-flow fans.

After fixing the specific speed, the impeller hub ratio $\psi = D_h/D_o$ is read off from the hub ratio-specific speed chart (Fig. 6.26). The dimensionless specific speed ω_s can then be obtained from the relation

$$n_s = 2.2\,\omega_s \left[\frac{(1-\psi^2)}{(1+\psi^2)}\right]^{\frac{1}{2}}$$

(this relationship can be derived from equation 6.38 by substituting the values of b_2, D_m and D_{ave} as shown in Fig. 6.12) in order to enter Fig 6.11. For the selected hub ratio, the chord spacing ratio l/t is determined from the equation

$$l/t = 4.75\psi \qquad (6.66)$$

and the number of vanes Z, from the empirical relation

$$Z = 6\psi/(1-\psi) \qquad (6.67)$$

or,

$$Z = 6\,\frac{D_h}{D_o - D_h} = \frac{3D_h}{b} \qquad (6.68)$$

where b=vane length. Table 6.2 gives the number of vanes for different hub ratios according to this relation.

Table 6.2 : Number of Vanes for Different Hub Ratios

Hub ratio	0.3	0.4	0.5	0.6	0.7	0.8
Number of vanes	3	4	6	9	14	24

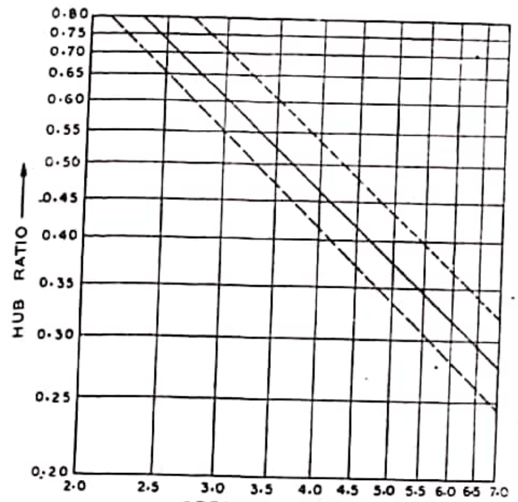

Fig. 6.26 Hub ratio vs specific speed—dotted lines indicate the limits of variation (*after Stepanoff*).

Now a value of β_2 is assumed. It is usually assumed at 0.44 rad (25°); though a higher value of β_2 gives a higher output for a given size of machine (values of β_2 as high as $\pi/4$ rad (45°) are often used in auxiliary fans). It may be noted here that by altering the

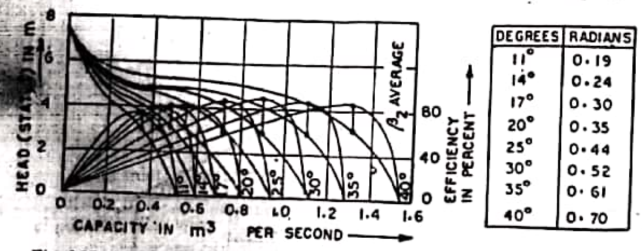

Fig. 6.27 Performance of a 500mm dia four-vane impeller running at 28.67 rads⁻¹ (860 r.p.m.) at various vane angles (*after Stepanoff*).

vane setting (which means the alteration of both β_1 and β_2 through the same amount) the capacity of the fan can be increased without practically any variation in the head as shown in Fig. 6.27. This clearly indicates that the head developed by the axial-flow fan is almost entirely dependent on the vane angle difference, i.e $\beta_2 - \beta_1$. That is why where the quantity requirement varies over a wide range, it is preferable to have a variable-pitch axial-flow fan. β_2 in this case refers to the mean effective diameter condition.

Now from Fig. 6.11 values of ψ and ϕ are calculated for the given n, and β_2 and from them the values of U_m (the tangential velocity of the impeller at the mean effective diameter D_m) and D_m can be calculated as for centrifugal fans. From D_m and the hub ratio, values of D_o and D_h can be calculated using the relation

$$D_m = \sqrt{\frac{D_h^2 + D_o^2}{2}} \qquad (6.69)$$

Then from ϕ, $V_{Rm} = V_R$ is calculated, knowing U_m. It is to be noted here that the hub ratio as computed from the ψ-n, chart may have to be adjusted so as to satisfy the equation $Q = V_R \, \pi D_o^2 \, (1-\psi^2)/4$. Having known U_m and β_2, the Euler's discharge velocity triangle ABC for the mean diameter is drawn as shown in Fig. 6.28. Velocity triangles for other values of U at various radii are also drawn and from them the values of β_2 for the different radii found out. Two such triangles A_hBC_h and A_oBC_o representing the hub and outlet conditions are plotted in Fig. 6.28.

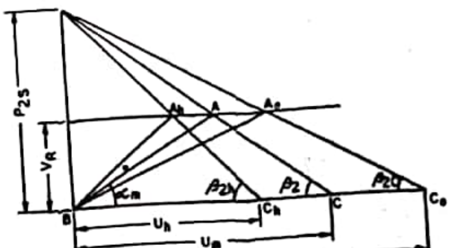

Fig. 6.28 Euler's discharge velocity triangles for different diameters.

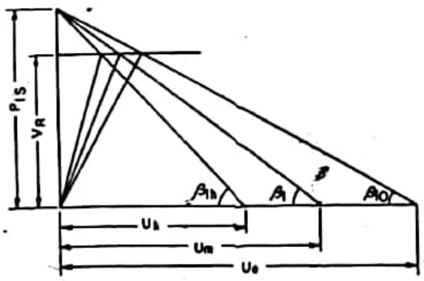

Fig. 6.29 Inlet velocity triangles for different radii.

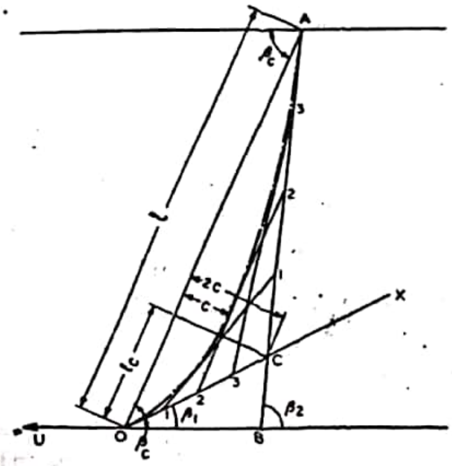

Fig. 6.30 Munk's method of drawing vane profile.

The inlet velocity triangles (Fig. 6.29) are then drawn for the various radii. A value of P_{1s}/V_R=1.15 to 1.25 is assumed for this purpose. Knowing β_2 and β_1 for a particular radius, the vane profile, i.e. mean camber line can be drawn by using Munk's method illustrated in Fig. 6.30. l can be calculated from the value of l/t

ratio and Z. This value of l is for the mean diameter. Usually l decreases progressively from the hub to the tip of the impeller, its value at the hub being 1.25 to 1.3 times that at the tip. The chord l is now drawn from a point O (Fig. 6.30) at an angle β_c with the direction of U. β_c is determined from the relation

$$\beta_c = \beta_1 + \tan^{-1}\left(\frac{2C}{l_c}\right)$$

and C, from $\tan \beta_2 - \tan \beta_1 = \frac{2C}{l_c(1-l_c)}$

where l_c and C are expressed as fractions of chord length. A line OX is then drawn from O making an angle β_1 with the direction of U. From A at the other end of the chord, a line AB is drawn making an angle β_2 with the direction of U. Let AB and OX intersect at C. Now OC and CA are divided into equal number of parts. Let the dividing points be 1, 2, 3 etc. The corresponding dividing points on both lines OC and CA are now joined to form lines 1 1, 2 2, 3 3 etc. The mean camber line of the vane will then be tangential to all these lines.

Design of axial-flow fans on the basis of aerofoil theory also assumes several experimental design factors such as (1) hub ratio, (2) l/t ratio at each radius, (3) r.p.s. or specific speed, (4) axial velocity and (5) impeller diameter from experience. The design procedure then consists of selecting suitable aerofoil profiles and determining the vane settings or chord angles β_c at various radii, using the aerofoil theoretical head equation (equation 6.70).

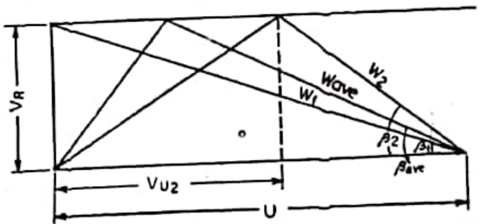

Fig. 6.31 Velocity triangles giving the values of of B_{ave} and W_{ave}.

$$C_L \frac{l}{t} = H_e \frac{2g}{W_{ave}^2} \cdot \frac{V_R}{U} \cdot \frac{\cos \lambda}{\sin (\beta_{ave} + \lambda)} \qquad (6.70)$$

where H_e, the theoretical head can be obtained from the relation $H_e = H/\eta_h$ (where η_h = hydraulic efficiency which has to be assumed). β_{ave} and W_{ave} can be obtained from the velocity triangle shown in Fig. 6.31 which can be drawn having known U, V_R and V_{U2}. V_{U2} is obtained from the Euler's equation

$$H_e = \frac{UV_{U2} - UV_{U1}}{g},$$

assuming $V_{U1} = 0$. W_{ave} is drawn for a value of V_U equal to $\frac{V_{U1} + V_{U2}}{2}$, or, in this case, $\frac{V_{U2}}{2}$.

Neglecting λ, equation 6.70 will give a value of C_L which is the determining factor in selecting a suitable aerofoil section.

6.3.3 Fan Casing

Fan casings are usually provided with fixed outlet guide vanes which are necessary for converting the tangential component of the absolute velocity of air leaving the impeller into pressure by mainly straightening the direction of flow to an axial one.

The curvature of diffuser vane or guide vane is so fixed that the fluid enters the guide passage with minimum loss which means that the angle between the guide vane inlet and the direction of the absolute velocity of air leaving the impeller should be equal to zero or as small as possible. As in the case of impeller vanes, the diffuser vane entrance angles are also laid out at different radii for a constant pitch P_3, so as to maintain a uniform axial flow at all radii.

It must be noted here that the angle of absolute velocity at the mean diameter α_m as represented in the Euler's velocity diagram (Fig. 6.28), is not the true one. The actual angle can be obtained by drawing a figure similar to Fig. 6.13 or from the relation $\tan \alpha'_m = \phi/\psi$. The actual impeller outlet velocity diagram can now be drawn (Fig. 6.32) from V_R, α_m and, of course, U_m. From this diagram, the values of α_o and α_h i.e. absolute velocity angles at outer diameter and hub respectively can be obtained. These will then be the guide vane inlet angles, the guide vane outlet angle being always $\pi/2$ rad so that the outlet velocity V has no tangential component.

Scanned with CamScanner

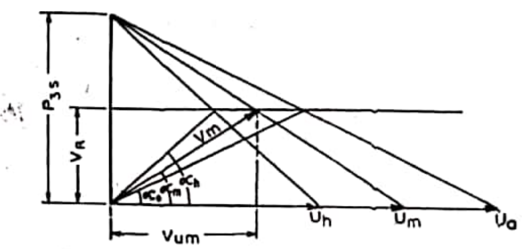

Fig. 6.32 Actual outlet velocity diagram for an axial-flow fan.

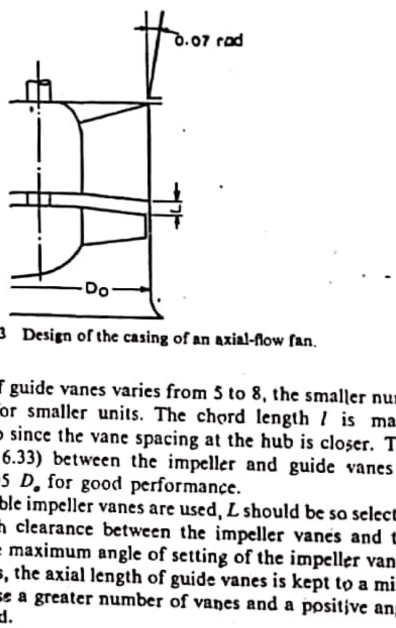

Fig. 6.33 Design of the casing of an axial-flow fan.

The number of guide vanes varies from 5 to 8, the smaller number being used for smaller units. The chord length l is made shorter at the hub since the vane spacing at the hub is closer. The distance L (Fig. 6.33) between the impeller and guide vanes is maintained at 0.05 D_o for good performance.

Where adjustable impeller vanes are used, L should be so selected as to give enough clearance between the impeller vanes and the guide vanes at the maximum angle of setting of the impeller vanes. For compact units, the axial length of guide vanes is kept to a minimum in which case a greater number of vanes and a positive angle of attack are used.

In addition to the provision of guide vanes, the casings are usually made of an expanding construction, the angle of divergence being 0.138 rad (Fig. 6.33), in order to further convert velocity head to static head. Tapering of the diffuser hub within the vaned part of the casing also helps in head conversion although its main purpose is to streamline the flow through the passage.

Sometimes instead of fixed guide vanes, another contra-rotating impeller may be provided in order to straighten out the flow. In such a case the fan should be considered as a two-stage fan as the total head developed by it is twice as much as would be developed by a single-stage fan. However, owing to difficulties of mechanical construction, such fans are not much used. These fans have adjustable vanes on both impellers so that by suitably adjusting them, a variation of capacity from 0.5 to 2 times the normal is possible.

6.3.4 Characteristics and Performance of Axial-flow Fans

Fig. 6.34 gives the characteristics of a fixed-vane axial-flow fan. In general, axial-flow fans are of higher efficiency than ordinary

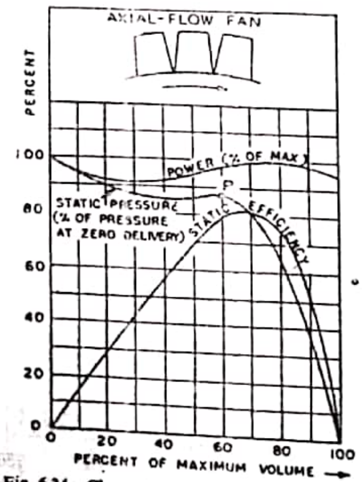

Fig. 6.34 Characteristics of an axial-flow fan (*after MacFarlane*).

centrifugal fans, although modern aerofoil-section backward-bladed fans can have equal or even greater (in case of high-head types) efficiency. The pressure characteristic of axial-flow fans is similar to that of forward-bladed fans, but the stall point occurs at a larger capacity, particularly at higher pitch (see Fig. 6.27) thus restricting the range of smooth operation of the fan to a narrower limit. Slight rise in mine resistance may lead to unstable operation of the fan. Should unstable operation develop, the mine resistance should be immediately lowered by short-circuiting the fan. More permanently however, the blade pitch should be changed or

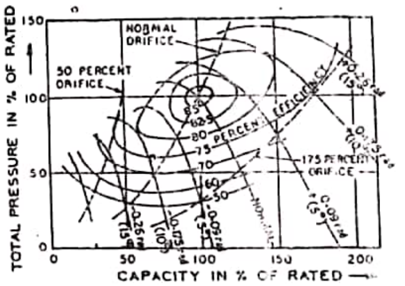

Fig. 6.35 Effect of the variation of blade angle on the performance of an axial-flow fan (*after MacFarlane*).

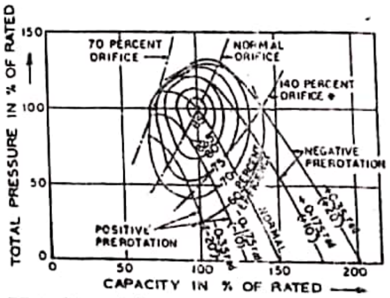

Fig. 6.36 Effect of the variation of inlet guide-vane angle on the performance of an axial-flow fan (*after MacFarlane*).

the mine resistance lowered. The power characteristic is of a non-overloading character and is fairly flat over a large range of duty. However, fixed-vane axial-flow fans have a limited range of efficient operation (as would be evident from the sharper peak of the efficiency curve) and hence are not suitable for operation over a wide range of mine resistance.

For covering a wider range of mine resistance, axial-flow fans can be fitted with adjustable blades whose angle can be varied up to ± 0.26 rad (15°). Fig. 6.35 shows the characteristics of an axial-flow fan at various blade angles. Another method is to have adjustable inlet guide vanes to give the air a certain amount of pre-rotation before it enters the impeller. The effect of variation in the inlet guide vane angle on the performance of the above fan is given in Fig. 6.36. A comparison of the two shows that the adjustment of blade pitch offers a wider range of efficient operation than that of inlet guide vanes. This is evident from the fact that with 75% as the limiting efficiency, the variation of blade pitch can cover a range of equivalent orifice of the mine from 50% to 175% of the normal whereas this range is only 70%-140% with adjustable inlet guide vanes. Besides, variable-pitch blades offer a larger volume range with a small variation in pressure while inlet guide vanes allow a wide range of pressure over a small volume range. Partial deblading helps in the reduction of flow as would be evident from Fig. 6.37. As in centrifugal fans, both quantity and pressure of an axial-flow fan can be varied by varying

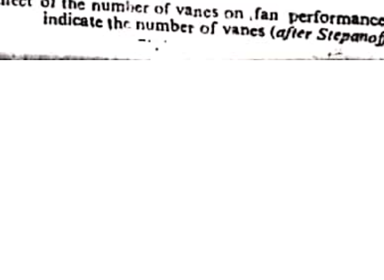

Fig. 6.37 Effect of the number of vanes on fan performance—figures indicate the number of vanes (*after Stepanoff*).

Scanned with CamScanner

the speed of the fan rotor with little variation of efficiency, if the system characteristic remains constant; but with varying system characteristic, the efficiency changes. In extreme cases, alteration in the duty of axial-flow fans can be achieved by changing the number of stages, or replacing the impeller for a new design. It may be noted that the same outlet static guide vanes also serve the new rotor with only a slight change in efficiency.

The greatest drawback of a screw-type axial-flow fan is its low head coefficient which requires that the tip speed be very high compared to a centrifugal fan for producing a given head. Tip speed can be increased by increasing either the diameter or the rotational speed. The latter is more practicable and is usually adopted. Sometimes it is an advantage, particularly in the case of a small fan, for then the fan can be directly driven by a motor and the capital cost of reduction gearing thus dispensed with. However, high tip speed necessitates stronger material of construction, the permissible tip speed for steel-sheet construction being 100 m s^{-1}. Aerofoil blades are usually constructed of strong silicon-aluminium alloy or manganese-bronze and sometimes of hollow fabricated stainless steel. High speed of revolution causes increase in noise. To minimize noise, the limiting tip speed in axial-flow fans is usually fixed at 70 m s^{-1}. This together with considerations of strength usually restricts the head per stage of axial-flow fans to 1-1.25 kPa. Hence for high heads, multi-stage axial-flow fans have to be used. Usually multi-stage axial-flow fans are made with a maximum of 3 stages which generate a head of about 3 kPa. Beyond this they become bulky and very costly. In such cases turbo-axial fans or aerofoil-section backward-bladed centrifugal fans may have to be chosen.

The greater popularity of axial-flow fans over backward-bladed centrifugal fans is mainly due to the flexible duty possible with the

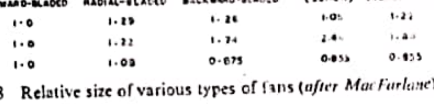

	FORWARD-BLADED	RADIAL-BLADED	BACKWARD-BLADED	AXIAL-FLOW (SCREW)	AXIAL-FLOW (TURBO-AXIAL)
DIAMETER	1·0	1·29	1·26	1·05	1·22
TIP SPEED	1·0	1·22	1·74	2·4[illegible]	[illegible]
POWER	1·0	1·08	0·875	0·855	0·855

Fig. 6.38 Relative size of various types of fans (*after MacFarlane*).

former, as well as the relatively small space occupied by it and its simpler housing. Fig. 6.38 gives the relative space occupied by various types of fans.

6.3.5 Turbo-axial Fans

These owe their origin to modification in the design of axial-flow fans for developing larger heads per stage. They are essentially single-stage fans capable of developing pressures up to 5 kPa. The vanes in this case are mounted on the curved portion of a dish-shaped hub (Fig. 6.39) instead of being mounted on a cylindrical hub, so that the air enters at moderate velocity through a large inlet area and leaves the rotor at a large velocity through a small outlet area. This causes most of the total head developed in this fan to be in the dynamic form which is subsequently converted to static head by a diffuser. The low static head developed in the rotor reduces recirculation so that rigorous control of the gap between the rotor and casing is not necessary. (It may be noted here that the clearance between the impeller and the casing of high-pressure axial-flow fans is of the order of 0.1% of the impeller diameter.) Special bearings to take up axial thrust as in the case of axial-flow fans become unnecessary. Besides, the rotors of these fans are usually of simpler plate-section construction and are lighter, though separately cast aerofoil blades of silicon-aluminium alloys are also used. These fans share the advantage of simple housing and easy installation of axial-flow fans while their efficiency equals that of axial-flow fans. At the same time they generate a much higher head than a single-stage axial-flow fan.

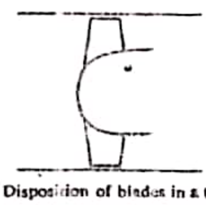

Fig. 6.39 Disposition of blades in a turbo-axial fan.

The disadvantages of the turbo-axial fans lie in their inflexible operation. It is not possible to vary the blade pitch though inlet guide vanes have been provided with some large fans. As in fixed-bladed axial-flow fans, the characteristic of the turbo-axial fans restrict their efficient operation to a small range only and hence these fans can be used only where the mine characteristic remains reasonably constant.

6.3.6 Mixed-flow Fans

These fans are hydraulically midway between the radial flow and axial-flow fans. They have vanes with double curvature as in Francis turbines.

They impart nearly equal velocity components to the air at discharge. However, they are of more recent origin and have not found use in mines.

6.4 SELECTION OF A MINE FAN

A fan has to be selected basically to meet the pressure and quantity demands of the mine which have to be carefully estimated not only for the present but also for the future covering the life of the fan. The following are the major factors that have to be considered in selecting a mine fan : (1) quantity required at various periods during the life of the mine, (2) pressure required for circulating these quantities (in other words, range of variation of the mine characteristic), (3) altitude or barometric pressure at the fan site and the temperature of air to be handled by the fan (primarily for obtaining the air density), (4) whether reversal of airflow required, (5) type and speed of motive power available, if any, (6) degree of permissible sound emission, (7) initial and running cost, (8) size of the fan, nature of housing and space required and (9) nature of the air to be handled, viz. humidity, dustiness etc.

The first two factors out of these are essential for selecting the size and type of the fan and theoretically any type of fan can be designed for these essential requirements, but it is the other factors which ultimately determine the exact type and make of fan.

The pressure-quantity duty of a fan is selected on the basis of the ventilation requirements of the mine. A fan should be so selected that it operates with as high an efficiency as possible during the major operational life of the mine. A high efficiency is essential not only from the point of view of minimizing running cost but also for keeping down noise. Usually fans are installed with constant-speed drives so that variations in the mine resistance shift the

operating point along the fan characteristic. The exact operating points for these mine resistances are given by the points of intersection of the mine characteristics with the fan characteristic (Fig. 6.40). The variation in mine resistance should be small so that it does not change the efficiency of the fan to a large extent. However, when large variations in the mine resistance do occur, other means of varying the duty of the fan such as varying the speed, adjusting blade pitch etc. have to be adopted. From this point of view, adjustable-vane axial-flow fans are more flexible and should be preferred where large variations in the mine resistance are likely to occur.

When the mine characteristic varies over a wide range over the life of the fan so that the operation of a single fan over its whole life becomes inefficient and hence uneconomical, multiple installation of fans may be considered at different stages in the life of the mine.

It is a conservative practice to use the fan static head characteristic for the determination of the duty of operation of the fan. However, main mine fans are generally installed with evasees. Where the fan is installed with a diffuser or evasee (the former with a forcing fan and the latter with an exhaust fan), a part of the fan velocity head is converted to static head.

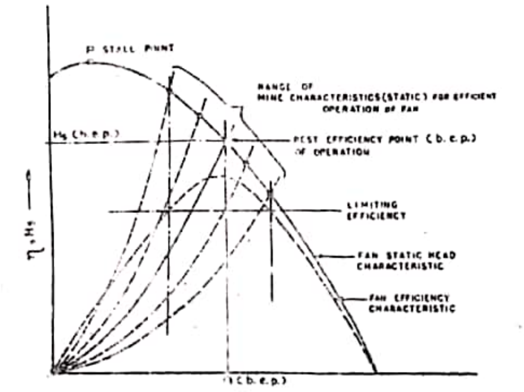

Fig. 6.40 Range of mine characteristics for efficient operation of fan.

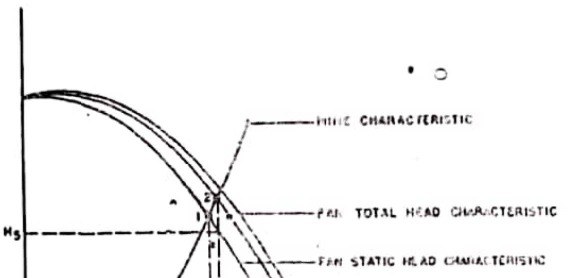

Fig. 6.41 Effect of an evasee on the performance of a mine fan.

In such a case the operating point is obtained from the intersection of the combined fan static head and evasee head characteristic with the mine characteristic as shown in Fig. 6.41. Point 1 in the figure gives the operating point without evasee while point 2 gives the operating point with an evasee. It should be borne in mind that while the evasee is a matter of choice in case of an exhaust fan, in case of a forcing fan blowing air into a mine or system, the diffuser has to be installed to connect the fan (usually of smaller diameter than the system) to the system. The benefit of the evasee however is evident from the increase in the quantity circulated from Q_1 to Q_2. The fan operates at a static head H_s corresponding to Q_2 on its static head characteristic.

The head duty of the fan should be determined after suitably accounting for the natural ventilation pressure. Natural ventilation pressure in shallow mines is negligible but cannot be ignored in deep mines. In selecting the head duty of the fan, the N.V.P. should be subtracted from the head required to overcome the mine resistance for passing the desired quantity when the N.V.P. aids

the fan. When it opposes the fan or there are seasonal reversals of natural ventilation, the N.V.P. should be added to the pressure required to overcome the mine resistance so as to obtain the head duty of the fan. Figs. 6.42 (a) and (b) show the effect of N.V.P. on fan characteristics and amply illustrate the point. Point 'a' in the figure is the operating point on the mine characteristic for the required quantity Q whereas point 'b' gives the corresponding duty of the fan. The above consideration of the simple series operation

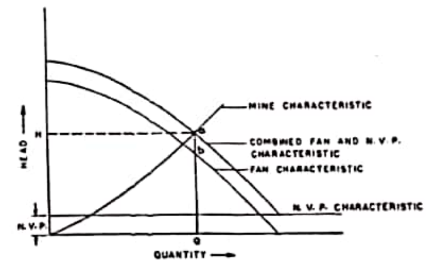

Fig. 6.42(a) Combined N.V.P. and fan characteristic with N.V.P. aiding fan.

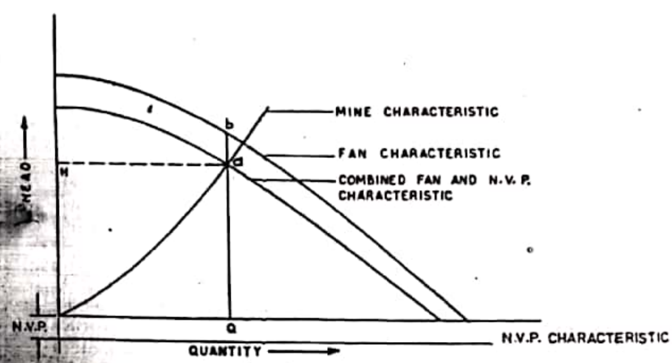

Fig. 6.42(b) Combined N.V.P. and fan characteristic with N.V.P. opposing fan.

of the fan with the N.V.P. holds good in single-level mines, but in multi-level mines such as metal mines, there are different natural ventilation pressures acting across different levels, thus complicating the calculation of the fan pressure. In practice however, the N.V.P. at the uppermost cross-connected level carrying an appreciable part of the total flow is taken to act in series with the fan. The fan duty and the total flow are very little affected by the N.V.P. developed below this level which merely changes the air distribution in the lower levels.

Fan capacity, particularly where an exhaust fan is to be used, should take into account the increase in the volume of air circulating in the mine workings as it rises in the upcast shaft and undergoes auto-expansion. This increase is about 1% for every 100m depth. In metal mines, where a large amount of compressed-air is used underground, the fan should be so designed as to handle this amount of extra air too.

From the point of view of reversal of air-current, axial-flow fans are superior to centrifugal fans since they do not need an elaborate arrangement for air reversal. The reversal of air-current with axial-flow fans can be effected by simply reversing the stator connections of the driving motor which changes the direction of rotation of the motor and hence of the fan. The fan when running in the reverse direction, of course, generates only about 65 percent of the normal volume at a lower efficiency (with a power consumption of 75% of the normal), but the reduced quantity is usually adequate to meet the exigencies of the situation requiring a reversal of the air-current. On the other hand, air reversal with centrifugal fans requires elaborate arrangements of doors and ducts (see Fig. 6.57) in a suitable housing which involves a large capital investment.

Noise in fans is a function of rotational speed and since axial-flow fans have usually high speed, they produce more noise. However, modern fan design so restricts the speed that noise is usually kept within tolerable limits. It must be remembered that a fan produces the least noise when operating at the maximum efficiency.

Axial-flow fans have a higher initial cost owing to the complicated design of the impeller and the better material of construction, but they require a less costly motor (since high-speed motors of similar power are less costly than low-speed ones) and a less costly housing. Axial-flow fans can have factory made steel housing

or can be installed in concrete housing while centrifugal fans are usually installed in brick or concrete housing. Moreover, axial-flow fans weigh about 40 to 60% less than centrifugal fans of similar capacity thus requiring less costly foundation. When all these have been taken into consideration, axial-flow fans cost as much as or even less than modern radial-flow fans of cast aerofoil-vane impellers for small heads, but for large heads where multi-stage axial-flow fans become necessary, centrifugal fans are cheaper in the initial cost. Centrifugal fans of welded plate construction are however much cheaper than those with aerofoil blades but their running cost is high due to their lower efficiency so much so that the advantage of the lower initial cost is well offset within a period of about 5 years of operation. The initial cost of a centrifugal fan of plate construction circulating 230 $m^3\ s^{-1}$ at a pressure of 3 kPa was about Rs. 80 000 while an axial-flow fan of similar duty cost about Rs. 288 000.

As regards maintenance, low-speed centrifugal fans are superior to high-speed axial-flow ones. In the former, the bearings are more accessible and the drive, always isolated from the air-stream whereas only large-size axial-flow fans have isolated drives. It must be remembered that an isolated drive is much preferred from the point of view of maintenance. However, the greater streamlining of flow through the impeller of an axial-flow fan causes less accumulation of dirt on the blades than in centrifugal fans. This, coupled with the better material of construction of axial-flow fan vanes, makes them less liable to corrosion.

Although most suppliers of fans require the user to specify chiefly the pressure and quantity duty at different times of operation, altitude of the fan site and temperature and nature of air (dusty, humid, corrosive etc.) to be handled, any preference for drive (speed of operation, type of gearing, flame-proofing and dust-proofing of motor etc.) and housing, any restriction on noise level and the preference for measurement and control gear for the fan should also be specified by the user. The design of fan drift and evasee should never be left to the manufacturer of the fan unless a standard factory-made housing is sought.

It would be in the interest of the user to supply the evasee design and pressure recovery characteristic along with the natural ventilating pressure so that the manufacturer upplier can choose a suitable fan characteristic. Even then the user should insist on

Scanned with CamScanner

the supply of detailed fan characteristics and satisfy himself as to the suitability of the fan for the mine before entertaining tender. It would be advisable to test the fan for the accuracy of the characteristics supplied by the manufacturer since the characteristic of a particular fan may differ from the standard ones for the type depending on manufacturing defects in the fan.

It is ultimately up to the ventilation planner to examine the tender documents submitted by various suppliers and select the right fan which meets all the physical requirements and at the same time offers the least capital (ownership) and operating cost (see Chapter IX for economic analysis of ventilation equipment and systems). The reliability of the supplier as to quality of goods supplied and ability to adhere to the schedule of supply weigh greatly in accepting a tender.

6.5 FAN TESTING

Fan testing is of two main types : (a) *rating test* used for determination of fan characteristics and (b) *field test*. Rating tests are more accurate and are done according to a standard test code. They need elaborate test set-up and hence are rarely used at mines except at large ones where a number of auxiliary fans may be in use. At such mines, it may be worthwhile to maintain a standard test set-up for verifying the performance of fans as specified by the makers. Normally however, fan tests are restricted to field tests in the fan drift where the operating point on the fan characteristic is fixed by the mine characteristic. Such field tests are necessary to verify the fan duty (mainly the capacity) and efficiency of operation of the fan. They also reveal the system (mine) characteristic and help in the design and modification of the system as well as the fan inlet and outlet etc., so as to obtain the most efficient operation. Field tests are usually less accurate. A rough idea of the fan characteristics can be obtained from field tests by varying the mine resistance by introducing different obstructions in the main airway.

6.5.1 Field Tests

Field tests are carried out on similar lines as rating tests, but are suitably adapted to field conditions. They involve the measurement of pressure and quantity of air as well as the power input to the driving motor. It is better to conduct quantity measurements

on the suction side of the mine fan as there is less turbulence on this side. With surface fans, it is usually conducted at a suitable point in the fan drift. The measuring station should have a regular cross-section and should be situated in a straight portion of the fan drift not less than six times the diameter in length. There should be no obstruction on the path of air at the test section. These tests should be carried out when there is no movement of cages or skips in the shaft and not much variation in the atmospheric pressure and temperature.

The fan total pressure can be obtained by deducting the inlet total pressure from the outlet total pressure as measured by a pitot (total pressure) tube connected to one limb of an inclined-gauge manometer, the other limb of which is exposed to the atmosphere. In case of exhaust fans which deliver air into the atmosphere, e.g. a surface exhaust fan, the static pressure at the outlet is equal to zero or, the total pressure is equal to the velocity pressure P_v whereas at the inlet, the total pressure is the algebraic sum of the static pressure P_s (which is negative in this case) and the velocity pressure P_v (assuming inlet and outlet velocities to be the same). Or, inlet total pressure $= -P_s+P_v$. Note that the velocity pressure is always positive. Now fan total pressure$=P_v-(-P_s+P_v)$ $=P_s$. This indicates that in case of a surface exhaust fan, the fan total pressure will be given by a static tube at the fan inlet (i.e. in the fan drift) while a pitot tube at the fan inlet will read the fan static pressure. On the other hand, a forcing fan drawing air from the ambient atmosphere has zero total pressure at the inlet while the outlet total pressure as recorded by a pitot tube at the outlet is the sum of the static pressure and the velocity pressure. Hence in such a case, the fan total pressure is equal to the outlet total pressure.

Velocity measurement in fan drifts is best done by pitot-static tubes. Air velocities in fan drifts are usually too high for anemometers. Anemometers or velometers can, however, be used with low air velocities. When anemometers or pitot-static tubes are used for measuring air velocity, the static pressure is usually measured by a static tube and the total pressure is obtained by algebraically adding the velocity pressure to it. For accurate velocity measurement, properly calibrated anemometers should be used and the measuring area should be divided into suitable sections by stretched wires.

Scanned with CamScanner

In testing underground or other auxiliary fans with both inlet and outlet ducts, two total-or static-pressure tubes, one at the inlet and the other at the outlet of fan are used as shown in Fig. 6.43. The two tubes are connected to the two limbs of an inclined-gauge manometer which reads the fan total pressure. The fan static pressure can be obtained by deducting the fan velocity pressure (measured at the fan outlet) from it.

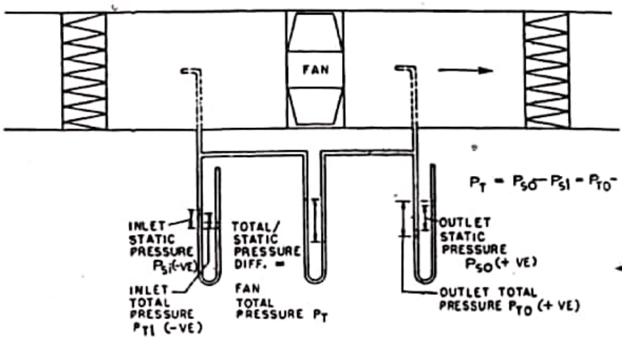

Fig. 6.43 Fan total pressure in auxiliary fans with both inlet and outlet ducts.

6.5.2 Rating Tests

Fig. 6.44 gives the *AMCA* standard test set-up*[95] suitable for fans with both inlet and outlet ducts or with outlet duct only. For fans with inlet duct only, a slightly modified set-up with the test duct on the inlet of the fan is used. For fans with no inlet or outlet ducts, the test set-up incorporates a chamber, but this test is not usually necessary for mine fans since most mine fans are installed with inlet and outlet ducts.

The test duct has a minimum length of 10 diameters and is connected to the outlet of the fan by a connecting piece whose sides should not converge at an angle greater than 0.26 rad (15°) or diverge at an angle exceeding 0.123 rad (7°). The diameter of the duct should be such that its cross-sectional area does not exceed

*Air Moving and Conditioning Association Inc., U.S.A.

that of the fan outlet by more than 12½% nor should it be less than the cross-sectional area at the fan outlet by more than 7½%. The duct should be straight and of perfect shape. The tolerable limit of roundness for circular ducts at the traverse section is ±½% of the diameter and this limit should hold good for a distance of at least ½D on either side of the traverse plane. An egg-crate straightener (Fig. 6.45) is used in the duct for straightening air-flow. A diffuser cone (as shown by dotted lines in Fig. 6.44) at the outlet end of the duct may be used in order to approach more nearly free delivery conditions. The dotted line at the fan inlet indicates an inlet bell which may be used to simulate inlet duct condition. The friction loss in the inlet bell however is not considered in test calculations. Variation of quantity circulated by the fan is done by a symmetrical throttling device provided at the outlet of the duct.

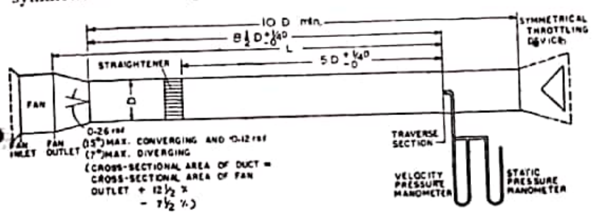

Fig. 6.44 *AMCA* standard fan testing set-up.

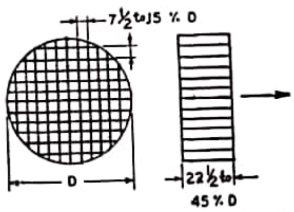

Fig. 6.45 Egg-crate straightener.

Rating test aims at finding out the fan static and total pressures, power input to the fan and total efficiency of the fan for various flow-rates at the rated speed so that the fan characteristics can be drawn. Static efficiency may also be calculated. With variable

Scanned with CamScanner

speed fans, all these readings are taken for different fan speeds. The results are stated for the inlet air density during the test. The necessary measurements are (a) static pressure and (b) velocity pressure (from which the velocity and hence the quantity can be calculated) at the traverse section, (c) the rotational speed of the fan, (d) power input to the fan, (e) barometric pressure, (f) dry- and wet-bulb temperatures on the path of the inflowing air and (g) dry-bulb temperature at the traverse section.

The static pressure and the velocity pressure are measured by a pitot-static tube connected to two manometers as shown in Fig. 6.44. Pressures greater than 500 Pa are usually measured by vertical U-tube water gauges graduated in millimetres whereas lower pressures should be measured on an inclined manometer having a least reading of 1-2.5 Pa. The inclined manometer should be calibrated against a sensitive micro-manometer. The pitot-static tube should be of the standard hemispherical-head type to be described later. It should not have a stem diameter less than 2.5mm, neither should the stem diameter exceed one-thirtieth of the test-duct diameter. Ten readings should be taken along each of two diameters of the duct at right angles to each other at the traverse section, the measuring points being located at distances of 0.052, 0.163, 0.293, 0.452 and 0.684 times the radius of the duct from the wall with a tolerance of $\pm\frac{1}{2}\%$ of the radius. Whereas the average static pressure is given by the arithmetic mean of the static pressure readings at the points of observation, the average velocity pressure can be calculated as given in Chapter VIII.

The fan velocity pressure is the velocity pressure at the fan outlet and can be calculated from the relation

$$P_v = P_{vo}\left(\frac{A_o}{A}\right)^2 \frac{\rho_o}{\rho_f} \qquad (6.71)$$

where
P_v = fan velocity pressure,
P_{vo} = velocity pressure in the duct,
A_o = cross-sectional area of the duct,
A = cross-sectional area of the fan outlet,
ρ_o = density of air in the duct
and ρ_f = density of air at the fan outlet.

Normally ρ_o is taken as equal to ρ_f. Velocity of air in the duct can be found from the relation

$$V_o = \sqrt{\left(\frac{2P_{vo}}{\rho_o}\right)} \qquad (6.72)$$

where V_o = velocity in m s⁻¹
P_{vo} = velocity pressure in Pa
and ρ_o = air density in the duct in kg m^{-3}
ρ_o is obtained from the relation

$$\rho_o = \rho\frac{T}{T_o}\left(\frac{B+P_s}{B}\right) \qquad (6.73)$$

where ρ is the density of air at the fan inlet, T and T_o are the dry-bulb temperatures at the fan inlet and in the duct respectively, B is the barometric pressure and P_s, the static pressure measured in the duct in Pa.

T_o, T, B and P_s are measured, the barometer reading, of course, being corrected for temperature whereas ρ is calculated from equation 3.78. For fans generating up to 1 kPa pressure, ρ_o can be taken equal to ρ. The quantity circulating in the duct can be calculated by multiplying v_o by A_o.

The fan total pressure indicates the total pressure at the outlet of the fan and can be calculated by adding the pressure loss in the intervening duct as well as that in the straightener to the sum of the static and velocity pressures measured in the duct. Pressure loss in the duct is given by the relation

$$P_1 = 0.02\frac{L}{D}P_{vo} \qquad (6.74)$$

where P_1 = Pressure loss due to friction in the duct,
L = length of duct between the fan outlet and the traverse section,
D = diameter of the duct
and P_{vo} = velocity pressure in the duct.

Pressure loss in the straightener, P_2 is given by the relation

$$P_2 = 0.08\ P_{vo} \qquad (6.75)$$

The fan static pressure is found out by algebraically subtracting the fan velocity pressure from the fan total pressure. The fan quantity (quantity at the fan inlet) is calculated from the relation

$$Q = Q_o\frac{\rho_o}{\rho} \qquad (6.76)$$

where Q = quantity at the inlet and Q_o = quantity in the duct.

Scanned with CamScanner

The rotational speed of the fan is usually measured by a sensitive tachometer or by a stroboscope. It is necessary to control the speed within a limit of $\pm 1\%$. All measurements of pressure, quantity and power should be converted to the rated speed using the following relations :

$Q \propto$ speed, $P \propto$ (speed)^2 and power $\propto$ (speed)^3.

The power input to the fan can be obtained by dynamometers, torsion meters or from motor characteristics. When dynamometers are used, the power is given by the relation

$$\text{Power} = \omega m g L \times 10^{-3} \quad \text{kW} \tag{6.77}$$

where m=net mass of the beam in kg and L=length of arm from shaft centre to knife edge in m. With torsion meters,

$$\text{Power} = \omega \tau \quad \text{kW} \tag{6.78}$$

where τ =torque in kJ. With calibrated motors,

$$\text{Power} = \text{Power input to the motor in kW} \times \text{efficiency of motor} \quad \text{kW} \tag{6.79}$$

The power input to the motor can be directly measured by a watt meter or with a volt meter, an ammeter and a power-factor meter.

The air power is equal to PQ kW where P is the fan total pressure in kPa and Q, the quantity at the fan inlet in m^3 s^{-1}. This relation holds good for fans of low to medium pressure (less than 2.5 kPa) but for high-pressure fans, the effect of compressibility has to be taken into account in which case the air power will be given by the relation

$$\text{air power} = PQK_p \quad \text{kW} \tag{6.80}$$

where K_p is the compressibility factor and is given by the relation

$$K_p = \frac{\frac{\gamma}{\gamma-1}\left(r^{\frac{\gamma-1}{\gamma}}-1\right)}{r-1} \tag{6.81}$$

where $\gamma = C_p/C_v$=1.4 for air, $r=P_2/P_1$ and P_2 and P_1 are absolute total pressures at fan outlet and fan inlet respectively. Although an adiabatic compression of the air in the fan is assumed here, the process is not strictly adiabatic since some heat, corresponding to the losses in the fan, is added to the air.

The total efficiency of the fan can now be calculated by dividing air power by the power input to the fan. This calculation includes the bearing friction loss in the fan losses. However, it does not give an efficiency much different from the true fan efficiency since the bearing friction loss is only less than 1% of the power input.

Test results for a certain fan can be extrapolated for other fans of similar geometrical construction but larger in size than the test fan, by using the following affinity laws.

When tip speed remains constant, pressure remains constant, $Q \propto D^2$, rotational speed $\propto 1/D$ and power $\propto D^2$. These can be written in the form $Q \propto D^3\omega$, $P_s \propto D^2\omega^2$, power $\propto D^5\omega^3$.

where D =diameter of the fan,

ω =rotational speed,

P_s =fan static pressure,

and Q =quantity of the fan.

Also, test results at the stated air density can be extrapolated to any other density from the fan law that volume and efficiency are unaffected by change in density whereas pressure and power vary directly as density. This contingency, however, rarely arises in mines except in case of underground fans in very deep mines where there may be a substantial change in the air density.

The AMCA test set-up described above involves too long a duct for large-diameter fans for which the Indian standard test set-up for both centrifugal and axial-flow fans may be used.

The Indian standard test procedure[91] which is similar to the British standard, relies on the computation of flow rate from the pressure drop in the inlet cone incorporated in the test set-up (Fig. 6.46). Hence to maintain accuracy in flow measurement the shape of the inlet cone has to be accurately maintained in fabrication so that there is no variation in its discharge coefficient.

The test set-up comprises a short test duct (minimum length equal to 4 times the diameter D) fitted with a $\pi/3$ rad (60°) inlet cone with a flange. The duct should be truly circular within a tolerance of $D/200$. The junction between the cone and the duct should be smooth and free from ridges. Four pressure taps spaced $\pi/2$ rad apart measure the static pressure at section AA, $-P_{sA}$ so that P_{sA} equals the pressure drop in the conical inlet. The pressure taps should have a bore not exceeding 4.76mm at the

Scanned with CamScanner

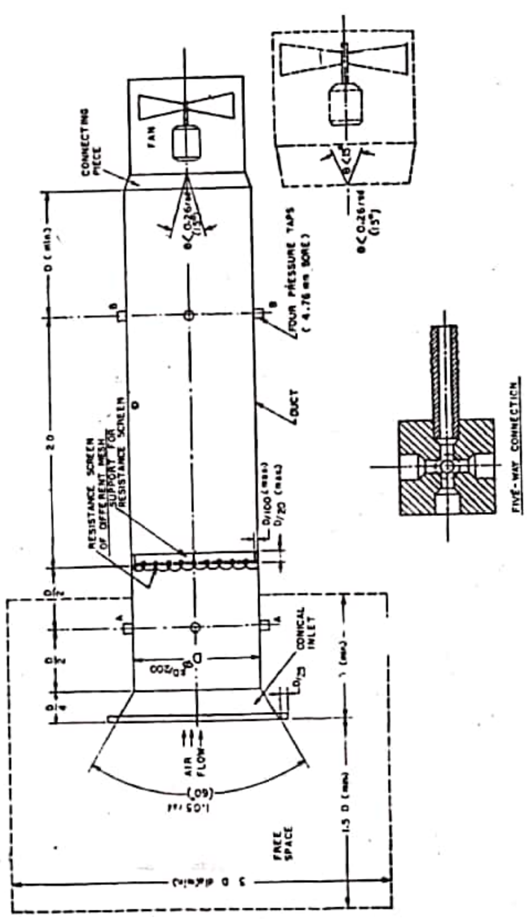

Fig. 6.46 Indian standard fan test set-up.

surface of the airway and should be straight, of uniform bore and at right angles to the duct for atleast 2-bore diameters. The openings should be flush with the duct and free from burrs and countersinks. The pressure taps should be connected by tubings of equal length to a manometer through a 5-way connector.

A resistance-screen support is mounted inside the duct 0.5 D behind the plane AA. Screens of different mesh can be fixed on to this for uniformly throttling the flow to different extents. A second set of pressure taps provided at BB are used for obtaining the static pressure at the fan inlet. The fan is connected to the duct by a connecting piece with an angle of contraction or expansion not exceeding 0.262 rad (15°). The duct diameter should not be more than 20% larger than the fan-inlet diameter nor should it be more than 5% smaller.

Fan quantity (flow-rate at the fan inlet) Q is obtained from the relation

$$Q = 1.11\ \alpha D^2 \sqrt{\frac{P_{sA}}{\rho_A}} \cdot \frac{\rho_A}{\rho_i}\ \mathrm{m^3\,s^{-1}} \tag{6.82}$$

where α = discharge coefficient given in Table 6.3,
ρ_A and ρ_i are the density of air in kg m^{-3} at section AA and fan inlet respectively and D is in m and P_{sA} in Pa.

Normally ρ_i is taken equal to ρ_A for static pressures in the duct less than 1 kPa so that equation 6.82 reduces to

$$Q = 1.11\ \alpha D^2 \sqrt{\frac{P_{sA}}{\rho_A}}\ \mathrm{m^3\,s^{-1}} \tag{6.83}$$

Even for high-pressure fans, it is complicated to estimate ρ_i which is generally approximated to ρ_B, the density of air at section BB, so that equation 6.82 can be modified to

$$Q = 1.11\ \alpha D^2 \sqrt{\frac{P_{sA}}{\rho_A}} \cdot \frac{\rho_A}{\rho_B}\ \mathrm{m^3\,s^{-1}} \tag{6.84}$$

ρ_A is obtained from the relation

$$\rho_A = 1.2\,\frac{B - 0.001\,P_{sA}}{101.33} \cdot \frac{293.15}{T}\ \mathrm{kg\,m^{-3}} \tag{6.85}$$

where B = barometric pressure in kPa and
T = ambient air temperature at the inlet to the test duct in K.

The above equation is based on the standard density of air at 293.15 K and 101.33 kPa being taken at 1.2 kg m^{-3}. More accurately however, ρ_A can be obtained from the relation

$$\rho_A = \frac{(B-0.001\, P_{sA}) - 0.378\, e}{287.1\, T} \times 10^3 \text{ kg m}^{-3} \qquad (6.86)$$

where e = vapour pressure of moisture in the air in kPa.

ρ_B is given by the relation

$$\rho_B = \rho_A \frac{B-0.001\, P_{sB}}{B-0.001\, P_{sA}} \text{ kg m}^{-3} \qquad (6.87)$$

where $-P_{sB}$ = static pressure at section BB.

Table 6.3 : Discharge Coefficient of Inlet Cone at Various Reynolds Numbers of Flow

Re	20 000*	40 000	60 000	100 000	200 000	300 000	400 000
α	0.930	0.940	0.945	0.953	0.967	0.973	0.975

*A conical inlet shall not be used below Re=20 000. α for intermediate values of Re can be obtained by linear interpolation.

Fan total pressure

$$P_{tf} = P_{vo} - (-P_{si} + P_{vi}) = P_{vo} - P_{vi} + P_{si} \qquad (6.88)$$

where P_{vo} = velocity pressure at fan outlet

$$= \frac{\rho_o v_o^2}{2} = \frac{\rho_o Q_o^2}{2A_o^2} = \frac{Q^2 \rho_i^2}{2A_o^2 \rho_o} = \frac{Q^2 \rho_B^2}{2A_o^2 \rho_A} \qquad (6.89)$$

taking $\rho_o \simeq \rho_A$,
v_o = velocity at fan outlet,
Q_o = quantity at fan outlet,
A_o = fan outlet area,
ρ_o = density of air at fan outlet,

P_{vi} = velocity pressure at the fan inlet

$$= \frac{\rho_i v_i^2}{2} = \frac{\rho_i Q^2}{2A_i^2} = \frac{\rho_B Q^2}{2A_i^2}, \qquad (6.90)$$

v_i = velocity at fan inlet,
A_i = fan inlet area,
$-P_{si}$ = static pressure at fan inlet
$= -P_{sB} - \Delta P + P_{vB} - P_{vi}$, (6.91)
ΔP = pressure loss in the duct between section BB and fan inlet

$$= 0.02 \frac{L}{D} P_{vB} \qquad (6.92)$$

L = length of duct between section BB and fan inlet,
P_{vB} = velocity pressure at section BB.

$$= \frac{\rho_B v_B^2}{2} = \frac{2\, Q^2 \rho_i^2}{\rho_B \pi D^2} = \frac{2\, Q^2 \rho_B}{\pi D^2} \qquad (6.93)$$

and v_B = velocity at section BB

Combining equations 6.88 and 6.91, we have

$$P_{tf} = P_{vo} + P_{sB} + \Delta P - P_{vB} \qquad (6.94)$$

Fan static pressure

$$P_{sf} = P_{tf} - P_{vo} = P_{sB} + \Delta P - P_{vB} \qquad (6.95)$$

Example 6.3

Makers' tests conducted at dry-/wet-bulb temperatures of 308 K/298 K and a barometer of 101.33 kPa give the b.e.p. duty of a fan as 5 m^3 s^{-1} at 500 Pa. The power output of the motor driving the fan is 2.9 kW. Calculate the b.e.p. duty of the fan and the power of the driver when it is installed in an underground working at a depth of 3000m below sea level. The underground air temperatures are 318 K/288 K d.b./w.b. The mean downcast shaft temperature is 310 K with the barometer reading 100 kPa at the shaft top.

Scanned with CamScanner

Vapour pressure at 101.33 kPa barometer and 308/298 K dry-/wet-bulb temperatures = 2.48 kPa.

Therefore, air density $= \frac{101.33-0.378\times2.48}{287.1\times298}\times10^3 = 1.17$ kg m^{-3}.

From equation 3.3

$3000=67.4\times310\log(B/100)$

Or, B (barometric pressure at a depth of 3000m) = 139.18 kPa.

Vapour pressure at 139.18 kPa and 318/288 K dry-/wet-bulb temperatures$\approx$0.

Therefore, density of air underground =

$$\frac{139.18-0}{287.1\times318}\times10^3 = 1.52 \text{ kg m}^{-3}.$$

Let P and Q represent the b.e.p. duty of the fan when installed underground.

Q =5 m^3 s^{-1}

P =500$\times$1.52/1.17=649.6 Pa.

Power =2.9$\times$1.52/1.17=3.77 kW.

Example 6.4

The following data were obtained from tests on a surface fan exhausting air from a mine. Calculate the efficiency (both total and static) of the fan and gearing assuming a moto fficiency of 80%. If the fan is speeded up to 73.33 rad s^{-1}, calculate the duty of the fan and the power output of the motor. Take fan velocity pressure equal to the fan-drift velocity pressure.

Cross-section of the fan drift=3$\times$3m.

Average air velocity in the fan drift=6.5 m s^{-1}.

Reading of fan-drift water gauge (fan total pressure)=70mm.

Speed of fan=62.86 rad s^{-1}.

Line voltage of power supply=3200 V.

Line current in the three-phase motor=13.5 A.

Power factor=0.9

Pit-top barometer reading=99.99 kPa.

Hygrometer reading in the fan drift=301 K d.b./300 K w.b.

Now, quantity circulated by the fan at 62.86 rad s^{-1}

=3$\times$3$\times$6.5=58.5 m^3 s^{-1}.

Fan total pressure=70$\times$9.81=686.7 Pa.

Air Power=686.7$\times$58.5=40 171.95 W.

Power input to the motor=$\sqrt{3}\times$3200$\times$13.5$\times$0.9=67 342.14 W.

Power output of the motor=67 342.14$\times$0.8=53 873.7 W.

Therefore, efficiency (total) of the fan and gear

$$= \frac{40\,171.95}{53\,873.7}\times100 = 74.57\%.$$

e at 99.99 kPa barometer and 301/300 K temperatures=3.5 kPa.

$$\rho \text{ (density of air)} = \frac{(99.99-0.378\times3.5)}{287.1\times301}\times10^3 = 1.142 \text{ kg m}^{-3}.$$

Velocity pressure of air=$v^2\rho/2$=(6.5$^2\times$1.142)/2=24.13 Pa.

Therefore, fan static pressure=686.7$-$24.13=662.57 Pa.

Air power based on static pressure=662.57$\times$58.5=38 760.35 W.

Therefore, efficiency of fan and gear (static)

$$= \frac{38\,760.35}{53\,873.7}\times100 = 71.95\%.$$

When the fan is speeded up to 73.33 rad s^{-1},

Q=58.5$\times$73.33/62.86=68.24 m^3 s^{-1}.

P (total pressure)=686.7 (73.33/62.86)^2=934.5 Pa.

Power of motor=53 873.7 (73.33/62.86)^3=85 526.1 W=85.5 kW.

6.6 OUTPUT CONTROL IN FANS

Control of the capacity of a centrifugal fan can be achieved in three main ways.

(a) Constant speed of drive and fan with capacity control by devices which modify the fan or the system characteristics : Such devices include (I) damper control and (ii) inlet-vane or inlet-louvre control. These devices are, however, not commonly used in mine fans.

(b) Constant-speed drive with provision for variation of fan speed by auxiliary intermediate devices between the fan and the drive : Such devices include (i) hydraulic coupling (ii) electro-magnetic coupling and (iii) V-belt of gear drive.

Scanned with CamScanner

(c) Variable-speed drive directly coupled to the fan : Such drives can be (i) D.C. motors, (ii) slip-ring induction motors, (iii) multi-speed A.C. motors (iv) A.C. commutator motors or (v) steam turbines.

Any of the above methods can be used for the control of capacity of axial-flow fans. In addition, capacity of axial-flow fans can be varied by altering the pitch of the rotor blades where the fan is provided with variable-pitch blades. Sometimes adjustable inlet guide vanes are used for imparting a swirl or counter swirl to the inlet air-flow for the purpose of varying output. These are less costly than adjustable rotor blades but their range of efficient performance is not so wide (see Fig 6.36).

6.6.1 Damper Control

This is achieved by introducing a damper or variable throttle between the fan and the system. The damper adds to the resistance of the system depending, of course, on the degree of throttling and this makes the fan work at a lower capacity on the characteristic. Though dampers are cheap, simple in operation and have a long life as well as a wide range of operation, they are wasteful and hence incur a high running cost.

6.6.2 Inlet-vane and Inlet-louvre Control

These consist of a set of vanes at the inlet of the fan, the position of which can be adjusted to give a desired amount of prerotation to the air before it enters the fan wheel. Such an adjustment effects a modification in the fan characteristic, resulting in the necessary capacity control. This process is less wasteful than damper control and hence has a lower operating cost, though its initial cost is slightly higher. Inlet vanes or inlet louvres are also simple in operation and have a wide range of regulation as well as a relatively long life.

6.6.3 Hydraulic Coupling

This comprises a centrifugal pump run by the constant-speed drive which pumps oil that, in turn, drives the runner of a turbine which is mechanically connected to the fan shaft. The speed of the runner can be varied by varying the amount of oil in the pump-turbine system. Hydraulic coupling has the advantage of having a smooth speed regulation over a wide range. Its initial cost though higher than the above two devices, is comparable to that

of multi-speed drives. It is less wasteful than the damper or inlet-vane and inlet-louvre controls, but its efficiency decreases with reduction in the runner speed.

6.6.4 Electro-magnetic or Eddy-current Coupling

This fundamentally consists of a ring driven by a constant-speed motor. A magnet element connected to the fan rotates inside the ring. The speed of the magnet and hence the fan is varied by adjusting the D.C. excitation of the magnet. This device, like the hydraulic coupling, gives a smooth speed control over a wide range, but its efficiency falls as the speed of rotation of the fan is reduced. The efficiency of an electro-magnetic coupling falls from 95% to 83% when the speed of the fan is reduced from one equal to the speed of the driver to two-thirds of the speed of the driver.

6.6.5 V-belt and Gear Drive

V-belt drives offer a good range of speed variation with constant-speed drivers. Speed variation can be achieved by simultaneously varying the pitch of the driver and the driven sheaves thus maintaining constant belt tension or by varying the pitch of the driver sheave with a corresponding shift in the position of the motor base in order to maintain belt tension. Changing the pitch of belt sheaves is usually done manually by stopping the motor, but where frequent speed changes are needed, arrangements can be made for making such changes automatically without stopping the motor. Gear drives offer a smaller range of speed control than belt drives. Normally the motor is stopped for changing gears, but if frequent speed changes are needed, it is preferable to use a variable-speed gear box.

6.6.6 Variable-speed Drives

The best speed variation is offered by a direct-current motor with a high starting torque, but D.C. is rarely available at mines and it becomes too costly to convert A.C. into D.C. for such purposes. A good speed regulation down to approximately 35% is possible with D.C. motors. Slip-ring induction motors offer a speed regulation down to 50% without necessitating special controlling equipment. The speed regulation is obtained by introducing resistance in the rotor circuit which is a wasteful process and hence slip-ring induction motors should not be used for speed variation except as a

Scanned with CamScanner

temporary measure. Alternating-current commutator motors offer a wide range of speed variation at relatively high efficiency, but they are costly. Multi-speed squirrel-cage motors offer two to one, or, even three to one, speed variation but they are suitable for light and medium duties only. Steam turbines offer a smooth speed variation down to 35% and should be considered for use where exhaust steam is available. The initial cost of a large steam turbine compares well with that of a constant-speed induction motor. Fig. 6.47 gives a comparative study of the power consumption at different capacities with various methods of capacity control.

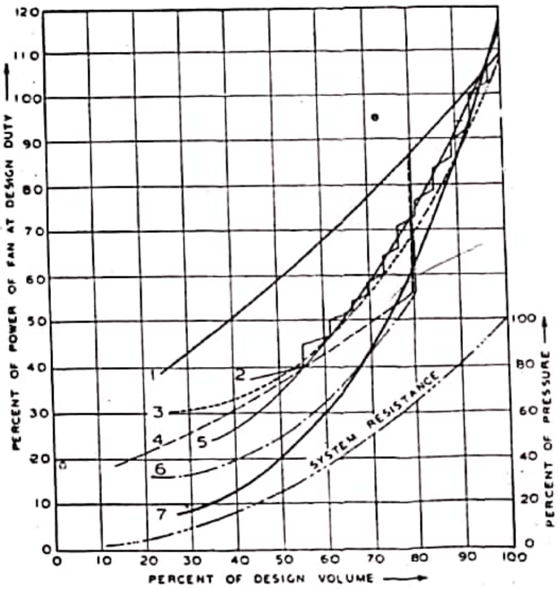

Fig. 6.47 Power input to fan motor for various types of capacity control—1 : damper control with constant-speed motor ; 2 : rotor control in variable-speed motor ; 3 : sirocco semicircle inlet control with constant-speed motor ; 4 : damper control with two-speed motor; 5 : variable-speed hydraulic or magnetic coupling; 6 : sirocco semicircle inlet control with two-speed motor ; 7 : variable-speed commutating motor (*after MacFarlane*).

6.7 COMMON DRIVES FOR MINE FANS

In coal mines, where speed variation is not frequent, constant-speed motors are commonly used. They are usually of the squirrel-cage type for small and medium size motors whereas for large ones, slipring induction motors are chosen for their superior starting duty. In some cases auto-synchronous motors are chosen because of their high power factor. Normally modern centrifugal fans and large-diameter axial-flow fans are driven at speeds varying from 10π-20π rad s^{-1} (300 to 600 r.p.m.) though much higher speeds ranging above 50π rad s^{-1} (1500 r.p.m.) are used in small axial-flow fans. High-speed fans should be directly coupled to motors since direct drives are cheap, compact and efficient in operation. Even medium-speed fans can be direct-driven since the higher efficiency of direct drives often offsets the higher initial cost of a medium-speed motor. Low-speed motors are, however, too costly and hence for low-speed fans, a high-speed motor with reduction gearing is preferable. The defect with a direct drive is that no speed variation of the fan is possible unless a variable-speed motor, which has a high initial cost, is provided. That is why direct drives are often restricted to fairly constant-speed operations.

Where speed variation is required, V-belt or gear drives in conjunction with constant-speed motors of 25π-50π rad s^{-1} (750 or 1500 r.p.m.) are preferable. V-belt drives, though more flexible for speed variation, are less efficient than gear drives, their efficiency varying from 96% to 84% (an average figure being 90%), whereas gear drives have an efficiency of 96%. That is why for large installations (i.e. above 200 kW), gear drives are preferred : the saving in the cost of running of such drives well compensates for their higher initial cost.

In metal mines where more frequent speed variation over a wider range is required, a variable-speed motor may be used. Though electro-magnetic or hydraulic couplings give a smooth speed variation, they are not commonly used with mine fans probably because of their low efficiency at reduced speed.

6.7.1 Stand-by Drives

Stoppage of main mine fans due to breakdown of fan or drive or due to failure of power supply is undesirable in coal mines,

Scanned with CamScanner

particularly in gassy ones, if there is not enough natural ventilation in the mine. Law in certain countries requires men to be withdrawn from the mine in the event of stoppage of fan after 30 minutes in gassy coal mines and after 60 minutes in non-gassy ones. That is why it is necessary to provide alternative drives for the fan, if not a complete fan installation as a stand-by. Alternative fan installations also allow for adequate inspection and maintenance of fans and drives. Alternative drives are, however, unnecessary in metal mines since a short stoppage of the fan does not lead to any danger there. Natural ventilation and the compressed-air used underground usually suffice to maintain a tolerable environmental condition for a short time in metal mines.

The stand-by drives may be designed for circulating only 70% of the normal quantity of air, in which case the power requirement will be only 35% and smaller drivers will serve the purpose. It is better to have a steam engine (if steam is available at the mine) or a diesel engine as the stand-by drive. Stand-by electric drives can be used if they are fed from an independent source of power supply. Quick changeover of drives is essential since explosive mixtures of gas may be formed within a few minutes of the stoppage of fan. This can be achieved by providing a clutch between the stand-by drive and the fan together with a device for disconnecting the normal drive quickly. A special gear box with each of its two separate driving shafts connected to a motor through a quick-connecting flexible coupling can also be used for the purpose.

6.8 COMBINATION OF FANS

Although the use of a single fan to meet the demands of pressure and quantity of a mine is the most efficient practice, a second fan may also be necessary in case of inadequate selection of the fan or considerable variation of pressure and quantity requirements from their projected values. Provision of combined operation of fans may also be made at different stages in the life of a mine involving large variations in air requirement or mine characteristic. When the mine resistance is higher than what can be negotiated satisfactorily by a single fan, the second fan is installed in series, but for increasing the quantity, the second fan has to be used in parallel.

6.8.1 Fans in Series

Each of the fans in series circulates the same volume as the system, the pressure required to overcome the resistance of the system being shared by both of them. The performance of each of the two fans operating in series can be obtained graphically by plotting a combined characteristic for the two fans as illustrated in Fig. 6.48. The combined characteristic is obtained by plotting

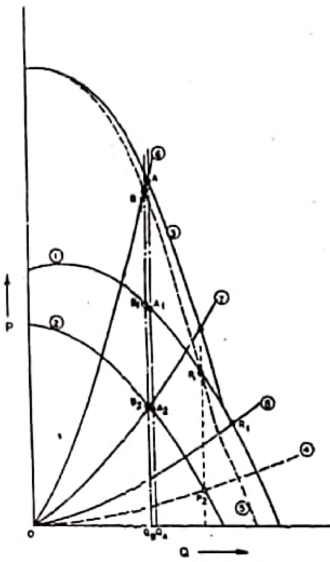

Fig. 6.48 Combined characteristic of two fans in series—1 : Characteristic of fan 1; 2 : Characteristic of fan 2; 3 : Combined fan characteristic; 4: Intervening airway characteristic ; 5: Combined fans and intervening airway characteristic ; 6, 7 and 8 : Mine characteristic, A: Operating point on combined fan characteristic (mine characteristic 6) ; B : Operating point on combined fans and intervening airway characteristic ; A_1 & A_2 : Operating points of fans 1 and 2 respectively with no intervening airway ; B_1 & B_2 : Operating points of fans 1 and 2 respectively with the intervening airway ; R_1 : Operating point with mine characteristic 8 ; P_1 & P_2 : Operating points of fans 1 and 2 respectively with mine characteristic 7.

the sum of the pressures of the two fans for different quantities. The mine characteristic is plotted on the same figure. The point of intersection of the mine characteristic with the combined fan characteristic gives the point of operation. The pressure, power and efficiency of the individual fans can then be found out from their respective characteristics corresponding to the capacity at this operating point.

When the two fans are separated by an intervening airway of appreciable resistance, it is better to draw a combined fans and intervening airway characteristic by deducting the pressure consumed in the intervening airway from the sum of the fan pressures for different quantities. The operating point is then the point of intersection of this combined characteristic and the mine characteristic.

Alternatively, the intervening airway characteristic could be combined in series with the mine characteristic and the operating point obtained from its intersection with the combined fan characteristic.

As is evident from Fig. 6.48, series operation of fans is suitable for steep mine characteristics (6). With flatter mine characteristics (7), the operating points on the characteristics of the individual fans, P_1 and P_2 shift to lower efficiency ranges. With very low mine resistances (characteristic 8) the operating point falls on the characteristic of only one fan (1) and the entire load shifts to that fan while the other (2) only offers resistance on its path.

6.8.2 Fans in Parallel

In parallel operation, all the fans develop the same pressure, i.e. the pressure required to overcome the resistance of the system. The quantity of each individual fan corresponds to this pressure on its own characteristic and the quantity circulating in the system is the sum of these individual fan quantities. The combined characteristic of two fans in parallel can be drawn by plotting the sum of the quantities of the two fans at different pressures as illustrated in Fig. 6.49. If now the mine characteristic is plotted on the same figure, the point of intersection of the combined fan characteristic and the mine characteristic gives the operating point. The quantity, power and efficiency of the individual fans can be obtained from their respective characteristics corresponding to the pressure at the operating point. Here too it is necessary that the

operating point falls on the combined fan characteristic rather than on the characteristic of any individual fan for proper sharing of load. If the operating point falls on the characteristic of one fan only, the load is taken up totally by that fan and it may even circulate some air through the other fan depending on its resistance relative to that of the mine.

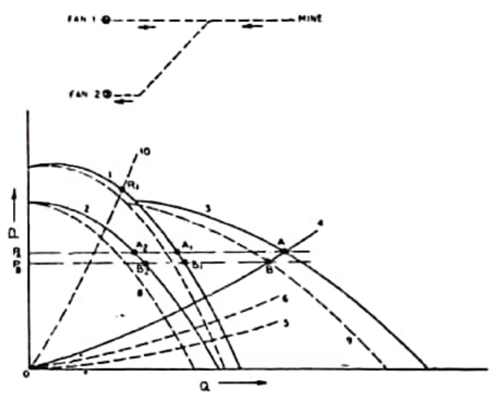

Fig. 6.49 Combined characteristic of two fans in parallel—1 : Characteristic of fan 1 ; 2 : Characteristic of fan 2 ; 3: Combined fan characteristic ; 4 : Mine characteristic ; 5 : Characteristic of roadway in series with fan 1 ; 6: Characteristic of roadway in series with fan 2 ; 7 : Combined characteristic of fan 1 and accompanying roadway ; 8 : Combined characteristic of fan 2 and accompanying roadway ; 9 : Combined fans and roadways characteristic ; 10 ; Mine characteristic for the entire load being taken up by fan 1 (operating point—R_1) : A : Operating point on combined fan characteristic ; B : Operating point on combined fans and roadways characteristic : A_1 & A_2 : Operating points of fans 1 and 2 respectively corresponding to A ; B_1 & B_2 : Operating points of fans 1 and 2 respectively corresponding to B.

Where connecting airways intervene between the fans and the mine or system, the combined fan and accompanying airway characteristic should be plotted for each fan and these characteristics then further combined, as shown in Fig. 6.49, to obtain the overall characteristic of the fans and accompanying airways. The

Scanned with CamScanner

operating point will then be the point of intersection of this overall characteristic and the mine characteristic.

When fans work in parallel, there is always a slight fluctuation in the ratio of quantities shared by them. Such fluctuations are corrected quickly and the operation becomes stable if the fans operate on the steep parts of their characteristics where there is a large variation of pressure for small changes in quantity. Stable operation is obtained with backward-bladed centrifugal fans as well as axial-flow fans. With forward- or radial-bladed centrifugal fans which have flatter head characteristics, particularly at the point of maximum efficiency, parallel operation of fans often tends to be unstable. This is because of the fact that a reduction in the quantity circulated by one of the fans involves only a small rise in its pressure which is inadequate to restore the normal operation quickly so much so that there is a continual shift in the load taken up by the fan. In extreme cases, the fan may reach a point where there is no further rise of pressure with a drop in quantity. At this point it loses its load entirely and can never recover it. Thus forward-bladed fans are unsuitable for parallel operation except when they are operating at large quantities and low heads where their efficiency is low. Unstable operation can also occur with any fan when the system characteristic is too steep so that the operating point falls on the flatter portion of the fan characteristic to the left of the stall point.

For efficient operation of fans both in series and in parallel, the two fans, should, as far as possible, be of the same size. Too large a difference in size leads to the inefficient operation of one of the fans, and when in parallel, there may be a tendency for the larger fan to take up the entire load.

Operating points for more than two fans in series or parallel can be obtained graphically in a similar way as for two fans.

It may be noted here that for accuracy, fan total pressure characteristics should be combined and the operating point obtained from their intersection with the total pressure characteristic of the mine or system. However, where velocity pressures are low compared to static pressures developed by the fans, the error involved in using static pressure characteristics is negligible.

Example 6.5

Following gives the test data on two fans available at a mine. Fan A installed on the mine circulates 10.5 $m^3 s^{-1}$ of air through the mine at a pressure of 500 Pa. It is proposed to augment the flow through the mine by adding fan B in parallel. Find the increased flow through the mine and the operating point of each fan.

Fan A		Fan B	
Pressure, Pa	Quantity, $m^3 s^{-1}$	Pressure, Pa	Quantity, $m^3 s^{-1}$
250	12.75	250	8.9
500	10.5	500	7.4
750	6.5	750	5.5
		1000	2.4

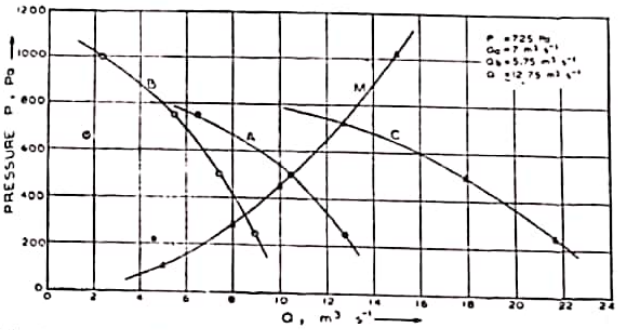

Fig. Exp. 6.5 A—characteristic of fan A, B—characteristic of fan B, C—combined fan characteristic, M—mine characteristic.

When operating in parallel the quantities for a given pressure are added together. Hence for the combined characteristic, the quantities at different pressures, are as given in the table below which also gives the data for the mine characteristic where for any flow the pressure is calculated from the relation :

$$\text{Pressure} = \frac{500\,Q^2}{(10.5)^2}\ \text{Pa.}$$

Q is the flow in $m^3\,s^{-1}$

Combined fan characteristic		Mine characteristic	
Pressure, Pa	Quantity, $m^3\,s^{-1}$	Pressure, Pa	Quantity, $m^3\,s^{-1}$
250	21.65	18.1	2
500	17.9	113.4	5
750	12.0	290.3	8
		453.5	10
		1020.4	15

The combined fan characteristic as well as the mine characteristic are drawn in Fig. Exp. 6.5. The point of intersection gives a pressure of 725 Pa at which both the fans will operate. The quantity through the mine is 12.75 $m^3\,s^{-1}$ of which fan A circulates 7 $m^3\,s^{-1}$ and fan B, 5.75 $m^3\,s^{-1}$.

6.9 COMMON TYPES OF MINE FANS

Early mine fans such as the Guibal, Waddle or Walker's indestructible fans were of backward-bladed centrifugal type. They were very large in diameter and operated at low speeds. Owing to their unwieldy size, they were soon replaced by multi-vane forward-bladed fans of Sirocco type which were much smaller in diameter, though wider than the backward-bladed fans. Sirocco fans have a large number of short blades (up to a maximum of 64) as compared to a small number (8 to 10) of long blades in backward-bladed fans. Though the efficiency of backward-bladed fans is slightly higher than that of the Sirocco-type fans, the latter became more popular due to their smaller size and quieter operation for the same water gauge. Sirocco fans, though still in operation in a few mines, have been generally superceded nowadays by axial-flow fans and modern backward-bladed centrifugal fans because of their superior efficiency.

The main mine fans now in common operation can be classed as (a) screw-type axial-flow fans, (b) turbo-axial fans and (c) aerofoil-section backward-bladed centrifugal fans. Surface fans of the two-stage axial-flow type are generally used for pressures of 2-2.5 kPa. For pressures varying from 3 to 3.75 kPa, three-stage axial-flow fans, turbo-axial fans or aerofoil-section backward-bladed centrifugal fans are used. For higher pressures, the last type of fan is the most suitable as it can generate pressures upto 7.5 kPa. Axial-flow fans are invariably preferred for underground installations because of their compact size.

6.10 INSTALLATION OF MAIN MINE FANS

Main mine fans are mostly installed at the surface. For maximum volumetric efficiency of ventilation they should be directly connected to the top of a shaft entirely meant for ventilation [Fig. 6.50 (a) and (b)]. They can be directly mounted over the shaft with their axis vertical or horizontally on the ground connected to the shaft by a suitable bend. The latter is essential in coal mines with the fan being located atleast 5m away from the shaft in order to protect it from possible explosions.

Where separate ventilation shafts cannot be provided and fans have to be installed on operating shafts, they are connected to the shafts by well designed fan drifts [Fig. 6.50 (c) and (d)]. Fig. 6.50 shows installation of exhaust fans. Forcing fans can be connected directly to a ventilation shaft or a fan drift connected to an operating shaft by a suitable diffuser.

Normally the drive of the fan, instruments and control devices are housed in a rainproof, dustproof, fireproof building provided with locking arrangement and lightening arrester. The top of the evasee in an exhaust fan and the fan inlet in a forcing fan are covered with protective wire netting. It is a good practice to provide a fence enclosure around surface fan installations.

6.10.1 Surface vs Underground Installation

Main fans at collieries are required by law to be installed at the surface so that they are readily accessible in the event of floods, fires or explosions. They are easier and cheaper to install and maintain. Besides, it may be difficult to find a suitable underground site for a main fan. Underground fans cannot be installed until the workings are ready to receive them. They are usually of the axial-flow type owing to the restriction on space and hence are of limited head. Another disadvantage with underground fans is that they usually require air-locks on main levels which become a constant source of leakage and recirculation.

On the other hand, underground fans avoid leakage at surface air-locks and shaft collars. Leakage at surface air-locks can amount

Scanned with CamScanner

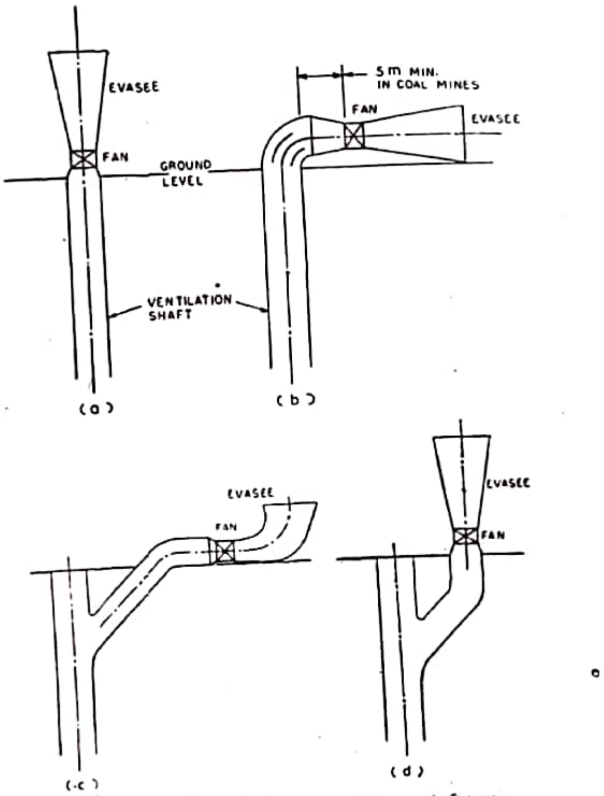

Fig. 5.50 Modes of installation of fans on shaft-tops.

to 10-20% of the quantity circulated by the fan. Even in case of fans installed at shafts entirely meant for ventilation, it is difficult to make the lining at the shaft collar completely air-tight and if caved ground or old workings exist near the shaft collar, as may happen in metal mines, leakage through the shaft collar can be

appreciable. (It is of interest to note that though surface fans cause leakage at the surface installation, they cause less leakage across underground stoppings and doors as compared to underground fans.) Underground fans assist natural ventilation (due to the heat produced by them being added to the upcast air) and may be of a smaller size, though of the same power, as they handle denser air. However, these considerations are of little practical importance. Underground fans are commonly used in metal mines where separate fans for different levels may be chosen for a more flexible control of ventilation. Also, where all the openings are required for active operation, it may be a better practice to install fans underground rather than have air-locks at the shaft-tops.

It is more economical in certain metal mines with many shafts and sections of workings to install several fans rather than a single fan for meeting the needs of ventilation. Besides, several fans offer a more flexible, though somewhat difficult, control of ventilation. However, there is a tendency in coal mines to have a single fan or sometimes fans located at a single point, though there is no reason why several fans cannot be used in extensive coal mines.

6.10.2 Forcing vs Exhaust Installation

Both forcing and exhaust type of installations are used in metal mines whereas exhaust fans are invariably used at collieries. Forcing fans handle denser and hence a lesser quantity of air. The air handled by them is cleaner and less corrosive. Besides, they help in holding back the gas in goaves from getting into the workings. (This, however, is a disadvantage in the event of the stoppage of the fan when the gas from goaves gets into the workings forming a dangerous concentration there.) On the other hand, forcing fans add some heat to the intake air.

One of the main considerations to be borne in mind when installing a surface fan is that the main exit from the mine should be through fresh intake air. This also helps in tackling emergencies such as fires etc. from the intake air. Also, as far as possible there should be no fan at the top of an active operating shaft such as a production shaft in order to avoid surface air-locks which not only hinder fast operation, but also cause considerable leakage of air. These considerations favour the installation of an exhaust fan on the top of a non-operating or a comparatively less busy shaft. Normally hoisting is done in downcast shafts so that tubs can pass

Scanned with CamScanner

from the face right to be surface in the intake without passing through shaft-bottom air-locks. In such cases an exhaust fan is desirable. With homotropal ventilation however, where the air travels in the same direction as the mineral, or the transport of the mineral is in the return air, a forcing fan on the top of the downcast shaft may be preferable. This system merits consideration where a lot of dust is produced in the hoisting shaft (as may sometimes happen with skip hoisting) and in haulage roads, so that the dust is carried out of the mine in the return air. Arrangements have however, to be made for transporting men in the downcast shaft.

6.10.3 Reversal of Air-current

In Indian mines it is required by law to provide arrangements for the reversal of air-current in order to meet with eventualities of fires in the downcast shaft or near the downcast shaft-bottom. Air reversal may well serve the purpose in coal mines where the number of openings are usually limited, but it is of not much use in metal mines where there are many shafts and outlets and there is usually a strong natural ventilation. In such cases, a more elaborate ventilation control by doors and readily erected stoppings becomes more important than reversal of air-current for controlling underground fires. However, in metal mines with a limited number of openings it is wise to provide for reversal of air-current particularly since it is the intakes which are usually dry and liable to fire hazards. In mines where there is a strong natural ventilation aiding the fan ventilation, it should be ensured that the fan generates enough pressure to overcome the opposing natural ventilating pressure in the event of a reversal of air-flow. It must be noted here that the decision for the reversal of ventilation is a very important one which can be taken only by responsible officials and hence reversing arrangements should be kept locked and operated by such responsible persons only.

6.10.4 Installation of Axial-flow Fans

Axial-flow fans can be installed with their axis either vertical or horizontal, the latter being more common. Where speed variation is not essential, the fan rotor can be directly coupled to the shaft of the driving motor, but this arrangement is unsuitable for gassy

mines where the motor has to be outside the air-stream. Besides, most fans have either V-belt or gear drives. In horizontal installations, the fan rotor can be driven by an extended shaft through the bend in the evasee as shown in Figs 6.51 and 6.52 with V-rope, gear or hydraulic drives outside the air-stream. This arrangement is common for large fans. It offers easy access to the drive and a stand-by motor can be easily accommodated.The extended shaft is usually of forged nickel steel and is connected to the fan and the motor at either ends through flexible couplings. For smaller fans, a long driving shaft can be avoided by fitting the pulley for V-ropes at the end of the runner shaft. The V-ropes pass through streamlined fairings in the air-stream (Fig. 6.53). The same can be achieved by using bevel gear drives as shown in Fig. 6.54. It is a modern trend to have two separate fans each with its own drive in which case they should be so housed that any one of them can be quickly connected to the mine and the other simultaneously isolated from the circuit in order to prevent recirculation through it.

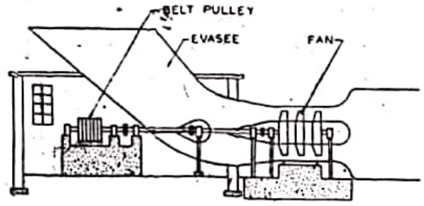

Fig. 6.51 2920mm dia three-stage axial-flow fan driven by a 370 kW motor through a rope drive at North Gauber Colliery, U.K. (*after MacFarlane*).

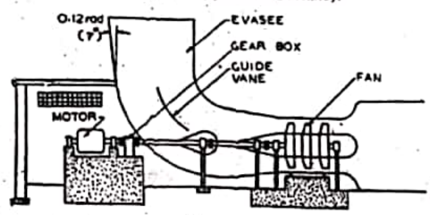

Fig. 6.52 3810mm dia three-stage axial-flow fan driven by 550 kW motor through a gear box at Bold Colliery, U.K. (*after MacFarlane*).

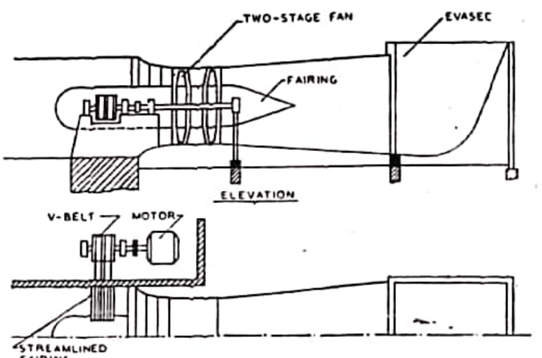

Fig. 6.53 V-belt drive for axial-flow fan (*after MacFarlane*).

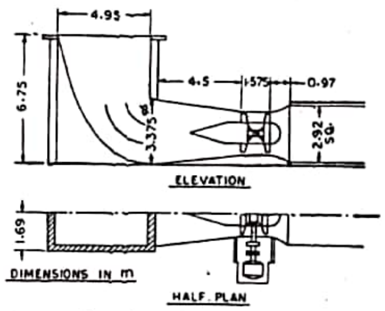

Fig. 6.54 2275mm dia contrarotaing axial-flow fan driven through gear box by a 132 kW motor (*after MacFarlane*).

Vertical installations are quite common on the European continent. They save space for fan drifts and evasees and obviate pressure loss in the fan drift. The best drive for a vertical fan is a motor directly connected to the impeller shaft as shown in Fig 6.55, but when this cannot be used as in the case of gassy mines, belt or gear drives (Fig. 6.56) can be used, access to the gear box

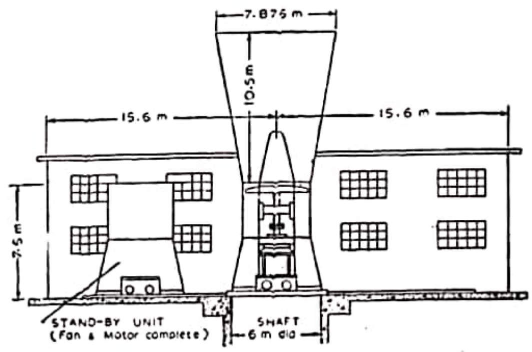

Fig. 6.55 5335mm dia vertically installed fan mounted on a bogie carriage with a 535 kW direct-coupled motor (*after MacFarlane*).

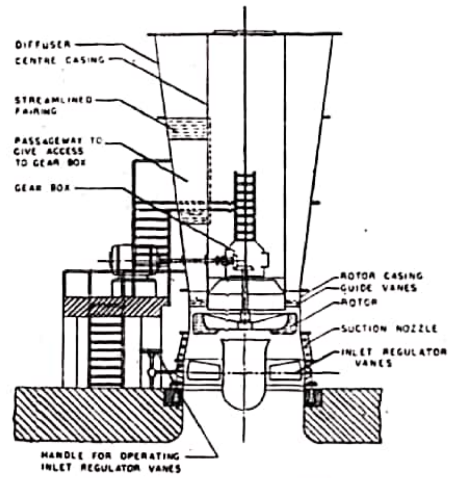

Fig. 6.56 Vertical installation of a Schicht (turbo-axial) fan (*after MacFarlane*).

being maintained through a passage covered by streamlined fairings. An interesting arrangement for a stand-by fan installation is shown in Fig. 6.55 where the fan and drive are mounted on a bogie carriage with an interchangeable stand-by fan unit. Vertical installation of axial-flow fans can be made directly over air shafts, but if the shaft is required for hoisting, the fan can be installed on a bypass shaft connected to the main shaft at a short distance below the collar.

6.10.5 Installation of Centrifugal Fans

Centrifugal fans, particularly of the double-inlet type, require much space and civil engineering work for their housing, if provision for the reversal of air-current has to be made. This calls for the provision of an elaborate set of doors and ducts as shown in Fig. 6.57. In normal operation of the fan, the doors are in the position as shown by the firm lines, but when reversing the air-current, the doors are thrown to the position as indicated by the

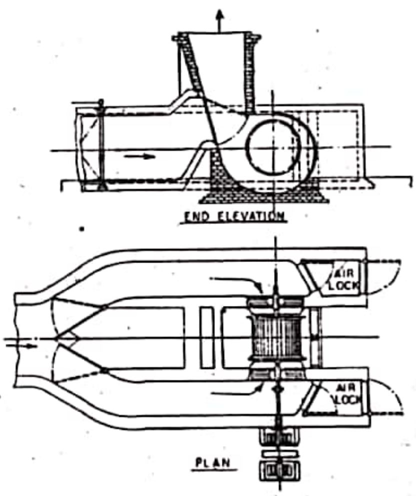

Fig. 6.57 2845mm dia double-inlet sirocco mine fan with arrangements for the reversal of air-current (*after MacFarlane*).

dotted lines. Fig. 6.58 shows the housing for two centrifugal fan units, one of which serves as a stand-by and Fig. 6.59, the housing for a single fan with a stand-by drive.

6.10.6 Fan Drifts

Fan drifts should be carefully designed for minimizing pressure loss in them. For this reason, they should be short (the distance between the shaft and the fan should not exceed 30m), smooth-lined and with gradual area change. Bends should be as few as possible and of large radius. The drift should open into the shaft

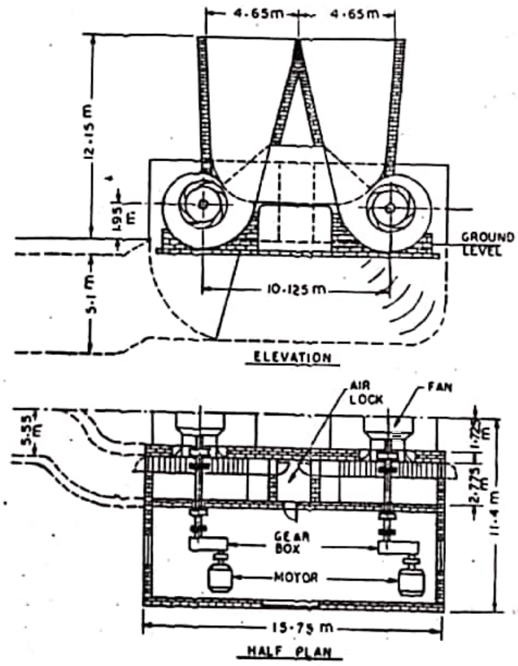

Fig. 6.58 3050mm dia aerofoil-section backward-bladed centrifugal fans complete with drives one unit acting as a stand-by (*after MacFarlane*).

Scanned with CamScanner

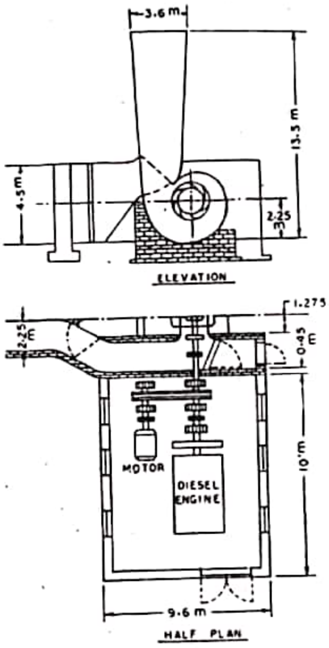

Fig. 6.59 2845mm dia double-inlet backward-bladed (aerofoil-section) fan driven by a 370 kW motor through V-ropes with alternative direct-coupled diesel-engine drive at Silverhill Colliery, U.K. (*after MacFarlane*).

well below the banking level to accommodate the surface air-lock and should have a large area of opening with well rounded edges. Where cage winding is adopted, opening of the fan drift into the shaft on the side corresponding to the narrow ends of the cages causes less obstruction to air-flow. It is usual to have the drift rising from the shaft at a sharp inclination and then flattening out to a horizontal stretch before the fan. Alternatively the

horizontal portion may be connected to the shaft by a continuous large radiused bend. The provision of the horizontal section offers a conventient position for air measurements and an easy access to the drift and fan through an air-lock in this section. Ducts serving other fans or air reversal systems are more conveniently connected at the horizontal section. The area of cross-section of the fan drift should be large and connected to the fan by a gradually converging section. Velocity of air in the fan drift should not exceed 15 m s^{-1} (preferably 10 m s^{-1}). Fan drifts should be of leakproof construction. Fan drifts can be of circular or rectangular section, the latter being more convenient to build and hence most commonly used. However, the connection to the fan should be well shaped.

It must be noted here that in coal mines where there are chances of underground explosions damaging surface fans, the fan should be at least 5m away from the mine opening. The fan drift, as indeed the entire housing of the fan, should be of fireproof construction and *explosion doors* which blow open to the atmosphere under high explosion pressures should be provided in the fan drift.

6.10.7 Diffusers and Evasees

Diffusers and evasees both refer to a gradually expanding duct meant for converting a part of the kinetic energy in the air leaving the fan to useful pressure energy. While diffusers are fitted to forcing fans, evasees are attached to exhaust fans. They are fitted to the fan outlet in order to reduce the velocity of air by increasing the cross-sectional area of discharge. The increase in area should be gradual and symmetrical in order to minimize shock loss in the diffuser or evasee. From this point of view a suitable angle of divergence of the sides of the evasee is 0.105-0.122 rad (6°-7°). Smaller angles make the evasee too long and costly. Besides, long evasees incur substantial frictional pressure loss which reduces their efficiency of head recovery. On the other hand, larger angles of divergence increase the shock loss in the evasee and consequently reduce its efficiency of head recovery. The efficiency progressively decreases with increasing angle of divergence till there is no head recovery at an angle of 0.524 rad or 30° (see Fig. 6.60)[137].

Complete conversion of velocity energy to pressure energy is impossible in an evasee since it would mean the velocity of discharge to be zero or the area of discharge to be infinitely large, which would need an infinitely long evasee. Cost considerations

Scanned with CamScanner

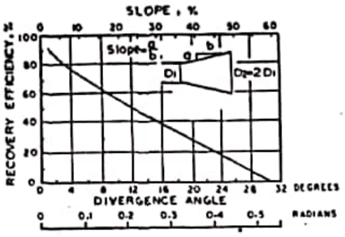

Fig. 6.60 Efficiency of head recovery in an evasee (*after Madison*).

usually restrict the ratio of the area of discharge of the evasee and that of the fan outlet to 4:1. An evasee with this area ratio and its sides diverging at an angle of 0.105 rad gives an efficiency of head recovery of about 70 percent. Larger area ratios involve a costlier evasee without any perceptible gain in the efficiency of head recovery. In fact too large area ratios involve a loss of efficiency.

If v_1 and v_2 are the velocity of air at the fan outlet and the evasee outlet respectively, then the static head h recovered in the evasee is given by the relation

$$h=\frac{v_1^2-v_2^2}{2g}\eta \tag{6.95}$$

where η=efficiency of head recovery in the evasee.

Expressing in terms of pressure recovered P_e, quantity of flow Q and the fan outlet area A, equation 6.95 becomes

$$P_e=\frac{0.328\,Q^2\rho}{A^2} \tag{6.96}$$

for an area ratio of 4:1 and $\eta=70\%$.

With large fans, an area ratio of even 4:1 may involve a large evasee with high cost when a smaller area ratio may be considered even though the pressure recovery is somewhat reduced. The final choice should be however, on the basis of minimum total cost of ventilation. Fig. 6.61[138] gives a plot of evasee *pressure recovery coefficient* k_p defined by the relation

$$k_p=\frac{P_e}{\rho v_1^2/2} \tag{6.97}$$

for different area ratios and angles of divergence and can serve as a guide for the design of evasees.

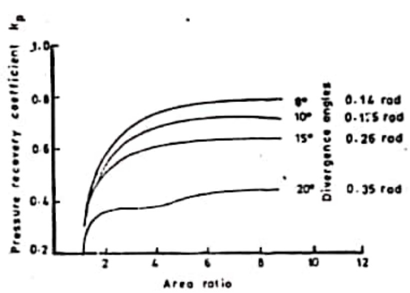

Fig. 6.61 Evasee pressure recovery coefficient (*after Ferrett*).

With centrifugal fans, the evasee is of a rectangular cross-section corresponding to the shape of the fan outlet. Usually the side of the evasee nearest the fan wheel is made vertical whereas the opposite side has a slope of 0.122 rad with the vertical (Fig. 6.57). The other two sides slope at an angle of 0.061 rad with the vertical. Sometimes all the sides of the evasee have the same slope, i.e. 0.061 rad with the vertical (Fig. 6.59).

With axial-flow fans, there can be several arrangements of evasees. With vertically installed fans, the evasee, usually made of steel or sometimes of concrete, is constructed about the vertical extension of the fan axis. With horizontally installed axial-flow fans, a horizontal steel evasee can be used provided there is ample open space for the polluted air to be discharged without causing incovenience to inhabited areas nearby. If there be populated areas nearby, it is better to discharge the air to the atmosphere at a height which necessitates a rising evasee. Such evasees also minimize noise at the ground level.

Fig. 6.53 illustrates an axial-flow fan fitted with an evasee with a long horizontal diverging section made of steel or concrete and a short vertical section made of brick or concrete to divert the air-stream upwards. But where the driving shaft passes through the wall of the evasee, the latter has to have a short horizontal section connected to a long vertical section by a sharp bend fitted with guide vanes (Fig. 6.52) for reducing shock loss. Alternatively an inclined evasee as shown in Fig. 6.51 may be used.

11 MAINTENANCE AND MONITORING OF MAIN MINE FANS

Main mine fans should be regularly inspected and maintained. Lubrication of bearings, cleaning of fan blades and painting (particularly in corrosive atmosphere) are among the major preventive maintenance measures. Periodic fan tests indicate the state of operation of the fan and should be carried out as a matter of routine.

All fans are provided with a fan-drift water gauge to indicate the fan pressure. Many countries require the fan pressure to be continuously recorded and suitable instruments should be chosen depending on the range of pressure to be recorded (see Chapter VIII). With forward-bladed centrifugal fans it is more desirable to monitor the quantity than pressure since quantity is a more sensitive measure of fan performance with a flat pressure-quantity characteristic. Warning devices should be installed to indicate failure of power supply or mechanical failure of the fan. Arrangements may also be made for automatic cutting off of power supply to the mine in case of fan stoppage. Ammeters and volt meters are usually provided on the motor control panel. Provision of a watt meter or power factor meter is desirable to keep a check on power input to the fan. It is also desirable to have a continuous record of motor current and fan speed.

Example 6.6

An 80m long and 560mm diameter ducting provides ventilation for an engine room with the fan installed inside the ducting. The following are the test readings on the fan :

Fan Quantity, $m^3\ s^{-1}$	3.0	4.0	5.0
Fan Static Pressure, Pa	880	723	450

The density of air handled by the fan is 1.29 kg m^{-3}. The value of k for the duct determined at an air density of 1.2 kgm^{-3} is 0.004 $Ns^2\ m^{-4}$. Assuming shock pressure loss at the entrance to the duct to be 18% of the friction pressure loss in the duct, calculate the quantity circulated by the fan.

What will be the increase in the fan quantity if an evasee of an outlet diameter of 1120mm and an efficiency of 80% is fitted at the delivery end of the duct ?

k at an air density of 1.29 kg m^{-3} $= 0.004 \times \frac{1.29}{1.2}$

$= 0.0043\ Ns^2\ m^{-4}$

Resistance of the duct (frictional)

$$= \frac{0.0043 \times \pi \times 0.56 \times 80}{\left\{\frac{\pi \times (0.56)^2}{4}\right\}^3}$$

$$= 40.5\ Ns^2\ m^{-8}$$

Taking 18% of friction loss as shock loss at entrance to duct, total resistance of the duct system $= 1.18 \times 40.5$

$= 47.79\ Ns^2\ m^{-8}$.

Table below gives the pressure drop in the system for various quantities of flow and the accompanying figure, the fan and the duct characteristics.

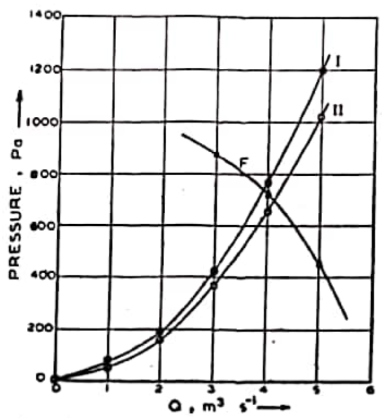

Fig. Exp. 6.6 F—fan characteristic, I—duct characteristic, II—duct characteristic compensated for evasee head recovery.

Flow through the duct, $m^3 s^{-1}$	Pressure loss, Pa
2	191.2
3	430.1
4	764.6
5	1194.8

From the intersection of the two characteristics, it is found that the fan circulates 3.9 $m^3 s^{-1}$ at 740 Pa.

With installation of the evasee,

Evasee inlet velocity $= \dfrac{3.9}{\frac{\pi}{4}(0.56)^2}$

$= 15.83 \text{ m s}^{-1}$

Velocity pressure $= \dfrac{(15.83)^2 \times 1.29}{2}$

$= 161.63$ Pa.

Evasee outlet velocity $= \dfrac{3.9}{\frac{\pi}{4}(1.12)^2}$

$= 3.96 \text{ m s}^{-1}$

Velocity pressure $= \dfrac{(3.96)^2 \times 1.29}{2}$

$= 10.1$ Pa.

$\therefore$ Pressure gain in the evasee $= (161.69 - 10.1) \times 0.8$

$= 121.2$ Pa.

Fan pressure—evasee pressure gain$=740-121.2=618.8$ Pa.

Now the system characteristic is redrawn (curve II in the figure) for a pressure of 618.8 Pa and a flow of 3.9 $m^3 s^{-1}$ from the following table,

Flow$_b$ $m^3 s^{-1}$	Pressure drop$=(\text{Flow})^2 \times \dfrac{618.8}{(3.9)^2}$ Pa
2	162.7
3	366.2
4	650.9
5	1017.1

From the intersection of this characteristic with the fan characteristic, the fan operating point is 4.15 $m^3 s^{-1}$ at 700 Pa.

The increase in quantity $= 4.15 - 3.9 = 0.25$ $m^3 s^{-1}$

6.12 BOOSTER FANS

As the name suggests, booster fans are those installed underground for boosting up or supplementing the air circulated by the main mine fan. They may assist the surface fan for ventilating the whole mine when they act in series with the surface fan, but such installations are rare since it is always better from the point of view of capital cost and efficiency to choose a single fan. However, in fiery coal mines where a single high-pressure fan may cause excessive leakage, several low-pressure fans suitably spaced in series ensure safer conditions. It may be noted here that in coal mines which are highly liable to spontaneous combustion, it is often necessary to restrict the pressure difference between intake and return to 1 kPa. Most boosters are however, used to overcome unusually high resistances of certain splits or districts in the mine or to circulate extra quantities to certain districts which need more air due to concentrated production or excessive gas emission in them.

Booster fans usually circulate 25 to 50 $m^3 s^{-1}$ at pressures varying from 0.25 to 1 kPa, though boosters circulating as much as 140 $m^3 s^{-1}$ at 1.5 kPa have been installed. Because of their compactness, axial-flow fans have been found most suitable for installation as boosters underground where economy of space is essential. Besides, axial-flow fans with adjustable vanes and variable-speed drives offer a wide range of output control which is so necessary for boosters that are often required to operate over a wide range of duty. Booster fans are normally installed in the return airway so that they do not interfere with haulage. Belt drives are common with the driver (a flame-proof motor for gassy coal mines) being placed in an adjacent room connected to the intake (Fig. 7.72). The motor room is ventilated by intake air leaking through the recess in the partition between the fan and the motor room provided for the passage of driving belts. A bypass with a suitable air-lock is provided alongside the airway housing the fan in order to provide access across the fan. Sometimes, if the main airway is required for occasional transport, the booster may be installed in a bypass airway while a suitable air-lock is provided in the main airway. However, it must be borne in mind that for efficient operation, the booster fan should be installed in straight airways of uniform cross-sectional area and bends, particularly sharp ones, should be avoided near the fan inlet or outlet.

Scanned with CamScanner

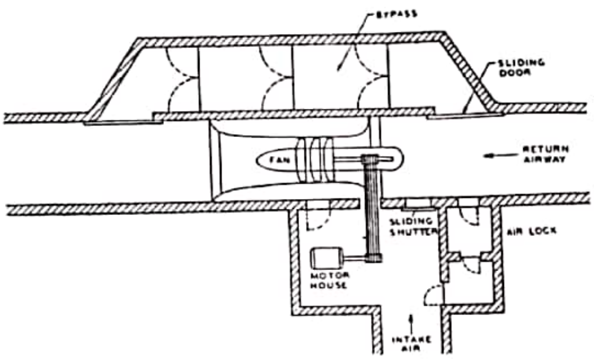

Fig. 6.62 Installation of a 1750mm dia booster fan underground (*after MacFarlane*).

It is well known that the installation of a booster fan in one district reduces the flow of air in other districts and may even completely stop the air-flow through them if the booster is not judiciously selected and installed. That is why it is necessary and is also required by law that a careful ventilation survey be made and the ventilation needs of the different splits in the mine carefully assessed before deciding on the installation of the booster fan. Installation of a booster underground increases the total quantity circulating in the mine which shifts the operating point on the main fan characteristic. However, installation of boosters normally becomes necessary when the overall resistance of the mine is high leading to the inefficient operation of the main fan and under such circumstances the shift of the operating point due to the installation of the booster only tends to increase the efficiency of operation of the main mine fan.

Booster fans are liable to damage by underground explosions. To guard against such contingencies as well as the stoppage of the booster fan due to any other reason, it is necessary to ensure that in the event of the failure of the booster fan, a sufficient quantity of air is circulated to the split by the main mine fan in order to prevent the development of a dangerous atmosphere there. It is also for this reason that good maintenance by a separate underground crew is vital for ensuring continuous running of boosters

even though it involves an increase in the maintenance cost of ventilation.

6.13 AUXILIARY VENTILATORS

Unlike boosters, auxiliary ventilators are much smaller in size and are used for ventilating shafts, drifts, tunnels and other development ends, particularly in metal mines, where the small size of openings does not permit bratticing. Auxiliary fans have now found use even in short headings or rooms in coal mines where large-scale mechanization prohibits the use of brattices. The size of an auxiliary fan depends on the air requirement at the face. Whereas under normal conditions in metal mines, a development face about 100 metres away from the main airway can be tolerably ventilated by convection and compressed-air escaping from machines, under hot and humid conditions, adequate mechanical ventilation becomes necessary to create comfortable environmental conditions at the working face. Besides, lack of mechanical ventilation often holds up progress due to slow dispersal of blasting fumes from the face by diffusion and convection. Hence it is expedient to use at least a small air driven fan or venturi for blowing air (about 0.5 $m^3 s^{-1}$) at the face where it has advanced more than 30m.

Larger quantities have to be circulated by auxiliary fans in longer headings, particularly mechanized ones, for dilution of gas, dust and quick removal of blasting fumes. Normally the quantity of air circulated to such headings varies from 1 to 2.5 $m^3 s^{-1}$, though in some deep and hot mines of South Africa, it is a practice to circulate as much as 5 $m^3 s^{-1}$ of air at drift faces of fairly small areas.

The pressure requirements of an auxiliary fan can be fairly high depending on the length of the drift to be ventilated. Normally the fan is so selected as to operate to the right of the stall point even when used with the longest ducting, i.e. with maximum system resistance. For this reason it is preferable to have a continuously drooping pressure characteristic of the fan. When operating with shorter ducting, the fan will have a tendency to overloading and that is why it is essential to select a type of fan for auxiliary ventilation which not only has a non-overloading, but also a fairly flat power characteristic. From this point of view, forward-bladed centrifugal fans are unsuitable as auxiliary ventilators

Scanned with CamScanner

even though they have a high head coefficient. Of the other types of fans, the backward-bladed centrifugal fans, though very suitable for high head requirements, are rarely used nowadays as auxiliary ventilators underground because of their bulkiness so that auxiliary fans today are invariably of the axial-flow type. Axial-flow fans are compact, portable and sturdy in construction which is so very necessary for auxiliary fans that are to be moved from place to place at frequent intervals. Axial-flow fans have the added advantage of being able to be easily connected to co-axial ducts which are often of the same diameter as the fan. However, for long tunnels and deep shafts where fans of high head are required to be installed more or less permanently and where enough space is available near the tunnel mouth or shaft collar, backward-bladed centrifugal fans may be chosen.

Arrangements for capacity control are not provided on auxiliary fans since they make the fan heavy and less portable. In some large fans however, provision is made to control excessive quantities produced by the fan operating with short ducting by the use of an inlet-vane or damper control. With small fans, excessive quantities are usually controlled by placing improvised obstructions on the path of air in the duct, though this process is wasteful. Because of the low power consumption (of the order of 4-8 kW) of auxiliary fans, only a small saving of power is effected by the introduction of a more efficient means of capacity control. Besides, the incorporation of such a control makes the fan less portable and more complex in operation.

Single-stage axial-flow fans varying from 450 to 750mm in diameter are most commonly used as auxiliary ventilators. Auxiliary axial-flow fans are now specially designed for negotiating widely varying system resistances. Their head characteristic is almost in the form of a straight line falling steadily from a maximum at zero capacity. This allows for operation of the fan over a wide range of system resistance without the fear of unstable operation, though the efficiency of operation falls at both high and low system resistances. These fans have a flatter efficiency characteristic which gives them a wider range of efficient operation, although the maximum efficiency is somewhat lower than that of axial-flow fans of usual designs. They develop about 1 kPa at the maximum efficiency and are capable of negotiating with heads up to 2 kPa at lower efficiencies.

Where pressure requirements are of the order of 2 kPa or more, two-stage or *contra-rotating axial-flow fans* (Fig. 6.63) may be chosen. Contra-rotating fans have the advantage of being operated as single-stage fans, where necessary, as in the case of the early stages of driving a long drift when the pressure requirement is less. Axial-flow fans of more than two stages are, however, unsuitable as auxiliary ventilators because they become too heavy and unportable. Several single-stage fans placed in series at suitable intervals in the duct are generally used for meeting with high pressure requirements. Low-pressure fans in series have the advantage of minimizing leakage, a fact worthy of consideration in case of leaky ducts. However, with series installation, the fans should be so placed that at no point inside the duct the pressure is lower than the ambient pressure in the case of forcing fans or higher than the ambient pressure in the case of exhaust fans. This is necessary to avoid recirculation of air.

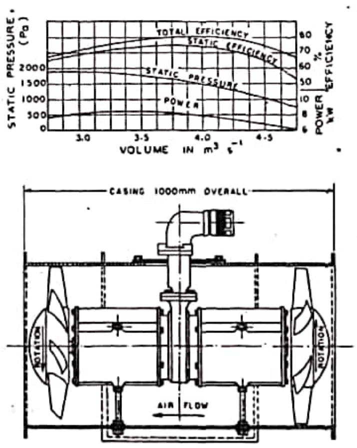

Fig. 6.63 500mm dia, 4.5 kW contra-rotating axial-flow fan and its characteristic curves (*after MacFarlane*).

Most axial-flow fans are electrically driven, the motor usually of 300 rad s^{-1} (2900 r.p.m.) for 50 Hz supply, being directly coupled to the fan wheel. For gassy coal mines, a suitable flameproof motor is used, but the arrangement of placing the motor outside the fan casing and driving the fan through belts is now obsolete since it makes the unit bulky and less portable.

6.13.1 Compressed-air-Driven Fans

Compressed-air-driven axial-flow fans are often used for small pressure-quantity duties. They are essentially single-stage axial-flow fans driven by a compressed-air turbine whose buckets are provided along the periphery of the fan wheel. The whole fan-turbine unit is cast in one piece in light aluminium alloy. Fig. 6.64 gives the characteristic of a compressed-air fan. The speed of these fans varies with the system resistance and hence their

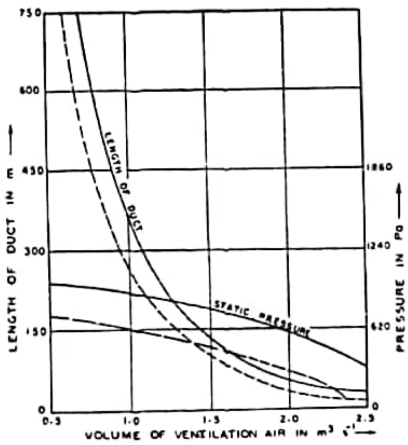

Fig. 6.64 Performance curves for a 400mm dia 'Sirocco' compressed-air driven fan on 400mm canvas duct—full line curves are for a compressed-air pressure of 570 kPa and compressed-air quantity of 2.29 m^3 min^{-1}; dotted-line curves are for a compressed-air pressure of 428 kPa and compressed-air quantity of 1.78m^3 min^{-1} (*after MacFarlane*).

characteristics, unlike those of other fans, are not drawn for constant speeds. On the other hand, they are drawn for constant compressed-air pressures. The head characteristic is similar in nature to that of other fans. The amount of compressed-air consumed and hence the power, remains constant for all volumes at a fixed compressed-air pressure, but the efficiency of these fans is low varying from 10% to 30%. It is for this reason that they are restricted to small pressure-quantity duties. Variation of duty is achieved by controlling the compressed-air pressure by a suitable valve.

Compressed-air fans, in spite of their low efficiency and noisier operation, are compact and easy to install and are preferable where excessive quantities of gas are found in coal mines. In metal mines they may be used in far off places where electric power supply is not available. Sometimes compressed-air fans are preferred to electrically-driven fans in hot places where the cool exhaust air from the compressed-air driven fans helps in improving the environmental condition.

6.13.2 Venturi Blowers

These are compressed-air ejectors which are sometimes used in stopes with sluggish ventilation, in short headings or as forcing ventilators in the overlap system of ventilation of drives where compressed-air supply is available. The performance of air ejectors[100] depends on the nozzle pressure, shape, size and location as well as the characteristics of the throat (length and diameter), diffuser (angle of divergence) and inlet (angle of convergence). For a given ejector, the head ratio β (ratio of the head at the discharge end to the velocity head of the primary stream at throat inlet) is related to the mass ratio $\propto$ (ratio of mass flow-rate of secondary fluid to that of the primary fluid) by the relation

$$\beta = A+B\propto+C\propto^2 \tag{6.98}$$

where A, B and C are constants depending on the construction of the ejector. This equation is comparable to equation 6.27 for centrifugal fans running at constant speed.

Theoretically efficiency of ejectors η is given by the relation

$$\eta = \frac{\propto\beta}{\sigma} \tag{6.99}$$

Scanned with CamScanner

where σ is the ratio of the densities of air of the secondary and primary streams. η is maximum where β equals the ratio of the throat area to the cross-sectional area of the primary stream at the throat inlet. However efficiency of ejectors is low (of the order 7-10%) and falls for both higher and lower values of β.

Venturi blowers at mines commonly operate at the available compressed-air pressure of around 500-600 kPa with nozzle diameters ranging between 5 and 10mm. Fig. 6.65 illustrates the Modder Deep type of venturi blower the design of which was perfected after much experimental work. A typical venturi blower delivers around 0.6-0.7 $m^3 s^{-1}$ of air at a pressure of 250 Pa with a compressed-air consumption of about 0.025 $m^3 s^{-1}$ of free air. With increase of pressure to around 500 Pa, the quantity falls to 0.5 $m^3 s^{-1}$ and to only 0.2 $m^3 s^{-1}$ at a pressure of 1 kPa. Venturi blowers are still used in mines in spite of their low efficiency because of their low initial cost (venturis cost about one-twentieth of the cost of air fans of similar duty), easy availability (they can be easily made at the mine), low maintenance cost owing to the absence of moving parts and less noisy operation. However, venturis are rarely used in series for ventilating long headings because of their low efficiency as compared to fans which are the right choice in such cases.

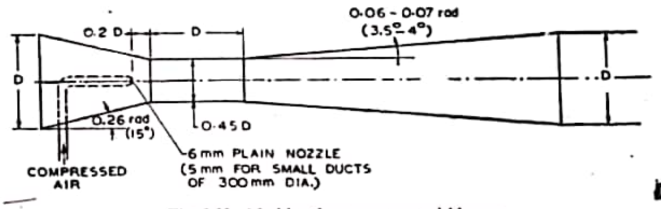

Fig. 6.65 Modder deep-type venturi blower.

Sometimes compressed-air jets are placed centrally in cylindrical ducts to form ejectors, but these are highly inefficient and can hardly deliver 0.17 $m^3 s^{-1}$ at a pressure of 250 Pa.

EXERCISE 6

6.1 Estimate the power of the motor required to drive an auxiliary fan forcing 1.5 $m^3 s^{-1}$ of air through a 100m long and 300mm

diameter steel duct having a Darcy-Weisbach resistance coefficient f=0.018. Assume the shock resistance of the system to be 15% of the frictional resistance and the fan to have an efficiency of 70%.

6.2 A fan forcing 840 $m^3 min^{-1}$ of air through a mine gives a total pressure (as measured by a pitot or facing tube) reading of 750 Pa and a velocity pressure reading (as measured by a pitot-static tube) of 250 Pa at the outlet. Calculate the overall efficiency of the fan and motor (a three-phase slip-ring induction motor) if the latter draws a current of 13.5 A at 440 V with a lagging power factor of 0.9.

6.3 A mine having a resistance of 0.01 $Ns^2 m^{-8}$ is 300m deep. Calculate the fan pressure required to circulate 100 $m^3 s^{-1}$ through the mine if the average temperatures of the upcast and downcast shafts are 305 K and 299 K respectively and the average barometric pressure in the shafts is 101.3 kPa.

6.4 Owing to a large deviation in the mine resistance from the projected value, the fan now supplying the mine 130 $m^3 s^{-1}$ at 700 Pa runs inefficiently with a power input of 200 kW. It is proposed to replace the fan by a new one with a more favorable characteristic so that it operates at the same point on the mine characteristic but with 80% efficiency. The same motor will be used with the new fan and is expected to operate at an efficiency of 92%. Taking the cost of the new fan inclusive of the cost of installation to be Rs. 100 000.00, examine if it will be economical to install the new fan if the mine has a projected life of 16 years. Take 8% interest on annuity.

6.5 A fan running at 10π rad s^{-1} (300 r.p.m.) circulates 7000 m^3 of air per minute through a mine at a pressure of 650 Pa. Calculate the power consumed if the combined efficiency of the fan and drive is 65%. Also determine the increase in the quantity circulated and the power consumed, if the fan speed is increased to 11π rad s^{-1} (330 r.p.m.).

6.6 A fan running at 293.3 rad s^{-1} (2800 r.p.m.) delivers a quantity of 3.3 $m^3 s^{-1}$ at a pressure of 1 kPa. It is desired to increase the pressure to 1.15 kPa by increasing the fan speed. Calculate the

Scanned with CamScanner

required fan speed and the quantity after the fan has been speeded up. Also examine if the 7.5 kW motor now provided with the fan will be adequate for the higher speed of operation assuming the fan and drive efficiency to be 60%.

6.7 A fan circulates 50 $m^3 s^{-1}$ of air through a mine having a resistance of 0.3 $Ns^2 m^{-8}$. The power input to the fan motor is recorded at 73.6 kW. What is the combined efficiency of the fan and motor ? It is desired to raise the quantity circulating through the mine to 65 $m^3 s^{-1}$ by speeding up the fan. Examine if the motor rated at 120 kW will be adequate.

6.8 A 900 Pa fan has been selected for a mine without taking into account the natural ventilating pressure which is 250 Pa. It is now decided to reduce the fan speed to save power of ventilation. What is the required reduction in the fan speed ? The motor-shaft pulley which is 300mm in diameter is to be replaced while the fan-shaft pulley of 600mm diameter is to be retained. What would be the new size of the motor-shaft pulley ?

6.9. A fan circulates 50 $m^3 s^{-1}$ of air through a mine at a pressure of 1000 Pa. Calculate the equivalent orifice of the mine. Calculate the quantity that will circulate through the mine and the pressure of the fans, if another identical fan is added (a) in series, (b) in parallel. Assume the power of the fans to remain constant.

6.10. A forcing fan, the test data on which is given in the table below, circulates 62 $m^3 s^{-1}$ of air through an airway at a pressure of 700 Pa, the pressure drop in the first half of the airway being 500 Pa. A second airway having a resistance of 0.2 $Ns^2 m^{-8}$ joins it midway. It is proposed to install an identical fan to force air into the second airway in order to augment flow through the system. Determine the flow through the system and the operating pressure and quantity of each of the two fans when they operate in parallel.

Static pressure, Pa	820	700	540	410	230	30
Quantity, $m^3 s^{-1}$	58	62	69	75	82	87

6.11. Figure gives static pressure characteristics of two types of fans A and B. A fan of type A is installed at a mine and circulates

110 $m^3 s^{-1}$ at a pressure of 500 Pa, but the quantity is inadequate. There are two fans of type B available. Examine which of the following combinations will give the maximum flow. Also calculate the operating point (quantity and pressure) of each of the three fans for maximum flow through the mine.

(a) All the three fans in series.

(b) All the three fans in parallel.

(c) The fan of type A in parallel with two fans of type B in series.

(d) The fan of type A in series with two fans of type B in parallel.

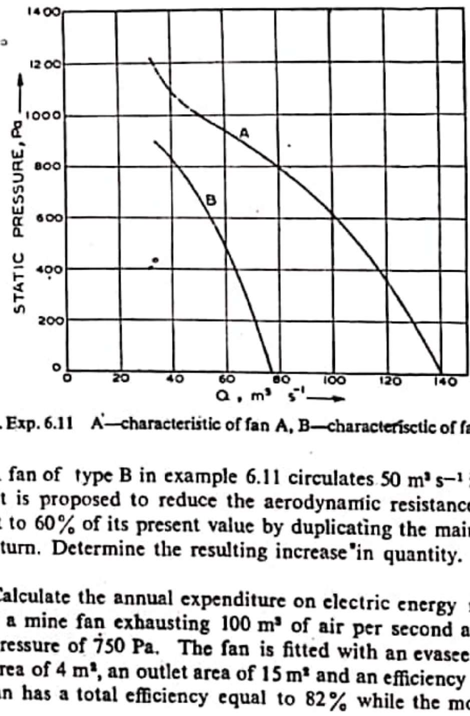

Fig. Exp. 6.11 A—characteristic of fan A, B—characteristic of fan B.

6.12 A fan of type B in example 6.11 circulates 50 $m^3 s^{-1}$ in a district. It is proposed to reduce the aerodynamic resistance of the district to 60% of its present value by duplicating the main intake and return. Determine the resulting increase in quantity.

6.13 Calculate the annual expenditure on electric energy required to run a mine fan exhausting 100 m^3 of air per second at a fan-drift pressure of 750 Pa. The fan is fitted with an evasee with an inlet area of 4 m^2, an outlet area of 15 m^2 and an efficiency of 70%. The fan has a total efficiency equal to 82% while the motor and

Scanned with CamScanner

drive efficiency is 88%. Take the density of air at 1.15 kg m^{-3} and power rate at Rs. 0.10 per kWh.

6.14 The area of an evasee at the outlet is 12 m^2 which is 3 times that at the throat. Calculate the useful pressure recovery in the evasee for a fan discharge of 200 $m^3 s^{-1}$ assuming 75% efficiency for the evasee. Also calculate the static pressure of the fan if the mine resistance is 0.04 $Ns^2 m^{-8}$, and the flow through the mine without the evasee assuming the static pressure of the fan to remain constant with or without evasee. What is the hourly saving in the cost of power wasted as velocity head with the installation of the evasee, if the combined fan and motor efficiency is taken constant at 60% and the cost of power is Rs. 0.12 per kWh ?

6.15 An 86m long 570mm diameter ducting provides ventilation for a substation with the fan installed at the midpoint of the ducting. Following gives the test data on the fan :

Quantity, $m^3 s^{-1}$	Fan static pressure, Pa
3.0	880
4.0	723
5.0	450

The density of air circulated is 1.3 kg m^{-3}. The shock loss at the entrance to the ducting is 20% of the frictional pressure loss in it. What is the flow handled by the fan ? What will be the increase in flow if a diffuser with an outlet diameter of 1140mm and efficiency of 81% is fitted at the duct outlet. Coefficient of friction for the duct measured at an air density of 1.2 kg m^{-3} is 0.0037 $Ns^2 m^{-4}$.

6.16. Field tests conducted on a surface exhaust fan fitted with an evasee gave the following readings :

Static pressure measured at the fan inlet = −900 Pa.
Static pressure measured at the fan outlet = −280 Pa.
Static pressure measured in the fan drift at its junction with the converging piece connecting the fan = −630 Pa.
Average air velocity measured in the fan drift = 10 m s^{-1}
Cross-sectional area of fan drift = 12 m^2

Cross-sectional area of the cylindrical casing of the axial-flow fan = 4.5 m^2
Cross-sectional area of the evasee outlet = 15 m^2.

The fan drift is connected to the fan by a gradually converging connecting piece. Calculate (a) the pressure loss in the converging piece connecting the fan drift to the fan, (b) the head loss in the evasee as well as its efficiency, (c) fan static pressure (excluding head recovered in the evasee) and (d) fan total pressure. Draw the total and static pressure gradients between the fan drift (at its junction with the converging piece) and the evasee outlet. Assume air density to remain unchanged (from fan inlet to fan outlet) at 1.2 kg m^{-3}.

Scanned with CamScanner

CHAPTER VII

DISTRIBUTION AND CONTROL OF AIR-CURRENTS

7.1 GENERAL

Controlled distribution of air is necessary for supplying the required quantities to various parts of a mine as well as for minimizing the dangers due to fires, explosions etc.

The quantity of air flowing through an airway can be reduced by increasing the resistance of the airway, as $Q \propto 1/\sqrt{R}$. This is generally done by introducing a regulator in the airway, but the method is wasteful though most practicable. The airflow can be completely stopped (except for small leakage) by erecting stoppings in the airway if the latter is not to be used as a travelling road or haulage-way, but in case access through the airway has to be maintained, doors have to be used for stopping the airflow. Another method of reducing flow in an airway with less wastage is to reduce the main fan pressure causing flow. This method however is rarely practised since it involves special adjustments in the fan. Also, a reduction in the main fan pressure affects flow in other airways.

Similarly, the flow through an airway or a circuit of airways can be increased, either by reducing the resistance of the circuit or by increasing the pressure causing flow. Increasing quantity by increasing the pressure causing flow is not as efficient as the other method since as we know, $Q \propto \sqrt{P}$ or for doubling Q, P has to be increased four times. Again, since power $\propto PQ \propto Q^3$, $Q \propto (\text{power})^{1/3}$; or in other words, for doubling Q, the power has to be increased eight times. However, this method is sometimes adopted, when booster fans are used in series with main mine fans to increase the quantity flowing through a certain district. Decreasing the resistance of an airway or circuit of airways for increasing the quantity flowing through it can be achieved by (a) increasing the cross-sectional area of the airway, (b) smooth-lining the airway or by (c) using several airways in parallel.

From equation 4.29, $Q \propto \sqrt{A^3/S} \propto \sqrt{D^5}$ for constant ventilating pressure, where D is the diameter or the side respectively of a circular or square airway. Or, to double Q, D has to be increased $4^{1/5}$

times or A has to be increased $16^{1/5}$ times. This method of increasing quantity by increasing the size of the airway can be practised only in special cases of short sections of airways, since stripping of airways involves high cost and other problems of support.

Smooth-lining of the airways increases the quantity flowing through it by decreasing the value of k. From equation 4.29, $Q \propto 1/\sqrt{k}$; or doubling Q necessitates the reduction of k by four times. The value of k can, however, be reduced considerably by smoothlining the airway, though it may involve some additional capital expenditure.

The best method of increasing air-flow through a district is by providing more than one airway in parallel serving the district.

Let us consider n similar openings (i.e. their lengths, cross-sectional areas and nature of surface are the same) supplying air to a district or face. If the resistance of each of them is R, then the total resistance R_n of all the openings is given by the relation

$$1/\sqrt{R_n} = n/\sqrt{R} ;$$

or,

$$R_n = R/n^2 \tag{7.1}$$

as the openings are in parallel. Now, if the pressure across the openings is P, and the quantity flowing through, Q_n, then

$$Q_n = \sqrt{(P/R_n)} = \sqrt{(Pn^2/R)} = n\sqrt{(P/R)} = nQ \tag{7.2}$$

where Q is the quantity circulating through a single opening of resistance R with pressure P acting across it. Or, the quantity is multiplied as many times as the number of splits. The air power also increases n times. It is thus evident that by providing parallel airways, the power consumption is doubled when the quantity is doubled, whereas if quantity is doubled by increasing pressure, the power consumption goes up eightfold. It must be noted here that as required by law nowadays, double intake airways have to be provided in gassy coal mines. This not only reduces the effective resistance of the intake but also provides a travelling way separate from the haulage way. Also, sufficient ventilation can be maintained even if one of the intakes is temporarily blocked by a roof fall.

Scanned with CamScanner

7.2 SPLITTING

When a mine has several working districts, it is preferable to divide or split the air required for the mine to the respective quantities needed in these districts and supply them through separate ventilation routes or circuits in parallel. Just as combination of airways in parallel reduces their resistance, splits reduce the overall resistance of the mine and increase the fan quantity. Control of quantities delivered to different districts to suit their needs can be done easily by controlling the resistance of the splits. Besides, splitting helps in providing fresh uncontaminated air to each district. Explosions or fires occurring in one district can be easily confined to that district by suitable ventilation control measures. Splitting helps in keeping down air velocities in roadways by distributing the quantity through several openings instead of one.

However, splitting has its disadvantages such as (a) the necessity of maintaining a larger number of airways and (b) addition of a greater amount of heat to the air by virtue of its low velocity and contact with a larger rock surface in the splits.

Splitting, as a means of distributing air from the shaft to the face, was first adopted by John Buddle in 1810 in the coal mines of U.K. Since then it has been the mainstay in ventilation planning. For ideal air distribution, (a) the splits should have resistances commensurate with their air requirements ; (b) they should be fairly long so that the trunk airways connecting them to the shafts at both ends are as short as possible, as these trunk airways are usually overloaded and can cause large friction losses ; and (c) the number of splits should be neither too large nor too small. Too few splits cause a large number of faces to be ventilated by a single split whereas too many splits may produce sluggish ventilation at the face. According to German regulations there should be one split for every 100 men in gassy coal mines.

Example 7.1

A 300m long airway passes 10 m³ of air per second. A new airway of the same cross-section and similar surface but 250m long is added in parallel to it. Calculate the quantity of air passing through the new airway as well as the total quantity.

Let us first assume that the pressure across the airway remains unchanged after the addition of the new airway. This means that

the quantity in the original airway remains unchanged after the addition of the new airway.

Let P = pressure causing flow in Pa,

Q_1 = quantity flowing through the longer airway $= 10$ m³ s⁻¹,

Q_2 = quantity flowing through the shorter airway in m³ s⁻¹,

Q = total quantity in m³ s⁻¹,

R_1 = resistance of the longer airway in Ns² m⁻⁸

and R_2 = resistance of the shorter airway in Ns² m⁻⁸. Since the two airways are similar in cross-section and nature of surface, their resistances are proportional to their lengths.

Or, $R_2 = 250\, R_1/300$.

$$\text{Or, } Q_2 = \sqrt{P/R_2} = \sqrt{\frac{100\, R_1}{250\, R_1/300}} = 10.95 \text{ m}^3 \text{ s}^{-1}$$

since $P = R_1\, Q_1^2 = 100\, R_1$.

Therefore $Q = 10 + 10.95 = 20.95$ m³ s⁻¹.

The above solution, assuming that the pressure remains constant, is not very accurate since the addition of the new airway increases the total quantity owing to the overall reduction of resistance and this shifts the operating point on the fan characteristic, so that the fan now operates at a lower pressure. That is why sometimes air power is assumed to be constant in such calculations.

But this is not strictly correct either, since even though the power characteristic of a fan shows much less variation with flow than the head characteristic, the efficiency characteristic which has a large variation introduces a substantial variation in the air power with flow rate. That is why for accurate calculation, the process of solution has to be iterated with a new fan pressure value in between the original one P and the value read off from the fan characteristic corresponding to the total flow Q. All the same the assumption of constant air power gives a more accurate solution than the assumption of constant fan pressure and hence may be used for rough calculations.

Let P and Q_1 be the pressure across the airway and the quantity

Scanned with CamScanner

flowing through it respectively before the addition of the new airway. After the addition of the new airway

let P' = pressure across the airways in P_a,
Q = total quantity in $m^3\ s^{-1}$,
Q' = quantity in the longer airway in $m^3\ s^{-1}$,
Q'' = quantity in the shorter airway in $m^3\ s^{-1}$
and R = combined resistance in $Ns^2\ m^{-8}$.

Air power after the addition of the new split$=P'\,Q=RQ^3$ W,
and air power before the addition of the new split

$$=PQ_1=R_1Q_1^3 \quad \text{W}.$$

Assuming air power to remain constant, $R_1Q_1^3=RQ^3=R_1Q^3/4.4$,

since $1/\sqrt{R}=1/\sqrt{R_1}+1/\sqrt{R_2}=1/\sqrt{R_1}+1/\sqrt{250\,R_1/300}$,

$$\text{or, } R=R_1/4.4.$$

Therefore, $Q^3/4.4=Q_1^3=1000$, or, $Q=16.4\ m^3\ s^{-1}$.

Now, $Q=Q'+Q''=16.4$ and $Q'/Q''=\sqrt{P'/R_1}/\sqrt{P'/R_2}=0.9$.

Therefore, $Q''=8.6\ m^3\ s^{-1}$ and $Q'=7.8\ m^3\ s^{-1}$.

Example 7.2

A fan installed in a drift connected to an exhaust shaft develops a pressure of 650 Pa and circulates 150 $m^3\ s^{-1}$ of air. The fan drift consumes a pressure of 250 Pa and the exhaust shaft 100 Pa. A quantity of 50 $m^3\ s^{-1}$ leaks through the surface air-locks on the exhaust shaft. A second shaft with a drift aerodynamically similar to the existing one is added in parallel with a view to reducing the system resistance. Assuming similar resistance of the leakage paths at the air-locks on the top of the second shaft, determine the change in the flow through the mine, assuming the fan pressure to remain unchanged.

Resistance of exhaust shaft $=\dfrac{100}{(100)^2}=0.01\ Ns^2\ m^{-8}$.

Resistance of fan drift $=\dfrac{250}{(150)^2}=0.0111\ Ns^2\ m^{-8}$.

Resistance of leakage paths through air-locks $=\dfrac{650-250}{(50)^2}=0.16\ Ns^2\ m^{-8}$.

Resistance of the rest of the mine $=\dfrac{650-(250+100)}{(100)^2}=0.03\ Ns^2\ m^{-8}$

Let the fan quantity after connection of the new shaft be $Q\ m^3 s^{-1}$ and the leakage through the shaft-top air-locks be $Q_L\ m^3 s^{-1}$. Since the resistances of the two drifts as well as the leakage paths through air-locks at the top of the two shafts are equal, the flow through each drift is $Q/2$ and the leakage at each shaft top, $Q_L/2$.

Also quantity through each exhaust shaft $=\dfrac{Q-Q_L}{2}$

Considering the mine circuit through any shaft,

$$650=(Q/2)^2\times0.0111+\left(\frac{Q-Q_L}{2}\right)^2\times0.01+(Q-Q_L)^2\times0.03 \quad \text{(a)}$$

Again considering the leakage path over any shaft-top,

$$\left(\frac{Q_L}{2}\right)^2\times0.16=\left(\frac{Q-Q_L}{2}\right)^2\times0.01+(Q-Q_L)^2\times0.03 \quad \text{(b)}$$

Combining equations, (a) and (b),

$$650=\frac{0.0111}{4}Q^2+\frac{0.16}{4}Q_L^2$$

Or, $Q_L=\sqrt{16\,250-0.07\,Q^2}$

Substituting this value of Q_L in equation (a), we have,

$$650=0.0028\,Q^2+0.0325\left(Q-\sqrt{16\,250-0.07\,Q^2}\right)^2$$

Or, $Q=226\ m^3\ s^{-1}$ (from a graphical solution of the above equation).

$Q_L=112.6\ m^3\ s^{-1}$.

$\therefore$ Flow through the mine$=226-112.6=113.4\ m^3\ s^{-1}$.

Change in flow through the mine$=113.4-100=13.4\ m^3\ s^{-1}$. There is a small increase in flow, but the leakage increases considerably from a third to almost half of the quantity circulated by the fan.

In fact if fan pressure is taken to vary along its characteristic instead of being taken constant, there may not be a rise in the flow through the mine at all while leakage will increase considerably.

7.3 STOPPINGS

Stoppings may be temporary or permanent. Temporary stoppings, though commonly used in coal mines (particularly with bord-and-

Scanned with CamScanner

pillar method of working), are rare in metal mines where most stoppings or bulkheads are of a permanent nature.

Temporary stoppings in coal mines are usually made of brattice cloth, tarred paper or plastic cloth with wire netting reinforcements. They can be hung as curtains for allowing access through the roadway or nailed on to a framework, the former allowing more leakage. Even the latter can allow substantial leakage at the periphery of the airway. Inflatable plastic stoppings have been designed to minimize such leakage. These materials are, however, rarely used in metal mines where the stronger blasting concussion might damage them easily. Besides, they make a poor fit against the rough walls of the drives in metal mines and hence cause a lot of leakage. Temporary bulkheads in metal mines are usually made of wooden boards nailed on to a skeleton frame of wood, the gaps between different boards as well as those between the boards and the rock wall being closed air-tight by stuffing them with rags and plastering with clay.

Permanent stoppings in coal mines are usually made of brick or cement-concrete walls. A good foundation reaching up to solid unfractured ground surrounding an airway is essential for preventing leakage, particularly in case of stoppings erected to seal off fire areas. According to Indian coal mines regulations, all stoppings between main intakes and returns should be either of brick work or masonry of a minimum thickness of 250mm and suitably plastered by lime or cement mortar. They should be accessible for inspection. British regulations require that stoppings between main intakes and returns should be explosionproof and made of either (a) at least 4.5m thick compact packing of stone, sand etc. or (b) at least 2.7m thick tight packing of the above material faced on the intake side with a brick, masonry or concrete wall of a minimum thickness of 230mm, plastered with a layer of mortar. The Director General of Mines Safety, India recommends a 1.5m thick brick wall for explosionproof stoppings. Important fireproof and explosionproof stoppings in coal mines should preferably be made of brick (two-brick thick) or concrete walls, spaced out a certain distance, depending on the strength desired, and with the intervening space filled tight with broken rock, sand and clay etc. Though permanent stoppings in coal mines become essential for sealing off inter-connecting openings between main intakes and returns, their use is less frequently called for in the ventilation systems commonly adopted in metal mines. Caved or filled material usually acts as

stopping in abandoned workings in metal mines where one often finds doors instead of stoppings even in unused airways. Things are, however, altogether different in gassy coal mines where a more rigid control of ventilation is necessary for preventing accumulation of gas. This demands the use of stoppings wherever possible, in preference to doors which are likely to be left open by irresponsible workers.

Permanent bulkheads in metal mines usually consist of wooden stoppings made air-tight by coating them with a layer of gunite (a mixture of sand and cement applied as a coating by means of compressed-air) reinforced with wire-netting, but more permanent stoppings, particularly those used for sealing off fire areas, are preferably made of lightly reinforced cement-concrete walls. These rigid stoppings are, however, liable to crack where ground pressure is heavy and in such cases, stoppings made of timber or timber and rock packs are used. Such packs are eventually compressed to form an air-tight stopping.

7.4 DOORS

Where access through stoppings is essential, doors are used. The term door usually means the assembly of both door and frame. The frames are set in suitable air-tight stoppings, made usually of cement concrete and the doors hung from them vertically by means of two to three strong strap iron hinges. Indian coal mines regulations require that the thickness of the masonry or concrete wall in which the door frame is set should not be less than 250mm. Single doors are most common in use though double doors are sometimes installed where a wide opening is required. Most double doors close in one plane though double V-doors operated manually or by compressed-air or electricity are sometimes used on rope-haulage roads. In some cases automatic sliding doors have been used on rope-haulage roads. The size of doors is often as large as that of the stopping itself except in airways which are infrequently used for the passage of men only ; in such cases small doors of 0.6×0.9m size may serve the purpose. Doors range in size from about 1.5×2m in metal mines up to 2×4m in coal mines, depending on the width of cars that have to pass through the door.

Door-frames and doors are often made of wood suitably treated with a fire retardant though steel or light metal doors in angle-iron door-frames are used in mines where corrosion by acid mine water

Scanned with CamScanner

is negligible. Metal construction is preferable for fire doors. Indian coal mines regulations require all ventilation doors to be of fireproof construction.

Wooden door-frames are usually made of 150×150mm or 200×200mm timber and the doors, of two layers of 25mm thick wooden boards with tarred cloth or paper between the layers. The boards in each layer are placed at right angles to each other, i.e. one horizontally and the other vertically and are held together by clinched nails. Reinforcing strips are sometimes used, but they add to the weight without much improving the construction. Single-layer doors are sometimes used where a little leakage can be tolerated, but they are weaker in construction and have to be well braced. Groove-and-tongue jointing of boards becomes essential for minimizing leakage. The door may be covered with a layer of tarred paper for avoiding leakage through joints between boards. However, single-layer doors are more prone to warping than double-layer doors with horizontal and vertical placing of boards. Steel doors should have a minimum thickness of 3mm.

Doors should preferably open on one side, i.e. the high-pressure side, opening in the other direction being checked by the frame. They should be so installed that they close automatically if left open. In coal mines, this is commonly achieved by installing the frame at a small angle of about 0.175 rad (10°) with the vertical so that the door closes by its own weight. In metal mines, counter-weights or springs along with manually operated catches are usually relied upon for keeping the doors shut. In spite of this arrangement for automatic closing of doors, they are often blocked open by irresponsible trammers so much so that in gassy coal mines it becomes necessary to place special operators at the doors. In coal mines, regulations provide that when a door is frequently used for the passage of men or material, an attendant shall always be placed at the door. Automatic doors are preferable from this point of view. Besides, automatic doors or remote-control doors are desirable in fast haulage roads whereas manually operated doors are sufficient for travelling roads.

Leakage across doors can be considerable if proper care is not taken to minimize it. For minimizing leakage the doors should overlap the frame and be provided with a gasket lining. Provision of wooden or concrete sill blocks (Fig. 7.1) are essential. Canvas or rubber strips fixed along the bottom edge of the door reduce

leakage appreciably. Drainage ditches should be provided with water seals in order to prevent leakage.

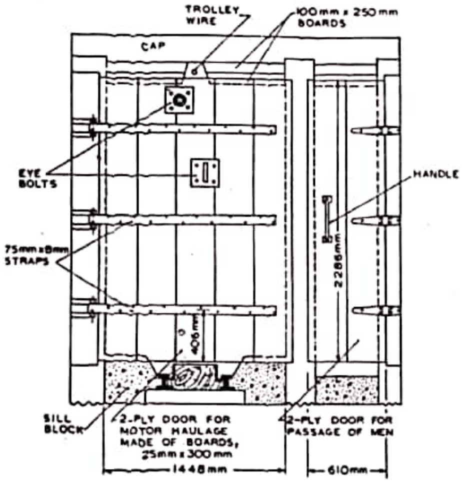

Fig. 7.1 Ventilation door.

7.4.1 Automatic Doors

The simplest of all automatically operated doors are those which open on either side and are bumped open by mine cars, but these are rarely used as they cause a lot of leakage and are damaged in a short time even though strong bumper springs are provided on either sides of the door. The more commonly used automatic doors are controlled by moving cars either (a) by their weight pressing a false rail which engages a bell crank lever operating the door through ropes and pulleys, or (b) by their engaging the studs on an endless chain moving on pulleys parallel to the track, or (c) by the sides of the cars pushing out and straightening spring bows which are linked to the doors. Doors operated by electric motors controlled by trolley-wire contacts are used in some metal mines while doors controlled by photo-electric relays are gaining favour in coal mines.

Scanned with CamScanner

7.4.2 Remote-control Doors

Though automatic doors are common in coal mines, they are less frequently used in metal mines where the purpose is as well served by remote-control doors. Remote-control doors are usually operated by compressed-air, the door being opened by a piston operating in a compressed-air cylinder (Fig. 7.2) and closing with the help of a heavy counter-weight on the release of air pressure. The three-way valve operating the compressed-air cylinder is controlled from the moving train by operating a lever attached to the valve through a system of wire ropes. Sometimes the valve may be operated through solenoids which can be switched by a lever operated from the passing train. Use of water under pressure instead

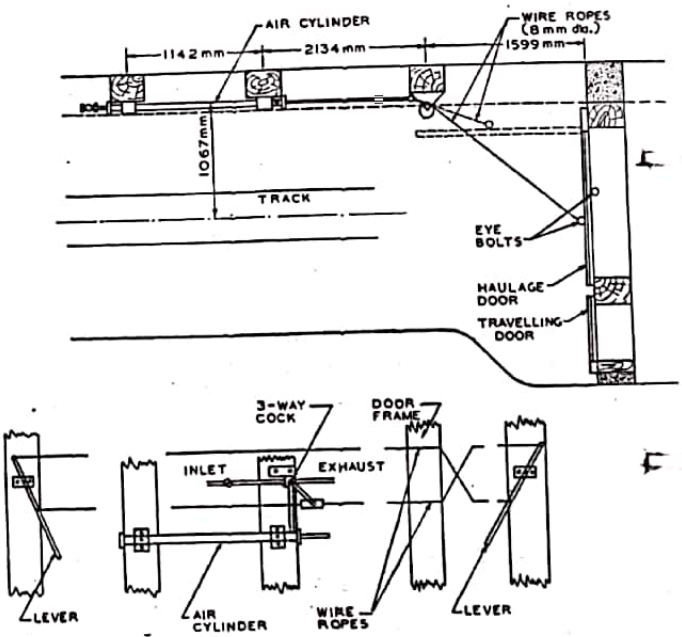

Fig. 7.2 Compressed-air operated remote-control device for ventilation door.

of compressed-air in the cylinders ensures a more economic and smoother operation of the door, but poses the problem of corrosion and disposal of water. Sometimes motor-operated doors are also controlled from a distance through a contacting switch operated by a lever from the passing train.

Automatic or remote-control doors are sometimes provided with a smaller side door for travelling of men (Fig. 7.1), a feature desirable from the point of view of safety. When such side doors are not provided, suitable safety measures such as warning lights or whistles, along with glass panels in the doors should be introduced.

7.4.3 Fire Doors

These doors are, as a rule, made fireproof. They are normally kept open but are shut in case of fire in order to prevent air reaching the fire area. Such doors are usually provided in all open airways off the main or operating shafts and are sometimes remote-controlled. The remote-control can be effected by compressed-air, water pressure or electric power which releases a catch holding the door open during normal operation.

7.4.4 Air-locks

An air-lock is a set of two doors so installed that one of them is always shut when the other is opened to pass men, tubs or a train. This not only minimizes leakage but becomes essential where the ventilation system is likely to be disturbed seriously by too frequent or prolonged opening of the doors. Indian coal mines regulations require that air-locks should be provided between main intakes and returns. In fact air-locks should always be provided where the pressure across the door is high. It must be noted here that the pressure on single doors should not exceed 250 Pa, in order that they offer no difficulty in opening, whereas pressures up to 500 Pa can be allowed with air-locks. Beyond this pressure, however, even air-lock doors are difficult to open and small shutters have to be provided on each of the doors. The small shutter is more easily opened under high pressure and once it is open, air pressure across the door gets equalized, as a result of which it becomes fairly easy to open the main door.

On important airways in gassy coal mines, it is a common practice and even enforced by law in some countries to provide three or more doors so that the air-lock is maintained even if one of the doors goes out of commission. One of these doors should preferably open in the opposite direction to the others so that the air-lock remains effective in the event of reversal of air-current.

It must be remembered that any door can be kept closed if provided with suitable catches, but such devices are not foolproof. That is why the operation of the doors of important air-locks are interlocked so that when one of the doors is open, the other is automatically kept closed. Alternatively an automatic warning device should be installed on each door to indicate if the other door is open or closed. Needless to say that the doors in an air-lock should be so spaced as to accommodate the longest length of train required to pass through it.

7.5 CLOSING OF SHAFT-TOPS

In practice, most fan shafts are used for hoisting men and material if not mineral and arrangements for effectively closing the shaft-top in order to minimize leakage become essential.

In all fan shafts, the shaft-top is usually closed by a suitable air-tight decking leaving openings for passage of the cages or skips. The decking is usually made of thick wooden planks suitably jointed and supported on a framework of joists spanning the shaft-top. Suitable rubber-lined openings are left in the decking for the passage of guide rope shoes. In the simplest form, the cage openings are covered by flat wooden or metallic doors through which passes the winding rope. The doors are lifted up by the cages when they bank at the surface, the bottom of the cages now serving to keep the openings closed. These doors however, allow considerable leakage sometimes amounting to 30% of the fan quantity.

A better design is to provide a sheet-metal well of rectangular cross-section inside the shaft below the decking under the cage openings as shown in Fig. 7.3. To minimize leakage, the gap between the walls of the well and the cages should be as small as possible. The top of the cage opening is closed by a door in the shape of a rectangular or trapezoidal box made of wood or light metal (aluminium). It should be light in order to avoid undue weight on the bridle chains of the cage which lift the box up from its seating on the deck as the cage banks. There is a circular opening on the top of the door large enough for the passage of the safety hook which

is kept closed by a wooden cover with a central hole for the passage of the winding rope.

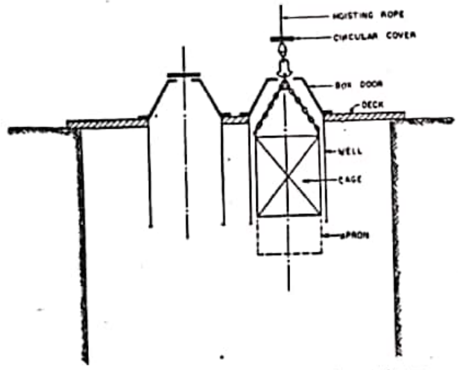

Fig. 7.3 Arrangement for closing of fan shaft-top.

The prior opening of this wooden cover helps in pressure equalization, so that the main door is easily lifted against the fan pressure. Sometimes a 0.5-1m long apron may be provided at the bottom of the cage in order to prevent leakage in the event of a slight overwind of the cage above the deck level.

The above method of closing the top of fan shafts reduces leakage to 7-20% of the fan quantity. It has the advantage of low cost compared to air-tight shaft chambers and can be easily constructed and repaired. However, for better control of leakage, it is desirable to completely enclose the shaft-top by an air-tight chamber provided with suitable air-locks for the passage of men and materials. Such chambers or buildings can be of sheet steel or preferably of plastered masonry construction provided with double sealed windows.

7.6 REGULATORS

Regulators are usually rectangular openings left in stoppings. The size of the opening can be normally calculated by using the equivalent orifice formula and is illustrated in the following example.

Scanned with CamScanner

Example 7.3

Two parallel splits A and B have a pressure of 500 Pa acting across them, causing a flow of 15 $m^3 s^{-1}$ in split A and 10 $m^3 s^{-1}$ in split B. It is desired to reduce the quantity in split A to 10 $m^3 s^{-1}$ by placing a regulator in it. Calculate the quantity in split B after the installation of the regulator as well as the size of the regulator if the surface fan pressure is 1 kPa.

Let R_A = resistance of split A$=500/15^2=2.2$ $Ns^2 m^{-8}$,

R_B = resistance of split B$=500/10^2=5.0$ $Ns^2 m^{-8}$,

R_T = resistance of the trunk airways and shafts $=500/25^2=0.8$ $Ns^2 m^{-8}$,

since the trunk airways and shafts consume a pressure of 500 Pa with a total quantity of 25 $m^3 s^{-1}$ passing through them,

Q_A = quantity flowing in split A after regulation $=10$ $m^3 s^{-1}$,

Q_B = quantity flowing in split B after regulation,

Q_T = total quantity flowing after regulation

and R_R = resistance of the regulator.

Let us assume the fan pressure to remain constant.

Considering flow in split B after the installation of the regulator in split A, we have

$$1000 = R_T Q_T^2 + R_B(Q_T - Q_A)^2$$
$$= 0.8\, Q_T^2 + 5(Q_T - 10)^2$$

or, $5.8\, Q_T^2 - 100\, Q_T - 500 = 0$

or, $Q_T = 21.3$ $m^3 s^{-1}$, neglecting the negative value.

Therefore, $Q_B = 21.3 - 10 = 11.3$ $m^3 s^{-1}$

Now considering split A,

$$1000 = R_T\, Q_T^2 + (R_A + R_R) Q_A^2$$
$$= 0.8\,(21.3)^2 + 2.2 \times 10^2 + R_R \times 10^2$$

or, $R_R = 4.2$ $Ns^2 m^{-8}$.

From the equivalent orifice formula (equation 4.105)

A (area of the regulator)$=1.2/\sqrt{R_R}$

$=1.2/\sqrt{4.2}=0.586$ m^2.

The use of equation 4.105 for the calculation of the size of regulators is not exact, though it is often used for simplicity. It is partly due to this and partly to the difficulty in foreseeing the requirements of a regulator that, in practice, the regulator openings are usually provided with a sliding shutter which helps in adjusting the size of the opening to suit the requirements.

Regulators can be permanent when they are constructed of steel in a concrete stopping, but more often they are temporary in nature, when they are in the form of an open wooden frame in a stopping made of brattice cloth nailed on to a wooden frame work. The air quantity can be adjusted by varying the size of the opening by nailing on strips of wood on the side of the opening.

Example 7.4

Two splits A and B pass 15 and 20 $m^3 s^{-1}$ of air respectively with a pressure drop of 500 Pa across them. The trunk airways consume a pressure of 300 Pa. Calculate the size of regulator required to equalize flow in the two splits. What will be the flow through the mine now ? Assume the fan pressure to remain constant.

Resistance of split A, $R_A = \frac{500}{15^2} = 2.22$ $Ns^2 m^{-8}$.

Resistance of split B, $R_B = \frac{500}{20^2} = 1.25$ $Ns^2 m^{-8}$.

Resistance of trunk airways, $R_T = \frac{300}{35^2} = 0.245$ $Ns^2 m^{-8}$.

Let the quantity through the mine be Q $m^3 s^{-1}$, when a regulator of resistance R_T has been installed in split B.

For flow to be equal in the two splits, $R_B + R_R = R_A$

Or, $R_R = R_A - R_B = 2.22 - 1.25 = 0.97$ $Ns^2 m^{-8}$.

Area of regulator $= \frac{1.2}{\sqrt{R_R}} = 1.22$ m^2.

$$800 = R_T Q^2 + R_A \left(\frac{Q}{2}\right)^2 = 0.245\, Q^2 + \frac{2.22}{4} Q^2$$

Or, $Q^2 = \frac{800}{0.8} = 1000$

Or, $Q = \sqrt{1000} = 31.6$ $m^3 s^{-1}$.

7.7 BOOSTERS

Booster fans are sometimes used for augmenting ventilation in certain districts. They increase quantity by increasing the pressure causing flow and the size of the booster fan can be calculated for any quantity as illustrated in the following example.

Scanned with CamScanner

Example 7.5

A mine fan generates pressure of 500 Pa which is sufficient to circulate 25 m^3 of air per second through the mine which consists of two splits, A and B, A circulating 15 $m^3 s^{-1}$ and B, 10 $m^3 s^{-1}$. It is desired to increase the quantity in split B to 15 $m^3 s^{-1}$ by installing a booster in it. Calculate the size of the booster if the resistance of the shafts and trunk airways is 0.2 $Ns^2 m^{-8}$.

Let R_A = resistance of split A,
R_B = resistance of split B,
R_T = resistance of shafts and trunk airways,
P_B = pressure generated by the booster fan,
Q_A = quantity in split A after installation of the booster,
Q_B = quantity in split B after installation of the booster
and Q_T = total quantity flowing through the mine after installation of the booster.

Before installation of the booster,

$$500 = R_T \times 25^2 + R_A \times 15^2 = R_T \times 25^2 + R_B \times 10^2$$

or, R_A = 1.67 $Ns^2 m^{-8}$

and R_B = 3.75 $Ns^2 m^{-8}$

since R_T = 0.2 $Ns^2 m^{-8}$.

After installation of the booster,

$$500 = R_T Q_T^2 + R_A (Q_T - Q_B)^2$$
$$= 0.2\, Q_T^2 + 1.67\, (Q_T - 15)^2 \text{ since } Q_B = 15 \text{ m}^3 \text{ s}^{-1},$$

assuming the fan pressure to remain constant.

Solving the above equation, $Q_T = 29$ $m^3 s^{-1}$, neglecting the negative value of Q_T.

Now considering flow in split B,

$$500 + P_B = R_B Q_B^2 + R_T Q_T^2$$
$$= 3.75 \times 225 + 0.2 \times 29^2$$

or, $P_B = 512$ Pa.

It will be seen from the above example that an increase in the quantity in the boosted district increases the total quantity passing through the mine which results in a greater pressure loss in the shafts and trunk airways thus reducing the pressure across the splits. Moreover, the fan when circulating a larger quantity, generates less pressure. These cause a reduction in the quantity circulating through the unboosted districts. Too large a booster in one split can cause stoppage of air-current or even reversal of air-current in the other splits, particularly, if the trunk resistance is high compared to the

resistance of the splits. That is why it is essential to have a judicious choice of the size of a booster fan. Positioning of booster fans also needs careful consideration, particularly, in leaky airways.

Let us consider a face served by an intake and a return airway separated from each other by a leaky barrier. It can be shown that depending on the amount of leakage, the pressure drop from the entrance of the intake to the face and again from the face to the outlet of the return will be in the form shown in Fig. 7.4. However, for the sake of simplicity let us assume a straightline pressure gradient between the entrance of the intake or the outlet of the return and the face as shown in Fig. 7.5. This assumption is approximately true for small leakages.

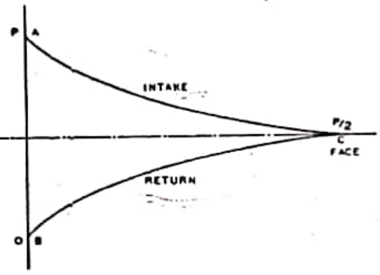

Fig. 7.4 Pressure gradient along the intake and return airways leading to a face.

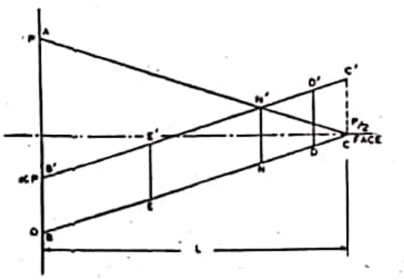

Fig. 7.5 Diagram illustrating the optimum positioning of a booster fan.

Referring to Fig. 7.5, if R_1 is the total resistance of the barrier between the intake and the return, the leakage Q_L will be equal to $P/2R_1$ assuming laminar flow for the leakage and hence a linear relationship between pressure and leakage quantity since $P/2$ is the average pressure difference between the intake and the return over the whole length of the airways. Now since R_1 is proportional to $1/L$, the leakage is proportional to $PL/2$=the area of the triangle ABC.

Let us assume the pressure P to be partly generated by a booster fan, developing a pressure αP and partly by a main fan, developing a pressure $P(1-\alpha)$. Let us consider the positioning of the booster at E in the return. Similar consideration will, however, hold good for the installation of the booster in the intake. The pressure profile is given by the line ACEE'B which means a saving in the leakage equal to the area B'E'EB. The saving in leakage will increase as the position of the booster is shifted progressively to the right of E. Let us now consider the position D where the pressure profile will be ACDD' B'. It is evident that between the points D and N the pressure in the return is higher than that in the intake so that leakage from return to intake or recirculation of air occurs. However, if the booster is located an N, the intake and return pressures at the booster become the same and this point is thus called the *neutral point*. Here, the saving in the leakage is the largest with no recirculation. That is why this is the most suitable position for the booster. The saving in leakage when the booster is installed at the neutral point is equal to $\alpha P(1-\alpha)L$, that is the area B'N' NB.

$$\text{or,}\quad \frac{\text{leakage saved}}{\text{total leakage}}=\frac{2\alpha P(1-\alpha)L}{PL}=2\alpha(1-\alpha)$$

This will be the maximum when

$$\frac{d}{d\alpha}\left\{2\alpha(1-\alpha)\right\}=0$$

$$\text{or,}\quad \alpha=1/2.$$

Hence, the maximum possible leakage saved by using a booster is half the total leakage when the booster position N is halfway in the return. Also, the pressure of the booster is the same as that due to the main fan. For other booster pressures, however, α varies, causing a variation in the position of the neutral point as well as the amount of leakage saved.

Extending the above argument, it will be seen that if n number of fans of equal pressure—one being the main fan and the rest, boosters—are used, the leakage will be reduced to $1/n$ parts of the total leakage. In such a case, the boosters will be placed at intervals of L/n along the return or intake airway.

Example 7.6

A main mine fan generates a pressure of 1.2 kPa of which 0.8 kPa is consumed in the shafts and trunk airways so that only 0.4 kPa is available to ventilate two splits A and B, A passing 15 $m^3 s^{-1}$ and B, 10 $m^3 s^{-1}$. It is desired to increase the quantity flowing through B by installing a booster fan in it. Calculate the size of the booster which will cause the stoppage of air-flow through split A.

Quantity passing through the trunk airways

$$=10+15=25\ m^3 s^{-1}.$$

Resistance of the trunk airways and shafts

$$=800/25^2=1.28\ Ns^2 m^{-8}.$$

No air flows through A when the booster is installed in B, or in other words, the whole of the main fan pressure is consumed in overcoming the resistance of shafts and trunk airways.

Let Q be the quantity flowing through the trunk airways as well as through B after the installation of the booster.

Assuming the main fan pressure to remain unchanged,

$1200=1.28\ Q^2$ or, $Q=30.62\ m^3 s^{-1}$.

Resistance of B$=400/10^2=4\ Ns^2 m^{-8}$.

Therefore, pressure of the booster$=4\times(30.62)^2$

$$=3750\ Pa=3.75\ kPa.$$

Example 7.7

A steeply dipping gold reef now being worked on the east section is ventilated by two boundary shafts. The exhaust fan located at the eastern boundary of the property circulates 25 $m^3 s^{-1}$ of air at a pressure of 1 kPa. The pressure drop in the intake shaft is measured at 250 Pa. It is proposed to work the west section of the lode and ventilate it by a separate exhaust fan located on a shaft at the western boundary of the property, the present intake shaft serving as the common intake for the two sections. The resistances of the west section workings and exhaust shaft are expected to be the same as for the east section, though the flow requirement in the west section

Scanned with CamScanner

is estimated at 30 $m^3 s^{-1}$. Calculate the required pressure of the west-section fan and any change in the flow in the east section when the west section goes into operation, assuming the east-section fan pressure to remain unchanged.

Let the changed quantity in the east section be Q $m^3 s^{-1}$ after commissioning of the west-section fan.

Considering the east-section circuit then

$$1000 = \frac{250}{(25)^2}(Q+30)^2 + \frac{750}{(25)^2}Q^2.$$

Or, $0.16\,Q^2+2.4\,Q-64=0$.

Solving the above quadratic equation, we get,

$Q=13.86$ $m^3 s^{-1}$

neglecting the $-$ve value.

The required west-section fan pressure

$$P = \frac{250}{(25)^2}(Q+30)^2 + \frac{750}{(25)^2}\times(30)^2$$

$$=1850 \text{ Pa} = 1.85 \text{ kPa}.$$

7.8 VENTILATION OF HEADINGS

Short headings in coal mines have hitherto been ventilated by line brattices commonly made out of treated hessian cloth nailed on to props placed at 1 to 1.5m intervals along the heading, thus dividing it into virtually two separate airways (Fig. 7.6). Use of hessian cloth makes the brattices very leaky and this had led to the use of iron sheets or wooden planks nailed to props in longer headings, but these were more difficult and time-consuming to erect and were, besides, costly. Sometimes brick partition walls were used for ventilating long headings, but they took long to erect and were very costly. Today rubberized as well as flameproof p.v.c.-coated hessian cloth is available for brattices. This material is leakproof. However, brattices in general leak mostly through the gaps at the roof and floor so that only 5% of the air entering the heading reaches a point 30 meters inbye. It is for this reason that brattices are now restricted to very short headings less than 20m in length. Besides, brattices need careful maintenance and have to be kept extended right up to the face which is essential for good face ventilation. They increase the effective resistance of the heading by doubling the length

of the airway and reducing the cross-sectional area. Brattices obstruct the movement of large-size machinery by reducing the effective size of the heading and hence in highly mechanized headings, brattices are invariably replaced by auxiliary ventilation through ducts. This is also desirable where methane emission or dust production at the face is high and cannot be adequately cleared by brattice ventilation. It has been found that where brattices are used, far better dispersal of dust from the face is obtained by dividing the heading in such a way that the return has a smaller cross-sectional area than the intake. Brattices, however, are rarely used in metal mines as the drives in such cases are usually long and narrow.

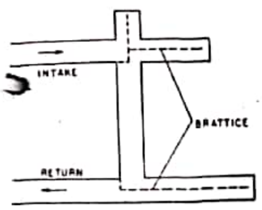

Fig. 7.6 Ventilation of headings by line brattices.

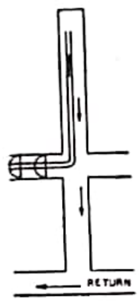

Fig. 7.7 Forcing ventilation with a tube.

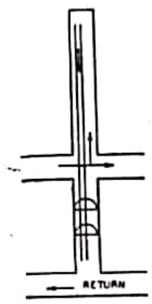

Fig. 7.8 Exhausting ventilation with a tube.

Where a connection between the intake and the return is available close to the heading to be ventilated and pressure difference between the intake and the return is sufficient, a tube may suffice for ventilating the heading. Fig. 7.7 gives the arrangement of the tube forcing air at the face and Fig. 7.8 shows the tube exhausting air from the face. Though forcing ventilation is preferable to exhausting ventilation in a heading, the former involves the provision of separation doors between the heading and the intake which obstructs haulage in the intake. Besides, in the forcing arrangement, the whole of the intake air has to pass through the duct which may be undesirable if other headings are also to be ventilated from the

Scanned with CamScanner

same intake. It may also necessitate the use of a large-size duct or the availability of a large pressure difference between the intake and the return if small-diameter ducts are to be used. However, ventilation by ducts alone utilizing the main fan pressure is less costly, simpler and more reliable in operation as compared to auxiliary ventilation.

Auxiliary ventilation can be of the following types : (a) *forcing*, (b) *exhausting*, (c) *overlapping* and (d) *reversible*. Ventilators should be placed at least 4.5m away from the entrance of the heading on the intake side of the main airway in case of forcing systems and the same distance away on the return side, in case of exhausting systems in order to prevent recirculation of air. On the same consideration, it is also desirable to circulate only half and preferably one-third of the air flowing in the main airway into the heading so that a steady flow of air is maintained in the main airway past the entrance of the heading. Circulation of only a part of the intake air into a heading becomes essential where other headings are also to be ventilated from the same intake so that the contaminated air from one heading is adequately diluted before reaching the other headings.

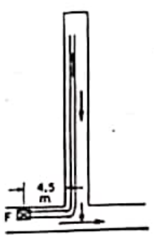

Fig. 7.9 Ventilation of a heading with a forcing fan F.

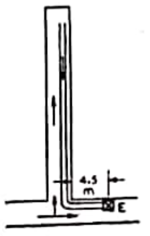

Fig. 7.10 Ventilation of a heading with an exhausting fan E.

The forcing system of ventilation (Fig. 7.9) is most commonly adopted since it delivers fresh and dry air at the face, much unlike the exhausting system (Fig. 7.10) where the air travelling to the face picks up gas and moisture from the exposed strata. The fan motor is placed in fresh intake air with a forcing system while with an exhaust system, the fan and motor are subjected to air contaminated

with gas, dust, moisture and corrosive blasting fumes. Besides, in the forcing system, air travels to the face at a higher velocity through a small duct so that it picks up less heat from the surrounding strata before reaching the face, although the heat produced by the fan is added to the air flowing to the face. In hot and humid conditions, a high velocity of air is desirable at the face and this is better achieved by a forcing system of ventilation. Fig. 7.11 shows the variation of air velocity with distance from the discharge end of a duct for various discharge velocities. Good air velocity at the face can be obtained by extending the duct to within 3-5m from the face by means of a flexible ducting. The flexible ducting can be folded back at the time of blasting to save it from damage by flying pieces of rock. Alternatively, a length of old duct can be used at the end. Flexible ducting without sufficient reinforcement cannot be used in exhausting systems where rigid ducts have to be used, but in order to be really effective in removing dust and gas from the face these have to be extended within a few hundred millimetres from the face (see equation 2.19), which is impracticable. On the other hand, in forcing ventilation, the air-stream impinging on the face scours the dust and gas fairly well. The main disadvantage of the forcing system is the slow movement of blasting dust and fumes from the heading—

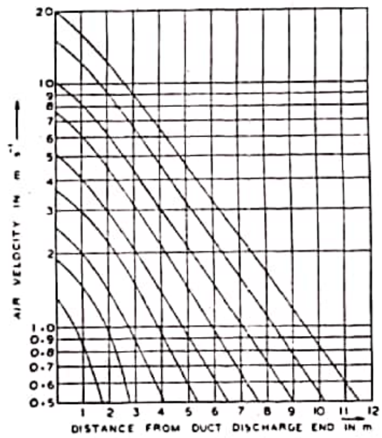

Fig. 7.11 Air velocity at different distances from the discharge end of a duct (*after MacFarlane*).

often at the rate of 0.15 m s^{-1}. The whole process may take over an hour in long headings with obvious hazard to men passing through the heading or working in it during this time.

In such cases an overlap or a reversible system should be selected. In the overlap system (Fig. 7.12) an exhausting duct is placed within 30m from the face along with a short forcing duct extending from about 10m (4.5m being the minimum) behind the end of the suction duct to within a convenient distance from the face. This system combines the advantages of both forcing and exhausting systems, but care must be taken to prevent recirculation of air by the forcing ventilator which may lead to an undesirably high concentration of dust and gas at the face. This can be done by maintaining proper overlap between the two ducts and by circulating about half or, preferably, one-third of the air drawn by the exhaust ventilator in the forcing duct. It is generally desirable and essential in gassy coal mines to stop the forcing ventilator if the exhausting ventilator stops in order that a dangerous concentration of gas may not be built up at the face. This can be done by interlocking the power supply to the two ventilators.

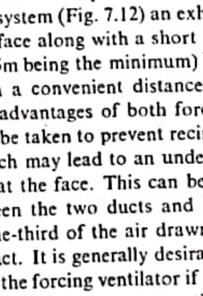

Fig. 7.12 Overlap system of ventilation of headings (F—forcing fan, E—exhausting fan).

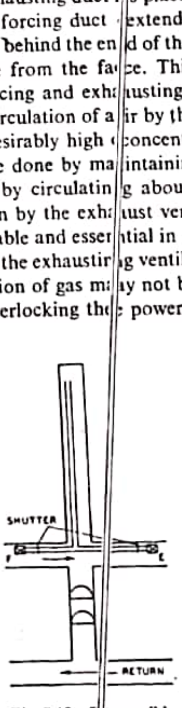

Fig. 7.13 Reversible system of ventilation of headings with two fans (F—forcing fan, E—exhausting fan).

The reversible system of ventilation has the combined advantages of both forcing and exhausting ventilation systems. Here a

single duct is used to force the air to the face at normal times, but after blasting, the direction of air-flow in the duct is reversed so that the dust and fumes produced by blasting are quickly cleared out from the heading. It is necessary to control carefully the time for which the forcing ventilation is continued after blasting in order to disperse the fumes and dust from the face before the air-flow is reversed so that the face gets completely cleared. Though this system utilizes a single duct, a single reversible fan is not enough because of the risk of recirculation and hence the duct is connected to two fans (Fig. 7.13), one forcing and the other exhausting through two separate branches. It will be clear from Fig. 7.13 that if only a forcing fan F is used, there will be recirculation of foul air to the face when the fan is reversed to act as an exhausting one. Similar argument also holds good for the location of the fan at E. With reversible ventilation, it is not feasible to use several fans in series spaced along the ducting and in such a case the fans have to be located at the entrance of the heading which means that, for long headings, the fans have to be of high-head type. That is why this system is not commonly used inside mines, though it is used in civil engineering tunnels and sinking shafts where centrifugal fans are used for generating a high head. Besides, high head produces much leakage and hence needs the ducting to be kept in good repair. Another arrangement of reversible ventilation with a single fan is illustrated in Fig. 7.14.

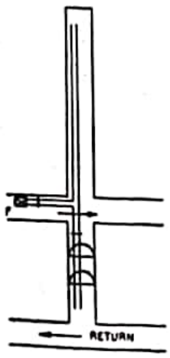

Fig. 7.14 Reversible system of ventilation of headings with a single forcing fan F.

Scanned with CamScanner

7.8.1 Ventilation of Headings and Tunnels Driven by Continuous Miners and Boring-type Machines

Continuous miners and tunnelling machines pose a special problem of heading ventilation since they (particularly the latter) almost completely occupy the whole cross-section of the heading. Besides, owing to their fast rate of advance, there is an increased rate of gas and dust production at the face. The rate of methane emission at faces in gassy mines worked by continuous miners averages 0.11 $m^3 s^{-1}$, though the peak rate at any time may be much higher. Continuous miners produce large quantities of dust, often exceeding 100×10^9 particles per minute. Also, these machines, being of high power, add a considerable amount of heat to the air at the face. All these necessitate the circulation of an excessively large quantity of air to a continuous-miner face for effective dilution of the contaminants. In gassy mines, the dilution of the methane emitted at the face becomes the major consideration and it may be necessary to circulate as much as 30-35 $m^3 s^{-1}$ of air at the face for diluting the methane evolved to a safe concentration of 0.5%.

Continuous-miner headings are usually ventilated by auxiliary exhaust fans. Forcing ventilation, though having a better scouring effect at the face, is undesirable as it exposes workers to high concentrations of dust. Besides, with the large quantities of air required to be circulated in such headings, the air velocity invariably becomes high enough to raise deposited dust. On the other hand, an exhausting ventilation system requires the ducting to be extended right up

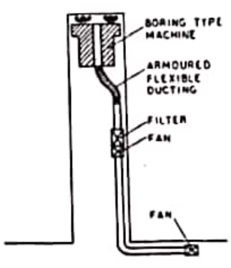

Fig. 7.15 Exhaust ventilation of a face worked by a boring-type machine.

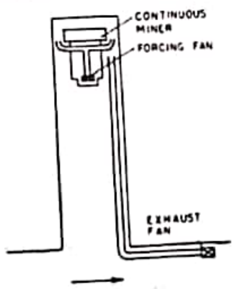

Fig. 7.16 Overlap system of ventilation for headings with continuous miners.

to the face for effective clearance of dust and gas from there. This can, however, be achieved by using armoured flexible ducting at the face (see Fig. 7.15).

Sometimes an overlap system of ventilation as shown in Fig. 7.16 is used for ventilating continuous miner headings. In any case it is often desirable to introduce a suitable filtration or scrubbing type of dust extractor (see Chapter II) in the exhaust duct so as to clean the air before discharging it to the general mine atmosphere. This also ensures better maintenance of the fan since it handles clean air. Besides, it reduces the quantity of air required to be circulated to the face, if the problem of gas is not acute.

In hot and humid headings, an exhaust fan alone may not be able to produce comfortable environmental conditions at the face where men work. In such a case a small blower may be installed for blowing fresh air on the workers.

7.9 DUCTS FOR AUXILIARY VENTILATION

The efficiency of most of the auxiliary ventilation systems depends more on the proper choice of the duct than the ventilator. Ducts have usually a low coefficient of friction as compared to other mine airways, the value of k being 0.003-0.005 $Ns^2 m^{-4}$, but for long headings, the resistance of small-diameter ducts becomes fairly high, thus necessitating a high ventilating pressure which in turn leads to excessive leakage.

New rigid steel ducts if properly jointed (with washers not projecting inside the duct) and aligned have a coefficient of friction of 0.0029 $Ns^2 m^{-4}$, but dented or rusted ducts can have up to 100% higher resistance. Improper jointing and alignment can cause further rise in the resistance. Straight lengths of p.v.c.-coated flexible ducting when properly inflated have a fairly low coefficient of friction (even as low as 0.002 $Ns^2 m^{-4}$ depending on the finish) but in actual installed condition where slight flexures cannot be avoided, the coefficient of friction can be taken around 0.004 $Ns^2 m^{-4}$.

The resistance can be reduced by having large-diameter ducts, but such ducts become costly, more difficult to carry and install and take up a large space which is undesirable in headings of small cross-sectional area. Thus the choice of the proper size of duct, commensurate with the length, is essential. National Coal Board, U. K.[104] recommend the use of 450mm diameter ducts up to a distance of 900m, beyond which the duct should have a minimum diameter of 600mm.

In practice however, a wide range of duct sizes varying from 300mm to 800mm are used, though the most common sizes are 500mm and 600mm.

Two types of ducts are commonly used, the flexible ducts and the rigid ducts.

7.9.1 Flexible Ducts

These are much easier to store, transport and install than rigid ducting. They are cheaper in initial cost, but have a shorter life. They are conveniently used for short headings up to a distance of 300m, where a more permanent steel ducting becomes unnecessary or at the face end of rigid ducts where they can be easily removed at the time of blasting. This, however, has the disadvantage of reducing the air supply to the face just after blasting when it is needed most. That is why many prefer to use old rigid ducts which can be subjected to damage by blasting rather than flexible tubes at the face end of forcing ducts so that ventilation is ensured at the face after blasting. Flexible ducts are very suitable in curved headings. They are made in longer sections thus reducing the number of joints and consequently leakage.

Flexible ducting is nowadays made of terylene, rayon or nylon fabric coated with p.v.c. which has superseded the older rubberized cotton cloth which was inflammable and less strong. Flexible ducts can be made of unsupported p.v.c. (0.5mm thick) or plastic, but these have less strength and are easily damaged, though they cost less. They are made in sizes varying between 300mm and 750mm in diameter and 4.5m to 30m (most commonly 15m) in length. These ducts usually have springy rings of stranded steel wire attached at their ends so that they can be joined to one another by pressing one ring and introducing it into the other. The joint may then be covered with a hinged steel clamp or hoop (see Fig. 7.17) with a locking lever. A more leakproof joint can be made by mounting the ends of the ducts on a short cylindrical metal coupling with an overlap of at least 10cm and then clamping with a suitable metal hoop.

The duct is fitted with brass eyelets at a maximum interval of 0.9m along its length for supporting it from a catenary wire stretched on the side of the heading for the purpose. Flexible ducting

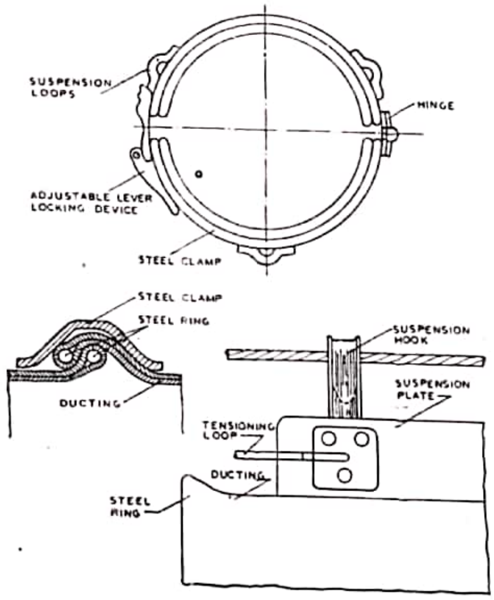

Fig. 7.17 Joint for flexible ducting.

is generally used for forcing ventilation. However, suitable designs of flexible ducting incorporating a spiral wire armouring embedded in the fabric, are available for exhaust ventilation. These do not collapse under suction but are expensive.

7.9.2 Rigid Ducting

Rigid ducts of round section are commonly used for all permanent installations. They can be made of steel, aluminium, plywood, fibre-glass-reinforced plastic or high-density polythene. Aluminium ducts are light and easy to transport. They have a smooth internal finish resulting in a low coefficient of friction, but they are costly and are easily damaged and deshaped. That is why

Scanned with CamScanner

they have not found common use in mines. Steel ducts are by far the most commonly used ones, because of their sturdiness and long life. However, where the air is highly corrosive as in mines with pyritic ores, they corrode quickly leading to high coefficient of friction and leakage. Fibre-glass-reinforced plastic and high-density polythene ducts which are used in the chemical industry can be used under such conditions, but they are very costly. Ply-wood ducts coated with laquer both inside and outside for water-proofing and giving a smooth finish are used in Europe. They are relatively cheap, light and corrosion resistant, but they are prone to fire hazards and warping and damage in hot and humid conditions.

Steel ducts are usually made of hot-rolled mild steel sheets of 1.6mm thickness, thinner sheets being more prone to damage. Welded seams are preferred to pressed lap jointed or rivetted seams which allow much leakage. The ducts should be galvanized or suitably painted with a fire-resistant resin-based enamel both inside and outside after thorough cleaning by shot blasting or wire-brushing. They are usually made in short sections of 2,3,or occasionally 4m length. Too long sections are difficult to carry and install while too short sections increase the number of joints and hence the cost as well as leakage.

The sections are jointed by flanged or push-in type of joints. In the former, angle-iron flanges are welded or rivetted to the ends of the duct section [Fig. 7.18 (c)]. Sometimes flat loose flanges may be used against upturned edges of the duct end. However, welded flanges of a minium height of 35mm and thickness of 6mm are essential in long ducts for minimizing leakage. The flanges are bolted by 12mm bolts spaced 100-150mm apart along the flange with a 5mm thick rubber or 6mm thick rubberized cork packing.

Push-in type of joints (where one end of the duct is made slightly larger in diameter than the other end) are more easily made and less expensive. They allow for curvature in the duct alignment more easily. Sealing of such joints with clay or putty as is often practised is not efficient as the sealing becomes imperfect with time and the joints start leaking badly. Rubber sealing rings of both internal and external type [see Fig. 7.18 (a) and (b)] can be used, but rubber also deteriorates with time and needs replacement. An overlap of 90-100mm is desirable and it is preferable to have some additional arrangement of clamping the two ends of the ducts

at three or more places by short welded flanges for mechanical rigidity of the joint.

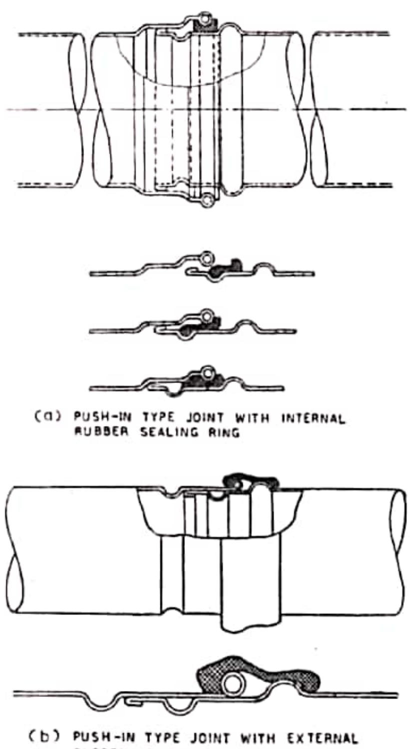

Fig. 7.18 (a) and (b) Joints for rigid steel ducts.

Sometimes in long tunnels permanent joints are made by welding duct lengths in place.

Temporary joints for quick assembly and dismantling are often of the victaulic type [Fig. 7.18 (d)]. The duct ends have short welded flanges. A suitable foam rubber packing is stuck to one of the

Scanned with CamScanner

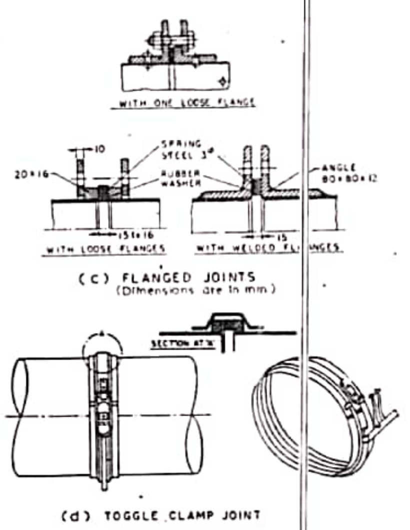

Fig. 7.18 (c) and (d) Joints for rigid steel ducts.

flanges and two semi-circular U-section clips are bolted together to tighten the flanges. Alternatively the two semicircular clips can be hinged at one end and drawn tight at the other by a quick-latching toggle clamp.

Flanged joints are the standard practice today and are much superior to push-in type spigot-and-socket joints or bayonet joints from the point of view of leakage. Rigid ducts should be suitably supported at intervals not exceeding 5m.

It is important to make the duct as leakproof as possible in order to maintain a high efficiency of ventilation. We have seen earlier that the leakiness of a duct as indicated by the ratio Q_E/Q_O, i.e. the ratio of the quantity of air delivered at the face and that entering the duct is dependent on the values of R_1 and R_2. R_1 can be calculated for a particular size of duct from the value of k. R_2 should be checked from time to time by measuring Q_E and Q_O and substituting their values in equation 4.94. If the value of R_2 so determined is less than the tolerable limit, it may be due to leaky

joints, which may be tightened up properly and gaskets replaced if necessary, or it may be due to perforations in the duct caused by mechanical damage or corrosion in which case it would be advisable to replace the duct.

7.10 AIR-CROSSINGS

Air-crossings become necessary when return air has to be taken across intake. In metal mines, the system of ventilation is usually such that air-crossings are rarely required, but in coal mines where main return and intake airways run close together, their use becomes essential. Air-crossings must be thoroughly leakproof since they generally involve main returns and intakes. They are usually made

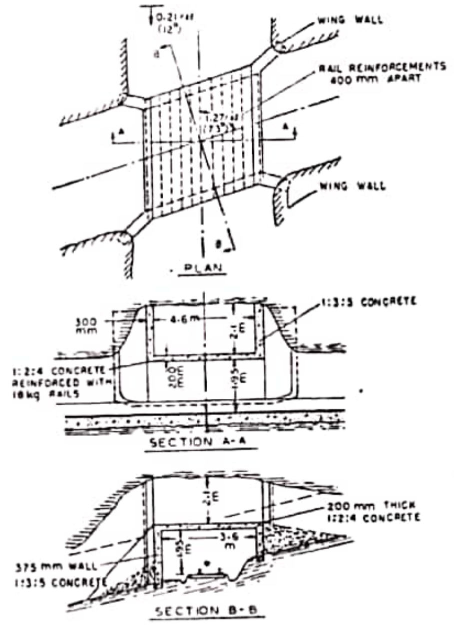

Fig. 7.19 Overcast air-crossing made of reinforced concrete.

of brick or concrete walls covered with a reinforced concrete roof. Wooden roofs, though sometimes used, are very leaky, and are inflammable. According to Indian regulations, air-crossings should be fireproof and in gassy coal mines, explosionproof too. They should be of a minimum thickness of 250mm if constructed of brick or lightly reinforced concrete or of 150mm if constructed of properly reinforced concrete. Fig. 7.19 shows a concrete air-crossing. Sometimes brick or concrete arches may be used instead of the rectangular construction as shown in the figure.

Natural air-crossings, where there are a few metres of rock separating the intake from the return, are the best from the point of view of leakage and are definitely explosionproof though they are costlier. Air-crossings can be overcast or undercast, the former (as illustrated in Fig. 7.19) being more common. Undercast air-crossings can be made by digging up the floor, but are less common because of their liability to get filled with debris or water. Sometimes minor quantities of return air can be taken across the intake through one or more large-diameter pipes or ducts.

7.11 VENTILATION FOR FIRE CONTROL

The design and operation of a ventilation system should have foolproof provision for meeting with emergencies such as fires underground. The primary aim of ventilation control in the event of fires is the withdrawal of men safely in fresh air as also helping fire fighters and rescuers so that they can operate in fresh air as far as practicable. This requires the ventilation system to be such as to have the escape routes at higher ventilating pressure so that smoke and gases from the fire area do not reach these openings. Ventilation should be ensured at any cost. Since underground fans may be damaged by the fire, surface fans are preferable. In mines prone to fires it is wise to keep a standby surface fan ready in case the mine is ventilated by underground fans. It is one of the reasons for which it is required by law to install main fans at coal mines on the surface.

The chief measure of ventilation control in the event of fire is the provision of fire doors. These are in the form of fireproof (usually steel) doors installed in suitable leakproof stoppings which are normally kept open. Sometimes the door flap may be taken off its hinges and stored alongside for quick installation in case of emergency. In some metal mines as in the Kolar Gold Field,

stoppings of brick or concrete are erected with vertical slots on the sides of the openings into which can be quickly fitted prefabricated concrete slabs (which are stored nearby) to build a fire stopping. Such fire doors are generally erected both at inbye and outbye ends of working panels and districts so that any fire in such a district can be quickly sealed after withdrawal of men.

Ventilation plans to be operative in the event of fire should be prepared both with or without reversal of air-current and the escape routes clearly marked on them. All persons should be acquainted with the evacuation plan in the event of fires. These plans should be kept updated with the ventilation staff fully apprised of the control measures to be taken in the event of fire.

A fresh-air zone is created behind fire fighters. Auxiliary ventilators may be used for the purpose. Use of brattice curtains helps in preventing smoke from the fire area getting into the fresh-air zone by convection.

EXERCISE 7

7.1 9000 m^3 min^{-1} of air is supplied to two splits of equal length and surface character, but having cross-sections of 2.5×3.5m and 2.5×4.5m. Calculate the flow in each split.

7.2 An airway 2.8×2.5m in cross-section and 150m long passes 10 m^3 s^{-1} of air. A new split of similar cross-section and surface but 200m long is added in parallel to the airway. Calculate the quantity that will flow through the new split assuming the air power to remain constant.

7.3 Pressure survey between the downcast and upcast shaft-bottoms in a mine gives pressure drops of 350 Pa each in the main intake and main return to the workings which comprise three equal splits in parallel and have a pressure drop of 250 Pa across them. Flow through each split is 800 m^3 min^{-1}. Calculate the flow in each split if an additional split of similar nature is added, assuming the pit-bottom water gauge to remain unchanged.

7.4 The surface fan at a mine exhausts 7200 m^3 of air per minute at a pressure of 2 kPa. 1420, 2000 and 2300 m^3 min^{-1} of air flow through three splits starting from the pit-bottom. The rest of the

Scanned with CamScanner

air leaks through the surface air-lock. The intake and exhaust shafts have a resistance of 0.01 $Ns^2\,m^{-8}$ each and the fan drift a resistance of 0.015 $Ns^2\,m^{-8}$. Calculate the flow through the mine, the flow in each of the remaining two splits and the leakage through the surface air-lock if the longest split is closed. Assume the fan pressure to remain constant.

7.5 A mine is ventilated by 3 splits two of 450m length each and the third of 250m length. However, flow in all the three splits is kept the same at 15 $m^3\,s^{-1}$ by installing a regulator in the short split. Pressure across the splits is 300 Pa while the main fan pressure is 900 Pa. Assuming the fan pressure to remain unchanged, calculate the flow through the different splits if the regulator were removed.

7.6 A mine is ventilated by two exhaust fans installed on the top of ventilation shafts at the two extremeties of the property. The intake is through a central shaft. One of the fans circulates 50 $m^3\,s^{-1}$ at a pressure of 450 Pa while the other circulates 40 $m^3\,s^{-1}$ at 500 Pa. The pressure drop in the intake shaft is 150 Pa. It is desired to reduce the quantity circulated by the first fan to 40 $m^3\,s^{-1}$ by installing a regulator in the fan drift. Calculate the change in the quantity circulated by the other fan assuming its pressure to remain the same. Also calculate the size of the regulator.

7.7 A mine having two districts in parallel is ventilated by a fan circulating 95 $m^3\,s^{-1}$ of air at a pressure of 850 Pa. The activities in one of the districts circulating 65 $m^3\,s^{-1}$ are to be curtailed so that the flow in that district is to be reduced to 40 $m^3\,s^{-1}$ by installing a regulator in it. Calculate the change in flow in the other district after the installation of the regulator assuming the fan pressure to remain constant. The resistance of the shafts and trunk airways feeding the two districts is 0.06 $Ns^2\,m^{-8}$.

7.8 Two splits A and B circulate 30 and 20 $m^3\,s^{-1}$ of air respectively with a pressure drop of 250 Pa across them, the main fan pressure being 500 Pa. It is required to boost the quantity in split B to 25 $m^3\,s^{-1}$. Calculate the required booster pressure and the change in flow in split A after installation of the booster assuming the main fan pressure to remain unchanged.

7.9 Two splits pass 20 and 30 $m^3\,s^{-1}$ of air respectively with a pressure of 600 Pa across them. The pressure drop in trunk airways being 1000 Pa, calculate the pressure of the booster fan in the longer split that will cause complete stoppage of flow in the other split. Assume main fan pressure to remain constant.

7.10 A district is supplied with 800 $m^3\,min^{-1}$ of air through a pair of parallel main intake and return airways 950m long separated from each other by permanent stoppings. The pressure across the district is 250 Pa while that across the main intake and return at the outbye end is 700 Pa. A booster is to be installed to raise the quantity supplied to the district to 1200 $m^3\,min^{-1}$. Determine the most suitable position of the booster to minimize leakage if the main intake and return airways are similar aerodynamically. Also calculate the size of the booster assuming the pressure across the main intake and return to remain unchanged.

7.11 A mine has three districts, A, B and C connected in parallel across the pit bottom. District A circulates 10 $m^3\,s^{-1}$, B, 17.5 $m^3\,s^{-1}$ and C, 22.5 $m^3\,s^{-1}$ with a pressure of 500 Pa across them; the fan pressure being 625 Pa. It is desired to increase the quantity in A to 12.5 $m^3\,s^{-1}$ by raising the fan pressure to 875 Pa and regulating districts B and C such that 17.5 $m^3\,s^{-1}$ still flows through B. Calculate the flow through C and the size of the regulators using the orifice formula $A=1.29Q/\sqrt{P}$ m^2 where Q and P are the flow in $m^3\,s^{-1}$ and pressure in Pa respectively. What will be the percentage of error in the size of the regulators calculated if the air density in the mine were 1.32 $kg\,m^{-3}$ instead of the standard density of 1.2 $kg\,m^{-3}$ assumed in the orifice formula ?

Scanned with CamScanner

CHAPTER VIII

VENTILATION SURVEY AND MEASUREMENT

8.1 GENERAL

8.1.1 Scope and Importance of Ventilation Surveys

A thorough ventilation survey should give a clear assessment of the quality of air and its effect on the mine environment as well as the adequacy of ventilation. The measurements should include (a) concentration of noxious and inflammable gases in the mine air, (b) concentration of pathogenic dusts, (c) dry- and wet-bulb temperatures of the air, (d) barometric pressure, (e) velocity of air, (f) quantity of flow and (g) pressure drop in different parts of the mine. Measurement of gas and dust concentration as well as that of temperature and humidity has been dealt with earlier. Besides, it is the quantity and pressure surveys which are of utmost importance in ensuring adequate ventilation. That is why the term ventilation survey usually denotes quantity and pressure survey.

The importance of systematic and regular ventilation surveys cannot be over-emphasized since such surveys provide the basis for (a) checking and supply of adequate quantity of air to any working face, which is particularly important in hot, humid and gassy mines ; (b) detecting and remedying leakage of air ; (c) determining the size of airways and sections of high aerodynamic resistance ; (d) suggesting possible modifications and alterations in the magnitude and course of air-currents, airway resistances, control devices etc. for improving the ventilation in the mine ; (e) planning suitable ventilation for the control of mine fires and dealing with other emergencies such as explosions, major falls etc. ; and (f) planning future reorganizations of the ventilation system. In general, ventilation surveys give a clear picture of the ventilation system and help in improving its efficiency.

8.1.2 Survey Interval

The interval of complete and systematic ventilation surveys should be commensurate with the requirements for safety and efficiency in a mine. In most of the mines, where there is no rapid

change in the mine characteristic, two such surveys, one in late summer and the other in late winter should generally suffice to begin with though quarterly surveys may be necessary in shallow and naturally ventilated mines where there are seasonal fluctuations in quantity and an annual survey may do for very deep mines. However, more frequent quantity measurements may become necessary where there is a rapid face advance causing frequent changes in the distribution of air to the faces, as may often happen in coal mines. Indian mines regulations provide that in all mechanically ventilated mines, quantity measurements should be made every 14 days in case of gassy coal mines and every 30 days in case of non-gassy mines. The measurements should be made (a) in the main intakes and returns of seams or sections near the entrance of the mine ; (b) in the splits, as near as possible to their starting points ; and (c) in ventilating districts, near the point where the air is sub-divided at the end of the split and also where it enters the first working place. Such quantity measurements are also to be made when any alteration in the ventilation system is effected. There is also provision for the determination of temperature, humidity and other environmental conditions every 30 days, if conditions so warrant.

8.1.3 Location of Survey Stations

It is customary to permanently fix the location of the points where ventilation measurements are to be taken. Such survey stations should be selected after careful reconnaissance so as to ensure the maximum accuracy of all observations. Although quantity surveys have to be done with a view to determining the distribution of air and possible leakage, pressure surveys should have the location and determination of pressure losses along mine airways as their objective. Whereas quantity-survey stations should be located before and after splitting and at points of possible leakage in addition to the pit-bottom as well as the faces, pressure-survey stations should be located before and after sections of airways where large changes of resistance occur due to obstructions, changes in the cross-sectional area of the airways etc. Besides, quantity-survey stations should be so selected that there be no obstructions nearby. It is a good practice to select a station where there is no area change for at least five roadway diameters, particularly on the upstream side. For accurate measurement of area,

Scanned with CamScanner

as well as of average velocity, the cross-section of the airway at the quantity-survey station should be as regular as possible. It may be worth while to dress the sides of the airway to a regular shape at quantity-survey stations, where accurate work is desired. Stations suitable for pressure surveying may not be found suitable for quantity surveys. However, in practice, common stations for both quantity and pressure surveys are selected wherever possible. After selection, the stations are surveyed, and their positions plotted on a ventilation plan. The reduced levels of the stations are also determined by suitable levelling. A fresh levelling of the stations is desirable before or after each survey where the ground is liable to heave or settle.

The time of ventilation surveys should be carefully chosen. Any variation in the ventilation system due to closing or opening of ventilation doors, movement of cages or skips in the shafts or tubs in roadways affects ventilation surveys. It is thus preferable to carry out such surveys at weekends or on holidays when the mine is idle. There must be no variation in the fan speed during the ventilation survey. Also, large changes in atmospheric pressure and temperature during the survey are undesirable and have to be corrected for. Changes in atmospheric temperature affect the natural ventilating pressure and consequently any pressure survey carried out underground. For this reason, it is necessary to keep a constant record of the pit-bottom water gauge over the duration of the survey.

8.1.4 Survey Records

Results of ventilation surveys should be suitably recorded and so tabulated as to reveal at a glance the changes in air quantity and pressure. A method of tabulation is shown in Table 8.1. It is also desirable to get the survey results plotted on a ventilation plan of a suitable scale, which should show the air quantities at the various survey stations. An idea of the variation in the resistance of the airways can be obtained by plotting the pressure drop along an airway against the distance. A good way of representing the pressure survey on the ventilation plant is to mark out sections of airways over which a fixed drop of pressure, say, 25 Pa takes place (see Fig. 8.1). A short section indicates a high resistance whereas a long one indicates a low resistance. Ventilation measurement data should be recorded at the survey station for ready reference.

Table 8.1 : Ventilation Survey Records

Station	Section	Pressure drop, Pa	Cumulative pressure drop, Pa	Distance, m	Air quantity, $m^3 s^{-1}$	Air power loss on section, kW	Cumulative air power loss, kW	Resistance of section, $Ns^2 m^{-8}$	Cumulative resistance, $Ns^2 m^{-8}$
A									
	1	200	200	200	20	4.0	4.0	0.5	0.5
B									
	2	50	250	35	20	1.0	5.0	0.125	0.625
C									

In India it is required to post a check board at all air-measuring stations in the return in gassy coal mines showing (a) the serial number of the station, (b) the quantity required to pass through the airway, (c) the cross-sectional area of the airway at the section, (d) the last date of air measurement, (e) measured air velocity, (f) measured air quantity, (g) percentage of inflammable gas in the general body of air and (h) the signature of the ventilation officer with date.

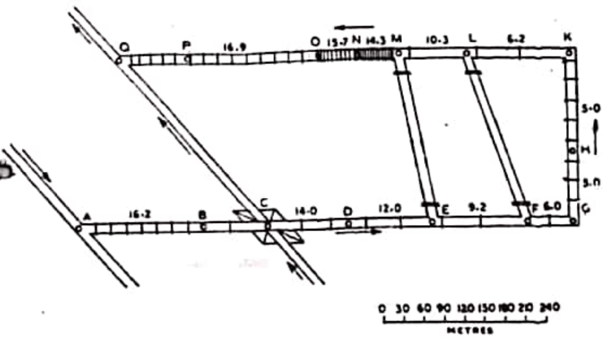

Fig. 8.1 Plan showing ventilation survey records—figures indicate quantity in $m^3 s^{-1}$.

8.1.5 Ventilation Plans

Ventilation plans are necessary for efficient control of ventilation in mines. It is also required by law that up-to-date ventilation plans of a mine showing the distribution of air be maintained. Ventilation plans are prepared based on the latest ventilation surveys and are essential for (1) giving a comprehensive picture of the mine air distribution system with the direction and amount of flow in various branches and circuits, (2) indicating the position of high resistance parts of branches and circuits, (3) indicating leakage or recirculation of air, (4) indicating the efficiency of the various ventilation control devices, (5) indicating possible ways of reorganization of the system for better air distribution, (6) indicating possible ventilation control measures in the event of emergency and (7) indicating the effect of introducing new airways, installation of fans etc. in the event of reorganization of the ventilation system.

Normally ventilation plans should clearly indicate (a) the direction of air-current in various branches and circuits, (b) quantity and pressure measuring stations, (c) air-crossings, doors, stoppings and other devices for controlling air distribution, (d) fire doors and stoppings with their serial number, (e) rooms used for storing inflammable materials, (f) position of fire fighting equipment, (g) water dams with dimensions, (h) pumping, telephone and ambulance stations and (i) haulage and travelling roads by suitable symbols. Table 8.2 gives the standard symbols prescribed for ventilation plans by the Indian Mines Regulations.

Apart from the above, quantities at the air measuring stations should also be shown on the ventilation plan. Wherever, the scale of the plan permits, airways with unduly high resistance should be specially marked with the pressure drop suitably indicated. While an elaborate plan must be maintained in the office, the ventilation officer should carry an abbreviated plan on his rounds in the mine.

8.2 MEASUREMENT OF QUANTITY OF FLOW

This involves the measurement of (a) the average air velocity at any point in a mine airway and (b) the cross-sectional area of the airway at that point. The product of the two gives an estimation of the air quantity.

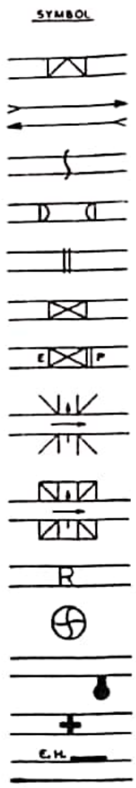

NAME	REMARK
WATER DAM	IN RED
DIRECTION OF AIR-CURRENT	INTAKE IN BLUE & RETURN IN RED
BRATTICE	IN RED
DOORS	IN RED
BRICK, STONE OR CONCRETE VENTILATION STOPPING	IN RED
FIRE DAM, SEAL OR STOPPING	IN RED
EXPLOSION-PROOF STOPPING	IN RED
AIR CROSSING	
EXPLOSION-PROOF AIR CROSSING	
REGULATOR	IN RED
AUXILIARY FAN	IN RED
TELEPHONE	IN RED
UNDERGROUND FIRST-AID STATION	THICK CROSS IN RED
ENGINE HOUSE	

Table 8.2 Prescribed Symbols for Ventilation Plans.

8.3 MEASUREMENT OF VELOCITY

Various methods are used for the measurement of air velocity depending on the degree of accuracy desired and the range of velocity to be measured.

Scanned with CamScanner

For low velocities up to 0.75 m s^{-1} the smoke-cloud method offers an easy and quick way of determining the air velocity with a fair degree of accuracy. The smoke-cloud measurement, if done carefully gives results varying from more precise measurements by only 10%. However, for accurate work, more precise low-velocity measuring instruments such as the Ower anemometer (suitable for velocities of 0.15 - 1 m s^{-1}, hot-wire anemometers, velometers, Kata thermometer etc. may be used. The relation between the dry Kata reading, dry-bulb temperature and air velocity is as follows:

$$v = \left\{\frac{K/(309.65-T)-8.37}{16.74}\right\}^2 \tag{8.1}$$

for velocities less than 1 m s^{-1} and

$$v = \left\{\frac{K/(309.65-T)-5.44}{19.62}\right\}^2 \tag{8.2}$$

for velocities greater than 1 m s^{-1} where

v =velocity in m s^{-1},

K_o =dry Kata reading in J m^{-2} s^{-1}

and T=dry-bulb temperature in K.

v can be calculated from the above equations by measuring K and T.

8.3.1 Smoke-Cloud Method

Fig. 8.2 shows a smoke-cloud generating device used by the U.S. Bureau of Mines. It consists essentially of a glass tube 125 to 150mm long and 12.5mm in diameter filled with granular pumice stone of 0.8-1.2mm size soaked with tin or titanium tetrachloride. The latter is often preferred as it is less corrosive. The two ends of the tube are plugged by glass wool and are sealed. When the tube is to be used, the sealed ends are broken off and the tube is attached to a rubber-bulb aspirator which, when squeezed, forces a current of air through the tube producing an atomized spray of the tetra-chloride which coming in contact with the moisture of mine air, develops a thick cloud of white smoke. The tube normally has a charge to last for eight hours.

Under ordinary conditions, the tube is held in the airway and the smoke released across its axis at a suitable point in the cross-section. The time taken by the smoke cloud to reach a

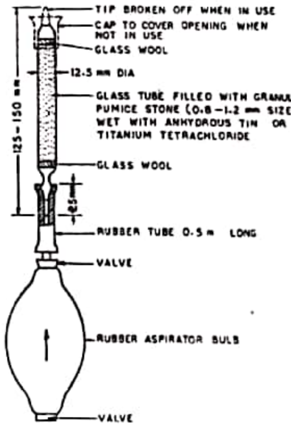

Fig. 8.2 Smoke-cloud generator.

distance of 8-10m is recorded by a stop-watch and the velocity computed thereform. However, this velocity may not represent the average velocity in the airway. The relation between the observed velocity and the average velocity depends on the position in the cross-section of the airway where the smoke cloud was released. The smoke cloud should not be released very near the sides lest it should be affected by eddy currents created by the rough surface of the airway. If it is released about quarter way from the side, it is found that the velocity obtained exceeds the average by 10% and this correction has to be applied to the observed velocity in order to get the average value.

Also, with very low velocities in airways of average cross-section, the smoke cloud may thin out considerably so as not to be discernable at the normal distance of observation of 8-10m. In such cases a smaller distance of 4-5m may be used whereas with velocities ranging from 0.55-0.75 m s^{-1} and good lighting in the airways, the distance of observation can be increased to 15-20m.

A straight portion of the airway with uniform cross-section should be chosen for velocity measurement by this method and the average cross-sectional area of the test section should be obtained.

Scanned with CamScanner

8.3.2 Tracer-Gas Method

Tracer gases[107] like oxides of nitrogen have been used for measuring air quantities, particularly small ones. With the help of infrared gas analysers, fairly low concentrations of nitrogen dioxide (of the order of 100 parts per million) can be estimated with an accuracy of $\pm 1\%$. The relative scarcity of nitrogen dioxide in normal mine atmospheres and the harmlessness of such low concentrations of the gas over a short period for the human system render it a very suitable tracer gas for use in mines. The procedure consists of releasing a certain volume V of nitrogen dioxide at a point in a mine airway and determining at regular time intervals its concentration in the mine air at a suitable distance downstream where complete diffusion would have taken place, till the tracer gas concentration in the air drops to zero again. A concentration-time curve is plotted and the area under the curve determined. The area divided by the time gives the average concentration c. The quantity of air Q flowing per unit time can then be obtained from the relation

$$Qc = V \tag{8.3}$$

Alternatively, nitrogen dioxide can be released at a constant rate of, say, V volumes per unit time and the concentration determined at any time during the release. In this case, too, the quantity Q will be given by the relation stated above. The tracer gas method can measure low air velocities with an accuracy of $\pm 5\%$.

Ree's torsion anemometer and the ionization anemometer are instruments sensitive to low air velocities, but the former is suitable for horizontal velocities only and the latter has been found to be fairly inaccurate where the air-stream is dust-laden. A very suitable method of measuring low air velocities is by hot-wire anemometers.

8.3.3 Hot-wire Anemometers

These are very sensitive instruments for measuring low air velocities.

The heat loss H per unit time per unit length of a wire of diameter D maintained at a temperature T above that of the surrounding air is given by the relation

$$H = kT + (2\pi k C_v \rho D)^{\frac{1}{2}} v^{\frac{1}{2}} T \tag{8.4}$$

where k = thermal conductivity of air,
C_v = specific heat of air at constant volume,
ρ = density of air
and v = velocity of air.

The above relation holds good down to a value of $vD = 1.87 \times 10^{-6}$ when v is in m s^{-1} and D, in m. This corresponds to a velocity of about 0.1 m s^{-1} for a wire diameter of 0.02mm. For an instrument with a hot wire of a certain diameter maintained at a certain temperature above that of the ambient air, equation 8.4 can be written in the following form assuming the values of k, C_v and ρ for air to remain constant :

$$H = K_1 v^{\frac{1}{2}} + K_2 \tag{8.5}$$

where K_1 and K_2 are constants.

If the wire is heated electrically, the heat produced per second in the wire of resistance $r\,\Omega$ with a current i A flowing in it will be equal to $i^2 r$ J.

$$\text{Or, } i^2 r = K_1 v^{\frac{1}{2}} + K_2 \tag{8.6}$$

If now the temperature is maintained constant, r will be constant when equation 8.6 will reduce to

$$i^2 = K_3 v^{\frac{1}{2}} + K_4 \tag{8.7}$$

where K_3 and K_4 are constants.

Plotting i as calculated from equation 8.7 against v we get a curve which shows a rapid variation in the current with velocity at low velocities, the variation gradually slowing down at higher velocities. This clearly indicates the high sensitivity of the instrument at low velocities.

The value of K_4 can be determined by noting the current i_0 in still air when $v = 0$.

$$\text{or, } i_0^2 = K_4 \tag{8.8}$$

Substituting this in equation 8.7, we have

$$i^2 = i_0^2 + K_3 v^{\frac{1}{2}} \tag{8.9}$$

Scanned with CamScanner

Equation 8.9 holds good for a fixed temperature of the hot wire and a particular difference in temperature between the hot wire and the surrounding air. It determines the values i_o and K_3 for a certain air temperature and any change in the air temperature will change these values. Also, change of air temperature will affect the value of ρ. The effect of these, however, is not much if the wire is maintained at a very high temperature (i.e., in the range of 1250-1300 K) as compared to the temperature of air.

There are two types of hot-wire anemometers, the constant-resistance type and the constant-current type. In the constant-resistance type of instrument the temperature and hence the resistance of the wire is maintained constant when the relationship of the air velocity and the heating current will be governed by equation 8.9. Alternatively, the current can be maintained constant and the change of temperature or resistance with change in air speed can be measured. Though the constant-current type of instrument has higher sensitivity except at low wire temperatures (less than 420 K), the constant-resistance type of instrument is more convenient to use.

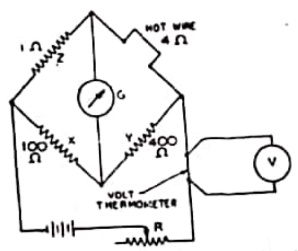

Fig. 8.3 Electrical circuit of a constant-resistance type of hot-wire anemometer.

Fig. 8.3 illustrates the principle of operation of a constant-resistance type of hot-wire anemometer. It consists of a Wheatstone bridge, the external circuit of which carries a variable resistance R, by varying which the current through the anemometer wire can be varied. The anemometer wire is usually of platinum. A volt thermometer consisting of a fine platinum wire is connected in series with the external circuit. It measures the current by noting

the voltage drop across the wire. When there is a change of current, the resistance of the volt thermometer changes and hence the voltage drop across it also changes. The two ratio arms X and Y are made of manganin wires (the resistance of which is not affected by temperature variations) of 100Ω and 400Ω resistances respectively. The standard resistance Z is of 1Ω and the anemometer wire, of 4Ω resistance when hot. Since the ratio arms have comparatively high resistances, the current through the volt thermometer can safely be taken as equal to that through the anemometer wire.

In the constant-current type of anemometer, there is no device to measure the current but a variation in the resistance of the anemometer wire causes an imbalance in the galvanometer G, the reading of which can be calibrated to give the resistance of the anemometer wire or more directly the air velocity.

For medium velocities of 0.75 to 10 m s^{-1}, vane anemometers and velometers are commonly used.

8.3.4 Vane Anemometer

The vane anemometer (Fig. 8.4) consists of a small windmill with vanes set at an angle of 0.785 rad to the direction of air-flow which rotates the vanes at a speed proportional to the air velocity. The number of revolutions converted to a scale of distance traversed by the air is recorded in a set of counting dials operated through gears. The air velocity can be obtained by dividing this reading by the duration of measurement recorded with a stop-watch. The commonly used type of anemometer is the Biram type which is 100 to 112mm in diameter with centrally placed counting dials. There is a small clutch which can be operated to engage the wheel with the counting system while measuring air velocity. A resetting device brings back the readings to zero. Provision can be made for mounting the anemometer on a shaft for more accurate measurements away from the body. In such a case arrangements are made to operate the clutch from a distance by means of a string. In some designs of anemometers the counting dials are placed on the top of the instrument perpendicular to the plane of the vanes. A recent development in anemometer design obviates the use of counting dials operated by the rotor through gears. Here, the number of revolutions are recorded by a fast photo-electric counter which can count up to 2400 π rad min^{-1} (1200 r.p.m.) and as a result, an air velocity up to 10 m s^{-1} can be recorded. The counter can be

Scanned with CamScanner

reset to zero and the air velocity obtained by referring to a calibration chart.

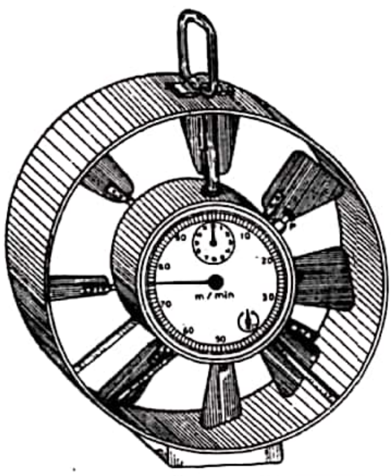

Fig. 8.4 One-minute vane anemometer.

Anemometers commonly used in mines cover a velocity range of 1-15 m s^{-1} though low-speed anemometers having a range of 0.15-1.5 m s^{-1} and high-speed cup-type meteorological anemometers having a range of 10-30 m s^{-1} have been designed.

There is a common belief that vane anemometers do not give accurate readings, but this is not true and the impression has been created by the use of instruments out of calibration. With proper care, anemometers have been found to give readings, accurate enough for mine requirements. Anemometer readings are practically independent of air density and temperature within the range commonly met with in mines and are only slightly affected by non-parallel flow. However, anemometers invariably record a velocity, different from the true velocity by up to 10%. The variation is usually given by the relation.

$$v_t = K_1 + K_2 v_r \tag{8.10}$$

where v_t = true velocity

v_r = recorded velocity

and K_1 and K_2 are constants depending on the anemometer.

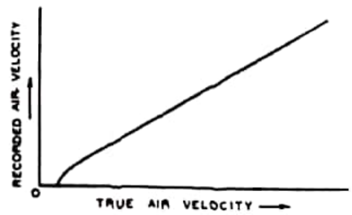

Fig. 8.5 Typical calibration curve for a vane anemometer.

This is because of friction in the instrument inhibiting the recording of the actual velocity of air as well as the constriction of the flow path by the dial, though the effect of the two are opposite in nature. Fig. 8.5 shows a typical calibration curve for a vane anemometer. It will be seen from the curve that at the measuring range of velocities, the curve is a straight line (the nature of the curve of course depends on the design of the instrument) though at very low velocities it is irregular in nature. Calibration curves are usually provided by manufacturers, but for accuracy of work it is necessary to check and, if necessary, recalibrate the instrument periodically. It is always desirable to recalibrate the instrument after an adjustment. Calibrations are also recommended before and after important measurement work such as fan testing or ventilation surveys.

Calibration of Anemometers. For low velocities, anemometers can be calibrated by mounting them at the tip of a horizontal arm which is rotated about a vertical axis. The relative air velocity is computed from the peripheral velocity or the linear velocity of rotation of the anemometer. At high velocities, however, the swirl in the air affects the reading of the anemometer and a suitable correction has to be applied. It is for this reason that today anemometers are usually calibrated in wind tunnels with constant velocity profiles or large-diameter ducts, particularly for calibration at high velocities. The air velocity in the duct can be determined by

Scanned with CamScanner

suitable orifices or nozzles incorporated in it. The position of the anemometer on the measuring cross-section of the duct should be such that it coincides with that of the average velocity as indicated by the orifice or nozzle flow-meter. The positioning is usually controlled by a pitot-static tube survey of velocities at various points on the measuring section of the duct. Alternatively the anemometer can be placed centrally in the duct and the velocity over its cross-section obtained from the velocity profile plotted from the pitot-static tube traverse. Variation of the air velocity in the duct is generally achieved by varying the fan speed.

The calibration, according to Ower[72] is not much affected by changes in air density except for very low velocities. Whereas a 32% change in air density can be neglected with an air velocity of 6 m s^{-1} with a velocity of 1.5 m s^{-1}, a variation of only 5% in density can be neglected for a limiting error of $\pm 1\%$. However, large differences in the density of air during calibration and actual measurement which may occur in deep and hot mines can substantially alter the calibration curve. In such cases, the constant, K_1 in the calibration equation 8.10 should be replaced by $K_1 \ (\rho_s/\rho)^{1/2}$ where ρ_s is the air density during calibration and ρ, the air density at the place of measurement. For calibration under ordinary temperature and pressure conditions, ρ_s can be taken as equal to 1.2 kg m^{-3}.

Ower has also shown that the accuracy of anemometers is only slightly affected if the anemometer does not exactly face the air-current. According to him, an anemometer facing the direction of air-current with its axis at an angle of 0.349 rad (20°) with the direction of air-flow gives readings with under 2% error. This fact has been well corroborated by other workers[109]. Hence non-parallel flows commonly met with in mines do not affect the anemometer reading to any appreciable extent. However Wilh Lambrecht, manufacturers of vane anemometers assert that an *angle of yaw* of greater than 0.175 rad (10°) affects the speed of rotation of the vanes to an uncontrollable extent.

Calibration of anemometers, however, can be seriously affected in dusty and wet atmospheres where dust may accumulate on the vanes and gearing thus changing the frictional resistance of the instrument. An instrument can be very quickly thrown out of calibration in a highly dusty and wet atmosphere and care should be taken not to expose anemometers to such conditions.

A special type of vane anemometer (Fig. 8.4) manufactured by Wilh Lambrecht of Germany has a single press button P, instead of the clutch and the resetting device, which (a) sets the pointer back to zero, (b) winds up the clock-work, and (c) releases a timing mechanism. The timing mechanism is automatically operated by the clock-work so that after 6 seconds of pressing the button or starting the instrument, the wheel gets geared to the recording unit for exactly 1 minute, after which it is automatically disengaged. The clock-work stops automatically after a slowing period of 4 more seconds. With this design, the handling of the instrument is much simplified. However, the use of this instrument in continuous traversing requires a judicious control of the traversing speed so that the roadway cross-section can be uniformly covered in the fixed time of 1 minute, although spot readings can be obtained without any difficulty.

Anemometers are suitably used for air measurement in all mine airways and ducts which have got a diameter of at least 6 to 8 times that of the anemometer. The readings become erroneous for ducts of lesser diameter. When used inside ducts, anemometers are usually placed centrally and the recorded velocity corrected by multiplying it with a suitable *method factor*. Northover[111] obtained the following method factors (Table 8.3) for ducts on the discharge side.

Table 8.3. : Method Factor for Anemometer Reading in Ducts

Diameter of duct in mm	Method factor
305	0.84
457	0.85
610	0.85
762	0.86

8.3.5 Velometer

The velometer (Fig. 8.6) consists of a double-pivoted spring-balanced aluminium vane mounted in jewelled bearings in a bakelite case. The vane moves in the passage in such a way that, as it is deflected more and more, the clearance between the vane and the walls of the passage increases or, in other words, the cross-sectional area of air-flow in the instrument increases.

Scanned with CamScanner

The deflection of the vane is directly proportional to the air velocity. Damping is done by eddy currents induced in an extension of the vane which moves in a permanent magnetic field. The deflection is recorded on a graduated scale so calibrated as to give the reading of velocity directly. Velometers can be made for one, two or three ranges of velocities, the lowest range being 0-1.5 m s^{-1} and the higher ranges, 0-5 m s^{-1} and 0-15 m s^{-1}. There are three scales for the three ranges. The lowest range is obtained by keeping the inlet port of the velometer open while suitable jets have to be fitted to the inlet port for obtaining the other two ranges. Velometers, if so designed, can also measure pressure (both static as well as total) on a separate scale by using suitable jets. The usual ranges of pressure are 0-500 Pa and 0-1500 Pa.

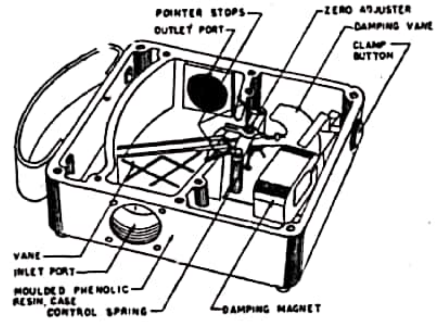

Fig. 8.6 The velometer.

The minimum reading obtainable by the common velometer is 0.15 m s^{-1} Special sensitive velometers with a range of 0-0.3 m s^{-1}, 0-0.5 m s^{-1} or 0-0.75 m s^{-1} with a minimum reading of 0.05 m s^{-1} have been designed. A continuous recording velometer has also been designed.

Velometers give indications within 3% of full scale in all ranges except in the case of special low-range velometers. It is claimed that there is no appreciable error in the reading of the velometer with an angle of yaw up to 0.524 rad (30°). Air density affects the velometer reading only slightly and a correction factor which is inversely proportional to the square root of the air density is to be

multiplied with the reading to get the correct value where great accuracy is desired. Usually a density correction chart is provided with the instrument. Velometers are usually calibrated at 291 K, standard barometer and 50% relative humidity where the air density is 1.2 kg m^{-3}.

Velometers are direct-reading instruments where no calculation or use of calibration charts is necessary. However, it is a spot reading instrument and cannot be used for continuous traversing. Another objection is that it is unsuitable for dusty atmospheres. However, a suitable flannel filter, which can be screwed on to the inlet of the velometer where the air is very dusty, has lately been designed by the manufacturers. The filter is claimed to affect the air velocity very slightly and correction charts are provided by the makers where necessary.

8.3.6 The German Velocity Meter

This instrument (Fig. 8.7) manufactured by Paul Gothe, Bochum has two blades A and B which are deflected by the air-current, the deflection being proportional to the air velocity. The deflection is recorded by a needle moving on a graduated scale. The air enters at D and passes through an orifice E, the size of which can be changed to read various ranges of velocities. The instrument is thus capable of reading four ranges of velocities, i.e. 0.017-1 m s^{-1}, 0.08-5 m s^{-1} and 0.33-20 m s^{-1}. The air passes through a sieve F where most of the dust is caught and then through holes G. One branch goes through H, impinges on the blade A and passes out through slot J to the exit ports N from where it leaves the ins-

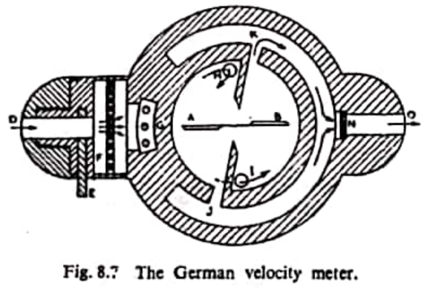

Fig. 8.7 The German velocity meter.

trument through O. The other branch goes through I, impinges on the blade B and then passes out to the exit ports N through slot K.

The smooth guiding of the air in the instrument prevents the blades from fluttering and thus makes damping unnecessary. Also, the dust in the air gets caught in the labyrinth and does not reach the blades. The velocities for any reading with a particular orifice can be obtained by referring to a calibration chart.

For high velocities above 8-10 m s^{-1}, ordinary anemometers cannot be used, as there is a chance of cracking of the jewelled bearings. High-speed anemometers with less number of vanes can be used in such cases. Velocities greater than 10 m s^{-1} can be measured by cup-type anemometers where there are four cups mounted on a cross with their axes horizontal and rotating about a vertical axis. Measurements with such anemometers are usually taken over a period of 3 minutes. Ordinary anemometers have been found suitable for measuring higher velocities when their frontal area is partly closed by a suitable shutter.[113] Velometers can be used for fairly high velocities. However, high air velocities are usually met with in ducts where anemometer or velometer measurements become inaccurate and may not be even possible at all. In such cases, a very simple and yet accurate instrument that can be used, is the pitot-static tube. This instrument is claimed to have an accuracy of 1% in the commercial types to 0.1% in special research types.

8.3.7 The Pitot-static Tube

The pitot-static tube, often erroneously referred to as the pitot tube consists essentially of a *pitot tube* or a *total-head tube* placed concentrically inside a *static tube*. It comprises a head which faces the air-stream and a stem bent at right angles to it. The pitot tube is nothing but a tube with an open end facing the air-stream so that it measures the total head whereas a static tube is one with its nose (which faces the air-stream) closed and with a few holes on the side of the tube for recording the static pressure only. In the pitot-static tube there are two concentric tubes, the outer of which has a few holes on the sides. The annular opening between the two tubes at the nose end is sealed so that the inner tube records the total pressure and the outer, the static pressure only. The nose is suitably shaped so as to avoid undue turbulence and hence offer the least resistance to flow. The two component tubes of the pitot-static tube are connected to the two limbs of a manometer which reads the velocity pressure. The velocity can be obtained from the velocity pressure by using the relation

$$P_v = \frac{Kv^2\rho}{2} \tag{8.11}$$

where v = velocity in m s^{-1}

P_v = velocity pressure in Pa,

ρ = density of air in kg m^{-3}

and K = correction factor for the particular pitot-static tube (for standard designs, K=1).

For a normal density of air of 1.2 kg m^{-3}, equation 8.11 reduces to

$$v = 1.29 \sqrt{P_v} \tag{8.12}$$

The pitot-static tube may or may not measure the true velocity pressure accordingly as it is designed. This deviation of a pitot-static tube reading from the true value is due to the effect of flow around the nose and the stem which affects the static pressure reading. Due to the effect of flow around the nose, a negative pressure is produced on the parallel sides of the head, the magnitude of which decreases away from the nose. On the other hand, the flow around the stem produces a positive pressure on the parallel sides of the head, the magnitude of which decreases away from the stem towards the nose. These two pressures oppose each other and with a certain length of head, a position can be found on it where the two pressures completely balance each other. If the static orifices are located at this position, a true static pressure reading will be obtained and hence the pitot-static tube will read the true velocity pressure. For such a design the correction factor K in equation 8.11 becomes unity. In practice, pitot-static tubes have been designed to give a correction factor of unity with an accuracy of 0.1% over a large range of velocities from 1 m s^{-1} to well over the speed at which compressibility becomes important i.e. a speed, much larger than the highest ever met with in mines. However, the accuracy of the pitot-static tube is affected by the angle of yaw or the angle between the direction of air-current and the axis of the head of the pitot-static tube. The permissible angle of yaw is

Scanned with CamScanner

0.175 rad (10°) which causes an error of 3% in the velocity measurement. Normally, during measurement, the head of the pitot-static tube is turned in different directions until the highest velocity pressure is recorded. This happens at the lowest angle of yaw.

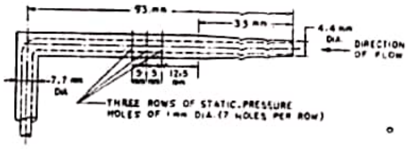

Fig. 8.8 Old N.P.L. standard pitot-static tube.

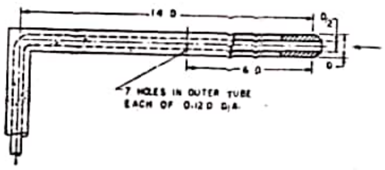

Fig. 8.9 N.P.L. standard pitot-static tube with hemispherical head.

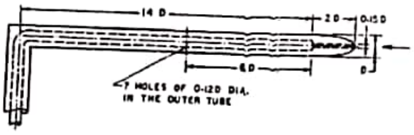

Fig. 8.10 N.P.L. standard pitot-static tube with ellipsoidal head.

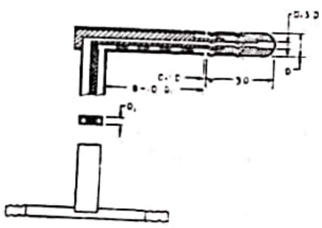

Fig. 8.11 Prandtl pitot-static tube.

It is found that the shape of the nose has very little effect on the accuracy of a pitot-static tube if the relative position of the static orifices on the head or the ratio of the length of the parallel portion of the head between the nose and the static orifices and that between the static orifices and the stem of the standard design remains unchanged. That is why the old British N.P.L. standard pitot-static tube with a pointed nose (Fig. 8.8) has been replaced by new standards with hemispherical (Fig. 8.9) and ellipsoidal (Fig. 8.10) noses which have the advantage of a sturdier construction and a shorter overall length of the head. Also, a round nose is less sensitive to yaw. In the Prandtl pitot-static tube (Fig. 8.11) the static orifices are replaced by an annular slit which is less likely to be clogged by dust and which attenuates any unequal distribution of pressure along the circumference. However, the static pressure in this instrument is very sensitive to the geometry of the slit. Though pitot-static tubes can be designed for any size, they are usually 8-10mm in diameter.

Pitot-static tubes are generally used for the measurement of air velocity in ducts. As the accuracy of the instrument is practically unimpaired for a large range of velocities, the minimum velocity that can be measured by a pitot-static tube is limited only by the sensitivity of the manometer that can be used under mining conditions. With an inclined-gauge manometer which has a sensitivity of say, 0.4 Pa, the lowest velocity that can be measured with 10% accuracy is of the order of 8 m s^{-1}. The use of the pitot-static tube is also limited by the size of the duct in which the measurement takes place. Pitot-static tubes of normal size should not be used in ducts less than 200mm in diameter, because in smaller ducts the circumferential measuring points become too close to the wall of the duct or may even touch it if sufficient number of measurements are to be taken across the duct with the measuring points located on equal area basis. The velocity in such small ducts can be measured by a small-diameter pitot tube (the outer diameter of a pitot tube should not exceed 2.5mm for measurement inside a 150mm duct) inserted inside the duct and connected to one limb of a manometer, the other limb of which is connected to a static orifice not exceeding 1.5mm in diameter on the side of the duct (Fig. 8.12). Besides, the pitot-static tube, unlike the anemometer, is a spot reading instrument.

Scanned with CamScanner

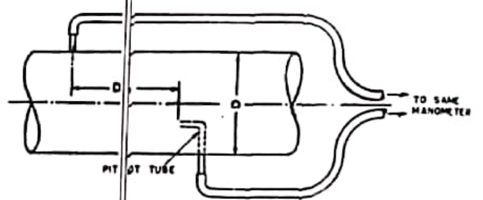

Fig. 8.12 Velocity measurement in narrow ducts.

Pressure-tube anemometers (Fig. 8.13) have been designed with correction factors greater than unity so that they can measure low velocities, but their efficacy is doubtful because of the fact that such correction factors vary appreciably with Reynolds number, particularly in the low-velocity range where the instrument is meant to be used. Moreover, even with a correction factor of 1.6, the reduction in the lower limit of velocity that can be read with a standard manometer used for the purpose is rather small, i.e. of the order of only 20%.

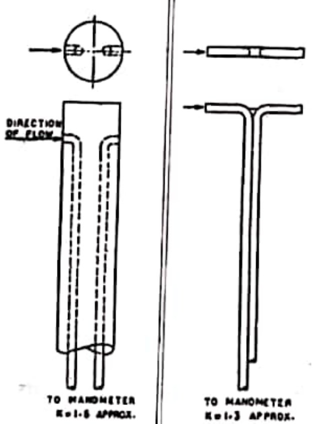

Fig. 8.13 Pressure-tube anemometers (diagrammatic).

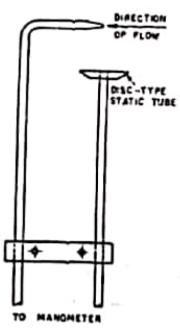

Fig. 8.14 Pitot tube with a disc-type static tube.

In heavily dust-laden air where the orifices in the standard pitot-static tube may get choked, a disc-type static tube may be used in conjunction with a pitot tube (Fig. 8.14). Such an instrument is claimed to have a fair degree of accuracy.

Example 8.1

A standard pitot-static tube placed at the centre of a 400mm diameter circular duct records a velocity pressure of 250 Pa. Calculate the quantity of air flowing in the duct if the air temperature is 303 K and the barometer reads 108 kPa. Assume the air to be dry and the method factor to be equal to 0.85.

Density of dry air at 303 K and 108 kPa pressure

$$= \frac{108\,000}{287 \times 303} = 1.242 \text{ kg m}^{-3}.$$

Velocity at the centre of the duct

$$= \sqrt{\frac{2P_v}{\rho}} = \sqrt{\frac{2\times 250}{1.242}} = 20.06 \text{ m s}^{-1}.$$

Average velocity $= 0.85 \times 20.06 = 17.05$ m s^{-1}.

Quantity flowing $= \frac{\pi}{4}(0.4)^2 \times 17.05 = 2.14$ m^3 s^{-1}.

8.3.8 Methods of Velocity Measurement

The velocity of flow varies from point to point over the cross-section of a mine airway and the variation is irregular in nature, particularly if the airway has rough sides and is not straight. The following methods can be adopted for computing the average velocity in such airways.

(*a*) *Single-point Measurement*. In this method, the measuring instrument (anemometer, velometer or pitot-static tube) is held at a fixed point on the cross-section of the airway and the reading multiplied by a method factor to get the average velocity. The instrument has to be held well away from the body of the observer. That is why anemometers should preferably be mounted on shafts. Usually readings at the centre are taken and these are multiplied by a method factor of 0.8 for getting the average values of velocity. It must be borne in mind that the method factor varies with the roughness of the sides of the airway and the Reynolds number, its value decreasing with decreasing Reynolds number. However, it can be taken to be constant for turbulent flow with high Reynolds numbers (>50 000) as in the case of mine air-currents commonly measured with anemometers or pitot-static tubes. The method factor is unity at one-seventh of the distance between opposite walls from any wall, or, in other words, the average velocity can be obtained directly by placing the instrument at this point. But readings at these points are not preferable to central readings as they are more likely to be affected by rough surfaces of the walls and unsymmetrical velocity profiles. An accuracy of 5% can be obtained with single-point measurement by an anemometer if the airway is straight and of uniform cross-section.

(*b*) *Continuous Traversing.* This is an approximate but quick method adopted with anemometers in minor airways which are neither very straight nor uniform in cross-section. This method gives an average accuracy of within 5% when used with a suitable method factor.

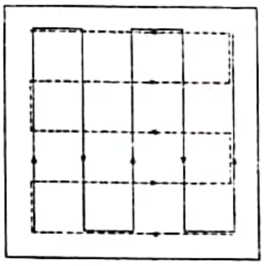

Fig. 8.15 Continuous traversing by anemometer.

The anemometer is held by hand or on a shaft away from the body and is traversed continuously either up and down or from side to side as shown in Fig. 8.15. The distance between adjacent legs of traverses should be about 300 mm for reasonable accuracy in

normal-size airways and this distance should be uniformly maintained. The duration of traversing varies with the area of cross-section. One minute is sufficient for an area of about 3 m^2 whereas 3 minutes may be necessary for an area of 9 m^2. A steady movement of the instrument is desirable for accuracy. Even for single-point measurements with anemometers, a minimum duration of reading of $\frac{1}{2}$ minute should be ensured so as to render the error due to acceleration of the counting gears at the start of measurement negligible. A fast rate of traversing of the anemometer introduces error in the measured air velocity and to keep down such errors below 2%, it is necessary to ensure that the speed of traversing does not exceed 1/10th of the speed of air being measured.

Owing to the presence of the observer standing in the airway the effective cross-sectional area of the airway is reduced and the observed air velocity is somewhat more than the average. In such a case the observed velocity has to be multiplied by a suitable method factor to get the true value. In airways of 3 to 4 m^2 cross-sectional area a method factor of 0.9 can be used if the observer always holds the anemometer at arm's length when standing in the airway or is shielded by a door frame or timber etc. during traversing. The method factor increases with increasing area of the airway as then the ratio of the area of the body obstructing flow to the total area of the airway gets reduced. A method factor of 0.92 is suitable for an area of 7.5 m^2 while for an area of 9 to 11 m^2 the method factor is 0.93. The effect of fluctuating air velocities on the anemometer reading is not much and since most air measurements are done under uniform flow conditions, this error is less likely to occur.

(*c*) *Precise Traversing.* This is a very highly accurate method of measuring air velocity by anemometers, velometers or pitot-static tubes. An accuracy of 2% can be obtained with this method of traversing by anemometers. However, this method is more time-consuming and hence should be confined to measurements in major airways only where a great deal of accuracy is needed.

Precise traversing should be done in straight portions of airways of uniform cross-section and preferably in smooth-lined portions away from any obstructions. The observer should stand at least 1.2m away from the instrument on the downstream side and the instrument should be mounted on a shaft. It is better if the observer stands in a suitable recess on the downstream side of the airway.

In this method, the cross-section of the airway is divided into equal areas of 300mm square for ordinary mine airways, the size being less for airways of lesser cross-sectional area as in the case of ducts. Wires are stretched across the airway in such a way that points of their intersection coincide with the centres of these areas where the observations have to be made. The instrument is then held at each of these observation points for a suitable length of time, say, a minute or so and the velocity is recorded. The average velocity can then be calculated from these velocities.

For circular airways such as ducts, the measurements are usually done along two diameters at right angles to each other. The measuring points are so located along the diameter (i.e., closer at the periphery and wider apart at the centre) that they represent equal areas. Referring to Fig. 8.16 the circle should be so divided that

$$r_1 = r\sqrt{\left(\frac{1}{2n}\right)},\ r_2 = r\sqrt{\left(\frac{3}{2n}\right)},\ r_3 = r\sqrt{\left(\frac{5}{2n}\right)},\ \ldots r_n = r\sqrt{\left(\frac{2n-1}{2n}\right)},$$

where n is the number of measuring points along a radius, r is the radius of the duct and $r_1, r_2, \ldots\ldots r_n$ are the distances of the measuring points from the centre of the duct along the radius. The number

Fig. 8.16 Location of velocity measuring points in a circular duct.

of measuring points depends on the diameter of the duct, but a practical minimum is 5 along a radius so that a minimum of 20 measurements are taken at a cross-section. For such a case, the measuring points are located at distances of $0.026D$, $0.082D$, $0.146D$, $0.226D$, $0.342D$, $0.658D$, $0.774D$, $0.854D$, $0.919D$ and $0.975D$ from the wall, where D is the diameter of the duct. Location of measuring points intended to represent equal areas in a duct often causes crowding of the measuring points towards the periphery of the duct and it may not be possible to accommodate the instruments suitably in these areas. In such cases the measuring points may be located at equal intervals along the diameter and the inequality of areas suitably accounted for by weighting the velocities according to areas they represent while averaging them.

Spot observations with anemometers take a long time and sometimes to economize on time, a reading is taken at one observation point for 10 to 20 seconds and then the instrument slowly moved on to the next point with the counting gear still engaged with the wheel of vanes and the process continued till all the points are covered. The anemometer then gives the average velocity directly, but this method is less accurate than that of separate spot observations.

8.3.9 Averaging of Velocities

When averaging spot velocities taken at various points on the cross-section of an airway, the velocities should be weighted according to the areas they represent, or, in other words,

$$Av_a = A_1v_1 + A_2v_2 + A_3v_3 \ldots\ldots\ldots\ldots + A_nv_n \tag{8.13}$$

where A_1, A_2 etc. are areas over which velocities v_1, v_2 etc. hold good respectively,

A = area of cross-section of the airway

and v_a = average velocity

When the areas are equal, equation 8.13 reduces to

$$Av_a = A_1(v_1 + v_2 + v_3 \ldots\ldots v_n)$$

$$= \frac{A}{n}(v_1 + v_2 + v_3 \ldots\ldots + v_n),$$

or, $$v_a = \frac{1}{n}(v_1 + v_2 + v_3 \ldots\ldots v_n) \tag{8.14}$$

where n = the number of observations.

Scanned with CamScanner

The readings obtained by a pitot-static tube are the velocity pressures. Since the velocity is proportional to the square root of the velocity pressure, the following relation is used to find the velocity pressure corresponding to the average velocity for measurements taken over equal areas.

$$P_v^{\frac{1}{2}} = \frac{1}{n}(P_{v_1}^{\frac{1}{2}} + P_{v_2}^{\frac{1}{2}} \ldots\ldots + P_{vn}^{\frac{1}{2}}) \tag{8.15}$$

where P_v = velocity pressure corresponding to the average velocity v_a, and P_{v1}, P_{v2} etc. are velocity pressures corresponding to velocities v_1, v_2 etc. respectively.

From P_v, the average velocity v_a can be calculated by using the relation given in equation 8.11, taking $K=1$.

8.4 QUANTITY MEASUREMENT BY PLATE ORIFICES, NOZZLES AND VENTURIS

These devices are particularly suited for measurement of the quantity of air flowing through ducts. They are permanently incorporated in the duct and can be utilized for continuously recording the air velocity in the duct. Such devices are sometimes used for the measurement of air quantity during testing of mine fans.

Let us consider an orifice of cross-sectional area A_2 in a thin plate placed across the path of flow in a duct of cross-sectional area A_1. Denoting, the cross-section of the pipe immediately before the orifice by suffix 1 and that at the orifice by suffix 2, the general energy balance equation for incompressible flow (equation 4.43) can be applied to flow through the orifice with $\triangle P$ taken equal to zero since the distance between sections 1 and 2 is negligible. $h_1 = h_2$ since there is no change in elevation between the two points with an orifice placed concentrically in the duct.

$$\text{Or, } P_1 - P_2 + \frac{v_1^2 - v_2^2}{2}\rho = 0 \tag{8.16}$$

Again for continuity

$$v_1 A_1 = v_2 A_2 \tag{8.17}$$

$$\text{or, } v_1 = m v_2 \tag{8.18}$$

where $m = A_2/A_1$ (area ratio of the orifice). Combining equation 8.18 with equation 8.16 we have

$$\frac{v_2^2(1-m^2)\rho}{2} = P_1 - P_2$$

$$\text{or, } v_2 = \sqrt{\frac{2(P_1-P_2)}{\rho(1-m^2)}} \tag{8.19}$$

$$\text{or, } Q = v_2 A_2 = A_2\sqrt{\frac{2(P_1-P_2)}{\rho(1-m^2)}} \tag{8.20}$$

where Q is the quantity flowing through the pipe in $m^3 s^{-1}$. Equation 8.28 holds good for incompressible flow where P_2/P_1 can be take as nearly equal to unity.

In case of compressible flow, the density will change with pressure. In pipes, the expansions and contractions at constrictions are sufficiently rapid so as to make the change adiabatic when

$$\frac{P_1}{\rho_1^{\gamma}} = \frac{P_2}{\rho_2^{\gamma}} = K \tag{8.21}$$

where γ = 1.4 for dry air and K = constant. In such a case

$$Q = A_2\sqrt{\left[2P_1\frac{\gamma}{\gamma-1}\left\{1-\left(\frac{P_2}{P_1}\right)^{\frac{\gamma-1}{\gamma}}\right\}\left(\frac{P_2}{P_1}\right)^{\frac{2}{\gamma}} \Big/ \rho_1\left\{1-m^2\left(\frac{P_2}{P_1}\right)^{\frac{2}{\gamma}}\right\}\right]} \tag{8.22}$$

The quantity of air flowing through a pipe of a certain diameter can thus be determined from equation 8.20 by noting the pressure drop P_1—P_2 across a constriction of a certain size in the pipe.

8.4.1 Plate Orifice

Fig. 8.17 shows a German standard plate orifice. Essentially it consists of a circular hole cut in a thin plate inserted across the pipe so that the hole or orifice is concentric with the pipe. A

Scanned with CamScanner

manometer connected to two holes or peripheral slots on the pipe wall on either side of the orifice plate records the pressure drop.

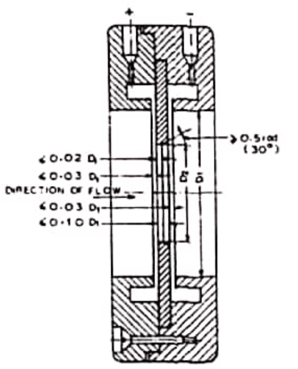

Fig. 8.17 German standard orifice.

Equation 8.20 assumes the cross-section of the flow-stream to change from A_1 to A_2, but in case of plate orifices, the cross-sectional area of the flow-stream reduces to a value lower than A_2 at the *vena contracta* so that equation 8.20 is modified to

$$Q_1 = CA_2\sqrt{\left\{\frac{2(P_1-P_2)}{\rho(1-C^2m^2)}\right\}} \tag{8.23}$$

were C=coefficient of contraction=area at the vena contracta/A_2. Even then the actual quantity Q_2 that flows through the orifice differs from the theoretical quantity Q_1 and if K is the ratio of the actual quantity Q_2 to the theoretical quantity Q_1, then equation 8.23 becomes

$$Q_2 = CKA_2\sqrt{\left\{\frac{2(P_1-P_2)}{\rho(1-C^2m^2)}\right\}} \tag{8.24}$$

In practice, the factor C and K are combined in the form of a *coefficient of discharge* $\propto$ when equation 8.24 becomes

$$Q_2 = \propto A_2\sqrt{\left\{\frac{2(P_1-P_2)}{\rho(1-m^2)}\right\}} \tag{8.25}$$

From equations 8.24 and 8.25, we have

$$\propto = CK\sqrt{\frac{1-m^2}{1-C^2m^2}} \tag{8.26}$$

$\propto$ is a function of v_2D_2/ϑ_2 (the Reynolds number), D_2/D_1 and e/D_1 where D_1 and D_2 are the diameters of the pipe and the orifice respectively, e=mean depth of roughness of the pipe wall, ϑ_2= kinematic viscosity=μ_2/ρ_2, μ_2=viscosity and ρ_2=density. With an orifice of a fixed size in a pipe of a fixed diameter, D_2/D_1 remains constant. For smooth-finished pipes of large diameter, e/D_1 tends to zero and its effect on the value of $\propto$ can be neglected. However, $\propto$ depends on the shape of the edge of the orifice if it is made in a thick plate which is normally done in practice and any change in this shape will alter the value of $\propto$. Also, in equation 8.25 we have assumed P_2 to be measured at the orifice, but in practice, this is impossible and P_2 is measured on the downstream side of the orifice. However, any variation in quantity due to this can be accounted for by suitably modifying the value of $\propto$. Table 8.4 gives the value of $\propto$ for the German standard orifice for various Reynolds numbers and pipe diameters.

It will be seen from the table that for m not exceeding 0.55, the value of $\propto$ can be assumed to be approximately constant at 0.603 with a limiting error of $\pm 1\%$ over the range of Reynolds numbers shown in Table 8.4. With lower Reynolds numbers the value of $\propto$ first rises and then falls rapidly with decreasing Reynolds number.

Table 8.4 : Discharge Coefficient for German Standard Orifice

m	$\propto$	lowest value of v_1D_1/ϑ_1 for which value of $\propto$ is valid	m	$\propto$	lowest value of v_1D_1/ϑ_1 for which value of $\propto$ is valid
0.05	0.597	20 000	0.40	0.606	125 000
0.10	0.599	30 000	0.45	0.605	145 000
0.15	0.601	40 000	0.50	0.603	170 000
0 20	0.603	50 000	0.55	0.599	195 000
0.25	0.604	65 000	0.60	0.594	225 000
0.30	0.605	80 000	0.75	0.585	260 000
0.35	0.606	100 000	0.70	0.574	300 000

Scanned with CamScanner

Presence of bends or obstructions near the orifice on either the downstream or the upstream side affects the value of α and to get α free from the effect of such obstructions, there should be a minimum length of straight pipe between the orifice and the obstruction. The minimum length for various conditions is given in Table 8.5.

Table 8.5 : Lengths of Straight Pipe Required between Obstruction and Orifice, in Pipe Diameters.

Type of obstruction (radii of all bends$=D_1$)	Position of obstruction (U-upstream D-downstream)	Type of orifice pressure tapping (S-single tap A-annular chamber)	Value of m					
			0.1	0.2	0.3	0.4	0.5	0.6
Single right-angle bend	U	S	5	8	12	18	26	—
	U	A	6	9	12	17	21	26
	D	S	5	5	5	5	5	5
	D	A	5	5	5	5	5	5
Double right-angle bend in one plane	U	S	5	5	5	8	15	24
	U	A	5	5	6	9	14	20
	D	S	5	5	7	9	13	17
	D	A	5	5	5	5	5	5
Double right-angle bend in two planes	U	S	28	28	28	28	28	28
	U	A	4	5	7	9	12	16
	D	S	5	5	5	5	5	5
	D	A	5	5	5	5	5	5
Stop valve	U	S	16	27	40	54	68	83
	U	A	8	11	14	18	22	27
	D	S	5	5	5	5	5	5
	D	A	5	5	5	5	5	5

Also, for small-diameter pipes using orifices with large values of m, the roughness of the pipe wall as compared to the pipe diameter affects α and in such cases α should be corrected for

according to the chart shown in Fig. 8.18. These corrections are applicable only to pipes with a roughness equivalent to that of cast-iron pipes which have rusted inside due to prolonged use out whose exteriors show no sign of serious corrosion.

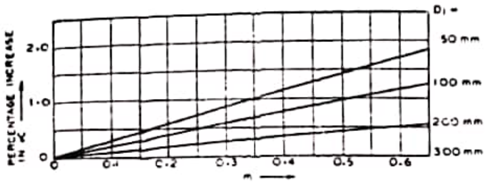

Fig. 8.18 Effect of pipe diameter on coefficient of discharge of German standard orifice.

The introduction of an orifice into a pipe range causes considerable irrecoverable pressure loss because of formation of eddies on the downstream side of the orifice resulting in inefficient recovery of velocity head. The irrecoverable pressure loss $\triangle P$ is given by the relation.

$$\triangle P=(P_1-P_2)\ (1-m) \tag{8.27}$$

That is why a shaped nozzle is often preferred to a plate orifice where pressure loss is to be minimized.

Example 8.2

A German standard plate orifice 400mm in diameter is installed in a duct of 600mm diameter. The manometer connected to the two sides of the orifice reads 30 Pa. Calculate the quantity flowing through the duct.

Let A_1 and A_2 be the cross-sectional areas of the duct and the orifice respectively.

$m=A_2/A_1 = 400^2/600^2 = 0.44.$

From Table 8.3 $\alpha=0.605.$

From equation 8.25, $Q=\alpha A_2\sqrt{2P/\{\rho(1-m^2)\}}$

where P=pressure difference across the orifice=30 Pa.

Or, $Q=(0.605\times3.14\times0.4^2/4)\sqrt{2\times30/\{1.2(1-0.44^2)\}}$

assuming $\rho=1.2$ kg m^{-3}.

Or, $Q=0.6$ m^3 s^{-1}.

Scanned with CamScanner

8.4.2 Shaped Nozzle

Fig. 8.19 shows a German standard nozzle and Table 8.6 gives the coefficient of discharge for such nozzles.

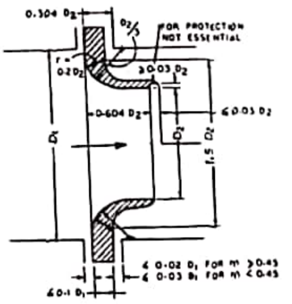

Fig. 8.19 German standard nozzle.

Since the discharge coefficient of a shaped nozzle is much larger than that of a plate orifice, the pressure drop $P_1—P_2$ for the same quantity Q_1 is much smaller and hence the irrecoverable pressure

Table 8.6 : Discharge Coefficient for German Standard Nozzle

m	$\propto$	Lowest value of $\frac{v_1 D_1}{\nu_1}$ for which value of $\propto$ is valid
0.5	0.986	70 000
0.10	0.984	73 000
0.15	0.982	80 000
0.20	0.979	90 000
0.25	0.975	100 000
0.30	0.969	115 000
0.35	0.963	130 000
0.40	0.954	145 000
0.45	0.946	170 000
0.50	0.936	185 000
0.55	0.925	195 000
0.60	0.914	200 000
0.65	0.899	200 000

loss across the nozzle is also correspondingly smaller than with a plate orifice. However, with a particular type of manometer of a certain sensitivity, one must measure a certain minimum pressure drop $P_1—P_2$ in order to maintain a particular degree of accuracy in the measurement of pressure. As for example, with a water gauge having a least graduation of 0.5mm, it is necessary to measure a pressure diffence of 50mm (490.5 Pa) so as to achieve an accuracy of 1% and from this point of view it may not be advisable to use a nozzle for reducing the pressure difference. On the other hand for the same pressure difference, the value of m can be considerably reduced with a nozzle which has the advantage of minimizing the errors due to roughness of pipe walls as well as any obstruction on either side of the nozzle.

$\propto$ for the German standard nozzle also needs correction for pipe diameter (i.e. roughness, similar to that in case of plate orifice) according to the chart given in Fig. 8.20. The lengths of straight pipes on either side of the nozzle necessary to avoid errors in $\propto$ are given in Table 8.7.

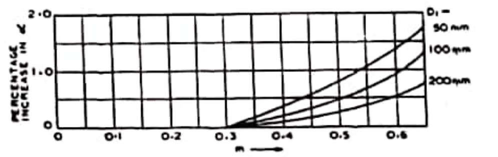

Fig. 8.20 Effect of pipe diameter on the coefficient of discharge of German standard nozzle.

8.4.3 Venturi Meter

Since a major part of the irrecoverable pressure loss in a nozzle is due to the abrupt expansion on the downstream side, the irrecoverable pressure loss can be greatly reduced if the expansion is made gradual as in the case of a venturi. The loss of head in a venturi, expressed as a percentage of pressure difference between inlet and throat, ranges from 13% for m=0.1 to 6½% for m=0.5 as against corresponding values of 83% and 33% for standard nozzles. Fig. 8.21 shows a British standard venturi tube and Table 8.8 gives its discharge coefficient with the limits of tolerance.

Table 8.7 : Lenghts of Straight Pipe Required between Obstruction and Nozzle in Pipe Diameters

Type of obstruction (radii of all bends = D_1)	Position of obstruction U=upstream D downstream	Type of pressure tapping S=single tap A=annular chamber	Value of m				
			0.1	0.2	0.3	0.4	0.5
Single right-angle bend	U	S	7	9	11	16	20
	U	A	7	9	11	14	18
	D	S	5	5	5	10	28
	D	A	5	5	5	5	5
Double right-angle bend in one plane	U	S	7	8	12	17	—
	U	A	6	6	7	14	—
	D	S	5	7	12	25	—
	D	A	5	5	5	5	5
Double right-angle bend in two planes	U	S	12	20	25	29	—
	U	A	5	6	8	12	16
	D	S	5	10	15	27	—
	D	A	5	5	5	5	5
Stop valve	U	S	15	28	43	63	—
	U	A	5	8	16	28	—
	D	S	5	5	5	5	5
	D	A	5	5	5	5	5

Table 8.8 : Discharge Coefficient for Venturi

$\frac{v_1 D_1}{\nu_1}$	$m=0.1$		$m=0.3$		$m=0.4$		$m=0.5$	
	α	tolerance, %	α	tolerance, %	α	tolerance, %	α	tolerance %
5 000	0.94	±1.25	0.94	±1.2	0.945	±1.1	0.96	±0.85
10 000	0.96	±0.8	0.96	±0.8	0.96	±0.75	0.97	±0.6
20 000	0.97	±0.6	0.97	±0.6	0.97	±0.5	0.975	±0.35
30 000	0.97	±0.4	0.97	±0.4	0.97	±0.4	0.98	±0.25
50 000	0.98	±0.2	0.98	±0.2	0.98	±0.2	0.985	±0.1
100 000	0.985	±0.1	0.985	±0.1	0.99	±0.1	0.99	±0.0

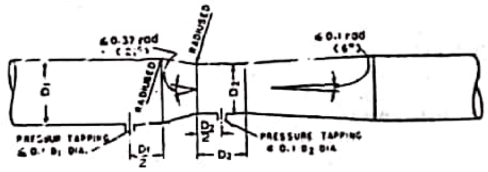

Fig. 8.21 Venturi Meter.

Discharge coefficients for venturis are also affected by pipe diameter and the correction factors are 0.985, 0.99, 0.995 and 0.997 for pipe diameters of 50, 100, 400 and 800mm respectively.

8.5 CONTINUOUS RECORDING AND MONITORING OF AIR VELOCITY AND QUANTITY

Continuous monitoring of air velocity is nowadays recommended for major airways subjected to large velocity fluctuations. Monitoring stations should be located in straight portions of airways with no obstructions up to 4.5m on the upstream side and 22.5m on the downstream side.

Instruments used for monitoring air velocity include (a) recording and telemetering type of vane anemometers such as the NCB MRE Airflow Transducer-type 815 or the 'Trolex' anemometer (b) mining-type hot-wire anemometers and (c) pitot-static tubes in conjunction with suitable pressure transducers. Sometimes the pressure drop across a section of an airway can be recorded as a measure of the quantity of flow through the airway. However, for accuracy of measurement the section of the airway should have a high resistance, which should remain constant.

Mining-type hot-wire anemometers for monitoring high velocities can be made in the form of constant-resistance heater coils cooling in the air-stream to different extents by different air velocities, the change in temperature being measured by a thermister through a suitable bridge circuit. One such instrument developed in South Africa comprises a 32mm long and 4mm outer diameter stainless steel tube supported on nylon bosses held in aluminium yokes. An 80-Ω coil made of 0.1mm diameter constant-resistance wire is wound over the tube with suitable insulation in between and coated with epoxy varnish. A heating current of 75 mA is passed through the coil giving a heat output of 0.45 W. A thermister placed inside the heater tube notes the change in temperature which ranges from 4.5-36 K for a velocity change of 0.125 to 30 m s^{-1}.

8.6 MEASUREMENT OF CROSS-SECTIONAL AREA

This is usually done by tapes. The work is simple if the airway cross-section is of a regular shape which can be divided into geometrical figures whose dimensions can be measured with a tape, but most commonly the shape of mine airways is irregular, where

Scanned with CamScanner

simple measurements by a tape will not do. In such cases any of the following methods can be used.

8.6.1 Tape Triangulation

In this method, a tape is stretched across the airway and with the help of another tape perpendicular offsets to the periphery of the airway on either side of the stretched tape are taken at regular intervals of 0.3-0.5 m. The measurements can be plotted to a certain scale and the area of the resulting diagram determined by a planimeter, or the area can be calculated using Simpson's rule for area as given below.

$$\text{Area} = \frac{L}{3} \text{ (sum of first and last ordinates +4 times the sum of even ordinates +2 times the sum of odd ordinates)} \qquad (8.28)$$

where L=distance between ordinates.

A modification of this method is to have a wooden frame of a size a little smaller than the cross-section of the airway but more or less resembling it in shape. Offsets are taken from the periphery of this frame to the sides of the airway.

8.6.2 Plane Table Method

This utilizes a drawing board with a sheet of paper pinned on to it and mounted in the plane of the section of the airway to be measured. Measurements are taken from a central point on the paper to various points on the periphery of the airway by means of a tape and the lengths are plotted on the paper to a suitable scale in the directions of measurement. The area of the resulting diagram can be estimated by a planimeter or by calculation (areas of individual triangles formed by adjacent rays can be calculated and added together to get the area of the cross-section).

8.6.3 The Profilometer[114]

This consists essentially of the equipment used in the plane table method except for the incorporation of a mechanical scaling device similar to that in a pantograph so that the profile of the airway is automatically plotted on the paper mounted on the plane table. This makes the measurement quicker and obviates any personal error in the plotting of the rays.

8.6.4 Craven Sunflower Method

This utilizes a graduated brass rod which is adjustable in length and can be rotated about a central point in the airway through a full circle. Measurements from a central point in the airway to the periphery are taken at various angles, the rod being adjusted every time so as to read the lengths at these angles. The measurements can be plotted to scale and the area computed thereform.

8.6.5 Photographic Method

The photographic method consists of marking the periphery of the section of the airway with white paint and photographing it with a scale placed in the plane of the section by means of a suitable photographic camera. Alternatively, the periphery can be marked out by moving along it a beam of light from a cap lamp while the camera shutter is kept open. In this method, computation of area can be done only after the photograph has been developed and printed. Computation of area can be done either from positive prints or from the image of the negative by screening it through a suitable projector. A wide angle lens obviates errors in rough airways.

Of the above methods, tape triangulation is the least accurate, particularly for irregular areas where it can have errors up to 10%. The sunflower method, according to Briggs, has a possible error of 3.5%. The photographic method has been claimed to have as high an accuracy as ±0.5%. This may well be true in airways of regular cross-section, but in highly rough airways this method is not very accurate since the rays from the periphery of the cross-section being photographed can get intercepted by adjacent projections from the the surface of the airway. In such cases the best accuracy can probably be obtained with the profilometer.

8.7 PRESSURE SURVEYS

Most pressure surveys in mines are required to measure pressure differences between two points so that the pressure loss over a certain section of an airway or its resistance can be obtained. This is the major requirement for ventilation planning. The resistance of an airway is indicated by the loss of pressure ΔP given by equation 4.43.

P_A+P_s in the above equation is the absolute static pressure normally read by a barometer placed at any point. However, a barometer can be made to read the absolute total pressure $P_A+P_s+\frac{\rho v^2}{2}$

Scanned with CamScanner

by putting it inside a container whose opening faces the air-current, though this may not be an accurate estimate of the total pressure since the velocity approaching the container may not be the average velocity v. That is why normally absolute static pressures are read on a barometer, while velocity pressures are computed from separate velocity measurements carried out with greater accuracy.

Equation 4.43 can thus be used to estimate the pressure drop ΔP and hence the resistance of any airway if the difference in the barometer readings at the two ends of the airway and the difference in height of the two points can be measured. This is the principle of pressure survey by aneroid barometers.

ΔP can also be measured directly on a U-tube water gauge (see equation 4.42) the two limbs of which are connected to two total-pressure tubes (tubes facing the air-current) placed at the two ends of the airway. The water gauge may be placed anywhere.

Here again, ΔP measured on a gauge connected to total-pressure tubes is not accurate as the average velocity pressures are not recorded. That is why it is a common practice to read the static pressure difference $P_{s1} - P_{s2}$ on the gauge by connecting its two limbs to two static-pressure tubes held at the two ends of the airway. The velocity-pressure difference is generally computed from the average velocities at the measuring stations as obtained from more elaborate velocity measurements. Equation 4.41 with ΔP substituted for ΔP_f can then be used to obtain ΔP.

In most mine airways with more or less uniform cross-section v_1 can be taken equal to v_2 so that the resistance is given by the difference in static pressures only.

Where the velocity of flow is so high that the velocity pressure nearly equals the static pressure (as may sometimes be the case at fan inlets and outlets), the method of calculating total pressure from average velocity gives a result which may be about 5% lower than the true mean total pressure which can be calculated in the following way.

Let us consider air flowing through a small element of area A on any section of the airway. The air flowing per unit time will have pressure energy equal to $P_s A v$ and kinetic energy equal to $\rho A v^3/2$, where v is the velocity of air passing through the area A. Hence,

Total energy of the airpassing through

$$\text{the area } A \text{ per unit time} = P_s A v + \frac{\rho A v^3}{2} \tag{8.29}$$

Also, the volume of air passing through the area per unit time $= Av$.

Now if the cross-section of the airway is divided into several such areas, say A_1, A_2, A_3 etc., with corresponding velocities of v_1, v_2, v_3 etc., respectively, the total energy of air passing per unit time through the whole section of the airway will be equal to

$\sum P_s A v + \sum \frac{\rho A v^3}{2}$ and the total volume of air passing through the section per unit time is equal to $\Sigma A v$.

So, the total pressure, (total energy per unit volume flow rate,

$$= \frac{\Sigma P_s A v}{\Sigma A v} + \frac{\sum \frac{\rho A v^3}{2}}{\Sigma A v} \tag{8.30}$$

If velocity measurements are taken over equal areas in the airway section and if ρ is assumed to remain constant all over the section, then

$$\text{Total pressure} = \frac{\Sigma P_s v}{\Sigma v} + \frac{\rho \Sigma v^3}{2 \Sigma v} \tag{8.31}$$

If the static pressure is further assumed to be constant all over the section of the airway, the total pressure will become equal to

$$P_s + \frac{\rho}{2} \frac{\Sigma v^3}{\Sigma v} = P_s + \frac{\Sigma P_v^{3/2}}{\Sigma P_v^{1/2}} \tag{8.32}$$

where P_v = velocity pressure as measured by the pitot-static tube in Pa (the same unit as of total pressure).

Measurement of absolute pressure is required mainly for the determination of air density, particularly in connection with natural draft, fan performance, air sampling and quantity change calculations. Absolute pressure can be approximately estimated from tables or by calculation if the reduced level and the temperature at the place are known. However, aneroid barometers are commonly used in mines for measurement of absolute pressure. They are also used

Scanned with CamScanner

for differential pressure measurements, but with less accuracy than inclined gauge and tube. Nevertheless, the mining type of aneroid is a very portable and handy instrument suitable for a rough but extensive survey in a short time. There are more accurate instruments such as Askania statoscope and Paulin aneroid for measuring small differences of pressure in mines, but they require extreme care in handling.

Example 8.3

A mine is ventilated by an exhaust fan at the surface connected to the exhaust shaft 6m in diameter by a fan drift 4.5×3m in cross-section. Two static-pressure tubes, one placed in the shaft just below its connection with the fan drift and the other in the fan drift at the fan inlet, give a reading of 310 Pa when connected to the two limbs of a manometer by suitable leakproof tubing. The manometer reading rises to 650 Pa when it is connected to the static-pressure tube in the fan drift with its other limb open to the atmosphere. The quantity readings in the fan drift and the exhaust shaft (measured below its connection with the fan drift) are 160 $m^3 s^{-1}$ and 138$m^3 s^{-1}$ respectively. Calculate the leakage through the surface air-lock when the fan is speeded up by 10%. Also calculate the shock factor for the junction of the shaft with the fan drift with respect to the fan-drift air velocity neglecting the frictional pressure loss in the fan drift.

Let static pressure in the exhaust shaft be P_{se} and that at the fan inlet, P_{si}. Both of these are negative since the fan is exhausting. From equation 4.41 with ΔP substituted for ΔP_f

$$\Delta P = P_{se} - P_{si} + (v_e^2 - v_i^2)\frac{\rho}{2}$$

where ΔP = pressure drop in the fan drift inclusive of its junction with the exhaust shaft.

v_e = average velocity of air in the the exhaust shaft

and v_i = average velocity of air in the fan drift.

$P_{se} - P_{si}$ = 310 Pa as measured on the monometer.

$$v_i = \frac{160}{4.5\times3} = 11.85 \text{ m s}^{-1}$$

$$v_e = \frac{138}{36\pi/4} = 4.88 \text{ m s}^{-1}.$$

$$\Delta P = 310 + (4.88^2 - 11.85^2)\times\frac{1.2}{2} = 240.03 \text{ Pa, taking } \rho = 1.2 \text{ kg m}^{-3}.$$

Neglecting friction loss in the fan drift, the above pressure gives the shock loss at the junction of the shaft with the fan drift.

$$\text{Shock factor} = \frac{240.03}{\frac{1.2\, v_i^2}{2}} = 2.85.$$

The current leakage through the surface air-lock $= 160 - 138 = 22 \text{ m}^3 \text{s}^{-1}$.

When the fan is speeded up by 10% the total quantity as also the leakage will increase by 10%.

Hence leakage on speeding up of the fan

$= 22 \times 1.1 = 24.2 \text{ m}^3 \text{s}^{-1}$.

8.7.1 Pressure Survey with Aneroids

Aneroids used for pressure surveys in mines should be periodically checked and calibrated for accuracy. When doing pressure surveys in mines, two aneroids are to be used, one as a stationary base instrument and the other for traversing. The readings of the traversing instrument should be corrected for any change in the atmospheric pressure during the survey with reference to the base instrument. Both the instruments should be taken down the pit slowly in order to avoid permanent set at least 24 hours before the survey starts so that they get adjusted to the increased pressure. Any movement from a high to a low-pressure area or vice versa should be slow and gradual in order to avoid lag or creep. The survey should usually proceed continuously in a single direction either from intake to return or vice versa. As far as possible, aneroids should not be taken from return to intake or vice versa through air-locks separating them. If however it cannot be avoided, there should be at least a ten minutes' gap between the opening of one door and that of the other and the same time should elapse between the closing of the last door and starting of the pressure survey. The traverse aneroid should normally be allowed 10-20 minutes to acquire the temperature of the surrounding air at any place before taking the reading.

Normally the aneroid reads the absolute static pressure. The velocity pressure as calculated from velocity measurements is added to the static pressure in order to obtain the total pressure. To obtain the differential pressure of ventilation alone without taking into account changes in barometric pressure, it is necessary to record the difference in height between the points of observation. This is simplified if the aneroid is always held at a fixed height from the floor so that the difference in height between the two positions of the aneroid is equal to the difference in the reduced levels on the floor at the two places of observation. A whirling hygrometer reading is usually taken along with the aneroid reading so that the temperature and density of air can be obtained for the computation of the variation in atmospheric pressure due to altitude difference. The following corrections have to be applied to aneroid readings for getting the differential pressure of ventilation between two points :

(a) *Correction for Variation of Temperature.* A temperature coefficient for any particular instrument is usually supplied by the calibrating authority and corrections to the aneroid reading have to be applied in accordance with the temperature of measurement as obtained on the whirling hygrometer.

(b) *Correction for Fluctuation in Atmospheric Pressure.* This is done by reading the control barometer at the base station every five minutes and noting the time of each reading of the traverse aneroid, the two timing devices being properly synchronized. Good results are obtained in calm weather when the barometer is steady. The survey should be discarded if there are large fluctuations in the reading of the control aneroid.

(c) *Correction for Changes in Natural Ventilating Pressure.* Changes in natural ventilating pressure affect the total ventilating pressure. However, such changes are negligible except in shallow mines with little mechanical ventilation.

(d) *Correction for Atitude of Stations.* This is calculated from the reduced level of the station obtained by levelling the traverse route just before or after the survey. An accuracy of 0.5m in determining the difference in levels is sufficient since it corresponds to a change in barometric pressure of the order of 6 Pa which is the usual sensitivity of aneroids commonly used in mines. The

difference in barometric pressure due to difference in altitude can be obtained from the relation given in equation 3.1.

A good check on the accuracy of the aneroid survey is provided by taking water-gauge readings across separation doors between intake and return airways if they occur en route. Table 8.9 gives a proforma for recording aneroid surveys.

Table 8.9 : Aneroid Survey Record

Station	Time (h)	Depth below datum (m)	Difference in level (m)	Control barometer reading (kPa)	Traverse barometer reading (kPa)	Corrected traverse barometer reading (kPa)	Hygrometer reading	
							d.b. (K)	w.b. (K)
						Correction +0.017		
Down-cast pit bottom	8-30	600.00	0	110.056	110.039	110.056	291	286
	8-40	601.00	–1	110.059	110.046	110.063	288	283

Correction for temperature		Correction for variation in atmospheric pressure (kPa)	Correction for level (kPa)	Corrected reading of traverse barometer (kPa)	Difference of pressure from base station (kPa)	Difference of pressure from base station (Pa)	Remarks
Difference in temp. (K)	Correction (kPa)						
—	—	—	—	110.056	—	—	
–3	+0.003	–0.003	–0.012	110.051	0.005	5	

Example 8.4

Two aneroid barometers are used to measure pressure loss in a horizontal airway. Though the aneroids have not been calibrated to indicate absolute pressure correctly, they are in good order so as to indicate changes in pressure with accuracy. The airway is 900m long and 3×3m in cross-section and is unsupported with a value of $k=0.01$ Ns^2 m^{-4}. The following are the readings of the two aneroids placed at either end of the airway with two different rates

Scanned with CamScanner

of flow (obtained by stopping one of the two fans ventilating the mine) in the airway. Calculate the pressure drop across the airway with the normal flow rate of 51 $m^3 s^{-1}$. Also calculate the shock resistance of the airway.

With a flow of 51 $m^3 s^{-1}$,
Aneroid reading at the upstream end = 104.26 kPa
Aneroid reading at the downstream end = 101.31 kPa.
With a reduced flow of 29 $m^3 s^{-1}$,
Aneroid reading at the upstream end = 102.2 kPa
Aneroid reading at the downstream end = 99.69 kPa.

Let resistance of the airway be R and P_1 and P_2 be the aneroid readings at the upstream and the downstream ends respectively with the subscripts f and r indicating full and reduced flow conditions.

Let P' be the calibration error in the reading of P_1-P_2. From equation 4.43

$\Delta P=P_1-P_2$ since $h_1=h_2$ and $v_1=v_2$ in a horizontal airway of uniform cross-section.

$$\therefore R=\frac{(P_{1_f}-P_{2_f})-P'}{Q_f^2}=\frac{(P_{1_r}-P_{2_r})-P'}{Q_r^2}.$$

$$RQ_f^2=(P_{1_f}-P_{2_f})-P'$$

and $$R.Q_r^2=(P_{1_r}-P_{2_r})-P'.$$

$$R(Q_f^2-Q_r^2)=(P_{1_f}-P_{2_f})-P'-(P_{1_r}-P_{2_r})+P'.$$

$$R=\frac{(P_{1_f}-P_{2_f})-(P_{1_r}-P_{2_r})}{Q_f^2-Q_r^2}$$

Substituting the respective values, we get

$$R=\frac{(104.26-101.31)-(102.2-99.69)}{51^2-29^2}\times 10^3=0.25 \text{ Ns}^2\text{ m}^{-8}.$$

Pressure drop $=0.25\times 51^2=650.25$ Pa.

$$\text{Friction pressure loss}=\frac{0.01\times 2(3+3)900\times 51^2}{9^3}=385.33 \text{ Pa.}$$

$\therefore$ Shock pressure loss $=650.25-385.33=264.92$ Pa.

$$\text{Shock resistance}=\frac{264.92}{51^2}=0.102 \text{ Ns}^2\text{ m}^{-8}.$$

8.7.2 Pressure Survey with Differential Barometers

A very suitable instrument for underground measurement of pressure differences is the differential barometer which has been successfully used in mines in the U.S.S.R.[118] This is free from the errors due to creep and set commonly met with in aneroid barometers although its sensitivity compares well with that of aneroids. It does not require much skilled operation and can take 15 to 20 readings in a shift.

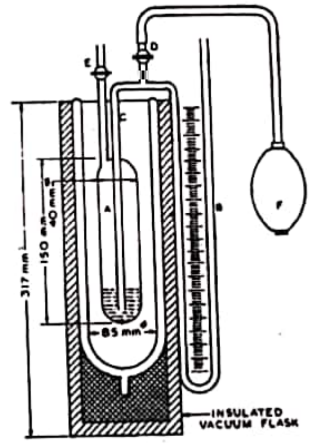

Fig. 8.22 The differential barometer.

The differential barometer (Fig. 8.22) consists of a vessel A connected to the atmosphere by a tube having a tap E. A tube C, one end of which extends nearly to the bottom of the vessel A, is connected at the other end to a U-tube manometer B. Tube C is connected to an aspirator bulb F through the tap D. The vessel A is encased in an insulating vacuum flask filled with ice and contains 50 cm^3 of alcohol.

At the base station, taps D and E are opened and the aspirator is squeezed until the alcohol rises in the tube C and fills it as well as the manometer. D is then closed. The liquid level in the exposed limb of the manometer B is the same as in the vessel A. The ice is

Scanned with CamScanner

then charged into the vacuum flask and 15 to 20 minutes allowed for the air in A to attain the temperature of ice. Tap E is now closed so that the air in the vessel A is maintained at 273.15 K temperature and at the atmospheric pressure of the base station. The instrument is now moved to the next station of measurement. If there is a change of atmospheric pressure, there will be a change in the liquid level in the exposed limb of the manometer. This difference in level can be measured by a suitable scale placed alongside the U tube. The level difference gives the difference in absolute pressure between the two stations since the change in liquid level in A is negligible. If the scale be graduated in millimetres and if alcohol be assumed to have a specific gravity of 0.8, a sensitivity of 7.8 Pa can be obtained. To have an accuracy of $\pm 5\%$ in the measurement, the minimum pressure difference to be measured should be 156 Pa.

As with aneroid barometers, here too corrections for altitude as well as variations in atmospheric pressure (as recorded by a control instrument at the base station) have to be applied for obtaining static-pressure differences.

8.7.3 Differential Pressure Survey by Gauge and Tube

The differential pressure between two points is measured by a suitable water gauge or manometer, the two limbs of which are connected by flexible tubes to the two points of observation. For measurement of static-pressure differences, the two ends of the tubes are usually held in manholes on the sides of the airway, where there is no air velocity. If there are no suitable manholes available, static tubes can be used. The static tube is so oriented that the nose exactly faces the air-current when the true static pressure is recorded. Pressure surveys with gauge and tube are more accurate than with aneroids or differential barometers and are to be adopted where more accurate pressure surveys covering less extensive areas are required.

For accuracy however, sufficiently thick-walled rubber hoses or polythene tubes at least 12mm in internal diameter are used so as to avoid kinks and collapse of walls. They also withstand rough use in mines and ensure a long leakproof life. They are also able to withstand their own weight when suspended in shafts without undergoing distortion. Joints should be as far apart as possible and should be mechanically strong and leakproof. Leakage can be checked by closing one end of the tube and blowing air into it while

it is placed under water. Choking of the tubes by kinking or by dirt and water should be avoided. The tube should be laid out in the airway sufficiently ahead of connecting to the gauge so that the air inside attains the ambient temperature.

The inclined manometer commonly used for the survey should be calibrated prior to the survey. Where the inclination of the gauge is variable, it should be properly set to the desired inclination. The instrument should be properly levelled. When a U-tube gauge is used better accuracy is obtained if the average of two readings is taken by interchanging the connection of the tubes to the two limbs of the manometer. As in the case of aneroid surveying, here also it is necessary to ensure constancy of fan speed during the survey. A check on the natural ventilating pressure is to be kept during the survey and corrections applied in case of appreciable variations in N.V.P. The pit should be idle during the survey in order to avoid changes in the system characteristics.

8.8 MANOMETERS

8.8.1 Vertical U-tube Manometer

The vertical U-tube manometer is commonly used for measuring pressures above 250 Pa. It consists of a glass tube of uniform bore bent in U shape. The upper limbs of the U tube are bent as shown in Fig. 8.23 for facilitating connection to flexible rubber tubes. The tube is normally of 6mm internal diameter. Tubes with smaller bores are liable to give erroneous reading owing to capillarity. The limbs are about 500mm long (the length of course depending on the range of pressure to be measured) and are about 20 mm apart.

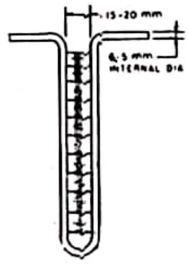

Fig. 8.23 U-tube manometer (diagrammatic).

A scale graduated in 1mm divisions is placed in between the two limbs. Vertical U tubes are usually filled with distilled water so that a sensitivity of 9.8 Pa can be obtained. Alternatively a least scale graduation of $10/g$ $(10/9.81=1.02$ mm) may be used when the manometer will have a sensitivity of 10 Pa. The U tube is usually mounted on a wooden board which is mounted vertically on a stand or suspended vertically.

A commercial type of vertical U-tube water gauge commonly used at fan drifts consists of two straight glass tubes mounted on a board and fitted into a brass reservoir at the lower end. A valve in the brass reservoir can be closed so as to steady the water meniscus where there are rapid fluctuations in pressure. A scale provided in between the tubes can be moved so as to have its zero coincide with the meniscus on the high-pressure limb in which case the pressure difference can be read directly on the scale.

8.8.2 Inclined-gauge Manometer

Owing to the limited sensitivity of a vertical U-tube water gauge, an inclined water gauge is preferred for accurate work. Here, the whole manometer along with the board on which it is mounted can be inclined at any angle commensurate with the degree of sensitivity desired. Usually, the inclined board is hinged to a horizontal board which can be levelled properly with the help of two spirit levels mounted on it with axes at right angles to each other. The inclination is usually fixed at 0.1 rad so that a magnification of ten times the reading on the vertical water gauge can be obtained. However, for reading pressures directly in pascals the inclination should be $1/g \simeq 0.102$ rad so that a least scale reading of 1mm gives a sensitivity of 1 Pa with water as the manometric fluid.

Inclined-gauge manometers can be filled with alcohol or paraffin instead of water in order to obtain a better sensitivity. Alcohol or paraffin has a lesser density (sp. gr.$=0.8$) than water so that an effective magnification of 12.5 times is obtained for a gauge inclined at at 0.1 rad. Besides, these liquids give a more clear meniscus. The least reading in such a gauge graduated in millimetres is ± 0.39 Pa by eye estimation (± 0.4 Pa with an inclination of 0.102 rad) and this manometer is thus about 15 to 20 times more sensitive than the high-grade aneroid. However, the density of paraffin may vary with temperature and hence the reading of the manometer may vary. This variation is normally negligible, but with large temperature

variations, it becomes important. In such a case the density of the manometer fluid, suitably corrected for the temperature of observation, should be taken for computation of the sensitivity of the manometer. Variation in temperature affects the scale graduation to a negligible extent, but it is essential for the scale to be graduated accurately.

8.8.3 Inclined-tube Manometer

This essentially consists of a U tube, one limb of which is a tube of uniform bore (6mm internal diameter) and inclined at a low angle with the horizontal while the other limb is a large reservoir whose cross-sectional area is 300 to 400 times that of the inclined tube so that any change in the level of the manometric fluid in the reservoir can be neglected in comparison with the change in fluid level in the inclined tube. In such a case, a scale placed along the inclined tube directly reads the pressure difference. For greater sensitivity, inclined-tube manometers can be filled with alcohol which also gives a better meniscus than water. Normally, in order to make the instrument suitable for use over a large range of pressure, arrangement is made for varying the inclination of the tube. For low-pressure measurements, a low value for the angle of inclination θ (see Fig. 8.24) is chosen, whereas for measurements in the high-pressure range, the value of θ is increased. The pressure measured by such a manometer is given by the equation

$$P \simeq L\rho' g \sin \theta \tag{8.22}$$

where P = pressure in Pa,
L = scale reading in mm,
ρ' = specific gravity of the manometer liquid
and θ = angle of inclination of the tube.

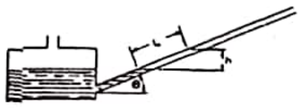

Fig. 8.24 Inclined-tube manometer (diagrammatic).

Inclined-tube manometers are very suitable for field use but are susceptible to errors due to lack of straightness of the tube or non-uniformity of bore ; so, it is desirable to get the instrument calibrated initially against a standard instrument.

8.8.4 Curved-tube Manometer

This (Fig. 8.25) was first designed by Hodgson particularly for reading velocity pressure. It is similar to an inclined-tube manometer, the tube of which is so curved (in the shape of a square parabola since $P_v \propto v^2$) as to give a uniform scale of velocity. Of course such manometers can be provided with pressure, velocity or even quantity scales.

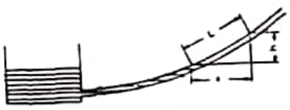

Fig. 8.25 Curved-tube manometer (diagrammatic).

However, it is difficult to shape the tube properly and the curved-tube manometer has to be calibrated initially against a standard instrument. Also, the velocity read from such a manometer is for a fixed air density (the calibration density ρ_a) and at another air density of, say, ρ'_a the velocity has to be multiplied by a factor equal to $\sqrt{(\rho_a/\rho'_a)}$ to get the correct velocity.

One advantage with the curved-tube manometer is that the angle of inclination of the curved tube increases at higher pressures so that the instrument can read a fairly large range of pressure. At the same time, the small inclination of the curved tube in the low-pressure range gives the instrument a high degree of sensitivity.

8.8.5 Two-liquid Differential Manometer

This type of manometer (Fig. 8.26) is a modified form of U tube where the two limbs contain two non-miscible and mutually insoluble liquids of nearly equal densities. A differential manometer with concentric limbs has an advantage over the other U-tube manometers that it avoids possible zero error due to tilt of the instrument. Usually the inner vessel contains the lighter liquid and the amount of liquid in the two vessels is so adjusted that the meniscus at the junction of the two liquids lies at the upper end of the stem when there is no pressure difference. When taking pressure measurements, the inner vessel is connected to the high-pressure side and the outer vessel to the low-pressure side so that the meniscus moves down the stem.

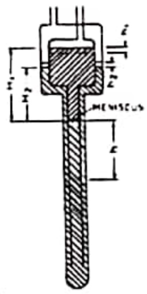

Fig. 8.26 Two-liquid differential manometer (diagrammatic).

Now let us consider a case when the meniscus moves through h and the levels of the liquids in the inner and the outer vessels through h_1 and h_2 respectively. For balance of pressure in the beginning,

$$H_1 \rho_1 = H_2 \rho_2 \tag{8.34}$$

where ρ_1 and ρ_2 are the densities of the liquids in the inner and the outer vessels respectively.

When a differential pressure P is applied to the manometer so that the meniscus moves through h, we have, for equilibrium,

$$P+(h+H_1-h_1)\rho_1=(h+H_2+h_2)\rho_2 \tag{8.35}$$

Again, since the volume of liquid displaced in the reservoirs as well as the tubes remains constant,

$$A_1 h_1 = A_2 h_2 = ah \tag{8.36}$$

where A_1, A_2 and a are the cross-sectional areas of the inner vessel, the annulus between the inner and the outer vessel and the inner tube respectively.

From equation 8.36, we get

$$h_1 = ah/A_1 \tag{8.37}$$

and

$$h_2 = ah/A_2 \tag{8.38}$$

Substituting these values in equation 8.35, we have

$$P = h\rho_2 + H_2\rho_2 + \frac{ah\rho_2}{A_2} - h\rho_1 - H_1\rho_1 + \frac{ah\rho_1}{A_1}$$

$$= h\left\{(\rho_2 - \rho_1) + a\left(\frac{\rho_2}{A_2} + \frac{\rho_1}{A_1}\right)\right\} \tag{8.39}$$

since $H_1\,\rho_1 = H_2\,\rho_2$.

For the same value of P, the lesser the difference between ρ_1 and ρ_2, the greater will be the value of h or, in other words, the sensitivity of the instrument increases with decrease in the difference between ρ_1 and ρ_2. However, in practice there is a limit to the extent to which the densities of the two liquids can be brought together, since too close densities produce a weak meniscus which breaks up easily and also, too high a sensitivity reduces the range of the gauge considerably. Sensitivity of the order of 1 Pa is a suitable standard and the densities of the liquids should be so chosen as to give this sensitivity.

The liquids used in the differential manometer should have low and approximately equal coefficients of thermal expansion and should not be volatile. Besides, they should be non-miscible and mutually insoluble. Ower[72] used benzyl alcohol stained with aniline black in the inner vessel and an aqueous solution of calcium chloride of specific gravity=1.048 in the outer vessel in order to get a magnification of 10 or a sensitivity of 0.98 Pa (0.1mm w.g.) with a least scale graduation of 1mm. The sensitivity can be changed by varying the specific gravity of the calcium chloride solution.

Ower suggests the following dimensions for differential manometers, the length of course depending on the range of pressure difference to be measured :

Diameter of the outer vessel	77.5mm
Diameter of the inner vessel	62.5mm
Diameter of the outer tube	12.5mm
Diameter of the inner tube	5.0mm

The instrument, like other manometers so far described, should be calibrated against a standard instrument, but large differences of temperature can introduce appreciable error in the readings of pressure difference, in which case it is advisable to calibrate the instrument at different temperatures.

For greater sensitivity and accuracy of work, micromanometers should be used.

8.8.6 Tilting Micromanometer

This is essentially a U tube having two glass vessels A and A connected by a long glass tube B (Fig. 8.27). The glass structure is mounted on a metal frame C which, in turn, is supported over the base frame D on three levelling screws. Two of the levelling screws E are on either side of the vessel A. They are in line with the vessel A and are so disposed that the line joining their centres is perpendicular to the axis of the tube B. C is held tight to D by means of spring F. The inclination of the tube B can be varied by rotating the third levelling screw G which is provided with a micrometer for recording the amount of tilt given to the tube. The two vessels are filled with a suitable manometric liquid, usually water, so that the level of liquid in the measuring vessel A′ coincides with a fixed mark. When a differential pressure is applied to the manometer, the water level in A′ changes, but it is brought back to the fixed index by turning the micrometer screw G, the coincidence being observed with the help of a microscope.

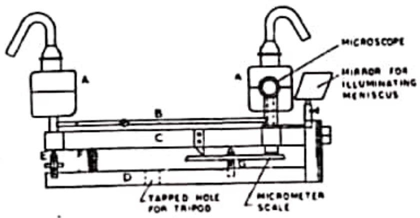

Fig. 8.27 Tilting micromanometer (diagrammatic).

The differential pressure P is then given by the relation

$$P = nt\,\frac{l_1}{l_2}\,\rho' g \quad \text{Pa} \tag{8.40}$$

Scanned with CamScanner

where n = number of turns through which the micrometer moves,
t = pitch of the micrometer screw in mm,
l_1 = distance between the centres of the vessels in mm,
l_2 = perpendicular distance between the micrometer screw and the line joining the other two levelling screws in mm
and ρ' = specific gravity of the manometric fluid.

When water is used as the manometric fluid, equation 8.40 becomes

$$P = nt\frac{l_1}{l_2}g \quad \text{Pa} \tag{8.41}$$

The usual values of l_1, l_2 and t for standard instruments are 330mm, 254mm and 1.25mm respectively and the maximum number of turns allowed for the travel of the micrometer screw is 20, giving the instrument a range of about 320 Pa. With a magnification of 20 to 30 of the microscope, the instrument is sensitive to a pressure of less than 0.25 Pa. For an increased range of pressure, it is preferable to double the length l_1 rather than to have a larger travel of the micrometer screw. However, for pressures higher than the range provided for in the instrument, an ordinary U-tube manometer can be used.

The tilting micromanometer is a standard instrument and needs no calibration, provided that the values of l_1, l_2 and t are accurately determined for the instrument.

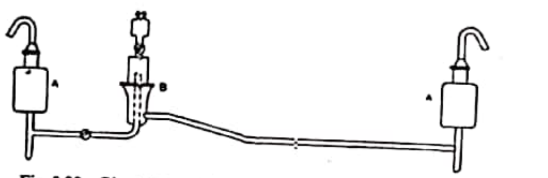

Fig. 8.28 Glass work of Chattock tilting micromanometer.

Chattock modified the glass work of the above manometer as shown in Fig. 8.28 in order to get a much higher sensitivity but at the expense of ease of manipulation and rapidity of working. Here the two vessels A and A′ are connected to a central vessel B as shown in the figure. The two vessels A and A′ as well as the lower part of the vessel B are filled with distilled water whereas the upper part of B is filled with liquid paraffin so that the surface of separation

between water and paraffin appears in the form of a bubble at the top of the central tube in the vessel B. The bubble is suitably illuminated from behind and its position observed through a microscope. When a small difference of pressure is applied to the micromanometer, the bubble tends to increase or decrease in size and is brought back to the original by turning the micrometer screw.

Such an instrument with a value of l_1=330mm has a sensitivity of the order of 0.025 Pa. However, these have a small range and with fluctuating pressures, the bubble often tends to break up thus necessitating resetting of the zero position. Besides, temperature changes affect the zero setting.

Micromanometers of larger ranges have been designed by manufacturers. *Askania minimeter* and *Casella micromanometer* are of this type and have a sensitivity of 0.098 Pa (0.01mm w.g.).

8.8.7 Askania Minimeter

This instrument contains two intercommunicating containers filled with distilled water (Fig. 8.29). Container F is the observation

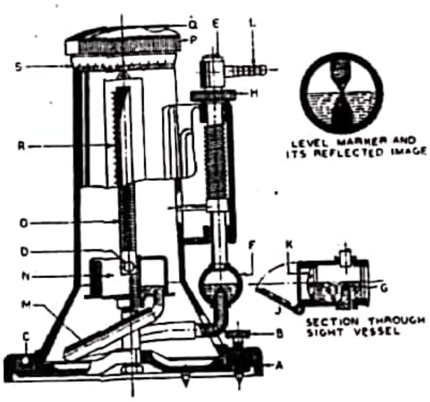

Fig. 8.29 Askania minimeter : A—Housing, B—Levelling screws, C—Spirit level, D—External pressure connection (—), E—Filler screw, F—Sight vessel, G—Level marker, H—Sight vessel adjustment screw, J—Hinged mirror, K—Lens, L—External pressure connection (+), M—Connecting tube, N—Balance vessel, O—Screwed spindle, P—Knurled ring for adjusting balance vessel, Q—Press button, R—Coarse scale, S—Fine scale.

Scanned with CamScanner

vessel and N is the balancing vessel. L is the nipple for connecting to the high-pressure side and D, to the low-pressure side. Vessel N can be raised or lowered by operating the knurled ring P, the amount of movement being noted on the scale R graduated in millimetres and the micrometer scale S having a least count of 0.01 mm.

At the outset, the central point of nipple D is brought to the zero of the scale R by the turning of the knurled ring P. Cock E is opened and vessel F is filled with water till the pointer G just touches the water level. E is then closed. The pointer is brought to touch the water level exactly by an adjustment of the milled head H, the exact coincidence being observed through the lens K.

The two nipples are then connected to the pressure lines when the level of water in F falls and that in N rises. Now the vessel N is raised by turning the knurled ring P until the water level in F again touches the tip of the pointer G (null point). The readings on the scale R and the micrometer S then give the pressure in mm w.g.

More sensitive manometers have been designed, but they are confined to the laboratory because of their delicacy of construction and manipulation.

One such instrument designed by Hodgson is an inclined-tube manometer, the liquid level in the reservoir of which can be altered by a plunger which is actuated by a micrometer screw. The liquid meniscus in the inclined tube is maintained at a fixed mark with the help of a microscope with a magnification of 60. The sensitivity of the instrument depends on the relative diameter of the plunger with respect to that of the reservoir, a higher sensitivity being obtained with a relatively smaller plunger diameter. The instrument is claimed to have a sensitivity of 0.0025 Pa.

Another very sensitive manometer designed by Ower is essentially a Chattock manometer, the central vessel of which is replaced by a capillary tube. The instrument is filled with xylol and an air bubble is introduced into the capillary tube, the position of the air bubble being observed through a microscope. Any change of pressure makes the air bubble travel along the capillary tube. The bubble is then brought back to the original position by adjusting the micrometer screw. The instrument is claimed to have a sensitivity of 0.0012 Pa.

8.8.8 Recording Pressure Gauges

It is necessary to maintain a record of the fan pressure which is

generally read by the fan-drift water gauge. Many recording pressure gauges are available which give a continuous record of the fan pressure on a chart. The pressure gauges may be of the water-filled U-tube manometer type, diaphragm or bellow type, ring balance type or bell type.

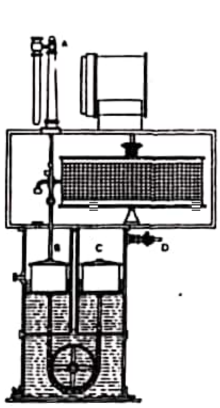

Fig. 8.30 Ochwadt automatic recording water gauge.

The U-tube manometer type has large-diameter limbs carrying floats which get displaced by change of liquid level in the limbs. The Ochwadt automatic indicating water gauge shown in Fig. 8.30 is of this type. The instrument consists of a U tube having two large-diameter limbs connected by a chamber at the bottom end. In the two limbs there are two floats connected to each other by a chain moving on a sprocket below them. One of the limbs, B is connected to the atmosphere through the drum box and the outlet A, the other C being connected to the fan drift through the nipple D. The float in the limb B carries a stylus which moves on a drum rotating at the rate of one revolution per week by a clock-work thus recording the variation in the fan-drift water gauge.

Diaphragm- or bellow-type pressure gauges usually magnify the deflection or displacement in the diaphragm produced by a differential pressure on either side of it by mechanical means and record it on a pen corder. The displacement can be converted to an electrical

Scanned with CamScanner

signal by a suitable transducer which can then be recorded. Electrical transducers help in remote recording of pressure. While the lowest range of pressure measured by bellow-type gauges is 0-1300 Pa, the lowest range with diaphragm type of gauges is 0-50 Pa. Bell-type pressure gauges comprise a bell inverted in a chamber with its lower end sealed by a liquid. The inside of the bell is connected to the high-pressure side while the chamber is connected to the low-pressure side. This causes an upward displacement of the bell which can be recorded mechanically or electrically. The bell-type pressure gauges can record small ranges of pressure.

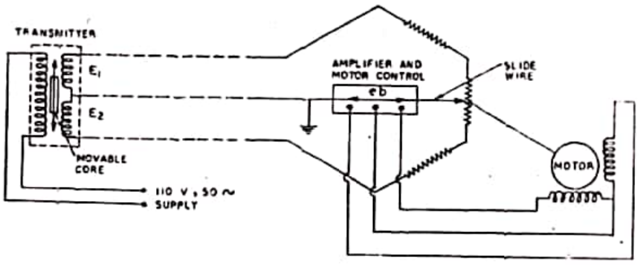

Fig. 8.31 Differential transformer measuring circuit.

Electrical pressure transducers are usually of the differential-transformer type illustrated in Fig. 8.31. The displacement produced in the pressure gauge shifts a movable core in a transformer comprising a single primary coil and two secondary coils E_1 and E_2 connected to a ratio bridge circuit. The position of the movable core determines the relative magnetic flux linkage of the two secondary coils which produces an unbalanced voltage eb. This is amplified and applied to a motor control unit which operates the balancing motor to position the sliding wire so as to rebalance the bridge. A cam and linkage system operated by the slide wire being driven by the balancing motor drives a recording pen or indicator pointer.

Example 8.5

An inclined-tube manometer has the vessel of 60mm internal diameter and the tube of 3mm internal diameter. The tube is graduated in millimetres and has an inclination of 0.1 rad. What is re

the sensitivity of the manometer if it is filled with a liquid of specific gravity equal to 0.82? What is the error in the reading of this instrument due to the change in level of manometric liquid in the vessel ?

The sensitivity of the manometer $= 0.82 \times \sin 0.1 \times 9.8$
$= 0.8023$ Pa,
taking $g = 9.8$ m s^{-2}.

Let a movement of the meniscus in the tube through 1mm cause a change in the liquid level in the vessel equal to l.

Then, $l = (3)^2/(60)^2 = 0.0025$mm.

The error is thus 0.0025mm in a reading of $1 \times \sin 0.1 = 0.1$mm of liquid column.

Or, the error $= 0.0025 \times 100/0.1 = 2.5\%$.

EXERCISE 8

8.1 An anemometer calibrated in the laboratory at 101.33 kPa barometric pressure and 303 K d.b./293 K w.b. temperatures reads a velocity of 216 m min^{-1} at the centre of a 600mm diameter duct installed underground where the barometric pressure is 107 kPa and the dry-and wet-bulb temperatures are 307 K/304.5 K. Calculate the correct average velocity of flow in the duct assuming a method factor of 0.85.

8.2 Calculate the rate of flow in a 400mm diameter duct fitted with a standard orifice of 300mm diameter, if the pressure drop across the orifice is 150 Pa. Assume air density to be equal to 1.2 kg m^{-3} and a discharge coefficient of 0.6. What will a manometer connected to a pitot-static tube placed centrally in the duct read, if the ratio of the average to central velocity in the duct is 0.84.

8.3 An aneroid barometer is taken from a point A in the intake to a point B in the return of a district situated at an elevation of 40m above A. Calculate the change in the reading of the aneroid if the air velocity at A is 2 m s^{-1} and at B, 3 m s^{-1} and there is a pressure drop of 200 Pa in the district. Assume there to be no change in the atmospheric pressure and neglect the effect of temperature on the reading of the aneroid.

Scanned with CamScanner

8.4 An inclined-tube manometer having a vessel of 100mm diameter and a tube of 6mm internal diameter inclined at 0.175 rad to the horizontal has a scale graduated in millimeters. The meniscus moves through 146mm on the application of a pressure source to the manometer. Calculate the pressure. What is the error in the reading due to the change in the water level in the vessel being neglected ?

8.5 An inclined-gauge manometer is filled with a manometric fluid having a specific gravity of 0.8 and is provided with a scale graduated in millimetres. What should be its inclination, so that each mm division reads 1 pascal ?

CHAPTER IX

VENTILATION PLANNING

9.1 OBJECTIVE

The primary objective of ventilation planning is to ensure adequate ventilation for safety, health and efficiency of workers in various parts of the mine at maximum possible economy. The ventilation system to be chosen depends on the method of development and working of the mine, particularly the number, size and position of openings and the way they are connected to the workings. It does not, however, mean that ventilation planning should always accommodate to a working plan of the mine determined from other considerations. On the other hand, it should form an integral part of the working plan and may so modify it as to result in an overall economy. For example, the production in a mine, the nature of the mineral mined or the environmental conditions may demand a quantity of ventilation that would call for larger or more number of openings than necessary for raising the mineral alone. Sometimes, requirements of adequate ventilation may substantially influence the choice of a mining method, as for example, longwall method may have to be preferred to board-and-pillar method in order to ensure a higher volumetric efficiency of ventilation in highly gassy pits with large productions. Indeed reorganization of the ventilation system in existing mines to suit modified production programmes often meets with greater difficulties and cost than if the system were designed for the production programme in the first place.

Ventilation plans should, therefore, be drawn up for various stages of the working of the mine integrated with the production plans. If there are major discreet changes in the development and production programme in the life of a mine, the ventilation plans should conform to these. Otherwise they can be drawn up at 5-year intervals over a period of 15-20 years. Planning over a longer period becomes futile since production programmes beyond this period are generally tentative and subject to major changes. Besides, fans do not generally have a life of efficient operation beyond this period because of corrosion, wear etc. apart from the fact that no single

Scanned with CamScanner

8.4 An inclined-tube manometer having a vessel of 100mm diameter and a tube of 6mm internal diameter inclined at 0.175 rad to the horizontal has a scale graduated in millimeters. The meniscus moves through 146mm on the application of a pressure source to the manometer. Calculate the pressure. What is the error in the reading due to the change in the water level in the vessel being neglected ?

8.5 An inclined-gauge manometer is filled with a manometric fluid having a specific gravity of 0.8 and is provided with a scale graduated in millimetres. What should be its inclination, so that each mm division reads 1 pascal ?

CHAPTER IX

VENTILATION PLANNING

9.1 OBJECTIVE

The primary objective of ventilation planning is to ensure adequate ventilation for safety, health and efficiency of workers in various parts of the mine at maximum possible economy. The ventilation system to be chosen depends on the method of development and working of the mine, particularly the number, size and position of openings and the way they are connected to the workings. It does not, however, mean that ventilation planning should always accommodate to a working plan of the mine determined from other considerations. On the other hand, it should form an integral part of the working plan and may so modify it as to result in an overall economy. For example, the production in a mine, the nature of the mineral mined or the environmental conditions may demand a quantity of ventilation that would call for larger or more number of openings than necessary for raising the mineral alone. Sometimes, requirements of adequate ventilation may substantially influence the choice of a mining method, as for example, longwall method may have to be preferred to board-and-pillar method in order to ensure a higher volumetric efficiency of ventilation in highly gassy pits with large productions. Indeed reorganization of the ventilation system in existing mines to suit modified production programmes often meets with greater difficulties and cost than if the system were designed for the production programme in the first place.

Ventilation plans should, therefore, be drawn up for various stages of the working of the mine integrated with the production plans. If there are major discreet changes in the development and production programme in the life of a mine, the ventilation plans should conform to these. Otherwise they can be drawn up at 5-year intervals over a period of 15-20 years. Planning over a longer period becomes futile since production programmes beyond this period are generally tentative and subject to major changes. Besides, fans do not generally have a life of efficient operation beyond this period because of corrosion, wear etc. apart from the fact that no single

Scanned with CamScanner

fan can generally cover the range of mine characteristics beyond this period with reasonable efficiency.

9.2 STEPS IN VENTILATION PLANNING

The various steps involved in ventilation planning are

1. Selection of ventilation norms for different parts of the mine in accordance with production, number of men employed, permissible concentration of noxious and explosive gases and respirable dust, permissible air velocities and environmental conditions such as dry and wet-bulb temperatures. Statutory norms should always be satisfied.
2. Calculation of the air requirement in various parts of the mine on the basis of selected norms.
3. Estimation of the extent of conditioning of air necessary, if any, in any part or whole of the mine to satisfy the environmental norms.
4. Selection of feasible ventilation systems.
5. Working out detailed air distribution and control arrangements for each system.
6. Estimation of the leakage at various parts, total quantity requirement and volumetric efficiency for each system.
7. Calculation of the aerodynamic resistance of various branches and circuits of each system.
8. Solution of the ventilation network for each system.
9. Estimation of the pressure requirement and drawing of the mine characteristic for each system.
10. Repetition of the above steps for different periods in the life of the mine.
11. Selection of fan or fans (inclusive of boosters, if any) to suit the varying mine characteristics taking due consideration of N.V.P. and evasee head recovery.
12. Estimation of the total cost of ventilation for each system.
13. Selection of the most economic ventilation system for the various stages of planning.
14. Working out the schedule of implementation of the ventilation plan.

9.3 DESIRABLE FEATURES OF A VENTILATION SYSTEM

The selection of a ventilation system has to be done carefully in order to ensure safety, reliability and economy. It should be flexible

enough to meet emergencies and future requirements. The following desirable features should be borne in mind in selecting a ventilation system

1. Openings used for travelling of men should as far as possible be intakes. Routes of egress of men in times of emergency such as fires and explosions underground should always be in the intake.

2. The overall resistance of the mine should be kept to a minimum for economy of ventilation. To this end all surface openings should, as far as possible, be utilized in the ventilation system. Similarly multiple airways where available, should be used for main intakes and returns subject of course to restrictions of air velocity.

3. Fresh air should be directly coursed to active workings through the shortest possible route. This not only reduces the resistance of the flow path but also minimizes the addition of heat and pollutants to the air reaching the face.

For the same reason splitting of air-current should be done as close to the surface as possible.

4. Hot gassy and dusty places should always be ventilated by separate splits. As far as possible, individual stopes, panels or districts should be ventilated by separate splits, particularly in gassy coal mines. Separate splits should also be provided for development and extraction areas in such mines.

Inactive sections in a gassy mine need ventilation, if not sealed off, though they may be ventilated by return air from active sections.

5. Leakage of air should be minimized and recirculation avoided. Leakage reduces the volumetric efficiency of ventilation and consequently increases the cost of ventilation. Recirculation is a hazard to safety and health of workers.

Minimization of leakage requires minimum use of ventilation control devices such as stoppings, doors, air crossings etc. Doors should always be avoided on active roadways. Coursing of air through roadways in broken ground can lead to substantial leakage, and should hence be avoided as far as practicable.

Injudicious positioning of booster fans underground is a major source of recirculation. That is why selection and use of booster fans underground should be given careful consideration.

6. Air should be circulated from active zones to caved ground rather than the reverse, which is unhealthy and can be extremely dangerous in gassy coal mines.

Scanned with CamScanner

In gassy coal mines in the U.S.A. (mainly worked by room-and-pillar method) it is often preferable to use controlled ventilation of goaf through bleeders in order to prevent methane getting into the workings, but this needs large quatities of air to be circulated particularly in extensive mines and leads to high cost of ventilation. Yet caved goaves, if not adequately ventilated should be suitably sealed in order to prevent spontaneous heating, particularly in fiery coal mines, where it is desirable to keep the ventilation pressure low for minimizing leakage.

7. Use of regulators should be minimized for effecting economy of ventilation as ventilation control by regulators results in wastage of power. The splits should therefore be so chosen as to have resistances in inverse proportion of the square of flow in them as far as possible.

8. Highly tortuous, constricted and obstructed airways should be avoided in good ventilation systems.

9. *Ascensional ventilation* (where fresh air is taken down to the bottom-most faces of a working district and is allowed to travel up the dip along the faces picking up heat from the freshly exposed rock at the faces) should, as far as practicable, be adopted as it leads to the development of N.V.P. that aids the fan pressure. *Descensional ventilation*[117] has been claimed to reduce the amount of heat added to the air in the workings, besides making the workings less dusty because of the air and mineral travelling in the same direction (*homotropal ventilation*). The advantages, however, are nominal in most cases.

In Russian coal mines[8], ascensional ventilation is adopted in all seams with dip exceeding 0.175 rad (10°), but with downward movement of air, its velocity should not be less than 1 m s^{-1} and the methane content, not more than 0.5%. For faces shorter than 50m, the angle of dip is immaterial.

10. Major airways such as intake and return shafts (including inclines) or adits as well as main intake and return roadways in the mine should be of adequate size (see Chapter IV for economic design of mine airways) and so designed and maintained as to satisfactorily serve the ventilation system throughout the life of the mine.

In relatively shallow metalliferous mines in steep lodes return air is often conducted to exhaust fans located on shallow ventilation shafts (usually driven down to the first level) through worked-out open stopes. Though such stopes in strong ground and at shallow depth provide excellent opening of almost negligible resistance for conducting return air, they are liable to closure by caving of hanging wall with time, particularly at greater depth when they can offer substantially high resistance. In such cases separate return shafts have to be provided. Alternatively one or more return airways of adequate size can be suitably supported and maintained through the worked-out stopes. Maintenance of such return airways is easy in filled stopes, but in open stopes, they have to be supported with suitable pack walls on either side.

The above practice however, should never be adopted in coal mines.

11. As will be seen later, method of mining has a profound effect on the ventilation system. Even with any method of mining certain measures like suitable distribution of working faces so as to have well balanced splits, minimum use of control devices etc. should always be considered for an efficient ventilation system. Stoping on the retreat often avoids contaminated air from the lower levels passing through the upper level stopes [see Fig. 9.1(b)].

An exhaust fan placed on the top of a ventilation shaft is the best for maintaining operating openings as intakes. (For a more detailed discussion of the location of main mine fans the reader is referred to Chapter VI.) Haulages are more conveniently placed in intakes as the intake air is less corrosive to equipment and operation in humid, dusty and foggy return airways becomes more difficult and hazardous. Electric haulages should not be used in the return in gassy coal mines. The only objection to the use of haulages in the intake is that the intake air may be contaminated by dust dispersed in the haulage road, a feature not negligible with fast haulages. But this can be obviated by the adoption of suitable dust control measures on the haulage road.

9.4 TYPES OF VENTILATION SYSTEM

Depending on the relative position of intake and return airways, ventilation systems in mines can be broadly divided into the following:

(a) Boundary or unidirectional
(b) Central or bidirectional
(c) Combined.

Scanned with CamScanner

9.4.1 Boundary Ventilation System

The boundary ventilation system where the air flows unidirectionally from the intake to the return through the workings is by far the most efficient system necessitating the least use of ventilation control devices and thus resulting in a high volumetric efficiency of ventilation (70-80%). It is commonly adopted in metal mines working steep lodes. In the simplest form, the intake and return shafts are located at the two strike boundaries of the mine as shown in Fig. 9.1 (b). But this is limited to mines having a small lateral extent only. Sometimes at shallow levels of a developing mine having a relatively large lateral extent, small fans may be installed on top of winzes as shown in Fig. 9.1 (a). When air requirement varies widely from level to level, each level may be ventilated by an independent underground fan as shown in Fig. 9.1 (c).

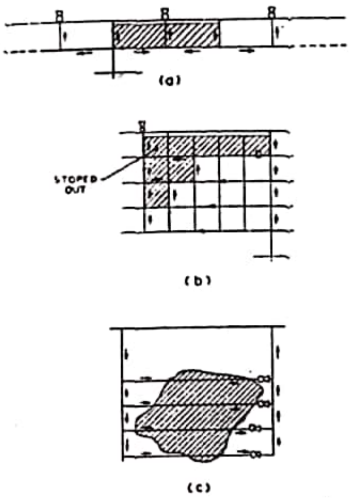

Fig. 9.1 (a), (b) & (c) Boundary ventilation systems in workings of steep ore bodies.

With larger lateral extent, it is preferable to have a central intake shaft with two return shafts or winzes at either boundary of the pro-

perty fitted with two exhaust fans [Fig. 9.1(d)]. Sometimes a single forcing fan may be used on the top of the intake shaft [Fig. 9.1(e)], but this necessitates air-lock on a hoisting shaft which is not very desirable. When the mine is extensive on the strike, it may be divided into several lateral sections with separate fans as shown in Fig. 9.1 (f).

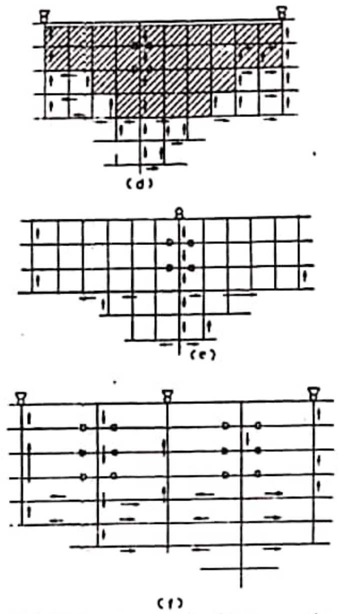

Fig. 9.1 (d), (e) & (f) Boundary ventilation systems in workings of steep ore bodies.

Mines having workings in multiple parallel lodes are generally ventilated by separate exhaust fans installed on each lode, though there may be a common intake [Fig. 9.1 (g)]. A less desirable alternative with a single forcing fan in shown in Fig. 9.1 (h).

In metal mines involving hard rock excavation it is often uneconomical to drive two parallel levels so that one can act as an intake and the other as a return. The return air from lower level stopes

Scanned with CamScanner

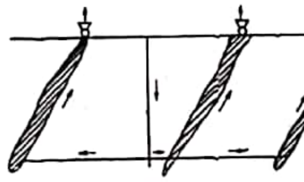

(g)

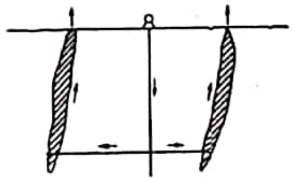

(h)

Fig. 9.1 (g) & (h) Boundary ventilation system in working of steep ore bodies.

therefore mixes with the intake into the upper-level stopes leading to a certain amount of contamination. This can be avoided if the stopes on a level are worked on the retreat [Fig. 9.1 (b)], but this is not generally adhered to. Where, absolutely necessary, return air from lower-level stopes can be taken across upper levels through sidecasts which may comprise one or two large-diameter tubes in the simplest form.

Air distribution through different stopes in a level is generally uncontrolled, though a certain amount of regulation can be achieved by closing raises and chute openings to different extents.

In mines working flat deposits, like coal mines, boundary ventilation is rarer, though the present trend in extensive mines involving large quantities of ventilation is to adopt boundary ventilation system for higher volumetric efficiency which more than compensates the extra cost of the ventilation shafts. Fig. 9.2 (a) illustrates such a system with two fan shafts at the two rise boundaries. Intake is through a pair of shafts located more to the dip side at the centre of the property. During development, one of these shafts acts as an intake and the other as a return, but later both are used as intakes. In more flat deposits, a pair of intake shafts may be located at the centre of the property with four return shafts at the four corners.

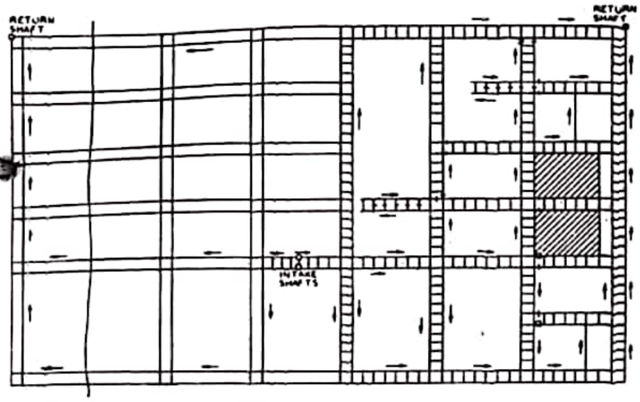

Fig. 9.2 (a) Boundary ventilation system in working of flat mineral deposits.

Advantages of Boundary Ventilation System

1. The boundary ventilation system necessitates the minimum use of ventilation control devices. This apart from saving the capital invested on them as well as the cost of their operation and maintenance, reduces leakage and results in a high volumetric efficiency.

2. Different sections of the mine can be independently ventilated by separate fans. This reduces the total flow handled by a single fan and hence its head requirement. Lower head results in less leakage. Airways of smaller cross-section can handle the flow. Ventilation of each individual section can be independently controlled and a section can be isolated easily in times of emergency.

3. There is greater safety because of larger number of outlets to the surface.

4. Since developments have to be extended to the boundary right in the beginning in this system, the mine characteristic remains almost constant throughout the life of the mine thus resulting in a uniformly efficient operation of the fan. On the other hand, the mine resistance goes on changing with the workings progressing towards the boundary of the property in the central system of ventilation where the fan has to negotiate a wider variation of mine characteristics.

Scanned with CamScanner

Disadvantages of the Boundary Ventilation System

1. Reversal of air-flow is more complex.
2. Separate fan installations increase the cost of their operation, supervision and maintenance.

9.4.2 Central or Bidirectional Ventilation System

This system is commonly adopted in in-the-seam coal mines where both the intake and return shafts are located close by at the centre of the property. Intake and return air from any district travel in opposite directions through parallel roadways usually separated by stoppings erected in the cross-connections between them. Also return air from a district has to cross the intake in order to join the main return. Obviously the central system of ventilation (Fig. 9.2(b)) allows a substantial leakage because of the large number of stoppings and air-crossings used so that volumetric efficiency is only 40-50% with this system.

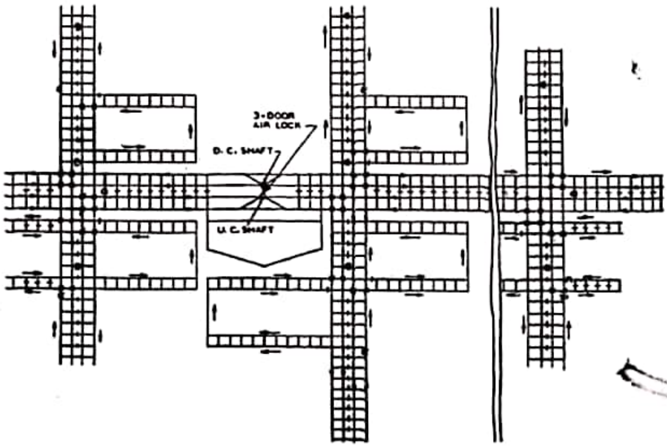

Fig. 9.2(b) Central ventilation system.

However, it has the following advantages :

1. The deposit can be worked after short development leading to a quicker start of production.

2. Long development headings are not necessary and hence there is no associated problem of their ventilation.
3. Sinking of deep pits close together economizes the cost of sinking as certain common facilities can be shared by the pits. On the other hand, boundary pits which are far off necessitate building of roads, extension of power lines etc. to the sinking site involving extra cost.
4. Central pits cause less loss of mineral in shaft pillars.
5. Both the central shafts can be used for hoisting, but boundary shafts are rarely used for hoisting as this would require extension of surface transport to these pits. They however serve well as stowing pits (with hydraulic stowing pipes installed in them) if located on the rise side.

9.4.3 Combined System

Fig. 9.2(c) illustrates a combined system where the main ventilation system as also that for ventilation of development headings is bidirectional in nature while the ventilation of the extraction panels is unidirectional through goaf connected to the return airways called bleeders. Connection of the goaf to the bleeders is generally regulated near the face where the goaf has not consolidated and is likely to lead to shortcircuiting of the air through that part of the goaf.

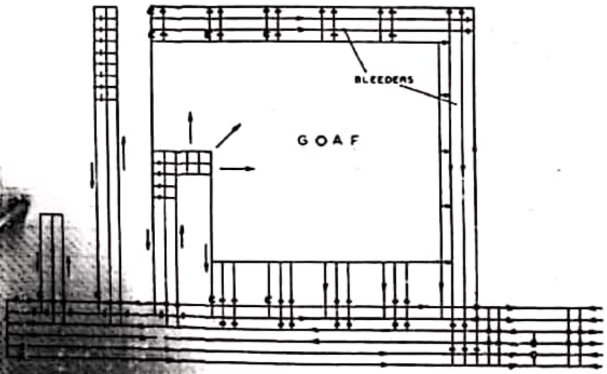

Fig. 9.2(c) Combined ventil tion system.

9.5 AIR DISTRIBUTION WITH DIFFERENT MINING METHODS

Air distribution to the faces depends primarily on the method of mining. Flat coal beds in India today are largely worked by the bord-and-pillar method though the longwall method is getting more popular. Metalliferous mines are worked by a variety of methods, the prevalent ones being shrinkage, sub-level, breast and cut-and-fill stoping.

9.5.1 Bord-and-Pillar Method

There are a large number of openings in a working district in this method. As a result, the air has to be guided to the working faces by means of numerous control devices such as stoppings (both permanent and temporary), doors, air-crossings etc. Air is coursed through the different faces in a working panel with the help of line brattices at the face and temporary stoppings generally made of brattice curtains in the galleries as illustrated in Fig. 9.3. However, this results in a substantial leakage through the brattices leading to poor face air velocity. Panels separated by solid coal barriers (see Fig. 9.3) reduce the number of permanent stoppings and to that extent reduce leakage.

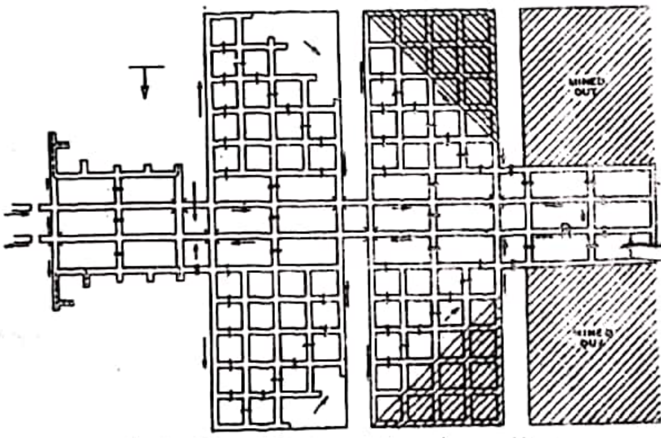

Fig. 9.3 Air distribution in bord-and-pillar workings.

9.5.2 Longwall Method

Ventilation of longwall faces is easier needing less control. Each face is normally ventilated by a separate split. Leakage is much less in the working district as compared to bord-and-pillar mining. Longwall workings with hydraulic stowing admit practically no leakage through the goaf, but there is a fair amount of leakage across the goaf in longwall caving districts, particularly with advancing faces.

With single-unit dip-rise longwall faces, the lower gate forms the intake and the upper gate, the return [Fig. 9.4(a)], but with

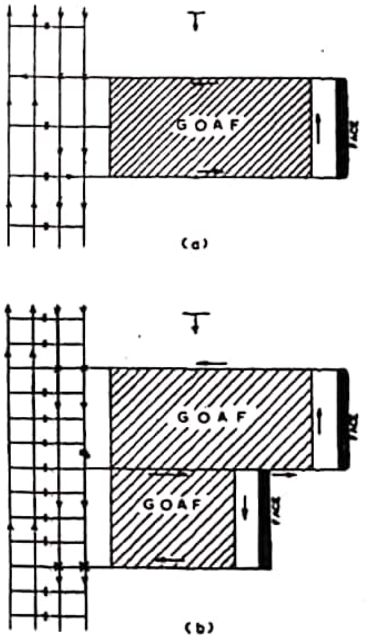

Fig. 9.4 Air distribution in longwall workings : (a) single-unit face, (b) double-unit face.

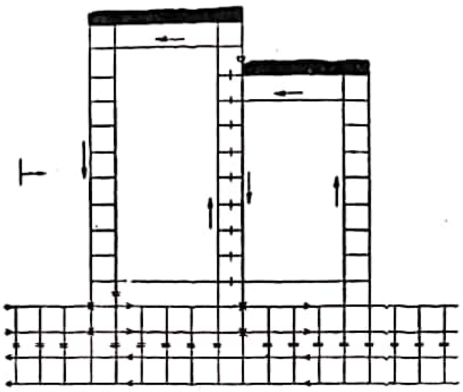

Fig. 9.4(c) Ascentional ventilation of both the units of a double-unit longwall face.

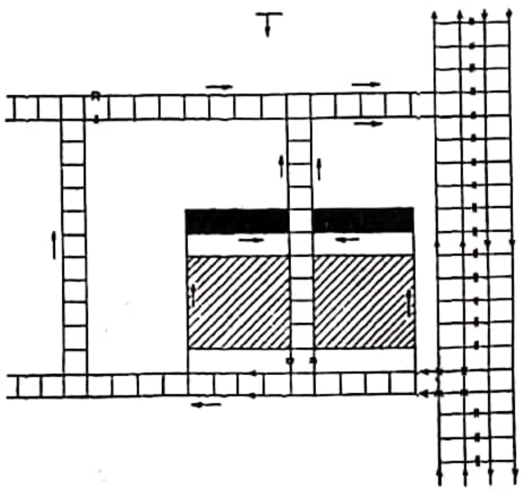

Fig. 9.4(d) Air distribution at a double-unit strike longwall face.

double-unit faces, the central gate usually forms the common intake with the lower unit ventilated descensionally. [Fig. 9.4(b)]. However, where twin gate roads are driven, both the units can have ascensional ventilation as shown in Fig. 9.4(c). Fig. 9.4(d) shows the ventilation system for a double-unit strike longwall face.

9.5.3 Shrinkage and Cut-and-Fill Stopes

Face ventilation is simple in shrinkage and cut-and-fill stopes. Air enters the face from the lower level along manways maintained at the two ends of the stope and leaves through the central raise to join the upper level (see Fig. 9.5). Owing to the restricted cross-section of the opening at the face, there is usually good face air velocity. Ventilation in filled square-set stopes is similar to that in cut-and-fill stoping.

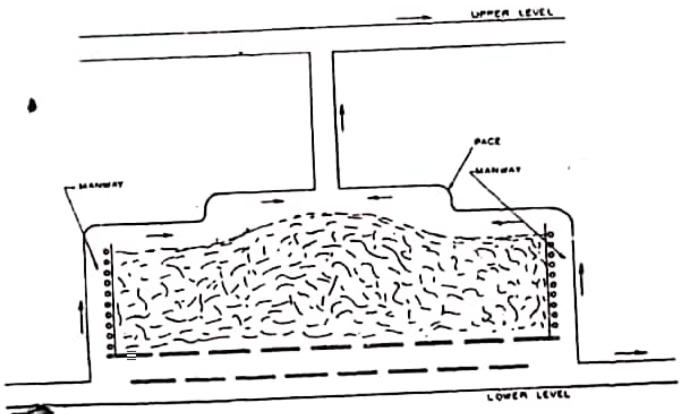

Fig. 9.5 Air distribution in a shrinkage stope.

9.5.4 Open Overhand and Underhand Stopes

Ventilation in open overhand and underhand stopes is poor compared to shrinkage stopes. Fig. 9.6 illustrates the ventilation of an open overhand stope where the air enters the stope at several points (each chute opening allowing air entry) from the lower level

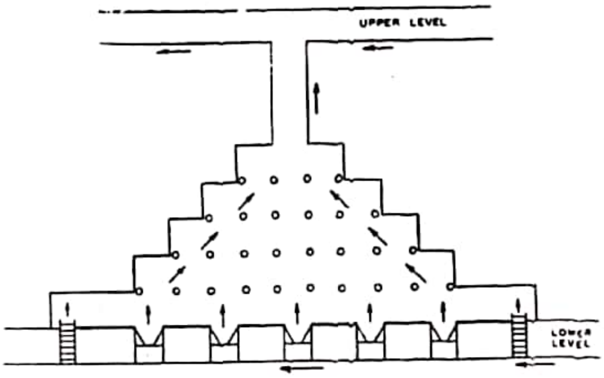

Fig. 9.6 Air distribution in an open overhand stope.

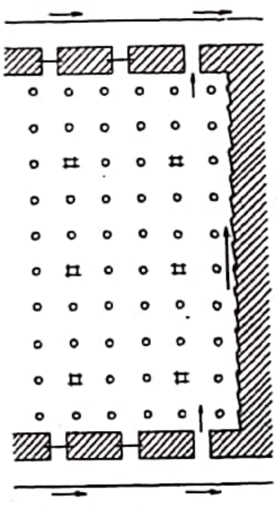

Fig. 9.7(a) Ventilation of a breast stope.

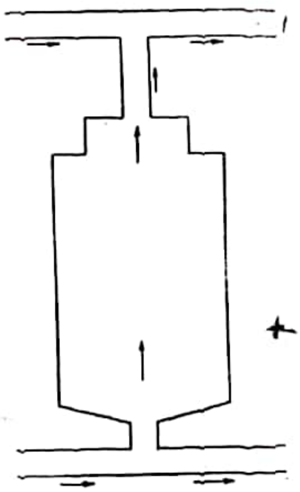

Fig. 9.7(b) Ventilation of a room in room-and-pillar mining.

and travels to the raise leading to the upper level. This coupled with the large volume of the open stope results in poor face air velocity.

Open breast stopes (Fig. 9.7a) and square-set stopes also suffer from similar defects though face ventilation is somewhat better in room-and-pillar mining (Fig. 9.7b).

9.5.5 Sublevel Stopes

The ventilation requirement in sublevel stopes is primarily in the sublevels and the grizzly level (or scraper level where scram drifts are used) where men work. However, grizzly levels should be ventilated by a separate split since a lot of dust is produced here which should be carried away directly to the return air. Fig. 9.8 illustrates the ventilation of a typical sublevel stope.

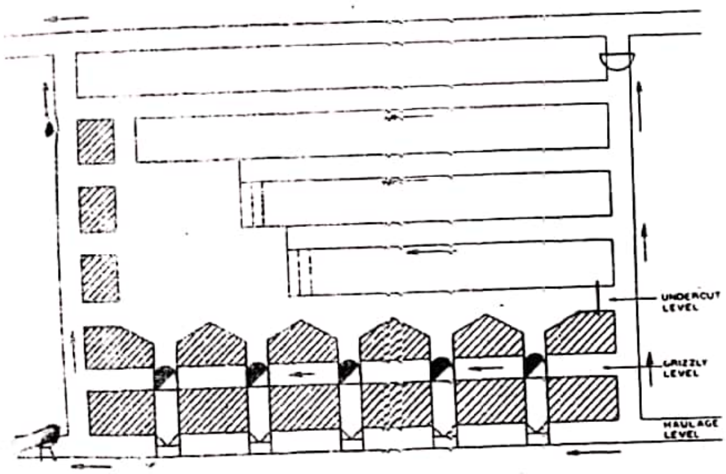

Fig. 9.8 Ventilation of a sub-level stope.

9.5.6 Top Slicing and Sublevel Caving

Of the caving methods, top slicing needs the least development and there is usually a single access opening leading from the haulage level to the slice drift or cross-cut through a raise. The ventilation of the face in this method is generally done by auxiliary fans through tubing. Yet top slicing faces need good ventilation to remove the heat produced by decaying timber in the mat.

Sublevel caving on the other hand provides more number of interconnected openings where separate raises can be used as intakes and returns. Individual faces may, however, have to be ventilated by tube ventilation.

9.5.7 Block Caving

The ventilation requirement in block caving is confined to the openings below the block used for ore handling. Ventilation of finger raises and the undercut level of the block is required during development only and is generally by auxiliary fans and tubing. *Fig. 9.9* illustrates the ventilation of the haulage and scraper drifts below a caving block. A boundary system of ventilation is provided by having separate fan shafts at the end of the property opposite to the hoisting shaft.

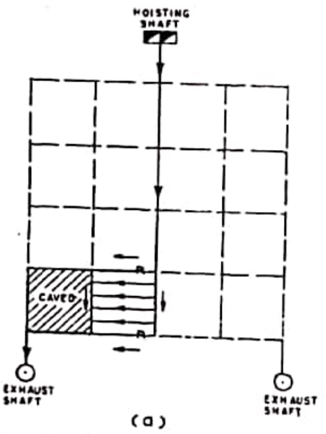

Fig. 9.9 (a) Ventilation of development openings in block caving ventilation system for the mine.

9.6 QUANTITY REQUIREMENT

9.6.1 Air Requirements in the Workings

Supply of an adequate quantity of air to the working face is necessary for the following reasons :

1. *Supplying the workers with breathable air.* As required by law in India and several other countries of the world, mine air should

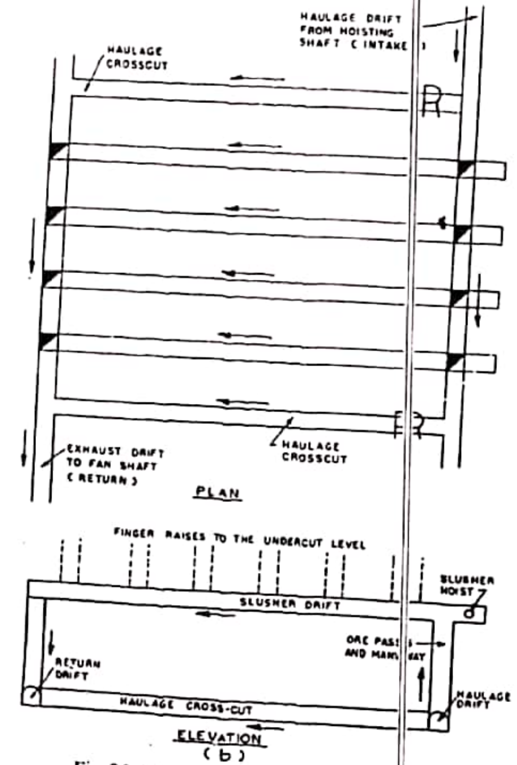

Fig. 9.9 (b) Ventilation system for each block.

Scanned with CamScanner

contain at least 19% oxygen. A man in confined space needs a fresh air supply at the rate of about 0.125 $m^3 min^{-1}$ (see Chapter 1) in order to maintain the oxygen content of the air at 19%. The quantity is to be still more (of the order of 0.5$m^3 min^{-1}$, see Example 1.2) if the carbon dioxide content of air has to be kept below 0.5% as required by regulations. Common industrial practice requires a fresh air supply rate of 0.3-0.9 $m^3 min^{-1}$ per man in buildings. However, besides workers, there are other agents in a mine such as burning lamps, oxidizing coal and timber etc. that deplete the oxygen content of air. The mine air may also be fed with other impurities such as methane. Hence the fresh air supply to a working face in a mine should be substantially more than the common industrial requirement.

2. *Diluting impurities in mine air such as inflammable and noxious gases as well as pathogenic and inflammable dusts to safe concentrations.* Indeed in gassy coal mines, the dilution of methane to a safe concentration is the determining factor in estimating the adequate quantity of ventilation. The DGMS (Director General of Mines Safety), India recommends that sufficient quantity of air should be circulated in a district so as to keep the percentage of inflammable gas in the return of the district below 0.75%. The general practice in this regard is to keep down the methane percentage at the face, particularly where electrical machinery are used, at a maximum of 0.5%. The air quantity should be so estimated that the gas produced at the face is diluted to this level of concentration. In very gassy mines however, the quantity of air required to dilute the gas to this level may cause undesirably high air velocities at the face. In such cases it may be necessary to use compressed-air machinery at the face so that the allowance limit of methane concentration at the return end of the face can be raised to 0.8%. It is well known that the gas content in the air at the outbye end of the return gate is more than near the face on account of methane emission from the goaf. Thus, if electrical apparatus or locomotives are to be used in the return gate, it would be desirable to maintain the methane percentage at the outbye end of the return gate at 0.5%. Otherwise, it would be sufficient to maintain the methane content of air at 0.5% about ten metres away from the outbye end of the face in the return gate.

The rate of air flow Q required to dilute the methane to the maximum allowable concentration c can be obtained from the gas balance equation per unit time

gas in intake air+gas added in the workings=gas in exhaust air

Or, $Q\,a+q=(Q+q)c$

$$\text{or,}\quad Q = \frac{q}{(c-a)} - \frac{qc}{(c-a)} \qquad m^3\,min^{-1} \tag{9.1}$$

where a = concentration of gas present in the intake air
and q = rate of gas emission, $m^3 min^{-1}$.

Note that the volume of exhaust air is increased by q, the amount of gas added in a unit time.

In planning for new mines, it becomes difficult to predict the rate of methane emission from the face. Relations have been developed (see equation 1.8) between the amount of methane emission and the depth of seam but such relations vary from seam to seam and locality to locality and hence are not of much general value. It would be worthwhile to study the rate of methane emission at the face per tonne of coal mined at various depths in the existing mines, if any in the area, before predicting a rate of methane emission for the projected mine. It has been suggested that half-hourly samples at the inbye end of the intake gate and the outbye end of the return gate have to be taken for three to six months in order that the rate of methane emission can be predicted with accuracy. If the mine is to be planned for depths for which no methane emission data can be obtained, it would be wise to allow a 10% increase in the rate of gas emission for every 100m depth. It is worth adding here that any estimation of air quantity for suitably diluting methane emitted at the face should be based on the peak rate of methane emission at any time.

As regards other noxious gases such as nitrous fumes and carbon monoxide it is recommended[119] that where explosives are used to win a mineral, arrangements should be made to send to the face such a quantity of air after every round of blasting as would dilute the carbon monoxide and nitrous fumes to less than 50 parts per million and 5 parts per million respectively within a period of 5 minutes. Radon gas and its daughter products are a source of danger in uranium mines and sufficient ventilation should be ensured to keep down their concentration in any part of the mine below the maximum permissible limit of 3700 $s^{-1} m^{-3}$ ($10^{-1} \mu Ci\, m^{-3}$). In any case a minimum of 0.5 $m^3 s^{-1}$ of air should be delivered from a tube outlet at a distance not exceeding 9m from the face for every pair of men mining uranium ore.

Scanned with CamScanner

3. *Diluting heat and humidity of the mine air.* It is difficult to estimate the quantity of air necessary to reduce the temperature of air at the face to a comfortable value since this depends on several variable factors. Heat from sources like men, lights, machinery, etc. are easily measurable. Heat from rock can be estimated from the various equations developed in Chapter III, though with a lesser degree of accuracy. Heat due to spontaneous heating is more difficult to estimate in projected mines, but spontaneous heating is not a universal phenomenon except in coal mines. In any case an attempt should always be made to estimate the heat addition in different parts of the mine and the quantity required to maintain the temperature rise within a tolerable limit calculated from equation 3.15.

4. *Producing sufficient face air velocity for comfortable working conditions.* A face velocity of 0.5 to 2.0 m s^{-1} is reasonable for comfortable working conditions. Velocities above this generally cause discomfort and raise dust. For efficient dilution of gases and dusts by turbulent diffusion, the flow at the face should be turbulent. Theoretically the velocity required to maintain turbulent flow in a mine (where the openings are fairly large) is well below the above figures. But with low air velocities, particularly in large openings, there is usually a substantial laminar sublayer formed at the boundary even though the flow in the opening is turbulent and it becomes necessary to maintain a high air velocity of the order 0.5 to 1.0 m s^{-1} at the face for efficient dilution of contaminants. Appendix 2 gives the minimum air velocities required at various parts in gassy coal mines in India.

Overall norms of air requirement. Taking into consideration the above requirements, certain empirical norms of air requirement for a mine have been developed which are either based on the number of men employed in the mine or on the output of the mine. Whereas the estimation of quantity based on the number of men employed seems all right for shallow non-gassy mines with small o.m.s. (overall man-shift production), in gassy coal mines with high o.m.s. it is more logical to estimate the air requirement on the basis of production since the rate of methane emission from the strata is to some extent dependent on the production. Besides, heat produced by machinery in mechanized mines with high o.m.s. is to a large extent dependent on the production. It is however wise to estimate the air quantity so as to satisfy both of the above norms. Some advocate the estimation of air quantity on the basis of a suitable air velocity at the face. Face air velocities should be sufficient to offer comfortable working conditions as well as clear the face quickly of dust, fumes etc., but not too high to raise dust.

Most countries in the world provide for a minimum quantity of air to be circulated at a working face based on the number of men working there. This varies from 3 m^3 min^{-1} per man in non-gassy mines to as much as 15 m^3 min^{-1} per man in very gassy mines, though a common figure for gassy mines is 6 m^3 min^{-1} per man. This is also the minimum quantity required to be circulated in gassy coal mines in India[104] as measured at the start of the split even though under more difficult conditions of ventilation as in the deep gold mines of Kolar, the minimum requirement has been kept down at only 0.85 m^3 min^{-1} per man.

On the basis of production, Penman[18] suggests a quantity of 2.8 m^3 min^{-1} per tonne of daily production for non-gassy coal mines and 4.2 m^3 min^{-1} per tonne in gassy mines. These figures compare well with the practice in German coal mines where a quantity ranging from 2 m^3 min^{-1} for non-gassy mines to 4 m^3 min^{-1} for fairly gassy mines is required per tonne of daily production. The usual practice in American coal mines is to use 6 tonnes of air per tonne of coal raised in the average for gassy mines and this ratio may even go up to 10:1. The quantity requirement in gassy coal mines in India is fixed at 2.5 m^3 min^{-1} per tonne of daily production.

The above norms are empirical and for a more accurate estimation of air quantity it is better to calculate the air requirement at the faces separately on the basis of the rate of gas emission, heat addition, dust production etc. The quantity requirement so calculated is then checked against the requirement based on production and the number of men employed at the faces. The highest of the values is taken for planning purposes. The overall air requirement for the whole mine (fan quantity) is then computed taking into account (a) air requirement at other parts of the mine, (b) leakage and (c) expansion in the upcast shaft.

Based on the ventilation practice in the deep South African gold mines for ensuring comfortable environmental conditions Lambrechts and Bracza[121] developed the empirical relationship between underground air requirement per 1000 t of monthly production and virgin-rock temperature as illustrated in Fig. 9.10. It is obvious that these values should apply where heat dilution is the major

Scanned with CamScanner

objective. Interestingly, the nature of the curve suggests the limitation of ventilation alone in controlling the environmental conditions at high values of V.R.T where air cooling becomes imperative.

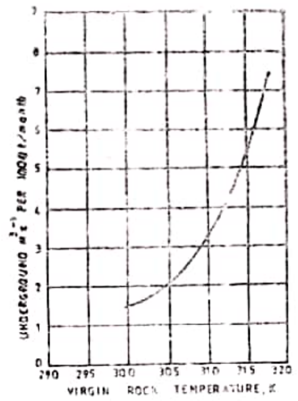

Fig. 9.10 Variation of underground air requirement with v.r.t. (*after Lambrecht*).

9.6.2 Air Requirement in Drifts and Tunnels

The quantity of air required at development headings, drifts and tunnels is usually greater than at longwall faces in order that the face is effectively cleared of gas, dust, fumes etc. and comfortable working conditions are offered. I.L.O (International Labour Organization) recommend a quantity of 0.175 $m^3 s^{-1}$ per m^2 of drift face area. Heavy dust, gas and heat production at the face requires the quantity to be further increased. In extremely hot faces quantities as high as 0.75 $m^3 s^{-1}$ per m^2 have been used. The above quantities are that delivered at the face and the fan quantity has to be still higher depending on the leakage through the duct.

In highly gassy coal headings, it would be desirable to circulate a quantity adequate to dilute the methane emitted at the face to a safe concentration. In any case, the quantity circulated should satisfy the statutory norm of ventilation of 6m^3 min^{-1} per man.

In long headings, the quantity required to be circulated is controlled chiefly by the need to quickly remove the blasting fumes from the drift face in order to minimize loss of working time. The Director[illegible] of [illegible] Safety, India requires the ventilation of drives [illegible] to dilute the nitrous fumes [illegible] blasting [illegible] p.p.m. and CO to 50 p.p.m. within [illegible] minutes. [illegible] is however a very stringent requirement in case of long drives with heavy blasting calling for circulation of [illegible] large quantity at the face. It would be more desirable [illegible] to increase the permissible time of dilution or use [illegible] system of ventilation.

Considering a diluting time t, the required rate of air-flow can be obtained from the gas balance equation for time t

$$[illegible]$$

$$\text{Or, } Q = \frac{q}{t(c-a)} - \frac{qc}{(c-a)} \tag{9.2}$$

where q = amount of gas added during time $t = M q'$,

M = mass of explosive blasted

and q' = volume of noxious gases produced per unit mass of explosive (Ammonia gelatines commonly used for tunnel blasting produce 0.1 mol (0.003 m^3) of NO and 0.1-0.3 mol (0.003-0.009 m^3) of CO per kg of explosive).

Taking $a=0$ and neglecting the second term on the right hand side, equation 9.2 reduces to

$$Q = \frac{M q'}{c\, t} \tag{9.3}$$

an equation often used to calculate the air-flow rate required to dilute blasting fumes. But this equation overestimates Q. A more exact solution can be obtained from the differential gas balance equation for a given volume of space V, say, that of the heading.

$$Q\, dt\, a + q\, dt = V\, dc + Q\, dt\, c + q\, dt\, c \tag{9.4}$$

where q = rate of gas-flow

and c = concentration at time t.

Scanned with CamScanner

Taking $a=0$ and neglecting $q\,dt\,c$ equation 9.4 becomes

$$V\,dc = q\,dt - Q\,c\,dt \tag{9.5}$$

Rearranging for integration we get

$$\int_{c_o}^{c} \frac{dc}{q-Qc} = \int_{o}^{t} \frac{dt}{V}$$

$$\text{Or, } \log \frac{q-Qc}{q-Q\,c_o} = -\frac{t\,Q}{2.303\,V} \tag{9.6}$$

where c_o=initial concentration of the gas in the space.
For blasting fumes c_o can be taken equal to $Mq'/(V+Mq')$ and the rate of gas flow q can be taken equal to zero, equation 9.6 then becomes

$$\log \frac{c\,(V+M\,q')}{M\,q'} = -\frac{tQ}{2.303\,V} \tag{9.7}$$

$$\text{Or, } t = \frac{2.303\,V}{Q} \log \frac{M\,q'}{c\,V+c\,M\,q'} \tag{9.8}$$

This equation is satisfactory in short tunnels where V is not too large. In long tunnels however, mixing and dilution occurs over a short length at the face in front of the ventilation tube while air movement in the rest of the tunnel can be considered as a plug flow. In such a case it would be more logical to use the following relation developed by the author.[19]

$$t = 2.303\,\frac{V_m}{Q} \log \frac{q}{V_m\,c} + \frac{V-V_m}{Q} \tag{9.9}$$

where V_m=volume of the tunnel over which mixing of the gases produced at the face and air delivered by the fan occurs,
V = volume of tunnel
and q = total volume of noxious gas produced$=M\,q'$.
Note that if V_m is taken equal to V in equation 9.9, we get

$$t = 2.303\,\frac{V}{Q} \log \frac{q}{V\,c} \tag{9.10}$$

which is the same as equation 9.8 if $M\,q'$ is neglected in comparison with V.

Voronin[3] gives the following empirical relation for Q which obviously ignores the effect of the fume quality of the explosive used :

$$Q = \frac{7.8}{6}\,(MV^2)^{\frac{1}{3}} \tag{9.11}$$

Note that equation 9.6 can also be used for finding the time required for cleaning a heading of accumulated methane by starting auxiliary ventilation. In this case both c_o and q have positive values.

Example 9.1

15 kg of explosive is fired in a 2×2.5m drive which is 100m long. Calculate the quantity of air to be circulated by an auxiliary fan to bring down the concentration of nitrous fumes in the drive to the tolerable limit of 5 p.p.m. within a period of 5 minutes. A kg of explosive produces 2000 cm³ of nitrous fumes.

The volume of the drive$=2\times2.5\times100=500$ m³

The volume of nitrous fumes produced

$$=15\times2000=30\,000 \text{ cm}^3$$
$$=0.03 \text{ m}^3$$

Maximum permissible concentration of gas=5 ppm=0.0005%.
Using equation 9.3, the quantity required to be circulated

$$Q = \frac{100\times0.03}{0.0005\times5} = 1200 \text{ m}^3\text{ min}^{-1} = 20 \text{ m}^3\text{ s}^{-1}.$$

Obviously this figure is unduly high.
Using equation 9.10 we have

$$5 = 2.303\times\frac{500}{Q} \log \frac{0.03\times100}{500\times0.0005}$$

$$\text{Or, } Q = 2.303\times100 \log \frac{30\,000}{2\,500}$$

$$= 248.5 \text{ m}^3\text{ min}^{-1} = 4.14 \text{ m}^3\text{ s}^{-1}.$$

Using equation 9.11,

$$\frac{7.8}{5}\Big[15(500)^2\Big]^{\frac{1}{3}} = 242.27 \text{ m}^3\text{ min}^{-1} = 4.04 \text{ m}^3\text{ s}^{-1}.$$

Scanned with CamScanner

Assuming the ventilation tube to discharge at a point 10m away from the face the mixing volume V_m can be taken equal to $10\times2\times2.5=50$ m³.
Now using equation 9.9 we have

$$5=2.303\,\frac{50}{Q}\log\frac{0.03\times100}{50\times0.0005}+\frac{500-50}{Q}$$

Or, $Q=137.9$ m³ min⁻¹ $=2.3$ m³ s⁻¹.
Note the lower value of Q obtained from this equation. However, for long tunnels, equation 9.10 or 9.8 gives a value of Q much lower than that obtained with equation 9.9 because the value of $c_o=Mq'/(V+Mq')$ in the former is underestimated owing to the high value of V. For example, for a 1000m long drive of the above cross-section equation 9.9 gives a value of $Q=17.3$ m³ s⁻¹ while equation 9.10 gives $Q=3.03$ m³ s⁻¹ which is lower than that required for the 100m drive, a fact not quite tenable. The high value of Q given by equation 9.9 is due to the need to clear the entire drive of gas, and not merely the face for which the last term on the right hand side of equation 9.9 has to be omitted.

9.6.3 Air Requirement at other Parts of the Mine

An air quantity of 2.3 m³ s⁻¹ is usually allowed for ventilating internal hoists, haulages, pump houses and other large electric motors, if any, though a better practice would be to exactly estimate the quantity for diluting the heat produced. Battery charging stations need an air quantity of 4.7 m³ s⁻¹.

Where diesel locomotives are used underground, the air requirement should take into consideration the proper dilution of the exhaust gases produced by these locomotives. British regulations provide that the percentage of carbon monoxide in exhaust gases of diesel locomotives should not exceed 0.2%. The percentage usually met with in practice is however lower when the locomotives are fitted with exhaust gas conditioners (see Fig. 9.11). Taking the rate of production of exhaust gases from diesel locomotives as 0.001 59 m³ s⁻¹ per kW of the locomotive[13], the maximum permissible rate of production of carbon monoxide by diesel locomotives is 0.000 0031 m³ s⁻¹ kW⁻¹. The quantity of air necessary to dilute this amount of carbon monoxide to 0.005% as required by regulations is thus 0.064 m³ s⁻¹ kW⁻¹. A safer practice, however, is to ensure an air-flow of 0.1 to 0.12 m³ s⁻¹ kW⁻¹ in haulage roads and 0.064 m³ s⁻¹ kW⁻¹ in locomotive garages and repair shops. Petrol engines, however, are never allowed in underground mines as they produce a large amount of CO.

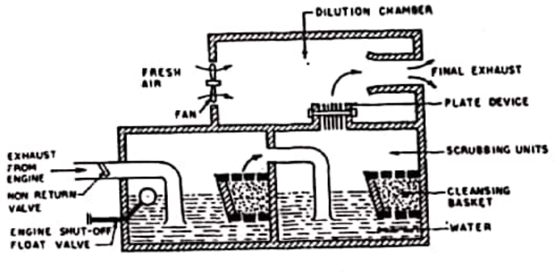

Fig. 9.11 Exhaust conditioner and flame trap used in underground diesel locomotives.

Air requirement in other excavations housing stores, rest rooms etc. should be calculated depending on the volume of the room on the basis of 4 to 6 air changes. However it is a common practice to provide about 0.5 m³ s⁻¹ of air to such rooms.

9.6.4 Leakage of Air

Between the fan and the face in a mine a lot of air is lost through leakage at stoppings, doors, air-crossings etc. so that a much larger quantity of air has to be circulated by the fan in order that the stipulated quantity of air reaches the face. The volumetric efficiency of distribution of air in mines may vary from only 10% in very poor conditions to 85% in very good conditions of ventilation. Under average conditions however, 45 to 55% of the air circulated by the fan reaches the working face in an in-the-seam coal mine. This figure is slightly higher (55 to 65%) in case of coal mines worked on the horizon system. The figure for metal mines is usually still higher.

Leakage is a function of the pressure of ventilation, higher pressure causing greater leakage. Whereas the quantity of leakage through large openings such as doors, loose packs etc. varies as the square root of the pressure, that through small openings as may be found in stoppings, compact packs or rock walls varies directly with pressure. For reducing leakage it is preferable to use a larger number of low-pressure fans in series than a single high-pressure fan. This is particularly true with mining in broken ground where leakage through the rock surrounding airways may be considerable. Besides, care must be taken to locate major airways in strong undisturbed ground in order to minimize leakage. Boundary ventilation, in which main intakes and returns are widely separated, is preferable from this point of view.

Leakage at permanent stoppings is negligible, the amount being only 0.03 $m^3 s^{-1}$ for a 200mm thick concrete wall built with a good foundation extending well beyond the broken zone at the periphery of the airway. Poorly built stoppings leak badly at the airway periphery. Patrushev[8] has given some values for resistance of stoppings to leakage which, according to his square law relation, give leakage values of 0.04 and 0.09 $m^3 s^{-1}$ respectively for differential pressures of 98 and 490 Pa across slag or rubble concrete stoppings in solid rock. The corresponding values for such stoppings in broken rock are 0.076 and 0.17$m^3 s^{-1}$. The leakage through temporary plank stoppings in solid rock is as high as 0.1 $m^3 s^{-1}$ even for a pressure difference of 98 Pa.

Leakage through separation doors between intake and return can be often considerable and is usually taken to be of the order of 1.4 $m^3 s^{-1}$. However, it has been seen in metal mines, where the ventilating pressure across doors is high, i.e. of the order of 250 Pa, that if the edges of the doors are suitably covered by canvas strips, the leakage of air can be reduced to only 0.47 $m^3 s^{-1}$ for active doors and 0.23 $m^3 s^{-1}$ for inactive doors. Skochinsky and Komarov[2] give the following values (see Table 9.1) for leakage through wooden doors and air-locks in masonry or concrete stoppings. A leakage of 1.4 $m^3 s^{-1}$ can be assumed for ordinary air-crossings (not explosionproof).

Values of leakage across newly-formed goaf as assumed by the N.C.B., U.K. for ventilation planning of coal mines are given in Table 9.2. No leakage is, however, assumed to take place across solidly stowed goaf.

In addition to the leakage of air underground, a lot of leakage often takes place at the top of the upcast shaft through the air-lock and the walls of the fan drift and the shaft collar. Leakage through the walls of the fan drift or the shaft collar can be minimized by suitably lining these with concrete, but it is difficult to prevent leakage through the air-locks. Leakage through air-locks at shaft-

Table 9.1 : Leakage Through Doors and Air-locks, $m^3 s^{-1}$

Pressure, Pa	Area of door, m^2 1.2	1.5	1.7	2.2	⩾2.6
		Doors			
98	0.15	0.18	0.22	0.28	0.33
196	0.22	0.27	0.30	0.33	
294	0.27	0.33			
392	0.30				
⩾490	0.33				
		Air-locks			
98-196	0.125	0.16	0.18	0.24	0.28
294-392	0.20	0.25	0.28	0.33	
490-589	0.25	0.30	0.33		
785-981	0.32				

Table 9.2 : Leakage Across Newly-formed Goaf

Distance between intake and return gates (m)	Leakage across goaf as percentage of the air on the face
45	20
90	10
180	5

tops depends on the fan-drift pressure, type and state of repair of the air-lock, number and type of entrances and the frequency of hoisting. Table 9.3 gives leakages for new pit-tops well constructed in concrete and laid out for regular winding of minerals. The values should be reduced by 70% if the shaft is not used regularly.

Scanned with CamScanner

Table 9.3 : Leakage at Pit-top

Fan-drift pressure, kPa	Leakage at pit-top ($m^3 s^{-1}$)
1.25	11.7
2.50	16.3
3.75	21.0
5.00	23.3
6.25	25.7

9.6.5 Expansion in Upcast Shaft

As the air from underground workings rises in the upcast shaft it expands due to the reduction of barometric pressure and if the air is circulated in the mine by an exhaust fan situated at the top of the upcast shaft, the fan will handle a larger quantity of air than that circulating in the workings. Thus provision should be made for this when estimating the quantity of air required to be circulated by the fan. The increase in the quantity of air due to expansion in the upcast shaft can be roughly taken as 1% for every 100m depth.

9.6.6 Air Velocities

In planning for the quantity of ventilation one should keep in mind the velocity of air in different parts of the mine. We have seen that from the point of view of economy, there is an optimum quantity or velocity for an airway of a given size. An increase in velocity over this value causes greater loss of pressure and hence greater power cost of ventilation whereas lower velocities mean unnecessary extra investment of capital in the excavation of airways of larger size. Besides, while low velocities are dangerous from the point of view of methane layering and can cause uncomfortable environmental conditions of working, too high velocities are equally undesirable from the point of view of safety and health. High velocities blow out naked lamps. Carbide lamps can withstand an air velocity of 5 m s^{-1} but for safe working, the velocity should not exceed 2.5 m s^{-1} where carbide lamps are to be used. Modern flame-safety lamps can withstand an air velocity of 12.5 m s^{-1}. Velocities greater than 2.5 m s^{-1} raise dust which not only is hazardous to the lung but also causes smarting of the eyes. Hodkinson[124] has shown that an air velocity of 5 m s^{-1} or more is required to raise an appreciable concentration of dust of dangerous size (1-5 μm) from stationary deposits. But with mechanical disturbances common at working faces, a velocity of 1.5-2 m s^{-1} is sufficient to raise a similar concentration of dust. However, velocities greater than 0.5 m s^{-1} are necessary for ensuring comfortable working conditions and effective dispersal of dust, gases etc.

It is a good practice not to exceed an air velocity of 1.7 m s^{-1} at the face ; 3 m s^{-1} in conveyor roads, loading points and transfer points; 5 m s^{-1} in main haulage roads; 7.5 m s^{-1} in smooth-lined airways not used for haulage purposes and shafts with rope guides ; and 12.5 m s^{-1} in shafts with rigid guides as well as fan drifts. High air velocities in shafts with flexible guides may cause too much swinging of cages. Appendix 2 gives the permissible maximum air velocities in different parts of a mine in India.

Air velocities in diesel locomotive sheds and battery charging stations should not be less than 0.75 m s^{-1}

9.7 PRESSURE REQUIREMENT

The pressure required to circulate a certain quantity through an airway can easily be calculated if the resistance of the airway is known either from measurement or from calculation as discussed earlier. It must be noted here that for accuracy, both friction and shock resistances should be estimated, though in practice it is the former which accounts for 70-90% of the total mine resistance, the rest being accounted for by the latter. Pressure loss in shafts should be calculated on the basis of the average quantity of flow in them. This becomes particularly necessary in case of deep shafts where there is a substantial variation in the volume of flow at the two ends of the shaft because of the large difference in the barometric pressure. Due consideration should be given to the effect of leakage, if there be any, on pressure loss across an airway.

Knowing the pressure requirement for each airway, the total pressure required for the whole mine can be calculated. If the mine consists of several parallel splits, the pressure required for the one with the largest resistance is generally taken as the actual pressure requirement. This involves the control of quantities flowing through the other splits by the installation of regulators in them. Installation of regulators, though wasteful, is a simple means of ventilation control and should be adopted if the degree of regulation is small or the regulation affects only a minor number of splits. If however,

Scanned with CamScanner

the adoption of the pressure requirement for the highest-resistance split involves a large degree of regulation in most of the other splits, it would be advisable to select a pressure requirement more congenial to these other splits. The required flow in the highest-resistance split could then be obtained by installing a booster fan in it.

The calculation of the resistance or pressure loss in a split is easy if it consists of branch airways so connected that the whole network can be resolved into a simple series-parallel circuit. In practice however, ventilation networks are usually complex and need special methods for solution.

9.8 SOLUTION OF COMPLEX VENTILATION NETWORKS

Kirchoff's law for electrical circuits holds good for air-flow circuits and hence is used for solving complex network problems. The law states that

(a) the total quantity of air flowing into a junction of airways equals that flowing out of it or, in other words, the algebraic sum of the quantities flowing into a junction is equal to zero ;

(b) in a closed circuit or a mesh, the algebraic sum of changes in pressure across each branch is zero.

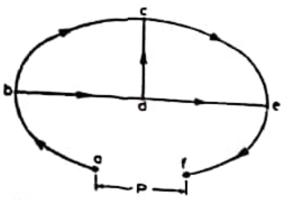

Fig. 9.12 Ventilation network.

Let us consider a simple network as shown in Fig. 9.12. A fan generating a pressure P is situated across a and f. Now, from Kirchoff's first law,

$$Q_{bd} = Q_{ab} - Q_{bc} \tag{9.12}$$

$$Q_{de} = Q_{ef} - Q_{ce} = Q_{ab} - Q_{ce} \tag{9.13}$$

since $\quad Q_{ab} = Q_{ef}$

and $\quad Q_{dc} = Q_{ce} - Q_{bc}$. (9.14)

Applying Kirchoff's second law, in mesh a b d e f a

$$(R_{ef}+R_{ab})Q^2_{ab}+R_{bd}(Q_{ab}-Q_{bc})^2+R_{de}(Q_{ab}-Q_{ce})^2-P=0 \tag{9.15}$$

in mesh b c d b

$$R_{bc}Q^2_{bc}-R_{dc}(Q_{ce}-Q_{bc})^2-R_{bd}(Q_{ab}-Q_{bc})^2=0 \tag{9.16}$$

and in mesh c e d c

$$R_{ce}Q^2_{ce}-R_{de}(Q_{ab}-Q_{ce})^2+R_{dc}(Q_{ce}-Q_{bc})^2=0 \tag{9.17}$$

where $\quad Q$ = quantity flowing in any branch airway,

$\quad R$ = resistance of the branch and the suffixes indicate the branch concerned.

From the above three equations it is possible to solve the three unknowns Q_{ab}, Q_{bc} and Q_{ce}, but the simultaneous solution of the above quadratic equations is difficult and hence a method of successive approximation as given below is adopted in solving them. For networks with larger number of branches, a larger number of equations have to be solved. If B=number of branch airways in a ventilation network and J=number of junctions, then the minimum number of meshes M to be considered or the minimum number of equations necessary to solve the network is given by

$$M=B-J+1 \tag{9.18}$$

In the above example

$\quad B$ = 8 (including the fan as a branch)

and $\quad J$ = 6 (each letter in Fig. 9.12 indicating a junction).

Therefore

$\quad M$ = 3.

9.8.1 Solution by Hardy Cross Method of Successive Approximation

In this method, suitable quantities for different branches are assumed giving due consideration to Kirchoff's first law, i.e. law of continuity of flow. The closer the assumed quantities to true ones, the less is the number of successive iterations. In the case of estimation of quantity in various airways after a reorganization of the ventilation system, the assumed quantities can be those flowing in the airways before the reorganization as obtained from pre-reorganizational ventilation surveys.

Meshes are now formed so as to include all branches, the minimum number of meshes selected being given by equation 9.18. Care should be taken to include not more than one high-resistance branch

Scanned with CamScanner

in each mesh nor should a high-resistance branch appear in more than one mesh in order to ensure rapid convergence.

Then for each mesh a correction factor X is found from the relation

$$X = \frac{-\Sigma P}{\Sigma 2R|Q|} = \frac{-\Sigma RQ|Q|}{\Sigma 2R|Q|} \qquad (9.19)$$

where ΣP is the algebraic sum of the pressure drop across the branches in the mesh, R is the resistance of a branch and $|Q|$ is the absolute value of flow-rate in the branch. All pressure drops are taken positive while all pressures generated such as by fans or N.V.P. are taken negative so that when fixed-pressure fans and N.V.P. are present in the mesh equation 9.19 modifies to

$$X = \frac{-(\Sigma RQ|Q| - \Sigma P_f - \text{N.V.P.})}{\Sigma 2R|Q|} \qquad (9.20)$$

When variation in fan pressure is allowed according to its characteristic, equation 9.20 modifies to

$$X = \frac{-(\Sigma RQ|Q| - \Sigma P_f - \text{N.V.P.})}{\Sigma 2R|Q| - \Sigma S_f} \qquad (9.21)$$

where P_f is the pressure of the fan and S_f the slope of its characteristic corresponding to the assumed quantity of flow.

The correction to the quantity in each branch ΣX is then equal to the algebraic sum of the corrections for the meshes in which the branch occurs.

The quantities can be successively corrected till the required degree of accuracy is achieved. In practice, while solving a complicated network, it is convenient to exclude branches of high resistance in the initial stages of computation until the quantities in major branches are corrected to a degree of accuracy where the error is of the order of the quantities passing through the high-resistance branches. The high-resistance branches can then be brought into computation.

Let us consider the above example accepting the values of P and R as shown in Table 9.4. The assumed values of Q are also shown in the 3rd column of the table. The successively corrected values are Q_1, Q_2 etc.

Table 9.4 : Solution by Successive Approximation of the Network Shown in Fig. 9.12

Branch	R	Q	$2RQ$	$P-RQ^2$	ΣX	Q_1	$2RQ_1$	RQ_1^2	ΣX_1	Q_2
ab	0.25	7	3.50	12.25	+0.06	7.06	3.53	12.46	+0.01	7.07
bd	0.16	3.5	1.12	1.96	+0.06 +0.19 +0.25	3.75	1.20	2.25	+0.01 −0.03 −0.02	3.73
de	0.20	3.5	1.40	2.45	+0.06 −0.09 −0.03	3.47	1.39	2.41	+0.01 −0.03 −0.02	3.45
ef	0.16	7	2.24	7.84	+0.06	7.06	2.26	7.97	+0.01	7.07
af (fan)	0	7	0	−25	+0.06	7.06	0	−25	+0.01	7.07
bc	0.20	3.5	1.40	2.45	−0.19	3.31	1.32	2.19	+0.03	3.34
dc	0.10	0	0	0	+0.19 +0.09 +0.28	0.28	0.06	0.008	−0.03 +0.03 0	0.28
ce	0.18	3.5	1.26	2.20	+0.09	3.59	1.29	2.32	+0.03	3.62
Mesh	$\Sigma 2RQ$		ΣRQ^2		X		$\Sigma 2RQ_1$	ΣRQ_1^2	X_1	
a b d e f a	8.26		−0.50		+0.06		8.38	−0.09	+0.01	
b c d b	2.52		+0.49		−0.19		2.58	−0.07	+0.03	
c e d c	2.66		−0.25		+0.09		2.74	−0.08	+0.03	

Scanned with CamScanner

The above method of computation is very time consuming, particularly for a network with a large number of branches. Digital computer programmes have, however, been developed to solve complex networks by the above method of successive approximation.

9.8.2 Ventilation Network Analysis by Digital Computor

Highly sophisticated digital computor programmes have been developed which can start with the selection of meshes from amongst the branches specified in the input data. Branches are normally identified by the junctions they connect, each junction being identified by a reference number. Branch resistances can be given as input data or a sub-programme provided to calculate the resistance of branches from survey data of pressures and quantities.

Fans with constant pressure or with variable-pressure characteristic can be provided between junctions. In the latter case the fan characteristic is generally represented by a table of pressures for different quantities in the input data. The pressure for any quantity is read by the computor by interpolation. Alternatively an equation may be fitted to the relevant part of the fan characteristic and the pressure computed from this equation. N.V.P. is generally represented as a constant-pressure fan. It can, however, be computed from temperatures and elevations of junctions with respect to a suitable datum.

Meshes are selected satisfying the following criteria: (a) the minimum number of meshes given by equation 9.18 are selected, (b) all branches are included in the meshes selected and (c) no high-resistance branch appears in more than one mesh. Mesh selection can be done in two ways. In one of them basic branches such as those with high resistance, fans or branches with fixed flow are first selected and the required number of meshes built around them by the *branch tree technique*. In the other method the computor starts with one branch and searches out alternative routes (*route finding technique*) which form a closed mesh back to the starting point. Unsuccessful routes are memorized by the computor and are avoided in the successive searches. The latter method leads to the formation of a larger number of meshes and hence takes more computor time for each iteration, but the number of iterations required for the solution is reduced.

After the meshes are formed, the appropriate iterative equation (9.19, 9.20 or 9.21) is used to compute X for each mesh and

therefrom ΣX for each branch. The branch quantities are then corrected and the process repeated until the difference between successive quantities for any branch falls within a tolerable limit.

In a mine there may be branches or circuits where a fixed quantity has to be supplied. The computor programme can incorporate the determination of the variation in the resistance of the branch required to keep the quantity fixed at a certain value. A rise in resistance indicates the need for a regulator while a fall indicates the need for the installation of a booster. The programme can also incorporate the determination of the size of the regulator or booster.

The programme can be made to incorporate modifications to the network such as (a) change in resistance values, (b) introduction of new branches and junctions, (c) removal of branches, (d) change in fan duty, (e) change in fan position and (f) variation in N.V.P.

9.8.3 Ventilation Network Analogue Computor

Electrical analogue computors have been developed for solution of ventilation networks. In these devices, air-flow in mine airways is considered analogous to the flow of current through a network of electrical circuits. The first computor developed in Belgium used tungsten filament lamps fed from an A.C. supply. Such lamps obey the law

$$V=i^2r \tag{9.22}$$

where V = voltage applied to the lamp,
i = current flowing through the lamp
and r = electrical resistance of the lamp.

The above law is similar to the law of ventilation $P=RQ^2$ generally applicable in mines and hence all that is to be done on the computor is to connect different bulbs of resistances corresponding to the resistances of branch airways in the ventilation network in the same way as the various branches are connected in the network. Then an A.C. voltage corresponding to the pressure of the ventilating fan is applied to the circuit and the current passing through each bulb is measured by a suitable ammeter which, if suitably calibrated, directly gives the quantity of air flowing through the branch. Such a computor was however soon replaced by one using ordinary

Scanned with CamScanner

resistors following the law $V=ir$ because, the square law for the tungsten lamps was found to hold good over only a small range of voltages varying between 25% and 100% of the rated voltage of the lamps.

The linear ventilation network analogue computor consists of several resistors with calibrated dials which are connected in the same fashion as the branch airways in the ventilation network. The fans in the network are simulated by applying suitable voltage corresponding to the pressures generated by them at the corresponding positions in the circuit.

We know that the law of air-flow is given by the equation $P=RQ^2$ whereas that of the flow of electrical current through a resistance, by $V=ri$. From the above two equations it can be easily seen that the airway resistance can be represented by the electrical resistance as shown in the following equation :

$$r=K(RQ) \tag{9.23}$$

where K is a constant of proportionality.

Since r is a product involving Q which is to be determined, the correct values of r cannot be directly set on the computor. First, a certain value of Q is assumed (the nearer this value to the true value, the lesser is the number of successive approximations) and r on the resistor is successively adjusted according to the following iterative equation until successive values of r become almost constant or the correct value of Q is reached :

$$r_{m+1}=\tfrac{1}{2}(r_m+KRQ_{m+1}) \tag{9.24}$$

where m is the number of the iteration (for mathematical proof see ref. 128)

The computor should be so constructed that it has an adequate number of resistors so as to cover all the branches in a ventilation network. Besides, the resistors should be of suitable ranges so as to cover the different values of RQ usually met with in mines. One such computor used by the N.C.B., U.K., uses 60 resistors as specified in Table 9.5.

There are usually three or four independent variable-voltage D.C. supplies provided on the computor in order to simulate the fans, though more fans may have to be provided for on a computor used

Table 9.5 : Specifications of the Resistors used in the N.C.B. Ventilation Network Analogue Computor.

Number of resistors	Range of Resistance, Ω
8	0 to 250
6	0 to 500
7	0 to 1000
7	0 to 2500
9	0 to 5000
7	0 to 10 000
6	0 to 25 000
4	0 to 100 000
6	0 to 250 000

for solving ventilation networks in metal mines. A voltmeter graduated in units of air pressure and an ammeter calibrated in units of quantity of air-flow are used to measure respectively the pressure across the fans and the quantity in each resistor or branch.

Apart from solving simple problems of air-flow in a ventilation network when resistances of branch airways and fan pressures are known, the computor can also solve certain special problems and apply with ease certain finer corrections which are generally left out in ordinary calculations.

Due account of natural ventilation can be taken by introducing a fan with a pressure equal to the N.V.P. in series with the main fan. It is of course assumed that there is no change in the N.V.P. with changes in the system of air-flow inside the mine. In multi-level workings, as in metal mines, where the N.V.P. acting across different levels is different depending on the depth of the level, the N.V.P., for each level can be represented by a fan in that level. In such a case, all these fans act in parallel with each other though together they are in series with the main mine fan. Similarly any addition of compressed-air or methane at any part of the mine can be represented by a fan with a resistance in series, the resistance being so adjusted that the current through it remains constant at a value representing the additional quantity of gas added to the air-current. It is possible to calculate the size of a booster to be installed in any district in order to increase the flow in it by adding a fan to the district and increasing its pressure until the resistor representing the

Scanned with CamScanner

district shows the required flow. In the subsequent adjustments the fan pressure is adjusted so as to maintain the flow constant. Similarly the size of a regulator can be determined by adding a resistor at the point desired and successively adjusting its resistance until the desired quantity through the regulator is maintained.

Any change in a ventilation system may alter the total quantity circulated by the fan thus shifting the operating point on the fan characteristic and causing a change in the fan pressure. Such changes in the main fan pressure can be easily corrected by just changing the fan pressure on the machine to a value corresponding to the quantity as obtained from the fan characteristic after every adjustment of quantity, until there is little difference between successive fan pressures.

Today square-law fluid-flow network analysers have been developed which make the solution of ventilation networks easier and less time consuming than on linear analogue computors. They comprise resistance cells composed of transistors and resistors which give a power-law relationship between applied voltage and current flowing through them.

$$V = ri^n \tag{9.25}$$

By suitable design, n can be made equal to 2 so that the electrical network can directly simulate the ventilation network.

However, these machines have not found wide use chiefly because of the use of digital computors for quick solution of complex ventilation networks.

9.9 ANALYSIS OF VENTILATION COST

In the choice of an optimum ventilation system or equipment, it may be necessary to evaluate several alternative systems or equipment.

The cost of ventilation comprises

(a) *Capital investment*

(i) On airways : Only those airways which are specifically required for ventilation may be included here. Sometimes an airway may have to be enlarged in cross-section or lined in order to meet ventilation needs. In such cases the capital cost under this head should cover the cost of enlargement or lining.

(ii) On ventilation control devices such as doors, air-locks, air-crossings, stoppings, regulators etc.

(iii) On air moving devices covering main fans, boosters and auxiliary fans : The capital investment under this head should cover the purchase cost of the fan, motor and drive, switch gear, instruments etc. inclusive of freight, insurance charges and duty, if any plus the cost of installation including housing for fan, motor and control units, fan drift, diffuser or evasee etc. When the fan has a resale value at the end of its term of use, the present value of the resale value should be deducted from the capital cost.

While smaller portable fans used for a short period or medium-size fans with standard factory-built housing have a fair resale value, large fans specially designed for a particular mine and installed in brick or concrete housing have little resale value except perhaps for the motor.

(iv) On ducts : This should include the purchase and installation cost minus the present value of resale value, if any.

Often the entire capital investment on a ventilation system is not done right in the beginning. Airways, control devices, fans or ducts may be added at different periods. The initial capital investment on these is then the present value of the investments.

(b) *Operating cost*

(i) Power cost : This is by far the most important operating cost in mine ventilation. It comprises the cost of power input to the fan motors and is computed for continuous operation of fans throughout the day and 365 days in a year. In project work the annual power cost A_p can be estimated from the relation

$$A_p = \frac{8.76\, P\, Q\, C}{\eta} = \frac{8.76\, R\, Q^3\, C}{\eta} \tag{9.26}$$

where P = pressure required to ventilate the system, Pa,
Q = flow through the system, $m^3\ s^{-1}$
R = resistance of the system, $N\ s^2\ m^{-8}$,
C = cost of power per unit (kW h)
and η = combined efficiency of fan, motor and gear.

(ii) Maintenance cost : This covers both materials and labour cost of maintenance on air moving devices, ducts, ventilation control devices and airways specially maintained for ventilation.

(iii) Direct labour and supervision cost.

(iv) Overhead cost.

Since the capital investment is done only once while the operating cost is a recurring expenditure, both must be brought to a

Scanned with CamScanner

common denomination for cost comparison purposes. For optimization purposes, both the costs can be reduced to either (a) a total annual ventilation cost or (b) a total current investment.

Total annual ventilation cost (*TAVC*) : This again may be computed in three different ways :

(a) $TAVC = A + Pr' + P/n$ (9.27)

where A = annual operating cost,
P = initial capital investment,
r' = a speculative rate of interest so that $P\,r'$ is the interest earnings on the capital invested
and n = life of the equipment, airway etc. so that P/n gives the annual depreciation cost by the straight line method of depreciation.

(b) $TAVC = A + Pr' + Pr/(R^n - 1)$ (9.28)

where $R = r + 1$
and r = a safe rate of interest used for amortization of capital.

The last term in equation 9.28 represents the amortization of capital invested through a sinking fund at a safe rate of interest r. It is indeed an annuity that accrues to the initial capital investment at the end of n years.

(c) $TAVC = A + \dfrac{P\,R^n\,r}{R^n - 1}$ (9.29)

In this equation there is a single rate of interest. The last term is an annuity over n years the present value of which equals the initial capital investment.

Of the three methods, the first amortizes more than the capital invested initially at the end of n years. However, with the value of money progressively going down with inflation, this will give a fund that may be able to meet the inflated cost of replacement of the equipment. For the purpose of cost comparison however, it is not necessary to go into economic complexities and any of the above methods can be used as long as all the alternative ventilation systems are analysed by the same method.

Total current investment (*TCI*) : This comprises the sum of the initial capital investment and the present value of the annual operating costs over n years.

$$TCI = P + \frac{A\,(R^n - 1)}{r\,R^n} \qquad (9.30)$$

Equation 9.30 leads to an exactly similar conclusion as equation 9.29.

Example 9.2

A mine having two sections is ventilated on the boundary system with a central exhaust shaft installed with a surface fan and two boundary intake shafts. The fan circulates 40 $m^3\,s^{-1}$ through one section and 60 $m^3\,s^{-1}$ through the other at a fan-drift pressure of 900 Pa of which 500 Pa is consumed in the exhaust shaft. It is required to increase the quantity flowing in the first section to 50 $m^3 s^{-1}$ by the following alternative methods : (a) installing a booster in the section, (b) speeding up the main fan, (c) speeding up the main fan with the installation of a regulator in the second section in order to maintain flow in it at the original level. Calculate the power consumption in each of the alternatives assuming the main fan and motor to have a combined efficiency of 72% and the booster fan and motor, 68%.

Case (*a*) : Assuming main fan pressure to remain unchanged, let new flow through the mine after the installation of the booster be Q $m^3\,s^{-1}$.

Exhaust shaft resistance (inclusive of fan drift)

$$R_T = \frac{500}{100^2} = 0.05\ Ns^2\,m^{-8}.$$

Resistance of the first section

$$R_1 = \frac{900-500}{40^2} = 0.25\ Ns^2\,m^{-8}.$$

Resistance of the second section

$$R_2 = \frac{400}{60^2} = 0.11\ Ns^2\,m^{-8}.$$

Now considering the unboosted split

$$900 = R_T Q^2 + (Q-50)^2 R_2$$
$$= 0.05\,Q^2 + 0.11\,(Q^2 + 2500 - 100Q)$$

Scanned with CamScanner

Or, $0.16Q^2-11Q-625=0$

$$\text{Or, } Q=\frac{11\pm\sqrt{121+4\times0.16\times625}}{2\times0.16}$$

$$=105.7 \text{ m}^3\text{ s}^{-1},$$

neglecting the negative value.
Considering the boosted split,

$900+P_B=0.05\,(105.7)^2+0.25\,(50)^2$

where P_B = booster pressure in Pa.

$\therefore P_B=283.62$ Pa.

$$\text{Power consumption}=\frac{900\times105.7}{0.72}+\frac{283.62\times50}{0.68}$$

$$=152\,979.4\text{ W}\quad=153\text{ kW}.$$

Case (*b*) : Let the speed of the main fan be increased x times. Its quantity will increase to $100x$ m³ s⁻¹ and its pressure to $900x^2$ Pa.

Considering the first section $900x^2=0.05\,(100x)^2+0.25\,(50)^2$

or, $x=1.25$.

The fan has to develop a pressure of $900x^2=1406.25$ Pa.

$$\text{Power consumption}=\frac{1406.25\times125}{0.72}=244\,140.63\text{ W}=244.1\text{ kW}.$$

Case (*c*) : Let the fan pressure be assumed to remain constant at 1406.25 Pa on regulation of flow in the second section at the original level of 60 m³ s⁻¹. There will then be a rise in the flow through the first section. Let the flow through the first section be Q m³ s⁻¹.

Considering the first section,

$1406.25=0.05\,(60+Q)^2+0.25\,Q^2$

$$\text{Or, } Q=\frac{-6\pm\sqrt{36+4\times0.3\times1226.25}}{0.6}=54.71\text{ m}^3\text{ s}^{-1},$$

taking the positive value.

$\therefore$ Total quantity circulated by the fan $=60+54.71=114.71$ m³ s⁻¹.

$$\text{Power consumption}=\frac{1406.25\times114.71}{0.72}=224\,042.97\text{ W}=224.\text{ kW}$$

Example 9.3

Figure shows the ventilation system for a section of a coal mine with two longwall faces and a set of dip development workings. The production from each of the longwall faces is 400 tonnes per day and that from the development headings, 100 tonnes per day.

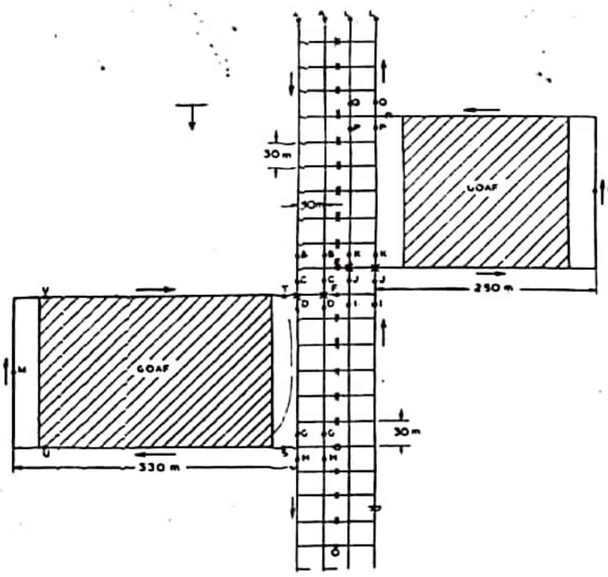

Fig. Exp. 9.3

The mine has a maximum methane emission rate of 12.5 m³ t⁻¹ of coal mined. The longwall faces have a resistance of 1.0 Ns² m⁻⁸. The gate roads as well as the trunk roads have a cross-section of 4×2.5m and have a coefficient of friction $k=0.009$ Ns² m⁻⁴. Calculate the quantities to be circulated in various parts of the system and the pressure required for the same. Also calculate the volumetric efficiency of the section.

Assume the following values for leakage :

Stoppings	0.03 m³ s⁻¹,
Doors	1.0 m³ s⁻¹,
Air-crossings	1.4 m³ s⁻¹,
Goaf (solid-stowed)	nil.

It is obvious that the maximum pressure drop will be along the split ventilating the longwall face M while the other districts are regulated.

Scanned with CamScanner

Quantity requirement at the longwall face M, on the basis of diluting methane to a permissible concentration of 0.75%

$$= \frac{400\times12.5\times100}{24\times60\times0.75} = 462.96 \ \text{m}^3\ \text{min}^{-1}$$

$$= 7.72 \ \text{m}^3\ \text{s}^{-1}.$$

But according to law the quantity requirement

$$= 400\times2.5 = 1000\ \text{m}^3\ \text{min}^{-1} = 16.67\ \text{m}^3\ \text{s}^{-1}$$

as the mine is a degree II gassy mine.

This quantity being higher, has to be circulated.

The quantity requirement at the development headings

$$= 100\times2.5 = 250\ \text{m}^3\ \text{min}^{-1} = 4.17\ \text{m}^3\ \text{s}^{-1}.$$

Taking the above quantities required in the districts and the leakage at various control devices at given rates, the flow at various parts of the section is given in the table below.

Position	Quantity, $\text{m}^3\ \text{s}^{-1}$
O	4.17
M	16.67
N	16.67
H	$4.17+3\times0.03=4.26$
G	$4.26+16.67+1.0=21.93$
D	$21.93+0.03\times5=22.08$
C	$22.08+2\times1.4=24.88$
F	$16.67+2\times1.4=19.47$
B	$24.88+16.67+2\times1.4=44.35$
E	$16.67+2\times1.4=19.47$
A	$44.35+8\times0.03=44.59$
I	$4.17+3\times0.03+1.0+5\times0.03=5.41$
J	$5.41+19.47=24.88$
K	$24.88+2\times1.4=27.68$
P	$27.68+5\times0.03=27.83$
Q	$27.83+0.03+16.67=44.53$
L	$44.53+2\times0.03=44.59$

Pressure loss in different branches in the M longwall face circuit is as follows :

Resistance per metre length of a single airway

$$= \frac{0.009\times2\,(4+2.5)}{(4\times2.5)^3} = 0.000\,117\ \ \text{Ns}^2\,\text{m}^{-8}.$$

Resistance per metre length of twin airways in parallel

$$= \frac{0.000\,117}{4} = 0.000\,029\ \text{Ns}^2\,\text{m}^{-8}.$$

Branch	Length, m	Pressure loss, Pa		
AB(twin)	270	$0.000\,029\times270\times44.59\times44.35$	=	15.48
BC(twin)	30	$0.000\,029\times30\times(24.88)^2$	=	0.54
DG(twin)	180	$0.000\,029\times180\times22.08\times21.93$	=	2.53
Split GS	—			3.00
SU (single)	330	$0.000\,117\times330\times(16.67)^2$	=	10.73
M(longwall face)	—	$1.0\times(16.67)^2$	=	277.89
VT (single)	330	$0.000\,117\times330\times(16.67)^2$	=	10.73
TF (single)	30	$0.000\,117\times30\times16.67\times19.47$	=	1.14
Junction FJ	—			2.73
JK (twin)	30	$0.000\,029\times30\times(24.88)^2$	=	0.54
KP (twin)	180	$0.000\,029\times180\times24.88\times27.83$	=	3.61
QL (twin)	90	$0.000\,029\times90\times44.53\times44.59$	=	5.18
		Total		334.1

Volumetric efficiency of the section

$$= \frac{(16.67+16.67+4.17)100}{44.59} = 84.12\%.$$

Note : Resistance of a longwall face is assumed at 1.0 $\text{Ns}^2\,\text{m}^{-8}$. Shock pressure loss at a split is taken equal to 1.5 times that of a bend and the shock loss at a junction equal to that of a bend with respect to flow in the branch airway. All bends are considered right-angle square bends with square inner corner so that shock factor $X=1.2$. Air density is taken equal to 1.2 kg m^{-3}.

$$\text{Pressure loss at split GS} = \frac{1.5\times1.2\times1.2}{2}\left(\frac{16.67}{4\times2.5}\right)^2 = 3.0 \text{ Pa.}$$

$$\text{Pressure loss at junction FJ} = \frac{1.2\times1.2}{2}\left(\frac{19.47}{4\times2.5}\right)^2 = 2.73 \text{ Pa.}$$

EXERCISE 9

9.1 Blasting in a raise liberates 6 m^3 of toxic fumes. The raise is 1.2×2m in cross-section and has advanced 14m from the level. If the auxiliary ventilator supplies 23.5 m^3 min^{-1} of fresh air to the face, how long will it take to dilute the fumes to a concentration of 100 ppm ?

9.2 1.25 m^3 of CO has been produced by blasting in a heading 2.5×3m in cross-section and 50m long. Calculate the quantity of fresh air to be circulated to the heading per second in order to dilute the CO to a safe concentration of 50 ppm in 5 minutes.

9.3 A heading off a main airway passing 19.7 m^3 s^{-1} of air is ventilated by an overlap system of ventilation. The forcing fan circulated 2.2 m^3 s^{-1} and the exhaust fan, 4.8 m^3 s^{-1}. The methane percentage in the exhaust duct is 1.2%. Calculate the rate of methane emission at the face and the percentage of methane in the main airway downstream of the heading.

9.4 Figure gives the layout of a section of a coal mine worked on the bord-and-pillar method with panels. Pillars are 40m centre to centre and galleries are 4.5m wide and 2.5m high. The mine has a maximum gas emission rate of 8 m^3 t^{-1} of coal produced. Projected production is 150 tonnes from each depillaring panel and 50 tonnes each from the development panel and dip development workings. Make a ventilation plan of the section showing the quantities

flowing in different parts, ventilation control devices and direction of air-flow. Calculate the pressure required to ventilate the section. Assume following values for leakage :

Permanent stoppings	0.03 m^3 s^{-1},
Temporary stoppings (brattice curtains)	0.5 m^3 s^{-1},
Doors	1.0 m^3 s^{-1},
Air-crossings	1.4 m^3 s^{-1}.

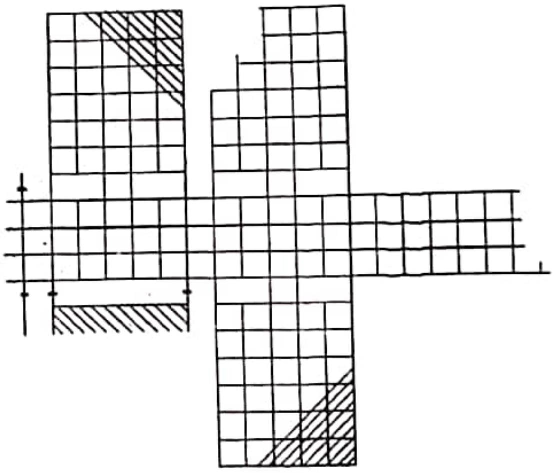

Fig. Exc. 9.4

Scanned with CamScanner

APPENDIX 1

PRESSURE LOSS WITH COMPRESSIBLE AIR-FLOW

In the main text we have assumed air flowing in mine airways to be generally incompressible. This introduces very little error in the calculation of pressure loss as long as it does not exceed about 2.5 kPa, but with higher pressure loss, the change in air density from one end of the system to the other can no longer be ignored. Such a contingency sometimes arises when long tunnels have to be ventilated through ducting by a single fan located at the tunnel entrance. Air-flow at subsonic velocities through uninsulated ducts can be considered as isothermal for which the pressure loss can be estimated from equation A7 derived below.

Equation 4.5 can be written as

$$\frac{dP}{\rho} + \frac{f v^2 \, dL}{2D} + g \, dh + v \, dv = 0 \qquad \text{(A1)}$$

For horizontal pipes of uniform cross-section, $g \, dh = 0$ and the continuity equation $M = \rho v A =$ constant can be written as

$$\rho v = \text{constant} \qquad \text{(A2)}$$

Or, $d(\rho v) = 0$

Or, $v \, d\rho + \rho dv = 0$

Dividing by ρv and rearranging, we get

$$\frac{dv}{v} = \frac{d\rho}{\rho} \qquad \text{(A3)}$$

For isothermal flow, $P/\rho = RT =$ constant.

$$\text{Or,} \quad \frac{dv}{v} = -\frac{dP}{P} \qquad \text{(A4)}$$

Substituting this in equation A1, dividing by v^2 and rearranging, we get

$$f \frac{dL}{2D} = \frac{P}{\rho} \frac{dv}{v^3} - \frac{dv}{v} = RT \frac{dv}{v^3} - \frac{dv}{v} \qquad \text{(A5)}$$

Again for isothermal flow the Reynolds number $Re = v D \rho / \mu$ is constant since the viscosity μ is dependent on temperature alone except at extreme pressures and hence is constant. Therefore f can be taken as constant and equation A5 integrated as follows :

$$\frac{fL}{2D} = \frac{RT}{2}\left(\frac{1}{v_1^2} - \frac{1}{v_2^2}\right) - \ln \frac{v_2}{v_1} \qquad \text{(A6)}$$

$$\text{Now } v = \frac{MV}{A} = \frac{MRT}{AP}$$

where M = mass flow rate
and A = cross-sectional area of pipe.

Expressing v in terms of P, we have

$$\frac{fL}{2D} = \frac{A^2}{2M^2 RT}\left(P_1^2 - P_2^2\right) - \ln \frac{P_1}{P_2} \qquad \text{(A7)}$$

APPENDIX 2

VENTILATION STANDARDS

Coal Mines

Indian Coal Mines Regulation 1971-2 requires that

(i) In every ventilating district, not less than six cubic metres per minute of air per person employed in the district on the largest shift or not less than 2.5 cubic metres per minute of air per daily tonne output, whichever is larger, passes along the last ventilation connection in the district which means the inbye most gallery in the district along which the air passes ;

(ii) at every place in the mine where persons are required to work or pass, the air does not contain less than 19% of oxygen or more than 0.5% of carbon dioxide or any noxious gas in quantity likely to affect the health of any person ;

(iii) the percentage of inflammable gas does not exceed 0.75 in the general body of the return air of any ventilating district and 1.25 in any place in the mine ;

(iv) the wet-bulb temperature in any working place does not exceed 33.5 degree centigrade (306.65 K); and where the wet-bulb temperature exceeds 30.5° centigrade (303.65 K) arrangements are made to ventilate the same with a current of air moving at a speed of not less than one metre per second.

The standards of ventilation specifying minimum velocity of air at various points in gassy seams of different degrees of gassiness have been laid down as in the Table A 2.1.

Table A 2.1 Recommended Air Velocity

Degree of gassiness	Place where velocity of air is to be measured	Velocity of air, m min^{-1}
First degree*	Immediate outbye ventilation connection from the face ;	30
Second degree**	(i) 4.5m from any face whether working or discontinued on the intake side of the brattice or partition ;	30
	(ii) 7.5m outbye of the discharge end of an air pipe ;	15
	(iii) at the maximum span of longwall face ;	60
Third degree***	(i) 4.5m from any face whether working or discontinued on the intake side of the brattice or partition ;	45
	(ii) 7.5m outbye of the discharge end of an air pipe ;	25
	(iii) at the maximum span of longwall face.	75

Scanned with CamScanner

*'gassy seam of the first degree' means a coal seam or part thereof lying within the precincts of a mine not being an opencast working whether or not inflammable gas is actually detected in the general body of the air at any place in its workings below ground, or when the percentage of the inflammable gas, if and when detected in such general body of air does not exceed 0.1 and the rate of emission of such gas does not exceed one cubic metre per tonne of coal produced ;

**'gassy seam of the second degree' means coal seam or part thereof lying within the precincts of a mine not being an opencast working in which the percentage of inflammable gas in the general body of air at any place in the workings of the seam is more than 0.1 or the rate of emission of inflammable gas per tonne of coal produced exceeds one cubic metre but does not exceed ten cubic metres ;

***'gassy seam of the third degree' means a coal seam or part thereof lying within the precincts of a mine not being an opencast working in which the rate of emission of inflammable gas per tonne of coal produced exceeds ten cubic metres.

Based on experience in this country as well as standards adopted by other countries like U.K., Poland, USSR, the following standards with regard to maximum air velocities are recommended (vide DGMS Circular No. 42 of 1974) for different locations as indicated in Table A 2.2.

Table A 2.2

Locality	Maximum velocity ($m\ s^{-1}$)
Ventilation shafts not provided with winding equipment, fan drifts	15
Ventilation shafts where man-winding is not carried out, or mineral hoisting shafts only	12
Shafts used for man-winding and haulage roads (other than conveyor roads)	8
Other roadways	6
Conveyor roads, loading points and transfer points	4
Working faces in development or depillaring/stoping areas including longwall faces	4

Metal Mines

It has been recommended (vide DGMS Circular No. 30 of 1973) that while using any explosive, be it NG-based, AN-based or a slurry in underground metalliferous mines the following precautions regarding ventilation should be observed

(a) Adequate arrangements should be made to circulate such quantity of air upto the site of blasting as to ensure, after every round of blast, dilution of carbon monoxide and oxides of nitrogen in the blasting fumes to less than 50 parts per million and 5 parts per million respectively within a period of 5 minutes.

(b) For drivages more than 50m long, a suitable auxiliary ventilator should be provided to ensure at least $15 m^3\ min^{-1}$ ventilation air-current within 4.5m of the faces.

In view of the difficulty of sampling and analysing for CO and nitrous fumes as well as paucity of suitable detector tubes for these gases, it is advised that no person should be allowed to re-enter the place where blasting has been carried out unless the fumes are cleared and unless a period of at least 15 minutes has elapsed from the time of blasting.

APPENDIX 3

Gaseous products of explosives, in percentage of volume[1]
(Tests with a Bichel gauge with 200g explosives)

	CO_2	CO	N_2O_3 +0.6% NO_2	H	CH_4	N	H_2S	Vol. of gas in $m^3 \times 10^{-3}$
40% Straight dynamite	27.3	26.9	—	18.0	0.4	27.4	—	88.5
60% Straight dynamite	22.2	34.6	—	23.2	0.8	19.2	—	128.9
40% Ammonia dynamite	41.4	3.8	—	3.1	0.8	45.5	5.4	65.6
40% Gelatine dynamite	50.8	3.0	—	1.8	0.8	39.5	4.1	60.3
40% Gelatine dynamite (when burned)	19.4	13.7	11.9	0.4	1.4	53.2	—	—
FFF Black powder	49.7	10.8	—	1.8	0.6	28.4	8.7	67.8
FFF Black powder (when fired in coal)	19.2	28.2	—	10.0	0.4	35.4	6.8	—

Scanned with CamScanner